IC 8853

Bureau of Mines Information Circular/1981

Proceedings of the Workshop on Techniques for Measurement of Thermodynamic Properties, Albany, Oreg., August 21-23, 1979

Compiled by N. A. Gokcen, R. V. Mrazek, and L. B. Pankratz

UNITED STATES DEPARTMENT OF THE INTERIOR

REPRODUCED BY
NATIONAL TECHNICAL
INFORMATION SERVICE
U.S. DEPARTMENT OF COMMERCE
SPRINGFIELD, VA 22161

50272-101

REPORT DOCUMENTATION PAGE	1. REPORT NO. BuMines IC 8853	2.	3. Recipient's Accession No. PB82 129446
4. Title and Subtitle: Proceedings of Workshop on Techniques for Measurement of Thermodynamic Properties, Albany, Oreg., August 21-23, 1979			5. Report Date: September 1981 6. 316022
7. Author(s): N. A. Gokcen, R. V. Mrazek, and L. B. Pankratz			8. Performing Organization Rept. No.
9. Performing Organization Name and Address: Albany Research Center Bureau of Mines, USDI P.O. Box 70 Albany, OR 97321			10. Project/Task/Work Unit No. 11. Contract(C) or Grant(G) No. (C) (G)
12. Sponsoring Organization Name and Address: Office of the Director--Minerals Resource Technology Bureau of Mines U.S. Department of the Interior Washington, DC 20241			13. Type of Report & Period Covered: Information Circular 14.

15. Supplementary Notes

16. Abstract (Limit: 200 words)

To improve communication among Government, industry, and academic researchers in the field of thermodynamics, the Federal Bureau of Mines sponsored a Workshop on Techniques for Measurement of Thermodynamic Properties in August 1979. Participants at the workshop presented 33 papers on the subjects of temperature measurement and control, general calorimetric techniques, low-temperature calorimetry, high-temperature calorimetry, galvanic cells, ionic solutions, and heterogeneous phase equilibria. A special invited lecture was presented by E. F. Westrum, Jr., on the resolution of lattice heat capacity. This Information Circular comprises the proceedings of the workshop and includes the texts of papers presented and discussion by attendees.

17. Document Analysis a. Descriptors

*Calorimetry
Thermodynamic properties
Gibbs energy
Enthalpy
Heat capacity (specific heat)
Heat of formation
Temperature
Galvanic cells
Ionic solutions
Heterogeneous equilibria
Data compilation

b. Identifiers/Open-Ended Terms

c. COSATI Field/Group 07/04 20/13

18. Availability Statement	19. Security Class (This Report)	21. No. of Pages
Unlimited release by NTIS.	Unclassified	447
	20. Security Class (This Page) Unclassified	22. Price

Bureau of Mines
Information Circular 8853

PROCEEDINGS OF THE WORKSHOP ON TECHNIQUES FOR MEASUREMENT OF THERMODYNAMIC PROPERTIES, ALBANY, OREG., August 21-23, 1979

Compiled by N. A. Gokcen, R. V. Mrazek and L. B. Pankratz

ERRATA

APPENDIX.- LIST OF ATTENDEES AND AUTHORS[1]

*Allibert, M. C.	University of Grenoble, France.
*Allred, G. C.	Brigham Young University, Provo, Utah.
Anderson, B. W.	University of Kansas, Lawrence, Kans.
Barclay, J.	Bureau of Mines, Washington, D.C.
*Bauman, J. E.	University of Missouri - Columbia, Columbia, Mo.
Bennett, R. R.	Consultant, Eugene, Oreg.
*Bennington, K. O.	Albany Research Center, Albany, Oreg.
*Beyer, R. P.	Albany Research Center, Albany, Oreg.
*Biltonen, R. L.	University of Virginia, Charlottesville, Va.
*Breslauer, K. J.	Rutgers University, New Brunswick, N. J.
Brown, R. R.	Albany Research Center, Albany, Oreg.
*Bulas, K.	Rutgers University, New Brunswick, N. J.
Bulau, J. R.	University of Oregon, Eugene, Oreg.
*Carling, R. W.	Sandia Laboratories, Livermore, Calif.
*Chang, Y. A.	University of Wisconsin - Milwaukee, Milwaukee, Wisc.
Chase, M. W.	Dow Chemical, Midland, Mich.
*Chatillon, C.	University of Grenoble, France.
*Christensen, J. J.	Brigham Young University, Provo, Utah.
*Criss, C. M.	University of Miami, Coral Gables, Fla.
Daut, G. E.	Albany Research Center, Albany, Oreg.
*Eatough, D. J.	Brigham Young University, Provo, Utah.
*Ferrante, M. J.	Albany Research Center, Albany, Oreg.
*Freeman, R. D.	Oklahoma State University, Stillwater, Okla.
Friedman, H.	General Foods, Tarrytown, N. Y.
*Furukawa, G. T.	National Bureau of Standards, Washington, D.C.
*Gammon, B. E.	Bartlesville Energy Technology Center, Bartlesville, Okla.
*Gokcen, N. A.	Albany Research Center, Albany, Oreg.
*Goldberg, R. N.	National Bureau of Standards, Washington, D.C.
*Good, W. D.	Bartlesville Energy Technology Center, Bartlesville, Okla.
*Hansen, L. D.	Brigham Young University, Provo, Utah.
Herrgott, J.	Hewlett-Packard, Mt. View, Calif.
Higuchi, T.	University of Kansas, Lawrence, Kans.
*Hildenbrand, D. L.	Stanford Research Institute, Menlo Park, Calif.

[1]* indicates author.

Hon, R.	Boston College, Boston, Mass.
*Izatt, R. M.	Brigham Young University, Provo, Utah.
Kirby, R. C.	Bureau of Mines, Washington, D.C.
*Knittel, D. R.	Stanford Research Institute, Menlo Park, Calif.
*Ko, H. C.	Albany Research Center, Albany, Oreg.
Landsberg, Arne	Albany Research Center, Albany, Oreg.
*Lau, K. H.	Stanford Research Institute, Menlo Park, Calif.
Leavenworth, H.	Albany Research Center, Albany, Oreg.
*Mah, A. D.	Albany Research Center, Albany, Oreg.
*Mangum, B. W.	National Bureau of Standards, Washington, D.C.
*Mountcastle, D. B.	University of Virginia, Charlottesville, Va.
Mrazek, R. V.	Oregon State University, Corvallis, Oreg.
*Neumann, J. P.	Albany Research Center, Albany, Oreg.
O'Hare, S. A.	Albany Research Center, Albany, Oreg.
*Otto, R. J.	University of California, Berkeley, Calif.
*Ozbek, H.	University of California, Berkeley, Calif.
*Pankratz, L. B.	Albany Research Center, Albany, Oreg.
*Parlee, N. A. D.	Stanford University, Stanford, Calif.
*Phillips, S. L.	University of California, Berkeley, Calif.
Poppleton, H. O.	Albany Research Center, Albany, Oreg.
*Prosen, E. J.	National Bureau of Standards, Washington, D.C.
Ritchey, J. L.	University of Oregon, Eugene, Oreg.
Rogers, P.	Lawrence Berkeley Laboratory, Berkeley, Calif.
Romans, P.	Albany Research Center, Albany, Oreg.
Russell, J. H.	Albany Research Center, Albany, Oreg.
*Rao, Y. K.	University of Washington, Seattle, Wash.
*Rytting, J. H.	University of Kansas, Lawrence, Kans.
*Schaefer, S. C.	Albany Research Center, Albany, Oreg.
Schenz, T.	General Foods, Tarrytown, N. Y.
Shaffer, M.	University of Oregon, Eugene, Oreg.
*Staples, B. R.	National Bureau of Standards, Washington, D.C.
Stephenson, J. B.	Bureau of Mines, Rolla, Mo.
*Stuve, J. M.	Albany Research Center, Albany, Oreg.
*Suurkuusk, J.	University of Virginia, Charlottesville, Va.
*Tavana, M.	University of California, Berkeley, Calif.
Thomas, R.	Department of Energy, Bartlesville, Okla.
*Vlach, K. C.	University of Wisconsin - Milwaukee, Milwaukee, Wisc.
*Walls, F. L.	National Bureau of Standards, Boulder, Colo.
Weill, D. F.	University of Oregon, Eugene, Oreg.
*Westrum, E. F.	University of Michigan, Ann Arbor, Mich.
*Williamson, K. D.	Union Carbide, South Charleston, W. Va.
*Witkowski, L.	Rutgers University, New Brunswick, N. J.
*Wooley, E. M.	Brigham Young University, Provo, Utah.

Information Circular 8853

Proceedings of the Workshop on Techniques for Measurement of Thermodynamic Properties, Albany, Oreg., August 21-23, 1979

Compiled by N. A. Gokcen, R. V. Mrazek, and L. B. Pankratz

UNITED STATES DEPARTMENT OF THE INTERIOR
James G. Watt, Secretary
BUREAU OF MINES

This publication has been cataloged as follows:

Workshop on Techniques for Measurement of Thermodynamic Properties, Albany, Oreg., 1979.

Proceedings of the Workshop on Techniques for Measurement of Thermodynamic Properties, August 21-23, 1979, Albany Research Center, Albany, Oreg.

(Information circular - U.S. Bureau of Mines ; 8853)

Includes bibliographies.

1. Calorimeters and calorimetry–Congresses. 2. Thermodynamics–Congresses. I. Gokcen, N. A. II. Mrazek, Robert V. III. Pankratz, L. B. IV. Series: United States. Bureau of Mines. Information circular ; 8853.

TN295.U4 [QC290] 622s [620.1'1296] 80-23912

CONTENTS

Page

Abstract 1
Introductory remarks, by R. C. Kirby 2

Section 1.- Temperature measurement and control

Platinum resistance thermometry, by G. T. Furukawa 7
Practical thermometers and temperature scales, by B. W. Mangum 27
Future of quartz resonator thermometry, by F. L. Walls 51
Panel discussion 63

Section 2.- Calorimetric techniques

General Techniques

Thermodynamic property measurements made at the Bartlesville Energy Technology Center, by B. E. Gammon and W. D. Good 66
Recent developments in calorimetric instrumentation: Application to problems of energy storage and recovery, by L. D. Hansen, J. J. Christensen, D. J. Eatough, and R. M. Izatt 81
Resolution of lattice heat capacity, by E. F. Westrum, Jr. (special invited lecture) 100

Low-Temperature Calorimetry

Automation of a low-temperature calorimeter, by R. P. Beyer 113
Design and operation of a differential scanning calorimeter based on the heat leak principle, by R. L. Biltonen, J. Suurkuusk, and D. B. Mountcastle 120
The thermodynamics of transfer of phenol and aniline between nonpolar and aqueous environments, by K. J. Breslauer, L. Witkowski, and K. Bulas 124

High-Temperature Calorimetry

High-temperature enthalpy measurements with a copper-block calorimeter, by M. J. Ferrante 134

Solution Calorimeter

Adiabatic solution calorimetry and standards, by E. J. Prosen 152
Sulfide solution calorimetry - a novel method, by J. M. Stuve 161
Determination of enthalpies of formation by solution calorimetry, by H. C. Ko 166
Some techniques and measurements with HF solution calorimetry, by K. O. Bennington 173

Section 3.- Galvanic cells

Determination of thermodynamic properties of systems by the galvanic cell technique, by Y. K. Rao 179
Electrochemical determination of Gibbs energy of formation of sulfides, by S. C. Schaefer 203

CONTENTS--Continued

Page

Section 4.- Ionic solutions

Determination of ionic activities of aqueous metal salt solutions, by J. P. Neumann and N. A. Gokcen 214
Calorimetry of ionic solutions, by C. M. Criss 225
Aqueous solutions database to high temperatures and pressures, NaCl solutions, by S. L. Phillips, R. J. Otto, H. Ozbek, and M. Tavana 244
Thermodynamic measurements of carbonate equilibria involving metal ions, by J. E. Bauman, Jr. 268
Determination of apparent molar heat capacities by flow microcalorimetry: $\Delta C\beta$ for ionization of water and heavy water at 10°, 20°, and 40° C, by G. C. Allred and E. M. Woolley 275

Section 5.- Data compilation

Evaluation of activity and osmotic coefficients for electrolyte solutions, basic methodology, by B. R. Staples 286
Evaluation of activity and osmotic coefficients for electrolyte solutions, applications to real systems, by R. N. Goldberg 293
Survey of Bureau of Mines critical compilations, by A. D. Mah 305
Thermodynamic data evaluation, by L. B. Pankratz 309
Analysis of equilibrium constant and temperature data: new equations for calculation of change in Planck function from $\Delta C\beta$, by R. D. Freeman 313

Section 6.- Heterogeneous phase equilibria

Thermochemical measurements of gas-solid reactions proposed for chemical heat pumps, by R. W. Carling 323
Differential mass spectrometry using effusion cells for activity measurements in complex liquid oxide mixtures, by M. C. Allibert and C. Chatillon 334
Vapor pressure and calorimetric studies of self-association, by J. H. Rytting 354
Torsion-effusive study of the catalyzed thermal decomposition of magnesium sulfate, by D. R. Knittel, K. H. Lau, and D. L. Hildenbrand 363
The use of the torsion-effusion and the mass spectrometric methods to study complex vaporization processes, by K. H. Lau and D. L. Hildenbrand 374
Experimental methods for determining the Gibbs energies of metal sulfides, by K. C. Vlach and Y. A. Chang 385
Thermodynamics of reactions, and interaction properties in some gas-liquid metal systems, by N. A. D. Parlee 407
Heats of mixing of hydrogen-bonded species, by K. D. Williamson 427

General discussion: Gas-condensed phase equilibria 434
Closing remarks, by N. A. Gokcen 436
Appendix.-List of attendees and authors..... 437

PROCEEDINGS OF THE WORKSHOP ON TECHNIQUES FOR MEASUREMENT OF THERMODYNAMIC PROPERTIES, ALBANY, OREG., AUGUST 21-23, 1979

compiled by

N. A. Gokcen[1], R. V. Mrazek[2], and L. B. Pankratz[3]

ABSTRACT

To improve communication among Government, industry, and academic researchers in the field of thermodynamics, the Federal Bureau of Mines sponsored a Workshop on Techniques for Measurement of Thermodynamic Properties in August 1979. Participants at the workshop presented 33 papers on the subjects of temperature measurement and control, general calorimetric techniques, low-temperature calorimetry, high-temperature calorimetry, galvanic cells, ionic solutions, and heterogeneous phase equilibria. A special invited lecture was presented by E. F. Westrum, Jr., on the resolution of lattice heat capacity. This Information Circular comprises the proceedings of the workshop and includes the texts of papers presented and discussion by attendees.

[1]Research Supervisor.
[2]Chemical Engineer (and Professor of Chemical Engineering, Oregon State University, Corvallis, Oreg.)
[3]Research Chemist.
All compilers are with the Albany Research Center, Bureau of Mines, Albany, Oreg.

INTRODUCTORY REMARKS

by

Ralph C. Kirby[1]

I regret that Dr. Thomas A. Henrie, the Chief Scientist of the Bureau of Mines, is unable to attend and present his introduction to the workshop. As much as he wanted to be here, there is an overriding responsibility. Today, he is giving testimony to a Congressional committee concerned with the Bureau's program.

The Bureau of Mines is proud of its Thermodynamics Group and its contributions, and we plan that thermodynamics will continue to be an important part of our research and development effort. This workshop represents a new part of the thermodynamics program and is a change in direction for the number of ways this group conducts its efforts at transferring the results of its investigations.

My first knowledge of the Bureau of Mines was in 1949 when I was a student. A chemical engineering thermodynamics course included a long problem on zinc metallurgy. The key material came from the publications of K. K. Kelley. The information simply exemplified the work of the Bureau of Mines in metallurgical thermodynamics, which began in 1930. In all there have been 430 publications, including 16 in the well-known series "Contributions to the Data on Theoretical Metallurgy."

As with all long-term research efforts, there must be periodic assessments of direction. In May 1976, we formed the Ad Hoc Committee on the Role of Thermodynamics in Metallurgy to

- review the role of thermodynamics in past and present metallurgical research in the Bureau of Mines,
- evaluate the usefulness of the present program in meeting the Bureau's short- and long-range needs, and
- determine areas where thermodynamic studies are needed.

The members of the committee were: Dr. Harry C. Allen, Jr., Head of the Chemistry Department at Clark University; Dr. Marshall M. Lih, Program Director for Thermodynamics and Mass Transfer at the National Science Foundation; Frank E. Block, then Research Director of the Reno Metallurgy Research Center, Chairman of the Ad Hoc Committee; and James A. Barclay, a chemical engineer on my staff.

[1]Director, Division of Mineral Resources Technology, Bureau of Mines, Washington, D.C.

One of the committee's recommendations was that a workshop be held, to be attended by industry and academic people recognized as leaders in the generation and correlation of thermodynamic data and its application to metallurgical research. This workshop is the result. For the first time, we are trying this new path to more effective communication with a specific segment of the scientific community.

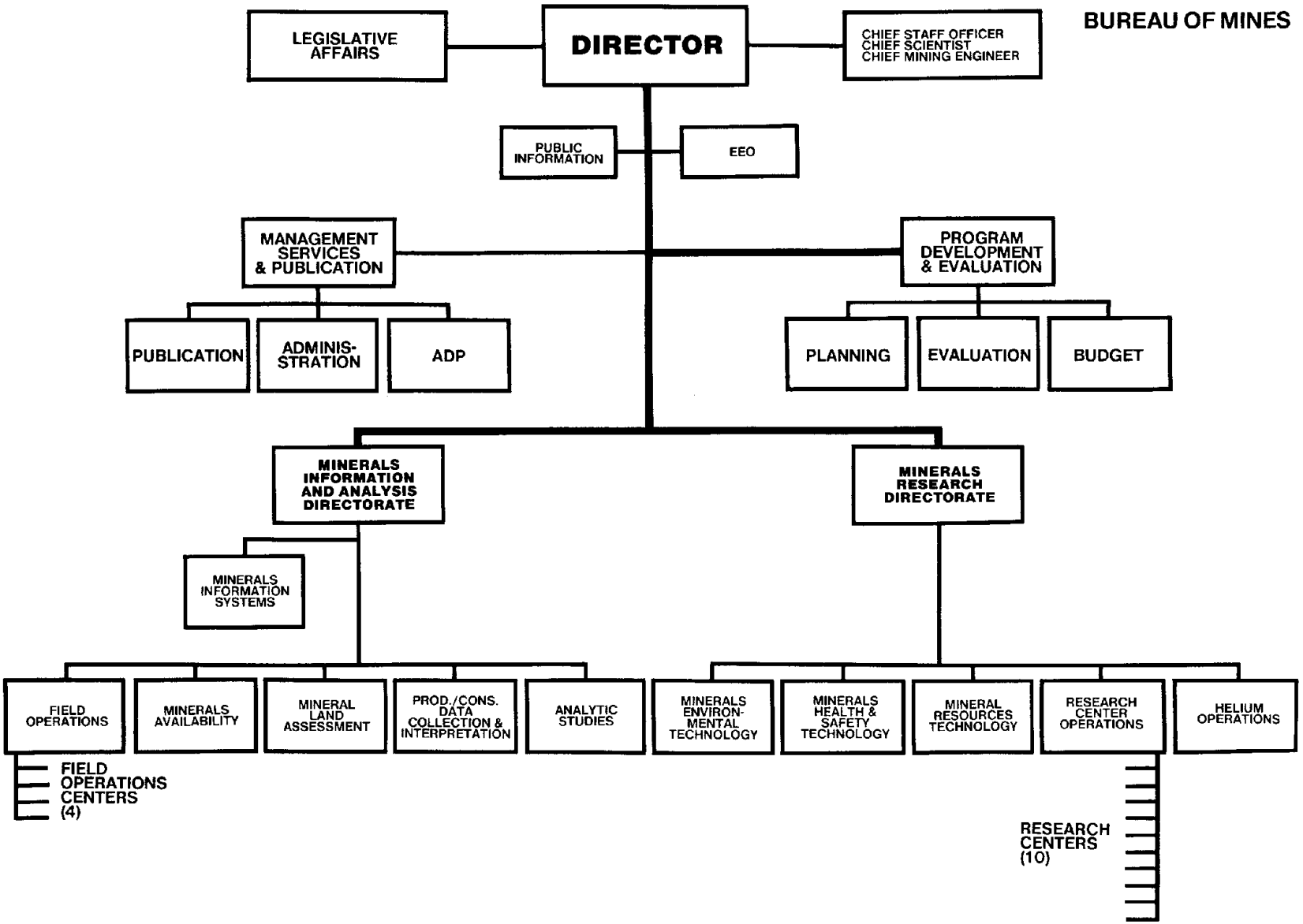
The Bureau of Mines uses many mechanisms for technology transfer, including

- Bureau publication series
- Technical journals
- Professional talks
- Films
- Facility open houses
- Open industry briefings
- Professional contacts
- Patents
- Demonstrations
- Cooperative agreements
- Interagency agreements
- Fellowships

The addition of this workshop to transfer the technology that we develop will also give us input for program planning. The workshop should, in part, result in an examination of the entire U.S. effort in applied thermodynamics as related to metallurgical research. We hope that it also will be an opportunity for the Thermodynamics Group to see how its efforts can be molded to help the Bureau of Mines accomplish its mission.

Since you received your first program in the mail, the Bureau has had a significant reorganization. It, too, resulted from a reassessment of mission, roles, and directions. Coupled with a strong program management, our plan is aimed at maintaining a vigorous research and development program. I would like to show you how thermodynamics will fit into the new Mineral Resources Technology program.

The new organization chart shows the integration of metallurgy and mining technology functions. By addressing the mineral cycle as a unit, this integration will result in more efficient planning, implementation, and management of research programs that address the Nation's mineral problems across the entire portion of the cycle that is the responsibility of the Bureau of Mines. The Mineral Resources Technology program is under the Minerals Research Directorate; other responsibilities of the Directorate are shown in the chart.



Organization chart of the Bureau of Mines.

The goal for the Mineral Resources Technology program is to promote a sound economy and national security through new and/or improved technologies for the development of domestic resources of essential minerals. The components of the program for are summarized in the following list:

- Advancing mineral science and technology
  - Mineral science base
  - Efficient extraction technologies

- Conserving domestic mineral resources
  - Maximum resource recovery
  - Scrap and waste utilization

- Developing domestic mineral resources
  - Use of plentiful resources
  - Substitutes for critical and strategic minerals.

The subprogram objectives for advancing mineral science and technology under which comes our thermodynamics effort, are

To assure an ample domestic supply of the essential minerals that provide the foundation of the Nation's economic and overall security by

- Expanding the mineral science base

- Developing more efficient mineral extraction technologies

The mineral science base program element can be summarized as follows:

- Provides basic scientific information required for development of new and innovative mineral technologies throughout the mineral cycle.

- Provides fundamental data required for mineral technologies
  - Having high impact on national needs
  - Potentially important to meeting future national needs

- Conducts anticipatory research aimed at helping solve future national problems

- Provides bridge between basic research and use of data in practice

Its major milestones will be:

- Develop handbook by 1983 for controlling massive rock failures

- Generate thermodynamic data for use in devising energy-efficient mineral processing sequences

- Complete by 1984 fundamental studies on the physical chemistry of mineral-reagent interactions in sulfide flotation

The mission of the Bureau of Mines is unchanged - to insure the continued viability of the domestic minerals and materials economy and the maintenance of an adequate minerals base, so that the Nation's economic, social, strategic, and environmental needs can be better served. The key words are still "adequate mineral base." The specific goals are slightly different and will no doubt continue to change somewhat, depending on future conditions. Thermodynamics, however, is basic to our research and development efforts, and we see a continued vital role for it in our efforts to fulfill the Bureau's mission.

To aid us in our planning, we solicit your input. If anyone has any comments about whether or not this workshop has been worthwhile to you, or about the Bureau's thermodynamics program, or about the Bureau's research program in general, please write to me in Washington, or speak to Mr. Barclay, who will be here for all 3 days.

SECTION 1.- TEMPERATURE MEASUREMENT AND CONTROL

PLATINUM RESISTANCE THERMOMETRY IN THERMODYNAMIC MEASUREMENTS

by

George T. Furukawa[1]

ABSTRACT

The standard platinum resistance thermometer (SPRT) is the interpolating instrument on the International Practical Temperature Scale of 1968 (IPTS-68) from 13.81 to 903.89 K. The IPTS-68 was designed to be a close approximation to the kelvin thermodynamic temperature scale within the limits of experimental uncertainty believed to exist at the time of the adoption of the scale. The procedure employed at the National Bureau of Standards in the calibration of SPRT's on the IPTS-68 is described. Except for the extremes of range, the temperature values of SPRT's are reproducible to about ±1 mK. Applications of SPRT's and other thermometers in thermodynamic measurements in the range of SPRT's as well as outside the range are discussed.

INTRODUCTION

The "absolute temperature" is basic to the description of thermodynamic properties. The understanding of the temperature function evolved with the development of thermodynamics. Temperature is a function that always has the same value for systems that are in thermal equilibrium with each other. (This is basic to thermometry and, hence, to the assignment of thermodynamic values to any system.) The concept of absolute temperature emerged from the study of Carnot heat engines and upon establishment of the second law of thermodynamics. The temperature function describes the distribution of kinetic energy in the motion of gas molecules; through statistical mechanics, the temperature function can relate the distribution of energy among the different degrees of freedom of any system - gas, liquid, solid, or thermal radiation. For the temperature function to have numerical values, at least one system in equilibrium must first be assigned a numerical value; then, in principle, the numerical values of thermodynamic temperatures of other systems can be obtained, relative to the defining fixed point; by means of Carnot heat engines or other thermodynamic thermometers, e.g., a gas thermometer. However, the difficulties of realization of accurate thermodynamic temperature measurements have

[1]Temperature and Pressure Measurements and Standards Division, Center for Absolute Physical Quantities, National Bureau of Standards, Washington, D.C.

led to the development of practical thermometers and practical temperature scales, leaving the determination of the differences between the practical temperature scale and the thermodynamic temperature scale to specialized laboratories.

In October 1954, the Tenth General Conference on Weights and Measures adopted the kelvin absolute thermodynamic temperature scale defined by assigning the value 273.16 K to the single fixed point - the triple point of water (39)[2], replacing an earlier thermodynamic temperature scale based on assigning a difference of 100° between two fixed points - the freezing and boiling points of water. In October 1968, the International Committee on Weights and Measures adopted the International Practical Temperature Scale of 1968 (34, 35), henceforth to be referred to as IPTS-68. The IPTS-68 has been designed in such a way that the temperatures measured on it closely approximate thermodynamic temperatures, the differences being within the limits of knowledge of the thermodynamic temperatures at the time of the first adoption of the IPTS-68. Temperatures on the IPTS-68 are more easily and accurately reproducible than the temperatures on the thermodynamic temperature scale. The IPTS-68 replaces the International Practical Temperature Scale of 1948 (38-39), which had replaced the International Temperature Scale of 1927 (10).

The IPTS-68 is based on the assigned values of the temperatures of specified, reproducible equilibrium states of pure substances (defining fixed points) and on standard instruments calibrated at these temperatures. Between the fixed-point temperatures, interpolation equations relate the indications of the standard instruments to temperature values of the IPTS-68. The platinum resistance thermometer is the specified standard instrument from 13.81 K (-259.34° C) to 903.89 K (630.74° C), the platinum 10 pct rhodium alloy versus platinum thermocouple from 903.89 K to 1,337.58 K (1,064.43° C), and the optical pyrometer above 1,337.58 K. (Platinum resistance thermometers that meet the IPTS-68 specifications for a standard will be abbreviated SPRT.) This paper includes a brief account of the procedures employed at the National Bureau of Standards (NBS) for the calibration of SPRT's on the IPTS-68, in the range 13.81 K to 903.89 K where a large fraction of thermodynamic measurements are made. The results of the calibration demonstrate the accuracy that can be achieved with SPRT's in calorimetry. The limitations on the application of SPRT's are described, and the recent gas thermometry data that show deviations of the IPTS-68 from the thermodynamic temperature are pointed out.

IPTS-68 IN THE RANGE 13.81 to 903.89 K

The assigned temperatures of 11 equilibrium states that define the IPTS-68 in the region of the SPRT are listed in table 1. The calibrations of SPRT's are made at these fixed points to determine the thermometer constants to be used in the specified interpolation equations. The specified interpolation equations relate the temperature and the resistance ratio:

---

[2]Underlined numbers in parentheses refer to items in the list of references at the end of the paper.

TABLE 1.- Defining Fixed Points of the IPTS-68[1]

Substance and equilibrium state[2]	Assigned value of the IPTS-68 temperature	
	T,K	t,° C
^{3}e-H_2, TP	13.81	-259.34
^{3}e-H_2, BP[4] (33,330.6 Pa)	17.042	-256.108
^{3}e-H_2, BP[4]	20.28	-252.87
Ne, BP[4,5]	27.102	-246.048
O_2, TP	54.361	-218.789
Ar, TP[6]	83.798	-189.352
O_2, CP[4]	90.188	-182.962
H_2O, TP	273.16	0.01
H_2O, BP	373.15	100
Sn, FP[7]	505.1181	231.9681
Zn, FP	692.73	419.58

[1]Except for the triple points and the equilibrium hydrogen point at 17.042 K, the assigned values of temperature are for equilibrium states at a pressure of 101,325 Pa (1 std atm). In the realization of the fixed points, small departures from the assigned temperatures occur as a result of small deviations from the specified pressure at the point of immersion of the thermometer. Adjustment is made for these small temperature differences.

[2]TP = triple point, BP = boiling point, CP = condensation point, FP = freezing point, and e-H_2 = equilibrium hydrogen.

[3]Hydrogen has 2 molecular configurations (nuclear spin arrangements), designated ortho and para. The equilibrium composition is temperature dependent. Equilibrium hydrogen means that the hydrogen has its equilibrium composition at the relevant temperature.

[4]Fractionation of isotopes or impurities dictates the use of boiling points (vanishingly small vapor fraction) for hydrogen and neon, and condensation point (vanishingly small liquid fraction) for oxygen.

[5]Good practice dictates that the neon used should have the normal isotopic composition: 0.905 mol ^{20}Ne, 0.092 mol ^{22}Ne, and 0.0027 mol ^{21}Ne.

[6]The triple point of argon may be used as an alternative to the condensation point of oxygen.

[7]The freezing point of tin (Note that t' = 231.9292° C) may be used as an alternative to the boiling point of water.

$$W(T) = R(T)/R(0^\circ\ C), \tag{1}$$

where R(T) is the thermometer resistance at IPTS-68 temperature T (kelvins) and R(0° C) is the resistance at 0° C. The SPRT resistor must be annealed pure platinum, supported in a "strain-free" manner, and have a value of W(100° C) not less than 1.39250. The resistor must be hermetically sealed inside a protective sheath filled with dry gas.

Below 0° C, the W(T) relation of the SPRT is given by

$$W(T) = W^*(T) + \Delta W(T) \tag{2}$$

where W*(T) is the reference function defined by

$$T = \sum_{j=o}^{20} a_j[(\ln W^*(T) + 3.28)/3.28]^j \tag{3}$$

and ΔW(T) is a deviation function which is a polynomial in T. (The coefficients a_j of equation 3 are given in reference (35). The reference function was developed from the results of comparison of SPRT's against gas thermometers.) The range from 13.81 to 273.15 K is divided into four subranges, each with its specified deviation function of the general form

$$\Delta W(T) = \sum_{i=0}^{n} k_i T^i \tag{4}$$

where $n \leq 4$. In the subrange 13.81 to 20.28 K, n = 3; 20.28 to 54.361 K, n = 3; 54.361 to 90.188 K, n = 2; and 90.188 to 273.15 K, n = 4. The coefficients k_i are determined from the deviation ΔW(T) at the fixed points, obtained by calibration (see equation 1), and by the requirement that the first derivative, dΔW(T)/dT, be continuous at the junction with the next higher subrange.

From 0° C to 630.74° C (930.89 K), the values of IPTS-68 temperature t (defined by t = T - 273.15 K) are defined by

$$t = t' + 0.045\ \left(\frac{t'}{100^\circ\ C}\right)\left(\frac{t'}{100^\circ\ C} - 1\right)\left(\frac{t'}{419.58^\circ\ C} - 1\right)\left(\frac{t'}{630.74^\circ\ C} - 1\right)^\circ\ C$$

where t' is defined by

$$W(t)' = R(t')/R(0^\circ\ C) = 1 + At' + Bt'^2. \tag{6}$$

Equation 6 is equivalent to

$$t' = \left[\frac{1}{\alpha}[W(t') - 1] + \delta\left(\frac{t'}{100^\circ\ C}\right)\left(\frac{t'}{100^\circ\ C} - 1\right)\right]^\circ\ C \tag{7}$$

where $$\alpha = A + B \times 100^\circ\ C \tag{8}$$

and $$\delta = -\frac{B(100^\circ\ C)^2}{A + B \times 100^\circ\ C}\ . \tag{9}$$

(Equation 5 is independent of the SPRT; it is intended to adjust the SPRT temperature scale, given by equation 6, to be closer to the thermodynamic temperature scale.) The thermometer constants R(0° C), A, and B are determined from calibration at the triple point of water, the steam point or the tin point, and the zinc point. The constants α and δ are derived from the constants A and B according to equations 8 and 9, respectively. When the steam point (100° C) is used in the calibration, the constant α can be obtained directly from equation 7, i.e.,

$$\alpha = [W(100^\circ\ C) - 1]/100^\circ\ C. \tag{10}$$

IPTS-68 AS MAINTAINED AT THE NATIONAL BUREAU OF STANDARDS

Above 0° C, the three defining fixed points - triple point of water, tin point, and zinc point - are employed in the calibration of SPRT's. Below 0° C, the defining fixed points are maintained on capsule-type reference standard SPRT's. The IPTS-68 maintained by these capsule-type reference standard SPRT's will be referred to in this paper as NBS-IPTS-68.

TRIPLE POINT OF WATER

Of the 13 defining fixed points that are specified in the text of the IPTS-68, the triple point of water, henceforth referred to as TP, is the most important. It is the single fixed point upon which the kelvin absolute thermodynamic temperature scale is defined. Also, it is the fixed point at which the values of temperature on the thermodynamic scale and on the IPTS-68 are, by definition, the same. Furthermore, the SPRT temperature scale is defined in terms of the resistance ratio R(T)/R(0° C); consequently, the accuracy of every temperature measurement depends on the accuracy of two observations, R(T) and R(0° C). In practice, the R(0° C) may be determined most accurately from resistance measurements at the TP, i.e., R(TP); hence, the accuracy of every temperature value depends ultimately on the accuracy of measurements at the temperature of the TP and on the reproducibility of the TP. In an intercomparison of 15 TP cells at the NBS, the averages of temperatures observed on each cell were within ±0.1 mK (22). In a recent test of the reproducibility of readings in TP cells, the spread of the readings obtained over 3 days on each of eight TP cells was 0.01 mK (23).

R(0° C) is obtained directly from R(TP) by employing equation 6. Since t' is close to 0.01° C, the term containing the constant B is assumed to be zero. (B is about -6×10^{-7} for SPRT's; hence, Bt'^2 is about -6×10^{-11}.) The value of A used is 3.98485×10^{-3}° C, which does not vary by more than $\pm 1 \times 10^{-6}$° C for SPRT's. The assigned TP temperature, t = 0.01° C, is first adjusted for the effect of hydrostatic head of water on the temperature where the SPRT coil is placed in the TP cell. The adjustment amounts to -0.23 mK for an immersion depth of 33 cm. (Adjustment is made for the effect of

hydrostatic head in the zinc and tin point cells also.) The adjusted temperature t is then converted to the corresponding value t' using equation 5. [At t = 0.00977° C, t'-t is only 4 x 10^{-6}° C; however, at t = 231.9681° C (the assigned value for the tin point), t'-t is -0.0389° C (37).]

FREEZING POINTS OF ZINC AND TIN

The freezing points of zinc and tin are realized by using exceptionally high purity samples of these metals in tube furnaces that are automatically controlled to be closely isothermal along the axis. (See reference 27 for details of the design and operation of the furnace.) Both zinc and tin samples have been purified by zone-refining techniques and are nominally 99.9999 pct pure. The freezing-point cells of each metal have been found to agree within ±0.1 mK (24-25, 37). Normally, the SPRT's are calibrated during the first 50 pct of the freeze, during which time the temperature change is not more than 0.2 mK. The complete freeze duration is 14 to 16 hours. The hydrostatic head corrections for the NBS zinc and tin point cells are +0.5 and +0.4 mK, respectively.

OXYGEN POINT

The SPRT's are calibrated at the oxygen point by a comparison method in terms of reference standard SPRT's, using a copper block apparatus which is maintained as nearly isothermal as possible close to the oxygen point. The temperature scale on the long-stem-type reference standard SPRT's for the oxygen-point calibration is made to be consistent with that of the capsule-type reference standard SPRT's that maintain the NBS-IPTS-68 scale in the range 13 to 90 K. The results of repeated measurements on "check SPRT's" show the standard deviation of the oxygen point calibration to correspond to ±0.16 mK (27). (See the section on check SPRT's.)

13.81 K TO 90.188 K RANGE (NBS-IPTS-68)

In the range from 13.81 to 90.188 K, the IPTS-68 is based on the average of four national temperature scales (1, 9, 36, 40) and on the selected IPTS-68 values for the defining fixed points. Each of the national scales, defined in terms of reference standard SPRT's calibrated against gas thermometers, is highly reproducible. The differences between the IPTS-68 and the individual national scales were published (2) to allow the use of the national scales and these differences to give a close approximation to the IPTS-68. The NBS-IPTS-68 was formulated using the NBS-1955 scale (29, 40) and these pub- lished differences (2, 34). Except for the triple point of oxygen, which is at present being investigated, all of the fixed points in the range 13.81 to 90.188 K have been realized in terms of the NBS-IPTS-68 at the National Bureau of Standards (13). [Instead of the boiling point of oxygen, its alternative, the triple point of argon, was realized (21).] After all of the fixed points have been thoroughly investigated, a new NBS-IPTS-68 scale based on fixed points could be developed. However, since a new IPTS is not far in the future, the new NBS scale will most likely be based on the new IPTS to avoid having an NBS scale that is used for only a short duration.

There was recently published (41) an intercomparison of IPTS-68 maintained in various national laboratories. Some of these scales are based, either partially or wholly, on the defining fixed points. The results of the intercomparison showed that differences in the realization of the fixed points contribute much to the differences in the national scales. Figure 1 shows the deviations of the realized fixed points of various laboratories from the NBS-IPTS-68 (12-14, 19-20, 41). In terms of the fixed points and their assigned values, figure 1 shows that the NBS-IPTS-68 tends to be "colder" at 90 K and "hotter" at 13 K. The fixed points that have been realized at the NBS are plotted as ⊘ , which tend to agree with the data of other laboratories.

At the time the IPTS-68 was formulated, an international comparison indicated that the NBS-1955 scale had lower values at the boiling point of oxygen and higher values at the triple point of e-H_2 than previously believed (2, 34). For example, 90.18 K was the designated oxygen point on the NBS-1955; but the comparison gave the value 90.1781 K as the oxygen point on the NBS-1955. In a recent publication, the oxygen point on the NBS-1955 scale was reported as 90.1815 K (14). It seems that the suggested shift for the NBS- 1955 scale was in the wrong direction. The corresponding shifts (approximate) at the other fixed points, based on published values for the fixed points on the NBS-1955 scale, are plotted in figure 1 (symbol ⊗) as NBS-68 minus NBS-55, where NBS-68 is the temperature on the NBS-1955 to which the shift would have been made (2, 34). The plot shows that if this "error" in the "hotness" of the NBS-1955 scale had not been incorporated in the formulation of the NBS-IPTS-68, the NBS scale based on the reference standard SPRT's would be within about 1 mK of the recently realized fixed points.

CALIBRATION OF SPRT's

There are two types of SPRT's received at the NBS for calibration, the long-stem type and the capsule type. The calibration tables for long-stem-type SPRT's are normally furnished for the range -183 to 631° C in W versus t. The calibration tables for capsule-type SPRT's are normally furnished for the range 13 to 500 K in R versus T, because the R(0° C) of capsule-type SPRT's is expected to be determined less often. This means that the users' instruments must be calibrated in terms of the NBS resistance unit to be consistent with the R versus T tables. With the W versus t tables, the principal requirement of the users' instruments is that they be calibrated to yield readings that are "linear."

Calibration of Long-Stem SPRT's

Prior to calibration, all long-stem SPRT's received at the NBS are normally annealed for about 4 hours at 480° C. This removes most of the strains in the SPRT caused by thermal quenching and mechanical actions (5). After annealing, the SPRT's are removed from the furnace and allowed to cool in air at ambient conditions. The rapid cooling of the SPRT's from 480° C by such procedures does not quench in significant amounts of strain (5). The calibration measurements are then obtained at the fixed points in the following sequence: TP, zinc point, TP, tin point, TP, oxygen point, and TP. Normally, six SPRT's are calibrated in a batch. For SPRT's that are used only

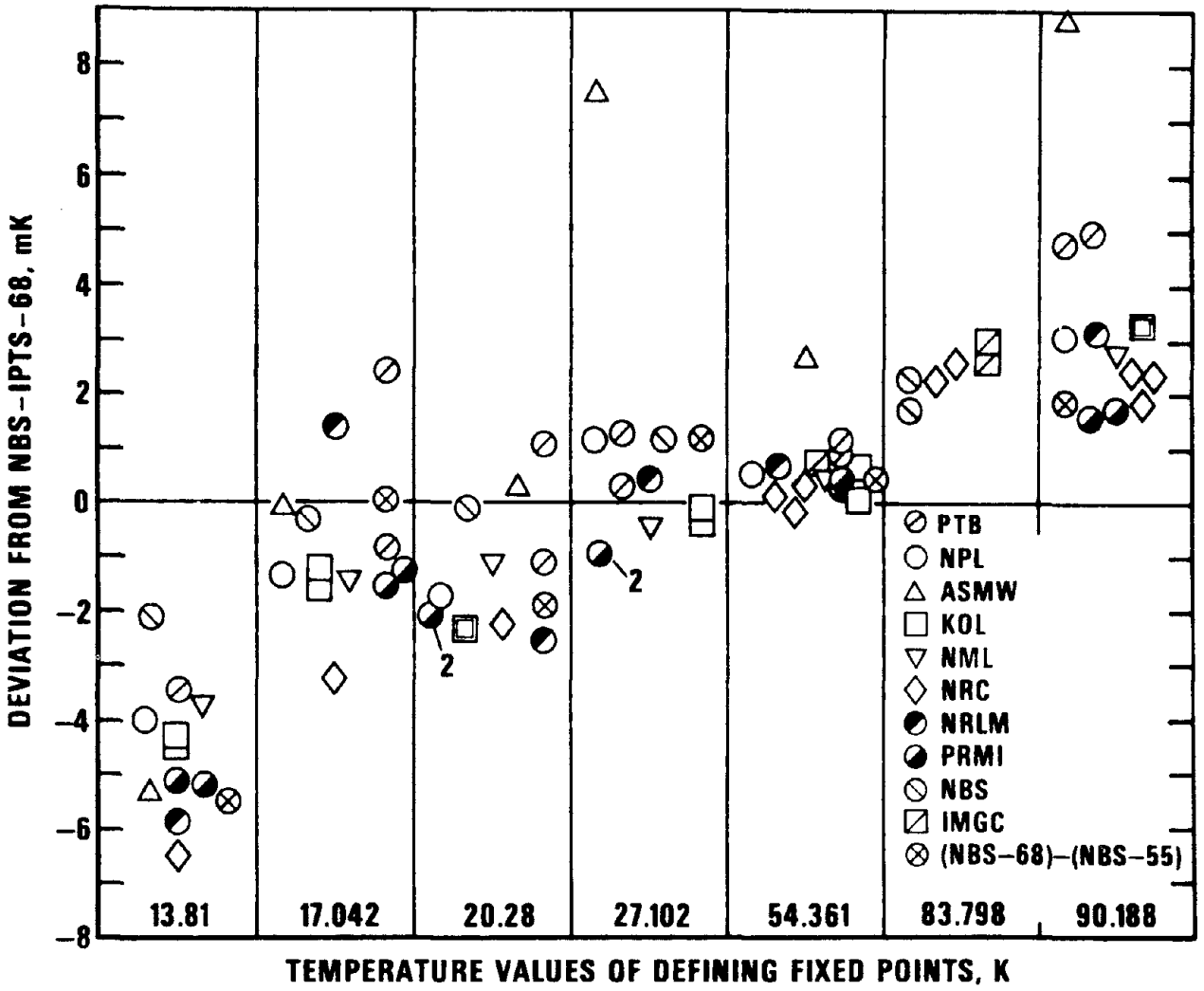


FIGURE 1. - Comparison of fixed points in the range 13 to 90 K realized in various laboratories in terms of the NBS-IPTS-68 scale. ASMW (Democratic Republic of Germany), IMGC (Italy), KOL (The Netherlands), NML (Australia), NPL (United Kingdom), NRC (Canada), NRLM (Japan), PRMI (USSR), PTB (Federal Republic of Germany).

above -50° C, the last two calibration measurements (oxygen point and TP) are omitted. The W value is calculated using the R(TP) reading immediately after the respective zinc, tin, oxygen point reading. The range of the R(TP) readings must be 0.75 mK or less; if not, the SPRT is reannealed and recalibrated. If the R(TP) readings of the second set are not within a 1-mK range, the SPRT is considered unstable and not suitable as an IPTS-68 standard. The average standard deviation of the R(TP) readings of 213 SPRT's that were calibrated between July 1972 and July 1974 was ±0.15.

It has been shown recently that the state of oxidation of platinum wire of the SPRT is dependent upon the temperature, the oxygen pressure inside the sheath, the thermal history, and time (6, 8). Even at room temperature detectable changes take place. Since the platinum oxide has higher resistance than platinum, oxide formation tends to increase the resistance of the SPRT. If the SPRT is heated to a temperature where the oxygen dissociation pressure of the platinum oxide is above the oxygen pressure in the sheath, the platinum would become free of oxide; however, the oxide begins to form when cooled to lower temperatures. This effect imposes a limitation on the precision that can be achieved with the SPRT's above room temperature when the oxide dissociation becomes detectable. For long-stem-type SPRT with 0.3 atm of dry air sealed in the sheath, the reported results suggest that observed values of R(TP) can differ by as much as 4 ppm(1 mK) depending upon the thermal history and time (6). However, the effect of the changes in the state of oxidation of the SPRT can be reduced by obtaining W from two readings with as nearly the same oxidation state as possible (7). Hence, as mentioned earlier, the W values are calculated from the R(TP) reading immediately after the zinc, tin, or oxygen point reading. From the values of W(ZN), W(SN), and $W(O_2)$ the calibration constants of the SPRT are calculated according to equations 6 and 4, and then the calibration tables are calculated using the constants.

Calibration of Capsule-Type SPRT's in the Range 13 to 90 K

The calibration of the capsule-type SPRT's in the range 13 to 90 K is carried out using a liquid helium cryostat. Details of the design and operation are given in references 26 and 37. Within the cryostat, the temperature of the copper block in which 6 SPRT's (2 reference standards and 4 test SPRT's) can be installed is successively controlled, as nearly isothermally as possible, at 16 temperatures including the 6 defining fixed-point temperatures in the range 13 to 90 K. The test SPRT's are calibrated by comparison in terms of the working reference standard SPRT. The second reference standard SPRT is used as a check and is calibrated in terms of the working reference standard SPRT in the same manner as the test SPRT's. The 16 observations are analyzed by a least squares method to obtain the best values at the 6 fix-point temperatures (13.81, 17.042, 20.28, 27.102, 54.361, and 90.188 K). Figure 2 shows the differences, obtained during a 2 1/2-year period, between the computed values of temperatures at the temperatures of intercomparison of the two reference standard SPRT's. Except for a few possible errors of recording of observations, the deviations are within ±0.2 mK above about 20 K; the scatter increases to ±1 or ±2 mK below 20 K.

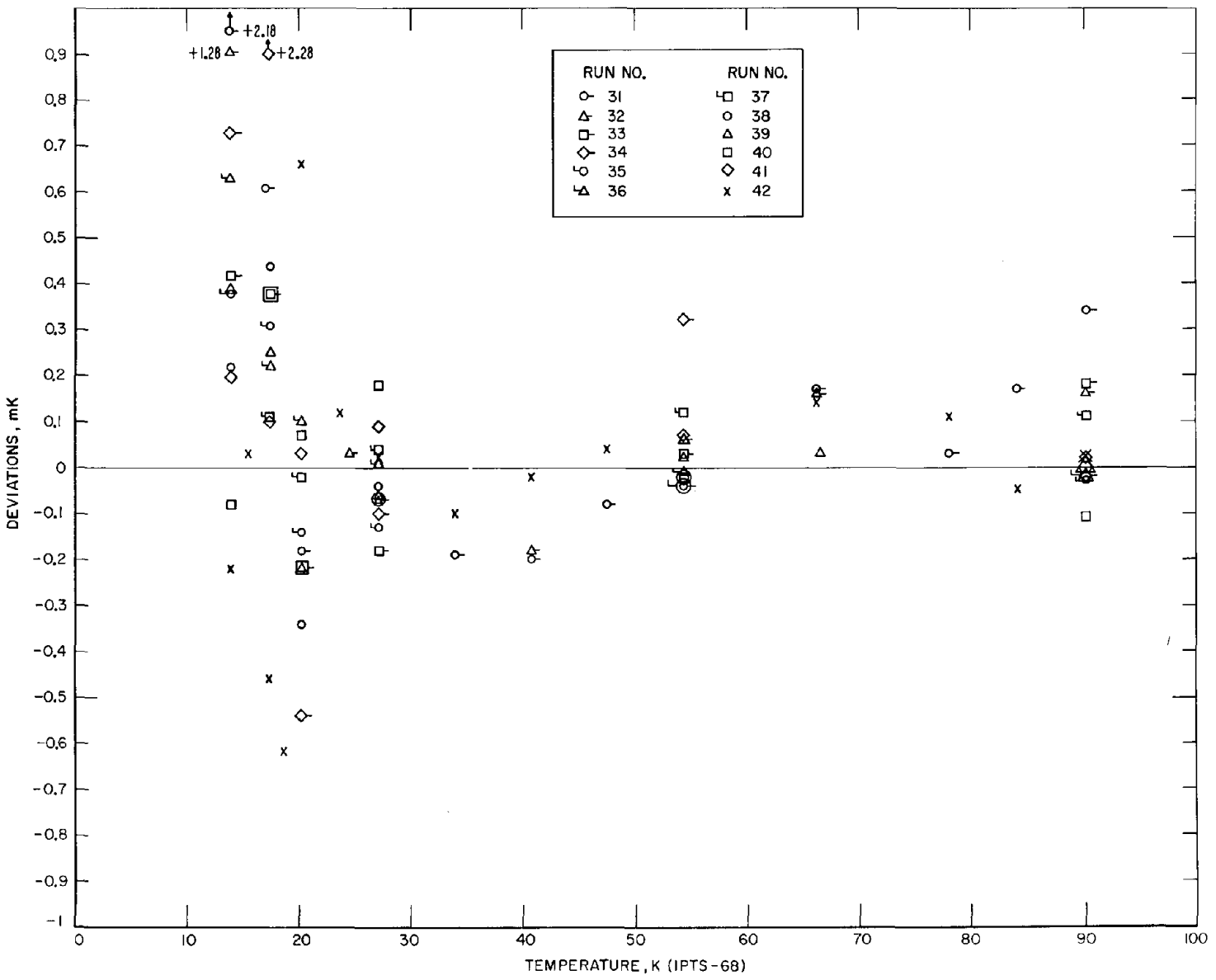


FIGURE 2. - Measured deviations of the values of temperature of the second reference standard SPRT from those of the first reference standard.

The calibration constants for the capsule SPRT are calculated according to equation 4 from the best values of W at the 6 low-temperature fixed points and the calibration data above 90.188 K. (See reference 26 for details.) Calibration tables are calculated from the constants at 0.1 K intervals from 13 to 90 K and at 1 K intervals above 90 K.

Check SPRT's

In a calibration laboratory, it is extremely important that its own measurement errors be small enough so that the decisions of the users of the calibrated instruments would not be affected by those errors. This means that the measurement process of the calibration laboratory must produce results that always lie within these allowable limits of measurement error. (The SPRT calibration laboratory is constantly seeking procedures to improve its measurement accuracy and to eliminate possible accidental calibration errors.) To establish the validity of a single calibration on a new SPRT, i.e., that the variability of the measurements is the same and that the calibration process is not drifting or has not abruptly shifted, there must be redundant measurements of a control or check SPRT. Any abrupt shift in the calibration of the check SPRT would indicate that there may be problems with the fixed-point devices or with the measurement instrument, or that the check SPRT was accidently "bumped." The long record of measurements on the check SPRT gives information on the limits of calibration of any new SPRT. (These considerations are very similar to the testing of a new calorimeter with a substance on which the results are well established. The difference is that the test is made with every batch of SPRT's that is calibrated.)

The procedure that is employed to monitor the calibration of every batch of SPRT's is as follows: Different long-stem-type check SPRT's are assigned to the zinc point, tin point, and oxygen point measurements. These check SPRT's are measured also in the TP cell to obtain the resistance ratio W. In the cases of the tin and zin point measurements, the freeze is initiated using the check SPRT and the first equilibrium readings are obtained on the check SPRT. This is followed by calibration of the test SPRT (usually six). After all of the test SPRT's are calibrated, the check SPRT is read again in the freezing-point cell. The second reading with the check SPRT for the given freeze must not differ from the first by more than 0.5 mK. Usually the difference is not more than 0.1 or 0.2 mK. Also, the readings should be consistent with those obtained in earlier freezes.

With the oxygen-point apparatus and with the cryostat used for the calibration of capsule-type SPRT's from 13 to 90 K, a second reference standard SPRT is calibrated in terms of the working reference standard SPRT in the same manner as the test SPRT's. Readings at the TP are always obtained on the long-stem-type check SPRT's with the calibration of every batch of SPRT's. The standard deviations of the values of W of the check SPRT's obtained from July 1972 to July 1974 were ±0.28 mK, ±0.30 mK, and ±0.16 mK for the zinc, tin, and oxygen point calibrations, respectively. The results on the check SPRT used in the calibration of capsule-type SPRT's in the range

13 to 90 K were shown in figure 2.

Repeatability and Stability of Calibration

The measurement data with the check SPRT's give information on the repeatability of calibration measurements at each of the fixed points. Hence, to test the repeatability of complete calibrations, a long-stem-type SPRT was repeatedly calibrated (including the annealing step) in seven successive batches of calibrations. The sequence of calibrations of this "test" SPRT was varied in each batch of SPRT's so that the location of the calibration on the freezing plateau of the zinc- and tin-point cells was varied for the SPRT. The ranges of the values of W at the zinc, tin, and oxygen points corresponded to about 2.2, 0.8, and 0.7 mK, respectively; the estimated standard deviations corresponded to ±0.75, ±0.25, and ±0.23 mK, respectively. The values of the estimated standard deviations for calibrations at the tin and oxygen points are comparable to the observations with the check SPRT's; however, the estimated standard deviation obtained for the zinc-point calibration is higher than that obtained with the check SPRT for the zinc point. These observations were reproduced in another type of experiment to be described next.

As part of the NBS Measurement Assurance Program (MAP) on platinum resistance thermometry, a set of three SPRT's was furnished to various participating laboratories for comparison of calibrations with the NBS.[3] While the SPRT's were at the participating laboratories they were subjected to the annealing temperatures (450° to 480° C) and to various temperatures (about -180°, 0°, 232°, and 420° C) that were employed in the calibration; while at the NBS the SPRT's were annealed and then recalibrated. Therefore, in the intervals between the calibrations at the NBS the SPRT's were exposed to a wide range of temperatures, including the higher temperatures where they were "annealed." In addition, the SPRT's were subjected to the usual handling process of shipment. The examination of eight intervening calibrations that were obtained at the NBS showed ranges and estimated standard deviations comparable to those for repeated calibrations for the single SPRT that were described above. These results suggest that the treatments to which the MAP SPRT's were subjected did not significantly affect the thermometers any more than if the SPRT's had remained at the NBS laboratory and been used. Also, the results show that, when properly used, a SPRT can give temperature values within ±1 mK over most of the range. Further work is needed to determine the source of the relatively larger imprecision at the zinc point. This may be related to the oxygen-activated cycling effects mentioned earlier.

Deviation of IPTS-68 From the Thermodynamic Temperature

Recent gas thermometry measurements above 0° C at NBS (28) show the

[3]Note that the Measurement Assurance Program is similar to the concept of the Calorimetry Conference samples initiated at the time of the organization of the Conference (1947), where the measurements could be used for comparison or for calibration of calorimeters.

thermodynamic temperature to deviate from the IPTS-68 (fig.3). The deviation is close to 81 mK at 460° C. It seems that the IPTS-48 is closer to the thermodynamic temperature than the IPTS-68. For the lower temperatures, table 2 compares the National Physical Laboratory (United Kingdom) gas thermometer values (NPL-75) with the IPTS-68 values at the fixed points (4). As seen, the gas thermometrv values are lower. A method similar to that described by Douglas (16) may be used to convert existing experimental thermodynamic values on one temperature scale to the basis to another temperature scale.

Recently the 1976 Provisional 0.5 K to 30 K Temperature Scale (17) was adopted to reduce the known irregularities in the IPTS-68 between 13.81 and 27.102 K and in the ^{3}He and ^{4}He vapor pressure scales at the lower temperatures. This scale, designated EPT-76, was designed to join the IPTS-68 smoothly at 27.102 K and to be consistent with the various magnetic scales and the gas thermometry values. The values assigned on this scale to the fixed points in the IPTS-68 range are given in table 2. It is expected that when the new IPTS is adopted (possibly 1986) adjustments for these various differences will be included and the scale will be extended below 13.81 K.

TABLE 2. - Values of temperatures at the fixed points on the IPTS-68, NPL-75, and EPT-76 K

Fixed point	IPTS-68	NPL-75	EPT-76
Ne, BP	27.102	27.0979	27.102
Ne, TP	24.561		24.5591
e-H_2, BP (1 atm)	20.28	20.2714	20.2735
e-H_2, BP (25/76 atm)	17.042	17.0357	17.0373
e-H_2, TP	13.81	13.8039	13.8044

BP=Boiling point TP=Triple point

APPLICATIONS OF CALIBRATED SPRT'S

The results of multiple calibrations show that when SPRT's are properly handled the calibrations at the fixed points can be reproduced to about ±1 mK. Between the fixed points, a comparison of some SPRT's shows a maximum spread of less than 1 mK (32) above 0° C.[4] Between 90 and 273 K, the spread

[4]Although different SPRT's, if calibrated perfectly, will agree exactly at the fixed points, they will show variations in the indicated temperatures at intermediate points. These variations are often referred to as nonuniqueness of the IPTS-68.

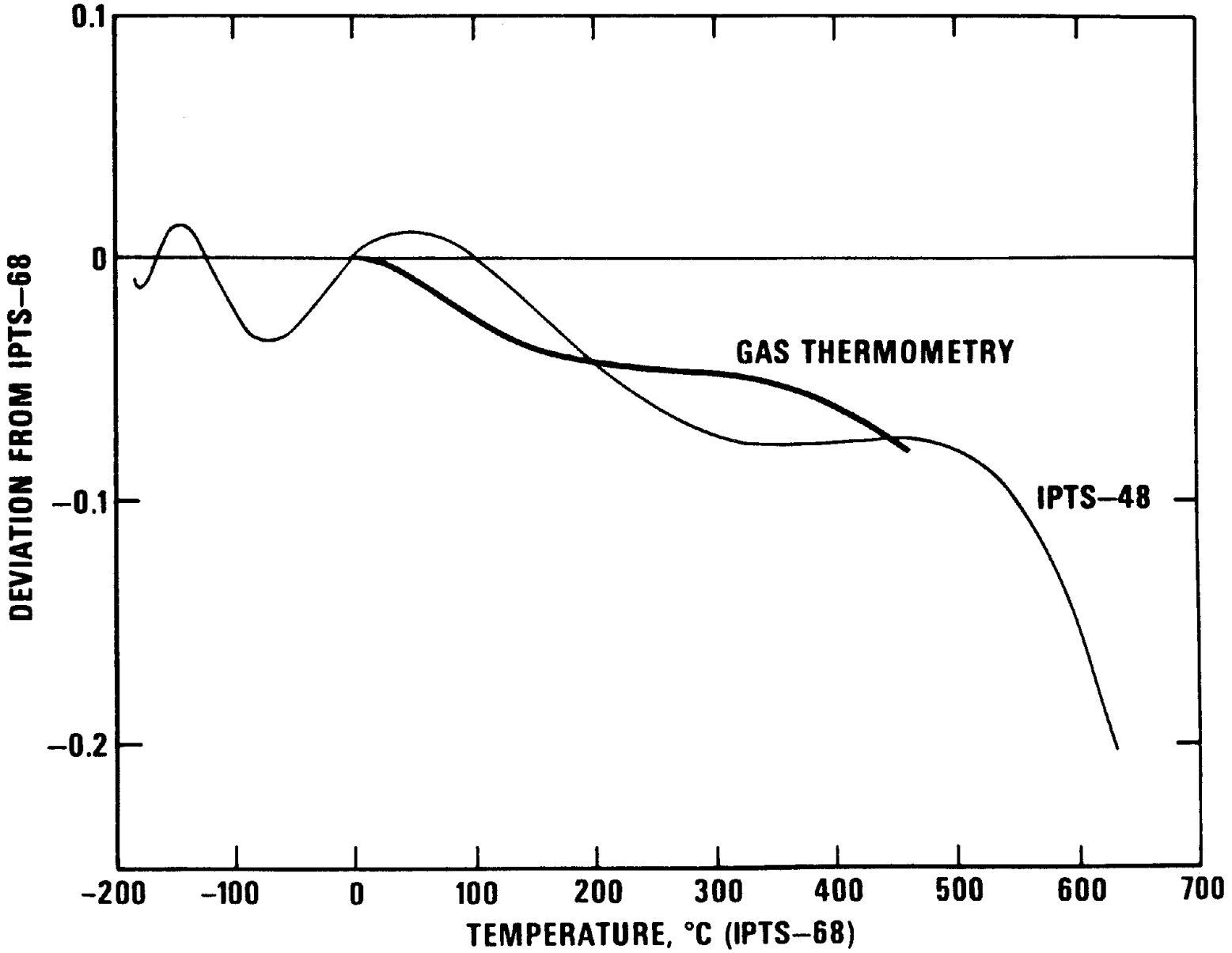


FIGURE 3. - Differences between the IPTS-68 and recent thermodynamic temperature measurements (28) and IPTS-48.

is believed to be close to 2 mK (3). When only the observations close to the fixed-point temperatures are used, the NBS calibration data on the capsule-type SPRT's give a maximum spread of 1.7 mK between 20 and 90 K and about 3 mK between 13 and 20 K. The lack of measurement sensitivity contributed to the spread below 20 K.

Thermometry is used in thermodynamic measurements to determine the temperature or the temperature change. In experiments where the SPRT is used to determine the temperature change, the temperature is determined as part of the measurement. In experiments where the temperature change or temperature difference is to be determined, the highest temperature resolution is desired. The sensitivity of the SPRT is sufficient for direct application in most measurements where the experiment permits fairly large temperature change (1° C or more). Where small temperature changes are involved, SPRT may not have the desired resolution. For measurements in a limited temperature range, thermistors or other resistance thermometers may be suitable, or a thermopile may be better suited. In experiments where two sources of power are compared by thermometry (or differential thermometry), the highest temperature resolution is also desired. Temperature controls require high temperature sensitivity.

In the description of thermodynamic properties (e.g., enthalpy or enthalpy change of a chemical process) the error in temperature must be small enough to have an insignificant effect on the property. For most thermodynamic measurements, an accuracy of the "absolute" temperature of ±0.01 K on the IPTS-68 is adequate. (The relation between the thermodynamic temperature and the IPTS-68 is known to about 0.002 to 0.01 K, depending upon the temperature, see references 4 and 28.) However, to achieve an accuracy of ±0.01 K the resistance of the SPRT must be determined with an accuracy of 0.001 ohm, or about 1 part in 26,000 at 0° C. To be certain that such accuracy is consistently achieved, regular calibration of instruments and check measurements are required. The simplest procedure to monitor the temperature measurement process is to include in the schedule of measurements the measurement of stable reference resistors of suitable value. The history of measurements on the reference resistors will yield information on the precision of resistance measurements and, hence, on that of the thermometry. If the resistance of the thermometer can be determined as a multiple of its resistance at some known temperature (usually 0° C), the demands on the instrumentation will be appreciably reduced.

The calibrated SPRT can be used to calibrate other SPRT's. For example, in a low-temperature adiabatic calorimeter the sample vessel can be replaced by a copper block with wells to calibrate a number of capsule-type SPRT's in terms of a calibrated SPRT. The calibration of long-stem-type SPRT's or other types of resistance thermometers in terms of a calibrated SPRT in fluid baths is a standard procedure in many laboratories. However, care must be taken to design the apparatus so that the test thermometers and the reference SPRT will be at the same temperature. Usually, a "temperature equalizing" copper block with wells for the thermometers is used with the bath. The

copper block is thermally lagged from the bath (e.g. a brass jacket that can be evacuated) to damp the effect of temperature fluctuations in the bath fluid. As a check on the calibration, the position of the test SPRT's and the reference SPRT should be changed and recalibrated, or a calibrated check SPRT should be used. With SPRT's, calibrations near the fixed points are sufficient; however, if the thermometers are not SPRT's, then the comparison calibrations may be necessary at smaller intervals of temperature. (Even SPRT's a least squares treatment of many observations can yield a more reliable W versus T relation.) The calibrations must be made so that the temperature units (size of the degrees) of the working thermometer are the same as those of the SPRT.

For high-temperature drop calorimetry in the region 631° to 1,064° C the platinum-10 pct rhodium alloy versus platinum thermocouple is used because the IPTS-68 in this range is defined by the thermocouple. The uncertainty of temperature measurements is about 0.1 to 0.3 K under optimum conditions (30, 33). It has been shown in recent measurements with specially designed platinum resistance thermometers that reproducibility of 0.03 or 0.04 K can be achieved in the 631° to 1,064° C region (11, 18). Such thermometers should improve the precision of relative enthalpy measurements in the range.

CONCLUSION

The results of calibrations at the NBS and literature data show that temperature values obtained with SPRT's agree with each other within ±1 mK over most of the specified temperature range. The SPRT's can be used directly in thermodynamic measurements and may be used to calibrate working thermometers. Temperature values given by the working thermometers must be consistent with those of the IPTS-68 (i.e., of an SPRT) in its range.

The future of measurements with SPRT's is bright. Instruments are now available, such as the Cutkosky a-c bridge (15) and the d-c comparator bridge (31), where measurement precision of seven or eight digits can be achieved with SPRT's of R(0° C) = 25.5 ohms. (At these levels of measurement, the insulation resistance of leads and thermometer coil support must be 10^9 ohms or higher.) This means that small temperature changes can be determined more precisely. Also, the measurements at the lower temperature limit of the SPRT scale can be made more precise. These instruments can be used to advantage with high-temperature SPRT's (which must have a lower resistance because of the lower insulation resistance of the coil form at high temperatures); for example, with an SPRT of R(0° C) = 0.25 ohm they give a resistance measurement precision that corresponds to about 0.05 mK. When the various possibilities of automatic measurements, testing, and calibrations are added, the instrumentation of thermodynamic measurements seems endless.

---

[4]Although different SPRT's, if calibrated perfectly, will agree exactly at the fixed points, they will show variations in the indicated temperatures at intermediate points. These variations are often referred to as nonuniqueness of the IPTS-68.

REFERENCES

1. Barber, C. R. Low-Temperature Scales 10 to 90° K. Ch. in American Institute of Physics, Temperature, Its Measurement, and Control in Science and Industry. Reinhold Pub. Corp., New York, v. 3, pt. 1, 1962, pp. 345-350.

2. Bedford, R. E., M. Durieux, R. Muijlwijk, and C. R. Barber. Relationships Between the International Practical Temperature Scale of 1968 and the NBS-1955, NPL-61, PRMI-54, and PSU-54 Temperature Scales in the Range From 13.81 to 90.188 K. Metrologia, v. 5, 1969, pp. 47-49.

3. Bedford, R. E., and C. K. Ma. A Note on the Reproducibility of the IPTS-68 Below 273.15 K. Metrologia, v. 6, 1970, pp. 89-94.

4. Berry, K. H. Fixed Point Values on NPL-75 and Virial Coefficient Data of ^{4}He. Comité Consultatif de Thermométrie, 11th session, Document 76-27, June 1976.

5. Berry, R. J. The Influence of Crystal Defects in Platinum on Platinum Resistance Thermometry. Ch. in Temperature, Its Measurement and Control in Science and Industry, ed. by H. H. Plumb, Instrument Society of America, Pittsburgh, Pa., v. 4, 1972, pp. 937-949.

6. _____. Oxygen-Activated Thermal Cycling Effects in Pt Resistance Thermometers. Metrologia, v. 10, 1974, pp. 145-154.

7. _____. Control of Oxygen-Activated Cycling Effects in Platinum Resistance Thermometers. Ch. in Temperature Measurements 1975, ed. by B. F. Billing and T. J. Quinn, Institute of Physics (London), ConSeries 26, 1975, pp. 99-106.

8. _____. Study of Multilayer Surface Oxidation of Platinum by Electrical Resistance Technique. Surface Science, v. 76, 1978, pp. 415-442.

9. Borovik-Romanov, A. S., P. G. Strelkov, M. P. Orlova, and D. N. Astrov. The I.M.P.R. Temperature Scale for the 10 to 90° K Region. Ch. in American Institute of Physics, Temperature, Its Measurement, and Control in Science and Industry, Reinhold Pub. Corp., New York, v. 3, pt. 1, 1962, pp. 113-128.

10. Burgess, G. K. The International Temperature Scale. J. Res. NBS, v. 1, 1928, pp. 635-640.

11. Chattle, M. V. Platinum Resistance Thermometry Up to the Gold Point. Ch. in Temperature, Its Measurement and Control in Science and Industry, ed. by H. H. Plumb. Instrument Society of America, Pittsburgh, Pa., v. 4, pp. 907-918.

12. Compton, J. P. The Realization of the Normal Boiling Point of Neon. II. Vapour Pressure Measurements. Metrologia, v. 6, 1970, pp. 103-109.

13. _____. The Realization of Low-Temperature Fixed Points. Ch. in Temperature, Its Measurement and Control in Science and Industry, ed. by H. H. Plumb. Instrument Society of America, Pittsburgh, Pa., v. 4, 1972, pp. 195-209.

14. Compton, J. P., and S. D. Ward. Realization of the Boiling and Triple Points of Oxygen. Metrologia, v. 12, 1976, pp. 101-113.

15. Cutkosky, R. D. An a-c Resistance Thermometer Bridge. J. Res. NBS, v. 74C, 1970, pp. 15-18.

16. Douglas, T. B. Conversion of Existing Calorimetrically Determined Thermodynamic Properties to the Basis of the International Practical Temperature Scale of 1968. J. Res. NBS, v. 73A, 1969, pp. 451-470.

17. Durieux, M., D. N. Astrov, W. R. G. Kemp, and C. A. Swenson. The Derivation and Development of the 1976 Provisional 0.5 to 30 K Temperature Scale. Metrologia, v. 15, 1979, pp. 57-63.

18. Evans, J. P., and S. D. Wood. An Intercomparison of High Temperature Platinum Resistance Thermometers and Standard Thermocouples. Metrologia, v. 7, 1971, pp. 108-130.

19. Furukawa, G. T. Vapor Pressures of Natural Neon and of the Isotopes ^{20}Ne and ^{22}Ne from the Triple Point to the Normal Boiling Point. Metrologia, v. 8, 1972, pp. 11-27.

20. _____. Vapor Pressures of ^{20}Ne and ^{22}Ne. Ch. in Temperature, Its Measurement and Control in Science and Industry, ed. by H. H. Plumb. Instrument Society of America, Pittsburgh, Pa., v. 4, 1972, pp. 127-135.

21. _____. Realization of Triple Point of Argon in a Transportable Sample Cell. Comité Consultatif de Thermométrie, 12th session, Document 78-14, May 1978.

22. Furukawa, G. T., and W. R. Bigge. Unpublished Data. NBS, 1975.

23. Furukawa, G. T., and E. R. Pfeiffer. Unpublished Data. NBS, 1979.

24. Furukawa, G. T., and J. L. Riddle. Comparison of Freezing Temperatures of National Bureau of Standards SRM-740 Zinc Standards. Comité Consultatif de Thermométrie, 12th session, Document 78-16, May 1978.

25. Furukawa, G. T., J. L. Riddle, and W. R. Bigge. Investigation of Freezing Temperatures of National Bureau of Standards Tin Standards. Ch. in Temperature, Its Measurement and Control in Science and Industry, ed. by H. H. Plumb. Instrument Society of America, Pittsburgh, Pa, v. 4, 1972, pp. 247-263.

26. Furukawa, G. T., J. L. Riddle, and W. R. Bigge. The International Practical Temperature Scale of 1968 in the Region 13.81 K to 90.188 K as Maintained at the National Bureau of Standards. J. Res. NBS, v. 77A, 1973, pp. 309-332.

27. _____. The International Practical Temperature Scale of 1968 in the Region 90.188 K to 903.89 K as Maintained at the National Bureau of Standards. J. Res. NBS, v. 80A, 1976, pp. 477-504.

28. Guildner, L. A., and R. E. Edsinger. Deviation of International Practical Temperatures From Thermodynamic Temperatures in the Temperature Range From 273.16 K to 730 K. J. Res. NBS, v. 80A, 1976, pp. 703-738.

29. Hoge, H. J., and F. G. Brickwedde. Establishment of a Temperature Scale for the Calibration of Thermometers Between 14° and 83° K. J. Res. NBS, v. 22, 1939, pp. 351-373.

30. Jones, T. P. The Accuracies of Calibration and Use of I.P.T.S. Thermocouples. Metrologia, v. 4, 1968, pp. 80-83.

31. Kusters, N. L., M. P. MacMartin, and R. J. Berry. Resistance Thermometry With the Direct Current Comparator Bridge. Ch. in Temperature, Its Measurement and Control in Science and Industry, ed. by H. H. Plumb. Instrument Society of America, Pittsburgh, Pa., v. 4, 1972, pp. 1477-1485.

32. McLaren, E. H., and E. G. Murdock. The Freezing Points of High-Purity Metals as Precision Temperature Standards. VIII b. Sb: Liquidus Points and Alloy Melting Ranges of Seven Samples of High-Purity Antimony; Temperature-Scale Realization and Reliability in the Range 0-631° C. Can. J. Phys. v. 46, 1968, pp. 401-444.

33. _____. New Considerations on the Preparation, Properties and Limitations of the Standard Thermocouple for Thermometry. Ch. in Temperature, Its Measurement and Control in Science and Industry, ed. by H. H. Plumb. Instrument Society of America, Pittsburgh, Pa., v. 4, 1972, pp. 1543-1560.

34. Metrologia. The International Practical Temperature Scale of 1968 (Adopted by the Comité International des Poids et Mesures). v. 5, 1969, pp. 35-44.

35. _____. The International Practical Temperature Scale of 1968 (Amended Edition of 1975). v. 12, 1976, pp. 7-17.

36. Moessen, G. W., J. G. Aston, and R. G. Ascah. The Pennsylvania State University Thermodynamic Temperature Scale Below 90°K and the Normal Boiling Points of Oxygen and Normal Hydrogen on the Thermodynamic Scale. Ch. in American Institute of Physics, Temperature, Its Measurement, and Control in Science and Industry. Reinhold Pub. Corp., New York, v. 3, pt. 1, 1962, pp. 91-102.

37. Riddle, J. L., G. T. Furukawa, and H. H. Plumb. Platinum Resistance Thermometry, NBS Monograph 126, April 1973, 129 pp.

38. Stimson, H. F. The International Temperature Scale of 1948. J. Res. NBS, v. 42, 1948, pp. 209-217.

39. _____. International Practical Temperature Scale of 1948. (Text revision of 1960). J. Res. NBS, v. 65A, 1961, pp. 139-145.

40. Swindells, J. F. National Burau of Standards Provisional Scale of 1955. Ch. in Temperature. Sec. in Precision Measurement and Calibration. Spec. Pub. 300, v. 2, August 1978, p. 56.

41. Ward, S. D., and J. P. Compton. Intercomparison of Platinum Resistance Thermometers and T_{68}. Metrologia, v. 15, 1979, pp. 31-46.

PRACTICAL THERMOMETERS AND TEMPERATURE SCALES

by

B. W. Mangum[1]

ABSTRACT

Since thermodynamic temperatures are very difficult to measure, a practical scale of temperatures approximating the thermodynamic temperatures at several fixed points, with a prescribed procedure for interpolating between those points with standard instruments, was developed. The latest version of the practical scale is the International Practical Temperature Scale of 1968 (amended edition of 1975) (IPTS-68), the lowest temperature of which is at the triple point of hydrogen. In 1978, a provisional scale (EPT-76) extending from 0.5 K to 30 K was promulgated by the International Committee of Weights and Measures in order to correct the lower end of the IPTS-68 and to extend it to lower temperatures. This new scale and its realization are discussed. The application of these scales is through suitably calibrated practical thermometers such as thermistors and other resistance thermometers, electronic and nuclear paramagnetic thermometers, nuclear quadrupole resonance thermometers, and several other less widely used thermometers. A discussion is given of some of the advantages and limitations of some of these practical thermometers, with special emphasis on thermistors.

INTRODUCTION

The temperature which is referred to in thermodynamic equations and which is the desired observable in thermometry and in various other thermodynamic investigations is the thermodynamic temperature T. Unfortunately, thermodynamic temperatures are very difficult to measure accurately. As a result, an internationally agreed upon practical scale of temperatures approximating the thermodynamic temperatures at several "fixed points," with a prescribed procedure for interpolating between those points with standard instruments, was developed. The practical scale has been revised over the years, and the latest version is the International Practical Temperature Scale of 1968 (amended edition of 1975) (IPTS-68) (11-12)[2]. The lowest temperature of this scale

[1]Temperature Measurements and Standards Division, Center for Absolute Physical Quantities, National Measurement Laboratory, National Bureau of Standards, Washington, D.C.

[2]Underlined numbers in parentheses refer to items in the list of references at the end of the paper.

is the triple point of hydrogen at 13.81 K. Since it had become evident that the low-temperature end of the IPTS-68 and the helium (^{4}He and ^{3}He) vapor pressure scales were inconsistent with each other and differ considerably from thermodynamic temperature, it was deemed prudent to have a provisional practical scale, which corrects the lower end of the IPTS-68 and extends it to lower temperatures, in use until a new International Practical Temperature Scale could be adopted. In 1978, such a provisional scale extending from 0.5 K to 30 K was promulgated by the International Committee of Weights and Measures.

The application of the temperature scales is through suitably calibrated practical thermometers such as thermistors, germanium resistance thermometers, rhodium-iron resistance thermometers, carbon resistance thermometers, capacitance thermometers, noise thermometers, quartz crystal thermometers, electronic salt thermometers, nuclear magnetic resonance thermometers, nuclear quadrupole resonance thermometers, and/or diode thermometers. The different types of thermometers have their own special advantages and limitations, of course, which make them particularly suited for certain applications and not for others. Stability is a feature of special concern for all thermometers.

In the next section, we will discuss the new low-temperature provisional scale, its objectives, and its realization. Then, in the following section, we will discuss some of the practical thermometers most widely used for the determination of temperatures on the provisional scale and on the IPTS-68. Some of their advantages and limitations will be given.

THE 1976 PROVISIONAL 0.5 K to 30 K TEMPERATURE SCALE

The NBS acoustical thermometer measurements, from which the NBS Provisional Scale of 1965 (2-20 K) (14) was derived, were the first measurements to show that the 1958 ^{4}He scale was in error Subsequently, magnetic thermometry additionally showed that the liquid helium vapor pressure scales and the IPTS-68 were inconsistent with each other. Because of the evidence that the helium vapor pressure scales and the low-temperature end of the IPTS-68 were not only inconsistent with each other but also indicated temperatures that differed from thermodynamic temperatures, the Comité Consultatif de Thermométrie (CCT) proposed to the Comité International des Poids et Mesures (CIPM) in 1976 that a provisional practical temperature scale be recommended for use in the range of 0.5 K to 30 K until a new International Practical Temperature Scale could be adopted. Subsequently, a provisional scale was derived and was promulgated in 1978. It is called "The 1976 Provisional 0.5 K to 30 K Temperature Scale" (6, 10) and temperatures on this scale are denoted by T_{76}. The scale itself is denoted by EPT-76, which is an abbreviation for the French title "Echelle Provisoire de Température de 1976 entre 0.5 K et 30 K."

The objectives that were striven for in deriving the scale were threefold. Firstly, the scale should be thermodynamically smooth in the sense that the second and higher derivatives of T_{76} with respect to T should be zero or small. For thermometer calibrations, this is especially important where the EPT-76 and the IPTS-68 join. Secondly, the EPT-76 should be continuous with the IPTS-68 at 27.1 K. Thirdly, within the constraints of the first two con-

ditions, temperatures on the EPT-76, T_{76}, should agree as closely as possible with the thermodynamic temperature.

The EPT-76 is defined in terms of several specified reproducible equilibrium states between phases of pure substances and in terms of the superconductive transition points of several pure metals (16), reference points to which values of temperature have been assigned. Table 1 gives the defining reference points and the values of temperature assigned to them. Realization of the EPT-76 is provided by the defining temperature reference points and by interpolation between them by any of a variety of methods. Values of T_{76} may also be obtained from specified existing laboratory scales. The four approved methods for realizing the EPT-76 over all or part of its range are

1. Through the use of a "thermodynamic" interpolating instrument, such as a gas thermometer or a magnetic thermometer, which has been calibrated at one or more of the defining reference points.

TABLE 1. - Reference points of the EPT-76

Reference point	Assigned temperature T_{76}, K
Superconducting transition point of cadmium. . . .	0.519
Superconducting transition point of zinc	.851
Superconducting transition point of aluminum . . .	1.179 6
Superconducting transition point of indium	3.414 5
Boiling point of ^4He[1].	4.222 1
Superconducting transition point of lead	7.199 9
Triple point of equilibrium hydrogen[2].	13.804 4
Boiling point of equilibrium hydrogen at a pressure of 33 330.6 pascals (25/76 std atm)[2]. .	17.037 3
Boiling point of equilibrium hydrogen[1,2]	20.273 4
Triple point of neon[3].	24.559 1
Boiling point of neon[1,2,3]	27.102

[1]Boiling point under a pressure of 101 325 Pa (1 std atm).

[2]These are the 4 lower defining points of the IPTS-68. (Note that the values of temperature assigned to these points in EPT-76 are not the same as those assigned in IPTS-68). The term equilibrium hydrogen means here that the hydrogen should have its equilibrium ortho-para composition at the relevant temperature.

[3]The 2 neon points are for neon with the natural isotopic composition of 2.7 mmol of ^{21}Ne and 92 mmol of ^{22}Ne per 0.905 mol of ^{20}Ne.

2. For temperatures above 13.81 K, the scale may be realized through the use of the IPTS-68, as realized at the National Physical Laboratory (NPL), and the differences given in table 2.

TABLE 2. - Differences between the EPT-76 (T_{76}) and the IPTS-68 (T_{68}) as realized at the National Physical Laboratory (NPL)

T_{68} K	$T_{68}-T_{76}$ mK	T_{68} K	$T_{68}-T_{76}$ mK	T_{68} K	$T_{68}-T_{76}$ mk
13.81	5.6	19.0	7.4	24.5	2.1
14.0	4.6	19.5	7.3	25.0	1.6
14.5	3.0	20.0	6.9	25.5	1.1
15.0	2.0	20.5	6.4	26.0	.7
15.5	2.2	21.0	5.8	26.5	.3
16.0	2.6	21.5	5.3	27.0	.0
16.5	3.6	22.0	4.8	27.1	.0
17.0	4.6	22.5	4.2	28.0	.0
17.5	5.6	23.0	3.7	29.0	.0
18.0	6.5	23.5	3.2	30.0	.0
18.5	7.2	24.0	2.7		

3. For temperatures below 5 K, the scale may be realized through the use of the 1958 ^{4}He vapor pressure scale, or below 3 K, through the use of the 1962 ^{3}He vapor pressure scale, and the difference given in

TABLE 3. - Differences between the EPT-76 and the helium vapor pressure scales (the 1958 ^{4}He scale and the 1962 ^{3}He scale)

$T_{58,62}$ K	$T_{58,62}-T_{76}$ mK	$T_{58,62}$ K	$T_{58,62}-T_{76}$ mK
0.5	-1.7	2.6	-5.5
.6	-2.0	2.8	-5.9
.8	-2.5	3.0	-6.3
1.0	-2.9	3.2	-6.6
1.2	-3.3	3.4	-6.8
1.4	-3.6	3.6	-7.0
1.6	-3.9	3.8	-7.0
1.8	-4.1	4.0	-7.1
2.0	-4.3	4.2	-7.1
2.2	-4.6	4.5	-7.1
2.4	-5.0	5.0	-7.1

NOTE - $T_{58,62}$ means T_{62} below 1 K, T_{62} and T_{58} between 1 K and 3.2 K, and T_{58} above 3.2 K.

4. Through the use of any of the existing laboratory scales for which the differences from the EPT-76 are given. (See tables 4 and 5. Differences between the magnetic scales and the EPT-76 and between the NPL-75 gas thermometer scale (2) and the EPT-76 are not given here.)

TABLE 4. - Differences between the NBS provisional temperature scale 2-20 K (1965) ($T_{NBS\ 2-20}$) and the EPT-76 (T_{76})

$T_{NBS\ 2-20}$[1] K	$T_{NBS\ 2-20}-T_{76}$ mK	$T_{NBS\ 2-20}$[1] K	$T_{NBS\ 2-20}-T_{76}$ mK
2.3	2.1	11.0	-1.0
2.8	-1.1	12.0	.2
3.2	1.0	13.0	-1.8
4.2	2.5	14.0	-2.2
5.0	3.0	15.0	-.6
6.0	1.7	16.0	.9
7.0	4.8	17.0	1.7
8.0	2.2	18.0	-.9
9.0	-1.5	19.0	-.2
10.0	-2.1	20.0	+7.0

[1]These temperatures are very close to the actual temperatures(acoustic points) at which the NBS 2-20 scale is defined.

TABLE 5. - Differences between the NBS version of the IPTS-68 (T_{NBS-68}) and the EPT-76 (T_{76})

T_{NBS-68} K	$T_{NBS-68}-T_{76}$ mK	T_{NBS-68} K	$T_{NBS-68}-T_{76}$ mK	T_{NBS-68} K	$T_{NBS-68}-T_{76}$ mK
13.8	1.7	19.0	4.9	24.5	2.9
14.0	1.8	19.5	4.9	25.0	2.5
14.5	2.1	20.0	4.9	25.5	2.1
15.0	2.0	20.5	4.8	26.0	1.7
15.5	2.2	21.0	4.7	26.5	1.3
16.0	2.4	21.5	4.6	27.0	1.1
16.5	3.0	22.0	4.5	27.5	1.1
17.0	3.5	22.5	4.2	28.0	1.1
17.5	3.9	23.0	4.0	29.0	1.1
18.0	4.4	23.5	3.7	30.0	1.0
18.5	4.8	24.0	3.4		

Thus, if thermometers have been calibrated against either the IPTS-68, the NBS version of the IPTS-68, the NBS 2-20 provisional scale, or any of the other specified laboratory scales, those thermometer calibrations can be put on the EPT-76 by making the appropriate corrections at the calibration points as given in the tables. Any calibration table for interpolation between the corrected temperature points (on the EPT-76) would have to be recalculated, of course, by use of the appropriate formulae.

Since a gap in temperature between 7.2 K and 13.8 K exists in the distribution of reference points of the EPT-76, the direct calibration of secondary resistance thermometers, such as germanium and rhodium-iron thermometers, is not realistic. Consquently, a "thermodynamic" interpolation instrument such as a magnetic thermometer or a gas thermometer is required for the practical realization of EPT-76 over all or certain parts of its range.

The various laboratory scales from which the EPT-76 may be realized, over the range in which the laboratory scales are defined, refer to scales maintained by sets of calibrated germanium or rhodium-iron resistance thermometers in various standards laboratories.

It should be noted that the EPT-76 is not an International Practical Temperature Scale and that it does not replace the IPTS-68 in the region of overlap. Nevertheless, its use is preferred for those applications in which smoothness with respect to thermodynamic temperature is desired or required.

It is possible that there may be some slight ambiguities produced by the different methods of realizing the EPT-76. These would arise because of possible internal inconsistencies among the different methods. Although such ambiguities and inconsistencies would not be acceptable for an International Practical Temperature Scale, it was thought that the advantages of having a working scale which is thermodynamically smooth and whose temperatures are in better agreement with thermodynamic temperature than is the IPTS-68, would outweigh these minor disadvantages.

Inaccuracy of the EPT-76

The uncertainty of the EPT-76 reference points and temperatures deduced from the helium vapor pressure is estimated to be 2 mK for the neon and hydrogen points, 1 mK for the lead point, 0.5 mK between 4.2 K and 0.9 K, and 1 mK for temperatures below 0.9 K. The ambiguities in the realizations of T_{76} that may arise as a result of using the different recommended methods of realization are also believed to be comparable with these numbers. The inaccuracy that one also wants to know is that relative to the thermodynamic temperature. The NPL-75 gas thermometer scale is the best approximation available to thermodynamic temperatures, and a comparison (2) of it with the EPT-76 indicated that T_{76} probably deviates from thermodynamic temperatures in a systematic way at temperatures above about 10 K. In this range, the thermodynamic temperature is thought to be lower than T_{76}, with a maximum deviation of about 4 mK at 27.1 K. At temperatures below 10 K, it is thought that T_{76} and thermodynamic temperatures are equal to within the uncertainties of the realization of the EPT-76 because of the equality at those temperatures of the EPT-76 and

the NPL-75 gas thermometer scale and of the EPT-76 and the magnetic scales. In addition to the uncertainty estimates of EPT-76 relative to the thermodynamic temperature, it is estimated that the slope of T_{76} with respect to thermodynamic temperature is unity to within 0.5 mK, i.e.,

$$\frac{d}{dT}\left(T_{76} - T\right) \leq \pm 5 \times 10^{-4}$$

PRACTICAL THERMOMETERS

What are practical thermometers? Practical thermometers are those that are convenient and fairly easy to use, do not require elaborate and complicated measuring equipment, do not require the expertise of a thermometrist or of an expert in a particular field of endeavor, are reproducible, are readily available or easily constructed, and are not terribly expensive. In this section, a brief review of some of the general characteristics of some practical thermometers is given, but it is not intended to be comprehensive, and certainly not all of the published data on the types of thermometers discussed here will be referenced.

Magnetic Thermometers

The usual magnetic thermometer is one that is based on the paramagnetic susceptibility χ of a weakly interacting system. Ideally, such a system would obey Curie's law

$$\chi = C/T \tag{1}$$

where C is the Curie constant. In real systems, magnetic interactions are always present, causing departures from Curie's law and eventual magnetic ordering at a sufficiently low temperature. In some cases, however, the departures from Curie's law are slight because the samples are magnetically dilute.

Two different types of magnetic thermometers are available, the choice dependent on the temperature range of interest. One type makes use of the electronic paramagnetism of a sample, and the other type makes use of the nuclear paramagnetism. The ratio of the sensitivities of magnetic thermometers based on the electronic and on the nuclear paramagnetism is given approximately by the relation

$$\left(\text{Bohr magneton/nuclear magneton}\right)^2 \cong (1{,}800)^2 \approx 3 \times 10^6.$$

Thermometers Based on Electronic Paramagnetism

Thermometers of this type are useful practical thermometers over the temperature range 0.005 K to 10 K, with no single thermometer suitable for use over the entire range.

A magnetic thermometer usually consists of a set of mutual inductance coils in which a paramagnetic salt, selected for the temperature range of interest, is located. The susceptibility, χ, of the salt is related to the

mutual inductance of such a system, measured in terms of the setting N of a mutual inductance bridge, by the equation

$$a\chi = N - N_\infty \tag{2}$$

where N_∞ (bridge setting for empty coils or with salt at infinite temperature) and a are constants. The susceptibility of the salt for ellipsoidally shaped samples is given by

$$\chi = C/(T_m + \Delta + \gamma/T_m) \tag{3}$$

so that

$$N = N_\infty + A/(T_m + \Delta + \gamma/T_m). \tag{4}$$

The constants N_∞ and A depend on the coil system, the mutual inductance bridge, and the salt. The constants Δ and γ represent the deviations of the susceptibility from Curie's law and are a function of the salt, its crystalline state, its orientation if a single crystal, and the external morphology of the sample. In general, these constants are determined by calibration at known temperatures. C is the Curie constant ($N_A g^2 \beta^2 S(S+1)/3k$), T_m is the temperature derived from the magnetic data, g is the spectroscopic splitting factor, β is the Bohr magneton, S is the effective spin, k is Boltzmann's constant, and N_A is Avogadro's number. An alternative formulation of equation 4 is

$$N = N_\infty + A/T_m + B/T^2_m + C/T^3_m + \ldots \tag{5}$$

which in many cases is a more convenient form to use.

For certain salts in which the magnetic interactions are weak, the coefficients of the $1/T^2$ and $1/T^3$ terms have been calculated and the validity of the results checked by experiments. Examples of salts with weak interactions are cerous magnesium nitrate (7-8), $Ce_2Mg_3(NO_3)_{12}\cdot 24H_2O$ (CMN), and neodymium ethyl sulfate (9), $Nd(C_2H_5SO_4)_3\cdot 9H_2O$ (NES). CMN has a useful temperature range from about 5 mK to 3 K and NES from about 15 mK to 10 K, as truly practical thermometers.

Other salts that are suitable for magnetic thermometers are chromic potassium alum, $CrK(SO_4)_2\cdot 12H_2O$ (CPA), chromic methylammonium alum, $CrCH_3NH_3\cdot(SO_4)_2\cdot 12H_2O$ (CMA), manganous ammonium sulfate, $Mn(NH_4)_2(SO_4)_2\cdot 6H_2O$ (MAS), gadolinium sulfate, $Gd_2(SO_4)_3\cdot 8H_2O$ (GS), gadolinium metaphosphate glass, $Gd(PO_3)_3$ (GP), and gadolinium molybdate, $Gd_2(MoO_4)_3$ (GM).

Figure 1 gives a comparison of the GP and NES temperature scales (9) as an example of the type of results that one can obtain with magnetic thermometers. The temperatures T_{ac} referred to in figure 1 are the acoustically

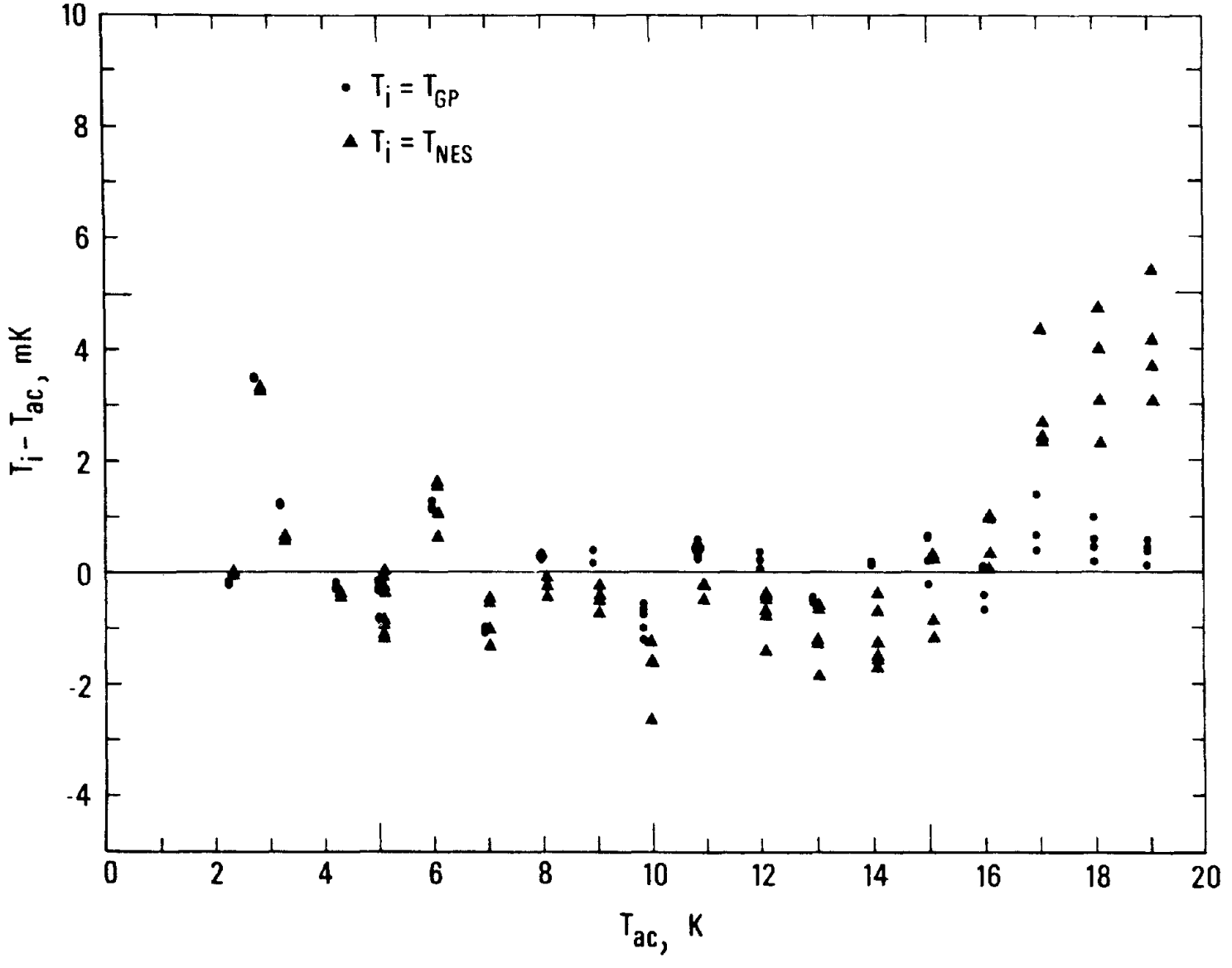


FIGURE 1. - Comparison of irreproducibilities of temperatures calculated from a least squares fit of GP and NES data to T_{ac}. For clarity, the calculated magnetic temperatures of GP and NES are displaced in temperature although measurements were made at the same T_{ac}.

determined temperatures, which have recently been recalculated by Plumb (13), taking into account at each isotherm the term quadratic in pressure.

The maximum sensitivity of a magnetic thermometer usually obtained by the mutual inductance technique ranges from about 1 μK at 0.005 K to 0.1 mK at 10 K. The repeatability of temperature measurements using a magnetic thermometer can be ≤ 0.1 mK. The smallest uncertainty that can be expected is dependent on the salt and on the temperature range and is approximately 0.1 mK to 1 mK.

In addition to the ac mutual inductance technique for the measurement of temperature via the paramagnetic susceptibility of salts, there is also a technique involving a superconducting quantum interference device (SQUID) magnetometer. This measures the magnetization of the paramagnetic salt in a small dc field and is highly sensitive.

Thermometers Based on Nuclear Paramagnetism

Magnetic thermometers based on nuclear paramagnetism are useful over the temperature interval 10^{-6} K to 1 K. As stated above, ideal paramagnetic systems do not exist and magnetic ordering will always occur at some characteristic temperature depending on the strengths of the interactions. For example, although CMN is magnetically very dilute and its interactions are thought to be purely dipolar in nature, it nevertheless orders magnetically at approximately 2 mK. For magnetic thermometers for use at lower temperatures, systems with even weaker interactions are required and since nuclear magnetic moments are about 1,000 times smaller than electronic ones, nuclear paramagnets are an obvious choice. For these types of thermometers, Curie's law is expected to be a good approximation down to temperatures of the order of 1 μK. For example, the nuclear spins in metallic copper, which are expected to order magnetically at about 0.1 μK, make a useful thermometer above about 1 μK.

Nuclear magnetic thermometers require the existence of a nuclear spin temperature, which can exist only if the spins are in equilibrium. The time required for spins to attain equilibrium among themselves is known as the spin-spin relaxation time, τ_2. The time required for the spins to come into equilibrium with the lattice, or actually the conduction electrons, is characterized by the spin lattice relaxation time, τ_1. Since a thermometer should respond repidly to changes in temperature, nuclear spin systems with short τ_1 are required, and, for this reason, only metals are used.

Although the nuclear susceptibility and magnetization obey Curie's law, the nuclear susceptibility is approximately 10^{-6} times smaller than electronic susceptibilities and, hence, is much more difficult to measure precisely. Two different practical techniques are used for measuring temperatures with nuclear magnetic thermometers (17), superconducting device magnetometers, and nuclear magnetic resonance.

A variety of superconducting devices, including the SQUID, have been made for magnetization measurements, and an important feature of all of them is that the devices respond to magnetic flux, with the response periodic in the flux quantum. With the appropriate circuitry, approximately 10^{-3} of the flux quantum ϕ_0 ($\phi_0 = h/2e = 2 \times 10^{-15}$ Wb or 2×10^{-7} gauss cm^2) can be detected. Such high sensitivity is ideal for measuring very weakly paramagnetic samples.

Nuclear magnetic thermometer samples are usually high-purity copper or platinum (99.9999 pct pure). With SQUID magnetometers, copper samples, and a magnetic induction of about 5×10^{-4}T, a temperature resolution of about 1 part in 10^4 at 1 mK is possible. Special precautions must be taken with these systems, however, to reduce stray pickup. Another limitation of the technique involving superconducting device magnetometers is that they are very sensitive to any magnetic impurities, especially those of electronic origin.

Nuclear magnetic resonance (NMR), either continuous wave (cw) or pulsed, offers a way of avoiding the stray contribution problem without going to great precautions as far as sample purity and background are concerned. The great sensitivity (and advantage) of this method comes from the fact that the spectrometer is in resonance with the precessing nuclear spins of interest and the signal is produced by only those spins that satisfy the resonance condition. Thus, impurity spins make no contribution to the signal. One common method of detecting NMR involves measuring the detuning of a spectrometer's "tank" circuit by the nuclear magnetization of the sample as this is being driven by a rotating magnetic field at the Larmor frequency given by $\omega_0 = \gamma B_0$. This is the cw method. Another method of detecting the NMR is by observing the voltage induced in the receiver coil of a crossed-coil system due to the nuclear magnetization that has been tipped by a pulsed rf magnetic field in the transmitter coil, where the pulsed field is at the resonant frequency. This is the pulsed NMR method. The temperature of the spin system is deduced from the strength of the absorption in cw measurements or from the amplitude of the signal picked up in the receiver coil for pulsed measurements. These signals are proportional to the reciprocal of the spin temperature. The thermometer is calibrated in the region from 0.1 K to 1 K.

One very important feature of the pulsed NMR method is that the temperature measured is the nuclear spin temperature of the sample just prior to the measurement. Although equilibrium times for the thermometer sample may be long, only about 10^{-4} second is required to measure the temperature by pulsed NMR, compared to approximately 30 seconds for cw measurements. Since a fast recovery time of the electronics is required for the pulsed NMR, it is necessary to have a low Q system. As a result, the cw method is more sensitive than the pulsed method, but the simplicity in measuring the temperature by the pulsed method makes it very useful.

The sensitivity and repeatability of the NMR methods are about 0.1 mK or better at 100 mK. The inaccuracy of NMR temperature measurements range from about 0.1 mK to 1 mK over the region of 0.02 K to 1 K; presently, it is rather uncertain at lower temperatures.

Nuclear Quadrupole Resonance Thermometers

Nuclear quadrupole resonance (NQR) is just nuclear magnetic resonance in the absence of magnetic fields. Nuclei with spin $I \geq 1$ possess electric quadrupole moments which, through interactions with electric field gradients produced by valence electrons and by the surrounding ions in the crystalline lattice, cause a splitting of the nuclear energy levels in the absence of a magnetic field. It is the temperature variation of these splittings, and hence of the resonance frequency, that gives rise to NQR thermometry. This technique was first suggested almost 30 years ago by Dean and Pound (4).

An NQR thermometer has the outstanding feature that once the frequency-temperature relationship has been determined for a suitable sensor material, such as $KClO_3$, that calibration will apply to all other samples of that material provided that the material has been prepared with consistent purity. This, then, eliminates the need to individually calibrate each thermometer as is required for most practical thermometers. Another advantage is that frequency, the thermometric parameter in NQR, can be easily and accurately measured, and the thermometer can be easily made a part of an automated system for temperature monitoring and control. Through the use of standard frequency broadcasts by NBS, the accuracy of the frequency counter used in making measurements can be easily checked.

The interaction of the nuclear electric quadrupole moment of ^{35}Cl ($I = 3/2$) of $KClO_3$ with the nonhomogeneous field, produced mainly by the valence electrons but with some from the surrounding ions, produces a splitting of the $I = 3/2$ energy level into two energy levels, each degenerate with respect to the sign of the magnetic quantum number, m_I. These energy levels are separated by an energy $h\nu$, where the frequency ν is given by

$$\nu = \frac{eQq_{zz}}{2h} \tag{6}$$

where e is the electronic charge, Q is the nuclear electric quadrupole moment, q_{zz} is the component of the field gradient tensor along the principal axis, and h is Planck's constant. The effects of an asymmetric electric field have not been considered here.

It has been found that fluctuations in the orientation of the electric field gradient tensor due to torsional vibrations of the ClO_3 group of $KClO_3$ account for the temperature dependence of the NQR freqency at low temperatures through changes in the values of the q_{zz}. Above 80 K, however, this does not adequately account for the variation since an expansion of the lattice occurs and the molecular vibrations cannot be approximated by harmonic oscillators. As the lattice expands, the distance between the ions increases, causing an additional decrease of q_{zz} and an increase in the sensitivity of the thermometer.

For $KClO_3$, the NQR of ^{35}Cl has been studied from about 10 K to 470 K (18). It was found that the resolution and accuracy of temperature measurements can be about ±1 mK in the range from 50 K to 470 K. The sensitivity at several temperatures throughout the range 10 K to 470 K is given in table 6. Since the width of the ^{35}Cl NQR line is approximately 500 Hz, at a resonant frequency of ~28 MHz, a determination of the center of the line to only 1 pct (or 5 Hz) gives 1 mK sensitivity.

TABLE 6. - Sensitivity of the $KClO_3$ NQR thermometer

T, K	Sensitivity kHz/K
15	0.109
30	0.674
60	1.965
100	2.907
150	3.563
200	4.072
250	4.586
290	5.057

The reproducibility of pure strain-free samples of $KClO_3$ is $\leq \pm 1$ mK near 300 K. This is as expected since the NQR frequency is an intrinsic property of the material. Over the entire range of 10 K to 470 K, the inaccuracy of a temperature measurement using this thermometer ranges from about 1 mK to 10 mK, depending on the temperature.

Resistance Thermometers

There are numerous types of resistance thermometers, but I shall discuss only three types and, even then, only briefly.

Rhodium-Iron Thermometers

Resistance thermometers consisting of an alloy of rhodium containing 0.5 at. pct iron have been developed over the past few years for use over the range 0.1 K to 300 K. They were developed primarily to provide an alternative to germanium thermometers. Although their sensitivity is much less than that of germanium thermometers below 30 K, being about 1.5 pct/K at 20 K and about 12 pct/K at 1 K, their repeatability or long-term stability is very good, and this offers a tremendous advantage. At 20 K, a repeatability of about ± 0.3 mK over about a 2-year period has been observed (15). Thus, these appear to be good practical thermometers on which to maintain the practical temperature scales.

The resistance values of thermometers commercially available are nominally 20 ohms, 47 ohms or 100 ohms at 273 K. The resistances are still sufficiently large at low temperatures that their voltage sensitivity at acceptable measuring currents (500 μA) is superior to that of the platinum thermometer

below 20 K and is comparable to that of the platinum thermometer at higher temperatures. For a 500-μA measuring current, typical voltage sensitivities are 300 μV/K at 1 K and 90 μV/K at 4.2 K.

The uncertainty of the rhodium-iron thermometer increases below 1 K, becoming about 10 mK at the lowest end of the temperature range.

Germanium Thermometers

Germanium resistance thermometers (GRT's) are small and have a high sensitivity, features that are required for most low-temperature thermometry, and they have been used extensively over the past decade or so. In fact, they have been used as the secondary thermometers on which basic thermometry results are retained. They have also been used extensively to transfer basic thermometry results to other laboratories, and to compare different laboratory scales. Nevertheless, many of them exhibit instabilities upon thermal cycling to room temperatures from 20 K or 4.2 K. Such effects are more important at the former, higher, temperature. As examples of the stabilities that can be expected of the GRT's upon thermal cycling, figures 2 and 3 present histograms of results of two investigations (3, 5). Figure 2 gives the results of Besley and Plumb (3) on 100 thermal cycles of 30 GRT's between 20 K and 300 K, with the reproducibility of the GRT's being evaluated at 20 K. The irreproducibilities ranged from 0.1 mK to 20 mK. The GRT's behavior on cycling fell into five groups: (1) stable--GRT reproducible to ±0.5 mK, (2) drifting-- resistances drifted continuously, some increasing and some decreasing, (3) jumping--sudden jumps in resistance, either increased or decreased, (4) bimodal--erratic, and (5) irregular--no pattern to the changes but irreproducibilities many times greater than the measurement precision. Overall, 50 pct of the GRT's were reproducible to within ±0.5 mK and 90 pct to within ±2 mK.

Figure 3 summarizes the results of Durieux (5) on 15 GRT's over 3 years; only slightly more than half of the GRT's studied had changes of 2 mK or less at 20 K. For short-term stability upon thermal cycling without demounting, Durieux found that about 85 pct were reproducible to within ±2 mK. Prior to Durieux's investigation, 3 of the 15 GRT's had changed by equivalents of 25 mK, 30 mK, and 45 mK at 20 K.

The above tests showed that changes in calibration are a serious problem in germanium thermometry and that it is necessary to check them repeatedly. For most of the GRT's, repeatability is $\leq \pm 0.5$ mK at 4.2 K but somewhat worse than that at 20 K. For selected GRT's, the inaccuracy can be as small as 0.1 mK to 0.5 mK at 20 K.

Another problem of which to be aware is that of the ac-dc effects (1). Resistance values may be different if measured by ac and dc techniques ($R_{dc}(T) > R_{ac}(T)$). Generally, such differences are negligibly small below 35 35 K, but they can be rather large above this temperature. For example, at 75 K the equivalent difference ($T_{dc} - T_{ac}$) may be as large as 60 to 100 mK.

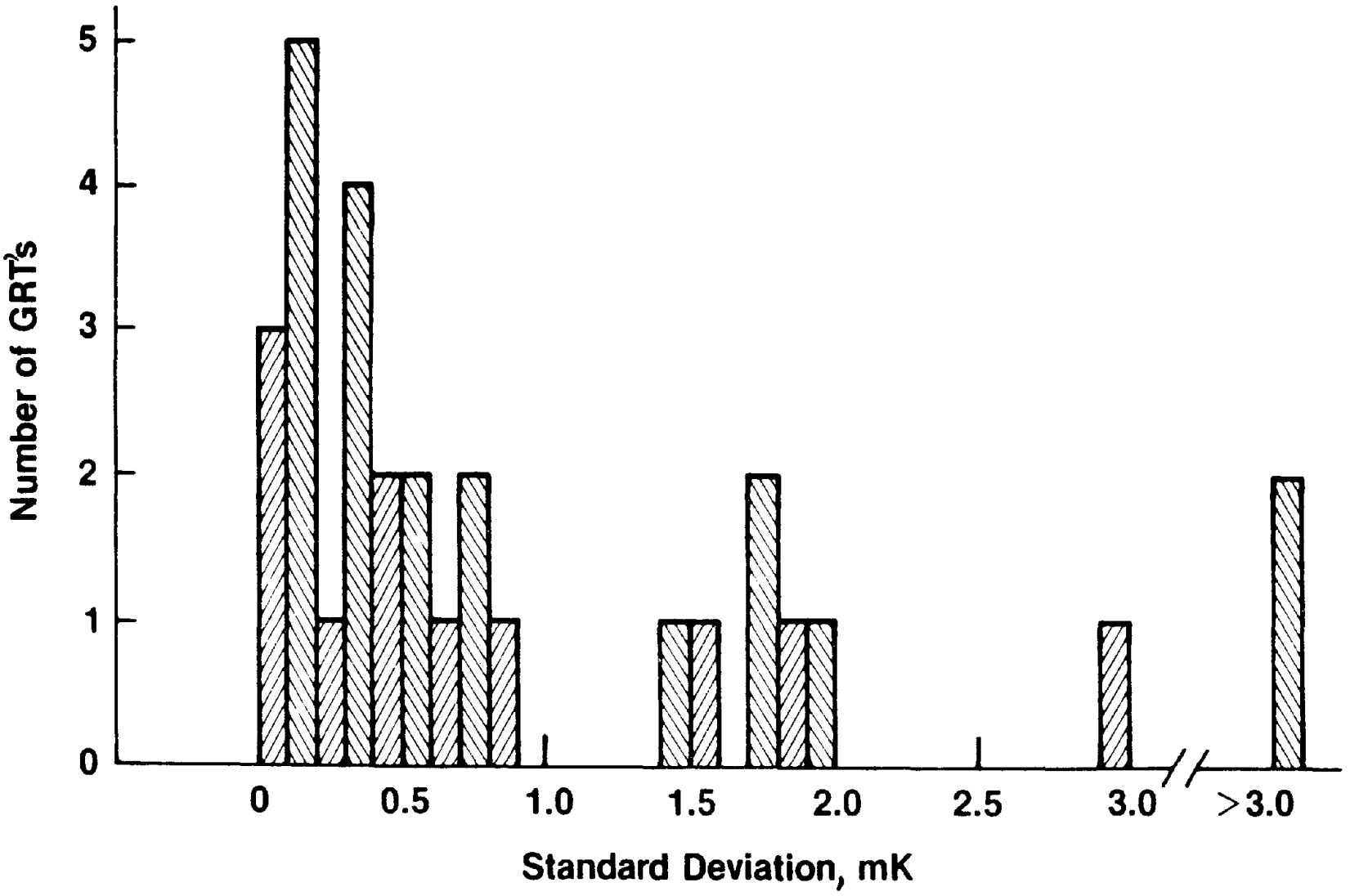


FIGURE 2. - Histogram of the standard deviations of equivalent temperature changes at 20 K for 100 thermal cycles of 30 GRT's (3).

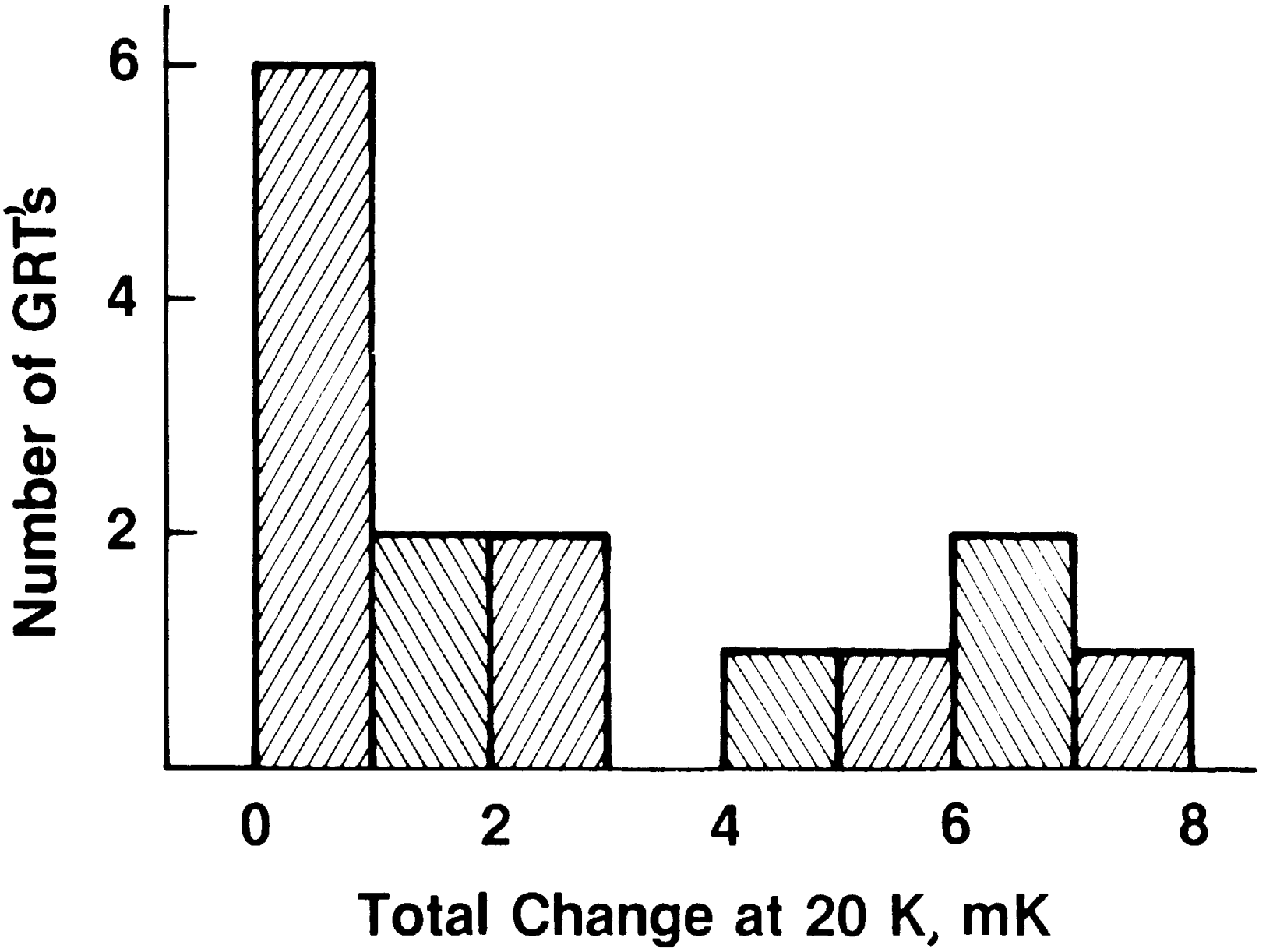


FIGURE 3. - Histogram of equivalent temperature changes at 20 K observed for 15 GRTs over 3 years (5).

In general, GRT's have a useful temperature range of 0.01 K to 100 K, although several GRT's will be required to cover the range. GRT resistance values are usually between 30 ohms and 5,000 ohms at 4.2 K. Their sensitivity is very good over limited ranges, and usually lies somewhere in the range of 3 pct/K to 15 pct/K at 20 K.

Thermistor Thermometers

Thermistors are ceramic semiconductors that exhibit large changes in resistance with small changes in temperature. They are small, rugged devices, composed primarily of manganese and nickel oxides, with dopants, and have a large negative temperature coefficient of resistance. The temperature range in which they are suitable thermometers is from about 1 K to 1,300 K, but very little information is available on applications below 0° C. The values of their resistances at 300 K vary from about 10^2 ohms to 10^6 ohms. Thermistor thermometers are available in various shapes and sizes, but the discussion here will be limited to bead-in-glass probes and disks (with passing reference to flakes), which are typical of other forms of thermistors in most of their characteristic features.

The sensitivity of thermistor thermometers is about 4 pct/K at 300 K and increases with decreasing temperature. Since they are commercially available at sizes as small as 0.1 mm in diameter, thermistor thermometers can have small masses and a relatively fast thermal response time (a few milliseconds in liquids). Flake thermistor thermometers are very useful for measurement of temperature changes since they also have a small mass and a short response time. The stability or reproducibility of the flakes as a function of time, however, is not good.

Although thermistor thermometers have been widely used in various applications, no precise testing of their reproducibility had ever been conducted until the study at NBS (19) over the past few years. A comprehensive investigation of some 135 thermistors, 65 bead-in-glass probes and 70 disks, in each of three constant-temperature baths (at 0° C, 30° C, and 60° C) was performed for about 2 years. The thermistors were in the baths continuously, and their resistances were monitored periodically with a resistance resolution equivalent to 1 mK or better. Beads having nominal resistances of 2 kohm, 10 kohm, 15 kohm, and 30 kohm and disks having nominal resistances of 1 kohm, 2 kohm, 5 kohm, and 10 kohm at 25° C were obtained from six manufacturers for the investigation. Those resistance values were selected in order to have representative sampling of units of the major different compositions.

The behavior of the thermistors falls into four categories: Stable, drifting linearly with time, drifting exponentially, and irregular. Figure 4 shows the typical exponential behavior of a disk at 60° C. Figures 5 and 6 and table 7 summarize the results of the investigation.

From these results, it appears that each manufacturer is producing very uniform lots of thermistors of a given resistance value, with variability, however, among different lots. It is also clear that bead-in-glass probes are much more stable than disks and should be selected for precision thermometry.

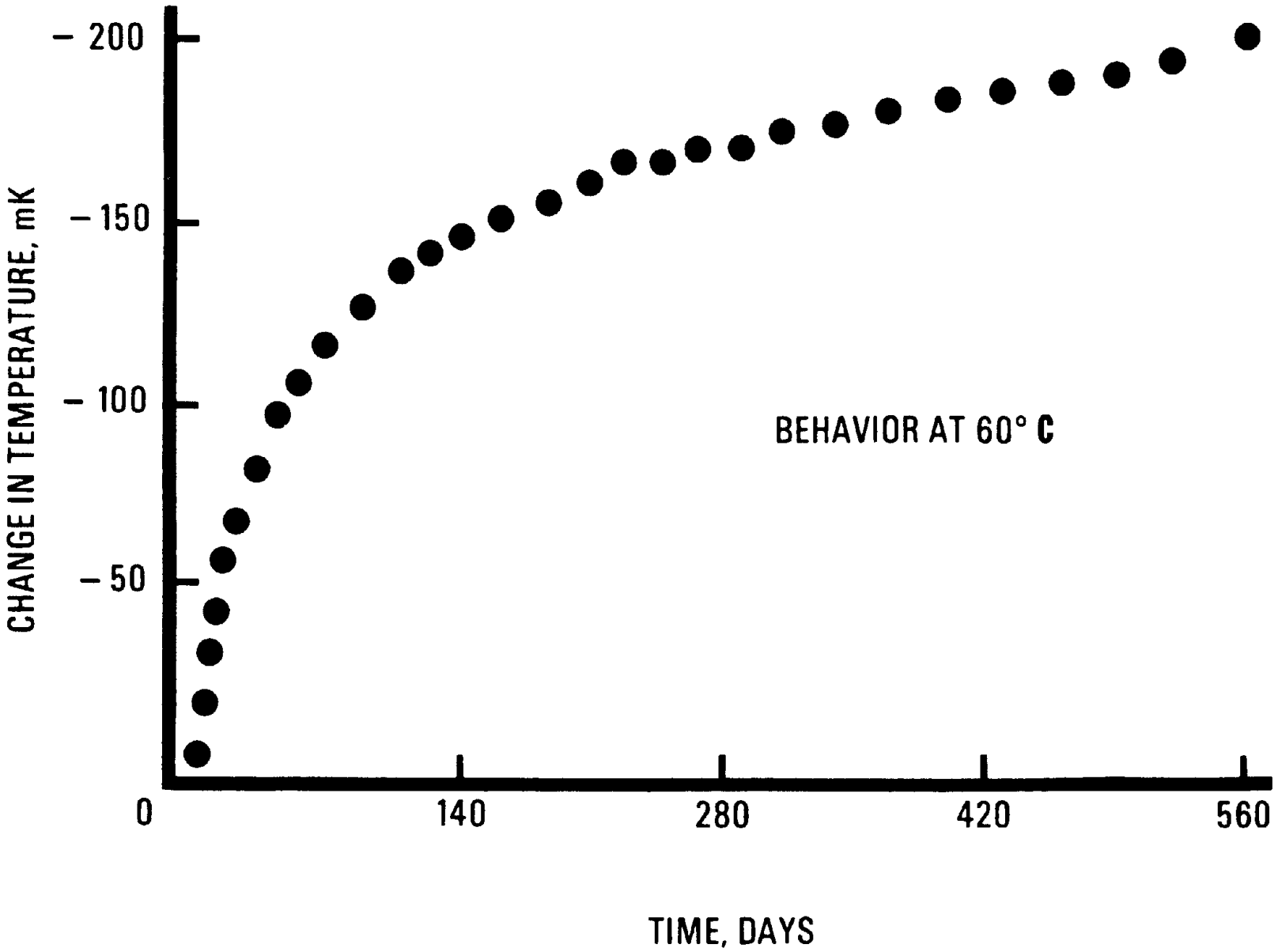


FIGURE 4. - Typical exponential drift of equivalent temperature of disks at 60° C.

TABLE 7. - Thermistor drift rates, mK/100 days

0° C								30° C								60° C, Days 2-554								60° C, Days 174-554							
Bead Resistance at 25° C, kohm				Disk Resistance at 25° C, kohm				Bead Resistance at 25° C, kohm				Disk Resistance at 25° C, kohm				Bead Resistance at 25° C, kohm				Disk Resistance at 25° C, kohm				Bead Resistance at 25° C, kohm				Disk Resistance at 25° C, kohm			
2	10	15	30	1	2	5	10	2	10	15	30	1	2	5	10	2	10	15	30	1	2	5	10	2	10	15	30	1	2	5	10
MANUFACTURER 1																															
-0	0		-3					-0	2		-1					-0	1		1					0	0		1				
2	0		-6					-0	-0		-0					-0	1		0					0	1		0				
0	0		ND					-0	-0		-1					-0	1		0					0	0		0				
-2	0		ND					-0	-0		-0					0	1		-1					0	0		-1				
-1	ND		ND					-0	0		-1					-1	1							-0	1						
MANUFACTURER 2																															
				-1	-3		-12					-6	-3		-0					-46	-25		-7					-38	-14		-5
				-2	-5		-16					-3	-3		-0					-53	-22		-5					-42	-12		-3
				-0	-38		-13					-3	-3		-1					-46	-25		-6					-36	-14		-5
				-1	-2		-15					-3	-4		-0					-54	-20		-8					-40	-11		-6
				8			-7					-3	-3		-1					-57	-21		-7					-44	-13		-6
MANUFACTURER 3																															
1	0		1				-2	-0	0		-0		-34	-15	-13	1	2		3		-54	-47	-35	0	1		2		-72	-21	-17
-0	1		-3				-10	-0	0		1		-127	-14	-13	0	1		4		-514	-54	-41	1	0		2		-89	-23	-21
-1	0		0				-6	-0	1		0		-107	-38	-20	0	3		2		-169	-44	-36	-0	2		1		-87	-20	-13
-1	1		1				-9	-0	0		-0		-12	-20	-19	1	-27		2		-471	-44	-101	1	-13		1		-807	-17	-72
1	1		-5				-10	-0	0		-0		-10	-16	-16	0	2		1			-43	-41	0	1		1			-17	-20
MANUFACTURER 4																															
-0		0	-1		-10	0	-10	-0		0	0		-41	-8	-10	0		2	2		-38	-49	-9	0		1	1		-14	-27	-6
-1		1	2		-8	-2	-10	-0		0	-0		-44	-7	-10	1		2	2		-33	-49	-12	1		1	1		-12	-27	-6
1		2	-0		-8	-0	-17	-0		-0	-0		-43	-7	-10	0		1	2		-44	-50	-11	1		1	1		-18	-26	-4
1		1	3		-4	1		-0		0	-0		-42	-8	-9	0		2	2		-39	-48	-20	-0		1	1		-13	-26	-17
		1	1		-9	-0		-0		-0	-0		-38	-9	-11			2			-36	-53				1			-12	-30	
MANUFACTURER 5																															
0	1		-23	-6		-0		-2	-0		-0	-15		-3		1	2		1	-37		-6		1	2		0	-25		-3	
-1	1		-2	-6		-1		-1	0		-1	-7		-3		0	3		3	-39		-11		0	2		1	-30		-6	
1	0		1	-4		-2		-1	0		-0	-8		-3		0	2		3	-21		-10		0	1		1	-13		-8	
-1	2			-5		-1		-0	-35		-0	-10		-4		-3	2		2	-27		-6		-0	1		1	-15		-3	
4	1			-8		-0		-1	-0		-1	-7		-3		-0	2		3	-29		-5		0	1		1	-22		-2	
MANUFACTURER 6																															
			0		-21	-16	-16				-2		-8	-9	-15				-1		-28	-87	-48				-0		-18	-43	-24
			3		-31	-11	-7				-2		-8	-14	-13				-1		-35	-88	-38				-0		-21	-44	-20
			1		-29	-11					-2		-6	-13	-16				-1		-29	-91	-41				-0		-20	-46	-22
			-5		-25	-13					-2		-8	-13	-12				-1		-32	-86	-51				-0		-21	-45	-25
			0		-46	-8					-1		-6	-13	-16				-2		-31	-90	-58				-1		-18	-48	-24
Median Mean																															
0	0.5	1.0	0	-3.0	-9.5	-1.0	-10.0	0	0	0	0	6.5	9.0	-9.0	-11.5	0	2.0	2.0	2.0	-42.5	-32.0	-48.5	-35.0	0	1.0	1.0	1.0	-30.5	-18.0	-24.5	-17.0
0.2	0.6	1.0	-3.5	-2.5	-17.0	-4.3	-10.7	-0.2	-2.1	0	-0.5	-6.5	-27.5	-11.0	-10.2	0	-0.2	1.8	1.1	-40.9	-88.2	-48.0	-30.0	0.3	0	1.0	0.6	-30.5	-67.7	-23.8	-16.6

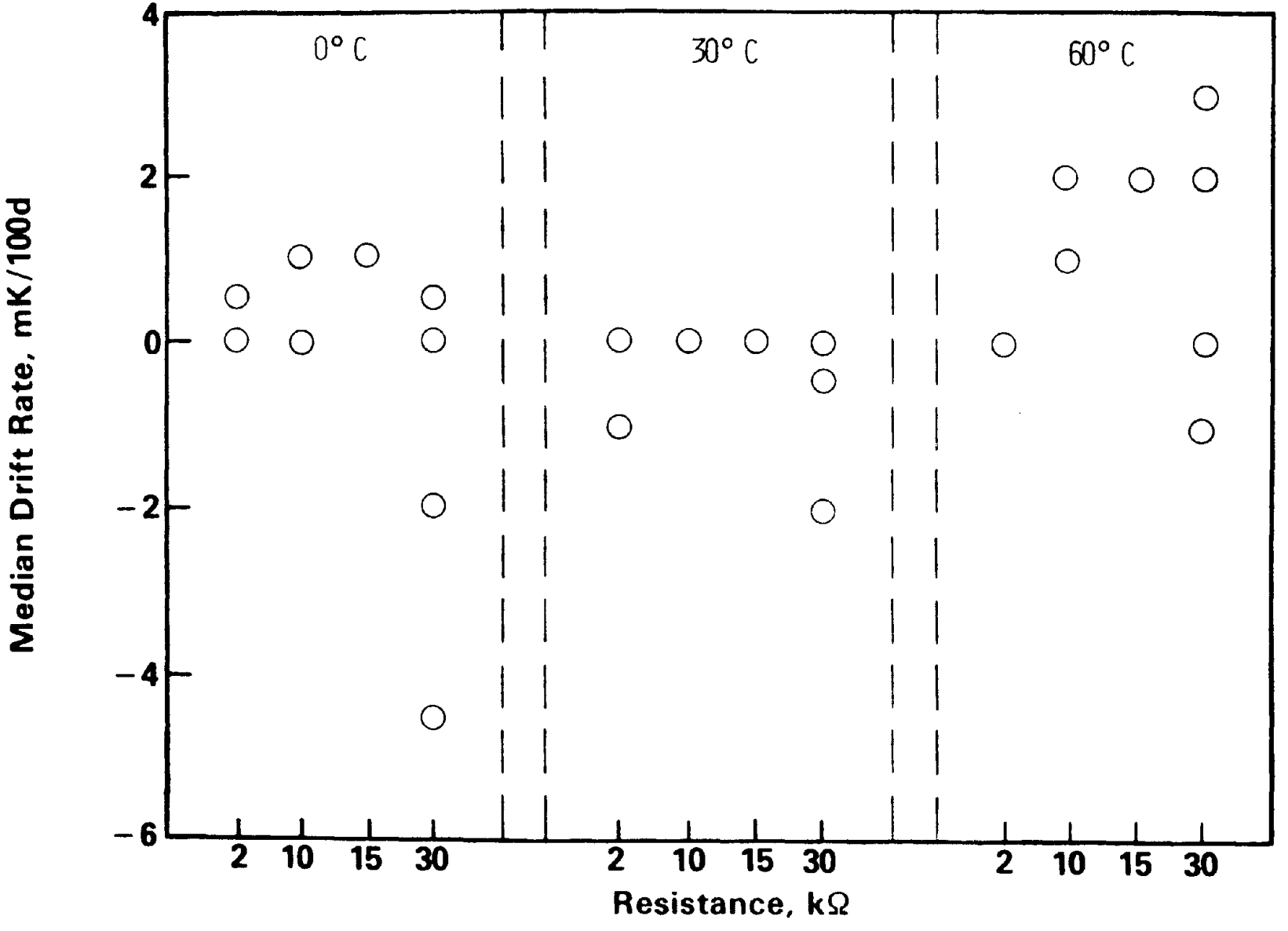


FIGURE 5. - Median drift rates at 0° C, 30° C, and 60° C of bead thermistors of various resistance values. (100d = 100 days.)

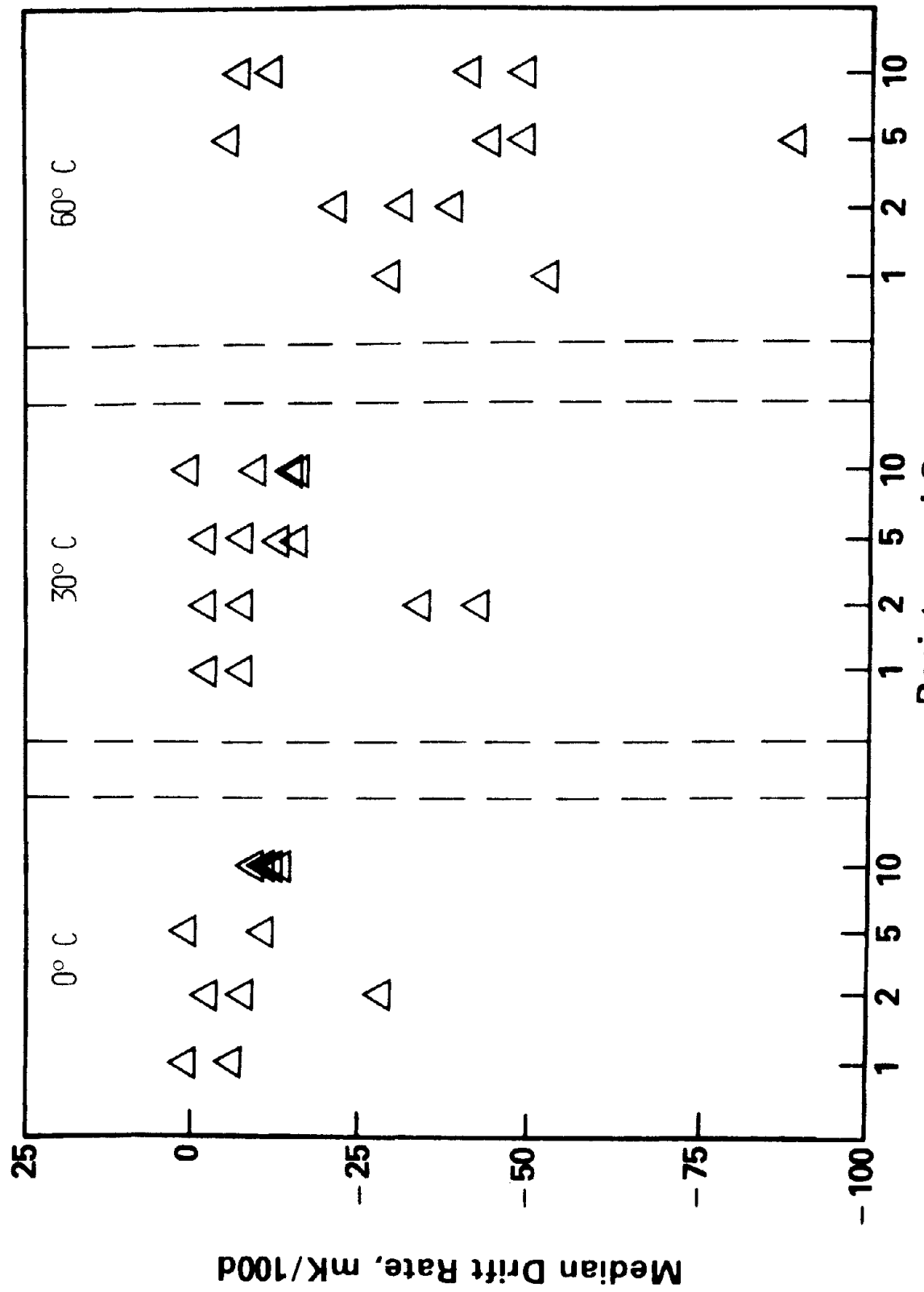


FIGURE 6. - Median drift rates at 0° C, 30° C, and 60° C of disk thermistors of various resistance values. (100d = 100 days.)

From precision thermometry investigations that we have conducted using bead-in-glass probe thermistors, it is clear that one can select units that have a repeatability of $\leq \pm 0.5$ mK at 300 K and that have an inaccuracy of $\leq \pm 1$ mK for temperatures below approximately 400 K over a period of about 2 years.

In a related investigation of thermistor thermometers, we have studied the dependence of the stability of bead and disk sensors upon time spent at 100° C, for a total time at 100° C of about 4,000 hours. The only time they were not at 100° C was when their resistances were being measured at the sequence of temperatures -40° C, 0° C, 30° C, 60° C, and -40° C. Resistances of disks generally changed a large amount and exponentially with time, while that of the bead-in-glass probes underwent a much smaller change. Only 11 disks and 12 beads, a total of 23 thermistors from 4 manufacturers, were involved in this study, however. The results are summarized in table 8.

TABLE 8. - Stability of 11 disk and 12 bead-in-glass probe thermistors heated for approximately 4,000 hours at 100° C

Resistance, kohm	Equivalent temperature change, ° C	
	Disks	Bead-in-glass probes
2	~0.25	~0.003 - 0.02
10	~0.25 - 1.5	~0.01 - 0.02

An investigation of the stability of bead and disk thermistor thermometers upon thermal cycling from about 25° C to 300° C and to 125° C, respectively, is currently underway at NBS. No results are yet available from this study.

CONCLUSIONS

In this paper, I have attempted to present in a concise way the fundamentals of the 1976 Provisional 0.5 K to 30 K Temperature Scale, its objectives, and methods of its realizaton. In addition, an attempt was made to give a brief review of the salient features of some practical thermometers used over parts of the range 0.005 K to 1,400 K.

REFERENCES

1. Anderson, M. S., and C. A. Swenson. Characteristics of Germanium Resistance Thermometers from 1 K to 30 K and The ISU Magnetic Temperature Scale. Rev. Sci. Instr., v. 49, 1978, pp. 1027-1033.

2. Berry, K. H. NPL-75: A Low Temperature Gas Thermometry Scale from 2.6 K to 27.1 K. Metrologia, v. 15, 1979, pp. 89-115.

3. Besley, L. M., and H. H. Plumb. Stability of Germanium Resistance Thermometers at 20 K. Rev. Sci. Instr., v. 49, 1978, pp. 68-73.

4. Dean, C., and R. V. Pound. The Temperature Dependence of the Chlorine Quadrupole Coupling in Solid Benzene Compounds. J. Chem. Phys., v. 20, 1952, pp 195-196.

5. Durieux, M. Cryogenic Thermometry Between 0.1 K and 100 K. Ch. 2 in Temperature Measurement 1975 (Inst. Phys. Conf. Ser. No. 26). Institute of Physics, London, 1975, pp. 17-31.

6. Durieux, M., D. N. Astrov, W. R. G. Kemp, and C. A. Swenson. The Derivation and Development of The 1976 Provisional 0.5 K to 30 K Temperature Scale. Metrologia, v. 15, 1979, pp. 57-63.

7. Hudson, R. P., and E. R. Pfeiffer. Dipolar Heat Capacity of CMN. J. Low Temp. Phys., v. 16, 1974, pp. 309-316.

8. Hudson, R. P., and E. R. Pfeiffer. Temperature Scale for Cerous Magnesium Nitrate. Ch. in Temperature, Its Measurement and Control in Science and Industry, ed. by H. H. Plumb. (Instrument Society of America, Pittsburgh, Pa., v. 4, pt. 2, 1972, pp. 1279-1285.

9. Mangum, B. W., and W. J. Bowers. Two Practical Magnetic Thermometers for Use Below 30 K. J. de Phys., v. 8, 1978, Supplement, Colloque No. 6, v. II, pp. C6-1175-C6-1176.

10. Metrologia. The 1976 Provisional 0.5 K to 30 K Temperature Scale. V. 15, 1979, pp. 65-68.

11. _____. International Practical Temperature Scale of 1968 (adopted by the Comité International des Poids et Mesures). V. 5, 1969, pp. 35-44.

12. _____. International Practical Temperature Scale of 1968 (Amended Edition of 1975). V. 12, 1976, pp. 7-17.

13. Plumb, H. H. Private communication.

14. Plumb, H., and G. Cataland. Acoustical Thermometer and the National Bureau of Standards Provisional Temperature Scale 2-20 (1965). Metrologia, v. 2, 1966, pp. 127-137.

15. Rusby, R. L. Resistance Thermometry Using Rhodium-Iron, 0.1 K to 273 K. Ch. 3 in Temperature Measurement 1975 (Inst. Phys. Conf. Ser. No. 26). Institute of Physics, London, 1975, pp. 125-130.

16. Schooley, J. F., R. J. Soulen, Jr., and G. A. Evans, Jr., Preparation and Use of Superconductive Fixed Point Devices, SRM 767, NBS Spec. Pub. 260-46, 1972.

17. Symko, O. G. Nuclear Magnetic Thermometry at Very Low Temperatures. Ch in Temperature, Its Measurement and Control in Science and Industry, ed. by H. H. Plumb. Instrument Society of America, Pittsburgh, Pa., v. 4, pt. 2, 1972, pp. 1239-1252.

18. Utton, D. B. Nuclear Quadrupole Resonance Thermometry. Metrologia, v. 3, 1967, pp. 98-105.

19. Wood, S. D., B. W. Mangum, J. J. Filliben, and S. B. Tillett. An Investigation of the Stability of Thermistors. J. Res. NBS, v. 83, 1978, pp. 247-263.

FUTURE OF QUARTZ RESONATOR THERMOMETRY

by

F. L. Walls[1]

ABSTRACT

This paper will attempt to predict the future of precision thermometry based on quartz crystal resonators used as thermal sensors. At present, quartz resonator thermal sensors exhibit considerable hysteresis after temperature cycling and, therefore, are not generally used for precision thermometry. However, we have shown that the sensors can be used to detect temperature fluctuations of approximately 20 μK over many seconds. Moreover, major advances in quartz resonators, including new crystallographic cuts, hold promise of producing quartz resonators with greatly reduced hysteresis. These new advances will be discussed in terms of their implication for thermometry from ≈100 to 400 K. A new technique for utilizing quartz resonators for thermal measurements will be discussed in detail. It is expected that a few of these improved resonators will become available for testing within a few months.

INTRODUCTION

Experimental thermodynamics can be said to be a study of thermometry as much as a study of fundamental properties of macroscopic systems. The present accuracy limit of temperature measurements near 300 K is of order 50 to 100 μK and is obtained using platinum resistance thermometers (14).[2] Thermistors used as thermal sensors yield a resolution of approximately 10 μK and a temperature stability of order 1 mK/100 days (4, 19). Quartz crystal thermometers presently have a temperature resolution of order 2 μK; however, they are plagued by hysteresis effects due to thermal shock and cycling. Several new experimental quartz crystal resonators show promise of achieving temperature resolutions of less than 1 μK with daily variations of less than 10 μK and greatly reduced thermal shock and/or cycling-induced hysteresis.

---

[1]Frequency and Time Standards Group, National Bureau of Standards, Boulder, Colo.

[2]Underlined numbers in parenthese refer to items in the list of references at the end of the report.

The development of a convenient thermal sensor with 1-μK resolution would provide an important new tool for many areas of science, especially thermodynamics. This paper will review the background, problems, and capabilities of present quartz crystal resonators used as thermal sensors, describe new advances in resonator design and fabrication which are likely to lead to much greater accuracy, and finally, describe some of the methods of using quartz crystal resonators as thermal sensors.

PRESENT STATUS OF QUARTZ THERMAL SENSORS

Quartz crystal resonators have long been known for their stable resonance frequency. Present high-quality commercial quartz-controlled oscillators have achieved frequency stabilities of order 3×10^{-13}.

The potential for using a quartz crystal resonator to obtain a high-resolution digital thermometer has long been recognized (7-9, 11, 15). Indeed, Smith and Spencer in 1962 used a high-quality quartz resonator as the frequency-determining element of an oscillator and obtained a temperature resolution of approximately 5 μK for a 10-s measurement time and a drift of less than 100 μK per hour, illustrated in figure 1 (15). The frequency dependence was approximately 74.6 ppm/K and was relatively linear from -20° C to +100° C. Presently available quartz thermometers are considerably more linear than the results obtained in references 15 and 9 (fig. 2). However, they suffer from thermal stress effects which result in spurious temperature reading of order 10 mK following thermal cycling (fig. 3). This apparent temperature typically drifts approximately 10 mK over several days immediately following a temperature shock of many degrees. Because of these hysteresis effects, quartz crystal resonators have generally not been used in precision thermometry where temperature cycling is required. An additional problem for using the commercial quartz sensors for μK resolution thermometry is the large heat conduction along the sensor cable. This can be overcome either by replacing the sensor cable or by very careful heat sinking of the sensor cable. The advantages of these sensors are that they dissipate only a few μW, they are easily made into a digital thermometer whose output can be manipulated with great precision using microprocessors, etc., and they have a thermal time constant of less than 1 s. Measurements made with these sensors indicate a temperature resolution approaching 2 μK and a drift of less than 100 μK/day (17).

Figure 4 shows the temperature versus time behavior of a single-stage oven that employs one commercial quartz crystal as the thermal sensor for controlling the heater power and a different quartz sensor for detecting temperature changes. These data were obtained after the system had operated on temperature for 2 days in order to allow some of the thermal-shock-induced transients to die out. Figure 5 shows the fractional temperature fluctuations for the single-stage oven, as measured by the quartz thermometer using experimental electronics (17). Note that for the averaging time of 1 s, the approximate thermal time constant for the sensor, the temperature resolution is approximately 3 μK, while at averaging times of 10 s it is approximately 30 μK. It is expected that temperature stabilities of order 2 μK could be obtained for times of many minutes in a two-stage oven if great care is used in

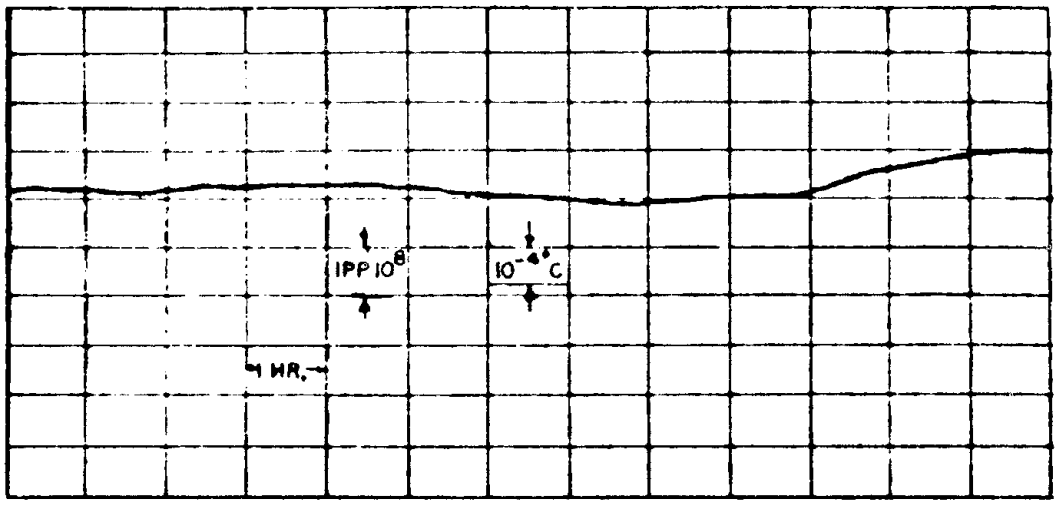


FIGURE 1. - Temperature variation of a double oven versus time measured using 5° Y cut quartz resonator (15).

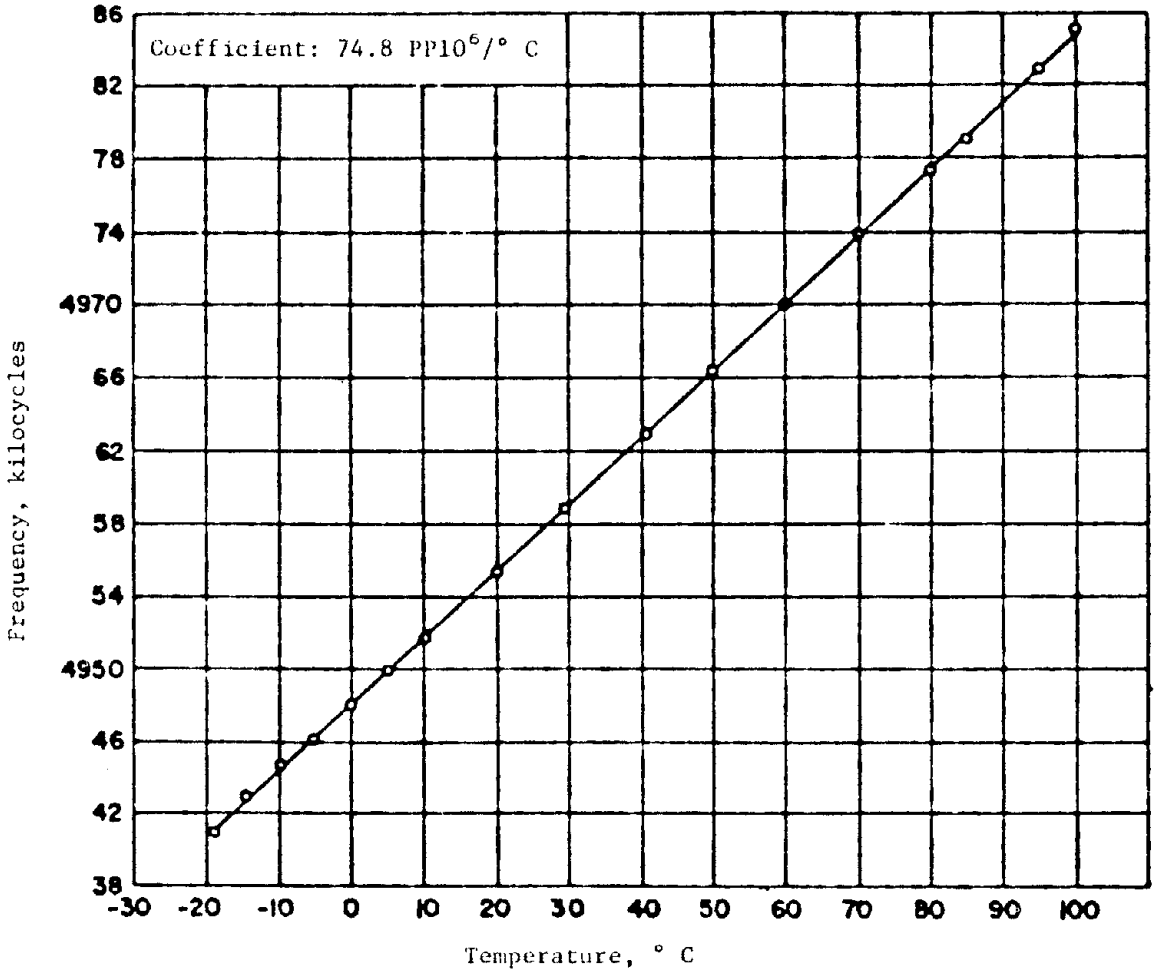


FIGURE 2. - Frequency versus temperature over a 120° C range for 5° Y cut quartz plate (15).

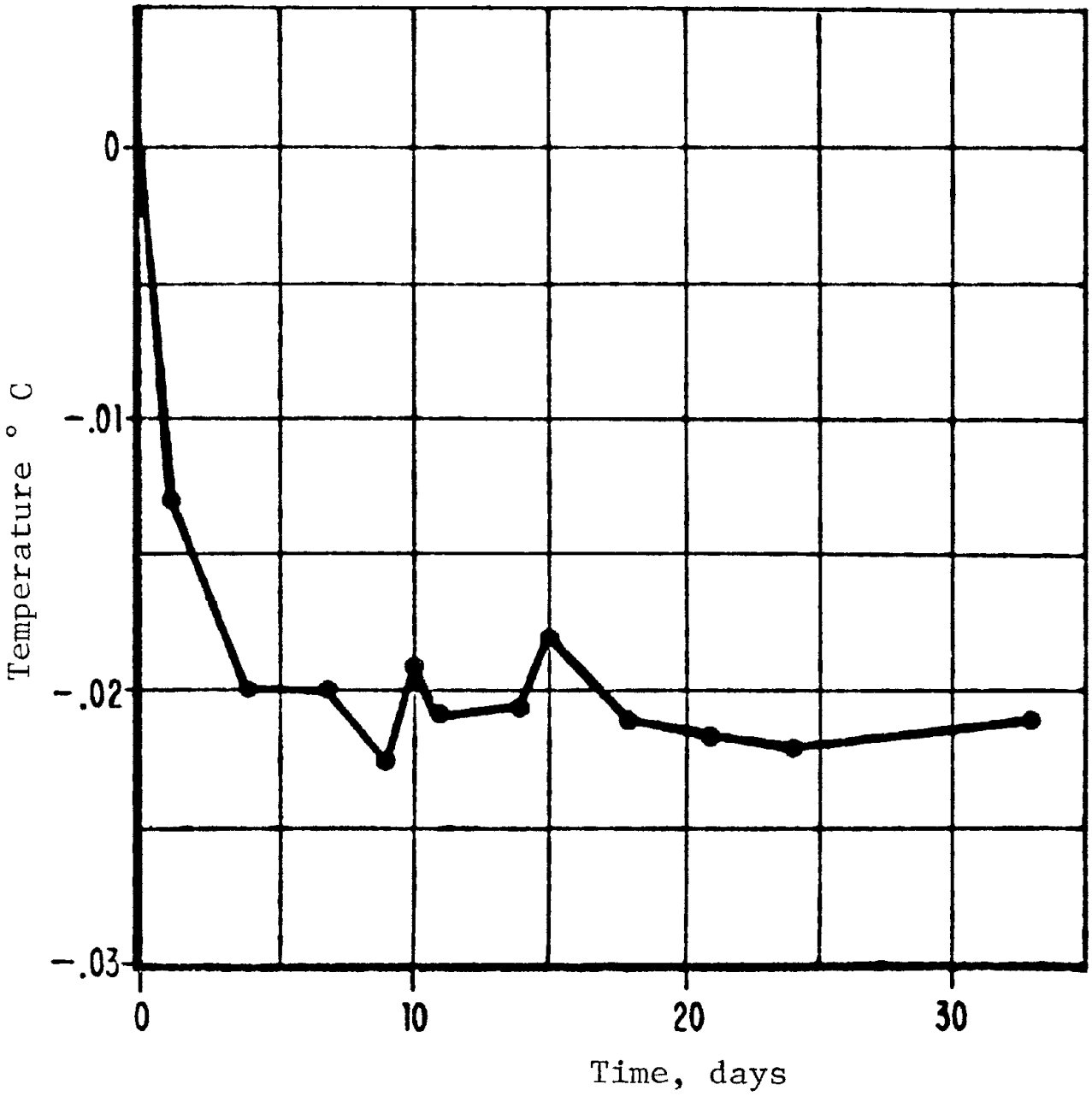


FIGURE 3. - Temperature error of an LC cut quartz thermometer as a function of time (9).

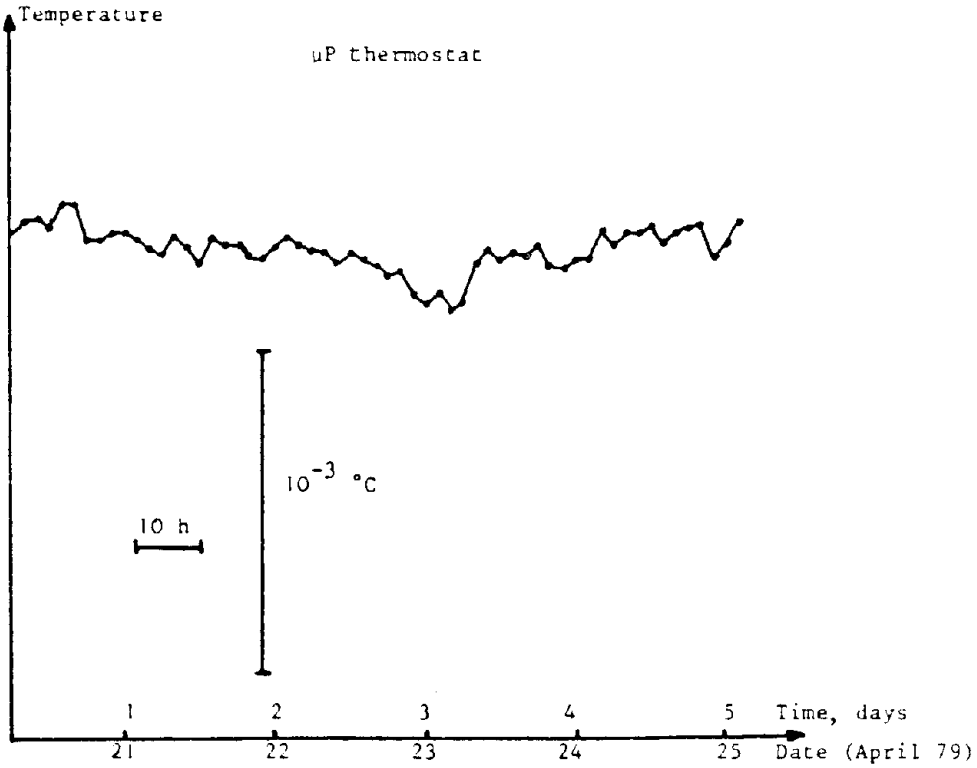


FIGURE 4. - Temperature stability of LC quartz thermometer-controlled oven as measured with a second LC cut resonator (17).

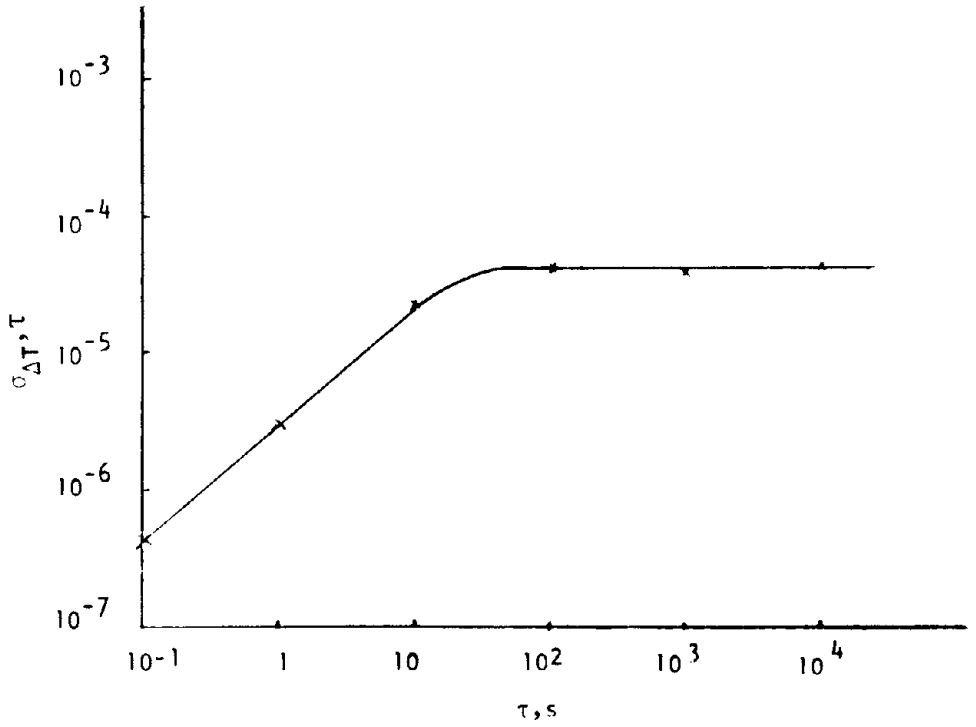


FIGURE 5. - Fractional temperature fluctuation as a function of measurement time (17).

heat-sinking the sensor cables. A resolution of 2 μK is probably close to the limit imposed by stress relaxation in this type of sensor.

NEW DEVELOPMENTS IN QUARTZ RESONATORS

Stress-induced frequency transients have received considerable attention in the past 5 years because they are responsible for much of the frequency instability of high-precision quartz crystal resonators used in frequency control (1, 10, 16-17). It appears likely that they are responsible for the thermal hysteresis as well as the noise in quartz sensors. In the past 2 years, great strides have been made in designing crystallographic cuts that are less sensitive to stress, and to new mounting techniques that help to minimize temperature (i.e., stress) induced transients (2-3, 5-6, 12, 17).

For example, a fifth-overtone, 5-MHz quartz resonator has a temperature sensitivity of approximately $\Delta v/v = 10^{-8}/K$, yielding a linearized sensitivity of $\sim \Delta v/v = 10^{-6}/K$, 10 K away from turnover. Since the frequency stability of such precision units is $\Delta v/v = 10^{-13}$, one would expect to achieve temperature resolution of 0.5 μK; however, the thermal-transient-induced response is $\Delta v/v = 10^{-5}\ dT/dt$, requiring that dT/dt be less that 10^{-8} K/s in order to achieve this 1-μK temperature resolution and stability. Most ovens and test systems do not have the low-temperature transients required to use AT cut resonators for temperature sensors.

The new SC[3] cut resonators (2-3, 12, 17) have a measured transient response which is 50 to 100 times smaller than that for AT cuts. Therefore, dT/dt of only 0.5 to 1 x 10^{-7} K/s is required in order to resolve 1 μK. SC cut resonators are therefore excellent candidates for thermal sensors. These new SC cut resonators have another very interesting feature; namely, they can be made to oscillate on both the B and C mode simultaneously (13). The C mode can be made with $\Delta v/v \approx 10^{-9}/K^2 + 10^{-7}\ dT/dt$, while the B mode has a linear response of $\Delta v/v \sim 2.5 \times 10^{-5}/K$, with a so-far-unmeasured transient response. It may be possible to use the C mode as the frequency reference for the microprocessor-based counter measuring the frequency of the B mode. With such a system, temperature resolutions of approximately 0.1 μK are contemplated. Using only the B mode temperature resolution of 1 μK over hours, and 10 to 20 μK per day resolutions appear likely. Precision SC cut resonator should be commercially available within 9 months.

Additionally, we have been studying the thermal transient process. From measurements on AT and SC cut resonators, it appears that the aging which leads to apparent frequency temperature drift can be greatly reduced by applying an exponentially decaying thermal sign wave to the final temperature. This process anneals out the bonding stress, thereby reducing the hysteresis effect observed in all resonators to date.[4]

Aging rates in the frequency of the C mode of an SC cut resonator are

---

[3]For SC and AT cuts, see reference 1.

[4]Private communication from S. R. Stein, C. M. Manney, Jr., and G. M. Kielian, National Bureau of Standards, Boulder, Colo.

dropped from approximately 10^{-10}/day (~10^{-4} K/day) to approximately 10^{-11}/day (~10^{-5} K/day) after a 2-hour annealing cycle. Normally, such an improvement in the aging rate would require more than 40 days. The effect on the B mode has not been measured yet.

A new approach to reducing bonding and plating stress is shown in figure 6 (2-3). The oscillating quartz resonator is the center portion of part C, shown in the cross section. The resonator is fixed at the ends between two auxiliary plates, D1 and D2. D1 and D2 carry the resonator electrodes, which are separated by ~20 μ from resonator C. This design greatly increases the isolation between the resonator C and the bonding points. This technique has been applied to precision SC cut resonators, yielding frequency stablities of order 1 x 10^{-13}, which should make thermal sensors with resolutions of 0.1 μK at 100 s possible.

The application of such technology to the LC cut used in the present commercial quartz thermometer (9) or the Y cut used by Smith and Spencer (15) could yield a thermal sensor with resolution of order 0.1 μK, a linearity of order 10 mK/100 K, and a daily stability of order 20 μK.

DISCUSSION OF MEASUREMENT TECHNIQUES

The traditional method of using a quartz crystal as a temperature sensor is to make it the frequency-determining element in a oscillator (fig. 7). The output frequency of the oscillator is then compared with a very stable reference, yielding a difference frequency dependent on temperature. For the resonator of reference 9, the frequency derivation is linear to approximately ± 0.01 pct over the range from 0° to 200° C. AT cut and C mode SC cut resonators have a cubic frequency dependence on temperature which can be locally linearized. To achieve enough resolution to detect 1 μK changes in temperature, it is necessary to detect frequency changes of order 10 to 100 μHz. To resolve 100 μHz with a direct-counting scheme requires a counting time of 10^4 s, or 2.4 hours. The same resolution (100 μHz) can be obtained in 10 s by deterodyning the temperature-controlled oscillator down to 1,000 Hz and measuring its period with a resolution of 1 μs, which is easily done using a frequency synthesizer. Such a scheme gives a direct digital readout of temperature which is easily processed.

The practical problem of such a circuit is that the electrical phase around the oscillating loop must be maintained extremely stable--of order 10^{-5} radians--in order to achieve μK stabilities. This, in turn, requires that the sensor cable be held mechanically very stable and that its temperature be held constant to ~1 K. It is very likely that much of the spurious temperature fluctuations observed with quartz sensors have been due to phase changes along the sensor cable because of mechanical and/or thermal disturbances.

Figure 8 shows the block diagram of a new technique for locking an oscillator to a quartz crystal where the electrical phase length of the sensor cable is relatively unimportant (16). Phase modulation sidebands at Ω_1 are impressed upon a carrier frequency originating from a frequency source. The carrier frequency probes the quartz crystal resonance, while the modulation

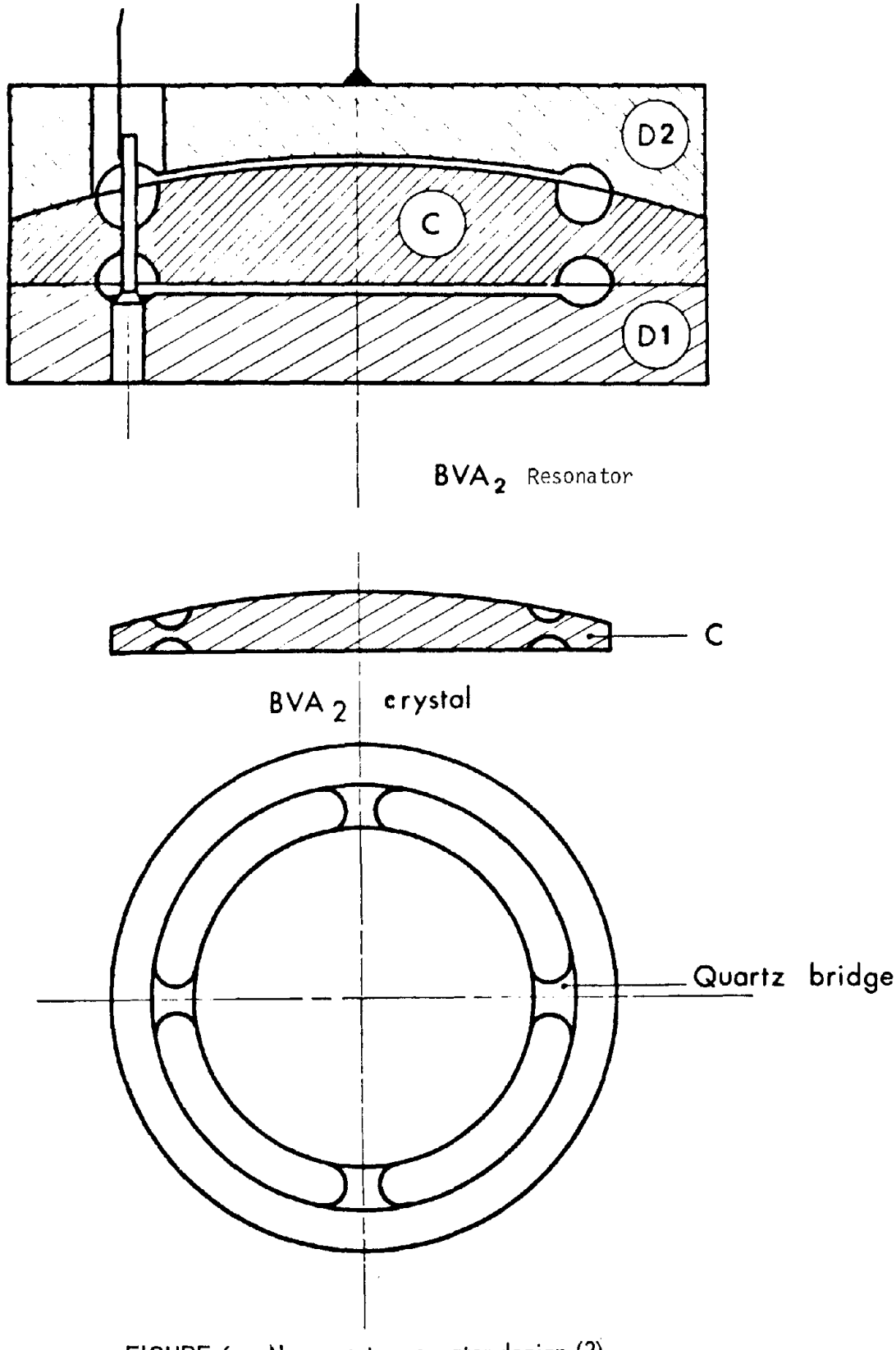


FIGURE 6. - New quartz resonator design (2).

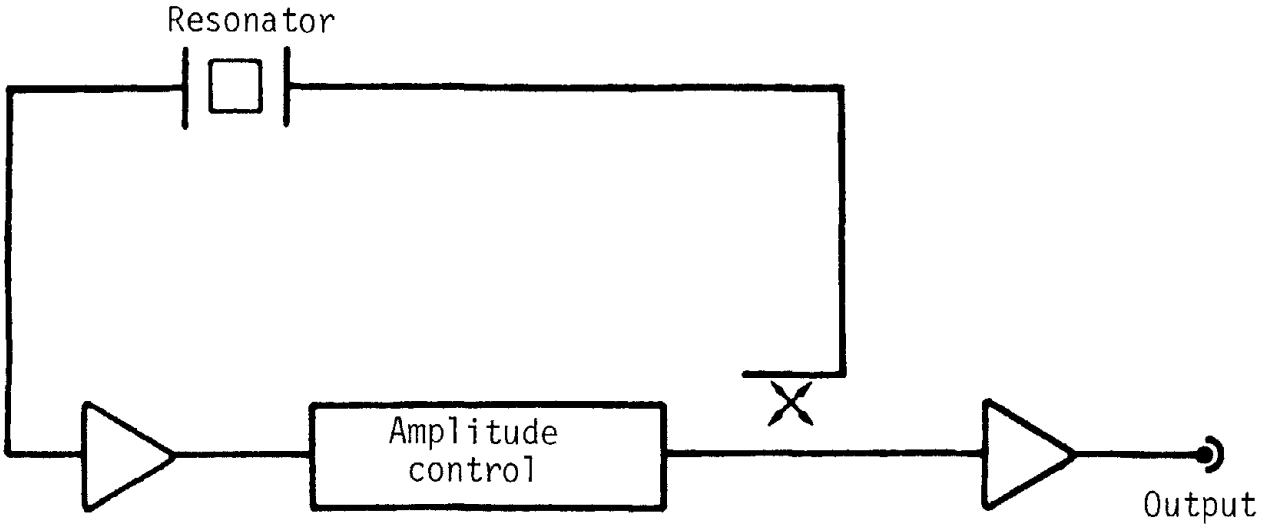


FIGURE 7. - Traditional crystal controlled oscillator.

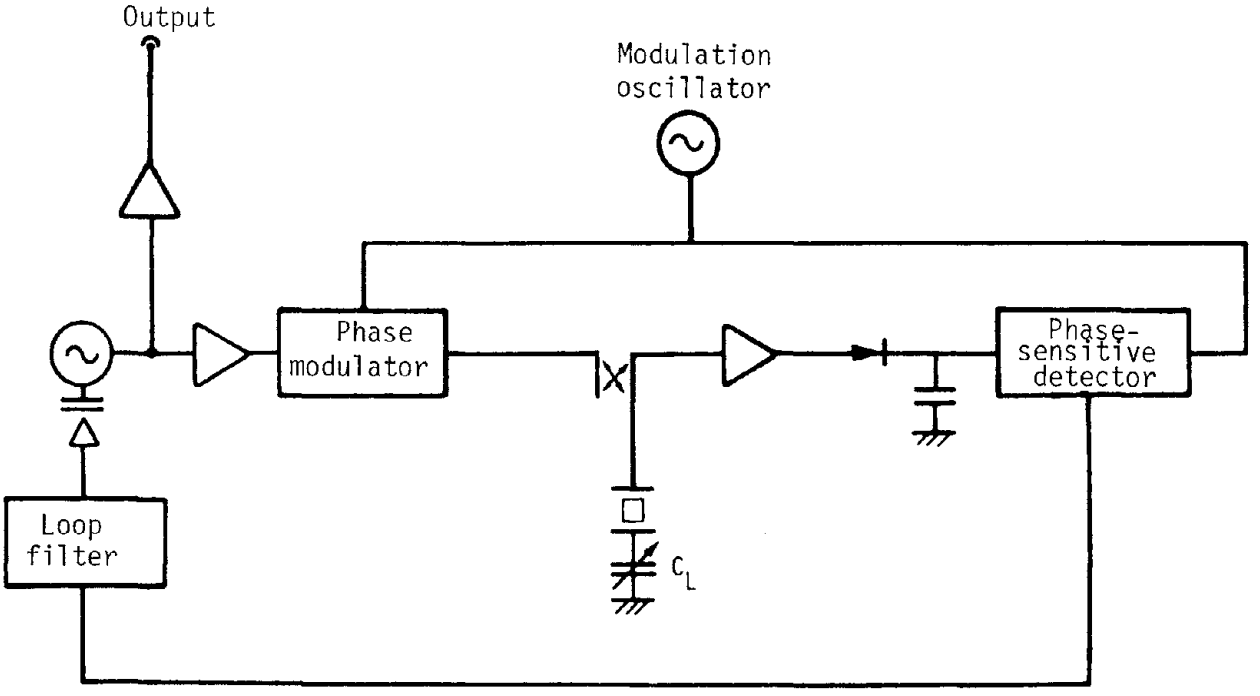


FIGURE 8. - New passive crystal oscillator design (18).

sidebands are reflected off a virtual short since they lie outside the crystal resonance. If the frequency source is detuned from the resonance frequency of the crystal, amplitude modulation at Ω_1 results. The phase of the amplitude modulation relative to the impressed phase modulation depends on whether the frequency source is higher or lower than the quartz crystal, thus enabling one to electronically steer the frequency source to the center of the quartz crystal resonance. The important new aspect here is that the phase of the carrier frequency, v_o, is measured relative to that of the modulation sidebands at $v_o \pm 167$ Hz, so that the phase change due to changes in electrical length of the sensor cable is reduced by approximately 10^5 relative to the traditional simple oscillator scheme described above. This technique has been used to obtain a frequency stability of 7×10^{-14} using a 5-MHz SC cut crystal, which is nearly five times better than that obtained previously (16). If the SC crystal had been operated away from its turnover point, this would correspond to a temperature resolution of approximately 0.07 μK.

Using this new technique, the author believes that temperature resolutions of much less that 1 μK, perhaps even as good as 0.1 μK, will be achieved in the near future. It appears that this temperature resolution should be obtainable from approximately 100 to 400 K and perhaps higher.

The above analysis and measurements have primarily addressed temperature resolution without regard to absolute reproducibility. At the present level of technology and understanding, it is likely that hysteresis effects following large temperature excursions will remain at least an order of magnitude above the best resolutions obtainable with the same devices. Therefore, it seems appropriate to suggest that, whenever possible, calorimetry experiments be designed to operate at constant temperature and constant heat loss, and that one measure the heat input necessary to maintain constant temperature. This would appear to have great advantages in terms of maintaining thermal gradients constant in space and time, and minimizing thermal transients, both of which make the measurement of temperatures to μK resolutions extremely difficult.

CONCLUSION

It has been shown that the present commercially available quartz crystal thermometer is capable of achieving a temperature resolution in excess of 20 μK over many seconds, provided care is taken in heat sinking the sensor cable and thermal cycling is avoided. Thermal cycling of the sensor by 100 K typically causes a spurious temperture reading of order 10 mK, which dies away in several days. Temperature stability of presently available quartz thermometers and also AT cut resonators normally used for frequency control application is typically dominated by residual mounting and/or plating stress which changes under thermal shock. New quartz resonator crystallographic cuts and new mounting techniques provide resonators that have thermal-shock-induced transients of order 50 times smaller than traditional resonators. It has been proposed to use these new quartz resonators, which were originally designed for frequency control, as thermal sensors. Calculated resolution based on the best achieved frequency stability at the temperature turnover point indicates

an ultimate temperature resolution in excess of 0.1 μK if the same frequency stability can be achieved away from the temperature turnover point.

The traditional oscillator scheme of using quartz crystal resonators as thermal sensors was briefly described, and the most serious cause of spurious temperature readings due to practical electronic problems was discussed. A new technique with several orders of magnitude smaller spurious readings due to electronic problems was described, and preliminary results were presented.

Finally, it is suggested that whenever possible, calorimetry experiments should be designed to operate at nearly constant temperatures, thereby reducing temperature measurement problems due to thermal cycling, changing gradients, etc. Instead of measuring temperatures during a process, one measures the amount of heat necessary to maintain constant temperature in the presence of a known constant heat leak. Under such conditions it was predicted that effective temperature resolutions of much better that 1 μK can be achieved in the near future.

REFERENCES

1. Ballato, A., and J. R. Vig. Static and Dynamic Frequency Temperature Behavior of Singly and Doubly Rotated Oven-Controlled Quartz Resonators. Proc. 32d Ann. Symp. on Freq. Control, 1978, pp. 180-189.

2. Besson, R. J. A New Electrodeless Resonator Design. Proc. 31st Ann. Symp. on Freq. Control, 1977, pp. 147-152.

3. ———. A New Piezoelectric Resonator Design. Proc. 30th Ann. Symp. on Freq. Control, 1976, pp. 78-83.

4. Dror, S., and D. S. Connel. A ± 15 Microdegree Temperature Controller. Rev. Sci. Instr., v. 45, 1974, pp. 1082-1088.

5. EerNisse, E. P. Calculations on the Stress Compensated (SC cut) Quartz Resonator. Proc. 30th Ann. Symp. on Freq. Control, 1976, pp. 8-11.

6. ———. Quartz Resonator Frequency Shifts Arising From Electrode Stress. Proc. 29th Ann. Symp. on Freq. Control, 1975, pp. 1-4.

7. Flynn, T. M., H. Hinnah, and D. E. Newel. An Improved Cryogenic Thermometer. Proc. Cryogenic Eng. Conf., v. 8, 1972, pp. 334-339.

8. Gorini, I., and S. Sartori. Quartz Thermometer. Rev. Sci. Instr., v. 33, No. 8, 1962, pp. 883-884.

9. Hammond, D. L., and C. A. Adamo. A Linear Quartz Crystal Temperature Sensing Element. ISA Trans., v. 4, 1965, pp. 349-354.

10. Holland, R. Nonuniformly Heated Anisotropic Plates: I. Mechanical Distortion and Relaxation. IEEE Trans. S.U., v. 21, 1974, pp. 171-178.

11. IRE Proceedings. IRE Standards on Piezoelectric Crystals, 1949. V. 37, December 1949, pp. 1378-1395.

12. Kusters, J. A., C. A. Adams, H. Yosida, and J. G. Leach. TTC's--Further Developmental Results. Proc. 31st Ann. Symp. on Freq. Control, 1977, pp. 3-7.

13. Kusters, J. A., M. C. Fischer, and J. G. Leach. Dual Mode Operation of Temperature and Stress Compensated Crystals. Proc. 32d An. Symp. on Freq. Control, 1978, pp. 389-397.

14. Riddle, J. I., G. T. Furakawa, and H. H. Plumb. Platinum Resistance Thermometry. NBS Monograph, v. 126, 1973.

15. Smith, W. L., and W. J. Spencer. Quartz Crystal Thermometer for Measuring Temperature Deviations in the 10^{-3} to 10^{-6} Range. Rev. Sci. Instr., v. 34, No. 3, 1963, pp. 268-270.

16. Stein, S. R., C. M. Manney, Jr., F. L. Walls, J. E. Gray, and R. J. Besson. A Systems Approach to High Performance Oscillators. Proc. 32d Ann. Symp. on Freq. Control, 1978, pp. 527-530.

17. Theshold, G., and J.-J. Gagnepain. Dynamic Behavior of Quartz Resonators Proc. 33d Ann. Symp. on Freq. Control, 1979.

18. Walls, F. L., and S. R. Stein. A Frequency-Lock System for Improved Quartz Crystal Oscillator Performance. IEEE Trans. Inst. and Meas. IM-27(3), 1978, pp. 249-252.

19. Wood, S. D., B. W. Mangum, J. J. Filliben, and S. B. Tillett. An Investigation of the Stability of Thermistors. J. Res. NBS, v. 83, 1978, p. 247.

PANEL DISCUSSION ON
TEMPERATURE MEASUREMENT AND CONTROL

E. F. Westrum, Jr.: How do the IPTS-68 and IPTS-48 compare with the thermodynamic scale?

G. T. Furukawa: At the National Bureau of Standards, Dr. L. A. Guildner has been conducting gas thermometry. His published results on the differences beween IPTS-68 and the thermodynamic temperatures between 0° and 460° C and the differences between IPTS-68 and IPTS-48 show that the IPTS-48 is closer than the IPTS-68 to the thermodynamic temperature in the range. The scales are compared in my paper. Dr. Guilder now has measurements above the aluminum point (660° C). The latter work has not been published.

E. F. Westrum, Jr.: Is the temperature scale better on the IPTS-68 than on the IPTS-48 in the region from the normal boiling point of oxygen to the triple point of water?

G. T. Furukawa: I am not aware of any gas thermometry work in the region 90-273 K, published since the formulation of the IPTS-68. The IPTS-68 in the region is based principally on the gas thermometry work at the National Physical Laboratory (United Kingdom, 1965) between 90 and 273 K and the National Research Council (Canada, 1968) between 70 and 373 K, which agree quite closely. There is no correlation between IPTS-48 and IPTS-68 below 90 K because the lower temperature limit of the IPTS-48 was 90 K. However, the National Bureau of Standards had a provisional scale, referred to as NBS-1955, from about 12 to 90 K. In the formulation of the IPTS-68, the NBS-1955 scale was averaged with the other national temperature scales, and the average and the NRC gas thermometry scale between 70 and 373 K were combined to generate the IPTS-68 reference function. As mentioned earlier, the NRC and the NPL gas thermometry scales in the region 90-273 K are in close agreement. The differences between the IPTS-68 and the NBS-1955 are tabulated in NBS Monograph 126 (1972) on platinum resistance thermometry.

E. F. Westrum, Jr.: I would like to ask Bill Mangum about rhodium-iron thermometers. Are they available; can they be cycled, are they useful for calorimetry; is the Bureau of Standards doing anything on this?

B. W. Mangum: The rhodium-iron thermometers were developed primarily as a replacement for the germanium resistance thermometers and are available. They were found to be exceedingly stable during a 2-year period of time that Rusby, NPL, studied them. He found that the reproducibility over that time was some 0.3 mK. The thermometers were cycled from 20 K to room temperature and back. NBS is looking at them now; they are being compared with germanium thermometers and with some noise thermometers. There is a comparison going on right now at NBS, and the results look very good. To describe the rhodium- iron resistance-temperature behavior, polynomials of high degree must be used; also, the resistors must be calibrated at very short intervals. But they really are very good. The main disadvantage of rhodium-iron resistors, in my

opinion, is that they are fairly large, maybe 4 cm long. They are not as small as the germanium thermometers, but they are usable up to 300 K.

E. F. Westrum, Jr.: How about the thermal and electrical cycling of the thermistors?

B. W. Mangum: I did not specify the currents or the voltages applied to them, but current was not flowing through them continuously, so they were electrically cycled. However, we were using maximum currents of only 10 microamps, which cases very small heating. We saw no effects. If measurements were made with 10 microamps and repeated several months later, at either 30° or 60° C; for beads, I do not think any effect would be observed. There would probably be an effect if you put high currents through them. It might cause an expansion around the leads, so that the leads for the bead would in fact become separated from the thermistor materials. That certainly would be true for the disks. I guess I didn't answer Dr. Westrum's question concerning the thermal cycling of a few specially treated thermistors (which had been kept at 300° C for 6 months), which were used in the range from 0 to 100° C, i.e., they were just normally cycled in use, show that over a 3-year period they drifted by no more than 0.5 mK per year.

M. W. Chase: How do the temperature scales compare below 90 K?

G. T. Furukawa: There is no correlation between 48 and 68 scale below 50 K, just in tabulation. First of all, the IPTS 48 scale started from 90 K up. The National Bureau of Standards had a provisional scale in the region of about 12-90 K. There is no comparison between IPTS 48 and 68 in the region of 50 K. There is in our platinum resistance thermometry monograph 126 a tabulation of difference between the NBS 55 and the IPTS 68.

E. F. Westrum, Jr.: Are there plans for an extension of IPTS scale? In other words, is it planned to have an IPTS 78, or 88 in the future?

B. W. Mangum: The next version of the IPTS is scheduled for 1985 to 1987. There will be a temperature symposium, the Sixth Temperature Symposium, to be held in the spring of 1982 in Washington. That is really sort of a prelude to getting the new scale in order.

L. D. Hansen: What are the advantages of quartz probe over a thermistor probe?

F. L. Walls: The built-in resolution of quartz crystal thermometers is much higher. If you look at the noise in thermistors, they bottom out at about 10 μk, whereas we have been able to look at the correlation between temperature fluctuations and crystal resonator performance on the 1- to 2-μk range which would have been masked out by the thermistor noise.

B. W. Mangum: What is the cost of the electronic equipment needed for your measurements?

F. L. Walls: Perhaps on the order of $10,000. But the new SC cut resonators are only available as a prototype from a university in France, Raymond Besson is fabricating them, and I think we are the only group in the United States that has ever looked at them. Hopefully, they will be available commercially within 1 year, being manufactured by a company in Switzerland. It is really speculation, but I assume that the resonators will be available, and then the electronics, including the sophisticated counters, for less that $10,000, perhaps even as low as $4,000.

SECTION 2.- CALORIMETRIC TECHNIQUES

THERMODYNAMIC PROPERTY MEASUREMENTS MADE AT THE BARTLESVILLE ENERGY TECHNOLOGY CENTER

by

Bruce E. Gammon[1] and William D. Good[2]

ABSTRACT

The Bartlesville Energy Technology Center maintains personnel and equipment for determining and/or predicting thermodynamic properties of fossil-fuel-related organic compounds. These measurements are made so that the properties may be specified over the range of temperature and pressure that may be encountered in utilizing such materials.

Calorimetric techniques are described for (1) bomb calorimetry, (2) solution calorimetry, (3) condensed-phase heat-capacity calorimetry, and (4) vapor-flow calorimetry. State-property measurements are described for (1) vapor pressures, (2) the pressure, volume, temperature surface, (3) the velocity of sound, temperature, pressure surface, and (4) gas solubilities at high pressures. Techniques for spectroscopic measurements and for statistical mechanical calculations are discussed. The relative region of the thermodynamic surface probed by these methods is identified and discussed.

INTRODUCTION

For many years, the Bartlesville Energy Technology Center has maintained laboratories devoted to the measurement of the thermodynamic properties of substances associated with petroleum and other fossil fuels. Many of our efforts are dedicated to systematic studies of pure "key" compounds within significant organic chemical families to provide sufficient data for chemical equilibria calculations through the well-known relationship

$$\Delta G^\circ = -RT \ln K, \qquad (1)$$

where K is the equilibrium constant. For these efforts, our concern has been

---

[1]Research chemist.

[2]Research supervisor.

Both authors are with the Department of Energy, Bartlesville Energy Technology Center, Bartlesville, Okla.

to supply data for the left side of this equation. Of course, most applications require appropriate mixing data to relate the activities in K to desired concentrations. Recently we added facilities to provide vitally needed data on mixtures encountered in technologies under development for the extraction and processing of fossil fuels.

For pure-compound studies, enthalpies of formation are derived from condensed-state combustion-calorimetry experiments for reactions such as

$$kC + (n/2)H_2 + mX \rightarrow C_kH_nX_m, \quad (2)$$

where X is a heteroatom and the reactants and products are in their "standard states." To determine the entropy and Gibbs energy change for such reactions and to relate the results to other regions of the phase diagram, other properties are measured over the ranges shown on the simple phase diagram in figure 1.

Starting from the lower left corner of figure 1, adiabtic calorimeters are used to measure the heat capacity of the stable crystalline form from sufficiently near-zero Kelvin, for use of Debye extrapolation, up through the solid-solid transitions (not depicted in the figure), then up through the triple point, and finally along the saturated liquid line to a point where the vapor pressure may be as high as 2 atm or where the temperature reaches 150° C. Enthalpies and temperatures of transition are also determined in this process. These results are used to derive values of the conventional entropy, Gibbs energy, and enthalpy relative to zero Kelvin.

Two different laboratories provide information to relate the entropy, etc., of the condensed state at low pressures with that of the vapor, and ultimately the ideal gas. We have equipment to measure vapor pressure from 0.01 mm of mercury to as high as 3 atm. It provides data to determine the enthalpies and entropies of sublimation and vaporization via the Clapeyron equation. In addition, a vapor-flow calorimeter is used to measure enthalpies of vaporization and vapor heat capacities at pressures from about 1/8 to 2 atm.

The ultimately obtained values of the thermodynamic properties for the ideal gas state are compared with statistical mechancially derived values based on spectroscopic data. In some cases, the experimental data are used to derive a correction function for statistical mechanical terms that are not amenable to direct evaluation for large molecules. The products from this procedure are functions for describing the thermodynamic properties of all members in the compound families in the low-density-gas state from zero Kelvin to experimentally inaccessible high temperatures where the molecule becomes too unstable and/or too reactive for direct experimental measurements. Such high temperatures are encountered in many reservoir and processing conditions, and thermodynamic data are needed to estimate complex reaction equilibria.

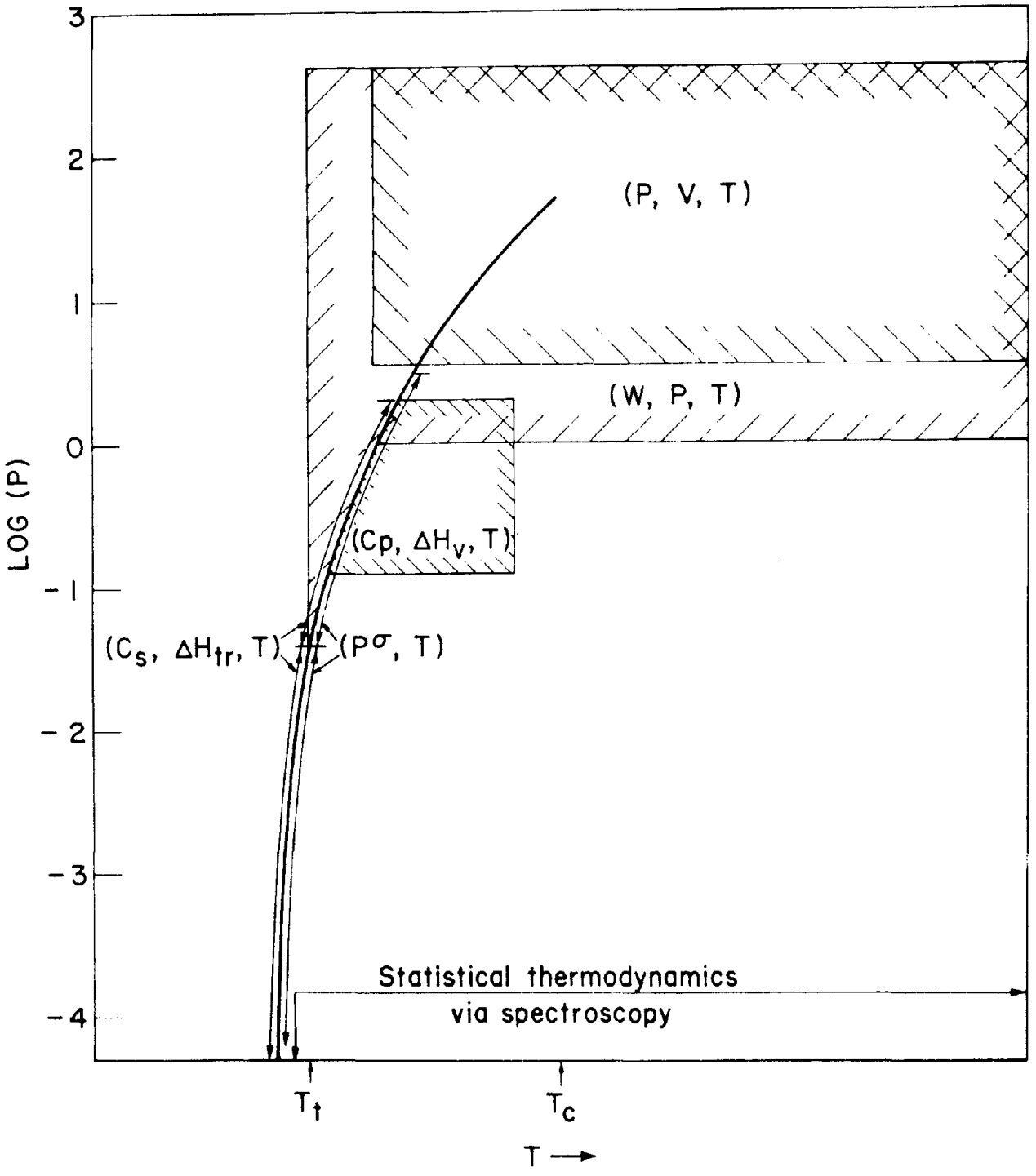


FIGURE 1. - Regions of application of experimental techniques in the (P,T) phase diagram. C_s and $P\sigma$ are heat capacity and pressure respectively at saturation, WPT is velocity of sound at constant P and T, and T_t and T_c are melting and critical temperatures respectively.

Most processes are operated at high pressure, and as an extension to the measurements at lower pressures, we have two methods primarily designed to study different features of the properties in compressed fluids, namely PVT and velocity of sound (WPT) measurements to pressures as high as 400 bars. These are shown in the upper right region of figure 1. Both techinques have been applied to low-molecular-weight substances. The critical points of high-molecular-weight substances are at temperatures too high for pure compound studies; however, studies on low-molecular-weight compounds serve to supply information on the compressed states of other substances through various statistical mechanical and empirical theories for fluids.

Figure 1 does not indicate our studies in mixtures, but some of the methods mentioned above have been or can be used for mixtures. In addition, we have recently developed equipment for determining the solubilities of gases in compressed fluids and the associated vapor and liquid compositions. We also have equipment devoted to the calorimetry and densimetry of solutions, as well as the calorimetry of absorption by solids from solutions.

Our present studies are devoted to determining (1) the properties of polycyclic ring compounds of hydrocarbons and similar compounds containing N, O, and S; (2) the properties of compounds with high heats of combustion per unit volume; (3) the properties of materials from coal conversion process streams; and (4) the thermodynamics of micellar solutions and fluid-solid interaction in tertiary oil recovery systems.

In the past, systematic studies have been made on hydrocarbons with as many as 20 carbon atoms. The families include alkanes and alkenes and their adducts to simple ring systems. Additionally, systematic studies have been made on compounds similar in structure to the hydrocarbons, but that contain either nitrogen or sulfur as heteroatoms. Other studies include those on organic fluorine compounds and on the organic derivatives of the lighter elements (B, Al, Si, Cl). Some limited studies were performed on the organic derivatives of lead and manganese. Finally, systematic studies have been made on the state properties of low-molecular-weight compressed fluids.

In the discussion that follows, our methods for the various measurements are briefly described.

COMBUSTION CALORIMETRY

The basic method consists of determining the energy released from a reaction such as

$$C_nH_mS_p + (n + m/2 + 2p)O_2 \rightarrow nCO_2 + m/2\ H_2O + pH_2SO_4. \qquad (3)$$

The energy released by the process is deduced from the temperature rise produced by the reaction when it is carried out in a calorimetric vessel with a known heat capacity and measured extraneous sources of energy. The instrument used in this work has been described (14, 20, 23).[3] It contains a combustion

[3]Underlined numbers in parentheses refer to items in the list of references at the end of this paper.

vessel which may be rotated end over end and about its cylindrical axis to insure that all of the internal parts of the bomb are bathed in a solution selected to produce a well-defined final state of reaction products. The rotation feature is particulary important for substances that burn to form acids, solids, and species of mixed oxidation states.

Until recently, the temperature rise of the calorimetric vessel was determined with a platinum resistance thermometer and an associated Mueller G-2 bridge, which employed a telescopically observed, mirrored galvanometer. Presently, the temperature rise of the system is automatically and equally as well determined with a quartz thermometer, which uses a desktop computer-controlled electronic counter with a high-stability ($<5 \times 10^{-10}$ per day) time base. The quartz thermometer inherently gives an integrated average of the temperature as a function of time, and by using averages of the temperature from 100-s intervals, corrections for heat leak and mechanically generated energy are made easily.

Simply implemented but clever sample partitioning and sealing schemes have been essential in the successful use of the rotating-bomb calorimeter for a variety of compounds. Techniques developed and often used employ sealed polyester bags (14) and sealed ampoules of borosilicate glass, soft glass, and quartz (17, 20-21). Characterization of the sample and its products is essential; carbon dioxide is quantitatively recovered from each experiment to check and sometimes supplant determinations of the mass of sample used in the experiments. A sampling of the chemical schemes devised for burning organic compounds containing heteroatoms can be seen in the following: For sulfur compounds, nitrogen was introducted in the bomb (17) to promote the oxidation of sulfur to the hexavalent state. Good and Mansson (18) burned organoboron compounds by mixing them with a fluorine-containing combustion promoter and by including hydrofluoric acid in the bomb solution so that a well-defined aqueous solution was obtained containing hydrofluoric and fluoroboric acid. A similar technique was used for organosilicon compounds and elemental silicon by Good and coworkers (16). Other notable examples include the burning of lead tetramethyl (19) and manganese decacarbonyl (15) in the presence of nitric acid solution to give final solutions containing metal nitrates.

CONDENSED-PHASE HEAT CAPACITIES

For application of our results to chemical thermodynamics, we obtain conventional entropies of pure substances with adiabatic calorimeters. Measured values of the heat capacities and enthalpies of transition, ΔH_i, are used to obtain the conventional entropies,

$$S = \int_0^T C_p/T \, dT + (\Delta H_i/T_i) + \ldots , \qquad (4)$$

where the T_i's are for the various condensed-phase transitions of the substance under study. Enthalpies and Gibbs energies relative to zero Kelvin are also derived. Sample purities are determined in studies on the melting transition.

The essential features of the adiabatic calorimetric equipment for heat capacity studies from near zero to 423 K have been described (24, 32). In the capacity studies from near zero to 423 K have been described (24, 32). In the present configuration, calorimeters are used in any one of four different cryostats, which provide the requisite refrigeration, vacuum insulation, radiation shields, and adiabatic shields for the calorimeter and its associated electrical leads. Three-action electronic temperature controllers for the adiabatic shields and equipment for temperature and energy measurements are provided from two essentially identical stations. The temperature in each calorimeter is measured with a platinum resistance thermometer which is mounted in a reentrant well within the calorimeter. Measured values of the energy are supplied to the calorimeter and sample through a resistance heater which is bifilarly wound on the same mica cross as the platinum coils in the resistance thermometer. For the thermometry and energy measurements, the necessary currents and potentials are measured using standard direct-current potentiometric methods, which employ suitable NBS-calibrated standard resistors and emf cells.

We are currently developing a microcomputer-controlled system that is expected to require very little human intervention for the calorimetric measurements. It will employ a high-resolution, AC-resistance bridge for temperature measurements and computer-controlled sources for current, timing, resistances, and potential in the energy measurements. Sufficient internal and random access computer memory will be available for making the necessary corrections to the results and for making decisions such as the rate and duration of heating required for the system, when the system is sufficiently near equilibrium, etc.

In conjunction with the adiabatic calorimeters, we also use a differential scanning calorimeter (Perkin-Elmer DSC II)[4] for preliminary studies in pure compounds, and for determining heat capacities and heats of transition with moderate accuracy. This instrument has been used to study many chars and coal-derived fluid distillates. We expect to exploit this versatile instrument for many other applications in the future.

VAPOR PRESSURE

Two different sets of equipment are used for the precise determination of vapor pressures below 3 bars. One uses ebulliometers (27, 36, 38) to reflux the substance under study and a standard of known vapor pressure under a common helium atmosphere. The boiling temperatures of the two substances are determined, and the vapor pressure is derived from the vapor pressure of the standard, water, or benzene. The ebulliometers have provisions for determining the difference in the boiling and condensation temperature; this provides a useful test of the purity of substance. This method is used at pressures from 70 to 2,026 mm Hg and at temperatures from 15 to 200° C. The other

[4]Reference to specific manfacturers, brands of equipment, or trade names is made for identification only and does not imply endorsement by the U.S. Department of Energy.

is a novel development of a piston-pressure gage (7, 9, 28). One end of a piston cylinder assembly is evacuated, and the other is exposed to the pressure produced by the sample. Varied pressures are determined from the angle at which the piston of known mass and cross section must be tilted relative to the horizontal to obtain a balance of force against that produced by the pressure. This system is used to measure vapor pressures from 0.01 to 40 mm Hg and at temperatures from -60° to 200° C. In both systems, the sample temperatures are measured with platinum resistance thermometers.

The vapor pressure data are used to obtain values of the enthalpies of vaporization from the Clapeyron equation. In such evaluations, the data are represented by a suitable vapor-pressure equation derived with least-squares procedures that employ weighting functions consistent with the experimental errors in the data.

VAPOR-FLOW CALORIMETRY

The equipment used for these measurements is commonly refered to as a nonadiabatic flow calorimeter and has been well described (25, 37, 39). It has been used to determine heats of vaporization at temperatures from 15° to 165° C and at pressures from 1/8 to 2 bars. In such measurements, a suitable amount of vapor is collected over a measured period of time from a well- insulated boiler supplied with accurately determined electrical power. During this process, the pressure and temperature in the boiler are held constant at set and determined values, and the liquid level is maintained constant by addition from an auxiliary container of fluid maintained at the same temperature as the boiler.

Vapor-heat-capacity measurements have been made in the apparatus at temperature from 25° to 250° C. For these measurements, power is supplid to the boiler to produce desired vapor-flow rates to a second secton of the apparatus, where the temperature rise is determined across a second resistance heater energized at a measured constant power in the flowing gas stream; the input temperature of the flowing stream to the second heater is regulated, and resistance thermomoeters mounted in the gas stream are used to measure the temperature rise produced across the heater. After small corrections for minor effects, these results are used to extrapolate the observed heat capacity to infinite flow rate and thus to eliminate effects from heat leaks. The methods used in the electrical measurements are similar to those used in the condensed-phase heat capacity work.

The measurements provide heats of vaporization at varied temperatures corresponding to vapor pressures from 1/8 to 2 bars and values of C_p along isotherms at pressures corresponding to the vaporization pressures. From these results, the heat capacities at zero pressure are determined, and second virial coefficients B are derived for the equation of state,

$$PV = RT(1 + B/V), \qquad (5)$$

with the Clapeyron equation and from

$$\lim_{P \to 0} (\partial C_p / \partial P)_T = -T(d^2B/dT^2). \quad (6)$$

Both of these derived properties, C_p° and B, serve as important tests and sources of adjustment for statistical mechanical calculations involving both the intramolecular and the intermolecular potential functions.

MOLECULAR SPECTROSCOPY AND STATISTICAL THERMODYNAMIC CALCULATION

The results from this laboratory provide important extrapolations of the thermodynamic properties to high temperatures. Also, procedures have been developed in this laboratory for correlating the significant intramolecular force constants and structure of molecules; these correlations are used in predicting the thermodynamic properties of substances for which measurements were not made (34).

Two different spectrometers are used in this laboratory. A far-infrared spectrometer with a gas cell and a laser Raman spectrometer are used primarily to determine the fundamental wave numbers in the vapor phase. The use of vapor spectra for the thermally significant low wave numbers is essential in the statistical mechanical calculation for the ideal gas state.

For the interpretation of the spectra and statistical mechanical calculations, well-established, but very detailed and complex, procedures are used in deriving the suitable information for the partition function. Basically, calculations are made assuming the molecules behave as rigid rotators, with harmonic oscillators for the internal modes of vibration. The subsequently derived values of the heat capacity, enthalpy, entropy, and Gibbs energy in the ideal gas state may not agree with the experimental thermodynamic data, and the differences are used as a basis for adjusting barrier heights to internal rotation and to establish empirical functions for contributions from anharmonicity, vibrational-rotational interaction, and centrifugal distortion.

The final functions produced from this process usually include values of the Gibbs energy function, $(G^\circ - H_0^\circ)/T$; the enthalpy function, $(H - H_0^\circ)/T$; the enthalpy, $H^\circ - H_0^\circ$; the entropy, S°; the heat capacity, C_p°; the standard enthalpy of formation, ΔH_f°; the standard Gibbs energy of formation, ΔG_f°; and the logarithm of the equilibrium constant of formation, $\log_{10} K_f$. These are for the ideal gas at 1 atm and are tabulated to at least 1,000 K. Extensive tabulations of these data from this laboratory may be found in a series of publications by Scott and coworkers (10, 33, 35).

PVT

For PVT measurements, the experimental method (1, 6, 8) is very accurate and simple to use and is faster than most PVT methods. It employs mercury in contact with the sample, which requires a minor correction that may appear objectionable; the use of mercury does not cause significant uncertainties, however. The equipment is designed to operate at temperatures from -35° to 350° C and at pressures from 3 to 400 bars. For the density determinations, a

calibrated screw injector is used to force mercury into a pressure vessel which contains a weighed amount of sample in an interior cell. The interior cell is completely immersed in mercury and has an opening on its lower end so that the sample container is subjected only to simple compression, and not to distortion from pressure imbalance. The pressure of the mercury is transmitted to a piston pressure gage through a high-pressure manometer, and the sample temperature is measured with a platinum-resistance thermometer.

The results are presented as values of pressure, density (ρ), and temperature and are used to graphically derive virial coefficients and the (P, ρ, T) locus of the vapor-liquid saturation line. Numerical procedures (22) are used to derive the functions ($H-H^\circ$), ($G-G^\circ$), and ($S-S^\circ$) where the superscript zero indicated ideal gas values at 1 atm.

The measured surface, along with the graphically derived virial coefficients and the thermodynamic functions derived from numerical integration, provides important test data for statistical mechanical functions and for equations of state devised to fit state property data of fluids.

VELOCITY-OF-SOUND (WPT) MEASUREMENTS

The velocity of sound equipment (12-13) is designed to operate with fluids at temperature from -175° to 300° C and at pressures from subatmospheric to 400 bars. This equipment can be operated at much lower temperatures than that for the PVT work. As a complement to recent PVT work done at Bartlesville (5), it was used to extent the state properties in ethylene down to the triple point.

The instrument used for this work is a double-crystal interferometer, which may be operated at any of the odd harmonics of the 500-kHz quartz crystals. The sound wavelength and thus the velocity are determined from lengths of a fluid column in acoustic resonance between the two crystals. The pressure and temperature are measured with a piston gage and a platinum resistance thermometer, respectively. Provisions are also made for determining the density of the fluid with limited accuracy; these density values facilitate corrections and provide an essential measure of the state of the fluid in regions where the pressure is a slowly varying function of density.

Some elaboration on the use of velocity of sound for state property measurements is made here because the method is not widely used, and its unique features and limitations are not generally recognized. The velocity of sound, W, may be related to other state properties through either of the following equations:

$$W^2M = (\partial P/\partial \rho)_T + (T/C_v)\,[(1/\rho)(\partial P/\partial T)_\rho]^2 \tag{7}$$

$$W^2M = \frac{(\partial G/\partial P)^2(\partial^2 G/\partial T^2)}{(\partial^2 G/\partial T^2)(\partial^2 G/\partial P^2) - (T\partial^2 G/\partial P\partial T)^2} \tag{8}$$

where M and G are molar values of the mass and Gibbs energy, and the derivatives in the second equation are taken along isotherms and isobars. A comparison of the second equation with those for other commonly measured thermodynamic functions (S, H, E, ρ, P, and T) reveals that the velocity of sound is unique in giving measures of second derivatives of G with respect to P and T. In these comparisons, one must recognize that experimental heat capacities are determined by numerical differentiations. The dependence of the velocity of sound on the second derivatives of G provides a stringent constraint to derived equations of state. Results for helium (11) were used to show that WPT data alone could be used to derive an equation of state, which accurately reproduces PVT data both within and, to a surprising extent, outside the range of the WPT measurements.

To insure that equilibrium values of the velocity of sound are obtained, measurements must be made as a function of frequency to correct for nonadiabatic effects. In fluids, the most troublesome of these is the frequency dependence of the heat capacity, which requires determination of temperature and density-dependent relaxation times and of the contributions to C_V from the vibrational modes of the molecules that fail to reach equilibrium during acoustic compression and rarefication cycles. An example can be found in the work on methane (13).

COMPRESSED GAS SOLUBILITY

The equipment for this work was designed to determine the solubilities of hydrogen in coal-derived fluids. It is installed in a special hazardous material laboratory to meet current safety standards. The design is similar to that of Prather and coworkers (31). The liquid under study is held in a stirred autoclave at temperatures as high as 425° C. The sample is subjected to measured pressures of hydrogen of up to 4,000 psi, and after suitable time for equilibration, vapor and liquid samples are withdrawn into small sampling vessels. The mass, the low pressure volumes of the gas, and the composition of the samples are determined to obtain solubilities and vapor-liquid compositions. The composition of the samples is determined with gas-liquid chromatography and mass spectral analysis by a separate laboratory dedicated to the analysis of fossil-fuel-related materials.

Recent work with this system includes studies with tetralin, a four-component recycle solvent, and coal liquids derived from the SRC process.

SOLUTION AND ADSORPTION CALORIMETRY AND DENSIMETRY OF SOLUTIONS

The measurements in this laboratory are devoted to the study of surfactant and cosurfactant systems in brines. These studies are made to provide fundamental knowledge of these systems for tertiary oil recovery. The equipment used in these measurements is commercially avalable, though with some modifications, and it is operated at 15° to 75° C at ambient pressure.

Enthalpies of dilution are made in a modified LKB microcalorimeter. It

is a heat-conduction-type flow calorimeter (26) with a power resolution of 0.2 μw. This instrument has been used to study the heats of dilution of surfacant systems to gain understanding of the effects of temperature, cosurfactants, and salts on the formation of micelles (2-4).

The flow system and a second LKB microcalorimeter operated in the batch mode have been used to study the enthalpies of adsorption and desorption of surfactants on solid substrates to gain an understanding of their interaction with reservoir surfaces. Several properties are of interest in these studies: enthalpy of adsorption, the amount adsorbed, the surface area of the solid, the reversibility of the adsorption, and the kinetics of the adsorption processes.

A third set of commercial equipment (SODEV) was recently obtained for determining the densities and the heat capacities of solutions. The densities are determined by a vibrating-tube method (30), and the relative heat capacities are determined by a microcalorimetric flow method (29). The heat capacities are to be used in extrapolating enthalpy data and in deducing micelle structures from the temperature variations. The density information is to be used in obtaining the partial molar volumes for determining changes in structure that occur in transitions of the surfactants from monomers to micelles. The effects of salts and cosurfactants are of particluar interest.

The calorimetric equipment in this laboratory produces a voltage versus time for the inference of the desired thermodynamic properties. The results are often displayed on integrating strip-chart recorders for interpretation, but efforts are underway to collect and reduce this information into a desktop computer, which employs a digital voltmeter on the voltage output of the calorimeters.

SUMMARY AND FUTURE EFFORTS

The framework of this presentation was chosen to present methods for providing measured and predicted chemical thermodynamic information on organic compounds. Our results are referred to in the ideal gas state where, for correlation purposes, the intermolecular effects are eliminated; however, this is not the only focus of our work. The different research methods are used to address questions important for general understanding of the properties under study. The bomb calorimetry studies are principally concerned with understanding the changes in chemical-bound energies that arise from variations in the molecular structure; conjugated systems, strained structures, and structures with strong steric interactions are of particular importance. The significant structural features from these studies may not always coincide with those that would be chosen for our other studies. In studies of some phase transitions of solids and in spectroscopic studies, the internal degrees of freedom, with barriers comparable to the thermal energies, are the features that require significant effort for their understanding. In studies of lattice effects in solids and of state properties in fluids, the internal structural features become less important, and the gross features of intermolecular potentials and of molecular shape become important.

It is evident in the foregoing presentation that our efforts on mixtures have been limited. This has been from a lack of resources for such studies and not from a lack of interest in their needs. In addition to our current mixture work, we are considering additional PVT studies in mixtures to answer fundamental questions about the phase behavior of fluids near the vapor-liquid phase boundary.

Our current equipment and procedures are suitable for many compounds that are candidates for study; however, we are currently making or planning improvements to our instruments to facilitate additional studies. Improved methods are needed for obtaining vapor spectra and enthalpies of sublimation and/or vaporization on high-molecular-weight compounds. Efforts are being made to extend the high-temperature range of the present vapor-pressure equipment. Methods for lower pressure measurements are being considered. New systems are being devised to obtain spectra on heated vapors to obtain sufficient vapor densities for the currently used spectrometers.

Efforts are being made to develop accurate methods that require smaller samples and thereby reduce the demands required for synthesis and purification of compounds.

Finally, in many of our measurements, we are developing equipment for automatic and more rapid methods of acquiring the data. The availablility of inexpensive microcomputers and of plug-to-plug compatible research-grade measuring instruments employing IEEE 488 interfacing has greatly facilitated developing these systems.

REFERENCES

1. Beattie, J. A. The Apparatus and Method Used for the Measurement of the Compressibility of Several Gasses in the Range of 0 to 325° C. Proc. Am. Acad. Arts and Sci., v. 69, 1934, pp. 389-405.

2. Berg, R. L. Thermodynamics of Aqueous Sodium Dodecyl Sulfate. BERC/TPR-77/3, 1977, 35pp.

3. Berg, R. L., and W. D. Good. ERDA In-House Reearch on Thermodynamics of Oil-Recovery Micellar Systems. 2d ERDA Symp. on Enhanced Oil & Gas Recovery, Tulsa, Okla., Sept. 9-10, 1976, (Petroleum Publishing Co.), pp. D-6/1--D-6/4.

4. Berg, R. L., L. A. Noll, and W. D. Good. ERDA In-House Research on Thermodynamics of Oil-Recovery Micellar Systems. 3d ERDA Symp. on Enhanced Oil and Gas Recovery & Imporved Drilling Methods, Tulsa, Okla., Aug. 30-31, Sept. 1, 1977, (Petroleum Publishing Co.), pp. B-10/1--B-10/8.

5. Douslin, D. R., and R. H. Harrison. Pressure, Volume, Temperature Relations of Ethylene. J. Chem. Thermodynamics, v. 8, 1976, pp. 301-330.

6. Douslin, D. R., R. H. Harrison, R. T. Moore, and J. P. McCullough. Tetrafluoromethane: P-V-T and Intermolecular Potential Energy Relations. J. Chem. Phys., v. 35, 1961, pp. 1357-1366.

7. Douslin, D. R., and J. P. McCullough. An Inclined-Piston Deadweight Pressure Gage. BuMines RI 6149, 1963, 11 pp.

8. Douslin, D. R., R. T. Moore, J. P. Dawson, and G. Waddington. The Pressure-Volume-Temperature Properties of Fluorobenzene. J. Am. Chem. Soc., v. 80, 1958, pp. 2031-2038.

9. Douslin, D. R., and A. Osborn. Pressure Measurements in the 0.01-30 mm Range With an Inclined-Piston Gage. J. Sci. Instr., v. 42, 1965, pp. 369-373.

10. El-Sabban, M. Z., and D. W. Scott. The Chemical Thermodynamic Properties of Hydrocarbons and Related Substances. II. Properties of 25 Organic Sulfur Compounds in the Ideal Gas State from 0° to 1,000° K. BuMines Bull. 654, 1970, 26 pp.

11. Gammon, B. E. The Velocity of Sound wtih Derived State Properties in Helium at -175° to 150° C With Pressure to 150 atm. J. Chem. Phys., V.

12. Gammon, B. E., and D. R. Douslin. A System for Measuring the Velocity of Sound in Compressed Fluids and its Application to Helium Between -175 and 150° C. Proc. 5th Symp. Thermophysical Properties, sponsored by the Standing Committee on Thermophysical Properties, Heat Transfer Division, ASME, 1970, pp. 107-114.

13. ———. The Velocity of Sound and Heat Capacity in Methene From Near-Critical to Subcritical Conditions and Equation-of- State Implications. J. Chem. Phys., v. 64, No. 1, 1976, pp. 203-218.

14. Good, W. D., D. R. Douslin, D. W. Scott, Ann George, J. L. Lacina, J. P. Dawson, and G. Waddington. Thermochemistry and Vapor Pressure of Aliphatic Fluorocarbons. A Comparison of the C-F and C-H Thermochemical Bond Energies. J. Phys. Chem., V. 63, 1959, pp. 1133-1138.

15. Good, W. D., D. M. Fairbrother, and G. Waddington. Manganese Carbonyl: Heat of Formation by Rotating-Bomb Calorimetry. J. Phys. Chem., v. 62, 1958, pp. 853- 856.

16. Good, W. D., J. L. Lacina, B. L. DePrater, and J. P McCullough. A New Approach to the Combustion Calorimetry of Silicon and Organosilicon Compounds. Heats of Formation of Quartz, Fluorosilicic Acid and Hexamethyldisiloxane. J. Phys. Chem., v. 68, 1964, pp. 579-586.

17. Good, W. D., J. L. Lacina, and J. P. McCullough. Methanethiol and Carbon Disulfide: Heats of Combustion and Formation by Rotating-Bomb Calorimetry. J. Phys. Chem., v. 65, 1961, pp. 2229-2231.

18. Good, W. D., and M. Månsson. The Thermochemistry of Boron and Some of Its Compounds. The Enthalpies of Formation of Orthoboric Acid. Trimethylamine-borane and Diammonium Decaborane. J. Phys. Chem., v. 70, 1966, pp.97-104.

19. Good, W. D., D. W. Scott, J. L. Lacina, and J. P. McCullough. Tetramethyllead: Heat of Foramtion by Rotating-Bomb Calorimetry. J. Phys. Chem., v. 63, 1959, pp. 1139-1142.

20. Good, W. D., D. W. Scott, and G. Waddington. Combustion Calorimetry of Organic Fluorine Compounds by a Rotating-Bomb Method. J. Phys. Chem., v. 60, 1956, pp. 1080-1089.

21. Guthrie, G. B., Jr., D. W. Scott, W. N. Hubbard, C. Katz, J. P. McCullough, M. E. Gross, K. D. Williamson, and G. Waddington. Thermodynamic Properties of Furan. J. Am. Chem. Soc., v. 74, 1952, pp. 4662-4669.

22. Harrison, R. H., and D. R. Douslin. Perfluorocyclobutane: The Thermodynamic Properties of the Real Gas. BuMines RI 6475, 1964, 14 pp.

23. Hubbard, W. N., C. Katz, and G. Waddington. A Rotating Combustion Bomb for Precision Calorimetry. Heats of Combustion of Some Sulfur-Containing Compounds. J. Phys. Chem., v.58, 1954, pp. 142-152.

24. Huffman, H. M. Low-Temperature Calorimetry at the Bartlesville Station of the Bureau of Mines. Chem. Rev., v. 40, 1947, pp. 1-14.

25. McCullough, J. P., and G. Waddington. Vapor-Flow Calorimetry. Ch. 10 in Experimental Thermodynamics, ed. by J. P. McCullough and D. W. Scott. Butterworths, London, v. 1, 1968, pp. 369-394.

26. Monk, P., and I. Wadsö. A Flow Micro Reaction Calorimeter. Acta Chem. Scand., v. 22, No. 6, 1968, pp. 1842-1852.

27. Osborn, A. G., and D. R. Douslin. Vapor Pressure Relations of 36 Sulfur Compounds Present in Petroleum. J. Chem. Eng. Data, v. 11, 1966, pp. 502-509.

28. ———. Vapor Pressures and Derived Enthalpies of Vaporization for Some Condensed-Ring Hydrocarbons. J. Chem., Eng. Data, v. 20, No. 3, 1975, pp. 229-231.

29. Picker, P., P. A. Leduc, P. R. Philip, and J. E. Desnoyers. Heat Capacity of Solutions by Flow Microcalorimetry. J. Chem. Thermodynamics, v. 3, 1971, pp. 631-642.

30. Picker, P., E. Tremblay, and C. Jolicoeur. A High-Precision Digital Readout Flow Densimeter for Liquids. J. Solution Chem., v. 3, No. 5, 1974, pp. 377-384

31. Prather, J. W., A. M. Ahangar, W. S. Pitts, J. P. Henley, A. R. Tarrer, and J. A. Guin. Solubility of Hydrogen in Creosote Oil at High Temperatures and Pressures. Ind. Eng. Proc. Des. Dev., v. 16, 1977, pp. 267-270.

32. Ruehrwein, R. A., and H. M. Huffman. Thermal Data XVII. The Heat Capacity, Entropy, and Free Energy of Formation of Cyclohexane. A New Method of Heat Transfer in Low-Temperature Calorimetry. J. Am. Chem. Soc., v. 65, 1943, pp. 1620-1625.

33. Scott, D. W. The Chemical Thermodynamic Properties of Hydrocarbons and Related Substances. III. Properties of the Alkane Hydrocarbons, C_1 Through C_{10}, in the Ideal Gas State from 0 to 1,500 K. BuMines Bull. 666, 1974, 187 pp.

34. ———. A Correlation of the Chemical Thermodynamic Properites of Alkane Hydrocarbons. J. Chem. Phys., v. 60, No. 8, 1974, pp. 3144-3165.

35. Scott, D. W., and J. P. McCullough. The Chemical Thermodynamic Properties of 100 Linear Alakane Thiols, Sulfides, and Symmetrical Disulfides in the Ideal Gas State From 0 to 1,000 K. BuMines Bull. 595, 1961, 68 pp.

36. Swietoslawski, W. Ebulliometric Measurements. Reinhold Pub. Corp., New York, 1945, p. 11

37. Todd, S. S., I. A. Hossenlopp, and D. W. Scott. Vapor-Flow Calorimetry of Benzene. J. Chem. Thermodynamics. v. 10, No. 7, 1978, pp. 641-648.

38. Waddington, G., J. W. Knowlton, D. W. Scott, G. D. Oliver, S. S. Todd, W. N. Hubbard, J. C. Smith, and H. M. Huffman. Thermodynamic Properties of Thiophene. J. Am. Chem. Soc., v. 71, 1949, pp. 797-808.

39. Waddington, G., S. S. Todd, and H. M. Huffman. An Improved Flow Calorimeter. Experimental Vapor Heat Capacities and Heats of Vaporization of n-Heptane and 2,2,3-Trimethylbutane. J. Am. Chem. Soc., v. 69, 1947, pp. 22-30.

RECENT DEVELOPMENTS IN CALORIMETRIC INSTRUMENTATION: APPLICATION TO PROBLEMS OF ENERGY STORAGE AND RECOVERY

by

L. D. Hansen[1], J. J. Christensen[1], D. J. Eatough[1], and R. M. Izatt[1]

ABSTRACT

Four major developments in calorimetric instrumentation have been made at the Thermochemical Institute at BYU during the last few years: (1) micro (<5-ml) reaction vessels and improved controllers have been developed for the isothermal calorimeter, (2) micro (<3-ml) reaction vessels and methods for heat loss correction for such vessels have been developed for the isoperibol titration calorimeter, (3) a controlled-plate design and a high-pressure flow cell have been developed for the isothermal calorimeter, and (4) a heat conduction calorimeter with a peak -to-peak noise level of 0.1 μw has been developed. All of these instruments are commercially available.

Each of these instruments has found recent application to problems of storage or recovery of energy. The isothermal solution calorimeters are being used for the study of heats of wetting of rock surfaces with crude oils and surfactant solutions. The micro isoperibol calorimeter is being used as an analytical tool in environmental studies on sulfur and nitrogen compounds. The high-pressure flow calorimeter is being used to measure heats of mixing of both volatile and viscous fluids, and the data so obtained are being used to develop better methods for predicting vapor-liquid equilibria. The heat conduction and controlled-plate calorimeters are being used to study mechanisms of energy loss and corrosion in batteries.

INTRODUCTION

Calorimetric methods have come of age during the past decade. Prior to this decade a calorimetric experiment usually began with the design and construction of the calorimeter. Today there is a wide range of commercially available calorimetric equipment which can be readily adapted to the needs of most investigators. Most of the recent developments in calorimetric instrumentation that have been made at the Thermochemical Institute at Brigham Young University have in fact been modifications or improvements of existing commercial designs (2-4, 12-13). While this does not mean that the modifications required a minor effort, much less effort was required than would have been

[1]Brigham Young University, Provo, Utah.

required to begin without the commercially available equipment as a starting point.

The object of this paper will be to present a series of problems in the area of energy storage or retrieval and then to demonstrate how we have applied calorimetric methods to find solutions to these problems. Since a modification of an existing commercially available calorimeter was required for most of the studies, the description of the modifications and the reasons for our specific choice of a calorimetric technique will be discussed as part of the solution to each problem presented.

TERTIARY OIL RECOVERY

Any approach to the problem of tertiary oil recovery must involve an understanding of the surface interactions among the rock in the oil-bearing formation, the crude oil, and the solution which is being used to remove the oil. Titration calorimetry has been shown to be a rapid way to study the adsorption of organic compounds on solids (8). Adsorption isotherms and heats of adsorbtion are quickly and easily determined with good accuracy by this method.

Continuous titrations in an isoperibol titration calorimeter of suspensions of crushed rock with surfactant solutions in oil or water quickly showed that some of the reactions required several minutes to reach thermal equilibrium. Because of the time required for the system to reach equilibrium (5-15 min) between additions of titrant, the isoperibol calorimeter was not suitable for this work. Because of the vigorous stirring required to maintain the rock in suspension, the available heat conduction calorimeters were also not suitable. We therefore chose to continue the work using the isothermal solution calorimeter (2) in a discontinuous titration mode. Two features made the Tronac isothermal calorimeter ideally suited to this work. First, the long-term flat baseline makes it possible to study slow reactions, and, second, the vigorously stirred reaction vessel makes the study of suspensions of solids in liquids possible.

The use of surfactant-cosurfactant systems for tertiary recovery of oil from fields has been proposed and is currently being evaluated by many laboratories and firms. The interaction between such surfactant systems and field rocks and/or dissolved minerals is not yet well understood. Using isothermal titration calorimetry we investigated the interaction of Ca^{2+} and Mg^{2+} with a long-chain sulfonate surfactant, S^-, and the binding of the surfactant to field core samples (sandstone and carbonate) in the presence and absence of Ca^{2+} and Mg^{2+} at 25° C. The results indicate that the Ca^{2+}-S^- system forms a bridge complex binding the sulfonate to the carbonate core.

Micellization of the surfactant system was studied by dilution of 0.08 M and 0.02 M solutions of the surfactant into water using a previously described technique (7). The cmc was found to be 0.32 ± 0.09 mM, and the heat of micellization was calculated to be 0.30 ± 0.15 kcal/mole. Dilution of the micelles to a concentration below the cmc results in a heat of -0.05 ± 0.09 kcal/mole

for the 0.08 M solution. Interaction of Ca^{2+} and Mg^{2+} with the surfacant was studied by titration of 0.08 M surfactant solution into either $MgCl_2$ or $CaCl_2$ solutions. The concentrations of the salts ranged from 0.3 mM to 3.0 mM. No precipitates were formed in any of these titrations. The ΔH values for the overall reactions

$$M^{2+} + 2S^{-} = MS_2 \qquad (1)$$

were 0.20 and -0.10 kcal/mole for Ca^{2+} and Mg^{2+}, respectively.

Adsorption of the surfactant and the metal ions into core rock samples could be conveniently studied by titration of solutions of the salts or the surfactant(0.08 M) into a suspension of 2 g of finely crushed ore in 50 ml of water. Sharp end points were seen, corresponding to quantitative interaction with adsorption sites on the core sample. Results are summarized in table 1. The adsorption is endothermic in all cases. Two apparent adsorption sites were seen for the interaction of the surfactant with the carbonate core sample, as summarized in table 1 and illustrated in figure 1.

TABLE 1. - Calorimetric results for adsorption of salts or surfactant in water by core samples at 25° C

Adsorbant	Core sample	Observed end point, μmole/g	ΔH, kcal/mole adsorbant
Surfactant	Carbonate	5.9 ± 0.5	0.9 ± 0.1
		12.8 ± .9	2.3 ± .3
	Sandstone	12.1 ± 1.8	1.2 ± .8
	Ceramic	too weak to measure	
$CaCl_2$	Carbonate	22.8 ± 0.7	.21 ± .05
	Sandstone	20.4 ± 2.0	.46 ± .12
	Ceramic	21. ± 3.	.21 ± .05
Surfactant	Carbonate + 3 mM $CaCl_2$.	7.2 ± 1.0	-.76 ± .18
		---	.30 ± .16
	Sandstone + 3 mM $CaCl_2$.	---	.20 ± .05
	Carbonate + 3 mM $MgCl_2$.	---	.5 ± .4
	Sandstone + 3 mM $MgCl_2$.	---	.3 ± .2

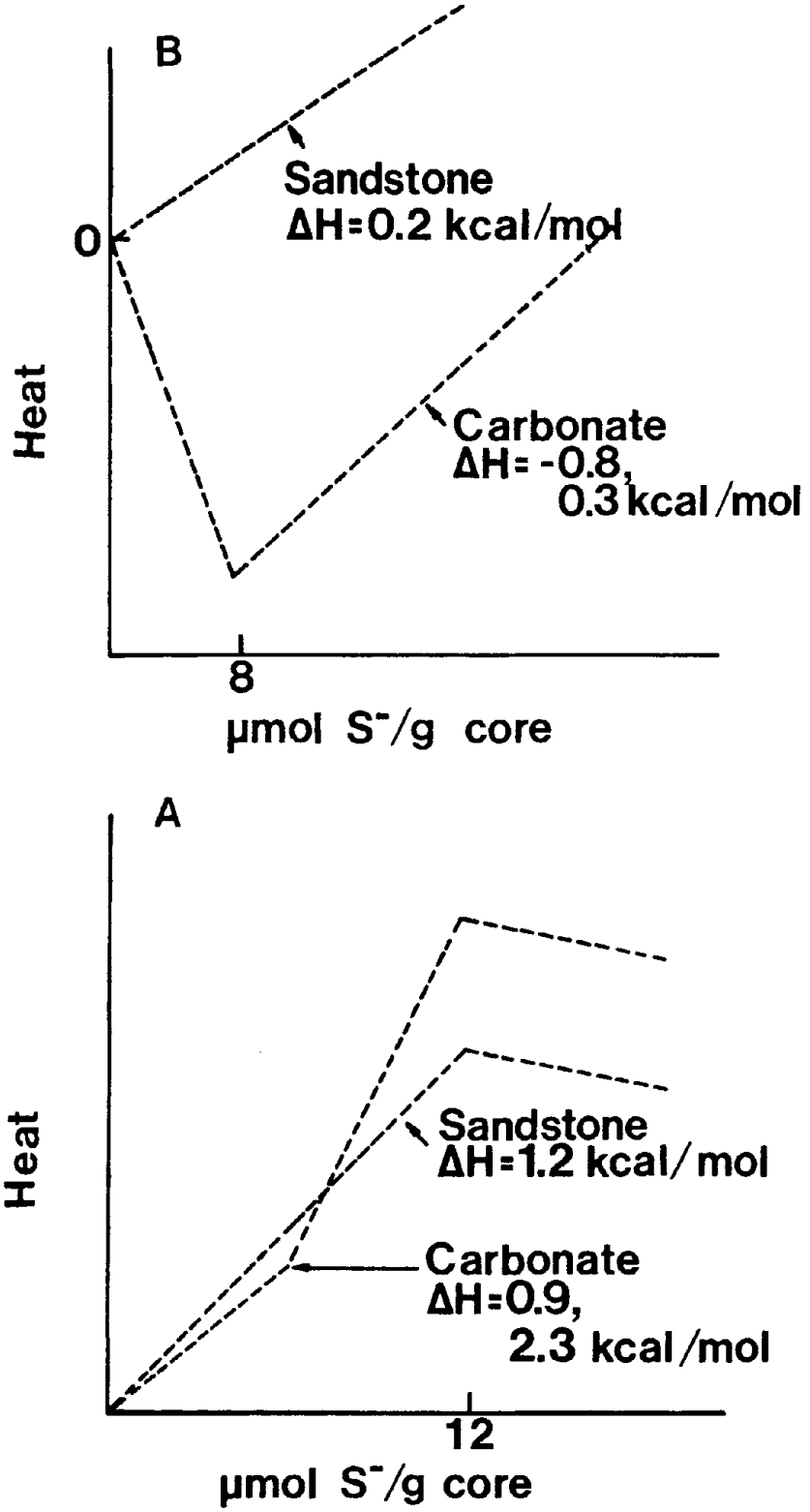


FIGURE 1. - Calorimetric titration curves for titration of surfactant (S^-) into core sample (A) and into core sample and Ca^{2+} (B).

Finally runs were made to investigate complexes that might form in a system containing surfactant, salt, and core sample by titration of the surfactant (0.08 M) into a suspension of the core sample in $MgCl_2$ or $CaCl_2$ solution, (table I). If interaction of the surfactant with the core samples is independent of the salt, an initial heat of about 1 kcal/mole should be seen, and an endpoint should be evident similar to that observed in the system with no added salt. If the surfactant binds to the core by displacing Ca^{2+} or Mg^{2+}, or if the surfactant binds the metal ion but not the core, a smaller endothermic heat would be expected. The exothermic heat observed for initial binding of the surfactant to carbonate core in the presence of Ca^{2+} (figure 1) indicates that none of these mechanisms predominate and suggests a complex is formed that is not present in any of the two-component systems. We postulate this involves the formation of a

$$S^- \ldots Ca^{2+} \ldots \underset{\text{core}}{\text{Carbonate}}$$

bridged complex, with the $CaCl_2$, carbonate core system only.

The study illustrates how the details of surface chemistry in such systems may be probed using titration calorimetry. We have also shown that hydration effects involved in the formation of oil-external or water-external micelle systems with sulfonate surfactants and alcohol cosurfactants may be studied using calorimetry (5).

DETERMINING CHEMICAL SPECIES IN AIRBORNE PARTICULATE MATTER

While extensive determinations of the elemental composition of airborne particulate matter have been made and can now be done routinely with automated equipment, little information is available concerning the exact chemical species and compounds present. This is especially true of the minor inorganic components. Interestingly enough, it is these same minor components that cause concern when released to the atmosphere. Specific information on the compounds present is extremely important in understanding the environmental impact of fossil fuel combustion because the behavior of an element in the environment can differ markedly with oxidation state and with the other species with which it is combined. Specifically we have been interested in identifying acids, bases, and the S, N, and As species present in airborne particulate matter produced by the smelting of metals and the combustion of fossil fuels.

The Tronac model 450 micro isoperibol titration calorimeter (12-13) has proven to be an extremely useful tool for these studies. A titration with $K_2Cr_2O_7$ solution followed by an injection of $BaCl_2$ solution and then by an injection of sulfamic acid solution suffices for the determination of S(IV), other reducing agents, sulfate, and nitrite (14-15). Figure 2 shows schematically the data collected. All of the acid-base active species present in a water extract of the particulate matter can often be determined in a separate experiment using the same model of calorimeter with the addition of a set of

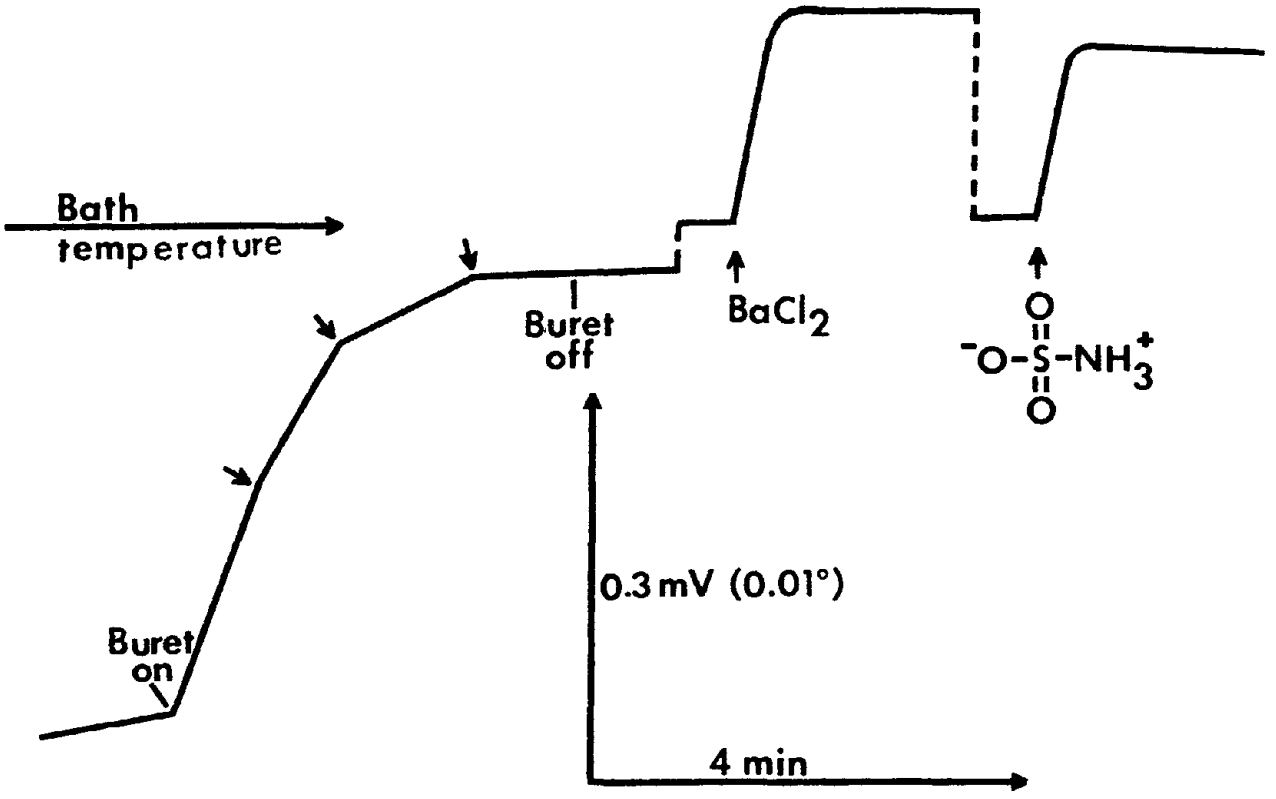


FIGURE 2. - Calorimetric titration curve for determination of S(IV), sulfate, and nitrite.

micro pH electrodes to the reaction vessel (6). The titrants in this case are $HClO_4$ and NaOH solutions. Figure 3 shows the data collected on a sample of airborne particulate matter collected in New York City.

The advantage of the titration calorimetry approach are (1) freedom from interferences, (2) rapidity, (3) ability to handle submilligram samples, and (4) the equipment is portable and relatively inexpensive. Because the thermogram produced by titration calorimetry provides data on both the amount (end points) and the identity (ΔH) of the substance undergoing reaction, it is essentially free from interferences. The direct injection enthalpimetric determinations of sulfate and nitrite are interference-free because of the specificity of the reagents used. Since a titration and an injection can be run in about 20 minutes, the method is fast enough for routine work. The detection limit of the method depends mainly on the ΔH value for the analytical reaction. Typically it ranges from about 30 nanomoles (ΔH~40 kj/mole) to about 3 nanomoles (ΔH~400 kj/mole) in 2 ml of solution. Development of a micro isoperibol titration calorimeter has made this analytical application of calorimetry possible.

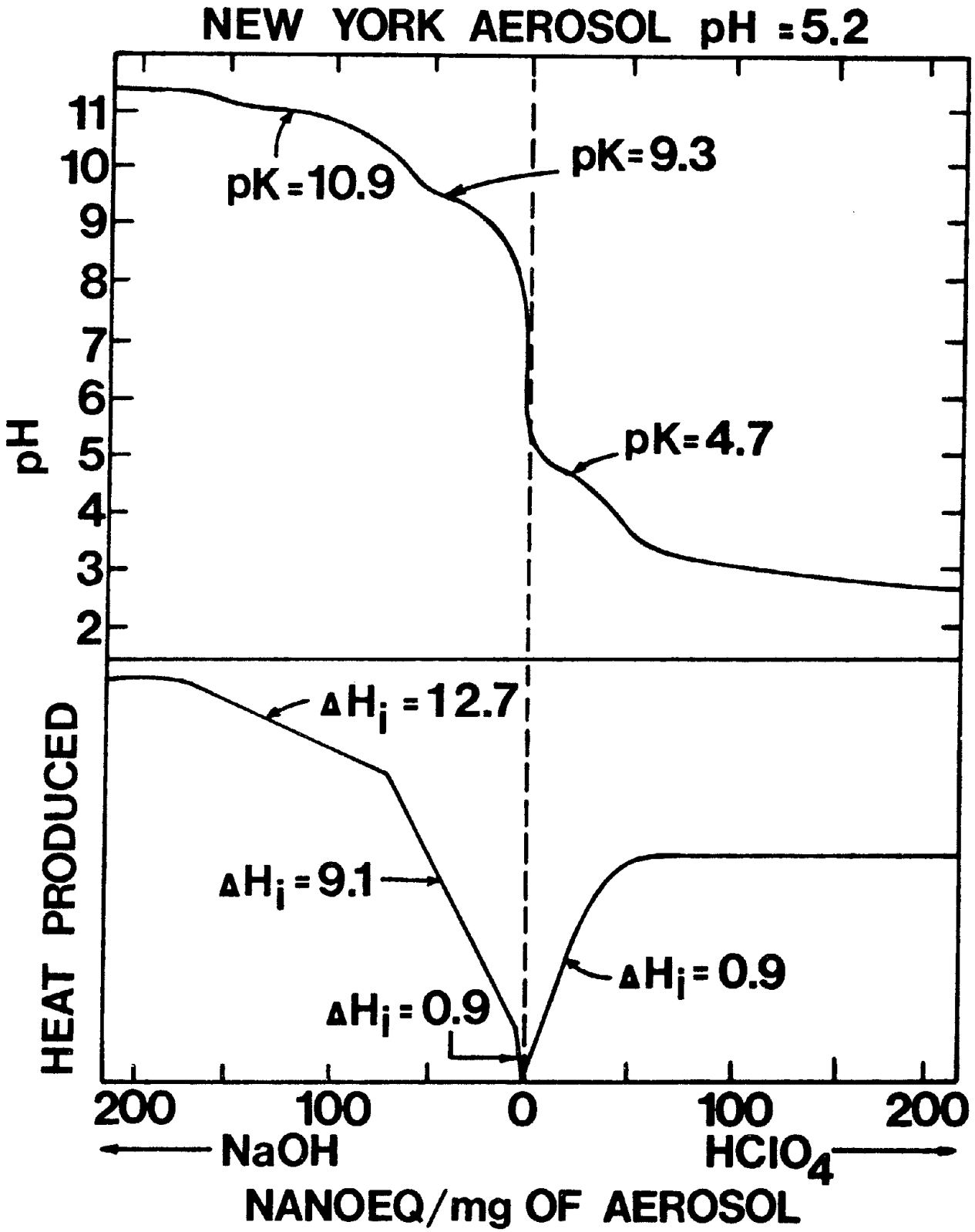


FIGURE 3. - pH and calorimetric titration curves for New York airborne particulate matter for titration with acid and base.

PREDICTION OF VAPOR-LIQUID EQUILIBRIA FOR NONIDEAL, MULTICOMPONENT MIXTURES

Designers of separation equipment for the chemical process and petroleum industries need accurate vapor-liquid equilibrium (VLE) data, often at a variety of conditions. Although large amounts of such data are available in the literature, one frequently finds that data are not available for the substances to be separated or for the conditions at which a design must be made. In such a situation the designer must either make new measurements of VLE data at appropriate conditions or estimate the required data by means of some data correlation or model. Because of the difficulties associated with obtaining good VLE data experimentally, especially at extreme conditions, the designer often turns to estimation methods to get his data.

The use of semitheoretical models to fit existing VLE data and to extrapolate to other conditions is common (16). Models of this type generally involve one or more adjustable parameters, the values of which must be determined by curve-fitting experimental data. The usual method for doing this is to curve-fit either the activity coefficients or the g^E data derived from the VLE data (1). However, reliable VLE data are relatively scarce for temperatures above 100° C and almost nonexistent above 200° C.

An alternative approach to the problem of estimating VLE data has been developed by Hanks and coworkers (9). In this method a model for the excess Gibbs energy, g^E, is first assumed. Then an algebraic expression for the h^E, the heat of mixing, is derived by use of the Gibbs-Helmholtz relation:

$$h^E = T^2 \left[\frac{\partial(g^E/T)}{\partial T}\right]_{P,x} \qquad (2)$$

The parameters of the assumed free-energy model are then determined by fitting the algebraic expression for h^E to a set of experimental h^E data. These parameters are then used in the g^E model to calculate activity coefficients and thence VLE data.

This method has been shown to be valid for isothermal binary systems, isobaric binary systems, and isothermal-isobaric ternary systems (9, 17-18). It has also been used to predict high-temperature VLE data from low- to medium- temperature h^E data (10). A variety of types of mixtures have been treated including those involving aromatic hydrocarbons, aliphatic hydrocarbons, and alcohols (9-10, 17-18).

This technique represents a rather significant simplification of the VLE data prediction process because accurate h^E data may be readily obtained at moderate temperatures and because experimental h^E data are not required over the entire temperature range. Also in many instances the h^E data are more easily obtained than the g^E data.

In figure 4 this method is illustratd for the cyclohexane(1)-n-heptane-(2) system at 25° C. The model assumed for g^E in this case is embodied in

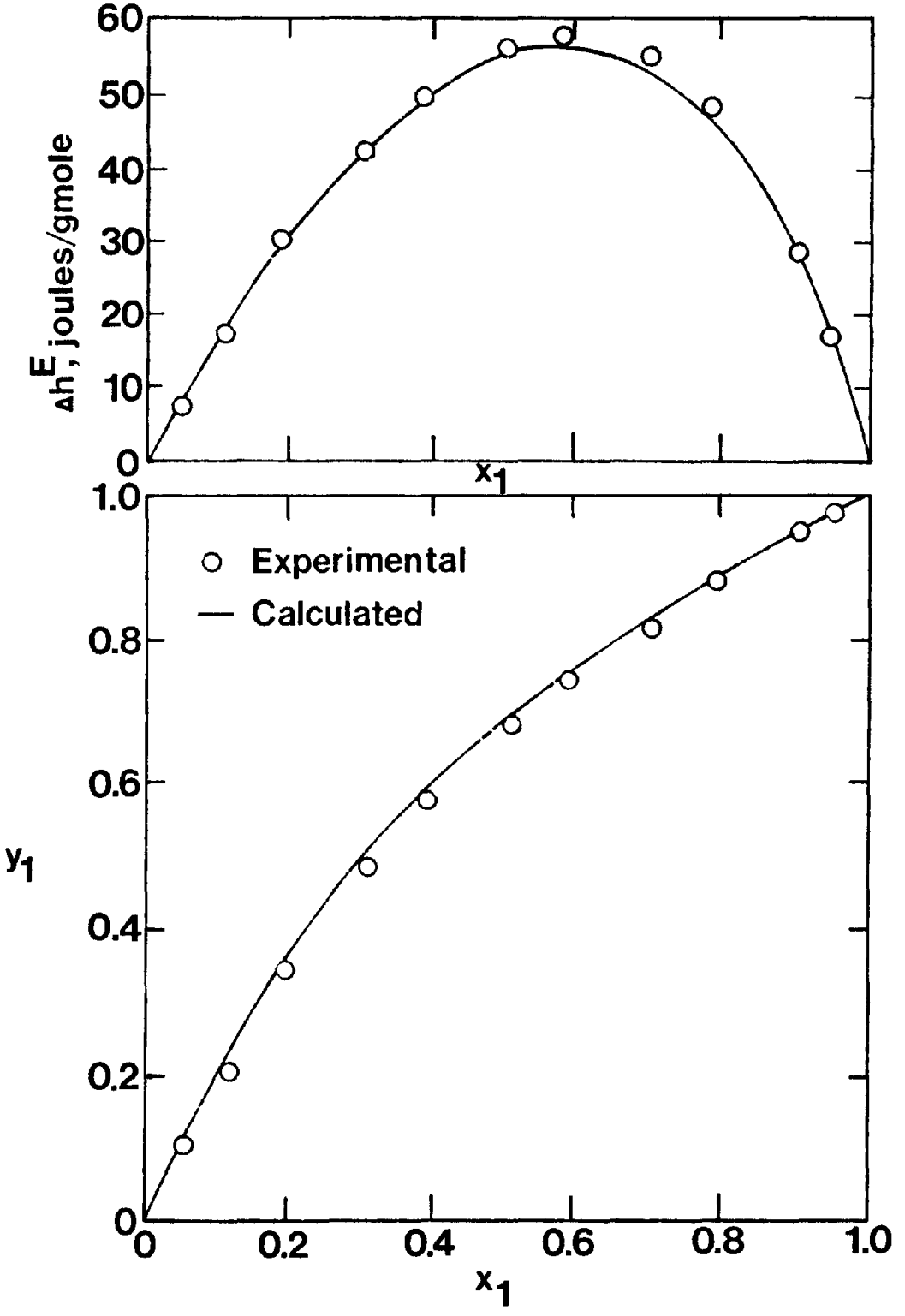


FIGURE 4. - Comparison of calculated and experimental data for cyclohexane(1)-n-heptane(2) system at 25° C. Curves calculated from the NRTL model. Y_1 is the mole fraction of (1) in the vapor, and X_1, in the liquid.

the Renon and Prausnitz Nonrandom Two Liquid (NRTL) equation, which has three adjustable parameters. In the upper graph the solid curve is curve-fitted to the h^E data to determine the three adjustable parameters. These parameters are then used in the activity coefficient equations to compute the binary VLE data as shown in the lower graph. Another example of the method is shown in figure 5 for the system toluene(1)-butanol(2) at 25° C. In this case the Continuous Linear Association Model (CLAM) equation is used.

There are numerous models for g^E in the literature, many of which provide excellent curve-fits of experimental VLE data. However, in using the h^E-VLE prediction method described above, the application of the Gibbs-Helmholtz relation imposes a rather severe constraint upon these g^E models since they must also fit the h^E data. Some models can meet this additional constraint only over limited ranges of their parameters, while some cannot meet it at all. Our results for over 30 hydrocarbon-hydrocarbon binary systems indicate that either the NRTL equation or the LEMF equation (NRTL equation modified by Marina and Tassios) gives VLE predictions from heats of mixing of better that 5 pct. For over 35 hydrocarbon-alcohol systems the CLAM equation was found to give VLE data better than 5 pct.

These results reveal the price one must pay to gain the simplicity of the h^E-VLE prediction method. It is that one must first choose a model which is capable of simultaneous g^E and h^E data representation. This in turn raises the question of how to select such a model. This question is not easy to answer. At present, work is in progress in our laboratories to find a suitable h^E-g^E model which will work for alcohol-alcohol mixtures and other systems with various types of complex physical and chemical interactions. We are also using the same approach to pursue the problem of predicting liquid-liquid equilibrium in multicomponent mixtures. In order to do this, h^E data on many different systems under a variety of conditions of P and T must be collected.

By modifying the reaction vessel of the Tronac model 550 isothermal calorimeter, we were able to construct a calorimeter to meet our needs. Substituting a coil of stainless steel tubing for the reaction chamber and coupling this coil to two high-pressure pumps with programmable delivery capability resulted in an isothermal high-pressure flow calorimeter (3). The unit retains all of the desirable operating characteristics and advantages of previous isothermal instruments (2, 4) while offering the additional advantage of operating as a flow instrument at pressures up to 400 atm with programmable solvent delivery rates. For example, binary, isothermal, and isobaric heat-of-mixing curves over the mole fraction range 0-1 are automatically produced in one continuous, 2 to 3 hour run at any temperature and pressure in the ranges of 0 to 70° C and 1 to 400 atm, respectively. The data can be printed out in digital form and/or obtained as a strip chart recording which is the differential heat of mixing curve.

The main component of the calorimeter are the reaction vessel containing the isothermal plate and the mixing and equilibration coil, the flow circuit which contains the high-pressure pump and the flow controller programmer, the water bath, and the isothermal control unit. A block diagram showing the main components of the unit is given in figure 6.

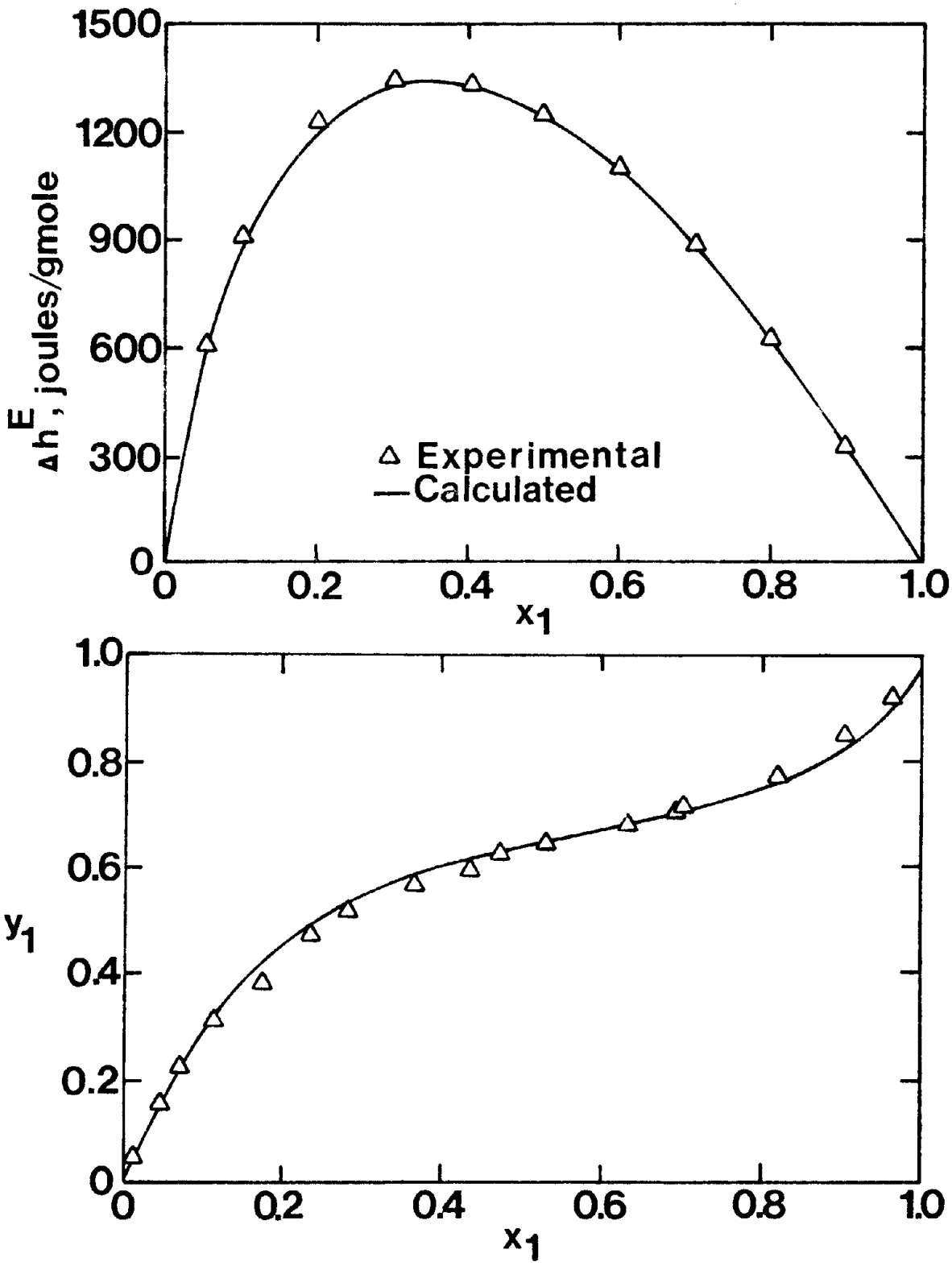


FIGURE 5. - Comparison of calculated and experimental data for toluene(1)-butanol(2) at 25° C. Curves calculated from CLAM model.

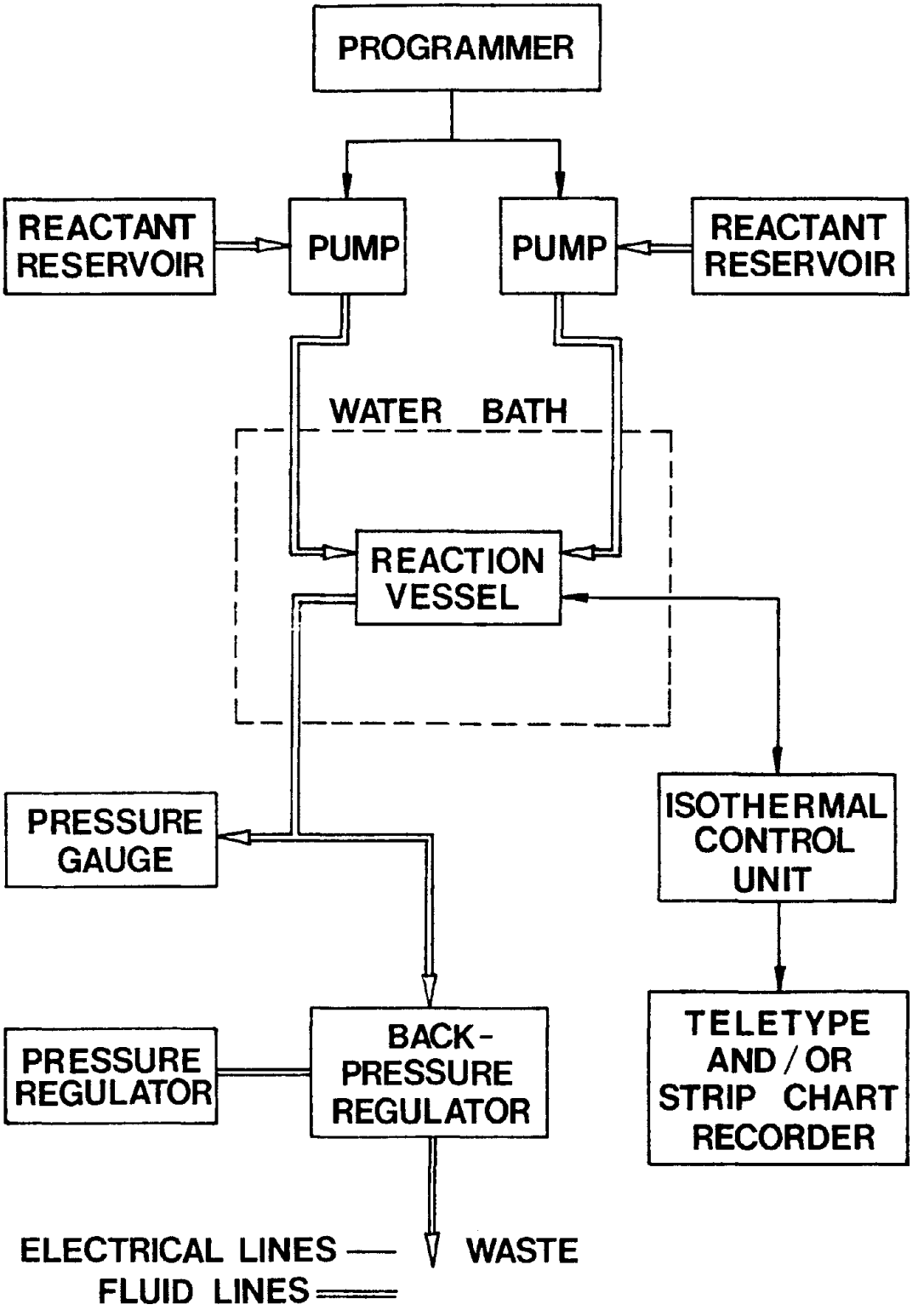


FIGURE 6. - Block diagram of the isothermal high pressure flow calorimeter. *(Reproduced from reference 3 by permission of the American Institute of Physics.)*

The precision and accuracy of the calorimeter have been determined by both electrical and chemical calibrations. Three chemical systems, $HClO_4$-NaOH, $HClO_4$-TRIS, and n-hexane-cyclohexane, were investigated over a wide range of flow rates and pressures. The results obtained showed that the calorimeter achieved an accuracy of ± 0.2 pct in the mean of several runs and a precision of ± 0.8 pct or less in any individual measurement point during a run. The rates of heat production in these runs were in the range of 1 to 5 mw.

This calorimeter thus can measure both heats of reactions and heats of mixing at constant temperature and pressure over a wide range of concentrations, flow rates, temperatures, and pressures. The lack of any dependence on the heat capacity of the solution makes the method particularly applicable to systems involving nonaqueous solvents and concentrated solutions which may undergo large heat capacity changes. In addition, no correction is necessary for heat exchange between the calorimeter and its environment. The calorimeter can be programed to automatically generate data as a function of composition over a given period of time.

BATTERY PROCESSES

Chemical batteries are probably the most convenient way of storing energy for many purposes. The wide range of sizes, chemistries, and applications of batteries is testimony to this. Currently available batteries have problems, however, which prevent or limit their usefulness in certain applications. All batteries are subject to internal self-discharge which may significantly decrease the efficiency of the battery for energy storage over long time periods. Rechargeable batteries which are cycled repeatedly between charged and discharged conditions are subject to a variety of chemical changes which eventually lead to battery failure. A third problem which can be serious in some batteries is dissipation of heat during the charging and/or discharging portion of the cycle. All of these problems are amenable to study by calorimetric methods.

The isothermal plate calorimeter, which was designed at BYU (3) and is now commercially available, has been used to study thermal effects during charge-discharge cycling of batteries. Among other applications, the data so collected will be used in designing extremely large batteries (in the megawatt range) for load leveling in electric power generating plants. This isothermal plate calorimeter is particularly useful for this type of measurement because fairly large heat flow rates can be measured (up to about 1.5 watt), the noise level is low ($\pm$ 20 μw peak-to-peak), and there is little limitation on the shape or size (up to about 7.5 by 15 cm) of battery that can be studied. In concept, this calorimeter is extremely simple since it consists only of an isothermal plate on which the battery rests and the associated circuitry which is used to measure the energy flow rate necessary to maintain the plate in an isothermal condition.

The study of internal self-discharge in batteries, particularly those

destined for very-long-life applications, requires a much lower detection limit on heat effects. For example, a 1-μw internal power leakage can shorten the expected lifetime of a battery by as much as 10 pct in some long-term, low- power applications such as cardiac pacemakers and remote data stations. Since the batteries in some of these applications are expected to last 10 years, this is a difference of a full year. Because of this requirement, that is, a detection limit less than 1-μw, we specifically designed a calorimeter for studying this type of battery (11).

The calorimeter is now commercially available (19). It is a twin-cell differential heat flow instrument as shown schematically in figure 7. The calorimeter has a peak-to-peak noise level of less than 0.3 μw on an open circuit battery measurement in which the two sides cannot be matched exactly. Peak-to-peak baseline noise is reduced to about ±0.1 μw if the heat capacity of the compartment used as a reference can be carefully adjusted to be the same as the compartment containing a battery by insertion of an aluminum block.

The calorimeter consists of an aluminum block 15 cm wide, 17 cm high, and 30 cm long with a tapered channel 10 cm wide, 10 cm deep and 25 cm long cut into it; four wedges of 2.5-cm-thick aluminum placed in the channel; and four thermoelectric measuring devices (Cambion Model 1052) which are mounted on the aluminum wedges together with two battery holders made of thin aluminum. The large aluminum block assembly was suspended by 0.6-cm bolts in the center of the watertight box which was then submerged in a Tronac Model 405 water bath controlled to ± 0.0002° C. Two pipes, sealed around holes in the box cover, give access through the water bath to the battery holders. During a measurement, the holes in the box cover and the battery holders are covered with aluminum plates to prevent heat transfer by air currents or radiation.

The outputs from the two sets of thermoelectric devices are connected with opposing polarities so that the effects of any temperatue fluctuations in the block are canceled in the output. The difference in the output voltages of the two compartments, which is proportional to the difference in the rates of heat production in the two compartments, is filtered with a simple R-C filter (time constant=6 min), amplified by a Keithley Model 150B amplifier, and recorded on a strip chart recorder.

Table 2 gives the results obtained for a series of open-circuit heat dissipation measurements on batteries of various kinds, shapes, and sizes. These results clearly show the capabilities of the calorimeter as well as the reproducibility of open-circuit heat dissipation in a set of supposedly identical batteries.

Calorimetric measurements of open-circuit heat dissipation of batteries may not accurately reflect that a primary chemical reaction is occurring in the battery with a consequent loss in ampere-hours available. Processes such as crystal growth, evaporation of liquids, curing of plastics and cements, and mechanical strain release can produce a change in the total energy content of the battery and, hence, an output signal to the calorimeter. These changes are not significant in determining battery life unless they lead to mechanical

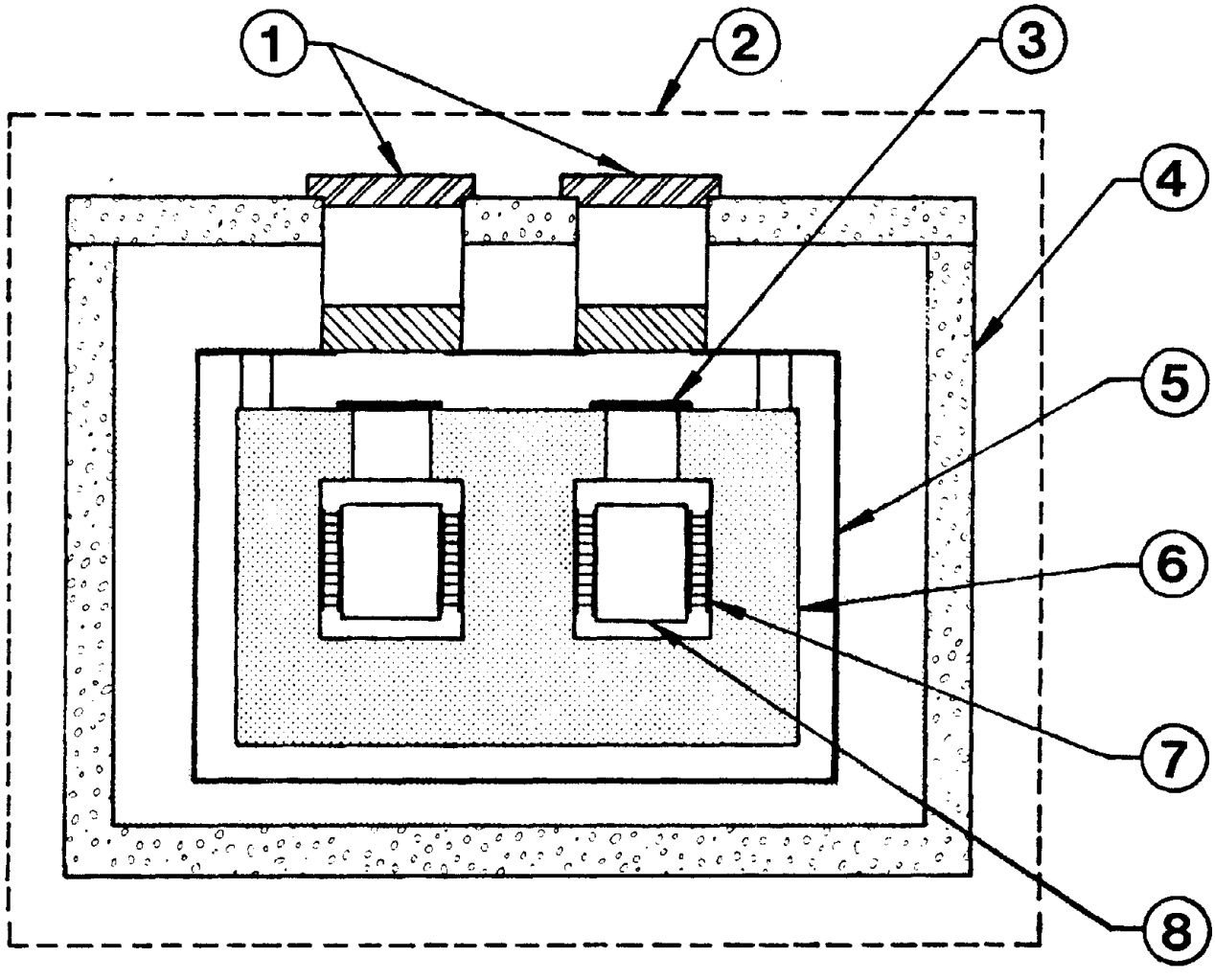


FIGURE 7. - Cross section of twin-cell differential heat flow calorimeter. 1, Access tubes and covers; 2, temperature-controlled air bath with electronics inside; 3, covers on block compartments; 4, temperature-controlled water bath; 5, watertight stainless steel box; 6, aluminum heat sink block; 7, thermoelectric sensors; 8, battery holder. *(Reproduced from reference 11 by permission of The Electrochemical Society.)*

TABLE 2. - Open-circuit battery measurements

Battery type	Ampere-hours	Volts	Power[1] μw	Number in sample
Mercury, HgO/Zn, pacemaker set I	1	1.4	4.1 ± 0.1	2
Mercury, HgO/Zn, pacemaker set II	1	1.4	7.5 ± 0.3	2
Alkaline, MnO_2/Zn, penlight	2	1.5	46 ± 2	2
Mercury, HgO/Zn, penlight	2	1.4	68 ± 5	2
Carbon-Zn, penlight	1	1.5	15	1
AgO/Zn watch battery set I	0.16	1.5	7 ± 1	8
AgO/Zn watch battery set II	0.16	1.5	10.2 ± 0.4	3
AgO/Zn watch battery set III	0.16	1.5	13 ± 1	5
Lithium-iodine pacemaker set I	1.2	2.7	5 ± 1	2
Lithium-iodine pacemaker set II	1.5	2.7	30 + 5	2
Lithium-iodine pacemaker set III	3.0	2.7	6 ± 2	2

[1]Deviations are the standard deviation with respect to the mean between batteries.

failure of some battery component. Calorimetric experiments can be done to determine the magnitude and source of most of these effects by measuring the heat output of each battery component separately. Open-circuit heat dissipation is also typically a function of age as shown in figure 8, and this must be taken into account in interpreting these kinds of data.

REFERENCES

1. Brown, I., and F. Smith. Liquid-Vapor Equilibriums. VI. The Systems Acetonitrile-Benzene at 45° and Acetonitrile-Nitromethane at 60°. Aust. J. Chem., v. 8, 1955, pp. 62-67.

2. Christensen, J. J., J. W. Gardner, D. J. Eatough, and R. M. Izatt. An Isothermal Titration Microcalorimeter. Rev. Sci Instr., v. 44, 1973, pp. 481-484.

3. Christensen, J. J., L. D. Hansen, D. J. Eatough, and R. M. Izatt. Isothermal High Pressure Flow Calorimeter. Rev. Sci. Instr., v. 47, 1976, pp. 730-734.

4. Eatough, D. J., J. J. Christensen, and R. M. Izatt. Determination of the Enthalpy of Solution of tris-(Hydroxymethyl)aminomethane in 0.1 M HCl Solution and the Enthalpy of Neutralization of $HClO_4$ With NaOH at Low Ionic Strengths by Use of an Improved Isothermal Titration Calorimeter. J. Chem. Thermodynamics, v. 7., 1975, pp. 417-422.

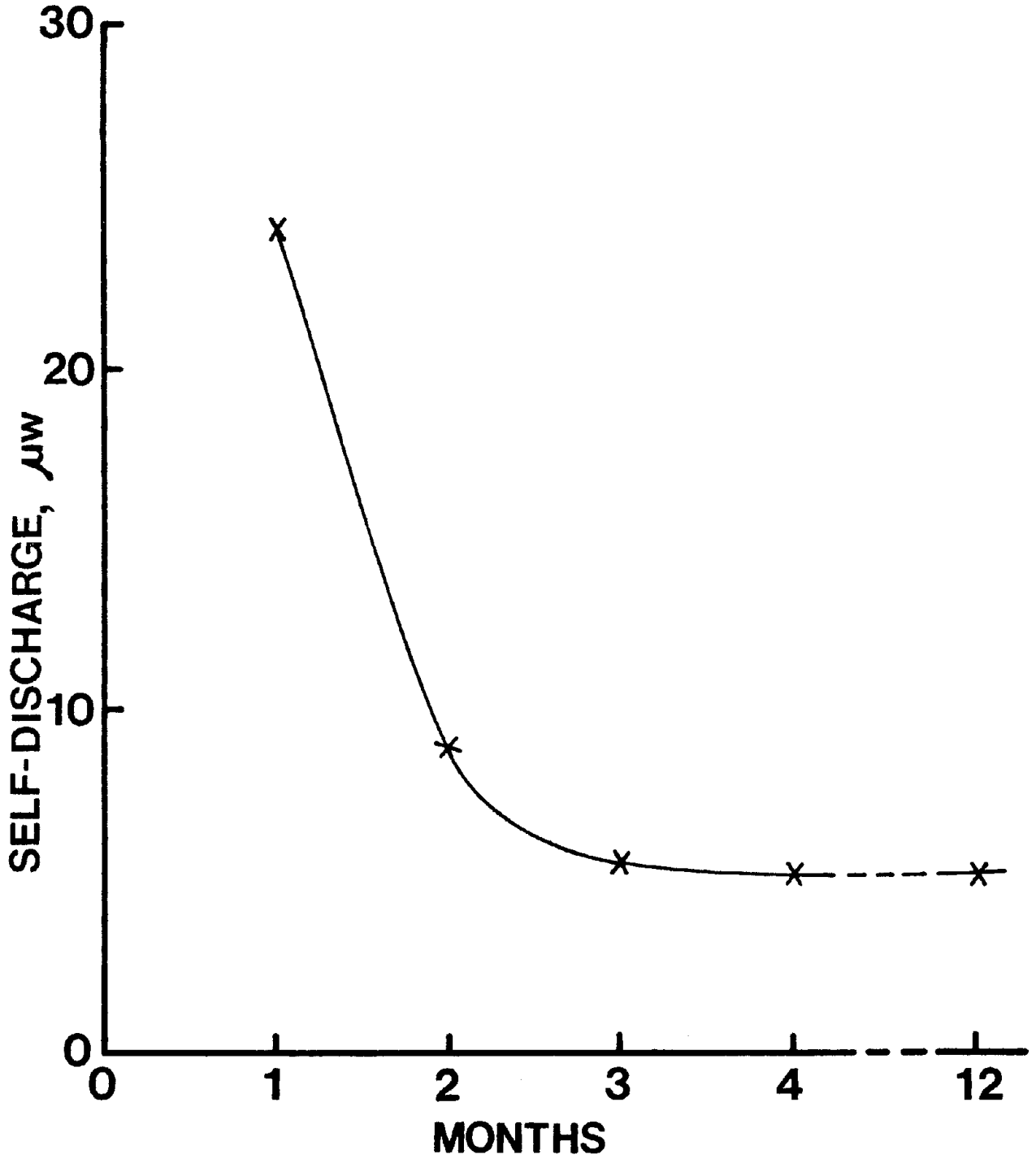


FIGURE 8. - Open-circuit heat dissipation of a typical pacemaker battery as a function of battery age. *(Reproduced from reference 11 by permission of The Electrochemical Society.)*

5. Eatough, D. J., K. D. Dreher, and R. D. Sydansk. A Calorimetric Investigation of Microemulsions. Proc. Symp. on Oilfield Chemistry, Soc. Petrol. Eng., Denver, Colo., May 1973.

6. Eatough, D. J., L. D. Hansen, R. M. Izatt, and N. F. Mangelson. Determination of Acidic and Basic Species in Particulates by Thermometric Titration Calorimetry in Methods and Standards for Environmental Measurements. Proc. 8th Materials Res. Symp., NBS Spec. Pub. 464, 1977, pp. 643-649.

7. Eatough, D. J., and S. J. Rehfeld. A Calorimetric Investigation of Micelle Formation in Aqueous Sodium Dodecylsulfate Solutions. Thermochim. Acta, v.2, 1971, pp. 443-456.

8. Eatough, D. J., S. Salim, R. M. Izatt, J. J. Christensen, and L. D. Hansen. Calorimetric Investigation of Adsorption of Aromatic Compounds by Linde Molecular Sieve 13X. Anal. Chem., v. 46, 1974, pp. 126-128.

9. Hanks, R. W., A. C. Gupta, and J. J. Christensen. Calculation of Isothermal Vapor-Liquid Equilibrium Data for Binary Mixtures From Heats of Mixing. Ind. Eng. Chem. Fund., v. 10, 1971, pp. 504-509.

10. Hanks, R. W., R. L. Tan, and J. J. Christensen. The Prediction of High Temperature Vapor-Liquid Equilibrium From Lower Temperature Heat of Mixing Data. Thermochim. Acta, v. 27, 1979, pp. 9-18.

11. Hansen, L. D., and R. M. Hart. The Characterization of Internal Power Losses in Pacemaker Batteries by Calorimetry. J. Electrochem. Soc., v. 125, 1978, pp. 842-845.

12. Hansen, L. D., R. M. Izatt, D. J. Eatough, T. E. Jensen, and J. J. Christensen. Recent Advances in Titration Calorimetry in Analytical Calorimetry, ed. by R. S. Porter and J. F. Johnson. Plenum Press, New York, v. 3, 1974, pp. 7-16.

13. Hansen. L. D., T. E. Jensen, S. Mayne, D. J. Eatough, R. M. Izatt, and J. J. Christensen. Heat-Loss Corrections for Small Isoperibol-Calorimeter Reaction Vessels. J. Chem. Thermodynamics, v. 7, 1975, pp. 919-926.

14. Hansen, L. D., B. E. Richter, and D. J. Eatough. Determination of Nitrite by Direct Injection Enthalpimetry. Anal. Chem., v. 49, 1977, pp. 1779-1781.

15. Hansen, L. D.., L. Whiting, D. J. Eatough, T. E. Jensen, and R. M. Izatt. Determination of Sulfur(IV) and Sulfate in Aerosols by Thermometric Methods. Anal. Chem., v. 48, 1976, pp. 634-638.

16. Prausnitz, J. M. Molecular Thermodynamics of Fluid-Phase Equilibria. Prentice-Hall, Englewood Cliffs, New Jersey, 1969, pp. 181-262.

17. Tan, R. L., R. W. Hanks, and J. J. Christensen. The Prediction of Isothermal Phase Equilibria for Nonideal Multicomponent Mixtures From Heats of Mixing. Thermochim. Acta, v. 21, 1977, pp. 157-170.

18. ———. The Prediction of Isobaric Phase Equilibria for Nonideal Multicomponent Mixtures From Heat of Mixing Data. Thermochim. Acta, v. 23, 1978, pp. 29-40.

RESOLUTION OF LATTICE HEAT CAPACITIES[1]

by

Edgar F. Westrum, Jr.[2]

ABSTRACT

Evaluation of the electronic (e.g., Schottky), magnetic, structural order-disorder, and other types of transitions and excess heat capactiies and other themodynamic contributions in the solid state usually rests upon an identification of the normal vibrational contribution of the vibrational modes of the crystal usually described as the lattice contribution. As appreciation of the morphology of heat capacity curves -- sensitive delineators of the energetics of matter -- has been enhanced, attempts to analyze and correlate -- as well as to understand and predict -- both these excess functions and the lattice contributions to the thermophysical properties have increased. Moreover, the realization of the major role made by Schottky contributions even at higher temperatures (where no anomaly can be readily perceived) has focused attention on the lattice. In silicate minerals, for example, the extrapolation of the heat capacities to terminal members invokes similar problems. With the accumulation of precise, equilibrium, cryogenic, calorimetric data especially on lanthanide compounds (notably the sesquioxides, the halides, and the trioxides) the importance of correlating lattice contributions with molal volumes as well as with cationic masses has become compounded. The development of this approach for lathanide series and its testing vis a vis resolution of Schottky functions will be demonstrated, and its relevance to other compounds will be discussed.

INTRODUCTION

Analysis of the morphology of heat capacity curves both provides a better appreciation of the substance under investigation and enables correlation of data and the ultimate estimation of thermophysical data for substances for which measurements are not available.

---

[1]The Research on which this paper is predicated was supported in part by the Structural Chemisty and Chemical Thermodynamics Program of the Chemistry Section of the National Science Foundation under grants GP-4252X and CHE-7710049 at the University of Michigan.

[2]Department of Chemistry, University of Michigan, Ann Arbor, Mich.

The principal problem of the calorimetric approach to the resolution of Schottky, magnetic, structural, and electronic contributions is the problem of how best to represent the lattice contribution, C_{latt},[3] to heat capacity of the particular compounds studied. In a slightly different -- but related -- context, for nearly half a century the Latimer scheme (11)[4] has been the favorite way of taking into account the differences between compounds in analogous series. This time-honored scheme is not without its flaws, despite the several times it has been adjusted by Latimer himself. C_{latt} is always treated as a contribution of the harmonic forces; the anharmonic terms are treated as the difference $C_p - C_v$. Since the thermal expansivity, α, and the isothermal compressibility, κ, needed to evaluate this difference are often not available, this results in a separate uncertainty in representing background contributions at higher temperatures, but is not the present concern. (The Latimer curve is shown in figure 1.)

In principle, the best way to evaluate C_{latt} is from the phonon dispersion relation, $k(\omega)$, determined by inelastic neutron scattering. Occasionally Einstein functions (in which ω_E = constant) or Debye functions (in which $\omega_D = \nu_o k$) can be used to get results within about 10 pct. Attempts to get an experimental estimate of C_{latt} by measuring an isostructural diamagnetic (10) compound are frequent. Here the corresponding states assumption

$$C_{latt}(X\ cpd)\ (T) = C_{latt}(ID) \times (k' \cdot T)$$

in which k' is experimentally deduced is often employed.

Alternatively, the Debye approximation is used:

$$\left[\frac{\theta_D(X)}{\theta_D(ID)} = \frac{M(ID)}{M(X)}\right]^{1/2}$$

or the more refined Lindeman's relationship using melting points, T_m, and molal volumes:

$$\theta_D^2 = \frac{k' T_m}{M V^{2/3}}$$

Since typically C_{latt} may amount to as much as 95 pct of the total heat capacity, it needs to be estimated accurately.

In the course of studies on the transition element chalcogenides, it was realized (as depicted in figure 1) that the Latimer scheme was predicting an entropic contribution for these cations diametrically opposed to experiment (16). Why? The lanthanide contraction, of course.

---

[3]Glossary of symbols is at the end of the paper.

[4]Underlined numbers in parenthese refer to items in the list of references at the end of the paper.

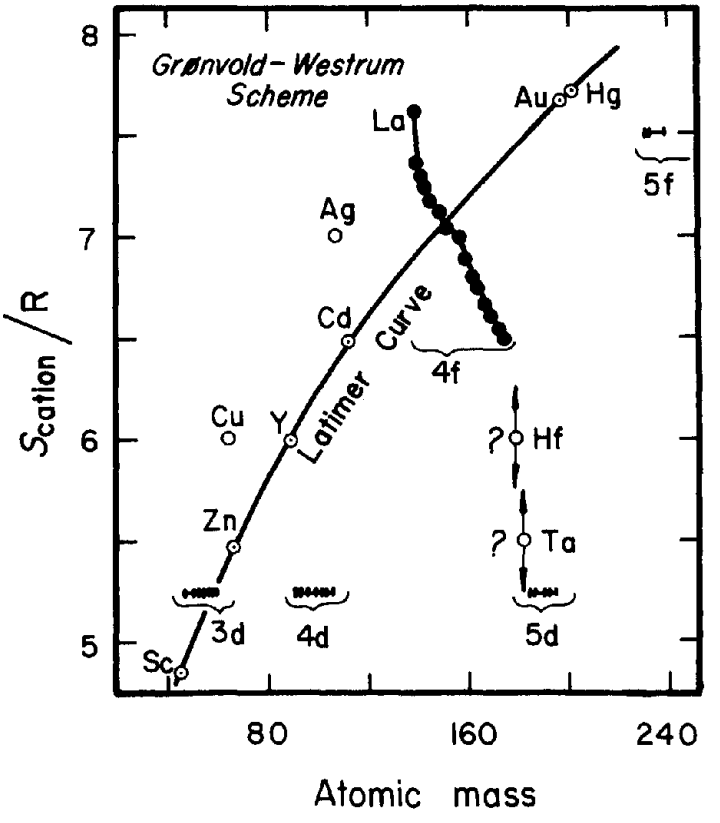


FIGURE 1. - The Latimer scheme (10) for cationic entropy contributions as modified by Grønvold and Westrum (7). Note the experimental trend of the lanthanides (4f-elements).

This led to the realization that molal volumes were too important to be neglected and that, although molal masses and molal volumes were often correlated, in the lathanides the trends were reversed. Interest in resolving Schottky functions from heat capacity data for the lanthanide compounds and the possibility of using the Schottky contribution calculated from spectroscopic data as a test of the quality of the lattice contribution resolution has provided an enhanced understanding of the importance of the volumetric correlation of C_{latt} over the region where entropic contributions are especially important.

THE SCHOTTKY FUNCTION

In this presentation the Schottky contribution is not the end product, but the "means to an end" of testing the quality of the C_{latt} estimate. However, for the benefit of thermodynamicists who may be "rusty", the details in figure 2 are presented. The simplest Schottky contribution arises from the presence of an excited electronic energy level separated from the ground state by $\Delta\varepsilon/R$ (fig. 2a). The magnitude of the heat capacity contribution (fig. 2) is fixed by the ratio of the degeneracies (g_1/g_0), and the maxi-

mum occurs at a temperature determined by the magnitude of $\Delta\varepsilon/R$. Simple Schottky functions are rigorously related to Einstein functions, as seen in figure 2c and even more dramatically in figure 2d. Additional excited energy levels are characteristic of lanthanide compounds, but typically fewer than 10 are signicant below 300 K.

LANTHANIDE EXPERIMENTAL APPROACH

Both in transition (d-element) compounds and in lanthanide/actinide (f-element) compounds, the Schottky contribution is becoming recognized as a major element in the morphology of heat capacity curves at both subambient and superambient temperatures. The trends were not entirely appreciated because crystal structure changes occurred in the series studied earlier.

Sesquioxides and Trihalides

Initial recognition of the importance of this thermophysical contribution came with a series of papers (9) on the lanthanide sesquioxides from which were obtained an unusually rich yield of data concerning the energetics of the trivalent ions in these compounds. Although the Schottky contributions may also be studied spectroscopically, the general unavailability of single-crystal samples for absorption spectroscopy or for paramagnetic resonance experiments had tended to favor the calorimetric approach. The initiatory measurement on neodymium sesquioxide yielded (table 1) levels more than an order of magnitude smaller than those estimated by Penney and his collaborators (12) from crystal field splittings. But any discredit was of short duration, since spectroscopy (8) soon confirmed, in this instance, the values that had been obtained by calorimetry.

TABLE 1. Stark levels for Nd_2O_3 (cm^{-1})

Level	g_i	Calc. (12)	Calorimetry (9)	Spectroscopy (8)
0	2	0	0	0
1	2	492	21	22
2	2	1,476	81	83
3	2	2,952	400	390
4	2	4,920	---	---

The method of approach involved measurement of the total heat capacity of Nd_2O_3 as well as that of a diamagnetic analog (La_2O_3), and the resolution of the difference in heat capacity of the two compounds in terms of a sequence of Schottky levels of the degeneracies predicted by crystal-field theory. The power of the cryogenic calorimetric approach thus demonstrated was later extended to include most of the lanthanide sesquioxides, even those containing C_2 and C_{3i} sets of levels. The levels were valid not only for the cryogenic heat capacity contribution, but also for temperatures in excess of 1000 K. Unfortunately, crystallization of the sesquioxides in A-, B-, and C-forms made recognition of the underlying trends difficult.

Subsequent examination of a number of trihalides (6, 14) provided further fuel for the study and further heightened the understanding of the trend and regularities involved and showed again the importance of the Schottky contribution to the thermophysical functions. The latter were in excellent accord with those predicted by the scheme of Westrum (15) based upon the treatment of Grønvold and Westrum (7). The excellence of the accord can be seen in table 2. (See also reference 4).

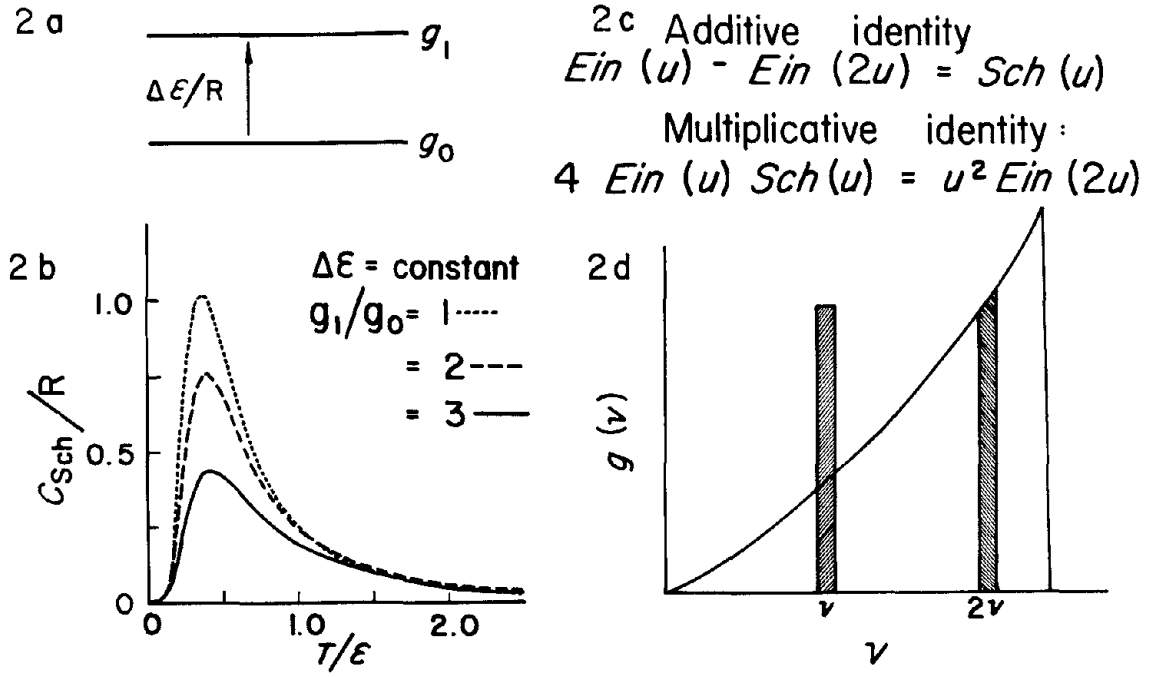


FIGURE 2. - The Schottky contribution to the heat capacity (2b) as a function of degeneracy ratio based on a simplistic two-level electronic structure (2a). Additive and multiplicative identities (2c) relate the Schottky function to Einstein functions; the former is shown graphically in (2d).

Trihydroxides

The trihydroxides have the great advantage of being isostructural across the entire lanthanide series. Moreover, they may be prepared by hydrothermal synthesis provided care is taken to preclude formation of the oxyhydroxide. The change in the lattice contributions across the series is significantly larger than in either the sesquioxides or the trihalides, and this series, therefore, provides a convenient testing ground for the evaluation of the lattice heat capacity and the trends with increasing atomic number across the lanthanide series. (As a matter of fact, even yttrium trihydroxide and uranium trihydroxide are outlying members which are also isostructural and ultimately can serve to provide extreme delimitation of the effects of volume and mass on the theories. The three definitive papers of Chirico and coworkers (2-3, 5) in which these works to date are being summarized provide an appreciation of the validity of the approach.

TABLE 2. - Comparison of some trihalide entropy estimation schemes

Compound	S°(298.15K) - S°(0)				
	Latimer	Latimer augmented[1]	Westrum[1,2] augmented	"Spectroscopic"	Reference 14
$LaCl_3$	34.5	34.5	3.1	32.47	32.88
$CeCl_3$	34.5	38.1	36.1	35.99	[3]36.0
$PrCl_3$	34.5	38.1	36.8	36.74	[4]36.64
$NdCl_3$	34.6	39.2	36.8	36.84	36.67
$PmCl_3$	34.7	39.5	36.8	36.82	[3]37.0
$SmCl_3$	34.8	38.4	35.7	36.10	35.88
$EuCl_3$	34.8	37.3	34.5	34.70	34.43
$GdCl_3$	35.0	39.1	36.0	36.60	36.19

[1]By R ln(2J+1); the $(Cl_3)^{-3}$ ion contribution is taken as 20.7 cal_{th} K^{-1} mol^{-1}.
[2]By R ln(2J+2); the $(Cl_3)^{-3}$ ion contribution is taken as 17.9 cal_{th} K^{-1} mol^{-1}.
[3]Values involve interpolated lattice and calculated Schottky contributions.
[4]Based on 0.294 K.

Perhaps the best way of testing the validity of a lattice contribution is in the calculation of the calorimetric Schottky contribution and the comparison of this excess heat capacity with that calculated from spectroscopic data on the sample itself. However, this comparison can only be made when one utilizes the Stark levels of the concentrated compounds. Measurements made on doped lanthanide halides, for example, need to be extrapolated by some technique (discussed elsewhere)(2-3, 5) or by calculation based on crystal-field parameters.

THE VOLUMETRIC SCHEME

The scheme developed by Chirico and Westrum is an interpolation on the basis of the molal volumes of the compounds in question between the corresponding lanthanum and gadolinium compounds. In particular, the formula by which the lattice heat capacity of praseodymium trihydroxide may be calculated is indicated below:

$$C_p[Pr(OH)_3 \text{ lattice}] = x\, C_p[La(OH)_3] + (1-x)\, C_p[Gd(OH)_3]$$

and in which x is the fractional molal volume increment:

$$x = \{V[Pr(OH)_3] - V[La(OH)_3]\}/\{V[Gd(OH)_3] - V[La(OH)_3]\}.$$

But does the volumetric scheme work? To test this, we compare the Schottky contribution for the lighter lanthanide trichlorides determined by calorimetric means with C_{latt} evaluated by the volumetric heat capacity resolution method with Schottky functions determined by spectroscopy. The

results are shown in figure 3. The accord is excellent except at the highest temperature. Similar comparisons have been made for the lighter trihydroxides (2).

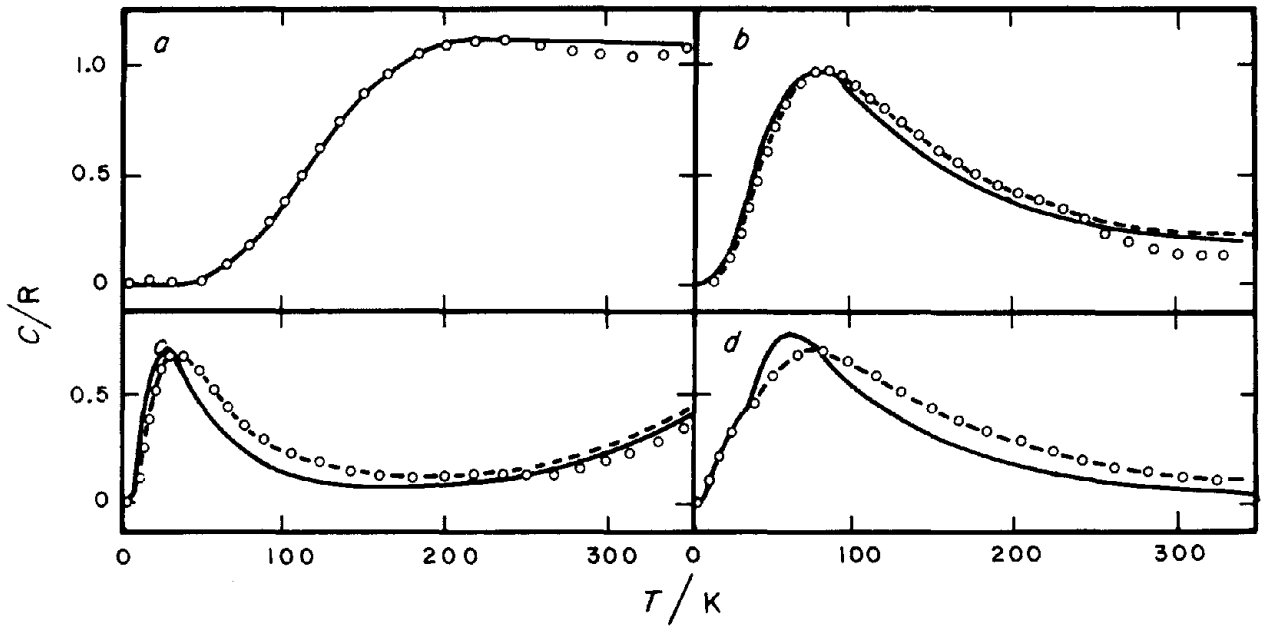


FIGURE 3. - The calorimetric Schottky curves are shown by dashed lines and the spectroscopic Schottky curves for doped $LaCl_3$ crystals by continuous lines; those deduced from estimated energy levels for the concentrated halides are shown by 0. *a*, $EuCl_3$; *b*, $NdCl_3$; *c*, $SmCl_3$; *d*, $PrCl_3$.

THE ADJUSTMENT OF STARK LEVELS

As may be seen in figure 3, the excellence of the agreement between the spectroscopic and calorimetric Schottky contributions is a consequence of the adjustment of levels from"doped" to "concentrated" samples. This may be done by several techniques. The most empirical of these is depicted in figure 4(b,c,d), where simple linear extrapolation to ordinates (corresponding to stronger crystalline fields) proportional to the position of the maximum heat capacity contribution is used. Such values are given in column c of table 3 based on the values observed for Pr^{+3} doped into $LaCl_3$.

The Schottky curves calculated from the energy levels deduced from calorimetry are represented by the dashed curves of figure 3(b-d) and are to be compared with the spectroscopic Schottky derived from energy levels extrapolated to those of concentrated halides. Spectroscopically derived energy levels for the concentrated slats are shown in figure 4(b-d) and listed in table 3 for comparison with the calorimetrically derived levels. Such simple energy level extrapolations may be useful to systems for which energy levels

TABLE 3. - Energy levels of praseodynium trichloride (cm^{-1})

μ	Pr^{+3} doped into $LaCl_3$ abs. fluor.	Concentrated $PrCl_3$				
		Calor.	CEF Calc.	ERS (I)	ERS (II)	Absorp.
a	b	c	d	e	f	g
		[SL]J-State: $^3H_4$				
2	[1]0	0	0	0	0	[2]0
3⁻	33.1	---	29	30.5	32	31.8
2'	96.4	---	99	99	100	99.6
1	130.2	155	152	145	139	---
3+	137.0	168	176	160	---	---
0	199.1	235	230	(238)	---	---
		[SL]J-State: $^3H_5$				
3⁻	2,137.2	---	---	2,134	2,136	---
2	2,169.8	---	---	2,168	2,169	2,167
1	2,188.5	---	---	2,190	2,190	2,191
3+	2,202.2	---	---	2,208	2,204	---
2	2,222.6	---	---	2,230	2,227	2,230
1	---	---	---	2,206	---	---
0	---	---	---	---	---	---

Explanation of columns:
[a]Assigned crystalline-field quantum numbers.
[b]Absorption and/or fluorescence spectral data.
[c]Deduced from calorimetry by lattice heat capacity interpolation method (fig. 4)
[d]Calculated from estimated crystal-field parameters (table 3).
[e]Electronic Raman scattering (Gruber).
[f]Electronic Raman scattering (Hougen and Singh).
[g]Adsorption spectral data.
[1]Sarup and Crozier.
[2]Dorman.

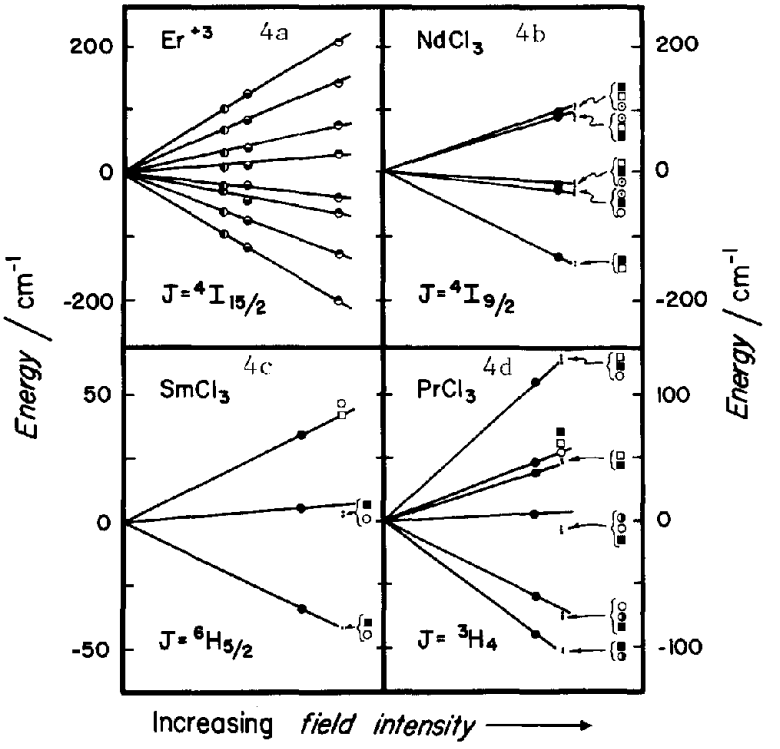


FIGURE 4. - Energy level diagrams. Ordinates are proportionate to Schottky maxima. For Er^{+3} the points represent values for this ion doped into $LaBr_3$, $GdCl_3$, and $Er(OH)_3$ with increasing field. For the three halides shown: ● represents values for $LnCl_3$ doped into $LaCl_3$; ○ values from electronic Raman scattering on concentrated samples; □ values calorimetrically deduced; ■ values deduced from crystal electric field parameters; ⊙ values from absorption spectra (Prinz); and ◑ values from absorption spectra (Dorman).

are unavailable or unobtainable by more sophisticated procedures. Figure 4a shows that even between several apparently (chemically) quite different systems, the simple linear extrapolation may be a fair approximation. Of course, caution must be observed.

A more theoretically based evaluation (2) from interpolated crystal-field parameters is shown in column d of table 3. Comparison values for these non-Kramers ions are provided by data cited in columns e through g. All are seen to be remarkably consistent.

The volumetric lattice approximation indeed effectively emphasizes the apparent dominance of volume over mass as a determining factor in C_{latt} over the subambient temperature region of major entropy development. However, from unpublished data on $Y(OH)_3$ recently obtained, a shift in the relative impor-importance of cationic mass and molal volume in determining C_{latt} is apparently observed near 50 K. At very low temperatures, low-frequency modes--roughly characterized as unit cell vibrations--are those primarily activated. On these the lanthanide contraction--an intramolar contraction--has little

effect. In essence, the force constants between the unit cells are unchanged, while the cell masses are increased across the series. This occasions a decrease in the vibrational frequencies of the unit cells with increasing atomic number and hence an increase in C_{latt}.

At higher temperatures an increasing proportion of the observed heat capacity is due to thermal activation of optical vibrational modes. The effect of the lanthanide contraction upon these modes is to increase their frequency by increasing the intramolecular force constants to such an extent that the counteracting effect of the increased cation mass is largely overshadowed.

SUMMARY AND CONCLUSION

It is already clearly evident that the excellence of the agreement between the Schottky functions for the condensed trichlorides and trihydoxides has verified the success of the volumetric approach to the development of lattice heat capacity contributions. We are in the process of extending this approach to other lanthanide systems and hope to test it also as a possibly more general approach to the estimation of lattice and compound entropy contributions in a Latimer-like scheme and to assist in the estimation, evaluation, and correlation of entropies of mineral systems and chemical compounds beyond the lanthanide series. Other authors, (1, 13) have been engaged in a polemic as to the relevance of volume and mass in providing interpolation schemes for lattice contributions Moreover, Kieffer (10) has undertaken a theroetical and experimental correlation of the lattice vibrations of minerals. This takes into account the many factors involved and discusses particularly the analysis of the vibrational contribution. This aspect has been discussed also by Sommers and Westrum (14).

In emphasizing the importance of volume, we do not mean to slight mass -- especially at lower temperatures. Data on $U(OH)_3$, which is isostructural with the $Ln(OH)_3$ series and $U(OH)_3$ should help to clarify and to test the role of mass.

GLOSSARY OF SYMBOLS

C_{latt}	Heat capacity contribution exclusively from vibrational degrees of freedom (under contraint of constant pressure)
C_p	Heat capacity at constant pressure per mole
C_v	Heat capacity at constant volume per mole
Ein(u)	Einstein heat capacity function in terms of $u = h\nu/kT$

g_i	Degeneracy of electronic energy state
g_ν	Frequency distribution function
h	Planck constant
(ID)cpd	Indicates property that of reference compound
J	Quantum number (Russell Saunders scheme)
k	Boltzmann constant
k(ω)	Phonon dispersion relation (deduced from inelastic neutron scattering)
k'	Arbitrary or emirical constant
M	Molar mass of the compound
M(ID),M(X)	Molar mass of the cation in the reference or selected compound
R	Gas constant
S	Entropy per mole
S_{cation}	Entropy contribution per mole of cation (in Latimer scheme)
Sch(u)	Schottky heat capacity function in terms of $u = h\nu/kT$
T	Temperature in Kelvins
T_m	Temperature of normal melting point
(X)cpd	Indicates property of the selected compounds
V	Molar volume of crystal
x	Fractional molar volume increment (defined more fully in text)
$\varepsilon, \Delta\varepsilon$	Energy of excited electronic levels referred to ground state
ω_D	Debye characteristic frequency expressed in wave numbers
ω_E	Einstein characteristic frequency expressed in wave numbers
ν_o	Limiting frequency of lattice vibrations
θ_D	Debye characteristic temperature
θ_E	Einstein characteristic temperature

REFERENCES

1. Cantor, S. Science, v. 198, 1977, pp. 206-207.

2. Chirico, R. D., and E. F. Westrum, Jr. Thermophysics of the Lanthanide Hydroxides. I. Heat Capacities of $La(OH)_3$, $Gd(OH)_3$, and $Eu(OH)_3$ From Near 5 to 350 K. Lattice and Schottky Contributions. J. Chem. Thermodyn., v. 11, 1979, pp. 71-85.

3. ———. Thermodynamics of the Lanthanide Hydroxides. II. Heat Capacities From 10 to 350 K of $Nd(OH)_3$ and $Tb(OH)_3$. Lattice and Schottky Contributions. J. Chem. Thermodyn., v. 12, 1980, pp. 311-327.

4. Chirico, R. D., E. F. Westrum, Jr., and J. B. Gruber. Thermodynamics of Some Lanthanide Trihalides. III. Reinterpretation of $LnCl_3$ Schottky Anomalies. J. Chem. Thermodyn., v. 12, 1980, pp. 717-736.

5. Chirico, R. D., E. F. Westrum, Jr., J. B. Gruber, and J. Warmkessel. Low-Temperature Heat Capacities, Thermophysical Properties, Optical Spectra, and Analysis of Schottky Contributions to $Pr(OH)_3$. J. Chem. Thermodyn., v. 11, 1979, pp. 835-850.

6. Deline, T. M., E. F. Westrum, Jr., and J. M. Haschke. J. Chem. Thermodyn. v. 7, 1975, pp 671-676.

7. Grønvold, F., and E. F. Westrum, Jr. Inorg. Chem., v. 1, 1962, pp 36-48.

8. Henderson, J. R., M. Muramoto, and J. B. Gruber. J. Chem. Phys., v. 46, 1967, p 2515.

9. Justice, B. H., and E. F. Westrum, Jr. J. Phys. Chem., v. 67, 1963, pp 339-345; v. 67,1963, pp 345-351; v. 67, 1963, pp 659-665; v. 73, 1969, pp. 333-340; v. 73, 1969, 1959-1962.

10. Kieffer, S. W. Reviews of Geophysics and Space Physics, v. 17, February 1979, pp. 1-39.

11. Latimer, W. M. J. Am. Chem. Soc., V. 43, 1921, p. 818; v. 73, 1951, p. 1480.

12. Penney, W. G. Phys. Rev., v. 43, 1933, p. 485.

13. Saxena, S. K. Science, v. 193, 1976, pp. 1241-1242.

14. Sommers, J. A., and E. F. Westrum, Jr. J. Chem. Thermodyn., v. 8, 1976, pp. 1115-1137; v. 9, 1977, pp 1-26.

15. Westrum, E. F., Jr., in Lanthanide/Actinide Chemistry, ed. by R. F. Gould. American Chemical Society, Washington, D. C. 1967.

16. ———. Exciting Developments in the Thermophysics of the Pnictides and Chalcogenides of the Transistion Elements. Uspekhi Khimii, v. 48, 1979, pp. 2194-2215.

DISCUSSION

Anonymous: Would you elaborate on the Verway transition?

E. F. Westrum, Jr.: I would like to give you a graphical presentation of this, but the Verway transition, first of all, is bifurcated; there are two peaks in it. Temperature of these two peaks, which are about 15 K apart in pure magnetite, can be moved independently by choice of n and p dopants and by whether they go on to the octahedral sites or the tetrahedral sites. In that instance, we found wonderful and exciting effects, but I know of no data on the lanthanide system.

AUTOMATION OF A LOW-TEMPERATURE CALORIMETER

by

R. P. Beyer[1]

ABSTRACT

An automated low-temperature adiabatic calorimeter operating over the range 5 to 300 K is described. The calorimeter instrumentation consists of automatic analog shield controls and digitally controlled data acquisition. Temperature measurements are made potentiometrically using a programmable dc voltage source and a digital nanovoltmeter. Energy measurements are made with a 6-1/2-digit voltmeter. Switching of low and high-level dc signals is done in a temperature-controlled, programmable scanner.

This research is a part of the effort by the Bureau of Mines to provide thermodynamic data for the advancement of mineral resource technology, environmental preservation, and energy economy.

INTRODUCTION

A manually operated low-temperature calorimeter used over the range 5 to 300 K, described previously by Stuve (8), has been modified to allow automatic control using a minicomputer. Automated calorimeters using both ac and dc methods have been described by other authors (1-2, 5-7). The method described here is potentiometric and is used to measure both the thermometer resistance and the heater resistance.

Our calorimeter used a double six-dial potentiometer. Although this instrument is of excellent accuracy and has been the workhorse for years in calorimetry work, it is tedious to run and requires constant operator attention for days at a time to complete a heat capacity curve over the range 5 to 300 K. With the advent of programmable instruments of comparable or superior accuracy, stability, and sensitivity, automation has become possible.

Automating the heat capacity measurements offers many advantages. The operator is freed from the repetitive task of resistance measurement. Possi-

[1]Chemical Engineer, Albany Research Center, Bureau of Mines, Albany, Oreg.

ble human errors in measurement and data logging are eliminated. Repeated measurements become more consistent and therefore more reproducible and accurate. Finally, an automatic calorimeter can be run unattended, around-the-clock, thereby making possible multiple runs on the same sample for a better confidence level.

APPARATUS

Calorimeter

The mechanical system, which includes the cryostat, vacuum system, sample vessel, shields, refrigerant reservoirs, and the wiring inside the cryostat, is the same as that described by Stuve (8).

Instrumentation

The programmable instrumentation includes a Keithley model 180 3-1/2-digit nanovoltmeter; an ICS Electronic Corp. model 4883 instrument coupler that is used to interface the nanovoltmeter to the IEEE-488 instrument bus, an Electronic Development Corp. model 501 J dc voltage standard, a Fluke model 8500 A 6-1/2-digit voltmeter, a Hewlett Packard model 6181B constant-current source, and a thermostatically controlled scanner specifically designed for switching low-level dc signals. A constant-current source for the resistance thermomometer circuit was built using a design that combined features from those designed by Chang (3) and by Field and Hesterman (4).

A block diagram of the instrumentation and wiring is shown in figure 1. The switches and instruments are computer controlled.

The measuring instruments are controlled by using the IEEE-488 instrument bus. The nanovoltmeter, which has a BCD digital output, is connected to the bus using an instrument coupler that does the necessary conversions from BCD output to the IEEE-488 bus. The heater constant- current source is voltage programmable and is controlled by the dc voltage standard. The dc voltage standard has an accuracy of ± 0.005 pct and a 24-hour stability of ± 0.001 pct, which makes it comparable to the double six-dial potentiometer.

The circuit of the constant-current source used for the thermometers is shown in figure 2. The important components are the operational amplifier (Precision Monolithics OP-07), the reference cell (Eppley Unsaturated Standard Cell), the low-level latching relay (Coto-coil CR-3207-5- 411), and the power supply (Analog Device Model 904). Although this current source is adjustable, the components have been chosen for a 1-ma output.

All switching of the dc signals is done in a thermostatically controlled enclosure. This enclosure is a box within a box, with the annular space controlled to ± 0.05 K. All the low-level dc switches are Coto-Coil single-pole latching relays (CR-3207-5-411) and are switched by another set of digitally controlled relay switches (Coto-Coil CR-2042-5- 1111). A diagram of one of these switch combinations is shown in figure 3. When the computer turns on switch A, a 10-μf capacitor discharges through a normally open switch and sets

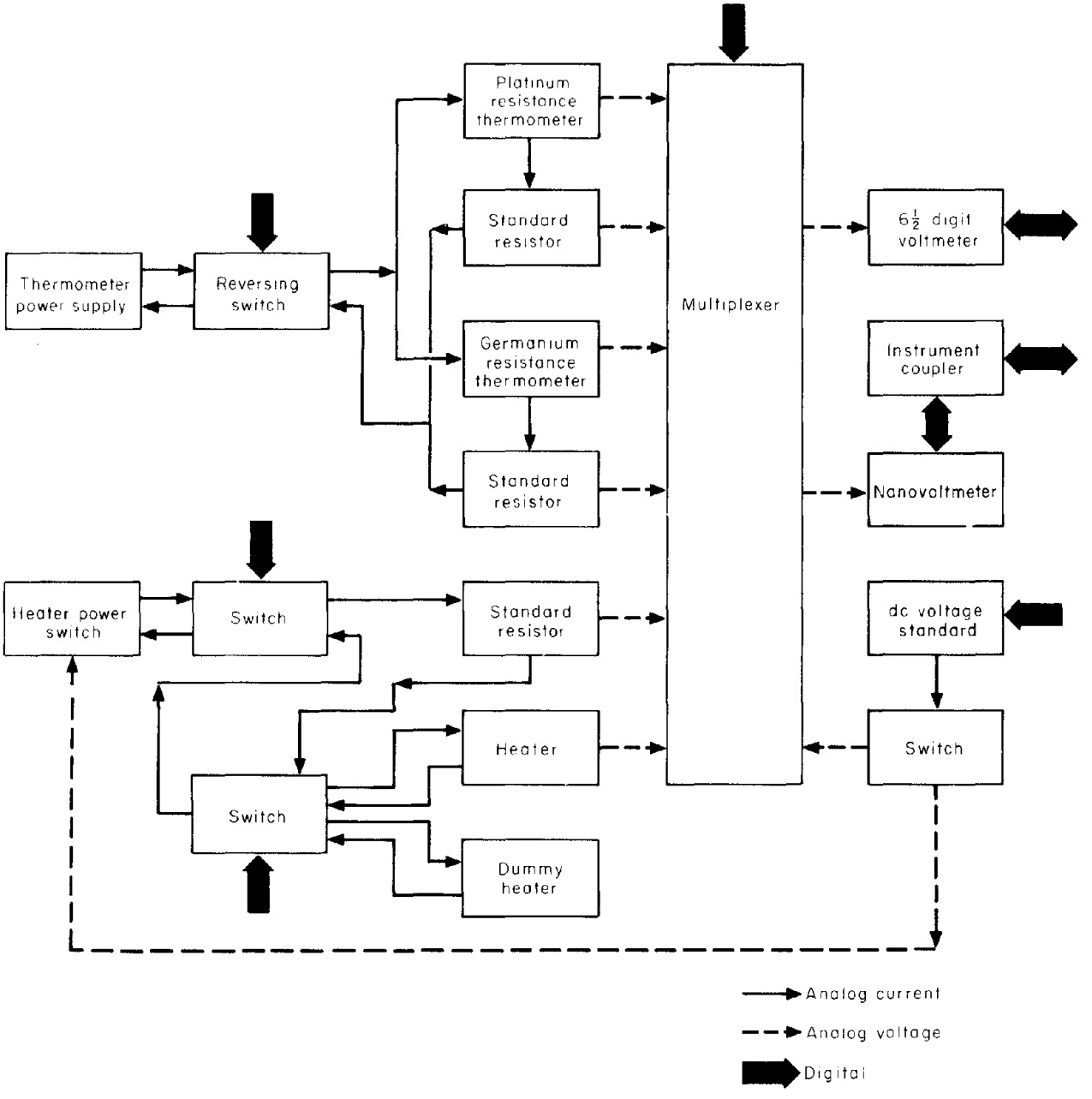


FIGURE 1. - Block diagram of automated low-temperature calorimeter instrumentation. All switches, multiplexer, standard resistors, and thermometer power supply are in a thermostated box.

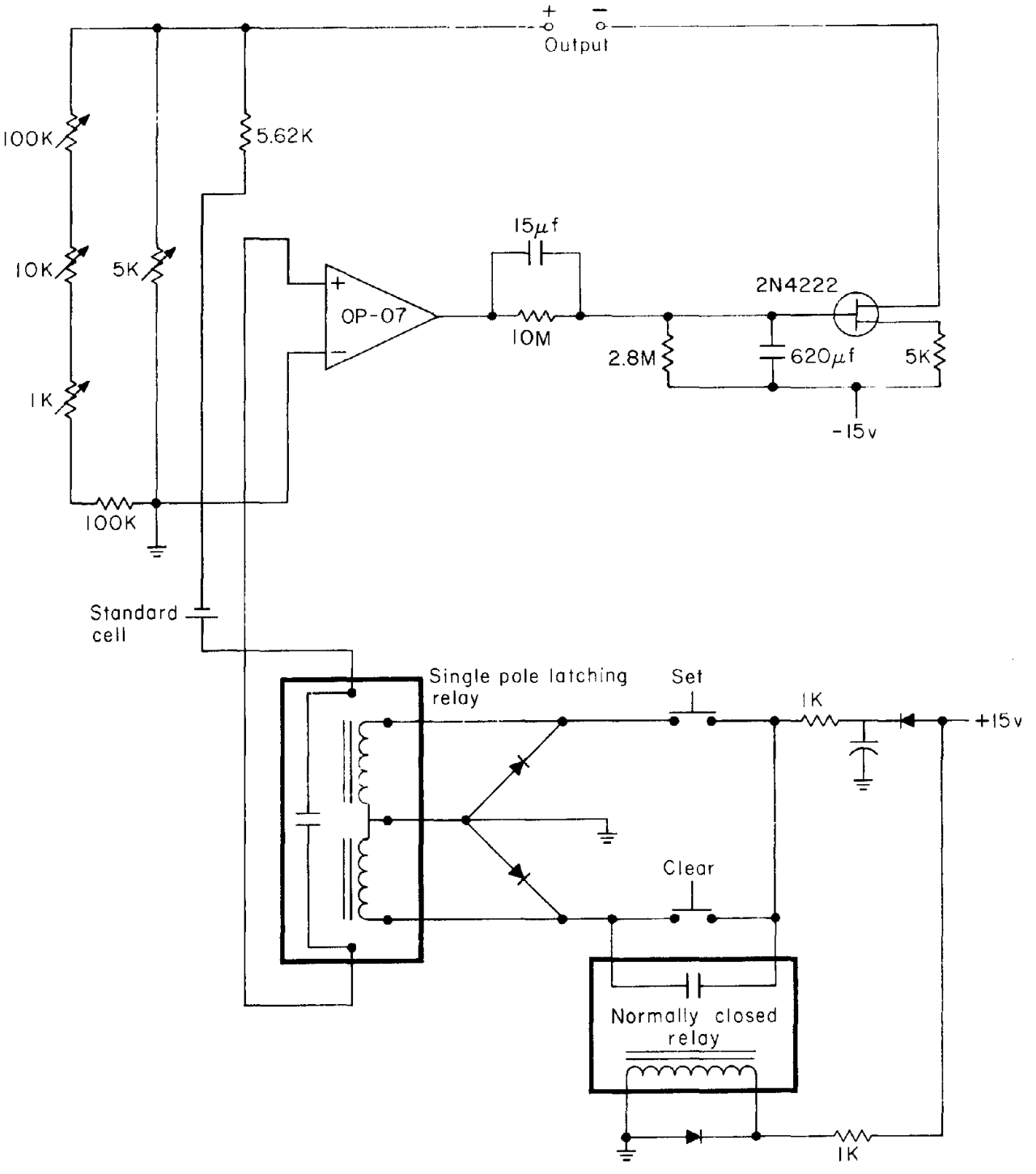


FIGURE 2. - Schematic of thermometer constant current source.

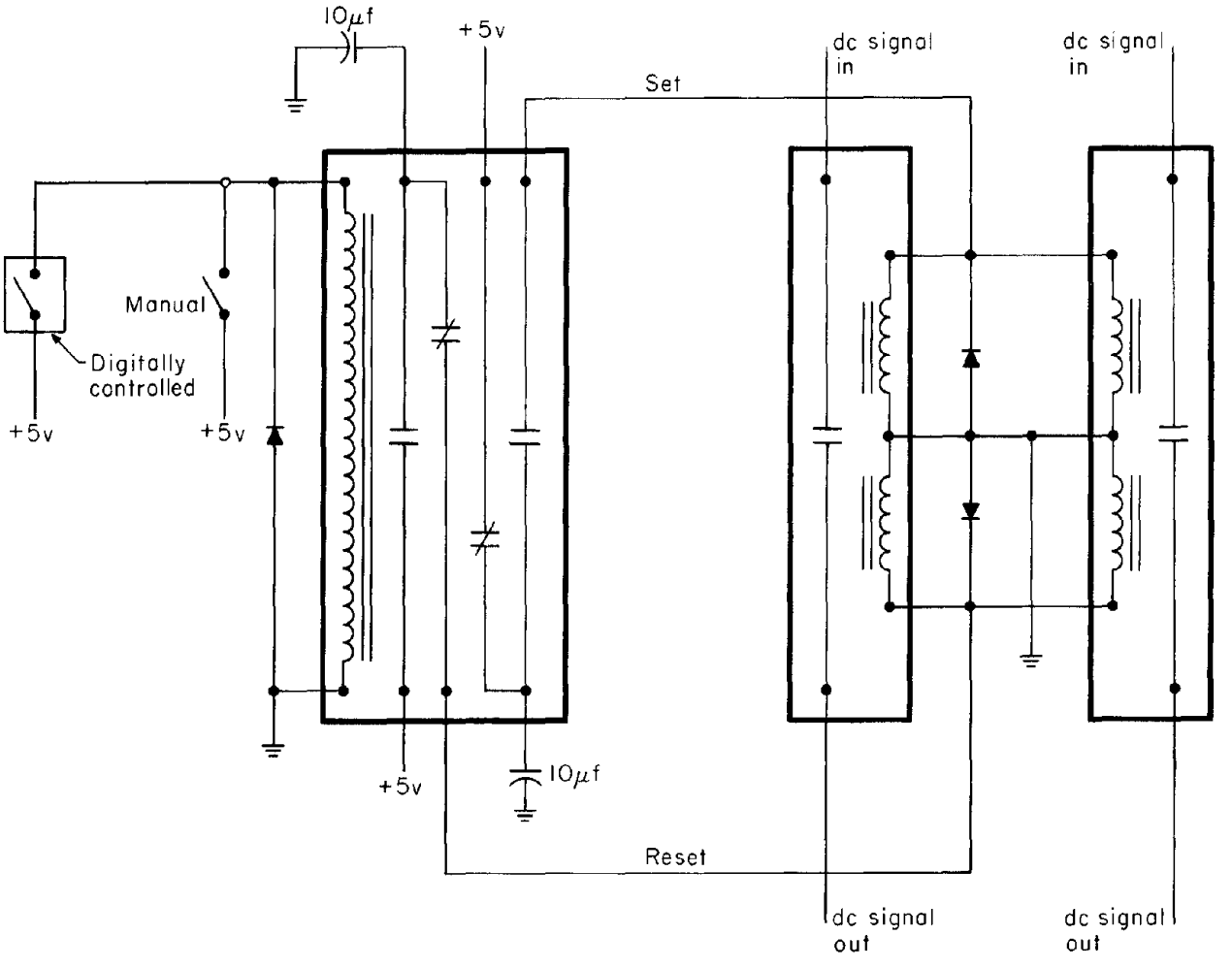


FIGURE 3. - Schematic diagram of one switching element.

switches B. When the computer turns off switch A, another 10-μf capacitor discharges through a normally open switch and resets switches B.

Temperature control of the adiabatic shields is essentially the same as previously described by Stuve (8) with only the modification of using Leeds and Northrup CAT 80 controllers for all four sections: the top, middle, and bottom shields, and the tempering ring.

Procedure

The procedure for making a temperature measurement follows: set the current direction through the thermometers; measure the potential of the thermometer with the 6-1/2-digit voltmeter; use this reading to set the dc voltage standard; measure the offset voltage between the dc voltage standard and the thermometer with the 3-1/2-digit nanovoltmeter; reset the dc voltage standard and measure the offset voltage between the dc voltage standard and the standard resistor in the thermometer circuit with the 3-1/2-digit nanovoltmeter. This prodecure is then repeated with the thermometer current reversed, and the readings are averaged to give a final thermometer resistance. This resistance is then used to calculate the temperature.

Once equilibrium has been established, a heating cycle is started. This consists of setting all the appropriate switches so that the heater constant-current source can be voltage-programmed by the dc voltage standard, setting the appropriate level of heater power through the dummy heater, switching on the power to the heater, measuring the voltage of the heater circuit standard resistor and the heater with the 6-1/2-digit voltmeter several times throughout the heating cycle, and turning off the heater constant-current source once the programmable clock in the computer signals that a preset amount of time has elapsed.

After the heating cycle, the temperature measurement algorithm is started again. In between thermometer voltage measurements, the computer calculates the heat capacity and temperature of the previous run.

REFERENCES

1. Andrews, J. T. S., P. A. Norton, and E. F. Westrum, Jr. An Adiabatic Calorimeter for Use at Superambient Temperatures. The Heat Capacity of Synthetic Synthetic Sapphire (α-Al_2O_3) From 300 to 500 K. J. Chem. Thermodyn., v.10, No.10, October 1978.

2. Chang, S. S. Automated Adiabatic Calorimetric System for Heat Capacity Measurement. Proc. 7th on Thermophysical Properties. The American Society of Mechanical Engineers, New York, 1977.

3. _____. A Self-Balancing Nonovolt Potentiometric System for Thermometry and Calorimetry. NBS-A, Phys. and Chem., v. 80A, No. 4, July-August 1976.

4. Field, B. F., and V. W. Hesterman, Laboratory Voltage Standard Based on 2e/h. IEEE Trans. on Instrumentation and Measurement, v. IM-25, No. 4, December 1976.

5. Martin, D. L., L. L. T. Bradley, W. J. Cazemier, and R. L. Snowdon. Automatic Calorimetry in the 3-30 K Range. The Specific Heat of α-Al_2O_3 Between 300 and 470 K. Rev. Sci. Instru., v. 41, No. 12, December 1970.

6. Martin, D. L., and R. L. Snowden. An Automatic Data Acquisition System for Calorimetry: The Specific Heat of α-Al_2O_3 Between 300 and 470 K. Rev. Sci. Instru., v. 41, No. 12, December 1970.

7. Moses, O., O. Ben-Aroya, and N. Lupu. Simple Calorimetric System for the Temperature Range 3 - 300 K With On-Line Computer. Rev. Sci. Instr., 4. 48, No. 8, August 1977.

8. Stuve, J. M., D. W. Richardson, and E. G. King. Low-Temperature Heat Capacities and Enthalpy of Formation of Copper Oxysulfate. BuMines RI 8045, 1975, 18 pp.

DISCUSSION

B. W. Mangum: After you switch the current, how long do you have to wait for the transients to settle?

R. P. Beyer: I believe it will be under a second. With the nanovoltmeter I have, I have to measure, if I want resolution in tens of manovolts, for 30-40 seconds. So, those transients are masked out.

E. F. Westrum: How long do you anticipate that this calorimeter will run in automated fashion, through the whole curve, or 2 hours?

R. P. Beyer: Several days anyway. The power supply is voltage programmable from 0 to 250 ma.

E. F. Westrum: On what basis is it programmable?

R. P. Beyer: You apply zero to 1 volt to the power supply, and depending upon what range you are on, you can get from 0-2.5 milliamps, or 0-25, or 0-250. So that zero to 1 volt gives you the power ranges.

G. T. Furukawa: With your computer-controlled measurement system, will you be able to calculate the heat capacity of the previous point while you are making heat or temperature measurements on the next point? Or, would the calculation be almost instantaneous when the temperature measurement is completed?

R. P. Beyer: I will have ample time to do all sorts of things. I will be calculating the heat capacity as I go along and estimating from that how much I want the next heating run to raise the temperature.

DESIGN AND OPERATION OF A DIFFERENTIAL SCANNING CALORIMETER BASED ON THE HEAT LEAK PRINCIPLE

by

Rodney L. Biltonen[1], Jaak Suurkuusk[1], and Donald B. Mountcastle[1]

A differential scanning calorimeter adapted from the original design of Ross and Goldberg (Thermochem. Acta 10, 143 (1974)) has been constructed. This calorimeter was specifically designed for measuring heat capacities and heat effects accompanying thermally induced transitions in dilute solutions. The accuracy of the instrument is approximately 3×10^{-4} cal/deg, and precision, in terms of relative C_p, is about 10^{-5} cal/deg. The temperature range of the instrument is -20° to 125° C, and it can operate at scanning rates of 3 to 60 deg/hr. The total volume of the sample cell is 0.7 ml.

Unique features of this apparatus are

1. The sample material can be weighed directly into the sample cell, and the mass within the calorimetric cell is invariant during an experiment.

2. The heat capacity functions of both liquid and solid materials can be determined.

3. The calorimeter can be operated in both heating and cooling modes.

4. The heat capacity of the sample can be determined as a function of temperature at different applied pressures (1 to 2,000 psi).

5. It is also possible that changes in heat content of a sample as a function of pressure at constant temperature can be determined.

The calorimeter consists of two rectangular aluminum cells each with a hole to contain a sample or reference ampule. Each cell is sandwiched between a pair of thermoelectric modules in thermal contact with a copper heat sink by means of a wedge system. The thermopiles surrounding the two cells are connected electrically in series with opposing polarity so that when the cell

[1]Department of Biochemistry, University of Virginia School of Medicine, Charlottesville, Va.

temperatures are equal, the differential voltage signal is zero. The heat sink is positioned inside a cylindrical adiabatic shield. The assembly is insulated from the surroundings by 5 cm of polyurethane foam. The differential voltage signal from the thermopiles is amplified, digitized, and recorded on a punch tape together with time and heat sink temperature. Recently the calorimeter has been placed "on line" with a microprocessor to control scanning rate and to provide more rapid data acquisition and processing.

The principle of operation is relatively simple. When the heat sink temperature is increased at constant rate, temperature differences are created because of thermal barriers between the heat sink and cells. The measured differential voltage signal is proportional to the temperature difference between the cells and thus to the heat capacity difference. For an ideal calorimeter the relation between heat capacity difference between cells, ΔC, and the voltage, V is given by

$$\Delta C = (\epsilon/\alpha)\ [V + (dV/dT)\tau\alpha],$$

where α is the scanning rate, ϵ is a calibration constant (calories $volt^{-1}$ sec^{-1}), and τ is the time constant (seconds). Owing to imperfectly matched thermoelectrical module pairs, a temperature dependence of the calorimetric constants, and a correction of the measured heat sink temperature to the actual sample cell temperature, an extensive computer calculation is necessary to obtain ΔC as a function of sample cell temperature. The details of the computational algorithm will be discussed, and examples of the conversion of the measured voltages to heat capacity will be presented.

To determine C_p at other than ambient pressure, a specially designed thick-walled stainless steel cell of approximately 0.4 ml volume was constructed. The top of the cell cap was connected to a stainless steel capillary tube which passed out of the calorimeter and connected to a helium pressurizing system. To avoid evaporation problems, the cell cap contained a miniature one-way valve maintained in the closed position by a light string. The cap assembly screwed onto the cell by means of an indium O-ring seal. The valve opened during pressurization with helium gas and closed when the pressures were equalized. This set-up allows the determination of C_p as a function of temperature at pressures up to 2,000 psi.

The calorimeter can also be operated in a cooling mode using Pelltier elements placed on the end plates of the heat sink to cool the calorimeter at a constant rate. The details of the calorimeter and its operation in the various modes will be discussed.

Editor's note: The authors submitted this expanded abstract without a detailed manuscript.

DISCUSSION

R. N. Goldberg: I wish to comment that I am very much impressed by the degree to which the scanning calorimetric technique has been developed at the University of Virginia. The computational techniques for reducing the data are particularly noteworthy.

K. D. Williamson: Are the eight parameters on which you base your correlation independent under your conditions of operation? Surely over a broad range there would be some confounding of variables.

R. L. Biltonen: We have to operate based on the assumption used in deriving equations, i.e., the steady-state situation that existed. The parameters are independent, but if we experience severe thermal nonequilibrium, we would be in very serious trouble and cannot assume that the first order correction is sufficient.

E. J. Prosen: There was a recent meeting in Washington using calorimetric data for kinetic work. Would you comment on it?

R. L. Biltonen: I think that AC calorimetry is an important approach. If one measuring a frequency-dependent signal, a time-dependent heat capacity under isothermal conditions will be observed. One can, in fact, get chemical kinetics from it by using pulses as a function of frequency. As far as we can tell, the resolution is insufficient to resolve anything faster than about 100 milliseconds, so I think our scanning rates are appropriate.

J. M. Stuve: I was interested in the relative accuracies you obtain for heat capacities using comparison standards. How well does the calorimeter perform, based on these standards, such as benzoic acid?

R. L. Biltonen: C_p of a series of compounds, the nucleic acid bases, had originally been determined with a drop calorimeter based on the design of Wadso. At that time, we were getting an accuracy of about 1 part in 10^4 for the whole system. We are now doing as well or better with this sytem. We could see no differences in the two methods. We do not know if truly accurate numbers were obtained because the water content could not be totally controlled. We see it working as well on an absolute basis as the drop calorimeter. Within an hour the temperature dependence of the heat capacity as well can be obtained.

B. E. Gammon: What is the diameter of the cell?

R. L. Biltonen: They vary, depending on whether the pressure cell or the usual cell is used. Some of them are about 7-8 mm.

B. E. Gammon: I am trying to get some scale to be used from the outside diameter of the cell itself.

R. L. Biltonen: It depends on the cell wall thickness. The new cells that have been built by Roger Hart for Tronac are about 12 to 15 mm in diameter, but they hold 2 ml. So, they are variable, but there is no apparent problem in their use.

Pamela Rogers: I am just trying to get a feel for the size of the calorimeter.

R. L. Biltonen: About the size of a tomato juice can. It is really quite small, the largest dimension is about 25 cm, and if it were not so heavy, I could take it home with me.

THE THERMODYNAMICS OF TRANSFER OF PHENOL AND ANILINE BETWEEN NONPOLAR AND AQUEOUS ENVIRONMENTS

by

K. J. Breslauer[1], L. Witkowski[1], and K. Bulas[1]

ABSTRACT

A flow calorimetric technique is described that allows the direct determination of the enthalpy change accompanying the transfer of compounds from nonpolar to aqueous environments. In conjunction with equilibrium studies, complete thermodynamic profiles are obtained for the transfer of phenol from octane, toluene, and octanol to water and for the transfer of aniline from toluene to water. These data are tabulated below.

Transfer process	ΔG°_t, kcal mol^{-1}	ΔH_t, kcal mol^{-1}	ΔS°_t, cal deg^{-1} mol^{-1}
PHENOL			
Octane → H_2O	-1.14	-3.9	-9.2
Toluene → H_2O	+0.27	-1.5	-5.9
Octanol → H_2O	+1.80	+2.6	+2.8
ANILINE			
Toluene → H_2O	+1.32	-1.2	-8.7

The data are interpreted in terms of solute-organic solvent and solute-water interactions. These results are discussed in light of currently accepted views concerning the nature of hydrophobic and hydrophilic forces.

INTRODUCTION

Several years ago we described the development of a new calorimetric technique that allows the direct determination of the enthalpy change accompanying the transfer of a molecule from a nonpolar to an aqueous environment (3).[2]

---

[1] Rutgers University, New Brunswick, N.J.

[2] Underlined numbers in parentheses refer to items in the list of references at the end of the paper.

Our work in this area was stimulated by the fact that many investigators were reporting thermochemical data on complex biochemical systems that they were unable to explain in terms of currently recognized molecular interactions. At the same time, several laboratories were suggesting that important contributions to the energetics of many biochemical processes arose from the transfer of groups from nonpolar to aqueous environments, or the reverse (6, 11-12). For example, in the denaturation of a globular protein those amino acid side-chains originally embedded in the relatively nonpolar interior of the macromolecule, upon unfolding, become exposed to the highly polar, aqueous environment of the solvent. In contrast, the binding of an inhibitor or substrate to a macromolecule was frequently envisioned as involving a change in the environment of the binding species from a purely polar, aqueous environment to the relatively nonpolar surroundings of the binding site (2).

In general, it was becoming clear that if one was to explain the molecular origins of the thermochemical data obtained on complex biochemical systems, one had to be able to define the thermodynamic contribution arising from such polar-nonpolar environmental changes. Unfortunately, these data are quite difficult to obtain by studying the biological systems themselves since these environmental changes invariably occur concurrently with charge-charge interactions as well as conformational changes.

To isolate the thermodynamic changes associated purely with the transfer of a macromolecular component from one environment to another, one can study the thermodynamics accompanying environmental changes for small molecules that can serve as models for the individual groups that make up these biopolymers. In this connection, the free energy change associated with the transfer of a small molecule from a nonpolar to an aqueous medium would be of interest. Such determinations can be and have been carried out by studying the equilibrium distribution of various compounds between water and some relatively nonpolar organic solvent (5). Alternatively, some workers have used solubility measurements to calculate partition coefficients (11). The results of such experiments have been used to construct free-energy tables (hydrophobicity scales) which reflect the relative affinity of various compounds and molecular groups for the organic and aqueous phases.

However, to begin to understand on a microscopic level what constitutes a hydrophobic or hydrophilic interaction as well as to explain much of the accumulated thermochemical data, one must dissect the free energy term into its constituent parts. That is to say, one must expand the model to include the determination of values for the enthalpy, entropy, and heat capacity changes accompanying these distribution experiments. Unfortunately, very few data exist for the enthalpy change accompanying the transfer of a molecule from a nonpolar to an aqueous environment. This probably has been due to the fact that no accurate and convenient method for measuring this parameter has in the past been available.

In an attempt to alleviate this situation, we initiated a program that has resulted in the development of a direct and accurate calorimetric technique for measuring the enthalpy change accompanying the transfer of a

molecule from a nonpolar to an aqueous medium. We present here the results obtained by application of this new technique to several molecules of general and biological interest.

EXPERIMENTAL SECTION

Chemicals

Phenol (99+ pct pure) and aniline were obtained from Fisher Scientific Co., Fairlawn, N.J., and used without further purification. Chromatoquality toluene and octane were purchased from Matheson, Coleman and Bell. Grade 1 99-pct pure octanol was obtained from Sigma Chemical Co., St. Louis, Mo.

Method

The Calorimeter

The experimental technique makes use of an extremely sensitive flow microcalorimeter developed by Sturtevant in collaboration with Beckman Instruments, Palo Alto, Calif. (11). The main components of the instrument are a precision fluid delivery system and a 10,000-junction thermopile, which is enclosed within a massive aluminum heat sink. The fluid delivery system consists of two glass syringes equipped with gas tight Teflon-tipped plungers which are independently driven by two variable-speed 10-rpm synchronous motors.

The two fluids are separately delivered to the calorimeter system by passage through Teflon tubes. At the entrance to the heat sink, the Teflon tubing is changed to platinum tubing (1.0-mm-ID) which is in good thermal contact with the heat sink. This insures proper equilibration of the liquids prior to their entering the thermopile. Upon reaching the thermopile the two platinum tubes are brought together by means of a Y-junction which serves to initiate the mixing process. The mixed liquids then pass through the platinum tubing, which is pressed tightly against the inside surface of a 10,000- junction thermopile. Thus, any heat evolved or absorbed upon mixing the two solutions is quantitatively conducted through the thermopile to the massive aluminum heat sink. The resulting electrical output (which is proportional to the heat evolved or absorbed) is amplified and recorded.

Enthalpies of Transfer

The technique employed involves the extraction of a compound of interest from an organic to an aqueous phase in the flow calorimeter described above. To avoid excessive heats of solvent mixing, it is essential to use immiscible phases. The extraction is readily accomplished by flowing a dilute alkaline (or acidic) aqueous solution against an organic solution of the compound to be transferred. Obviously, such a compound must possess a site for facile protonation or deprotonation so that either an acidic or an alkaline aqueous solution can be used to insure complete extraction during the calorimetric residence time. Previous work has shown that the extraction is in fact complete before the solution exits from the calorimeter (3).

The overall extraction process results in an enthalpy change which includes not only the heat associated with the transfer of the molecule between the two phases, but also the heat of ionization (or protonation) of the compound transferred. In addition, one must correct for the heat of formation of water whenever an alkaline extraction solution is used. This latter enthalpy is well known and thus can be subtracted from the overall heat of the process. On the other hand, a separate experiment must be performed in order to determine the heat of protonation (or deprotonation) for each compound transferred.

For the case of a molecule possessing an "active" hydrogen, the overall transfer process can be summarized as outlined in scheme 1. On the other hand, when dealing with compounds such as amines that are transferred (extracted) by means of aqueous acid, the overall set of reactions reduces to those shown in scheme 2. Thus, simply by adding the three processes illustrated in scheme 1 or the two processes illustrated in scheme 2, one obtains a value for the enthalpy change associated with transferring the uncharged molecule from a nonpolar to an aqueous environment.

SCHEME 1. Determination of enthalpies of transfer

$$\text{R-OH (organic solvent)} + {}^{-}\text{OH (aqueous)} \rightarrow \text{R-O}^{-}\text{ (aqueous)} + \text{H}_2\text{O} \qquad \Delta H_1$$

$$\text{R-O}^{-}\text{ (aqueous)} + \text{H}^{+}\text{ (aqueous)} \rightarrow \text{R-OH (aqueous)} \qquad \Delta H_2$$

$$\text{H}_2\text{O} \rightarrow \text{H}^{+}\text{ (aqueous)} + {}^{-}\text{OH (aqueous)} \qquad \Delta H_3$$

$$\text{R-OH (organic solvent)} \rightarrow \text{R-OH (aqueous)} \qquad \Delta H_{transfer}$$

$$\Delta H_{transfer} = \Delta H_1 + \Delta H_2 + \Delta H_3$$

SCHEME 2. - Determination of enthalpies of transfer

$$\text{R-NH}_2\text{ (organic solvent} + \text{H}^{+}\text{ (aqueous)} \rightarrow \text{R-}\overset{+}{\text{N}}\text{H}_3\text{ (aqueous)} \qquad \Delta H_1$$

$$\text{R-}\overset{+}{\text{N}}\text{H}_3\text{ (aqueous)} \rightarrow \text{R-NH}_2\text{ (aqueous)} + \text{H}^{+}\text{ (aqueous)} \qquad \Delta H'_2$$

$$\text{R-NH}_2\text{ (organic solvent)} \rightarrow \text{R-NH}_2\text{ (aqueous)} \qquad \Delta H_{transfer}$$

$$\Delta H_{transfer} = \Delta H_1 + \Delta H'_2$$

Repetition of the entire procedure at different temperature enables one to calculate the heat capacity changes associated with such transfer processes.

RESULTS AND DISCUSSION

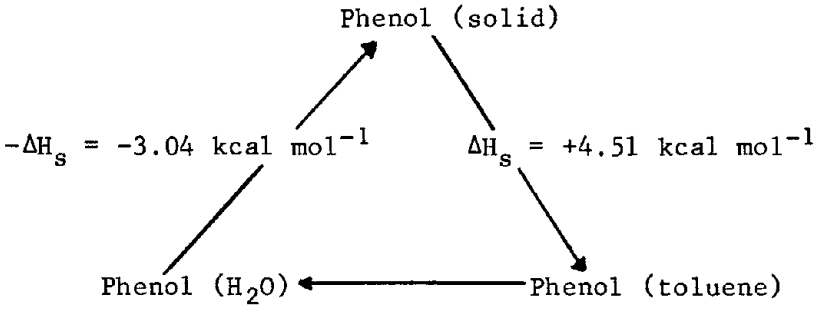
Table 1 summarizes the enthalpy data obtained for the transfer of phenol and aniline from toluene to water. As described below, these data can be used to test the new calorimetric technique employed in this work.

TABLE 1. _ Enthalpies of transfer of phenol and aniline from toluene to water at 25° C,[1] kcal mol^{-1}

Compound transferred	ΔH_1	ΔH_2	ΔH_3	ΔH transfer
Phenol	-9.19	-5.65	+13.34	-1.50
Aniline	-8.48	-7.28	--	-1.20

[1]See schemes 1 and 2 for meaning of symbols. All enthalpies are averages of at least 4 determinations.

The enthalpy of transfer of phenol from toluene to water is exothermic by 1.5 kcal mol^{-1} (note: 1 cal_{Th} = 4.184 J). This value should be compared with the corresponding enthalpy of transfer that can be derived from previously published heats of solution. Parsons and coworkers found the heat of solution (at 25° C) of solid phenol in water to be + 3.04 kcal mol^{-1} (8). Arnett and coworkers determined the heat of solution (at 25° C) of solid phenol in toluene to be +4.51 kcal mol^{-1} (1). From these data, one can derive a value for the enthalpy of transfer of phenol from toluene to water as shown below:



ΔH_t = -1.47 kcal mol^{-1}

The derived value of -1.47 kcal mol^{-1} for the toluene-to-water transfer is in very good agreement with the 1.5 kcal mol^{-1} determined by means of our direct calorimetric technique. This exothermicity probably reflects favorable hydrogen bonding between the phenolic hydroxyl group and water.

The enthalpy of transfer of aniline from toluene to water was found to be -1.2 kcal mol^{-1} at 25° C (table 1). Whetsel and Lady determined the enthalpy of complex formation between aniline and benzene to be -1.64 kcal mol^{-1} (13). By combining these two sets of data, one can derive a lower limit of -2.84 kcal mol^{-1} for the enthalpy of formation of a hydrogen bond between water and the aromatic amino group of aniline.

Influence of the Organic Solvent

Clearly, different organic solvents will provide different "nonpolar environments" so that the enthalpy data reported above should not be interpreted exclusively in terms of solute-water interactions. To determine the degree to which solute-organic solvent interactions contribute to the observed enthalpies of transfer, phenol was transferred to water from several different organic solvents. The results of these studies are summarized in table 2.

TABLE 2. - Enthalpies of transfer of phenol from various organic solvents to water at 25° C, kcal mol^{-1}

Transfer process	ΔH_1	ΔH_2	ΔH_3	$\Delta H_{transfer}$
Octane → H_2O	-11.60	-5.65	+13.34	-3.91
Toluene → H_2O	-9.19	-5.65	+13.34	-1.50
Octanol → H_2O	-5.04	-5.65	+13.34	+2.65

These data clearly indicate that the ΔH_t° values are strongly dependent upon the specific organic solvent selected. Furthermore, by combining the data of table 2 one can derive enthalpy values for the transfer of phenol between two organic solvents as illustrated in scheme 3. These data, which are summarized in table 3, provide considerable new insights into the nature of solute-organic solvent interactions and deserve further comment.

SCHEME 3. - Enthalpy of transfer of phenol (ϕ-OH) between organic solvents

ϕ-OH (octane) → ϕ-OH (H_2O)	ΔH = -3.9 kcal mol^{-1}
ϕ-OH (H_2O) → ϕ-OH (toluene)	ΔH = +1.5 kcal mol^{-1}
ϕ-OH (octane) → ϕ-OH (toluene)	ΔH = -2.4 kcal mol^{-1}

TABLE 3. - Enthalpies of transfer of phenol between two organic solvents at 25° C

Transfer process	$\Delta H_{transfer}$, kcal mol^{-1}
Octane → toluene	-2.4
Octane → octanol	-6.5
Toluene → octanol	-4.1

We have suggested earlier that the 1.5 kcal mol^{-1} exothermicity observed for the transfer of phenol from toluene to water reflects favorable hydrogen bonding between the phenolic hydroxyl group and water. We now see that for the octane-water solvent system phenol has a heat of transfer of -3.9 kcal mol^{-1} (table 2). By combining these data we can conclude that phenol has an energetically favorable interaction with toluene (relative to octane) of 2.4 kcal mol^{-1} (table 3).

This result is in excellent agreement with a spectroscopic study carried out by Pimentel and coworkers (9). These investigators found a favorable interaction of some -2.3 kcal mol^{-1} between phenol and benzene. Thus the derived value of -2.4 kcal mol^{-1} for the transfer of phenol from octane to toluene (table 3) is in very good agreement with their findings. In connection with these studies, it is interesting to note that Arnett and coworkers (1) found no free hydroxyl frequency in the infrared spectrum of phenol in a base as weak as benzene.

It should be emphasized that compilations such as table 3 are useful in that they clearly demonstrate that the enthalpy changes determined for these transfer processes are not all simply a result of interactions with water. In addition, as illustrated above for phenol, we are able to glean further useful information concerning molecular interactions by looking at the derived enthalpies of transfer between two organic solvents.

The data in table 2 also indicate that the transfer of phenol from octanol to water is accompanied by an enthalpy change of +2.65 kcal mol^{-1}. This endothermicity is probably due to the formation of a hydrogen bond between the hydroxyl group of the solute and that of the organic solvent. Such a value for this sort of interaction can be compared with that derived from heats of solution reported in the literature. Parsons and coworkers (8) found the heats of solution for phenol in methanol and water to be +0.88 and +3.04 kcal mol^{-1}, respectively. From these data one can derive a value of 2.16 kcal mol^{-1} for the enthalpy of transfer of phenol from methanol to water. Considering the differences in the solvent systems, this number agrees rather well with the +2.65 kcal mol^{-1} determined for the octanol-to-water transfer.

By combining this result with the data from the octane-water system, one can derive the ΔH_t for the transfer of phenol from octane to octanol. As seen in table 3, a value of -6.5 kcal mol^{-1} is obtained for the hydrogen bond assumed to be formed between phenol and octanol. Such a result is not unreasonable in light of the work of Nagakura (7) and Arnett (1). These investigators studied hydrogen bond formations between phenol and a number of different proton acceptors (ether, dioxane, ethyl acetate, N-methylformamide, N,N-dimethylformamide) and found ΔH values ranging from -4 to -6.8 kcal mol^{-1}.

Free Energies of Transfer

Free energies of transfer were calculated as previously described by determining partition coefficients of the compounds between water and various organic solvents (3). These partition coefficients were found to be

independent of solute concentration over the range of 10^{-1} to 10^{-4} M. This allows us to conclude that our data are not influenced by aggregation of the solute molecules.

The free energies of transfer, along with the calorimetrically determined enthalpies of transfer, allow the calculation of the entropy of transfer. As discussed below, knowledge of the sign and magnitude of this entropy change leads to further insights into the nature of the molecular interactions involved in a given transfer process.

Table 4 provides complete thermodynamic profiles for the transfer of phenol from several organic solvents to water and for the transfer of aniline from toluene to water. Significantly, the transfer of phenol from either octane or toluene to water is strongly entropy inhibited, as is the transfer of aniline from toluene to water.

TABLE 4. - Thermodynamics of transfer of phenol and aniline between various organic solvents and water at 25° C

Transfer process	ΔG_t°, kcal mol^{-1}	ΔH_t°, kcal mol^{-1}	ΔS_t°, cal deg^{-1} mol^{-1}
PHENOL			
Octane → H_2O	-1.14	-3.9	-9.2
Toluene → H_2O	+ .27	-1.5	-5.9
Octanol → H_2O	+1.80	+2.6	+2.8
ANILINE			
Toluene → H_2O	+1.32	-1.2	-8.7

Frank and Evans (4) and Kauzmann (6) have described models in which the transfer of nonpolar groups from organic to aqueous medium should result in a decrease in entropy due to the ordering of water molecules around the hydrophobic groups. The observed entropic inhibition to the transfer of phenol and aniline to water is consistent with their predictions.

In contrast, the transfer of phenol from octanol to water is accompanied by an increase in entropy. This may well reflect a high degree of order required for the formation of a phenol-octanol hydrogen bond. Clearly, in this solvent system octanol does not provide an "inert" nonpolar environment.

CONCLUSION

We have demonstrated that a great deal of new, fundamentally important information concerning the nature of solute-solvent interactions can be

obtained by investigating the thermodynamic changes accompanying the transfer of molecules between organic solvents and water.

In the past, such studies were limited to the calculation of free energies of transfer from partition coefficients. The calorimetric technique described here provides a convenient method for determining enthalpies of transfer, which in turn allows the calculation of entropies of transfer.

We strongly believe that further application of this general technique to additional compounds will lead to the recognition of the molecular forces responsible for the thermodynamic changes observed in many biochemical reactions.

REFERENCES

1. Arnett, E. M., L. Joris, E. Mitchell, T. S. S. F. Marty, T. M. Gorrie, and P. V. R. Schleyer. J. Am. Chem. Soc., v. 92, 1970, p. 2365.

2. Berezin, I. V., A. V. Larashov, and K. Martinek. FEBS Letters, v. 7, 1970, p. 20.

3. Breslauer, K. J., B. Terrin, and J. M. Sturtevant. J. Phys. Chem., v. 78, 1974, p. 23630.

4. Frank, H. S. , and M. W. Evans. J. Chem Phys., v. 13, 1945, p. 507.

5. Hansch, C., and T. Fujita. J. Am. Chem. Soc., v. 86, 1964, p. 1616.

6. Kauzmann, W. Advan. Protein Chem., v. 14, 1959, p. 1.

7. Nagakura, S. J. Am. Chem. Soc., v. 76, 1954, p. 3070.

8. Parsons, G. H., C. H. Rochester, and C. E. C. Wood. J. Chem. Soc. (B), 1971, p. 533.

9. Pimentel, G. C., and C. M. Huggins. J. Phys. Chem., v. 60, 1956, p. 1615.

10. Sturtevant, J. M., and P. A. Lyons. J. Chem. Thermodyn., v. 1, 1969, p. 201.

11. Tanford, C. J. Am. Chem. Soc., v. 84, 1962, p. 4240.

12. Tanford, C., and Y. Nozaki. J. Biol. Chem., v. 246, 1971, p. 2211.

13. Whetsel, K. B., and J. H. Lady. J. Phys. Chem., v. 69, 1965, p. 1596.

DISCUSSION

K. D. Williamson: Did you have a practical method for determining the Gibbs

energies of transfer between two organic solvents? The question was prompted by the fact that many organic solvents are miscible and thus do not permit measurements of partition coefficients. In many such cases vapor-liquid equilibrium data are available from the literature. These data can be used to determine the fugacity of the solute in the liquid phases, and hence transfer functions for the solute between the organic phases.

K. J. Breslauer: There is a well-established practical method. For two immiscible solvents, one carries out classical distribution experiments. Alternatively, for miscible solvents one performs independent solubility studies and then corrects for activities.

E. M. Woolley: Would you comment on molecular association?

K. J. Breslauer: In general, we have to concern ourselves with molecular association. In particular, wh;en we looked at some carboxylic acids the association process had to be taken into account by simply adding another equation to our interpretation scheme. However, this does not in any way reduce the general applicability of the method. In the case of phenol, we did not encounter any association in the concentration range investigated.

Anonymous: What is the effect of mutual solubilities?

K. J. Breslauer: We were concerned that the mutual solubilities of the organic solvents with water might give us a more complicated system than simply pure water and pure organic. Consequently, we checked our direct-transfer determinations against a separate set of experiments in which the heat of solution of solid phenol was determined in both pure water and pure organic solvent. With the latter approach there is no need to worry about mutual solubilities. The enthalpy of transfer derived from the solubility data was found to be identical with our directly determined value. Thus, we were able to conclude that mutual solubilities of the solvents did not affect our directly-determined enthalpies of transfer.

HIGH-TEMPERATURE ENTHALPY MEASUREMENTS WITH A COPPER-BLOCK CALORIMETER

by

M. J. Ferrante[1]

ABSTRACT

A copper-block calorimeter used to measure relative enthalpies above 298.15 K is described. The measurements involve heating a sample to a known temperature, dropping it into a copper block of known heat capacity, and measuring the rise in temperature of the block. The construction and operation of the calorimeter, related measuring equipment, and two furnaces are described. One furnace, containing a silver heat sink, is used for heating samples up to 1,200 K. The other furnace, containing a platinum heat sink, is used between 1,000 and 1,800 K. Results of typical enthalpy measurements for cupric sulfide are given.

INTRODUCTION

Enthalpies relative to 298.15 K are measured with a copper-block calorimeter at the Bureau of Mines, Albany (Oreg.) Research Center. In this method, a sample is heated in a furnace to a known temperature and dropped into a block calorimeter of known heat capacity that is operating near room temperature. The increase in temperature of the block is related to the change in enthalpy of the sample. Because the sample is dropped from the furnace into the calorimeter, the name "drop method" is applied to this technique.

The drop method is used with three types of calorimeters: (1) the fluid or water type as described by White (16),[2] (2) the phase change type as described by Ginnings and Corruccini (5-6) and modified several times (1, 4, 7), and (3) the metal-block type as described by Jaeger and Rosenbohm (8). The last type will be described here.

Results of typical enthalpy measurements made with the block calorimeter described in this report are given for cupric sulfide (Cu_2S). This investigation of synthetic Cu_2S was one in a series of thermody-

[1]Research chemist, Albany Research Center, Bureau of Mines, Albany, Oreg.

[2]Underlined numbers in parentheses refer to items in the list of references at the end of the paper.

namic studies conducted at the Bureau of Mines on copper compounds important in mineral technology. Despite the importance of Cu_2S in the processing of copper, thermodynamic data for Cu_2S were inadequate. Such thermodynamic data were needed for the more efficient extraction of copper from sulfide ores by roasting, and for the control of sulfur oxide pollutants that are formed during the roasting process. Thus, the thermodynamic data would foster maximum productivity and minimum energy requirements in the processing of copper and related substances.

APPARATUS AND OPERATION

The copper-block calorimeter was designed by Southard (15) and last described in 1968 by Douglas and King (2). Since then, this apparatus has been modified several times until only the calorimeter proper and the container remain unchanged. The present arrangement of the copper block and furnace is shown in figure 1. On the top of the furnace is the mechanism for dropping the sample capsule from the furnace into the calorimeter. This dropping mechanism consists of a tripping device, a plunger that fits snugly in the drop tube, and a suspension wire attached to the capsule containing a sample. The drop tube is slotted along most of its 115-cm length to permit the nearly free fall of the plunger. The lower 15 cm is not slotted, so that the fall of the plunger is checked by an air cushion when it reaches a position corresponding to the point where the capsule has entered the calorimeter. The air slowly escapes from the bottom of the drop tube through a small hole that provides passage for the suspension wire. Thus, the capsule drops from the furnace into the calorimeter in a minimum amount of time and settles gently into the copper block as the gates are momentarily opened and then closed. The rate of fall of the sample capsule is reproducible, and the gates are opened for no more than 2 seconds. Keeping the suspension wire attached to the capsule as it falls into the calorimeter enables easy retrieval of the capsule from the calorimeter or easy return to the furnace for another measurement. The wire is platinum-10 pct rhodium with a size of either Brown and Sharpe gage 32 or 30 depending on the weight of capsule and sample. The top of the furnace is closed with an alumina plug with holes just large enough for the suspension wire and the thermocouple. This calibrated thermocouple of platinum versus platinum-10 pct rhodium is used to measure the temperature of the sample capsule in the furnace. When the furnace is swung over the calorimeter, the steel tube at the bottom of the furnace is alined with the brass tube at the top of the calorimeter. Both tubes have an ID of about 2.7 cm.

The calorimeter proper is a cylindrical copper block 12.6 cm in diameter by 20.3 cm in height that weighs about 21 kg. This mass is large enough so that the highest heat absorption from a capsule and sample does not cause a temperature rise of more than 5 K. The copper block is supported by plastic knife edges that are glued to the bottom of the surrounding brass container. The block and the interior of the container are gold plated, and these surfaces are polished to minimize the heat exchange between them. The brass container is immersed in a vigorously stirred contant-temperature water bath maintained near 25° C. The temperature of the bath is controlled to $\pm$0.002° C by a combination of heating and cooling. The cooler uses mechanical refrigeration to

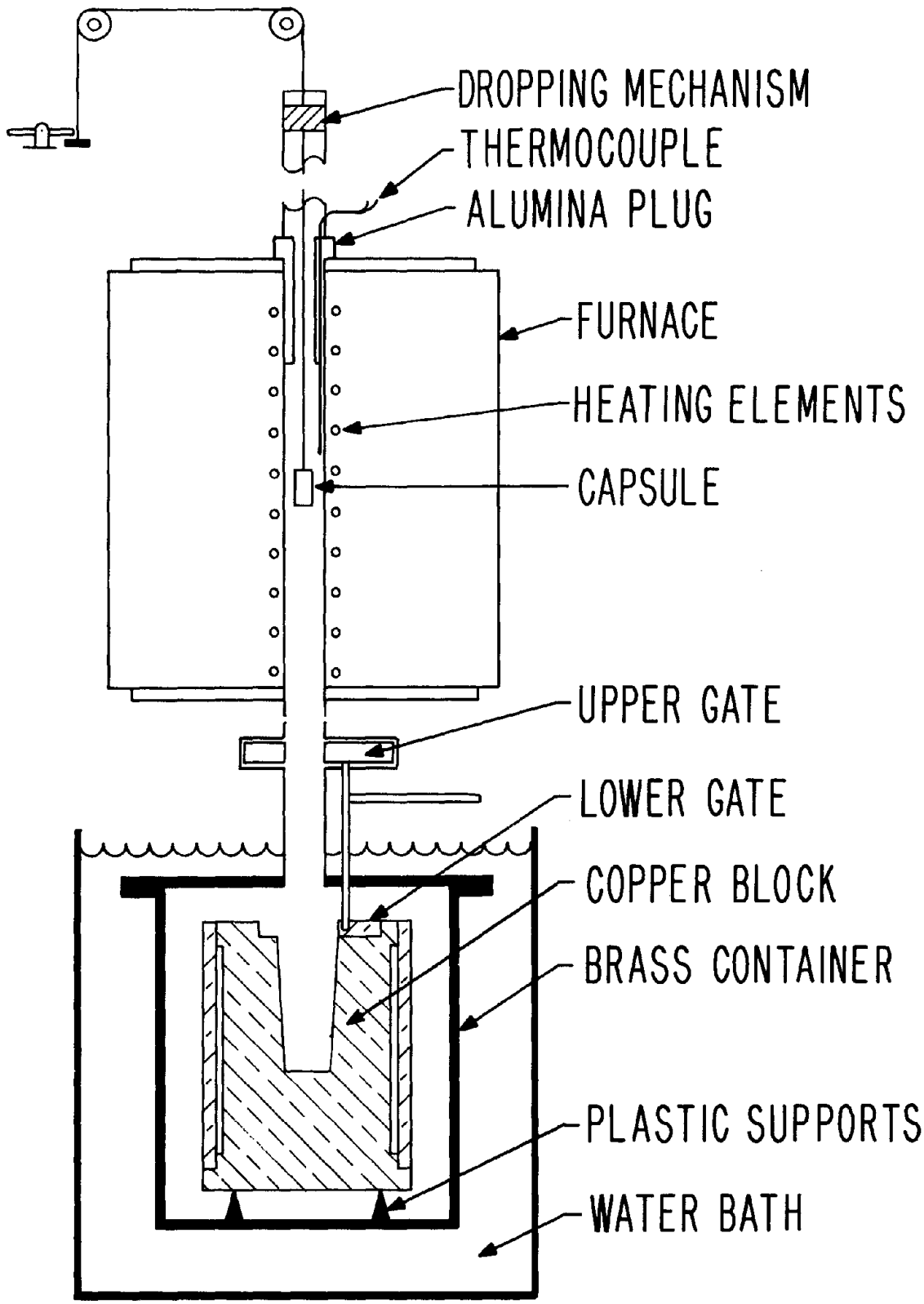


FIGURE 1. - Furnace and copper-block calorimeter.

supply continuous cooling at a constant rate. Heaters that have constant power inputs from variable-voltage transformers balance out almost all of the cooling, while a proportional temperature controller supplies power to the control heaters.

The upper gate is circular and hollow. It is made of copper about 1.3 cm thick with a hole 2.7 cm in ID. This gate rotates in a brass housing, and when closed, shields the calorimeter from radiation from the hot furnace. Even when the furnace is at 1,800 K with the gate closed, the heat exchange between the furnace and the calorimeter is negligible. The receiving well is covered by the lower gate. It is a circular, solid copper gate about 1.9 cm thick with a hole 2.7 cm in ID. In the closed position, this gate prevents heat losses from the calorimeter by convection from the hot capsule that is dropped from the furnace. Because the lower gate is part of the calorimeter proper, its bottom surface and the surface of its recess in the block were machined to a tight fit. These tight fits provide good contact for rapid attainment of thermal equilibrium. The lower and upper gates are manually rotated on the same shaft that is eccentric with the center line of the copper block. Both gates are normally closed except when briefly opened to allow the capsule to drop through into the well. Both gates have a slot that is on an arc of the proper radius and is just wide enough to allow the suspension wire to slide through when the gates are closing. A correction is made for the heat radiated into the calorimeter during the few seconds the gates are opened to permit the capsule to drop into the well. This heat gain is negligible below 1,025 K and does not exceed 0.1 pct of the sample heat at higher temperatures.

Additional details of the calorimeter are shown in figure 2. An atmosphere of dry carbon dioxide is maintained in the calorimeter by introducing a continuous flow of about 50 cm^3/min near the bottom of the brass container. Before the gas enters the calorimeter, it flows through a coil of copper tubing in the constant-temperature bath to attain the same temperature as the bath. This slow flow of carbon dioxide not only prevents condensation of atmospheric moisture in the calorimeter, but also decreases the heat exchange rates to about 60 pct of those in air. This rate of heat exchange in the calorimeter is about 0.002 K/min for a temperature difference of 1° between the block and bath and is reproducible to about 1 pct. There is a slight departure from this value for large temperature increases of the block from the hot capsule, but this variation is taken into account in the calculation of the measured heat exchange. The time for attainment of thermal equilibrium by the calorimeter is about 8 to 10 minutes after heating for an electrical calibration and 10 to 60 minutes after dropping a heated sample for an enthalpy measurement. The actual time depends primarily upon the thermal conductivity of the sample. After the furnace is swung over the calorimeter, the carbon dioxide flows up the furnace tube to enhance the heat transfer between the furnace and the capsule. It also maintains an oxidizing atmosphere around the furnace thermocouple. The flanged top is sealed to the bottom portion of the brass container by means of a gasket and machine screws. The removable top provides easy access to the block. The well is for receiving the capsule dropped from the furnace. This well is a tapered hole in a copper plug extending

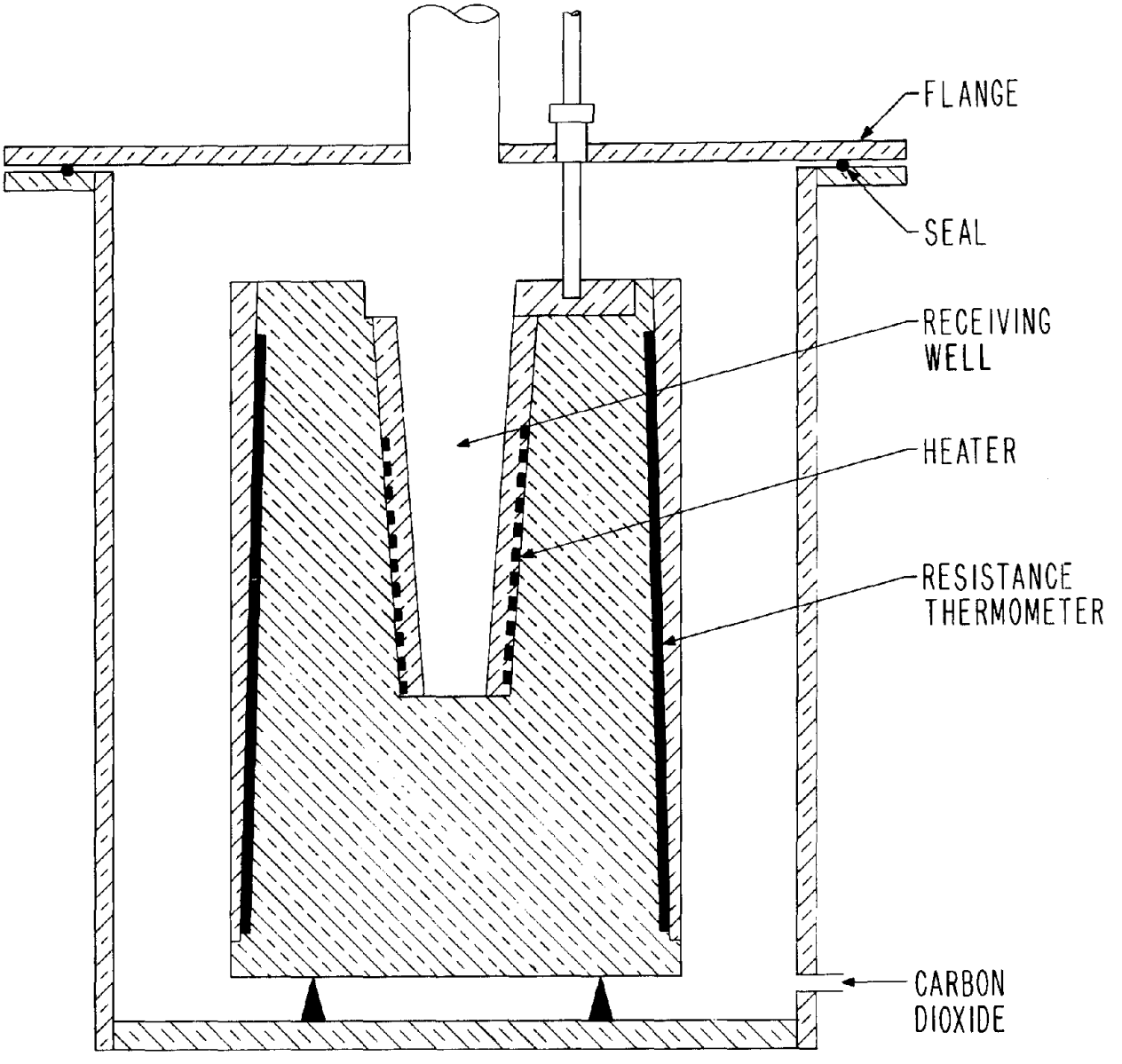


FIGURE 2. - Details of copper-block calorimeter.

from the top of the block to within 5 cm of its bottom. The plug is removable from the block and is wound with a 100-ohm manganin wire heater for electrical calibration of the heat capacity of the block calorimeter. The heat capacity of the copper block is 3.695 cal/μv change in the thermometer at 25.00° C. There is a small heat capacity change of less than 0.001 cal/μv-K of the block with temperature that is accounted for in the calculations.

The resistance thermometer of the calorimeter is wound around a recess in the block and covers about one-half of its outer surface. The winding is coated with Bakelite[3] varnish and is protected by a tapered copper sleeve that has a driving fit onto the similarly tapered block. The resistance thermometer is of the transposed (Wheatstone) bridge type described by Maier (13) and provides a significantly greater temperature sensitivity than a single winding. The thermometer consists of two copper and two manganin windings of approximately 210 ohms each. Therefore, the current passing through the thermometer is exactly divided at all temperatures, and the bridge is in balance only at 20.8° C. At temperatures other than the balance point, the copper windings have changed resistance significantly more than the manganin windings, and the bridge is unbalanced. This unbalance produces a potential difference, which is a measure of the temperature deviation from the balance point. The voltage drop across the thermometer is 1,765 μv at 25.00° C. The thermometer has a temperature coefficient of 416 μv/K with a current of 1 ma. Heat is generated by the thermometer at 0.003 cal/min, which is negligible. The use of a six-dial potentiometer in conjunction with a nanovolt null detector results in a system that can resolve changes equivalent to ±0.02 μv or ±0.00005 K.

The potentiometer-null detector system is also used in the electrical calibration of the calorimeter and in measuring the resistance of the manganin heater. In these cases, a 0.1-ohm standard resistance is used in the measuring circuit for electrical calibration, and a 100-ohm standard resistance is used in both measuring and checking the resistance of the manganin heater. The energy source for heating the block during electrical calibration is a dc power supply of the constant-voltage type. The time of the heat input to the block is measured with an electric timer with a crystal oscillator for a reference. The electrical calibration serves to determine the calibration factor for the heat capacity of the calorimeter. Over 100 electrical calibrations with the system described above have resulted in an average deviation of 0.02 pct. A calibration is made before and after measuring the complete series of enthalpies for each sample, and its constancy serves as a check on the precision of the measuring equipment. Each time an electrical calibration is performed, the enthalpy of a standard material is also measured and serves as an overall check of the entire equipment by comparing results with the best published values. Results with α-Al_2O_3 or MgO(periclase) have agreed with the published data within 0.1 pct.

The emf of the standard cell used with the potentiometer is checked periodically against a dc transfer standard. Both the transfer standard and the standard resistances were checked by comparison with standards

[3]Reference to specific brand names is made for identification only and does not imply endorsement by the Bureau of Mines.

calibrated by the National Bureau of Standards. Current sources for the potentiometer and resistance thermometer are lead cells of the charge-retaining type. The lead cells, standard cell, and standard resistances are housed in separate compartments within an insulated box. Air at 30 $\pm$0.05° C is circulated in a space between the insulated box and the outer shell.

Because the major error in drop calorimetry is usually the measurement of the temperature of the sample capsule in the furnace, special attention is given to the region of the furnace where the capsule is hung. The closer this region is to being isothermal, the smaller will be the problem of measuring the correct temperature of the capsule containing the sample. It should be remembered, however, that the actual temperature measurement of the sample capsule with a thermocouple must be done with care. Otherwise, this error can exceed the uncertainty of a nonisothermal region. In order to have a region near isothermal for the sample capsule and thermocouple, two furnaces were built with cylindrical heat sinks of silver or platinum. The furnace with the silver heat sink is used to heat samples up to 1,200 K. The other furnace containing the platinum cylinder is used between approximately 1,000 and 1,800 K to allow about a 200 K overlap with the lower temperature furnace. These furnaces are each about 61 cm in length and 30 cm in diameter. Both furnaces are mounted on bearings so that they can be swung aside for easy access to either the calorimeter or the furnaces.

The furnace with the silver heat sink is limited to near 1,200 K as a safety precaution to avoid melting of the silver at 1,235 K. Silver was selected because it has the highest thermal conductivity of any metal. Moreover, a relatively large mass of silver results in a high total heat capacity. This in turn provides a thermal inertia to temperature changes in the region occupied by the sample and thermocouple, and thereby permits easy control of the temperature in this region. A cross section of the furnace with the silver cylinders is shown in figure 3. The center cylinder has a length of 26.7 cm, an OD of 5.9 cm, a wall thickness of 1.4 cm, and a top cap with a thickness of 1.3 cm. The top and bottom silver cylinders are 5.1 cm in length and have 3.8-cm-long alumina spacers between them and the central silver cylinder. Additional alumina spacers are located above and below the end silver cylinders. The furnace core is centered and supported in alumina blocks and insulated with powdered alumina. For this furnace, the dropping mechanism is always attached to the top of the furnace.

Vertical holes in the silver cylinders and alumina spacers are lined with thin-walled Inconel tubes. The large Inconel tube has an ID of about 2.7 cm and is located in the central and bottom parts of the furnace. It encloses the sample capsule. This large Inconel tube is fitted with a smaller Inconel tube at the top for the suspension wire. Hence, the suspended sample capsule is pulled into the furnace from the bottom. Smaller holes (0.6 cm diameter) extend from the top and bottom of the furnace into the wall of the central silver cylinder. These holes were placed 90° apart azimuthally with one hole extending the length of the furnace, one hole extending about 7.6 cm into the top of the central silver cylinder, and two holes extending about 5.1 cm into both the top and bottom of the central silver cylinder. The construction

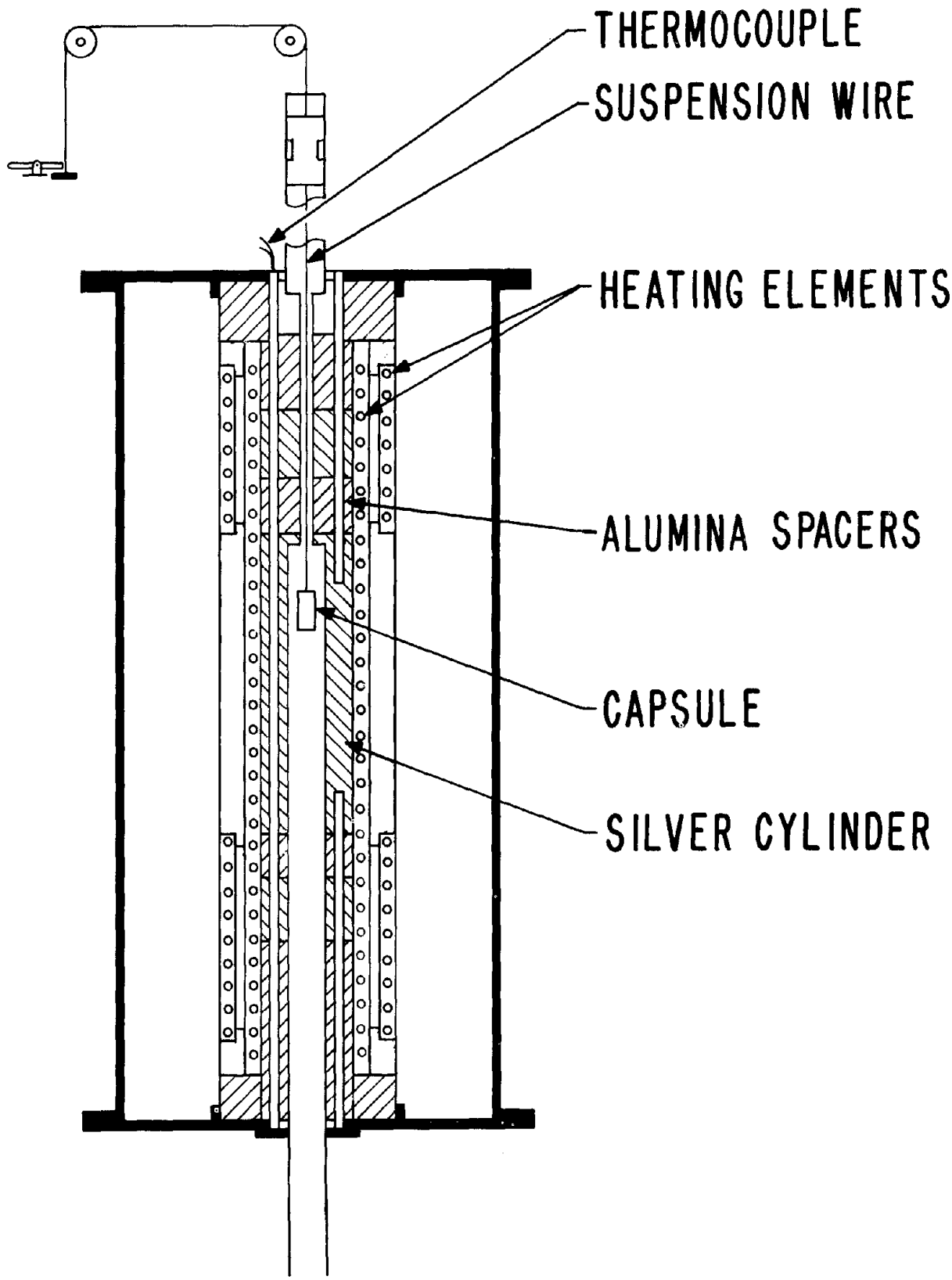


FIGURE 3. - Furnace with silver heat sink.

of the furnace to this point is essentially the same as that of the one at the National Bureau of Standards (1, 4, 7). The smaller holes house various thermocouples whose types and functions are described later. All thermocouples fit snugly in the Inconel tubes, which in turn fit snugly in the cylinders. These close fits are for good thermal contact so that heat conduction along the thermocouple leads is not a source of error.

The main heating elements extend the full length of the furnace and consist of coils of Nichrome wire that radiate directly to all three silver cylinders. Precision control of the main heater is accomplished with a proportional temperature controller that has rate and reset features. This temperature controller is used in conjunction with an iron-constantan thermocouple sheathed in Inconel. The thermocouple is placed in one of the smaller holes in the central silver cylinder with its junction at the same level as the sample capsule. Another iron-constantan thermocouple similarly placed in another small hole is used in conjunction with a strip chart for recording the temperature of the central cylinder. The iron-constantan thermocouple was selected for temperature controlling and recording because of its high sensitivity of about 60 μv/K. There are also auxiliary end heaters of Nichrome that surround the main heater at elevations corresponding to the top and bottom silver cylinders. These end heaters are controlled potentiometrically according to the difference in temperature between the main heater and the end heaters as sensed by differential thermocouples of Chromel-Alumel located in the center of their respective heating elements. The control circuit for each end heater is also trimmed with a variable-voltage transformer. In addition, the same Chromel-Alumel thermocouples are used in conjunction with high-limit temperature controllers to turn off all heaters if the temperature of one approaches the melting point of silver at 1,235 K.

The temperature in the central silver cylinder is measured with a calibrated platinum versus platinum-10 pct rhodium thermocouple insulated in an alumina tube and placed in one of the smaller holes of this cylinder. The junction of the thermocouple is at the same height as the middle of the sample capsule, Thus, precision temperature control of the main and end heaters usually allowed a negligible drift of a few hundredths of a degree from any set value. At these times, there was a negligible temperature gradient in the central silver cylinder below 700 K, and up to several hundreths of a degree above 700 K, particularly at the higher temperatures of 1,100 and 1,200 K. No correction is applied, because the error is very small. Consequently, it is considered safe to assume that the sample capsule attains the temperature of the central silver cylinder. However, it is also important to take temperature profiles of the actual region where the sample capsule is normally suspended. This is done by inserting a platinum versus platinum-10 pct rhodium thermocouple from the bottom of the furnace into the center of the large Inconel tube. These temperature profiles are used to verify that the temperature gradient of this region was small enough not to cause an error in the indirect temperature measurement of the sample capsule. Such a profile is taken before each measurement and showed the gradient in this region to be negligible below 700 K, 0.02 $\pm$0.01 K from 700 to 1,000 K, and 0.04 $\pm$0.02 K between 1,000 and 1,200 K. Because the

temperature of the sample capsule is measured indirectly, sufficient time must be allowed for the capsule to reach the temperature of the central silver cylinder. Since the central cylinder attains a steady temperature from 15 to 45 min after a capsule is pulled into the furnace, the minimum furnace residence times vary from 1 to 2 hours. An adequately long residence time is also verified experimentally for each sample by comparing the results of measurements with different times in the furnace, so that a deviation from normal results can be detected, and then a time can be selected that is clearly adequate.

The second furnace has a platinum heat sink and platinum-20 pct rhodium wire resistance windings that can be operated up to about 1,800 K. Figure 4 shows a cross section of the furnace. The dropping mechanism with the sample capsule and its measuring thermocouple is lowered into the furnace only when the furnace reaches a steady temperature. This is done to keep the calibrated platinum versus platinum-10 pct rhodium thermocouple out of the furnace as much as possible, and thereby minimize changes in its calibration at elevated temperatures, particularly about 1,500 K. The junction of the thermocouple is placed within 1 mm of the sample capsule, not touching it, to prevent sticking between the two surfaces. The capsule is usually placed near the center of the platinum heat sink. The heat sink is located in the central portion of the furnace with alumina spacers below and above it. The platinum cylinder is 22.9 cm long and 0.24 cm thick and weighs about 1.1 kg. A thin coating of alumina gives the cylinder an ID of about 2.7 cm. This coating is to avoid sticking between the cylinder and the capsule. Around the platinum cylinder are two concentric alumina tubes that support the heating elements. The main heating element was wound on the full length of the inner tube with about 18 m of number 18 Brown and Sharpe gage platinum-20 pct rhodium wire. The same type of wire was also wound on each end of the outer tube as end heaters to counteract the heat leakage from the top and bottom of the furnace. Both windings were coated with alumina cement and fired at about 1,500 K to confine the volatilization of the platinum-20 pct rhodium wire at elevated temperatures. The ends of the furnace core are supported and centered in alumina blocks. This core is then insulated with powdered alumina.

The thermocouple for control of the furnace temperature is made of platinum versus platinum-13 pct rhodium. The junction of this thermocouple is located adjacent to and in the center of the main heating element to make response time as short as possible. The proportional temperature control of the main windings and proper apportioning of power to the end windings are accomplished in a similar manner as for the furnace with the silver heat sink, and result in a minimum of temperature variation in the zone for heating the capsule containing the sample. Temperature profiles in the platinum cylinder where the capsule is suspended were conducted as previously described. These profiles showed a temperature gradient for this zone of 0.2 +0.1 K below 1,500 K, and normally less than 0.4 $\pm$0.2 K from 1,500 to 1,800 K.

TYPICAL RESULTS

Results of typical enthalpy measurements made with the copper-block calorimeter are given for Cu_2S. Cupric sulfide was selected because of

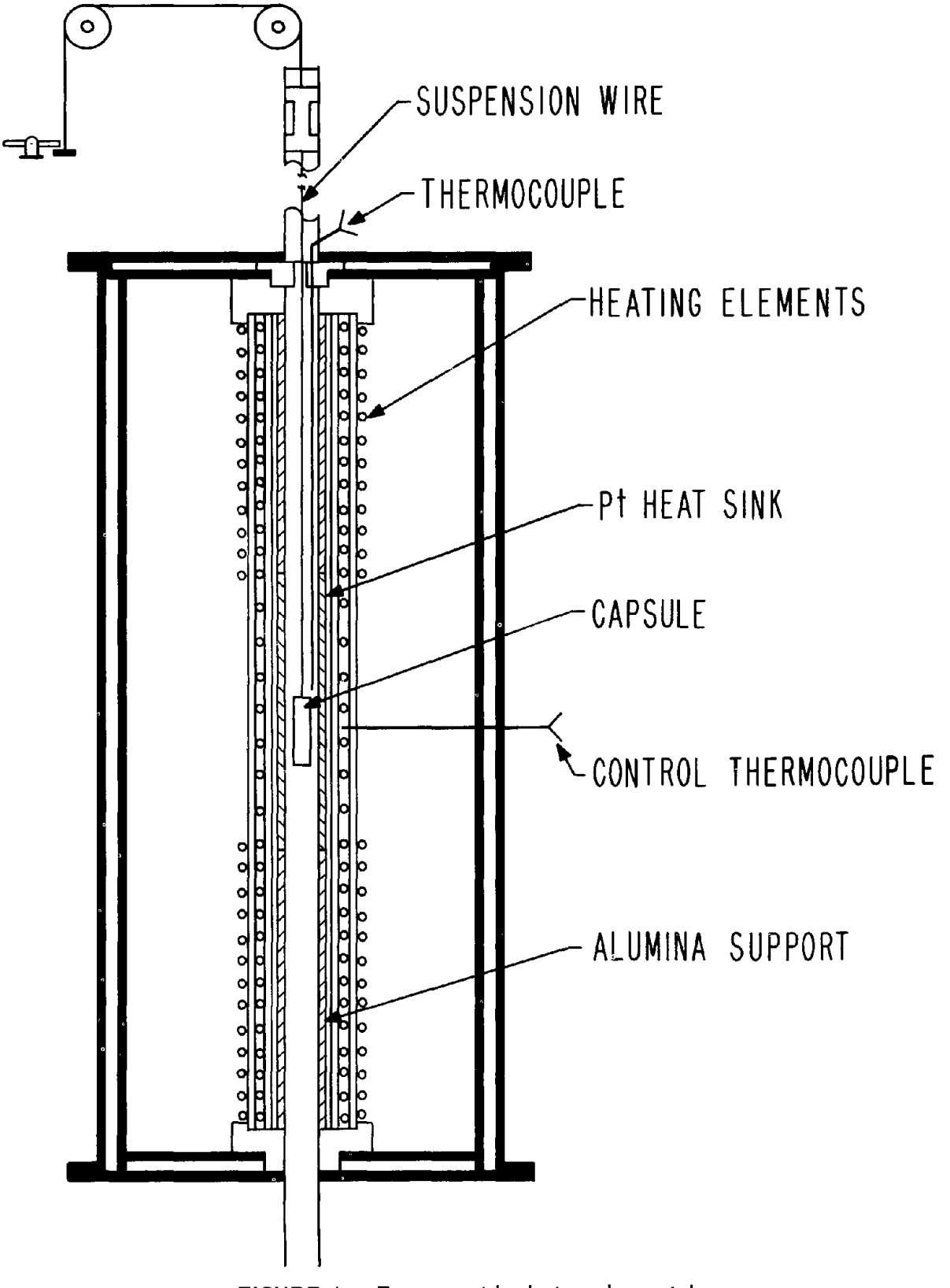


FIGURE 4. - Furnace with platinum heat sink.

its complex thermal behavior involving two solid-solid transitions and a solid-liquid transition. This investigation illustrates some experimental techniques that are encountered in high-temperature measurements by drop calorimetry, such as (1) verifying the reversibility of a phase transition, (2) substantiating that a phase transition is reasonably rapid or calorimetrically reversible, and (3) establishing the temperature of a transition that has shown slugglish behavior. In addition, data that could not be precisely determined in this investigation were obtained from other studies. A temperature for the transition at 376 K was needed to enable the calculation of the heat of transition, because enthalpy measurements under 400 K have poor precision. A temperature for the melting point was also needed to calculate the heat of fusion, because of the onset of early melting shown by an enthalpy measurement. Details of this investigation were reported in Bureau of Mines Report of Investigations 8305 (3), which included measurements of the low-temperature heat capacities and high-temperature enthalpies of cuprous and cupric sulfides.

Experimental enthalpies relative to 298.15 K for Cu_2S are listed in table 1. To obtain the best fit of smooth curves to these data, the values were computer-fitted with polynomial functions that were then used to calculate smooth values of enthalpies at the temperatures of the experimental measurements. These smooth enthalpies were in turn used to calculate the percent deviation from the experimental values that are listed in table 1. The percent deviation is defined as

$$\text{Deviation, percent} = 100 \left[\frac{(H^\circ - H^\circ_{298})_{\text{experimental}} - (H^\circ - H^\circ_{298})_{\text{smooth}}}{(H^\circ - H^\circ_{298})_{\text{experimental}}} \right].$$

The average percent deviation for the valid 32 measurements was 0.07 pct. This does not include 0.42 pct for the three measurements below the 376 K transition, where the precision of measurements is significantly less than that above 500 K. Likewise, the standard deviation of the measurements from the curves was 0.1 pct, not including 0.9 pct for the three measurements below 376 K. The standard deviation is calculated from the following equation, where d is the percent deviation of a measurement and n is the total number of measurements

$$\text{Standard deviation, percent} = \sqrt{\frac{d^2}{n - 2}}.$$

The complex thermal behavior of Cu_2S is shown by three reversible transitions in figure 5, which graphically shows the experimental measurements and the smooth curves. Solid-solid transitions were found at 376 and 720 K. Enthalpy measurements made above and then below the transitions at 376 and 720 K verified the reversibility of phase transitions by again being on the curve of the mean heat capacity. The third transition from solid to liquid was found at about 1,400 K. Rapid reversibility of phase transitions was confirmed by cooling separate samples from temperatures above the three transitions at 376, 720, and 1,400 K to 298 K in the calorimeter under the same conditions as for enthalpy measurements,

TABLE 1. - Experimental enthalpies and deviations for Cu_2S (c,ℓ)

T, K	$H^\circ-H^\circ_{298}$, cal/mole	Deviation,[1] pct	T, K	$H^\circ-H^\circ_{298}$ cal/mole	Deviation,[1] pct
350.7	990	-0.46	720.5	10,212	[2]
360.3	1,184	.05	720.9	10,283	[2]
370.2	1,391	.75	726.0	10,480	.10
380.2	2,462	-.09	727.1	10,489	-.01
399.4	2,910	-.33	735.5	10,667	.07
399.4	2,928	.36	740.6	10,743	-.13
453.5	4,197	.16	747.9	10,901	-.03
497.3	5,192	-.10	800.1	11,932	-.05
548.3	6.342	-.08	846.8	12.858	.01
595.9	7,402	.00	895.4	13,822	.02
597.3	7,435	.05	1,004.6	15,963	.01
603.7	7,573	.05	1,084.1	17,540	.11
619.2	7,911	.00	1,109.6	18,001	-.11
628.7	8,115	-.02	1,205.5	19,888	.00
639.2	8,347	.01	1,304.4	21,816	.01
686.5	9,356	-.05	1,381.9	23,587	[3]
700.5	9,671	.13	1,413.2	27,033	.06
710.3	9,870	.06	1,452.5	27,837	-.10
719.5	10,165	[2]	1,509.3	29,090	.04
719.7	10,059	.03			

[1]Deviation, pct = 100(experimental enthalpy - smooth enthalpy) experimental enthalpy.
[2]Partial phase conversion; not considered in smooth-curve-fitting process.
[3]Onset of early melting; not considered in smooth-curve-fitting process.

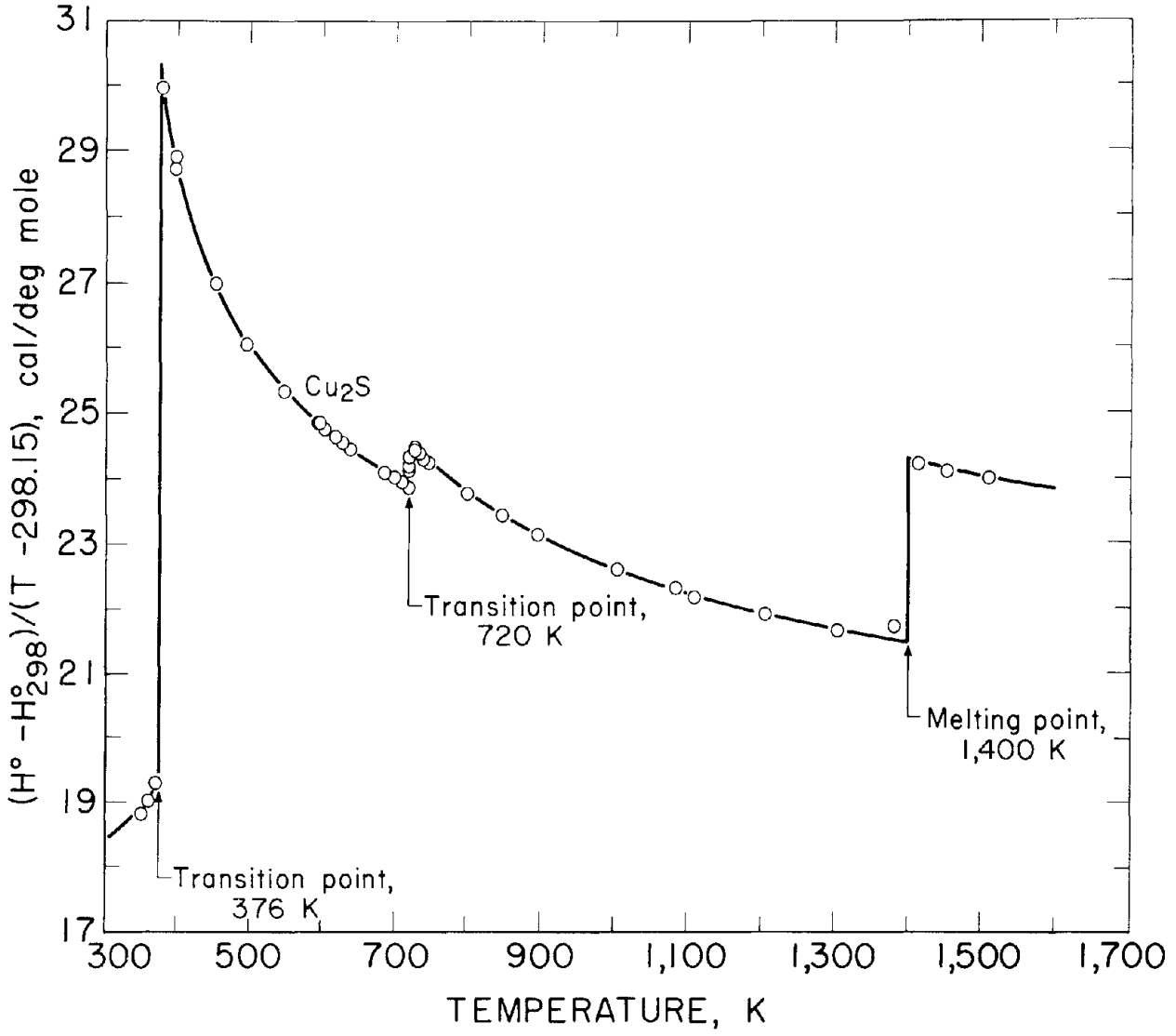


FIGURE 5. - High-temperature mean heat capacities of Cu_2S.

and then within minutes subjecting these samples to X-ray diffraction analyses. Such tests were made at approximately 600, 1,000, and 1,500 K. An additional test was made at about 350 K to have a sample heated below the transition at 376 K. All samples reverted to the stable reference form of monoclinic Cu_2S, and no metastable form was detected by X-ray analyses. Two months later, reanalyses of the same samples detected no structural change. This meticulous program was followed to be sure that the room-temperature form was the same after quenching in the calorimeter from each form encountered in this investigation, and to ensure that there were no slow transformations at room temperature. The quench from the liquid state, in particular, was suspect, in view of the small measured heat of fusion of 3,070 cal/mole. Only the room-temperature form of monoclinic Cu_2S was detected by X-ray diffraction analyses for samples used in enthalpy measurements.

For the first transition from the monoclinic to hexagonal structure, temperatures from 364 to 388 K have been given in the literature. The present investigation established this transition between 370.2 and 380.2 K for an average temperature of 375 K. However, 376 K was adopted from Jost and Kubaschewski (11) and Kubaschewski (12) because their heat capacity measurements by adiabatic calorimetry are more sensitive than enthalpy measurements by drop calorimetry below 400 K. Adoption of this more reliable transition temperature in turn permitted the more reliable calculation of a heat of transition after extrapolation of enthalpy data. The resulting isothermal heat of transition of 865 cal/mole compares favorably with the values of about 920 cal/mole reported by Jost and Kubaschewski and 889 cal/mole measured by Kubaschewski.

The second transition from the hexagonal to the cubic phase was established at a temperature of 720 K by 12 enthalpy measurements made within 34° of the transition temperature. Figure 5 and table 1 show the results of four of these measurements, all lying within 1° of the 720 K transition. This transition temperature was initially determined from enthalpy measurements with a minimum furnace residence time of 1.5 hours. Additional measurements were then made with residence times much longer than the minimum to more firmly establish the transition temperature, because a spread in temperatures from about 678 to 743 K has been reported for the transition due to sluggish behavior. The measurements with residence times 11 to 46 times longer than the minimum established relative enthalpies below, at, and above the 720 K transition at temperatures of 700.5 (17 hr), 720.5 (19 hr), 720.9 (43 hr), 727.1 (69 hr), and 740.6 K (21 hr). The temperature of 720 K and the heat of transition of 280 cal/mole that were determined for the transition from this investigation are in good agreement with results by adiabatic calorimetry of 717 K and 287 cal/mole reported by Jost and Kubaschewski and of 708 K and 306 cal/mole measured by Kubaschewski.

Other investigators have made limited high-temperature measurements for the solid phases of Cu_2S, but none of the liquid state. Heat capacity measurements between 203 and 803 K were reported by Jost and Kubaschewski; however, their values were not tabulated, but were presented graphically. Their data differed from the present investigation by ± 1 pct or less. Kubaschewski tabulated heat capacity values measured between 223 and 803 K. His values varied from the present investigation by ± 0.03 pct or less.

Enthalpy measurements of the liquid state resulted in cracking of the clear silica-glass capsules. The cracking of the glass capsules occurred inside the calorimeter without loss of sample, so that an adequate number of successful measurements were obtained for the liquid up to 1,509.3 K. X-ray diffraction analyses of the sample from the cracked capsules showed no differences from the starting material. Measurements were limited to three because the constancy of the heat capacity data in the liquid state permitted extrapolation of the smooth data to 1,600 K.

Enthalpy measurements could not determine the melting point due to the onset of early melting, as shown by the measurement at 1,381.9 K. This measurement has an abnormally high thermal effect of 1.2 pct above the smooth curve in figure 5. The early melting was probably caused by a trace amount of less than 0.01 pct of metallic impurities dissolved in the Cu_2S. This made it necessary to adopt the congruent melting point of 1,400 K from differential thermal analysis conducted by Jensen (9) in order to calculate the heat of fusion after extrapolation of the enthalpy data. The resulting heat of fusion was 3,070 cal/mole, compared with 2,700 cal/mole measured with a water calorimeter by Johannsen and Vollmer (10) and 2,700 cal/mole from differential thermal analysis measurements by Mendelevich, Krestovnikov, and Glazov (14).

REFERENCES

1. Ditmars, D. A., and T. B. Douglas. Measurement of the Relative Enthalpy of Pure α-Al_2O_3 (NBS Heat Capacity and Enthalpy Standard Reference Material No. 720) From 273 to 1173 K. J. Res. NBS, v. 75 A, 1971, pp. 401-420.

2. Douglas, T. B., and E. G. King. High-Temperature Drop Calorimetry. Ch. 8 in Experimental Thermodynamics, v. 1. Calorimetry of Non-Reacting Systems, ed. by J. P. McCullough and D. W. Scott. Butterworths, London, 1968, pp. 293-331.

3. Ferrante, M. J., J. M. Stuve, G. E. Daut, and L. B. Pankratz. Low-Temperature Heat Capacities and High-Temperature Enthalpies of Cuprous and Cupric Sulfides. BuMines RI 8305, 1978, 22 pp.

4. Furukawa, G. T., T. B. Douglas, R. E. McCoskey, and D. C. Ginnings. Thermal Properties of Aluminum Oxide From 0° to 1200° K. J. Res. NBS, v. 57, 1956, pp. 67-82.

5. Ginnings, D. C., and R. J. Corruccini. An Improved Ice Calorimeter - The Determination of its Calibration Factor and the Density of Ice at 0° C. J. Res. NBS, v. 38, 1947, pp. 583-591.

6. _____. Enthalpy, Specific Heat, and Entropy of Aluminum Oxide From 0° to 900° C. J. Res. NBS, v. 38, 1947, pp. 593-600.

7. Ginnings, D. C., T. B. Douglas, and A. F. Ball. Heat Capacity of Sodium Between 0° and 900° C, The Triple Point and Heat of Fusion. J. Res NBS, v. 45, 1950, pp. 23-33.

8. Jaeger, F. M., and E. Rosenbohm. On the Exact Determination of the Specific Heats of Solid Substances Between 0° and 1,625° C. I. Method and Apparatus. Proc. Acad. Sci. Amsterdam, v. 30, 1927, p. 905.

9. Jensen, E. Melting Relations of Chalcocite. Avhandl. Norske Videnskap-Akad., Oslo, Matematish-Naturvidenskapelig Klasse, No. 6, 1947, 14 pp.

10. Johannsen, F., and H. Vollmer. Untersuchungen im System Kupfer-Kupfersulfid (Investigations on the System Copper-Copper Sulfide). Z. Erz. u. Metallhuttenw., v. 13, 1960, pp. 313-322.

11. Jost, W., and P. Kubaschewski. Spezifische Warmen von Silber- und Kupfer (I) - Chalkogeniden von-70° C bis zu 550° C (Specific Heats of Silver and Copper (I) Chalcogenides From 70° to 550° C). Z. Phys. Chem. (Frankfurt), v. 60, 1968, pp. 69-78.

12. Kubaschewski, P. Spezifische Warmen und thermisch Fehlordnung von Kupferchalkogeniden Teil II: Die Systeme Cu_2S-CuS und Cu_2Se-CuSe (Specific Heats and Thermal Disorder of Copper Chalcogenides. II. Cu_2S-CuS and Cu_2Se-CuSe Systems). Ber. Bunsenges. Phys. Chem., v. 77, 1973, pp. 74-80.

13. Maier, C. G. Resistance Thermometers for Chemists. J. Phys. Chem., v. 34, 1930, pp. 2860-2868.

14. Mendelevich, A. Y., A. N. Krestovnikov, and V. M. Glazov. Phase Equilibria of Pseudobinary Group I Chalcogenide Systems in the Regular Solution Approximation. Russ. J. Phys. Chem., London, v. 43, 1969, pp. 1723-1724.

15. Southard, J. C. A Modified Calorimeter for High Temperatures. The Heat Content of Silica, Wollastonite, and Thorium Dioxide. J. Am. Chem. Soc., v. 63, 1941, pp. 3142-3146.

16. White, W. P. The Modern Calorimeter. Chemical Catalog Co., New York, 1928, 194 pp.

DISCUSSION

M. W. Chase: Why is the precision of enthalpy measurements by the copper-block calorimeter poor below 400 or 500 K?

M. J. Ferrante: The precision is poor because of the small amount of heat that is measured for a sample below those temperatures.

G. T. Furukawa: How were the temperatures of the Cu_2S sample measured in the furnace?

M. J. Ferrante: We do not use a resistance thermometer as done with the furnace having a silver heat sink for the NBS ice calorimeter. Our furnace is similar to the NBS furnace, particularly in respect to the silver cylinder. We measured the temperature of the sample with a thermocouple of platinum

versus platinum-10 pct rhodium. The thermocouple is inserted in the central silver cylinder as in the NBS furnace. The temperature of the central cylinder is taken as the temperature of the sample, which has been verified by experimental tests.

G. T. Furukawa: Was the temperature of the Cu_2S sample measured with a thermocouple as low as 350 K?

M. J. Ferrante: Yes, we used a thermocouple and not a resistance thermometer as done at NBS. NBS uses a thermocouple above 773 K. Although the resistance thermometer is more accurate than a thermocouple at 350 K, we do not use a resistance thermometer because a much larger error can be caused by the enthalpy measurement of the small amount of sample heat at this temperature. Thus, measurements usually are not made below 400 or 500 K. Even at these temperatures, the data from low-temperature heat capacity measurements takes precedence over the high-temperature enthalpy measurements during the merging of the two data sets to obtain smooth high-temperature values. In the case of Cu_2S, enthalpy measurements were made as low as 350 K because the low-temperature calorimeter was not yet capable of measurements above 310 K, and the transition at 376 K was known.

ADIABATIC SOLUTION CALORIMETRY AND STANDARDS

by

Edward J. Prosen[1]

ABSTRACT

The high-accuracy platinum-lined adiabatic solution calorimeter of the National Bureau of Standards is described briefly. Its capabilities for working with highly corrosive substances, at temperatures from 278 K (5° C) to 368 K (95° C) and for reaction times as long as 20 hours, are illustrated. Values for the enthalpies of reaction of four different standards of Standard Reference Materials are given.

THE ADIABATIC SOLUTION CALORIMETER

The National Bureau of Standards (NBS) adiabatic solution calorimeter was designed and built primarily to develop standards for solution calorimetry and to determine the enthalpies of solution or reaction of standard reference materials similar to the materials that other scientists might wish to measure at university, Government, and other research laboratories both in the United States and abroad. With such standard reference materials made available by the NBS and with descriptions of high accuracy measurements, procedures, and apparatus developed by NBS, the scientists can test their apparatus, procedures, and analytical techniques on materials and reactions similar to those that they need to measure. By this means the thermochemical measurements in all the laboratories will be upgraded and will be put on a uniform scale of energy and temperature so that the resulting data will form a consistent set.

The adiabatic solution calorimeter used for all the work on standards for solution calorimetry has been described in detail elsewhere (14).[2] A brief description is given here, together with some reasons for the way it was constructed and a statement about how we use the quartz oscillator thermometer and its stability over a period of years. A diagram of the calorimeter is shown in figure 1. The calorimeter vessel (A in fig. 1) consists of a

[1]Chemical Thermodynamics Division, National Bureau of Standards, Washington, D.C.

[2]Underlined numbers in parentheses refer to items in the list of references at the end of the paper.

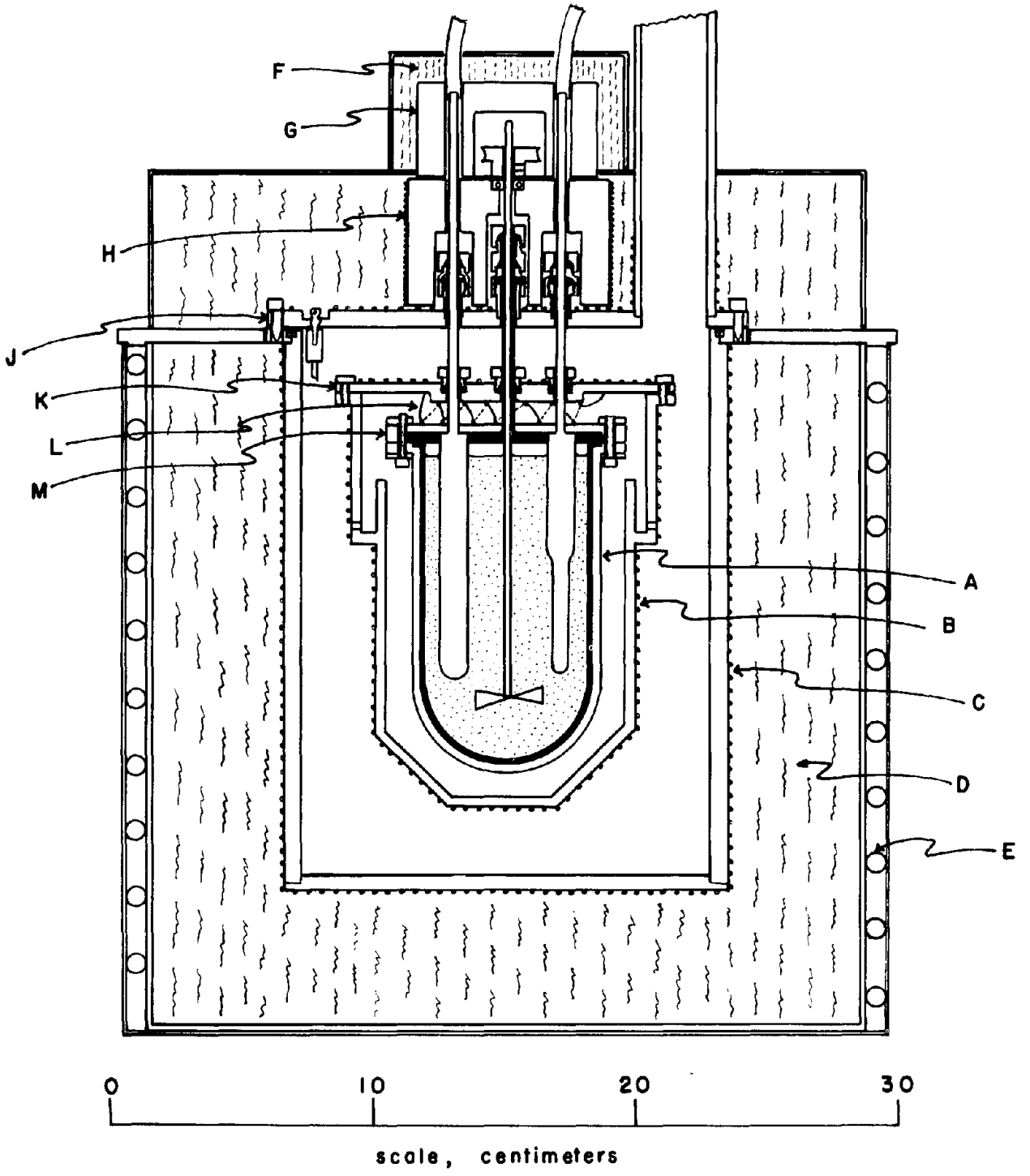


FIGURE 1. - Diagram of NBS Adiabatic Solution Calorimeter. (A) Calorimeter vessel. (B) Controlled adiabatic shield. (C) Copper jacket. (D) Fiberglass insulation. (E) Cooling coils. (F) Styrofoam insulation. (G) Aluminum block. (H) Controlled-temperature aluminum block. (J) Jacket cover (controlled-temperature). (K) Controlled-temperature shield lid. (L) Shield-control thermocouples. (M) Calorimeter vessel lid.

platinum-10 pct iridium cup, 0.8 mm thick, with a volume of approximately 350 ml. Pure silver was electroplated on the outside of this cup and then machined to a 3.2-mm layer. The silver was then plated with 0.08 mm of gold to provide good reflectivity. This construction was used because the high thermal conductivity of silver aids in providing an isothermal outer surface of the vessel which the adiabatic shield can follow in temperature. The lid of the vessel (M in fig. 1) is of the same layered construction but with a thicker platinum plate so that O-rings could be used for sealing the inserts. There are reentry wells made of Pt-10 pct Ir for the heater and for the platinum resistance thermometer capsule (later a quartz-oscillator probe) which protrude from the lid into the solution. There are also a platinum stirrer and a platinum sample holder held by the lid. The sample holder is sealed with polytetrafluoroethylene (PTFE), rubber, buna, or silicone rubber o-rings and can be triggered to open at the proper time. Thus the calorimeter can be used for highly corrosive materials such as 30 pct aqueous hydrofluoric acid up to about 368 K (95° C) since it only contacts platinum, Pt-10 pct Ir, or PTFE in the calorimeter. The adiabatic shield (B in fig. 1) was formed from vacuum-cast copper (to provide good thermal diffusivity) and was 3.2 mm thick and provided an annular space of approximately 10 mm around the calorimeter vessel. It consisted of a one-piece cup with a separate lid (K in fig. 1) from which the calorimeter vessel lid was suspended by the five thin platinum tubes which enter the calorimeter vessel. The platinum tubes also suspend the adiabatic shield from the outer nickel-plated copper jacket (C in fig. 1). The adiabatic shield has a heater wound around it and is automatically controlled to follow the calorimeter vessel temperature by means of a three-mode (proportional, reset, and rate) controller which can control the temperature to better than 1 mK. The differential (six junctions; L in fig. 1) thermocouples that drive the controller were placed between the lid of the adiabatic shield and the lid of the calorimeter vessel because the only heat conduction path from the calorimeter vessel is through the five platinum tubes (with the wires and the stirrer rod inside them). The jacket is evacuated to eliminate heat leak by air conduction and convection. The adiabatic shield very nearly eliminates heat leak by radiation. The jacket temperature is kept constant at a few degrees lower than the temperature of the experiment so that the adiabatic shield will always require some heating since there is no way of cooling it other than by radiation to the jacket. Conduction along the platinum tubes to the jacket lid is very nearly eliminated by separate controllers which keep the jacket lid (J in figure 1) and the tempering block (H in fig. 1) surrounding the platinum tubes (where they pass through the lid) at the same temperature as the adiabatic shield. A detailed diagram of the calorimeter vessel is shown in figure 2.

Further details on the calorimeter are given in the publications (1-12, 14-16) reporting work in which this calorimeter was used to measure various heats of solution or reaction. It has worked well even for reactions such as the solution of BeO(c) in aqueous HCl (10), which required a reaction period of approximately 20 hours for completion. It has been used for endothermic reactions by simultaneously adding electrical energy to compensate for the endothermic reaction such as the heat of solution of KCl(c) in water (8) or the endothermic reaction of tris (hydroxymethyl) aminomethane (c) in aqueous NaOH (15). It has been used for the heat of solution of various particle sizes of α-quartz and silica glass in 18 to 30 pct aqueous hydrofluoric acid at temperatures from 298 K (25° C) to 358 K (85° C) (12) with very good results.

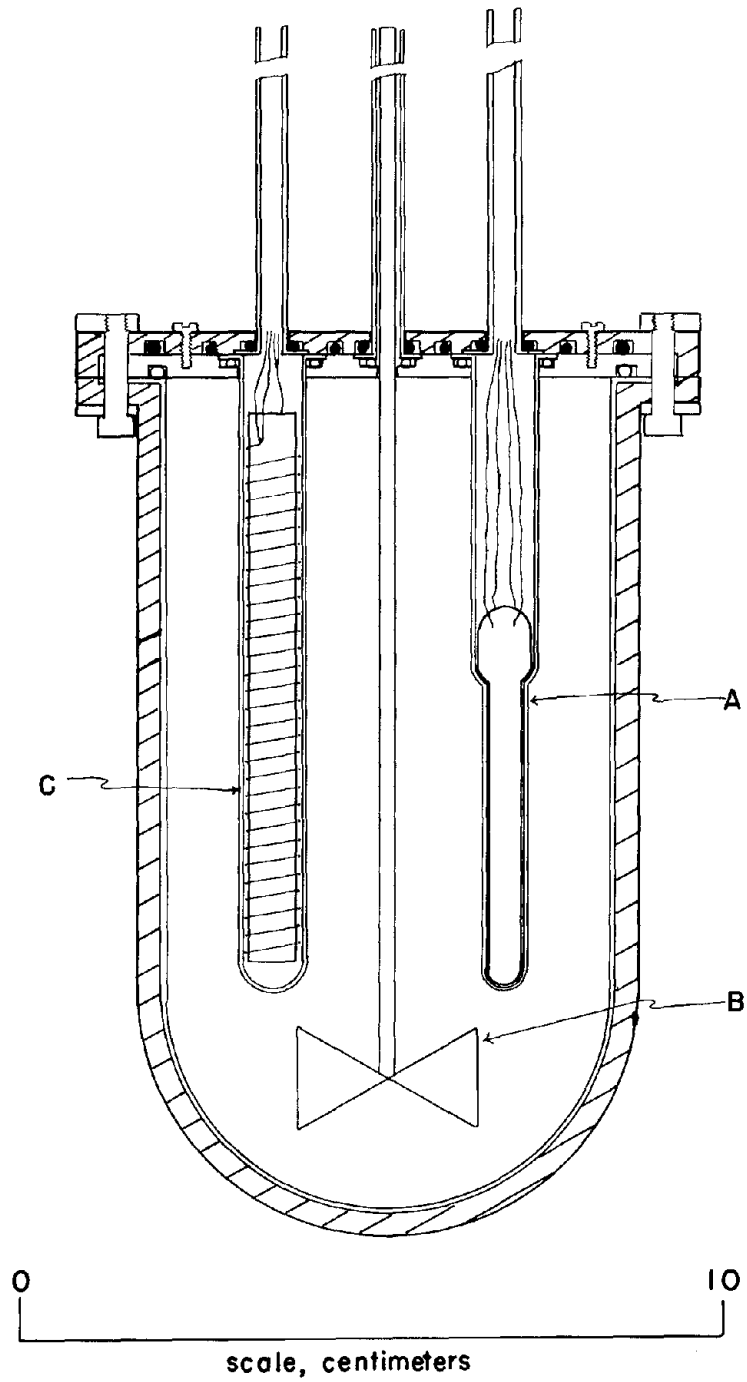


FIGURE 2. - Detailed diagram of Calorimeter Vessel. (A) Platinum re-entry well containing platinum resistance thermometer capsule. (B) Platinum stirrer. (C) Platinum re-entry well containing four-lead heater.

The use of a quartz-oscillator thermometer and digital recording equipment in place of a platinum resistance thermometer system for measuring the temperature rise of the calorimeter has made measurement and treatment of data much less cumbersome. We have now had about 10 years of experience in the use and stability of the quartz-oscillator thermometer and have made periodic calibrations against a platinum resistance thermometer. We found that the ice point drifts slowly with time, varying up to 20 mK. The absolute temperature is only important in assigning the enthalpy of reaction to a certain temperature, and 0.02 K is more than accurate enough for most reactions. We also found that the coefficient of change of frequency (f) with temperature in K, df/dT, stays constant to a few parts in 10,000 over the years. Thus for solution calorimetry, where electrical calibrations over the same range of temperatures are performed before and after each reaction experiment in the same day, df/dT is constant to 1 part in 100,000. Also the relation between temperature and frequency is very nearly linear (in most calibrations we could not find a significant quadratic term) from 293 K (20° C) to 363 K (90° C). Therefore it is not even necessary to convert from frequency to temperature, but we could just measure each rise in frequency (Hz). Thus the electrical calibration yields joules per kilohertz (kHz) rise, and the reaction experiment yields kHz rise per gram of reactant. The product of the two yields joules per gram of reactant. In our work we use a Hewlett-Packard (HP) 2850-D quartz probe and a HP 2830-A probe-oscillator. We use any 12 v ±0.02 pct power supply to drive it and a frequency counter (capable of direct counting at 30 MHz such as HP 5326-A) without a time base of its own. We trigger it to start counting with the NBS standard 100 kHz frequency (which is stable to 1 part in 10^{11}) and trigger it to stop after 100 seconds, or 10^7 pulses from the NBS standard frequency. The pulses occur at zero crossing on each cycle and are accurate to at least 0.01 cycle, thus providing a timing accuracy of at least one in 10^9. Since the quartz oscillator is 28,208 kHz at 273 K(0° C) with df/dT of 1 kHz/K, we get readings such as 2,823,812,345. Since we do not need the initial three significant digits, we let them overflow the seven-digit counter. The last significant digit represents 10 μK. For rating periods of 12 points, a least-squares straight line gives a standard error of 6 μK.

In retrospect, there are two changes that could have been made on the calorimeter: (1) The assembly of the vessel onto its lid requires inserting 12 screws and the assembly of the adiabatic shield onto its lid requires inserting 8 screws. These screws could have been replaced by some sort of quick-connect mechanism to eliminate the tedium. This was considered at the time, but those available were too bulky and the screws gave the best positive closure; (2) Stirring in the calorimeter vessel is very important. It must be sufficiently vigorous to dissolve solid materials quickly and the heat of stirring must remain as constant as possible. These have been achieved fairly well; however, at high speeds the stirrer tends to whip. Thus the propeller should perhaps be larger in diameter with larger blades and be shaped properly to achieve better, more stable stirring with slower speeds.

STANDARDS FOR SOLUTION CALORIMETRY

Several standard reactions have been developed for solution calorimetry. These are (1) sulfuric acid (aq) + sodium hydroxide (aq), (2) α-quartz (c) + hydrofluoric acid (aq), (3) tris(hydroxymethyl)aminomethane (c) + hydrochloric acid (aq) or sodium hydroxide (aq), and (4) KCl(c) + water (l). For the latter three there are Standard Reference Materials available from NBS together

with certified values for the heats (enthalpies) of solution at constant pressure. For sulfuric acid (aq) + sodium hydroxide (aq), CP or reagent grade materials are readily available from chemical manufacturers; the highest purity materials available should be used. The recommended enthalpy for this reaction and the certified enthalpies for the Standard Reference Material reactions are given below.

(1) Sulfuric Acid (aq) + NaOH(aq)

For the enthalpy of neutralization of $H_2SO_4 \cdot 8H_2O$ in $NaOH \cdot 262OH_2O$(~0.02M), the recommended value is (14)

$$H_2SO_4 \cdot 8H_2O + 2.36(NaOH \cdot 262OH_2O) = (Na_2SO_4 \cdot 36NaOH \cdot 6193H_2O)_{soln}$$

$$\Delta H(298.15\ K) = -590.692 \pm 0.101\ J \cdot g^{-1}\ \text{of}\ H_2SO_4.$$

In $NaOH \cdot 714H_2O$ (~0.08M) the recommended value is (14)

$$H_2SO_4 \cdot 8H_2O + 2.6\ (NaOH \cdot 714H_2O) = (Na_2SO_4 \cdot 0.6NaOH \cdot 1866H_2O)_{soln}$$
$$\Delta H(298.15\ K) = -590.828 \pm 0.193\ J \cdot g^{-1}\ \text{of}\ H_2SO_4.$$

(2) α-Quartz(c) + Hydrofluoric Acid (aq)

The enthalpy of solution of Standard Reference Material No. 1654 (α-quartz) at a concentration of 5 g in 1,000 cm^3 of 24.4 wt-pct HF(aq) at 353.15 K (80° C) is (9)

$$-\Delta H_{soln}(353.15\ K) = 2,362.2 \pm 1.1\ J \cdot g^{-1}.$$

The enthalpy of solution (in $J \cdot g^{-1}$) as a function of temperature, T, of the reaction in 24.4 wt pct HF(aq) in the range 298-358 K (9) is

$$-\Delta H_{soln}(T) = 2,275.0 + 1.586(T-298.15).$$

As a function of the concentration of the HF solution in the range 18 to 30 wt-pct (9) (corrected), the enthalpy per gram is

$$-\Delta H_{soln}(353.15\ K) = 2,362.20 + 1.398\ (Wp - 24.40) + 0.0714\ (Wp - 24.40)^2,$$

where Wp represents weight-percent HF (aq). The standard error of the estimate is $\pm 1.7\ J \cdot g^{-1}$.

(3) Tris(hydroxymethyl)aminomethane (c)

The enthalpy of reaction per gram of Standard Reference Material No. 724 [tris(hydroxymethyl)aminomethane(c)] with 0.100, N hydrochloric acid solution at a concentration of 5 g/l at 298.15 K (25° C) (15) is

$$\Delta H(298.15\ K) = -245.76 \pm 0.26\ J \cdot g^{-1}.$$

The enthalpy (endothermic) of reaction of the sample with 0.0500, N sodium hydroxide solution at a concentration of 5 g/l of solution at 298.15 K (25° C) (15) is

$$\Delta H(298.15\ K) = +141.80 \pm 0.19\ J \cdot g^{-1}.$$

The enthalpy of this reaction as a function of sodium hydroxide concentration is

$$\Delta H(298.15\ K) = +146.03 - 87.8(\underline{N}) + 43.2(\underline{N})^2,$$

where enthalpy change is in $J \cdot g^{-1}$, and $\underline{N}$ is the normality of the NaOH solution in the range 0.005 to 1.000$\underline{N}$. The standard error of the estimate is 0.19 $J \cdot g^{-1}$.

(4) Potassium Chloride (c) + Water (1)

The enthalpy (endothermic) of solution per gram of Standard Reference Material No. 1655 [KCl(c)] (dried at least 4 hours at 800 K) at infinite dilution in water at 298.15 K (25° C), (8) is

$$\Delta H(298.15\ K) = 231.18 \pm 0.27\ J \cdot g^{-1}.$$

The measured enthalpy change was corrected to infinite dilution, which is the reference state, using Parker's values in table XV-A (13) for the enthalpy of dilution of KCl.

REFERENCES

1. Cases, J. C., V. B. Parker, and M. V. Kilday. Enthalpy of Solution of Sodium Nitrite. J. Res. NBS, v. 82, 1977, pp. 19-28.

2. Efimov, M. E., G. N. Klevaichuk, V. A. Medvedev, and M. V. Kilday. Enthalpies of Solution of KBr, KI, KIO_3, and KIO_4 in H_2O. J. Res. NBS, v. 84, 1979, pp. 273-286.

3. Kilday, M. V. Enthalpies of Solution of the Nucleic Acid Bases. 1. Adenine in Water. J. Res. NBS, v. 83, 1978, pp. 347-370.

4. _____. Enthalpies of Solution of the Nucleic Acid Bases. 2. Thymine in water. J. Res. NBS, v. 83, 1978, pp. 529-537.

5. _____. Enthalpies of Solution of the Nucleic Acid Bases. 3. Cystosine in Water. J. Res. NBS, v. 83, 1978, pp. 539-546.

6. _____. Enthalpies of Solution of the Nucleic Acid Bases. 4. Uracil in Water. J. Res. NBS, v. 83, 1978, pp. 547-554.

7. _____. Enthalpies of Solution of the Nucleic Acid Bases. 5. Adenine in Aqueous Hydrochloric Acid, Aqueous Sodium Hydroxide, Methanol, and Ethanol. J. Res. NBS, v. 84, 1979.

8. Kilday, M. V. The Enthalpy of Solution of KCl (SRM 999) in H_2O. J. Res. NBS, v. 85, 1980, in press.

9. Kilday, M. V., and E. J. Prosen. The Enthalpy of Solution of Low Quartz (α- quartz) in Aqueous Hydrofluoric Acid. J. Res. NBS, v. 77A, 1973, pp. 205-215.

10. Kilday, M. V., E. J. Prosen, and D. D. Wagman. Enthalpies of Solution of BeO(c) in HF(aq) and in HCl(aq). J. Res. NBS, v. 77A, 1973, pp. 217-225.

11. Nuttall, R. L., K. L. Churney, and M. V. Kilday. The Enthalpy of Formation of MoF_6 (l) by Solution Calorimetry. J. Res. NBS, v. 83, 1978, pp. 335-345.

12. Nuttall, R. L., A. H. Laufer, and M. V. Kilday. The Enthalpy of Formation of Ketene. J. Chem. Thermodyn., v. 3, 1971, pp. 167-174.

13. Parker, V. B. Thermal Properties of Uni-univalent Electrolytes. Nat. Stand. Ref. Data Ser. NSRDS - NBS, v. 2, April 1965, 66 pp.

14. Prosen, E. J., and M.V. Kilday. An Adiabatic Solution Calorimeter and Measurements of a Standard Reaction for Solution Calorimetry. J. Res. NBS, v. 77A, 1973, pp. 179-203.

15. Prosen, E. J., and M. V. Kilday. Enthalpies of Reaction of Tris (hydroxymethyl)aminomethane in HCl(aq) and in NaOH(aq). J. Res. NBS, v. 77A, 1973, pp. 581-589.

16. Wagman, D. D., and M. V. Kilday. Enthalpies of Precipitation of Silver Halides; Entropy of the Aqueous Silver Ion. J. Res. NBS, v. 77A, 1973, pp. 569-579.

DISCUSSION

Anonymous: What would be the difference in the DC compared to the AC bridge for measuring platinum thermometry?

E. J. Prosen: I am not the expert on that. I think we have a better expert here from Bureau of Standards. The AC bridge is pretty much taken over as far as precision resistance thermometry goes. In our results, we put a straight line through the quartz versus platinum data. We would get agreement within 0.4 of a millidegree, but now when we use a quartz thermometer we can find a quadratic in the first place which we couldn't find before because it was in the band. The standard error of the fit is on the order of 0.1 of a millidegree, so it means our platinum thermometry is much better than with the quartz thermometer.

G. T. Furukawa: We have an AC bridge designed by R. D. Cutkosky of the NBS which operates at 400 Hz. AC and DC measurements yield different values depending upon the resistor configuration and measurement environment. The "AC effect" seems to be smaller with bifilarly wound platinum resistance thermometers. We have been using the AC bridge for comparison measurements under similar measurement conditions. In recent measurements at the triple point of water using the AC bridge with a Meyers-type bifilarly wound thermometer, we obtained among seven independent readings on a cell over a 3-day period, in which the thermometer was removed and reinserted between readings, a range of 0.01_4 mK.

E. J. Prosen: I think in summary you can do as good with a DC bridge, but

you have to be very careful. You have to do a lot of calibration, and you have to worry about the temperature much more than with an AC bridge. On the other hand, an AC bridge is very stable with time; you know the ratio, and the number of terms doesn't change with time. It can be automated much cheaper than automating a DC bridge, and overall it is easier to get high accuracy with an AC bridge than with a DC bridge. I am not saying that with a lot of work you can't do well with a DC bridge too.

G. T. Furukawa: We have a DC current comparator bridge based on the design by N. L. Kusters of the NRC. In recent measurements using the bridge with two capsule-type thermometers at the triple point of argon, the range of 8 or 10 observations over a 2-week period was not more than 0.01 mK.

E. J. Prosen: Yes, there was a paper on this at the recent calorimetry conference.

SULFIDE SOLUTION CALORIMETRY - A NOVEL METHOD

by

J. M. Stuve[1]

ABSTRACT

This presentation is a preliminary report of a novel calorimetric method investigated by the Bureau of Mines for determining formation enthalpies of sulfide minerals. The solution chemistry of sulfides in acidic bromine solutions and attendant problems related to accurate calorimetric measurement are discussed. Details of a bromine reaction calorimeter under development are described, and its application to a variety of complex sulfide minerals is outlined.

INTRODUCTION

A need for accurate thermodynamic data for metallurgically prominent sulfide minerals has interested the Bureau of Mines in investigation of improved calorimetric methods for obtaining formation energies. Many of the transition metal sulfides are not amenable to conventional methods of acidic solution calorimetry because of their poor solubility. Accordingly, the formation data for these important materials are often derived from indirect methods such as high-temperature dissociation pressure and electromotive force measurements.

METHOD

The Bureau has developed a novel approach to the calorimetric problem based on direct measurement of the formation enthalpies using acidic bromine solutions at elevated temperatures in a sealed reaction vessel. The composition of this solvent is 2.5 molar hydrobromic acid with 1 molar dissolved bromine complexed as the tribromide anion. Entensive tests of various other mineral acid compositions were made before selection of this hydrobromic-tribromide solvent.

The dissolution of a typical mineral sulfide such as covellite (CuS) proceeds in two distinct stages as shown by the following reactions:

[1]Research chemist, Albany Research Center, Bureau of Mines, Albany, Oreg.

$$2CuS(c) + 3Br_3^- \xrightarrow{fast} 2Cu^{++} + S_2Br_2(\ell) + 7Br^- \quad (1)$$

$$S_2Br_2(\ell) + 5Br_3^- + 8H_2O \xrightarrow{slow} 2SO_4^{=} + 17Br^- + 16H^+. \quad (2)$$

The overall net reaction is

$$CuS(c) + 4Br_3^- + 4H_2O = Cu^{++} + SO_4^{=} + 12Br^- + 8H^+. \quad (3)$$

At 40° C and with moderate stirring, reaction 1 occurs quite rapidly - in the order of 10 minutes to form a heavy oily phase of S_2Br_2, sulfur dibromide, which settles to the bottom of the reaction vessel - usually in a single globule. Reaction 2, which ultimately forms sulfate ($SO_4^=$), proceeds at a much slower rate. It usually takes about 2 hours to form a homogeneous solution using conditions required for accurate calorimetric measurement.

The above reactions are an obvious oversimplification of the actual chemistry involved; however, they do accurately reflect the overall stoichiometry. Undoubtably sulfate formation is preceded by a complex series of intermediate reactions producing various thionic species. In any case, the final composition of the acid-bromine solution in the postreaction period appears nominally reproducible and thermally stable.

After identifying the principal reaction paths, considerable effort was expended in finding a catalytic material to accelerate the reaction of sulfur dibiomide to sulfate. A wide variety of homogeneous and heterogeneous (surface active) types were evaluated. No effective catalyst was found.

Two important variables that increase the sulfur dibromide reaction rate are temperature and stirring. Unfortunately, temperature increases are restricted by the relatively high vapor pressure of bromine (normal boiling temperature = 59° C) and the extreme corrosiveness of the bromine solution. The rate of stirring must be moderated to limit the resulting heating effect to a reasonable level.

The details of the current calorimetric apparatus are shown in figure 1. A carefully sealed, adiabatic calorimeter was designed and constructed to overcome the inherent problems of this reaction scheme. All reaction vessel components exposed to bromine or its vapor were fabricated from high-purity tantalum alloy. The volume of the solvent chamber is approximately 500 cm^3. Demountable parts are sealed with polyfluorocarbon O-rings to provide gastight joints. The sample material is sealed in a thin-walled glass ampoule suspended at the top center of the reaction vessel. Stirring is accomplished by magnetic coupling at the bottom to avoid the leakage and heating problems of rotary shaft seals. The entire reaction vessel assembly and adiabatic shields

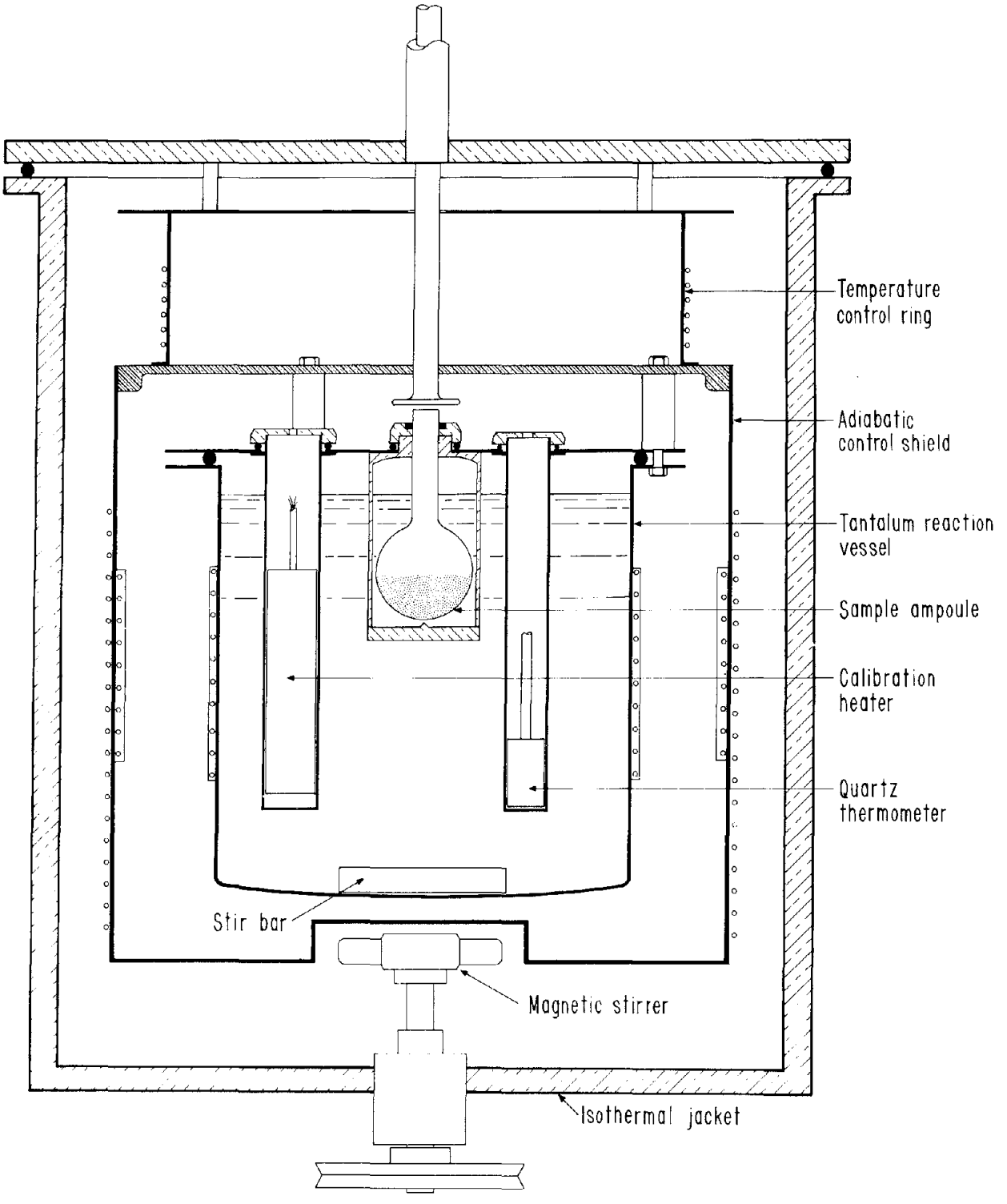


FIGURE 1. - Bromine reaction calorimeter.

are enclosed within a heavy, sealed copper jacket which is thermostated in a temperature-controlled water bath.

The primary adiabatic shield is concentric to the tantalum reaction vessel and has a control heater winding on its outer surface. The inner surface is partially covered with a resistance thermometer winding carefully matched to a similar winding on the outer surface of the tantalum reaction vessel. These thermometers are wired in a Wheatstone bridge configuration to accurately measure the temperature offset between the shield and the reaction vessel. The bridge is powered by a Zener diode stabilized constant-current source. Temperature imbalance is detected as a low-level dc voltage and is monitored by a high-gain current-adjusting controller with rate, reset, and proportional band adjustments. The analog output current of the controller drives a programable-gain power supply coupled to the shield heater winding to maintain quasi-adiabatic conditions. The temperature error band at steady state conditions is about ±0.001° C.

A secondary control system of similar design monitors the temperature difference between the adiabatic shield and the lead bundle components above. This control circuit is identical in function and design to the adiabatic shield circuit except the temperature differential sensors are copper-constantan thermocouples.

Precision temperature measurements of the reaction media are obtained using a quartz thermometer with a maximum resolution of 0.00001° C for a 100-sec counting period. Accurate energy calibration of the system is obtained for each solution run in situ with a 1,000-ohm Karma wire resistor located in a reentrant well. The heater current and voltage are alternately monitored with a high-impedance digital voltmeter during the calibration period.

DISCUSSION

The most appealing aspect of this novel method is its ability to dissolve a wide range of metal sulfides which resist conventional acidic calorimetry. Successful solution tests have been made on samples of Cu_3AsS_3, NiS, Ni_3S_2, PbS, HgS, CdS, AsS, Cu_5FeS_4, $CuFeS_2$, ZnS (sphalerite and wurtzite), CuS, Cu_2S, CeS, and FeS. Molybdenum disulfide (MoS_2) and Ag_2S are examples of sulfides that are not amenable to this solution technique.

One of the most important materials that reacts to form sulfate ion is elemental (rhombic) sulfur, which greatly simplifies the reaction sequence required to determine a formation enthalpy. For example, the calorimetric scheme for the mineral covellite would be composed of the following reactions:

$$CuS(c) + 4Br_3^- + 4H_2O = Cu^{++} + SO_4^{=} + 12Br^- + 8H^+ \quad (3)$$

$$Cu(c) + Br_3^- = Cu^{++} + 3Br^- \quad (4)$$

$$S(c) + 4H_2O + 3Br_3^- = SO_4^{=} + 9Br^- + 8H^+ \quad (5)$$

$$Cu(c) + S(c) = CuS(c) \qquad (6)$$

The formation enthalpy in this case is simply $\Delta H_6 = \Delta H_4 + \Delta H_5 - \Delta H_3$. Since rhombic sulfur, S(c), and copper metal do not react to any significant degree near ambient temperature, both materials could be weighed in the proper stoichiometric ratio and sealed in the same ampoule and dissolved together.

The major disadvantage of the method is the requirement of handling a highly corrosive and toxic material such as bromine. Access to a strong hood ventilation system is essential for safe operation.

From the viewpoint of accuracy, the method requires a relatively precise and sensitive calorimetric design because the heats of solution are quite large - about 200 to 300 kcal per mole of sulfide. The formation energy of many transition metal sulfides is about -5 to -30 kcal; thus the resulting experimental measurement is analogous of seeking accuracy in small differences of relatively large numbers.

DISCUSSION

Y. A. Chang: Have you considered the direct reaction of copper or any metal with sulfur as a basis of measuring its heats of formation?

J. M. Stuve: Yes we have, but the work in this area that I am aware of doesn't indicate a very high accuracy in some cases. It has been done, and it may be a good method for some sulfides, I don't know.

N. A. Gokcen: Incidentally, the method that John Stuve is going to use is useful not only for stoichiometric compounds, but also for nonstoichiometric compounds, such as iron-sulfur compounds that vary in sulfur-to-iron ratio.

J. M. Stuve: I would like to add to that. Probably the major problem you would find by direct-reaction calorimetry would be the formation of many different nonstoichiometric phases.

E. F. Westrum: Why did you choose to run Cu_2S? There are many values reported in the literature for it.

J. M. Stuve: The choice of Cu_2S was not by accident. We feel that Cu_2S has some of the best data available for it, so it would provide a good standard.

DETERMINATION OF ENTHALPIES OF FORMATION BY SOLUTION CALORIMETRY

by

H. C. Ko[1]

ABSTRACT

The basic principle of determining enthalpies of formation by solution calorimetry is described. Brief descriptions of the HCl solution colorimeter and experimental techniques are given. As examples of compounds studied at the Albany Research Center, results of enthalpies of formation of magnesium sulfates (α-$MgSO_4$ and β-$MgSO_4$) are discussed. Problems generally encountered in solution calorimetry are breifly discussed.

This research is a part of the effort by the Bureau of Mines to provide thermodynamic data for the advancement of mineral resource technology, environmental conservation, and energy economy.

INTRODUCTION

The enthalpy of formation of a compound AB is defined as the heat of the following reaction:

$$A + B = AB, \tag{1}$$

where A and B are the elements in their standard reference states and AB is in its standard state, all at 1 atm and 298.15 K. Often it is difficult or impossible to measure directly heats of reaction of this type. One has to resort to the indirect method of determining the enthalpy of formation of AB by the following route:

$$AB + CD = AD + CB, \tag{2}$$

$$\Delta H_2 = \Delta H_f^\circ(AD) + \Delta H_f^\circ(CB) - \Delta H_f^\circ(AB) - \Delta H_f^\circ(CD).$$

If ΔH_2, the heat of reaction of 2, and the enthalpies of formation, ΔH_f, of AD, CB, and CD are known, then the enthalpy of formation of AB can be obtained. The determination of the heat of the overall reaction 2 by HCl solution

[1]Research chemist, Albany Research Center, Bureau of Mines, Albany, Oreg.

calorimetry is the subject matter of this paper.

While the solution calorimeter cannot be used for direct determination of enthalpies of formation, it often provides the best, simplest, and often only means of determining enthalpies of formation or transition of inorganic compounds. The method is particularly valuable for silicates and other mixed oxides of two or more elements, hydrated salts, and other complex materials for which direct determination of enthalpy of formation would be extremely difficult or impossible.

The basic principle involved in determining heats of reaction by heats of solution is simple. The heat of reaction 2 mentioned above is simply the sum of the heats of solution of AB and CD minus the sum of heats of solution of AD and CB, provided the reactions are conducted at the same temperature and under conditions of strict chemical stoichiometry. Equimolar amounts of AB and CD are dissolved, either simultaneously or consecutively, in a weighed portion of solvent. Similarly, equimolar amounts of AD and CB are dissolved in a second weighed portion of the same solvent. The following reaction

$$AB = A^+(sol) + B^-(sol) \tag{3}$$

represents the dissolution and ionization of AB in a certain solvent. Similarly,

$$CD = C^+(sol) + D^-(sol), \tag{4}$$

$$AD = A^+(sol) + D^-(sol), \tag{5}$$

$$CB = C^+(sol) + B^-(sol), \tag{6}$$

The resulting solution from reactions 3 and 4 is identical with the resulting solution from reactions 5 and 6; that is,

$$(2) = (3) + (4) - (5) - (6)$$

where the numbers in parentheses refer to the reactions. Thus, the heat of the overall reaction can be obtained by

$$\Delta H_2 = \Delta H_3 + \Delta H_4 - \Delta H_5 - \Delta H_6,$$

where ΔH_3, ΔH_4, ΔH_5, and ΔH_6 are the experimentally determined heats of solution.

APPARATUS AND PROCEDURE

The Solution Calorimeter

The calorimeter is similar to that described by Southard (6)[2] with minor

[2]Underlined numbers in parenthese refer to items in the list of references at the end of the paper.

modifications by Young (8), Coughlin (2), and Mrazek(5). The reaction vessel shown in figure 1 is a narrow-necked glass Dewar flask having a capacity of about 2 liters. The flask is submerged in a constant-temperature water bath controlled at room temperature to ±0.003° C. The brass cover plate is sealed to the flask with an O-ring. The resistance thermometer and calibration heater are wound on the innermost of the two concentric thin-walled copper tubes, which are sealed at the ends and suspended from the cover plate by three tubes of low-conductivity copper-nickel alloy. These tubes also serve as conduits for the lead wires to the thermometer and the heater. To prevent corrosion from acid (calorimeter liquid), all exposed metal parts of the calorimeter are coated with acid-resistant OKUN's[3] liquid vinyl. The water level of the thermostat is approximately 2 inches above the copper plate of the Dewar flask.

The thin-walled, hollow tantalum stirrer shaft is supported by two ball bearings housed in a collar tube, which is welded on the top of the cover plate. The glass sample bulb is sealed at the end of a long glass rod that extends up through the stirrer shaft to the outside. The Teflon impeller is so constructed that the stirrer is rotated at about 1,000 rpm in the direction to force the calorimeter liquid down the center of the thermometer tube and against the bottom of the flask. This stirring forces any sample material settling at the bottom of the flask to continuous washing and thus hastens dissolution of the sample. Breaking of the sample bulb is accomplished by stopping the stirring momentarily and pulling the glass rod up against three sharp protruding prongs which are welded near the end of the stirrer shaft and below the impeller. Stirring is immediately resumed afterwards.

Temperature measurements are made with a copper-manganin resistance thermometer of the transposed bridge type described by Maier (4). It has a null point at about 20° C and a sensitivity of about 1,160 μv per degree when operated at a fixed thermometer current of 2 ma. A high-sensitivity nanovolt galvanometer, coupled with a Leeds and Northrup six-dial potentiometer, permits potential measurements accurate to 0.02 μv or approximately 0.00002° C. The calibration heater is made with manganin wire having a resistance of about 100 ohms. Energy input during calibration of the calorimeter system is supplied by a Hewlett-Packard dc constant-current source and is measured with the same galvanometer and potentiometer combination and a Monsanto counter-timer.

Experimental Procedure

The prodecure for a typical heat-of-solution experiment can be summarized as follows;

Approximately 2 liters of solvent liquid [4.360 molal hydrochloric acid or (HCl + 12.731 H_2O)], weighed to ±0.1 g, is poured into the Dewar flask. The temperature of the liquid is adjusted to slightly below 25° C. The glass rod with the sealed bulb containing a weighed amount of sample is assembled in place, and the entire calorimeter assembly is submerged into the bath and

[3]Reference to specific brand names is made for identification only and does not imply endorsement by the Bureau of Mines.

clamped in place. Stirring is started, and all electrical connections are made. Rough temperature measurements are recorded. If the temperarture of the calorimeter liquid is too much below 25° C, the calibration heater can be used to increase the temperature. After about 1 to 1-1/2 hours, the calorimeter attains equilibrium with the bath and a steady drift is reached . The experiment is begun at this point with temperature readings, in terms of microvolts, taken at regular intervals of 2 min which are registered with an electric timer accurate to 0.01 min. At a predetermined microvolt reading, the sample bulb is broken and readings are continuously taken. When the system reaches equilibrium again, as indicated by more or less steady drift, calibration of the system begins. The calibration heater is switched on, simultaneously turning on the counter-timer. A precisely determined amount of electrical energy is introduced into the calorimeter system. The heater current and duration of the heating period can be varied to simulate the condition of the solution run. During the heating period, the energy input is determined by measuring the potential drop across a standard resistor in series with the calibration heater. The resistance of the calibration heater has been previously determined. After the heating period, temperature versus time readings are taken again for about 30 min.

From the energy input and the temperature increase due to calibration heating, the heat capacity of the system is calculated. The heat of solution of the sample is calculated from the actual temperature change due to solution and the heat capacity of the system. The principle of calculation of results from recorded data is similar to that described by Coughlin (3).

EXAMPLES OF COMPOUNDS STUDIED

As an example for determination of enthalpies of formation by soltuion calorimetry, the results for α-$MgSO_4$ and β-$MgSO_4$ are presented in this paper. The calorimetric reaction schemes for α-$MgSO_4$ and β-$MgSO_4$ are shown in tables 1-2.

TABLE 1. - Calorimetric reaction scheme for α-$MgSO_4$(c) at 298.15 K

	Reaction	ΔH, kcal	Uncertainty, kcal
(7)	$(H_2SO_4+6H_2O)(\ell)=2H^+(sol) + SO_4^{2-}(sol) + 6H_2O(sol)$	-1.242	0.007
(8)	$MgO(c) + 2H^+(sol) = Mg^{2+}(sol) + H_2O(sol)$	-36.182	.033
(9)	$7H_2O(\ell) = 7H_2O(sol)$	-0.537	.007
(10)	α-$MgSO_4(c) = Mg^{2+}(sol) + SO_4^{2-}(sol)$	-13.327	.014
(11)	$MgO(c) + (H_2SO_4+6H_2O)(\ell) = \alpha$-$MgSO_4(c) + 7H_2O(\ell)$ $\Delta H_{11} = \Delta H_7 + \Delta H_8 - \Delta H_9 - \Delta H_{10} = -23.560 \pm 0.037$ kcal		

TABLE 2. - Calorimetric reaction scheme for β-$MgSO_4$(c) at 298.15 K

Reaction	ΔH, kcal	Uncertainty, kcal
(7) $(H_2SO_4+6H_2O)(\ell) = 2H^+(sol) + SO_4^{2-}(sol) + 6H_2O(sol)$	-1.242	0.007
(8) $MgO(c) + 2H^+(sol) = Mg^{2+}(sol) + H_2O(sol)$	-36.182	.033
(9) $7H_2O(\ell) = 7H_2O(sol)$	-0.537	.007
(12) β-$MgSO_4(c) = Mg^{2+}(sol) + SO_4^{2-}(sol)$	-14.243	.025
(13) $MgO(c) + (H_2SO_4+6H_2O)(\ell) = \beta\text{-}MgSO_4(c) + 7H_2O(\ell)$		

$\Delta H_{13} = \Delta H_7 + \Delta H_8 - \Delta H_9 - \Delta H_{12} = -22.644 \pm 0.043$ kcal

The symbols c, ℓ, and sol denote substances that are crystalline, liquid, and in solution, respectively. The solvent medium is 4.360 molal hydrochloric acid. The reactions are written so as to show that appropriate stoichiometry is maintained. The set of reaction 7-8 was measured consecutively in one batch of 2,260 g of solvent, and the set of reactions 9-10, as well as 9 and 12, was measured in 2,260 g of a fresh portion of solvent. Each reaction was carried out at least six times, and the average measured heat values and uncertainties are included in tables 1-2.

The overall calorimetric reactions 11 and 13 and their heats of reactions were obtained as mentioned earlier. the enthalpies of formation of α-$MgSO_4$ and β-$MgSO_4$ were calculated by combining reactions 11 and 13 and their heats with enthalpies of formation of MgO(c)(1), $H_2O(\ell)$(7), and $(H_2SO_4 + 6H_2O)(\ell)$(7) as shown in table 3. The enthalpy of transition from α-$MgSO_4$ to β-$MgSO_4$ was also calculated as shown in table 3.

TABLE 3. - Derivation of enthalpies of formation of α-$MgSO_4$(c) and β-$MgSO_4$(c) at 298.15 K

Reaction	ΔH, kcal	Uncertainty, kcal
(11) $MgO(c) + (H_2SO_4+6H_2O)(\ell) = \alpha\text{-}MgSO_4(c) + 7H_2O(\ell)$	-23.560	0.037
(13) $MgO(c) + (H_2SO_4+6H_2O)(\ell) = B\text{-}MgSO_4(c) + 7H_2O(\ell)$	-22.644	.043
(14) $Mg(c) + 1/2\ O_2(g) = MgO(c)$	-143.76	.07
(15) $H_2(g) + S(rh) + 2O_2(g) + 6H_2O(\ell) = (H_2SO_4+6H_2O)(\ell)$	-208.944	.100
(16) $H_2(g) + 1/2\ O_2(g) = H_2O(\ell)$	-68.315	.010

(17) $Mg(c) + S(rh) + 2O_2(g) = \alpha\text{-}MgSO_4(c)$

$\Delta H_f^\circ[\alpha\text{-}MgSO_4(c)] = \Delta H_{17} = \Delta H_{11} + \Delta H_{14} + \Delta H_{15} - \Delta_{16} = -307.95 \pm 0.13$ kcal/mole

(18) $Mg(c) + S(rh) + 2O_2(g) = \beta\text{=}MgSO_4(c)$

$\Delta H_f^\circ[\beta\text{-}MgSO_4(c)] = \Delta H_{18} = \Delta H_{13} + \Delta H_{14} + \Delta H_{15} - \Delta H_{16} = -307.03 \pm 0.13$ kcal/mole

(19) $\alpha\text{-}MgSO_4(c) = \beta\text{-}MgSO_4(c)$

$\Delta H^\circ_{trs} = \Delta H_{18} - \Delta H_{17} = 0.92 \pm 0.18$ kcal/mole

DISCUSSION

There are several aspects of solution calorimetry that deserve special attention:

1. The precise knowledge of the exact final thermodynamic state in any single reaction step is unnecessary so long as the final reaction steps from each series produce identical products. For example, $H_2SO_4(aq)$ is dissociated into $H^+(aq)$ and $HSO_4^-(aq)$ completely, but only less than 1 pct of $HSO_4^-(aq)$ dissociates further into $H^+(aq)$ and $SO_4^{2-}(aq)$. Even though reactions 7, 10, and 12 are written as formation of $SO_4^{2-}(sol)$, it is immaterial so long as they are identical thermodynamic states. The exact stoichiometry in a series of heat-of-solution steps, however, is important. If x millimoles of $MgSO_4(c)$ are used in reaction 9, then x millimoles of $(H_2SO_4 + 6H_2O)(\ell)$, x millimoles of MgO(c), and 7x millimoles of $H_2O(\ell)$ must be used.

2. Auxiliary compounds should be chosen with the following criteria in mind: stability in handling, dissolution feasibility in the chosen solvent medium, and accurately known enthalpy of formation.

3. If the reaction steps involve formation of precipitates, it must be determined definitely that the sample has completely dissolved or reacted. The precipitates should be collected and examined for any evidence of trapped or undissolved sample. If any doubt exists, a chemical analysis should be made to determine whether any undissolved sample remains.

4. When a series of compounds of a multivalent metal is being studied, it is usually necessary to use oxidizing or reducing agents in the reaction scheme. The choice of suitable oxidizers is actually limited because it is necessary to make measurements with both the oxidizing agent and the reduced form of the oxidizer, while being restricted to soluble compounds of accurately known enthalpy of formation.

5. When gas evolution is involved in a reaction, the assumption is generally made that all of the gas formed leaves the calorimeter. Quite often, only part of it escapes and some of it remains in the solution. In this case, two correction terms must be applied to the apparent heat of solution: correction for the heat of vaporization of water and other volatile components of the solution by the escaping gas, and correction for removal of the remaining dissolved gas from the solution to the gas phase.

In summary, the determination of enthalpies of formation by solution calorimetry can be the best and only means, especially for some inorganic complex materials when a direct determination would be difficult or impossible. The calorimeter described is capable of high precision and accuracy when operated under carefully controlled conditions as discussed earlier.

REFERENCES

1. Committee on Data for Science and Technology, International Council of Scientific Unions. CODATA Recommended Key Values for Thermodynamics. CODATA Bull. 17, 1976.

2. Coughlin, J. P. High Temperature Heat Contents, Heats of Transition and Heat of Fusion of Anhydrous Sodium Sulfate. J. Am. Chem. Soc., v. 77, 1955, pp. 868-870.

3. ———. Solution Caliorimetry and Silicate Thermochemistry. Ch. 14 in Experimental Thermochemistry, v. II, ed. by H. A. Skinner. Interscience Publishers, New York, 1962, pp. 293-320.

4. Maier, C. G. Resistance Thermometers for Chemists. J. Phys. Chem., v. 34, 1930, pp. 2860-2868.

5. Mrazek, R. V., D. W. Richardson, H. O. Poppleton, and F. E. Block. Determination of the Heat of Formation of Vanadium Trichloride. BuMines RI 7096, 1968, 15 pp.

6. Southard, J. C. Heat of Hydration of Calcium Sulfates. Ind. and Eng. Chem., v. 32, 1940, pp. 442-445.

7. Wagman, D. D., W. H. Evans, V. B. Parker, I. Halow, S. M. Bailey, and R. H. Schumm. Selected Values of Chemical Thermodynamic Properties. NBS Tech. Note 270-3, 1968, 264 pp.

8. Young, F. E. Heats of Formation of $Al_2(SO_4)_3.6H_2O$, $Al_2(SO_4)_3$, $KAl(SO_4)_2.12H_2O$, and $KAl(SO_4)_2$. J. Am. Chem. Soc., v. 67, 1945, pp. 257-261.

DISCUSSION

J. E. Bauman: Have you considered sulfate ion pairs in your analysis of these measurements?

H. C. Ko: I guess, in our experiments, we are mainly concerned with the overall reaction of the series. So, whatever the products, as long as you produce identical products in both series, they cancel out; therefore, we didn't look into the ion pair reactions that you mentioned.

SOME TECHNIQUES AND MEASUREMENTS WITH HF SOLUTION CALORIMETRY

by

K.O. Bennington[1]

ABSTRACT

Recent changes made in the 1-liter platinum alloy reaction vessel for the aqueous hydrofluoric acid solution calorimeter are presented. The top of the container was altered to use cone-shaped grease trap seals that matched the lid which carried the wells housing a miniature platinum resistance thermometer and Karma wire calibration heater. Heat of solution determinations provide the following data according to the associated reaction.

$$2Si_{(c)} + Fe_{(c)} + Na_{(c)} + 3O_{2(g)} \rightarrow NaFe^{3+}(Si_2O_6)_{(c)}$$

for which $\Delta H^{\circ}_{f298} = -615.98 \pm 0.72$ kcal.

This research is a part of the effort by the Bureau of Mines to provide thermodynamic data for the advancement of mineral resource technology, environmental preservation, and energy economy.

INTRODUCTION

A hydrofluoric acid solution calorimeter is used to obtain the enthalpies of formation of difficultly soluble silicates, titanates, zirconates, and oxides. The original Bureau of Mines apparatus was described by Torgeson and Sahama (8)[2] in 1948. It was built and operated at the Pacific Experiment Station by this laboratory, which was then located in Berkeley, Calif. Recent changes have also been published (1). An earlier HF solution calorimeter was described by Troitzsch (9) in a dissertation presented in Leipzig in 1935. Other similar equipment was built and operated at the Geophysical Laboratory, The Carnegie Institution of Washington by Kracek, Neuvonen, and Burley (4) and in Helsinki by Sahama and Neuvonen (7). The next generation of HF solution calorimeters were vacuum jacketed and were capable of making determinations on

[1]Research chemist, Albany Research Center, Bureau of Mines, Albany, Oreg.
[2]Underlined numbers in parentheses refer to items in the list of references at the end of the paper.

much slower reactions. A solution calorimeter was built and operated at the Geological Survey by Robie and Hemingway (6), and an adiabatic solution calorimeter was built, used and described by Prosen and Kilday (5) at the National Bureau of Standards.

Some variations from established practice and innovations pertinent to our measurements will be presented here.

THE APPARATUS

The reaction vessel, composed of a Pt-10 pct Rh alloy, has a capacity of approximately 1,100 ml and is fitted with three suspension eyes. There are two openings in the top: one is near the edge to accommodate the sample drop tube, and the other is slightly off center and accommodates the stirring rod and the thermometer and heater wells, which are mounted on the lid. The lid has a cone-shaped rim that fits over the cone-shaped flange on the reaction vessel. The cone-shaped flange is ringed with a shoulder that acts as an oil retention vapor seal. The reaction vessel is suspended from the jacket top by three Nichrome wire hooks, which are insulated from the jacket by small micarta block couplers. A radiation shield of copper foil surrounds the reaction vessell spaced between the vessel and the jacket. The jacket is of heavy copper and is sealed with an O-ring. The entire device is suspended in the constant-temperature water bath to a depth of 16 cm.

The bath temperature is controlled at approximately 74° ±0.001° C by a Bayley[3] proportional precision temperature controller.

The thermometer well, a part of the reaction vessel lid, was designed and built to accommodate a quartz thermometer. To date, however, a miniature platinum resistance thermometer has been used. Readings are made through a potentiometer and an electronic null detector. Complete automation is planned in the near future.

The calibration heater, also mounted in a well on the reaction vessel lid, is of Karma wire wound on a copper mandrel. Heater current is supplied by an adjustable dc constantcurrent source.

The temperature calibration of the reaction solution is made with an L & N certified platinum resistance thermometer. Heat of solution measurements are calibrated with very pure SiO_2, α-quartz, which has been compared against the NBS standard (3).

MATERIALS AND TECHNIQUES

To obtain consistent and uniformly reproducible results requires careful sample preparation and handling. Uniform particle sizes are necessary to obtain good dispersion, and to avoid clumping and prolonged reaction times.

[3]Reference to specific brand names is made for identification only and does not imply endorsement by the Bureau of Mines.

Washed and dried samples of silicates with particle sizes of minus 100 to plus 200 mesh for readily soluble minerals and minus 200 to plus 400 mesh for more difficultly soluble minerals generally circulate with the stirring and give reproducible results.

To disperse some samples quickly has required development of suitable mechanical means such as a bundle of Teflon thread attached to the gold ballast in the capsule, or Teflon granules mixed with the sample. Soluble chemical dispersion agents, such as carbonates, have never been used.

All samples, solid and liquid, are contained in Teflon tape capsules and are dropped at 25° C into the calorimeter. The capsules are sealed with paraffin and will spring open when the seals melt. These cylindrical capsules are sized to fit the individual sample and have an attached gold weight at the lower end; a fine Teflon or polyethelene retaining thread, or lanyard, is fastened to the drop tube stopper at the upper end. The capsule remains suspended and does not become entangled with the stirring apparatus. Samples must fall free and circulate unrestricted.

Compositions that react with great heat generation are restrained in concentric capsules. The outer capsule is perforated and latched so that it does not spring completely open. Particles are prevented from floating to the acid surface where they react with spattering.

Particular attention has been given to the handling of the calibration standard, α-quartz (SiO_2), which appears in many reaction schemes. Spectrographically pure natural material is sized carefully by eleutriation between plus 10 and minus 20 μM. It was repeatedly leached with hydrochloric acid until the solution remained clear and no iron test, with a sensitivity of 50 ppm, could be obtained. It was then repeatedly digested with hydrogen peroxide until no evidence of organic matter existed, following which it was thoroughly dried. Individually weighed samples were heated through the α-β transition before use. This last step has proved essential in obtaining uniform reaction rates, characteristically less than 30 min.

MEASUREMENTS

Acmite ($NaFe^{3+}Si_2O_6$) is a pyroxene mineral characteristic of many slag compositions, easily prepared synthetically, and of geochemical interest. A synthetic sample was used to determine the thermodynamic properties because of the need for high purity; the naturally occurring aegirine may contain many impurities. Manganese is a particularly common substituting element in this group of minerals; consequently, knowledge of acmite would later merge with the planned study of manganese pyroxene minerals.

The reaction scheme for acmite is presented in the following table, together with the heat of solution values, determined in the HF calorimeter, and their precision uncertainties. Reactions 1 through 4 are determined consecutively in the same acid solvent, and reactions 5 and 6 are determined

consecutively after a change of solvent. Stoichiometry requires that both reaction solutions be identical.

Sample sizes for all reactions are calculated stoichiometrically against the 0.601 g (0.01 mole) of SiO_2 that is used, and substituted, in reaction 1 (table 1). The smallest quantity for each reaction that will give reproducible results is most desirable. This is characteristically 0.3 to 0.7 g for solids and 2 to 4 g for liquids. Sample sizes for samples in these size ranges, used in the same stoichiometry, provide the same heat of solution value if an individual sample size is changed by a factor of from 1/2 to 2. Some very soluble salts, such as alkali chlorides, that do not show solution concentration effects and that provide a very small heat change may be increased in size by a factor of 3 or 4 in order to provide reproducible results.

The value from reaction 7, the overall calorimetric reaction, must be corrected with values from the literature to provide the standard enthalpy of formation for acmite. When this is accomplished, the standard reaction becomes

$$2Si_{(c)} + Fe_{(c)} + Na_{(c)} + 3O_{2(g)} \rightarrow NaFe^{3+}(Si_2O_6)_{(c)}$$

for which the enthalpy of formation is determined to be

$$\Delta Hf^{\circ}_{298} = -615.983 \pm 0.720 \text{ kcal.}$$

DISCUSSION

Hydrofluoric acid solution calorimetry is a long-established and well-proved method for providing otherwise unobtainable enthalpy of formation data at room temperature on difficultly soluble compounds. There are, however, several severe limitations, such as the generation of gas upon the dissolution of metals which precludes their use, the formation of insoluble precipitates with the alkaline earths, and the insolubility of a number of oxides, particularly corundum (Al_2O_3) and rutile (TiO_2) and some of their compounds. Using very carefully controlled stoichiometry and sample sizes on both sides of the overall calorimetric reaction minimizes the error introduced by precipitation. The insolubility of corundum prevents its use in liquid acid solution calorimetry. Rutile, when prepared by precipitation as described by Kelley, Todd and King (2), retains sufficient lattice H_2O to be soluble; however, when fired to complete dryness, it becomes insoluble. Kelley's (2) value for the heat of solution of TiO_2 was determined by extrapolation to dryness. A scheme for separately determining a heat of solution value for rutile (2) became apparent in the planning for the current study of manganese compounds. The investigation could be completed, according to the following reactions, by measuring

the heats of solution of MnO, MnO_2, TiO, and $MnTiO_3$ in a suitable acid mixture. These compounds are either in stock or obtainable commercially in high purity.

$$MnO_2 + TiO \rightarrow MnTiO_3$$

$$MnO + TiO_2 \rightarrow MnTiO_3$$

Studies of this nature may improve the capability of HF solution calorimeter to provide enthalpy of formation data.

REFERENCES

1. Bennington, K. O., M. J. Ferrante, and J. M. Stuve. Thermodynamic Properties of Two Lithium Silicates, Li_2SiO_3 and $Li_2Si_2O_5$. BuMines RI 8187, 1976, 19 pp.

2. Kelley, K. K., S. S. Todd, and E. G. King. Heat and Free Energy Data for Titanates of Iron and the Alkaline-Earth Metals. BuMines RI 5059, 1954, 37 pp.

3. Kilday, M. V., and E. J. Prosen. The Enthalpy of Solution of Low-Quartz (α-Quartz) in Aqueous Hydrofluoric Acids. J. Res. NBS, v. 77A, No. 2, March-April 1973, pp. 205-215.

4. Kracek, F. O., K. J. Neuvonen, and G. Burley. Petrology-Thermochemistry of Mineral Substances. J. Wash. Acad. Sci., v. 41, No. 12, 1951, pp. 373-383.

5. Prosen, E. J., and M. V. Kilday. An Adiabatic Solution Calorimeter and Measurements of a Standard Reaction for Solution Calorimetry. J. Res. NBS, v. 77A, No. 2, 1973, pp. 179-203.

6. Robie, R. A., and B. S. Hemingway. Calorimeters for Heat of Solution and Low-Temperature Heat Capacity Measurements. U.S. Geol. Survey Prof. Paper 755, 32 pp.

7. Sahama, T. G., and K. J. Neuvonn. A Solution Calorimeter for Silicates, Extrait des Comptes rendus de la Societe Geologique de Finlande, No. 24, 1951, pp. 177-180.

8. Torgeson, D. R., and T. G. Sahama. A Hydrofluoric Acid Solution Calorimeter and the Determination of the Heats of Formation of Mg_2SiO_4, $MgSiO_3$, and $CaSiO_3$. J. ACS, v. 70, 1948, pp 2156-2160.

9. Troitzsch, H. Beitrage zur Thermochemie der Silikate. (Contribution to Thermochemistry of Silicates) Dissertation Leipzig, 1935, pp. 1-46.

DISCUSSION

L. D. Hansen: Does very finely ground material have a surface effect?

K. O. Bennington: Yes it does, and that is why the sorting was of 10-20 mn sizes. The surface effect becomes noticeable below about 8 mn and these are elutriated very carefully in distilled water to sort out all fines. I have saved them because I was going to make some runs and see what the effect was, someday when I have enough time. I think Dr. Prosen did some work on that.

E. J. Prosen: Yes, we've done it on some elutriated samples and that is in one of our papers. On quartz, it is pretty straightforward. There are surface effects on other things. For example, we did the heat of combustion of diamond dust. This was done quite a while back. You can see it there if you get the diamond dust small enough.

M. W. Chase: Do the samples you use have to be as pure for solution calorimetry as they are for combustion calorimetry?

K. O. Bennington: Yes.

E. J. Prosen: It depends on the purity and on the sample. If you have an inert impurity in solution, it is just going to have a weight ratio effect. In combustion calorimetry, you usually burn everything but you could have inert ones there too. You could have some ground glass in there that ends up as ground glass. You have to consider the impurity separately for each material.

K. O. Bennington: If it is crystal the impurities are bonded in, then the correction can be made stoichiometrically and calorimetrically. But it can be corrected, or you can put a reaction in the reaction scheme for the impurity, if you know where the impurity sits; in other words, you cannot have just a mixture. Discrete, separate impurities are forbidden. There is no point in working on these, but impurities that are substituting - proxying - for some other element can be handled very accurately.

E. J. Prosen: I would like to add a little bit. In combustion calorimetry you are measuring a big heat and you've got to measure it to 1 part in 10,000 to get the answer you want for heat of formation to a tenth of a kilocalorie. In solution calorimetry, you are usually working with a lot smaller heats and adding these up, and you end up with a heat of formation within a few tenths of a kilocalorie also. In other words, 1 pct accuracy on a heat of solution may be equivalent to 1 part in 10,000 on a heat of combustion. Depends on the situation. If you only need 1 pct accuracy, then 1 pct impurity, an inert impurity, is okay. Whereas, if you need a hundredth of a percent accuracy in combustion, you've got to have your inert impurity down to a hundredth of a percent also.

N. A. Gokcen: I would like to make this discussion between Bert Staples, Hon Ko, and myself. I think we are going to be able to use the HCl solution calorimeter for heat of formation of some of the ionic solutions. For example, if you want to get the integral heat of solution of some of these electrolytes, then from that we can get the partial molar heat of solution. Are you planning to coordinate that sort of effort, Bert?

SECTION 3.- GALVANIC CELLS

DETERMINATION OF THERMODYNAMIC PROPERTIES OF SYSTEMS BY THE GALVANIC CELL TECHNIQUE

by

Y. K. Rao[1]

ABSTRACT

The galvanic cell technique is a convenient and accurate method for determining the changes in Gibbs energy entropy, and enthalpy associated with chemical processes. The standard Gibbs energies of formation of halides (and sulfides) have been determined from the electromotive force measurements on the formation cells of the type

$$A(s \text{ or } \ell)/AX\ (1)/C(gr),\ X_2(g).$$

In this cell, X may be a halogen or sulfur vapor. The concentration cells have been extensively used to determine the activities and relative partial molar enthalpies of components in binary and ternary metallic solutions.

Galvanic cells incorporating solid electrolytes are finding ever-increasing application in thermodynamic property measurements. Notable applications include determination of standard Gibbs energy of formation of oxides, measurement of oxygen activities in metal-oxygen solutions, and determination of thermodynamics of alloy systems. Among the solid oxide electrolytes, the calcia-stabilized zirconia and yttria-doped thoria have been used extensively. Of the various solid halide electrolytes that have been developed, calcium fluoride remains the most attractive.

INTRODUCTION

The measurement of the electromotive force (emf) of a galvanic cell is a convenient and accurate method for determining the changes in Gibbs energy, entropy, and enthalpy accompanying chemical processes. One type of cell, the formation cell, consists of a metal (A) anode, an electrolyte (AX), and a nonmetal (X_2) at a graphite electrode and may be represented as follows:

and $$A(s \text{ or } \ell)/AX\ (s \text{ or } \ell)/C(gr),\ X_2(g).$$

[1]Professor, Division of Metallurgical Engineering, FB-10, University of Wash.

Frequently X is a halogen or sulfur. The electrode reactions are

$$A = A^{n+} + ne^- \quad (1)$$

and

$$1/2X_2 + ne^- = X^{n-} \quad (2)$$

The overall cell reaction then becomes

$$A + 1/2X_2 = AX \quad (3)$$

The thermodynamic quantities are determined from the emf (E) measurements by means of the following relationships:

$$\Delta G_{AX} = -nFE, \quad (4)$$

$$\Delta S_{AX} = nF(dE/dT), \quad (5)$$

and

$$\Delta H_{AX} = -nFE + nFT(dE/dT) \quad (6)$$

where ΔG_{AX}, ΔS_{AX}, and ΔH_{AX} are the Gibbs energy, entropy, and enthalpy of formation of the compound AX, and F is the Faraday constant(=96,487 coulombs /g.equivalent). When A, AX, and X_2 are all in their respective standard states, the values determined are ΔG°_{AX}, ΔS°_{AX}, and ΔH°_{AX}, respectfully.

A concentration cell, on the other hand, consists of a metal electrode, the electrolyte, and one or more alloy electrodes. This may be represented as follows:

A(s or ℓ)/AX(in alkali or alkaline-earth salts)(s or ℓ)/A in A-Y(s or ℓ)

where Y is the alloying element. The half-cell reactions are

$$A_{(pure)} = A^{n+} + ne^- \quad (1)$$

and

$$A^{n+} + ne^- = A_{(A-Y)}. \quad (7)$$

The partial molar Gibbs energy and the activity of the metal A in the alloy can be calculated from the emf of the cell as follows:

$$G^M_A = RT\ln a_A = -nFE. \quad (8)$$

The partial molar entropy and the enthalpy of component A in the alloy can be determined from the emf and the temperature coefficient of the emf.

There is an important class of concentration cells which, unlike the foregoing, involve the transfer of anions through a solid electrolyte. Oxygen-ion-conducting solid-state electrolytes such as calcia-stabilized zirconia (CSZ) and halogen-ion-conducting solid-state electrolytes such as calcium

of systems Schematically these cells may be represented as follows·

$$Pt',X_2(\mu'_{X_2})/\text{Solid Electrolyte } (A.B)X_2/X_2(\mu''_{X_2}),Pt''.$$

where μ'_{X_2} and μ''_{X_2} represent the chemical potentials (or partial molar Gibbs energies) of X_2 at the respective electrodes. These chemical potentials are established by setting the partial pressures of X_2 at P'_{X_2} and P''_{X_2} respectively, or alternatively by means of appropriate condensed-phase equilibria.

CELLS WITH MOLTEN ELECTROLYTES

Formation Cells

One of the earliest studies is that of Salstrom and Hildebrand (48)[2] who employed a molten silver bromide-lithium bromide solution as the electrolyte; pure silver was one electrode, and bromine gas bubbling over an inert graphite electrode was the other.

$$Ag(s)/AgBr\text{-}LiBr(l)/Br_2(g,1\text{ atm}),\ C(gr).$$

The overall cell reaction is

$$Ag(s) + 1/2Br_2(g,1atm) = AgBr(\text{in fused-salt solution}). \qquad (9)$$

A general expression for the emf of this cell is given by

$$E = E^\circ - \frac{RT}{nF} \ln(a_{AgBr}/a_{Ag}P_{Br_2}^{1/2}). \qquad (10)$$

When silver is in its standard state, and bromine gas is bubbled over the graphite electrode at 1 atm pressure, the above expression becomes

$$E = E^\circ - \frac{RT}{nF} \ln a_{AgBr}. \qquad (11)$$

Measurements of E together with data on the standard emf E° were utilized by these authors (48) to calculate the activities of AgBr in the molten binary solution.

It should be emphasized that the validity of this method hinges upon the reversibility of the cell employed. The only measurements that can safely be used to evaluate the thermodynamic quantities (Gibbs energy changes, activities, etc.) are those of the reversible emf. With careful design, judicious selection of appropriate materials, and proper operation of the cell, it is possible to obtain emfs that are very nearly reversible. Chipman, Elliott, and Averbach(7) have identified a number of factors that may affect the reversibility of the cell. These are (1) Conductivity of the electrolyte - it must be high and at the same time it should be exclusively ionic. (2) Separation of electrode compartments - in order to prevent irreversible mixing of

[2]Underlined numbers in parentheses refer to items in the list of references at the end of the paper.

electrode constituents, it is necessary to partially isolate the electrode compartments from each other. This may be accomplsihed by the use of fritted tubes or small cuplike holders to contain the electrode constituents. (3) Valency state of the ionic species - a given type of ionic species may be present in two or more valency states which would introduce uncertainty in the value of 'n' in equations 4 and the like. For instance, it is known (47) that finite amounts of Mg(1) can dissolve in $MgCl_2$(1) with the result that there will be present in the molten-salt solution both Mg^{2+} and Mg_2^{2+} ionic species. The solubility of Mg(1) can, however, be substantially reduced by the addition of a second salt to the electrolyte. (4) Undesirable reactions - there may occur reactions between electrode constituents and container materials and also between the electrolyte and the leads which may result in spurious cell potentials. In addition exchange reactions may take place between one constituent of the alloy electrode and an ingredient of the electrolyte. (5) Concentration gradients - Both the electrolyte and the alloy electrode must be free of these. (6) Polarization effects - In high-temperature cells using liquid electrodes and molten electrolyte, diffusion occurs fairly rapidly and no appreciable polarization sets in when a small current is passed through the cell, as it may during the measurement of emf. With solid electrodes or solid electrolyte or both, diffusion is much slower; polarization appears readily, and adequate time must elapse for it to disappear. Proper care must be exercised in the electrolyte preparation and also in the design and operation of the cell to insure that the abovementioned impediments are overcome.

Belton and Rao (4) determined the Gibbs energy, entropy, and enthalpy of formation of $MgCl_2$(1) from the emf measurements of the galvanic cell,

$$Mg(1)/MgCl_2(1)/Cl_2(g,1\ atm),\ C(gr).$$

The cell (fig. 1) was constructed for the most part with fused quartz. In designing the electrode compartments, use was made of porous (or fritted) disks to achieve separation of one solution from the other while at the same time maintaining sound electrical contact. The chlorine electrode consisted of two concentric, cylindrical fused quartz tubes, the larger tube having been sealed with a fritted disk at the bottom. A graphite rod (3 mm in diam. by 23 cm long) over which the chlorine gas was passed made the contact with the molten electrolyte. A tungsten wire fitted through a rubber stopper was used to provide the electrical contact between the graphite electrode and the external circuitry. Pure recrystallized alumina tubes were used to make the metal (and alloy) electrode compartments. One end of the 5-mm-ID alumina tube was sealed with Morganite (Triangle 961) high-temperature Al_2O_3 cement and was dried at 200° C for about 4 hours. It was then fired at 1,200° C for about 10 hours. This procedure gave a porous sealed end.

Since magnesium chloride is highly hygroscopic, special care was exercised in the preparation and subsequent handling of the electrolyte. Anhydrous magnesium chloride was prepared by heating reagent-grade $MgCl_2.6H_2O$ with an appreciable amount of ammonium chloride under a dry argon atmosphere.

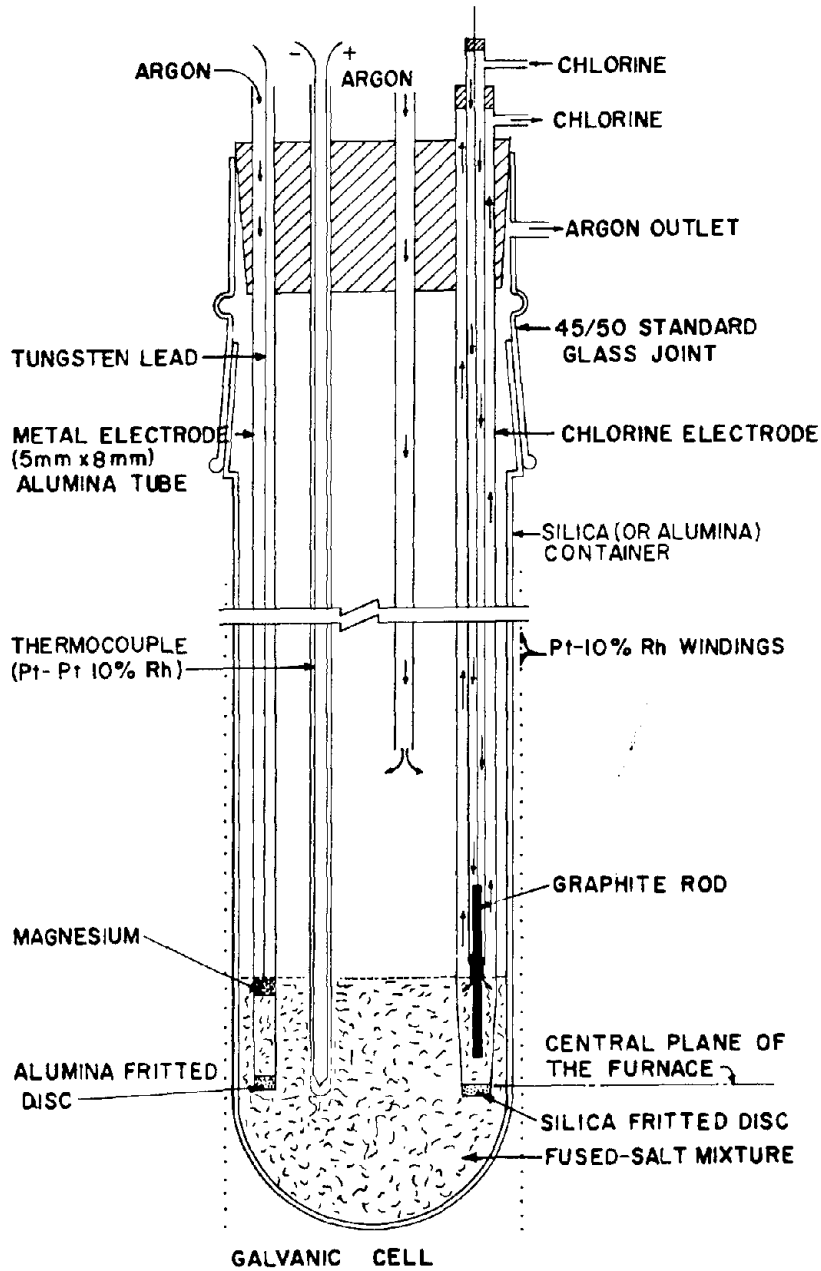


FIGURE 1. - Magnesium-chlorine formation cell.

The anhydrous salt thus produced was stored in a dry box. A similar procedure was used to prepare anhydrous calcium chloride. In setting up the cell, pure magnesium chloride was first melted in the quartz vessel (fig. 1) under an argon atmosphere, and the melt temperature was raised to 800° C. The electrode assembly was then lowered slowly into the molten electrolyte. Slight suction was applied to accelerate the seepage of the electrolyte through the porous disks into the respective electrode compartments. Magnesium was added to the metal electrode compartment (i.e., alumina tube), and

the bubbling of chlorine gas was commenced. At a constant temperature, it took about 6 to 8 hours with the pure $MgCl_2$ electrolyte for the emf to stabilize. The cell was tested for reversibility as follows: at a constant temperature, E° was measured; then an external voltage of equal magnitude was applied momentarily in the opposite direction, and the subsequent cell emf was measured. If the emf rose to the initial value, it was concluded that the data represented reversible emf values. All emf measurements were made with a Leeds and Northrup potentiometer operating in conjunction with an electronic null detector. The emf measurements were made in a staggered sequence within the range 720° to 870° C, and the data are shown plotted in figure 2. These results, which show good internal agreement between four different experiments, each with a fresh electrolyte, can be represented by the following linear relationship:

$$E° = 3.135 - (6.5 \times 10^{-4})T, \text{ volts}, \qquad (12)$$

where T is in degrees Kelvin. Assuming that n=2, we obtain for the standard Gibbs energy of formation of liquid $MgCl_2$:

$$\Delta G° = 144{,}600(\pm 2{,}000) + 29.98\ (\pm 1.85)\ T, \text{ calories}. \qquad (13)$$

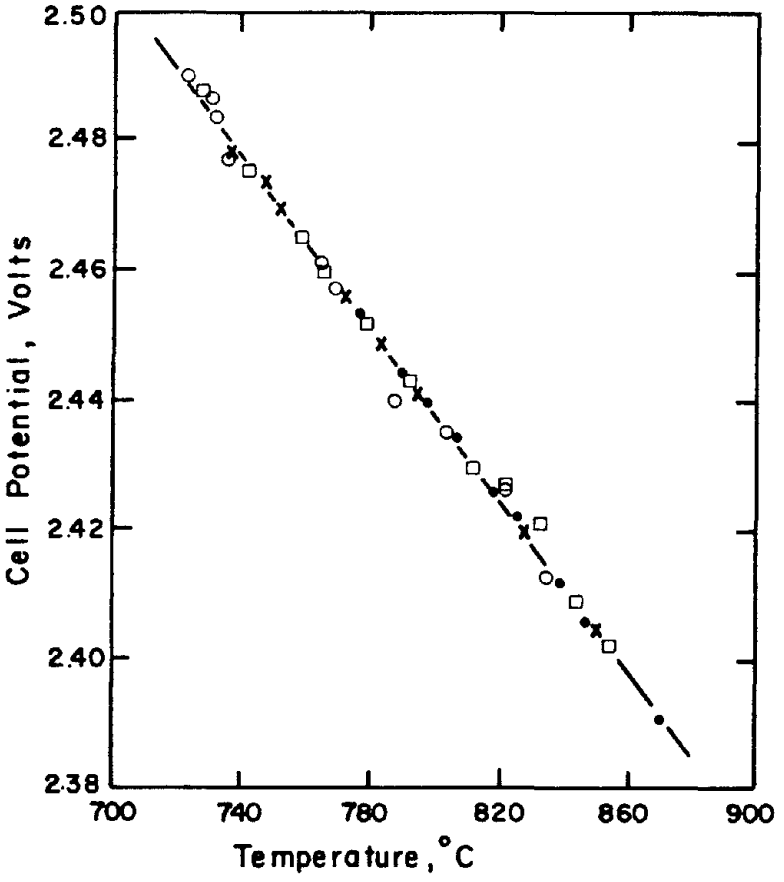


FIGURE 2. - Experimental results for the standard cell reaction: $Mg(l) + Cl_2(g) = MgCl_2(l)$.

At 780° C, $\Delta G°$ was found to be -113.0(±0.2) kcal, which is in very good agreement with the value of -113.3 kcal from the galvanic cell study of Lorenz and Velde (38). It does, however, differ from the value of -115.5 kcal reported by Markov and coworkers (40). The thermochemical value for $\Delta G°$ at 780° C is -113.9(±0.2) kcal (10) which is in good agreement with the present value.

Janz and Dijkhuis (30) published a critical evaluation of the excess Gibbs energies of formation of binary molten-salt mixtures determined by the galvanic cell technique. They (30) have also provided a concise summary of the data on $E°$ for a number of formation cells involving halides.

Thompson and Flengas (55, 56) investigated the reversibility of a sulfur vapor electrode and used it in an H-shaped cell to determine the Gibbs energies of formation of silver and lead sulfides. They (57) also determined the relative partial molar properties of lead sulfide-lead chloride system using the cell

$$C(gr),\ Pb(l)/PbS\text{-}PbCl_2(l)/S(g),C(gr).$$

The thermodynamic properties of Ag_2S-AgCl molten-salt mixtures were also determined by means of an analogous galvanic cell.

Ghosh and Kay (21) determined the standard Gibbs energy, entropy, and enthalpy of formation of $Al_2O_3(s)$ using the following cell:

$$Pt(s) - Al_2O_3(s),\ Al(l)/Al_2O_3 \text{ in liquid slag}/O_2(g),\ Pt(s).$$

A schematic diagram of the cell used by these authors (21) is shown in figure 3. The electrolyte consisted of a molten CaF_2-Al_2O_3 slag which was saturated with $Al_2O_3(s)$; the mode of conduction in this slag was overwhelmingly ionic. The cell assembly consisted of a graphite crucible, an Al/Al_2O_3 electrode, and an oxygen electrode. The half-cell reactions are

$$2Al(l) + 3O^{2-}_{(slag)} = Al_2O_3(s) + 6e^- \qquad (14)$$

and

$$3/2\ O_2(g) + 6e^- = 3O^{2-}_{(slag)}. \qquad (15)$$

The overall cell reaction becomes

$$2Al(l) + 3/2\ O_2(g) = Al_2O_3(s). \qquad (16)$$

Since the reactants and the products of this reaction were in their respective standard states, the measurements represented standard emf ($E°$) values from which the standard Gibbs energy of formation of Al_2O_3 was determined. These authors have also made use of a second type of galvanic cell in which the oxygen electrode was replaced by a carbon monoxide electrode. Over the temperature range of 1,640° to 1,830° K, the magnitude of the standard Gibbs energy of formation of $Al_2O_3(s)$ found in this work (21) was consistently

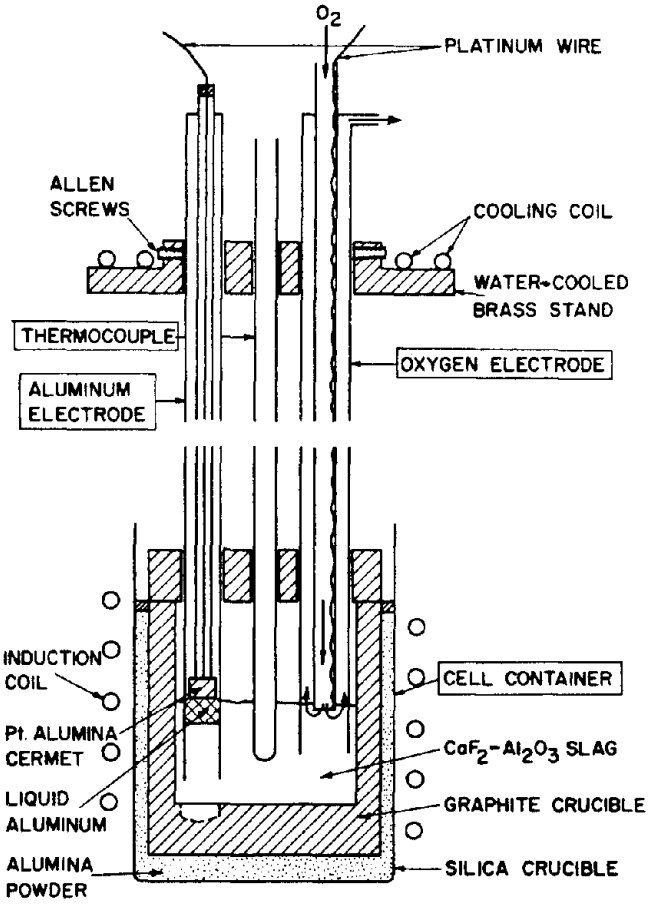


FIGURE 3. - An aluminum-oxygen formation cell.

lower than the thermochemical value (10) by about 8 kcal. One possible explanation for this discrepancy is the occurrence of undesirable side reactions in the cell.

Concentration Cells

Concentration cells which employ liquid electrodes and a molten electrolyte have been used extensively to determine the thermodynamic properties of metallic solutions. A typical cell is

$$Mg(l)/MgCl_2\text{-}CaCl_2(l)/Mg\text{-}Y(alloy)(l)$$

for which the overall reaction is

$$Mg_{(pure)} = Mg_{(alloy)}. \qquad (17)$$

The list of studies dealing with the concentration and other types of galvanic cells in quite extensive. Excellent bibliographies covering many of the previous studies have been published (26, 34, 35, 41, 62).

The choice of electrolyte is an important consideration in setting up a concentration cell. The electrolyte in most concentration cells is prepared by dissolving a few mole-percent of the salt of the least noble of the metals in the alloy system being investigated in a fused-salt solvent mixture. This practice has the advantage of preventing the side reactions and minimizing liquid-junction potentials. The LiCl-KCl eutectic mixture (m.p. 352° C) has often been used as the solvent mixture in concentration cell studies. Other combinations such as an equimolar mixture of KCl and NaCl have also found frequent application. Wilder (67), Wilder and Elliott (68-69), and Yazawa and coworkers (72) made use of concentration cells having an $AlCl_3$-KCl-NaCl electrolyte to determine the thermodynamic properties of alloy systems containing aluminum. In general there is some possibility that displacement reactions involving the alloy ingredients and the electrolyte may occur. Wagner and Werner (64) developed a thermodynamic treatment that enables the prediction of the extent of displacement reactions. In the case of $AlCl_3$-KCl-NaCl electrolyte the extent of displacement reactions as well as the errors introduced therefrom is negligible. A schematic diagram of the concentration cell used by Wilder (67) for investigating the Al-Cu liquid solutions is shown in figure 4. Partial isolation of the metal and alloy electrode compartments was achieved by using small Al_2O_3 crucibles to contain the metal (or reference) and the alloy electrodes respectively.

Rao and Patil (44) have used a similar cell but with a $MgCl_2$-KCl-NaCl electrolyte to determine the relative partial molar properties of Mg in liquid Mg-Sb solutions. Figure 5 shows the experimental results of this work [the three data points at high X_{Mg} values are from Kubaschewski and Catterall (35)] compared with the more recent work of Egan (11), who made use of a cell having a solid CaF_2 electrolyte. The agreement between the two studies is quite good. Belton and Rao (3, 43) investigated the thermodynamic properties of Mg-alloy systems using a concentration cell that was very similar in design to that shown in figure 1 except that the chlorine electrode was replaced by an alloy electrode. Fused $MgCl_2$-$CaCl_2$ salt was used as the electrolyte. The data for liquid Mg-Tl alloys (measured against liquid Mg reference electrode) are shown in figure 6. Also shown in the same figure are the data reported by Terpilowski and Slaby (54) who used a concentration cell having a molten salt electrolyte and a solid Mg reference electrode. The agreement between the two sets of data (fig. 6) is reasonably good. The relative partial molar Gibbs energy of magnesium (G^M_{Mg}) in liquid Mg-Ge solutions determined by means of the galvanic cell technique (3) is shown in figure 7 and is compared with the isopiestic measurements reported by Eldridge and coworkers (15). There is good agreement between the two studies.

Kleppa (32) made extensive use of the galvanic cell technique and determined the thermodynamic properties of binary liquid solutions Au-Pb, Au-Sn, Au-Bi, Au-Tl, Zn-Bi, and Zn-Pb. Kleppa and Thalmayer (33) extended the same technique to study the thermodynamics of binary liquid alloys rich in zinc.

CELLS WITH SOLID ELECTROLYTES

In the past 20 years there has beenremarkable progress in the development of galvanic cells having solid electrolytes. One of the principal applications of these cells has been in the measurement of thermodynamic data of

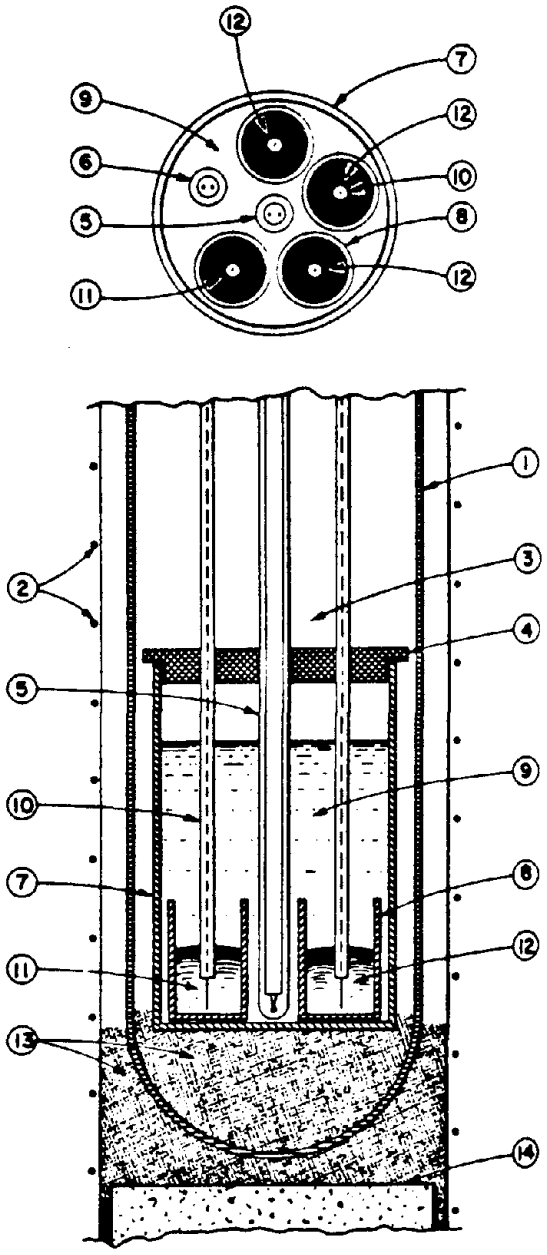


FIGURE 4. - Concentration cell having a fused-salt electrolyte. (1) Mullite cell tube, (2) furnace windings, (3) argon atmosphere, (4) Alundum radiation shield, (5) thermocouple, (6) control thermocouple, (7) alumina cell crucible, (8) alumina electrode crucibles, (9) $AlCl_3$-KCl-NaCl fused electrolyte, (10) tantalum contact in alumina sheath, (11) aluminum electrode, (12) Al-Cu alloy electrode(s), (13) alumina insulating grain, (14) firebrick.

metallurgical systems. Since several excellent reviews (16, 22, 45, 49, 52, 53, 58, 70) have been published on the subject of solid electrolyte techniques, it is deemed appropriate to concentrate here on a few selected topics. As in the case of molten electrolytes, it is imperative that the solid electrolytes used in thermodynamic measurements possess only negligible electronic conduction for most applications, it is sufficient if the electronic conductivity is less than 1 pct of the total conductivity of the electrolyte. In other words, the transference number (t_e) of electrons in the electrolyte must not exceed 0.01. Thus for a given electrolyte, one may define an electrolytic (or ionic) domain, a region that spans a wide range of temperatures and pressures (P_{X_2}, where X, the nonmetallic constituent of the electrolyte, may be oxygen or a halogen), within which the electronic contribution to the total conductivity remains below 1 pct.

The electrolytic domains for some of the more frequently used solid electrolytes are shown in figure 8 (53). It should be noted that at all temperatures and pressures (P_{X_2}) that fall within the boundary lines demarcated in this figure, the ionic conductivity constitutes better than 99 pct of the total electrical conductivity of the electrolyte. For instance, the electrolytic domain for the ZrO_2 (plus 15 mole-pct CaO) electrolyte lies between $\sim 10^{5}$ and $\sim 10^{-18}$ atm P_{O_2} at 1,000° C (71). At the same temperature, the electrolytic domain for the ThO_2 (plus 15 mole-pct $YO_{1.5}$) electrolyte is from $\sim 10^{-6}$ to $\sim 10^{-25}$ atm P_{O_2}. Figure 8 also shows that the width of the electrolytic domains diminishes with rising temperature.

The following relationship between the emf (E) of a galvanic cell and the chemical potential (μ_{X_2}) of the electrodes was derived by Wagner (63):

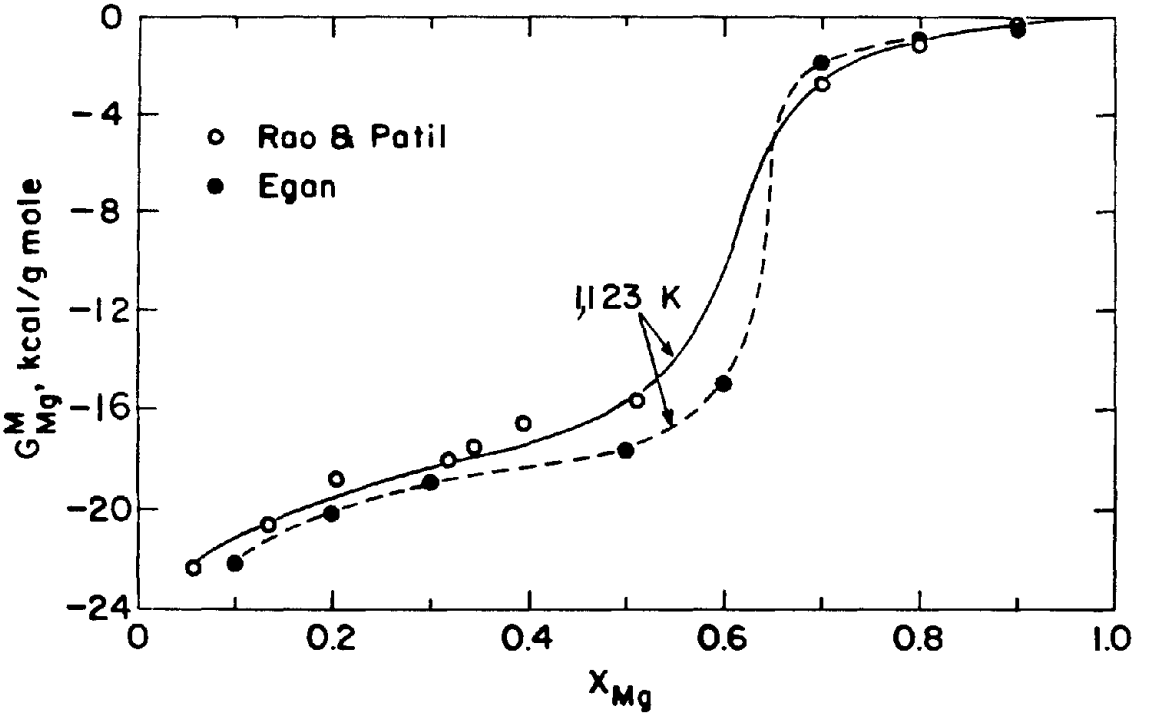


FIGURE 5. - Relative partial molar Gibbs energy of magnesium (G^M_{Mg}) in Mg-Sb liquid solutions at 1,123 K.

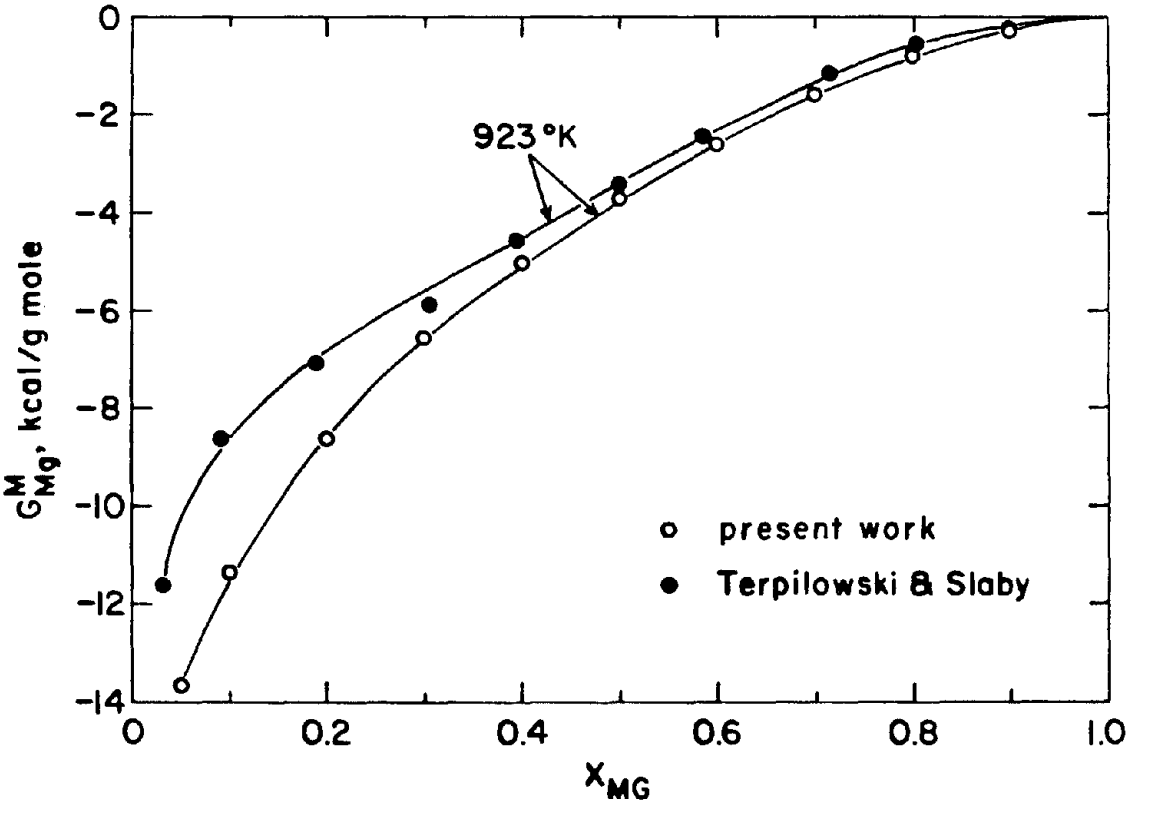


FIGURE 6. - Relative partial molar Gibbs energy of magnesium (G^M_{Mg}) in Mg-Tl liquid solutions at 923 K.

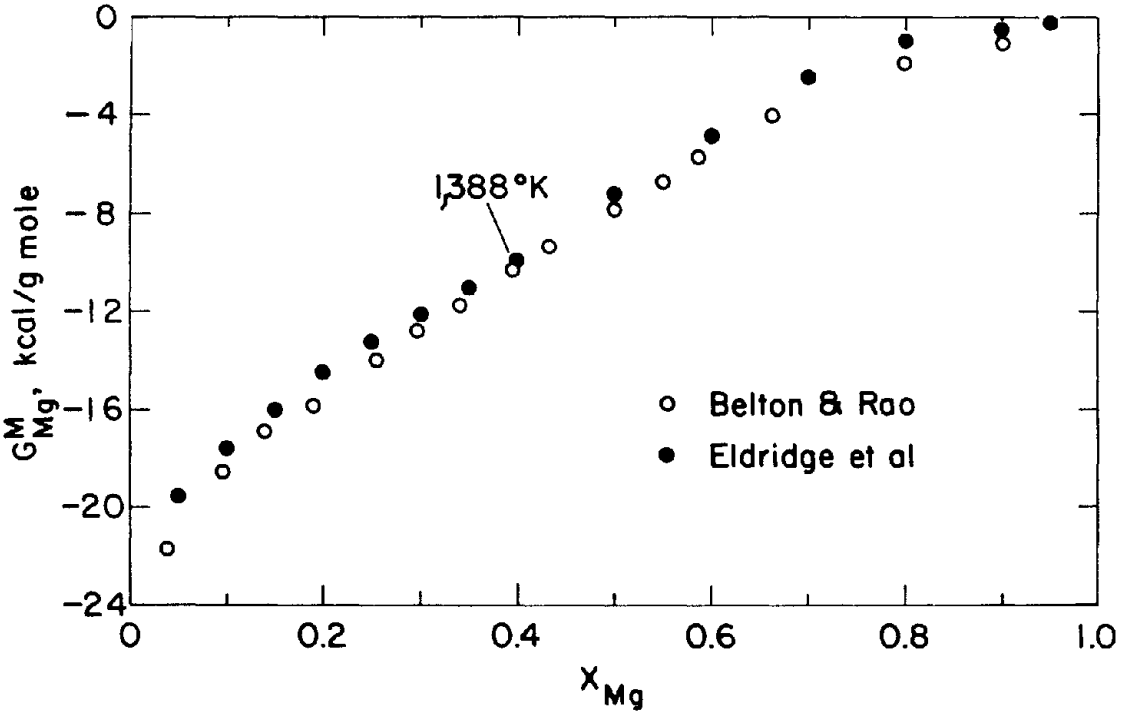


FIGURE 7. - Relative partial molar Gibbs energy of magnesium (G^M_{Mg}) in Mg-Ge liquid solutions at 1,388 K.

$$E = \frac{1}{2Z_X F} \int_{\mu'_{X_2}}^{\mu''_{X_2}} t_{ion} d\mu_{X_2} \qquad (18)$$

where Z_X is the absolute value of the valency of the X-ion in the electrolyte and t_{ion} is the ionic transference number (i.e., the fraction of the current carried by anions and cations in the electrolyte). The chemical potential μ''_{X_2} at the right electrode is greater than the chemical potential μ'_{X_2} at the left electrode, and X-ions are transferred from right to left through the electrolyte. When $t_{ion}=1$, equation 18 simplifies to

$$E = (\mu''_{X_2} - \mu'_{X_2})/(2Z_X F). \qquad (19)$$

Equation 19 can still be applied when t_{ion} is less than unity but greater than 0.99. If t_{ion} falls below 0.99, however, experimental difficulties are encountered (71).

Solid Oxide Electrolytes

Galvanic cells incorporating solid oxide electrolytes have been used in a variety of thermodynamic investigations since the pioneering work of Kiukkola and Wagner (31). These investigations may be classified as follows:

1. Determination of the thermodynamic stabilities of oxides and intermediate phases.

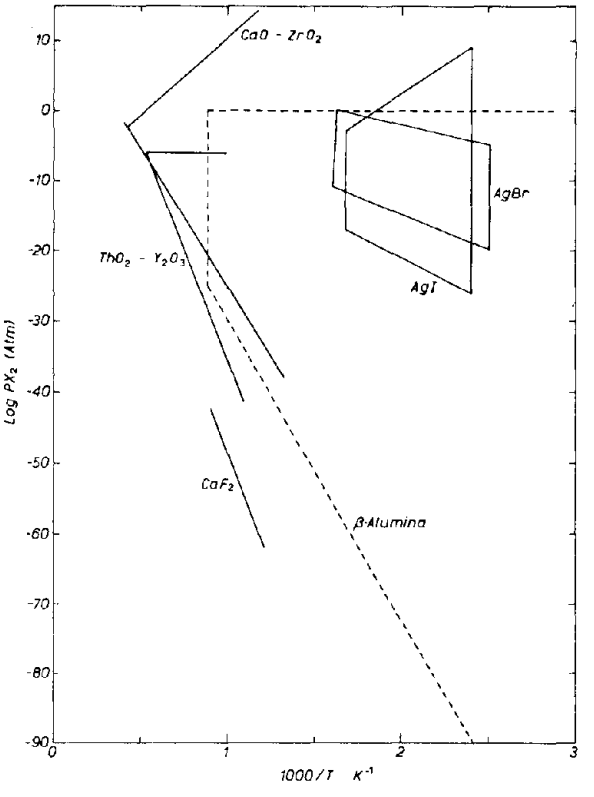


FIGURE 8. - Electrolytic domains for some solid electrolytes (53).

2 Measurement of the chemical potentials of oxygen dissolved in metals and alloys

3 Determination of the thermodynamic properties of alloy systems

Among the oxide electrolytes calcia-stabilized zirconia and thoria doped with yttria have received the widest application in the high-temperature galvanic cells. In general, ZrO_2-CaO and ThO_2-$YO_{1.5}$ solid solutions containing about 15 mole-pct of the second constituent (i.e., CaO, $YO_{1.5}$) are preferred because this composition corresponds to the maximum in their ionic conductivity (70). Electrical conductivity measurements indicate that ZrO_2(CaO) solid electrolyte has a higher ionic conductivity than ThO_2($YO_{1.5}$) solid electrolyte. The addition of CaO to ZrO_2 results in a cubic structure which does not undergo any solid-state phase transformations and remains stable over a wide range of temperature. Calcium substitutes randomly for zirconium in the fluorite-type cubic lattice, producing a defect structure in the oxide ion sublattice. Conduction occurs almost wholly by the movement of oxide ion vacancies. A similar phenonmenon occurs in ThO_2 when $YO_{1.5}$ is added to it. Electrical conductivity results show that zirconia electrolytes exhibit n-type electronic conductivity at P_{O_2} values less than 10^{-22} atm and that thoria electrolytes become p-type electronic conductors at P_{O_2} values greater

than 10^{-6} atm at a temperature of 1,000° C (70). Consequently zirconia electrolytes cannot be used in highly reducing atmospheres and thoria electrolytes are unsuitable for use in air or oxygen.

Electrode separation is much more easily achieved in cells with solid electrolytes than in those with molten electrolytes. In the operation of the solid electrolyte cells, the choice of gaseous environment within the cell must be made with care. In cells operating in an argon (or inert gas) atmosphere, provision must be made to thoroughly purify the gas in order to remove O_2, CO, CO_2, H_2O, and traces of hydrocarbons. In some instances it may be necessary to incorporate "getters" into the cell assembly to remove any harmful gaseous products liberated (through desorption or dissociation) during operation at high temperatures.

Kiukkola and Wagner (31) designed a simple cell with a calcia-stabilized zirconia electrolyte for use in the determination of standard Gibbs energies of formation of metal oxides. The cell may be represented as follows:

$$\text{Fe(s), Wustite (s)/0.85 } ZrO_2 + 0.15 \text{ CaO (s)/Me(s),MeO(s).}$$

The cell consisted of a pellet of a mixture of iron and wustite, a pellet of the electrolyte, and a pellet of a mixture of metal Me and its oxide MeO placed between Pt disks connected with Pt leads. The emf of this cell is given by

$$E^\circ = \frac{1}{2F} \left(\Delta G^\circ_{MeO} - \Delta G^\circ_{wustite}\right) \qquad (20)$$

ΔG°_{MeO} may be evaluated from the cell emf measurements and the published data on the standard Gibbs energy of formation of wustite. These authors employed this cell design for determining the standard Gibbs energies of formation of NiO, CoO, and Cu_2O (31).

There have been considerable improvements and modifications in the cell design in response to problems stemming from the high affinity for oxygen exhibited by electrode systems which have low oxygen potentials (52). The modified cell design which incorporates separate electrode compartments and Zr or Ti oxygen "getters" is shown in figure 9 (52). The reference electrode selected for use in the solid oxide cells must be capable of maintaining the fixed oxygen potential at the electrode/electrolyte interface. Metal-metal oxide mixtures, which are frequently chosen as the reference electrodes, have a tendency to polarize if appreciable current is drawn through the cell during the measurements. Under these conditions the two-phase mixture fails to maintain the correct oxygen potential and in fact may develop a concentration gradient. Recent work (70, 71) on overvoltage-current relationships in metal-metal oxide electrode systems indicates that Cu-Cu_2O electrode can accommodate small cell currents more easily than either the Fe-FeO or the Ni-NiO electrodes. Steele and Shaw (53) suggest the following sequential ordering of the electrode systems, the kinetically more responsive being on the left-hand side of this sequence:

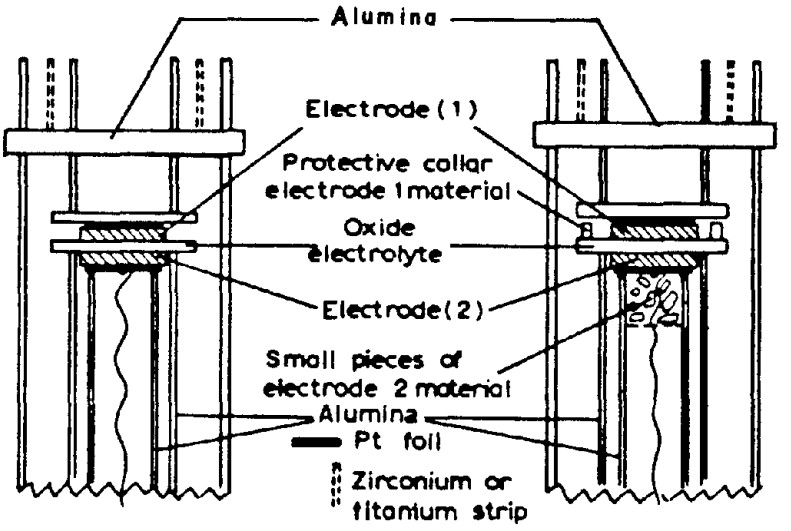


FIGURE 9. - Schematic diagram of cells with solid oxide electrolytes (52).

$$Ga\text{-}Ga_2O_3 > Cu\text{-}Cu_2O > Fe\text{-}FeO > Ni\text{-}NiO.$$

This means that the Ni-NiO electrode is not as attractive as the Ga-Ga2O3 for use as reference electrode.

Besides the judicious choice of the reference electrode there are other problems associated with the use of galvanic cells for high-temperature thermodynamic measurements which the experimentalist must be aware of. Since the reviews referenced earlier (22, 70) give excellent accounts of these problems and also suggest methods to overcome them, discussion here will be limited to few remarks. The original porosity as well as microcracks developed during rapid heating or cooling of the solid electrolyte cell can cause direct and irreversible flow of oxygen gas between the electrodes. Reactions within the electrode system and reactions between electrode and electrolyte can cause oxygen potential variations within the electrode.

Air or oxygen in contact with a suitable metal substrate (eg., Pt) have also been used as reference electrodes. Chatterji and Smith (6) employed a $ZrO_2(0.85) + CaO(0.15)$ solid electrolyte in conjunction with an air reference electrode to determine the standard free energy of formation of Bi_2O_3, Sb_2O_3, and TeO_2. Petot-Ervas and coworkers (42) employed the cell assembly shown in figure 10 to measure the standard Gibbs energy of formation of SnO_2. The cell consisted of an yttria-stabilized zirconia solid electrolyte and an Ni-NiO reference electrode. The measurements are in reasonably good agreement with those reported by Belford and Alcock (2). Jacob and coworkers (29) determined the thermodynamic properties of $CuFe_2O_4$-Fe_3O_4 solid solutions by means of the galvanic cell technique using a calcia-stabilized zirconia solid electrolyte and an Ni-NiO reference electrode. Using a $Cu\text{-}Cu_2O$ reference electrode and a $ThO_2 + YO_{1.5}$ solid electrolyte, Jacob (27) measured the standard Gibbs energy of formation of indium oxide.

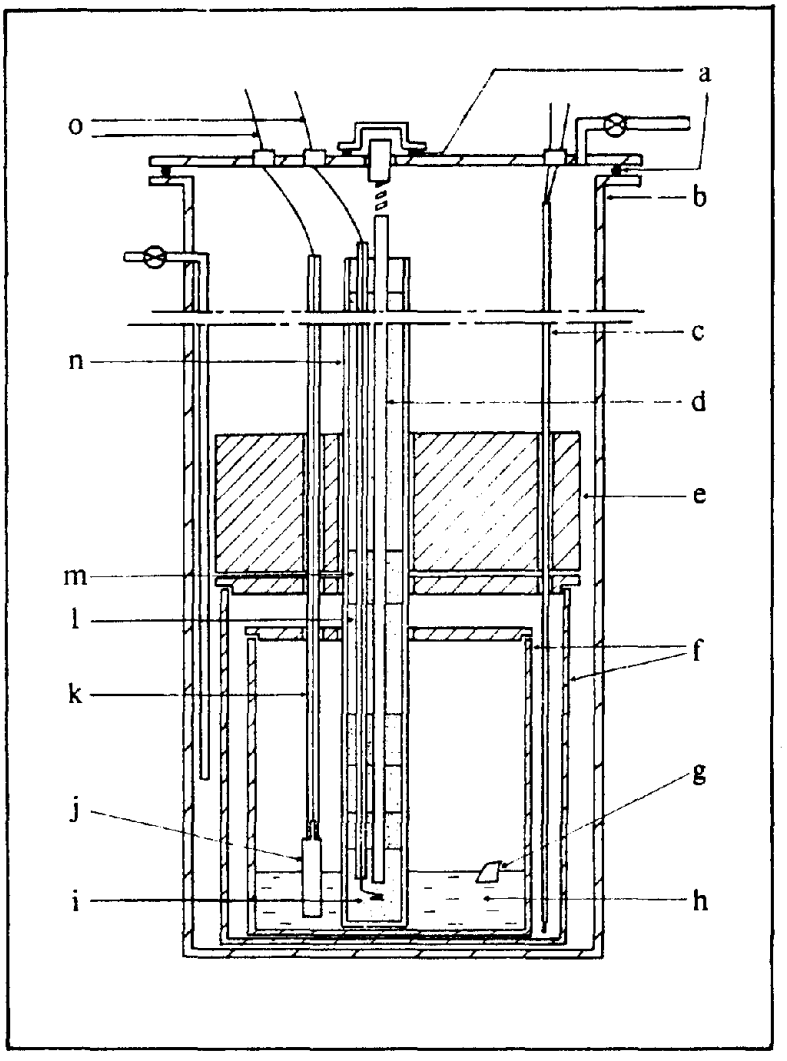


FIGURE 10. - Cell assembly: a, Rubber O-ring; b, stainless-steel container; c, thermocouple; d, alumina rod; e, alumina radiation shield; f, alumina crucibles; g, SnO_2(s); h, molten tin; i, Ni(s) + NiO(s) reference electrode; j, electrical junction SnO_2; k, alumina tube; l, Ni(s) + NiO(s) powder acting as a buffer for O_2(g); m, alumina powder; n, electrolyte crucible; o, Pt leads.

Galvanic cells with solid oxide electrolytes have found active practical application as oxygen sensors. The oxygen sensor, a device capable of providing the in situ determination of dissolved oxygen in liquid metals and alloys, consists of a solid oxide electrolyte, a reference electrode, and the electrode whose oxygen potential is to be determined. The reference electrode may be air or gas mixtures (e.g., CO/CO_2) or two-phase mixtures (such as Me/MeO). Oxygen sensors have been used to measure the oxygen content of liquid copper and its alloys (36, 37, 66), liquid silver (9), liquid steel (17, 18, 19, 20, 50, 59, 60), and liquid sodium (24).

Typical cell disigns used in the oxygen sensors for molten steel are shown in figure 11 (59). In cell I (17, 50), air or a mixture of CO and CO_2 was used as the reference electrode. With gaseous reference electrodes, difficulties are experienced in maintaining sound electrical contact between the electrode and the electrolyte. Moreover, the electrolyte tube used in this design was noted for its inferior thermal shock resistance. Fitterer (18), in cell II design, overcame this problem by fusing a ZrO_2(CaO) disk into a silica tube. But he too employed a gas reference electrode. Cell III design, developed by Turkdogan and coworkers (19, 20, 59, 60), incorporates a

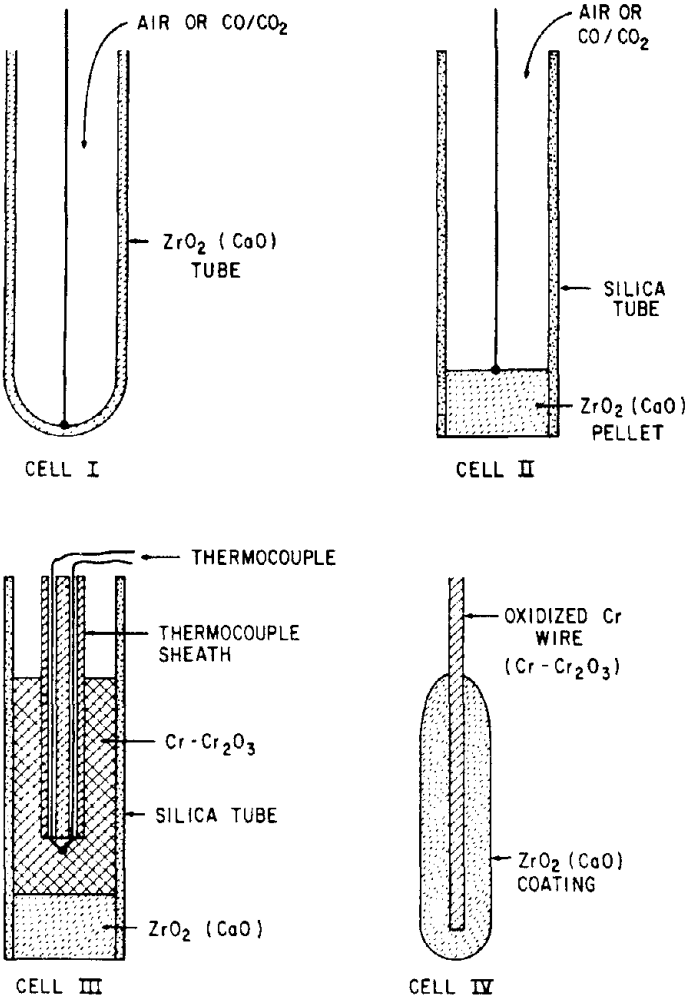


FIGURE 11. - Design of solid oxide cells used in oxygen sensors (59).

solid $Cr-Cr_2O_3$ reference electrode. It is seen that the same type of reference electrode is also used in the cell IV design.

Turkdogan and coworkers (20, 60) employed cell III design to determine the oxygen content of molten iron. The galvanic cell may be represented as follows:

$$(Pt),\ Cr(s),\ Cr_2O_3(s)\ /\ ZrO_2(CaO)\ (s)\ /\ \underline{O}\ (\text{in Fe melt}),\ (Mo).$$

The platinum lead of the thermocouple (fig. 11) served as the contact wire for the $Cr-Cr_2O_3$ electrode, and an Mo wire that was periodically dipped into the molten iron provided the second electrical lead for the emf measurements. The cell reaction is

$$2\ \underline{O}\ (\text{in Fe melt}) = O_2(g,\ P_{O_2})(Cr-Cr_2O_3\ \text{equilibrium}). \qquad (21)$$

The oxygen content of the melt was derived from the cell emf (E) as follows:

$$E = \frac{RT}{4F} \ln \frac{(\text{pct } O)^2}{K P_{O_2}}, \quad (22)$$

where P_{O_2} is the oxygen pressure in equilibrium with pure solid Cr and Cr_2O_3, and K is the equilibrium constant for the dissolution of pure oxygen in molten iron, viz.,

$$O_2 \text{ (g, 1 atm)} = 2 \underline{O}(1 \text{ wt pct in Fe melt}). \quad (23)$$

The temperature dependences of K and P_{O_2} were ascertained from standard sources and were combined with equation 22 to obtain the following result (60):

where P_{O_2} is the oxygen pressure in equilibrium with pure solid Cr and Cr_2O_3, and K is the equilibrium constant for the dissolution of pure oxygen in molten iron, viz.,

$$O_2 \text{ (g, 1 atm)} = 2 \underline{O}(1 \text{ wt pct in Fe melt}). \quad (23)$$

The temperature dependences of K and P_{O_2} were ascertained from standard sources and were combined with equation 22 to obtain the following result (60):

$$\log(\text{pct } O) = 4.62 - \frac{13580}{T} + \frac{10.08E}{T}. \quad (24)$$

where (pct O) refers to the weight-percent of oxygen dissolved in liquid iron, E is in millivolts, and T is in degrees Kelvin. The authors (60) found good agreement between the electrochemically determined oxygen contents and the chemical analysis results.

Solid oxide electrolyte cells have also been used in the investigation of thermodynamic properties of alloy systems (37, 46). Thermodynamic activities of PbO in ternary $PbO-Na_2O-SiO_2$ melts were determined by means of a solid electrolyte (0.95 ZrO_2 + 0.05 CaO) cell (23). A tabulated list of recent galvanic cell studies of alloy and oxide systems has been provided by Steele and Shaw (53).

Solid Halide Electrolytes

Cells with solid halide electrolytes have been used in a variety of thermodynamic measurements. $PbCl_2$ doped with KCl (31), solid $BaCl_2$ (14), and solid CuBr (65), and solid CaF_2 (1, 5, 11, 12, 13, 28, 39, 51) are some of the solid halide electrolytes that have proved satisfactory. Galvanic cells incorporating the latter (i.e., CaF_2) will be discussed here in some detail. Tretyakov and Kaul (58) have given a useful review of thermodynamic applications of CaF_2 solid electrolyte.

CaF_2 is an anionic conductor with fluorine ions migrating mostly as in-

terstitials. One advantage of CaF_2 is that it remains an ionic conductor even under extremely reducing conditions. The problem of electronic conduction in CaF_2 has been studied by several investigators (8, 25, 61). The electronic conductivity of CaF_2 was observed to decrease with decreasing Ca activity (8). It has been established (8) that over a wide range of Ca activities the fractional ionic conductivity (t_{ion}) of CaF_2 is greater than 0.99. Heus and Egan (13) have measured the standard Gibbs energy of formation of several metal fluorides using the setup shown in figure 12. The electrode and electrolyte arrangement for one of these cells may be represented as follows:

$$Al,\ AlF_3(s)/CaF_2(s)/PbF_2(s),Pb(l).$$

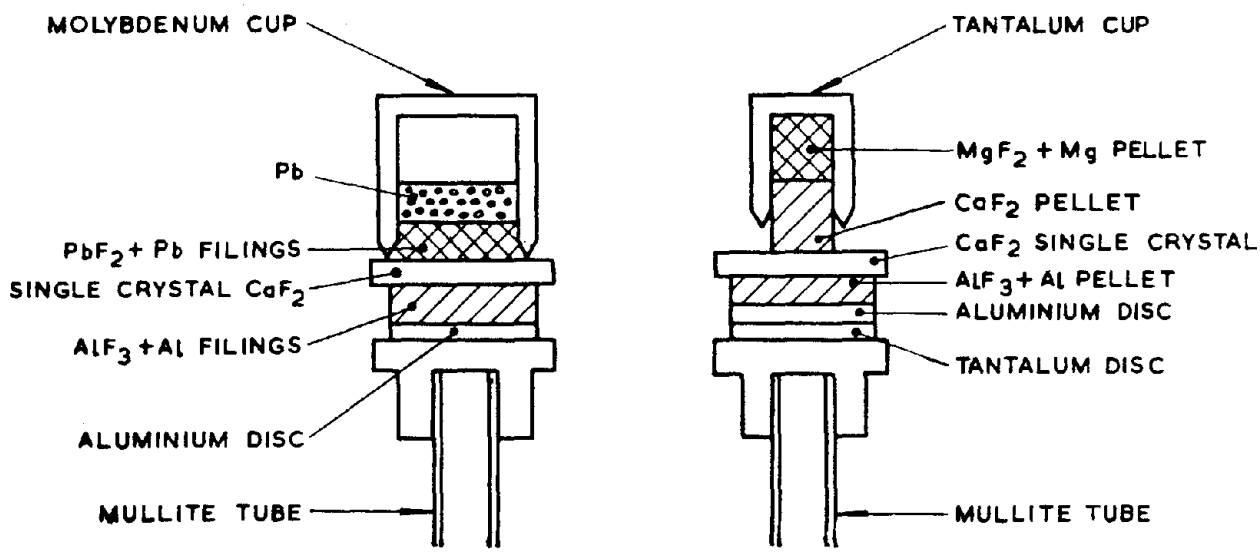


FIGURE 12. - Details of galvanic cells incorporating CaF_2 solid electrolyte (1, 12–13, 39).

$$2/3Al(s) + PbF_2(s) = 2/3AlF_3(s) + Pb(1). \quad (25)$$

The electromotive force (E°) of the cell is related to the difference in the standard Gibbs energies of formation of the fluorides as follows:

$$2/3(\Delta G^\circ_{AlF_3}) - \Delta G^\circ_{PbF_2} = -2FE^\circ. \quad (26)$$

Egan (12) also investigated the thermodynamics of thorium carbide by means of the cell

$$Mo \ / \ Th,ThF_4(s) \ / \ CaF_2(s) \ / \ ThF_4, \ ThC_2,C(s) \ / \ Mo.$$

The overall cell reaction taking place upon passing 4 Faradays of electricity is

$$Th(s) + 2C(s) = ThC_2(s). \quad (27)$$

Egan (11) studied the thermodynamics of magnesium alloys using CaF2 solid electrolyte. The cell arrangement may be represented as follows:

$$Mg(1), \ MgF_2(s) \ / \ CaF_2(s) \ / \ MgF_2(s), \ Mg\text{-}Me(1).$$

The overall cell reaction is

$$Mg(1) = Mg\text{-}Me \ (1), \quad (28)$$

where Me = Bi, Sb, or Sn, respectively. The activities of Mg in these binary systems determined by Egan (11) agree reasonably well with other measurements (44). Benz and Wagner (5) used the following solid CaF_2 cell,

$$Pt,O_2(g) \ / \ CaO(s) \ / \ CaF_2(s) \ / \ CaO\text{-}SiO_2(s) \ / \ Pt,O_2(g),$$

to investigate the thermodynamics of the binary system CaO-SiO2. They were able to deduce the standard Gibbs eneriges of formation of three different calcium silicates from the electromotive force measurements; these values compared facorably with the calorimetric measurements.

CONCLUDING REMARKS

The application of the galvanic cell technique to the measurement of thermodynamic properties has reached a well-developed state. Further refinements of the technique, especially with cells incorporating solid electrolytes, will take place, and the main thrust of the future developments will probably be toward understanding the microscopic processes occurring at the electrode-electrolyte interface.

REFERENCES

1. Behl, W. K., and J. J. Egan. J. Electrochem. Soc., v. 113, 1966, p. 376.

2. Belford, T. N., and C. B. Alcock. Trans. Faraday Soc., v. 61, 1965, p. 443.

3. Belton, G. R., and Y. K. Rao. Met. Trans., v. 2, 1971, p. 2215.

4. _____. Trans. AIME, v. 245, 1969, p. 2189.

5. Benz, R., and C. Wagner. J. Phys. Chem., v. 65, 1961, p. 1308.

6. Chatterji, D., and J. R. Smith. J. Electrochem. Soc., v. 120, 1973, p. 889.

7. Chipman, J., J. F. Elliott, and B. L. Averbach. 1B, N.P.L. Symposium No. 9, The Physical Chemistry of Metallic Solutions and Intermetallic Compounds, H.M. Sta. Office, London, 1959.

8. Delcet, J., R. J. Heus, and J. J. Egan. J. Electrochem. Soc., v. 125, 1978, p. 755.

9. Diaz, C. M., and F. D. Richardson. In Electromotive Force Measurements in High Temperature Systems, ed. by C. B. Alcock, American Elsevier Pub. Co., New York, 1968, p. 29.

10. Dow Chemical Co., Thermal Research Laboratory, JANAF Thermochemical Tables, 2d ed., NSRDS-NBS-37, S/N 003-003-00872-9, U.S. Government Printing Office, Washington, D.C., 1971, p. 1141.

11. Egan, J. J. J. Nucl. Mat., v. 51, 1974, p. 30.

12. _____. J. Phys. Chem., v. 68, 1964, p. 978.

13. Egan, J. J., and R. J. Heus. Z. Phys. Chem., v. 49, 1966, p. 38.

14. Egan, J. J., W. McCoy, and J. Bracker. In Thermodynamics of Nuclear Materials. International Atomic Energy Agency, 1962, Vienna, p. 163.

15. Eldridge, J. M., E. Miller, and K. L. Komarek. Trans. AIME, v. 236, 1966, p. 1094.

16. Etsell, T. H., and S. N. Flengas. Chem. Rev., v. 70, 1970, p. 339.

17. Fisher, W. A., and W. Ackerman. Arch. Eisenhuttenw., v. 36, 1965, p. 643; v. 37, 1966, p. 43.

18. Fitterer, G. R. J. Metals, v. 19, 1966, p. 961; v. 19, 1967, p. 92; v. 20, 1968, p. 74.

19. Fruehan, R. J. Met. Trans., v. 1, 1970, p. 3403.

20. Fruehan, R. J., L. J. Martonik, and E. T. Turkdogan. Trans. AIME, v. 245, 1969, p. 1501.

21. Ghosh, D., and D. A. R. Kay. J. Electrochem. Soc., v. 124, 1977, p. 1836.

22. Goto, K., and W. Pluschkell. In Physics of Electrolytes, ed. by J. Hladik. Academic Press, Inc., New York, v. 2, 1972, p. 539.

23. Grau, A. E., and S. N. Flengas. J. Electrochem. Soc., v. 123, 1976, p. 352.

24. Grundy, B. R., E. Berkey, E. T. Weber, and W. A. Ross. Trans. Am. Nucl. Soc., v. 14, 1971, p. 186.

25. Hinze, J. W., and J. W. Patterson. J. Electrochem. Soc., v. 120, 1973, p. 96.

26. Hultgren, R., P. D. Desai, D. T. Hawkins, M. Gleiser, and K. K. Kelley. Selected Values of Thermodynamic Properties of Binary Alloys. American Society for Metals, Metals Park, Ohio, 1973.

27. Jacob, K. T. Trans. Inst. Min. Met. (London), v. 87, 1978, p. C165.

28. Jacob, K. T., D. B. Rao, and H. G. Nelson. J. Electrochem. Soc., v. 125, 1978, p. 758.

29. Jacob, K. T., K. Fitzner, and C. B. Alcock. Met. Trans. B., v. 88, 1977, p. 451.

30. Janz, G. J., and Ch. G. M. Dijkhuis. In Molten Salts, v. 2. NBS1, 1969.

31. Kiukkola, K., and C. Wagner. J. Electrochem. Soc., v. 104, 1957, pp. 308-16, 379-87.

32. Kleppa, O. J. J. Amer. Chem. Soc., v. 71, 1949, p. 3275; v. 72, 1950, p. 3346; v. 73, 1951, p. 385; v. 74, 1952, p. 6052.

33. Kleppa, O. J., and C. E. Thalmayer. J. Phys. Chem., v. 63, 1959, p. 1953.

34. Kubaschewski, O., and C. B. Alcock. Metallurgical Thermochemistry. Pergamon Press, Inc., New York, 5th ed., 1979.

35. Kubaschewski, O., and J. A. Catterall. Thermochemical Data of Alloys. Pergamon Press, Inc., New York, 1956.

36. Kulkarni, A. D. Met. Trans., v. 4, 1973, p. 1713.

37. Kulkarni, A. D., and R. E. Johnson. Met. Trans., v. 4, 1973, p. 1723.

38. Lorenz, R., and H. Velde. Z. Anorg. Allgem. Chem., v. 183, 1929, p. 81.

39. Markin, T. L. In Electromotive Force Measurements in High-Temperature Systems, ed. by C. B. Alcock, American Elservier Publishing Co., New York, 1968, p. 91.

40. Markov, B. F., I. U. Delimarskii, and I. D. Panchenko. Zhur. Fiz. Khim., v. 29, 1955, p. 51.

41. Oriani, R. A. J. Electrochem. Soc., v. 103, 1956, p. 194.

42. Petot-Ervas, G., R. Farhi, and C. Petot. J. Chem. Thermodynam., v. 7, 1975, p. 1131.



43. Rao, Y. K., Ph.D. Thesis, Metallurgical Engineering, University of Pennsylvania, 1965.

44. Rao, Y. K., and B. V. Patil. Met. Trans., v. 2, 1971, p. 1829.

45. Rapp, R. A., and D. A. Shores. In Techniques in Metals Research, ed. by R. F. Bunshah, John Wiley & Sons, Inc., New York, v. 4, pt. 2, 1970, p. 123.

46. Rezukhina, R. N., and T. A. Kashina. J. Chem. Thermodynam., v. 8, 1976, p. 513.

47. Rogers, P. S., T. W. Tomlinson, and F. D. Richardson. In Physical Chemistry of Process Metallurgy, Metallurgical Society Conferences, No. 8, Interscience Publishers, Inc., New York, 1961, p. 909.

48. Saltrom, E. J., and J. H. Hildebrand. J. Amer. Chem. Soc., v. 52, 1930, p. 4650.

49. Schmalzreid, H., and A. D. Pelton. Ann. Rev. Mater. Sci., v. 2, 1972, p. 143.

50. Schwerdtfeger, K. Trans. AIME, v. 239, 1967, p. 1276.

51. Skelton, W. H., and J. W. Patterson. J. Electrochem. Soc., v. 118, 1971, p. 1033.

52. Steele, B. C. H. In Electromotive Force Measurements in High Temperature Systems, ed. by C. B. Alcock, American Elsevier Publ. Co., New York, 1968, p. 3.

53. Steele, B. C. H., and R. W. Shaw. In Solid Electrolytes, ed. by P. Hagenmuller and W. Van Gool, Academic Press, Inc., New York, 1978.

54. Terpilowski, J., and H. Slaby. Bull. de L'Acad. Polonaise des Sci., Serie des Sci. Chimiq., v. 11, No. 6, 1963, p. 317.

55. Thompson, W. T., and S. N. Flengas. Can J. Chem., v. 46, 1968, p. 1611.

56. _____. J. Electrochem. Soc., v. 118, 1971, p. 419.

57. _____. J. Electrochem. Soc., v. 119, 1972, p. 399.

58. Tretyakov, Y. D., and A. R. Kaul. In Physics of Electrolytes, ed. by J. Hladik, Academic Press, Inc., New York, v. 2, 1972, p. 623.

59. Turkdogan, E. T., and R. J. Fruehan. Can. Met. Quart., v. 11, 1972, p. 371.

60. _____. Yearbook AISI, 1968, p. 279.

61. Wagner, C. J. Electrochem. Soc., v. 115, 1968, p. 933.

62. _____. Thermodynamics of Alloy, Addison-Wesley Publ. Co., Reading, Mass., 1952.

63. Wagner, C. Z. Phys. Chem, v. B21, 1933, p. 25.

64. Wagner, C., and A. Werner. J. Electrochem. Soc., v. 110, 1963, p. 326.

65. Wagner, J. B., and C. Wagner. J. Electrochem. Soc., v. 104, 1957, p. 509.

66. Wilder, T. C. Trans. AIME, v. 236, 1966, p. 1035.

67. _____. Trans. AIME, v. 233, 1965, p. 1202.

68. Wilder, T. C., and J. F. Elliott. J. Electrochem. Soc., v. 107, 1960, p. 628.

69. _____. J. Electrochem. Soc., v. 111, 1964, p. 352.

70. Worrell, W. L. Ceram. Bull., v. 53, 1974, p. 425.

71. _____. In Topics in Applied Physics, v. 21, Solid Electrolytes, ed. by S. Geller, Springer-Verlag, New York, 1977, p. 143.

72. Yazawa, A., and Y. K. Lee. Trans. Japan Inst. Metals, v. 11, 1970. p. 411.

DISCUSSION

Anonymous: You made a reference to Janz's work. Can you give us more details?

Y. K. Rao: Yes, certainly. Janz and coworker (Dijkhuis) prepared a critical compilation of thermodynamic data for molten salt systems. This work was published by the National Bureau of Standards (Molten Salts, v. 2), Washington, D. C., in 1969.

N. A. D. Parlee: In the cell with the sulfur vapor electrode, how large are the sulfur pressures?

Y. K. Rao: The cell was operated at a fairly high temperature (about 870° K) and the sulfur pressures were appreciable (1-10 mm Hg).

ELECTROCHEMICAL DETERMINATION OF THE GIBBS ENERGIES OF FORMATION OF SULFIDES

by

S. C. Schaefer[1]

ABSTRACT

Standard Gibbs energies of formation of sphalerite (ZnS, β), molybdenite (MoS_2), and tungsten disulfide (WS_2) have been determined with high-temperature galvanic cells employing stabilized zirconia as the solid electrolyte. The emf method is discussed with emphasis on requirements, limitations, and applications. Experimental results and a thermodynamic treatment of the data are presented. This research is part of the effort by the Bureau of Mines, U.S. Department of the Interior, to provide thermodynamic data for the advancement of minerals resource technology, environmental preservation, and energy economy.

INTRODUCTION

A high-temperature emf technique was developed to provide accurate thermodynamic data for compounds, minerals, and alloy systems. Specifically, Gibbs energy changes of cell reactions are obtained directly from open-circuit potential measurements of appropriate cells. These potentials are related to the Gibbs energy change of the cell reaction by the Nernst equation

$$\Delta G(\text{cell reaction}) = -nFE,$$

where n = electrochemical equivalent, F is the Faraday constant (23.061) kcal/v equivalent), and E is the electromotive force in volts.

Two recent developments that have enhanced the reliability of this method are (1) advancement of electronic instruments, specifically high-input impedance electrometers, which are capable of measuring open-circuit potentials of these galvanic cells with essentially zero current drain, and (2) development of solid electrolytes such as fully stabilized zirconia and single crystals of calcium fluoride, which exhibit essentially complete ionic conductivity over a wide range of oxygen (2,5)[2] and fluorine (6) potentials.

---

[1]Metallurgist, Albany Research Center, Bureau of Mines, Albany, Oreg.

In addition, cell reactions must be identified and reversible. Measurements obtained from galvanic cells employing fused-salt or aqueous electrolytes are difficult to interpret owing to side reactions, electronic conduction, and junction potentials of unknown magnitude.

Development of a satisfactory electrochemical technique to determine $\Delta G°f$ of sulfides has been difficult and challenging because no solid electrolyte has been found that exhibits complete sulfide ion conductivity and is amenable to more than a few selected systems. Recent reports (7) indicate that CaS may be a satisfactory candidate. Calcium fluoride has been used as the electrolyte to indirectly measure sulfur potentials of a few systems in terms of well-defined fluorine potentials (1).

Pioneering work by Kiukkola and Wagner (2) demonstrated the usefulness of stabilized zirconia as an oxygen-ion electrolyte for investigation of metal-oxygen systems. Within limitations of the ionic properties of stabilized zirconia (5), any equilibrium involving oxygen may be investigated with this technique. The method is based on the measurement of the difference in chemical potential between an electrode of unknown oxygen potential and a reference electrode of known oxygen potential. A modification of this technique was designed to determine Gibbs energies of formation of some of the more stable sulfide compounds.

EXPERIMENTAL WORK

Materials

High-purity reagents were obtained commercially. Analyses of these reagents were confirmed by X-ray emission and analytical procedures. Anhydrous-grade sulfur dioxide, ultra-high-purity argon, and a certified standard of a mixture of 1 mole-pct oxygen in nitrogen provided the stabilizing atmospheres.

Apparatus and Procedure

Two types of high-temperature galvanic cells, employing stabilized zirconia as the electrolyte, have been developed. Figure 1 illustrates the internal arrangement of the components for a cell of the first type. A solid reference electrode consisting of a 1:1 mixture of Cu and Cu_2O was used to determine the Gibbs energy and formation of sphalerite (ZnS, β). Figure 2 illustrates a second type of high-temperature cell in which the solid reference electrode ($Cu + Cu_2O$) was replaced with a gas reference electrode consisting of 1 mole-pct oxygen in nitrogen. Gibbs energies of formation of MoS_2 and WS_2 were determined with this type of cell. Greater overall precision is possible for measurements from cells with gas reference electrodes. Detailed descriptions of these cells and the operating procedures have been published in Bureau of Mines Reports of Investigations (3-4).

---

[2]Underlined numbers in parentheses refer to items in the list of refe

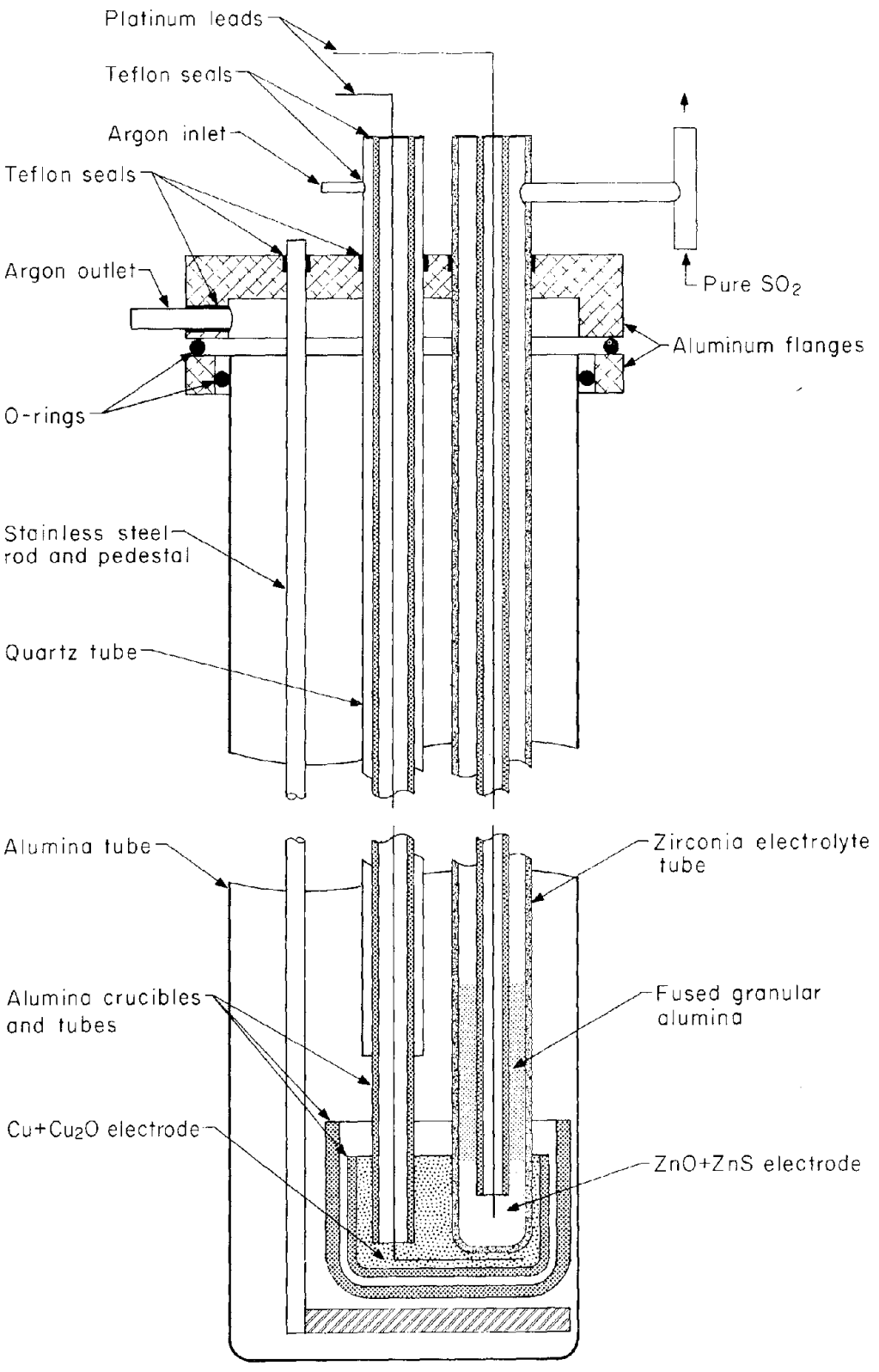


FIGURE 1. - High-temperature galvanic cell with a solid reference electrode.

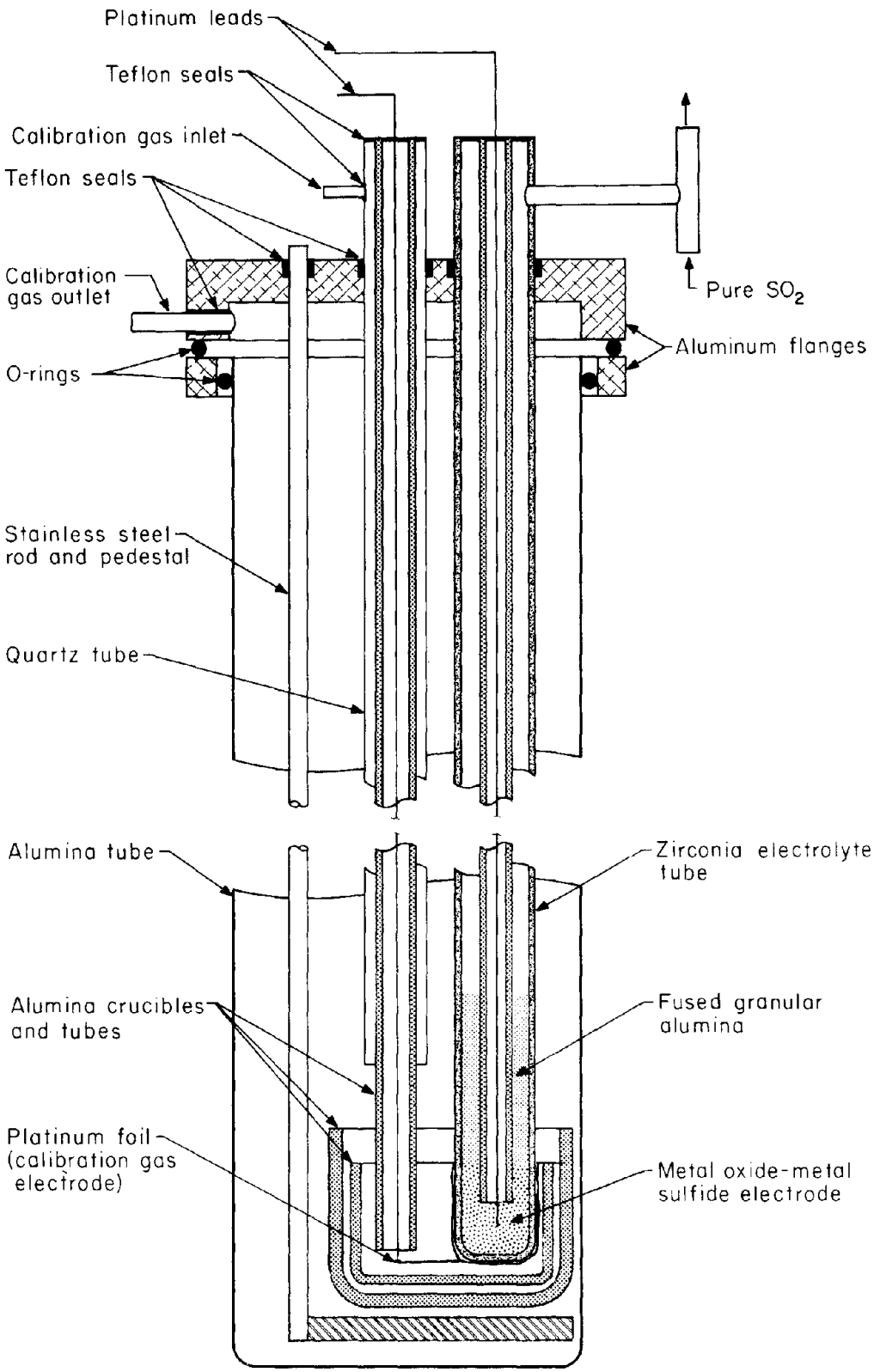


FIGURE 2. - High-temperature galvanic cell with a gas reference electrode.

RESULTS

Potential measurements were obtained from two cells for each system. Results for the cell reaction

$$ZnS(c) + 3\ Cu_2O(c) = ZnO(c) + 6\ Cu(c) + SO_2(g) \quad (1)$$

may be expressed as a function of temperature by the least-squares equation and standard error of estimate as follows:

$$E = -98.5039 + 0.2361T \pm 0.39 \quad (948.7 - 1{,}209.4\ K), \quad (2)$$

where E is expressed in millivolts and T in kelvins. Similar data for the cell reactions

$$MoS_2(c) + 3\ O_2(g,\ 0.0112\ atm) = MoO_2(c) + 2\ SO_2(g) \quad (3)$$

and

$$WS_2 + 3.5\ O_2(g,\ 0.0114\ atm) = WO_3(c) + 2\ SO_2(g) \quad (4)$$

may be expressed by the linear equations

$$E = 776.418 - 0.2116T \pm 0.62 \quad (867.9 - 1{,}209\ K), \quad (5)$$

and

$$E = 861.533 - 0.24574T \pm 0.52 \quad (872 - 1{,}210\ K). \quad (6)$$

Representative emf versus temperature data for ZnS, MoS_2, and WS_2 investigations are illuatrated in figures 3 and 4.

The Gibbs energies of formation of ZnS, MoS_2, and WS_2 were deduced from the foregoing cell reactions by substituting the proper values of the Gibbs energy change of the cell reactions, together with the standard Gibbs energies of formation of the metal oxides, SO_2, the quantity RT ln pSO_2, and the oxygen potential of the reference electrode.

The quantity RT ln pSO_2 requires resolution of the partial pressures of SO_2 at the reaction site, which involves evaluation of the following equilibria and relationships:

$$\Delta G(\text{cell reaction}) = -nFE = RT\ \ln\ pO_2 - RT\ \ln\ pO_2', \quad (7)$$

$$P_{(total)} = \text{barometric pressure} = pSO_3 + pSO_2 + pS_2 + pO_2 \quad (8)$$

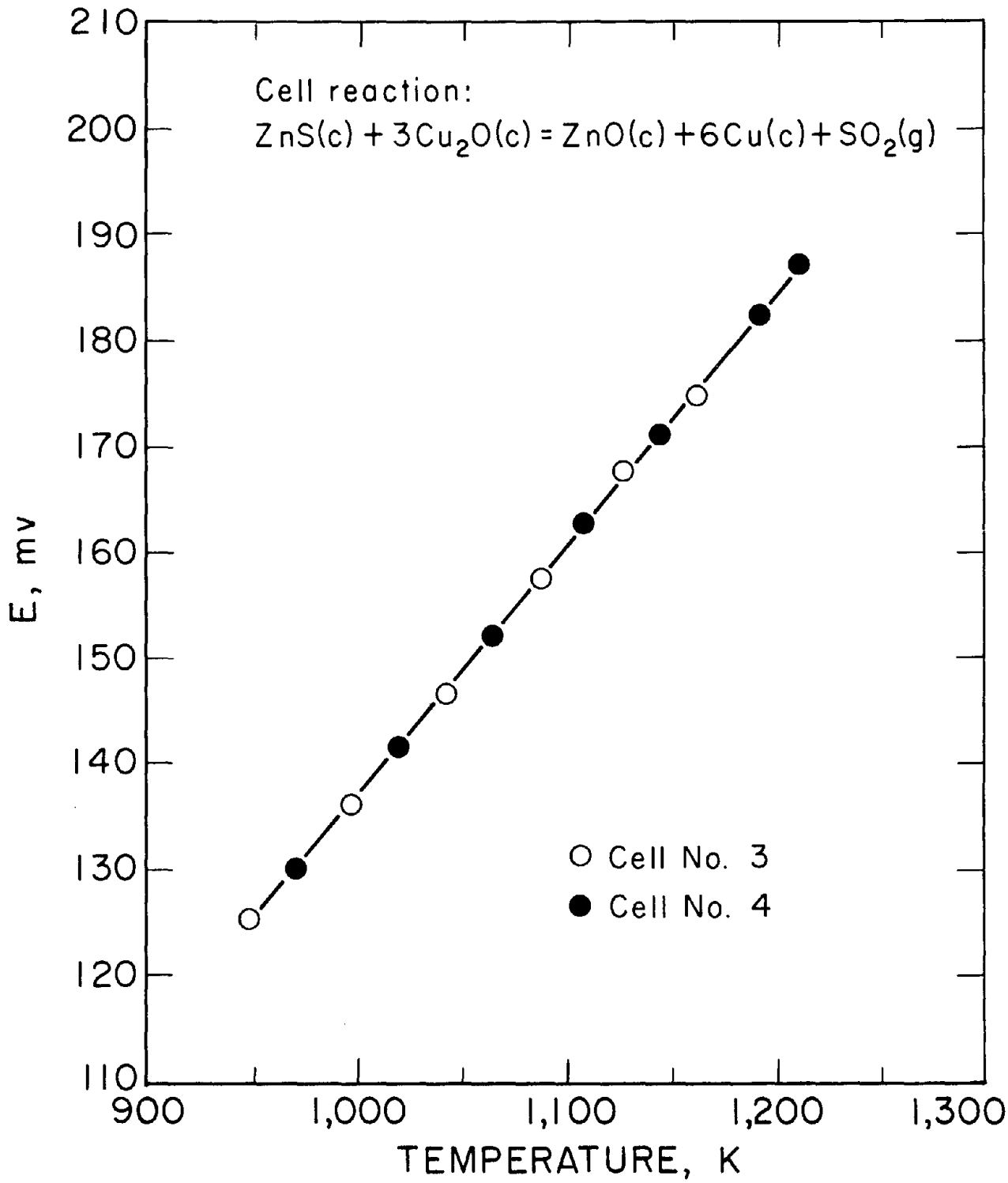


FIGURE 3. - Electromotive force versus temperature for cell reaction (ZnS data).

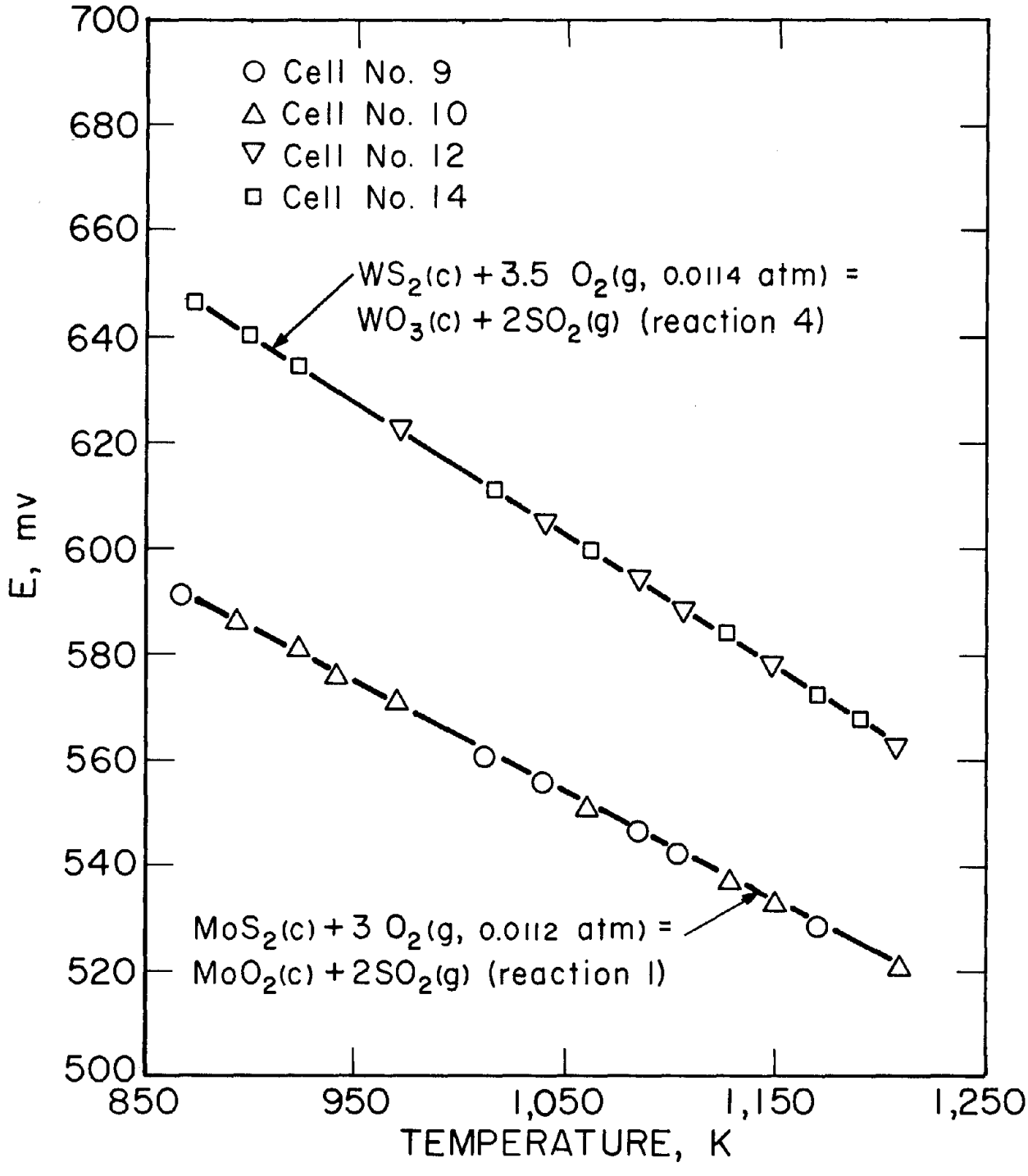


FIGURE 4. - Electromotive force versus temperature for cell reactions (MoS_2 and WS_2 data).

$$SO_3(g) = SO_2(g) + 0.5\ O_2(g) \quad (9)$$

$$SO_2(g) = 0.5\ S_2(g) + O_2(g), \text{ and} \quad (10)$$

$$P_{(total)} = pSO_2 + pSO_2(pO_2)^{0.5}/K_{p,9} + (K_{p,10})^2(pSO_2)^2/(pO_2)^2 + pO_2, \quad (11)$$

where $P_{(total)} = P_{atm}$ and pSO_3, pSO_2, and pS_2 are the partial pressures of the gaseous components. The quantity pO_2' is the partial pressure of oxygen at the reference electrode. $Kp,_9$ and $Kp,_{10}$ are the equilibrium constants for the dissociation of SO_3 and SO_2 as noted by the foregoing reactions. Results of a simultaneous solution of the foregoing relationships are given in table 1.

TABLE 1. - Effect of temperature, total pressure, pSO_3, pS_2, and pO_2 on pSO_2 at reaction site

Temperature, K	Pressure, atm		
	$P_{(total)}$	pO_2	pSO_2
		Zn-S-O	
950	1.000921	2.478×10^{-14}	1.0009205
1,210	1.000921	8.046×10^{-11}	1.0009187
		Mo-S-O	
870	0.99920	2.1048×10^{-1}	.99915
1,210	.99920	2.3915×10^{-1}	.99514
		W-S-O	
870	.99946	1.1125×10^{-17}	.98836
1,210	.99946	4.5303×10^{-12}	.90595

Within the temperature range of these measurements, the standard Gibbs energies of formation of ZnS(β), MoS_2, and WS_2 may be expressed as linear equations. Coefficients for the expression $\Delta G°f = \Delta H°f - T\Delta S°f$ together with a standard error of estimate for these compounds are presented in table 2. Details of these results for the three systems have been published (3-4).

CONCLUSION

The emf method, using solid zirconia stabilized with calcia as the electrolyte, offers a convenient and productive method to determine Gibbs energies of formation of the more stable sulfides. Direct measurement of the oxygen potential at the reaction site avoids some of the problems inherent in experimental techniques that rely on determination of gas compositions, particularly if these compositions lie near the limits of analytical procedures.

TABLE 2. - Coefficients in linear Gibbs equation $\Delta G°f = \Delta H°f - T\Delta S°f$(cal)

Formation Reaction	Temperature range, K	$\Delta H°f$	$\Delta S°f$	Standard error of estimate
$Zn(\ell) + 0.5\ S_2(g) = ZnS(\beta)$	958-1,180	-64,223	-24.02	±650
$Zn(g) + 0.5\ S_2(g) = ZnS(\beta)$	1,180-1,210	-92,720	-48.17	±650
$Mo(c) + S_2(g) = MoS_2(c)$	867-1,210	-96,681	-43.76	±538
$W(c) + S_2(g) = WS_2(c)$	872-1,210	-92,429	-43.88	±280

REFERENCES

1. Aronson, S. Free Energies of Formation of Thorium Sulfides From Solid State E.M.F. Measurements. J. Inorg. Nucl. Chem., V. 29, 1967, pp. 1611-1617.

2. Kiukkola, K., and C. Wagner. Measurements on Galvanic Cells Involving Solid Electrolytes. J. Electrolytes. J. Electrochem. Soc., v. 104, No. 6, 1957, pp. 379-387.

3. Schaefer, S. C. Electrochemical Determination of the Gibbs Energy of Formation of Sphalerite (ZnS). BuMines RI 8301, 1978, 16 pp.

4. _____. Electrochemical Determination of the Gibbs Energies of Formation of Molybdenite (MoS_2) and Tungsten Disulfide (WS_2). BuMines RI 8405, 1980, 17 pp.

5. Steel, B. C. H., and C. B. Alcock. Factors Influencing the Performance of Solid Oxide Electrolytes in High-Temperature Thermodynamic Measurments. Trans. AIME, v. 233, 1965, pp. 1359-1367.

6. Ure, R. W., Jr. Ionic Conductivity of Calcium Fluoride Crystals. J. Chem. Phys., v. 26, No. 6, 1957, pp. 1363-1373.

7. Worrell, W. L., V. B. Tare, and F. J. Bruni. Development of a High-Temperature Solid-Sulfide Electrolyte. High-Temperarture Technology (IUPAC), Butterworths, London, 1967, pp. 503-509.

DISCUSSION

N. A. D. Parlee: The equilibrium data and the emf data also yield the heats of formation. The difference with the calorimetric data is not that great, but it really shows that the emf leads to a different value than the heat of formation by calorimetry.

S. C. Schaefer: I don't have an authoritative explanation for this variation; however, these are saturated phases. Since I operate at fairly low temperatures, the intersolubility of the oxide and sulfide phases is negligible and side reactions would be minimal. At these lower temperatures (900-1,200 K) this source of error would not affect the Gibbs energies of formation appreciably. In addition, the lattice parameters of the final products of the cell reaction agree favorably with published parameters.

J. Haygarth: How did X-ray diffraction of the electrolyte interface establish that the reaction assumed was actually taking place? In view of the very small current flow needed to make measurements of emf, how could the X-ray powder diagrams distinguish between the products of the assumed reaction and some other? I recognize that they can show that formation of solid solutions between ZnS and ZnO was undetectable, and that direct reaction between the phases in contact, e.g.

$$2ZnO + ZnS \rightarrow 3Zn + SO_2,$$

was not taking place, but I am unconvinced that they can be appealed to as proof positive that the cell reaction assumed was taking place solely.

S. C. Schaefer: X-ray diffraction analysis identified the final products of the cell reaction. Starting mixtures consisting of a 1:1 ratio of sulfide and its coexisting oxide were blended and thoroughly mixed. These mixtures and the final products were analyzed by X-ray diffraction. In addition, lattice parameters were obtained. Other reactions that occur simultaneously at the reaction site at the interface of the ZnS + ZnO electrode with the electrolyte are $SO_3 = SO_2 + 0.5O_2$, and $SO_2 = 0.5S_2 + O_2$. Since equilibrium exists, the oxygen pressure is the same for all the reactions of the heterogeneous system. The oxygen pressure, pO_2, is obtained directly from the emf measurements and the independent relationship

$$\Delta G(\text{cell reaction}) = -nFE = RT \ln pO_2 - RT \ln pO_2'$$

where pO_2' is the partial pressure of oxygen at the reference electrode.

J. Haygarth: So it was the same mixture before and after?

S. C. Schaefer: Correct, in the case of ZnS and MoS_2. X-ray diffraction analysis was used to identify products after emf measurements were completed.

N. A. Gokcen: I think that in the case of nickel sulfide, what you put in the cell did not turn out to be the same as what you were studying in the cell.

S. C. Schaefer: That is correct. In the investigation to determine $\Delta G°f$ of Ni_3S_2, the coexisting phases in equilibrium with SO_2 at 1 atm were identified as $Ni_{3-x}S_2$ and NiO. High-temperature X-ray and chemical analyses are being

made to determine the composition of $Ni_{3-x}S_2$ and thereby establish the exact cell reaction. X-ray diffraction methods were used to identify the final products after the emf measurements were completed for each system.

N. A. D. Parlee: Considerable disagreement often exists between high-temperature equilibrium data and calorimetric data for oxide systems. This is apparently in contrast to the excellent agreement which was shown for the sulfides (ZnS and MoS_2). Is there a possible explanation for the variations in ΔH° and ΔS° that are obtained for the oxides, especially when the equilibrium data are extrapolated to higher or lower temperatures?

S. C. Schaefer: I would like to say one thing. We ordinarily don't extrapolate too far outside our own measurements. If you wish to use this type of measurement for ΔS°_T, then T refers to the average temperature.

N. A. D. Parlee: Do you assume that ΔH°_T and ΔS°_T are constant?

S. C. Schaefer: Yes, within a narrow range of temperature.

SECTION 4.- IONIC SOLUTIONS

DETERMINATION OF IONIC ACTIVITIES OF AQUEOUS METAL SALT SOLUTIONS

by

J. P. Neumann[1] and N. A. Gokcen[2]

ABSTRACT

A novel method for determination of ionic activities of aqueous electrolyte solutions is described. The method is based on precise measurements of the water vapor pressure of solutions by a differential capacitance pressure transducer. A number of flasks, each containing a solution of different concentration, are connected to the transducer, so that several measurements can be made successively within a short time. The vapor pressure data yield the activity of water, from which the activity of the electrolyte is computed by an equation satisfying the Gibbs-Duhem relation. The activities are expressed as a function of the molal concentration in the form of an empirical power series with adjustable parameters; a series with half-integer exponents of the molality is preferable to a series with integer exponents.

This research is part of the effort made by the U.S. Department of the Interior, Bureau of Mines to provide fundamental thermodynamic data for the advancement of mineral resource technology, corrosion protection, environmental preservation, pollution control, and energy economy.

INTRODUCTION

A thorough knowledge of the thermodynamic properties of aqueous electrolyte solutions is useful for the improvement of existing and the development of new processes (9, 12, 13).[3] In particular, ionic activity data are important for understanding processes such as leaching of minerals, purification of solutions, and precipitation of selected constituents. Extensive activity data are available for moderately dilute, single-electrolyte solutions at 25° C, but little work has been done in the area that is of principal technical interest, namely concentrated, multicomponent electrolyte solutions at various

[1]Metallurgist, Albany Research Center, Bureau of Mines, Albany, Oreg.
[2]Supervisory research chemist, Albany Research Center, Bureau of Mines, Albany, Oreg.
[3]Underlined numbers in parentheses refer to items in the list of references at the end of the paper.

temperatures. A number of empirical equations have been proposed for the estimation of ionic activities (3, 10-11) but presently accurate data can be obtained only from experimental measurements.

This report describes a novel method for determination of activities of aqueous single- and multi-electrolyte solutions. The method is based on precise measurements of the water vapor pressure of these solutions. Highly accurate electronic pressure sensors have recently become available (2, 4); they offer a promising means for convenient, rapid, and accurate determination of the ionic activity of aqueous electrolyte solutions.

THERMODYNAMIC BACKGROUND

The relationships between the vapor pressure of the solvent and the activities of solvent and solute for aqueous electrolyte solutions have been discussed recently in detail (5), and therefore only a brief review will be given here. Definitions of all symbols used in this paper are given in the Appendix.

The activity, a_w, of water - the solvent - is obtained from measurements of the vapor pressure of water, P, over the electrolyte solution by

$$a_w = P/P^\circ, \tag{1}$$

where P° is the vapor pressure over pure water, at the same temperature T as the solution. For concentrated solutions at elevated temperatures, P and P° must be replaced by the fugacities f and f° respectively.

The activity of water, a_w, and the mean ionic activity of electrolyte ij, a_{ij}, dissolved in water, are related by the Gibbs-Duhem equation

$$55.508\ d\ln a_w + \Sigma[m_{ij} \cdot d\ln(a_{ij}^{\nu_{ij}})] = 0, \tag{2}$$

where m_{ij} is the molality and ν_{ij} is the sum of the stoichiometric coefficients ν_i and ν_j of electrolyte ij; cations are denoted by i with odd subscripts (1,3,5,. . .), while anions are denoted by j with even subscripts (2,4,6,. . .). The summation Σ extends over all the electrolytes in the solution. The mean ionic activity, a_{ij}, is related to the mean ionic molality, $m_{ij\pm}$, and the mean ionic activity coefficient γ_{ij}, by

$$a_{ij} = (m_{ij\pm}) \cdot \gamma_{ij}. \tag{3}$$

The definitions of $m_{ij\pm}$ and γ_{ij} are given in the appendix ; they are analogous to the definition for a_{ij}. It should be noted that $m_{ij\pm}$ is generally different from m_{ij}; only for $\nu_i = \nu_j = 1$ are $m_{ij\pm}$ and m_{ij} equal. The reference state for γ_{ij} is the infinite dilute solution of electrolyte ij, that is, $\gamma_{ij} \to 1$ for $m_{ij} \to 0$. The activity of water, a_w, is based on pure water as the standard state, with the concentration of water in solution expressed by its mole fraction, x_w, given by

$$x_w = 55.508/(55.508 + \Sigma m_i + \Sigma m_j). \quad (4)$$

The activity coefficient of water, γ_w, is related to a_w by $a_w = \gamma_w x_w$. After determining the activity of water a_w at constant temperature as a function of molality of an electrolyte 12, from $m_{12} = 0$ to any desired molality m_{12} at a sufficient number of points, a_w can be expressed by a power series with half-integer exponents of m_{12},

$$55.508 \ln a_w = Bm_{12}^{1.5} + Cm_{12}^{2.0} + Dm_{12}^{2.5} + \ldots - \nu_{12} m_{12}. \quad (5)$$

The selection of the power series - apart from the requirement that the Debye-Hückel limiting law be obeyed - is empirical. However, it has been found that for a given number of terms, a half-integer series describes the experimental data more precisely than a full-integer series (7). The values of the coefficients B, C, and D are determined by a nonlinear regression analysis, using a computer. Since the equations for a_w and a_{12} must satisfy the Gibbs-Duhem relation 2, it can be shown that, in terms of the coefficients obtained for a_w, a_{12} is given by

$$\nu_{12} \ln(a_{12}) = -\frac{1.5}{0.5} Bm_{12}^{0.5} - \frac{2.0}{1.0} Cm_{12}^{1.0} - \frac{2.5}{1.5} Dm_{12}^{1.5} - \ldots + \nu_{12} \ln m_{12\pm}. \quad (6)$$

Obtaining the coefficients of the terms in this equation from those in equation 5 is far more convenient than the graphical integration of Gibbs-Duhem relation (6). The coefficient B is proportional to the Debye-Hückel constant α in $\ln \gamma_{12} = \alpha m_{12}^{0.5}$ for 1:1 electrolytes. Because of the large factor, 55.508, associated with $\ln a_w$ in equation 5 compared with the term $\ln a_{12}$ in equation 6, small errors in a_w will result in relatively large errors in a_{12}. It is therefore necessary to measure a_w as precisely as possible.

EXPERIMENTAL METHOD

The apparatus for the vapor pressure measurements is presently under construction. A general description of the various parts of the equipment is presented in this section. The solutions whose vapor pressure is to be measured are contained in six 100-ml Pyrex[4] flasks as shown in figure 1; all six flasks are attached to one side of the pressure sensor. Glass stopcocks permit connecting only one flask at a time to the pressure sensor. A seventh flask, containing pure water, identical to the others but separated from them, is connected to the other side of the pressure sensor. The system can be evacuated by a mechanical vacuum pump which, according to the manufacturer, has a free air displacement of 60 l/min (Sargent-Welch Scientific Co., Skokie, Ill.; model 1405). The pump is capable of achieving an ultimate vacuum of 10^{-4} torr. The vacuum is monitored by a Penning-Thermistor combination gage, which provides continuous automatic pressure readings from atmospheric pressure to less than 10^{-7} torr (CVC Products, Inc. Rochester, NY, model GPT-450).

[4]All references to specific manufacturers or equipment brands are made for identification purposes only and do not imply endorsement by the Bureau of Mines.

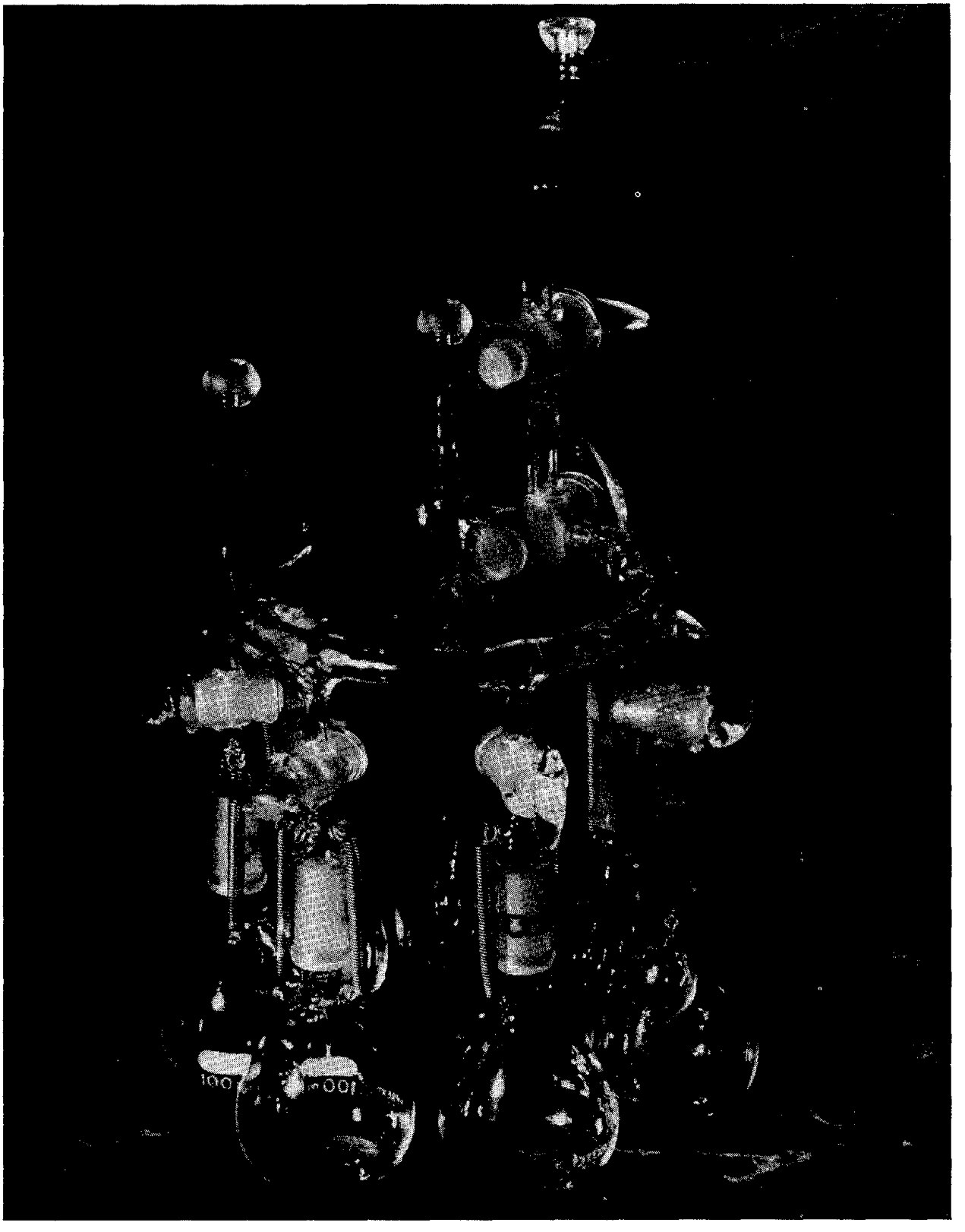


FIGURE 1. - Glass apparatus for aqueous electrolyte solutions.

The flasks are immersed in a temperature controlled water bath, which has a capacity of approximately 60 liters. The square-shaped container is constructed of polycarbonate sheet; it is mounted in a wooden bench. The sides and the bottom of the bath are thermally insulated by a 5-cm thick layer of Styrofoam. To be able to measure the vapor pressure as a function of temperature in the range from 10° C to 60° C, the bath is equipped with cooling and heating elements; the heating elements and the stirring mechanism are shown in figure 2. The inner element is a 1,000-W heater, which is controlled manually by a powerstat. The outer element is a 125-W heater, which is regulated by a precision temperature controller (Bayley Instrument Co., Kenwood, Calif., model 252). The stirrer is driven by a 60-W variable-speed motor (0-2,500 rpm). The temperature of the bath is measured by a quartz thermometer with digital readout (Hewlett-Packard Co., Mountain View, Calif., model 2804 A). Using a triple-point-of-water cell for periodic calibration, it should be possible to measure the temperature with an absolute accuracy of ±0.01° C with this instrument (1). An uncertainty of ±0.01° C in the absolute value of the temperature corresponds to a relative error of approximately ±0.05 pct in the vapor pressure of pure water, P°, over the temperature range from 10° to 60° C. This error is of approximately the same order of magnitude as the relative accuracy of the experimentally determined vapor pressure of pure water (14), but the error in $a_w = P/P^\circ$ is considerably smaller than 0.05 pct as will be shown later.

The vapor pressure is measured by a diaphragm-type differential capacitance pressure transducer (MKS Instruments, Inc., Burlington, Mass., model 315 BH-1000 SP), having a measuring range of 0 to 1,000 torr. One side of the sensor head is connected through the P_X port to the flask containing pure water; the other side is connected through the P_R port to the flasks containing the aqueous electrolyte solutions. The transducer measures the difference between the vapor pressure of pure water, P°, and that of the solutions, P, that is $\Delta P = P^\circ - P$. The transducer is connected via a preamplifier to a digital readout unit, calibrated in torr. To minimize mechanical vibrations, the transducer is suspended, together with the preamplifier, from a steel frame which is mounted rigidly to the wall and the ceiling of the laboratory above the bath, as shown in figure 3. The sensor, as well as the connections between the sensor and the glass apparatus, is heated to a temperature higher than that of the bath to prevent condensation of water vapor.

According to the manufacturer, the transducer has a resolution of 0.001 pct of the full-scale pressure, while the overall accuracy is about 0.1 pct of the pressure reading for pressures between 1 and 1,000 torr. However, the accuracy of the activity of water, a_w, will actually be better, since the differential transducer measures directly the small difference $\Delta P = P^\circ - P$ between two pressures P° and P and not the individual values of P and P°. By substituting the pressure difference ΔP in equation 1, the following expression for the activity, a_w, is obtained

$$a_w = 1 - (\Delta P/P^\circ). \qquad (7)$$

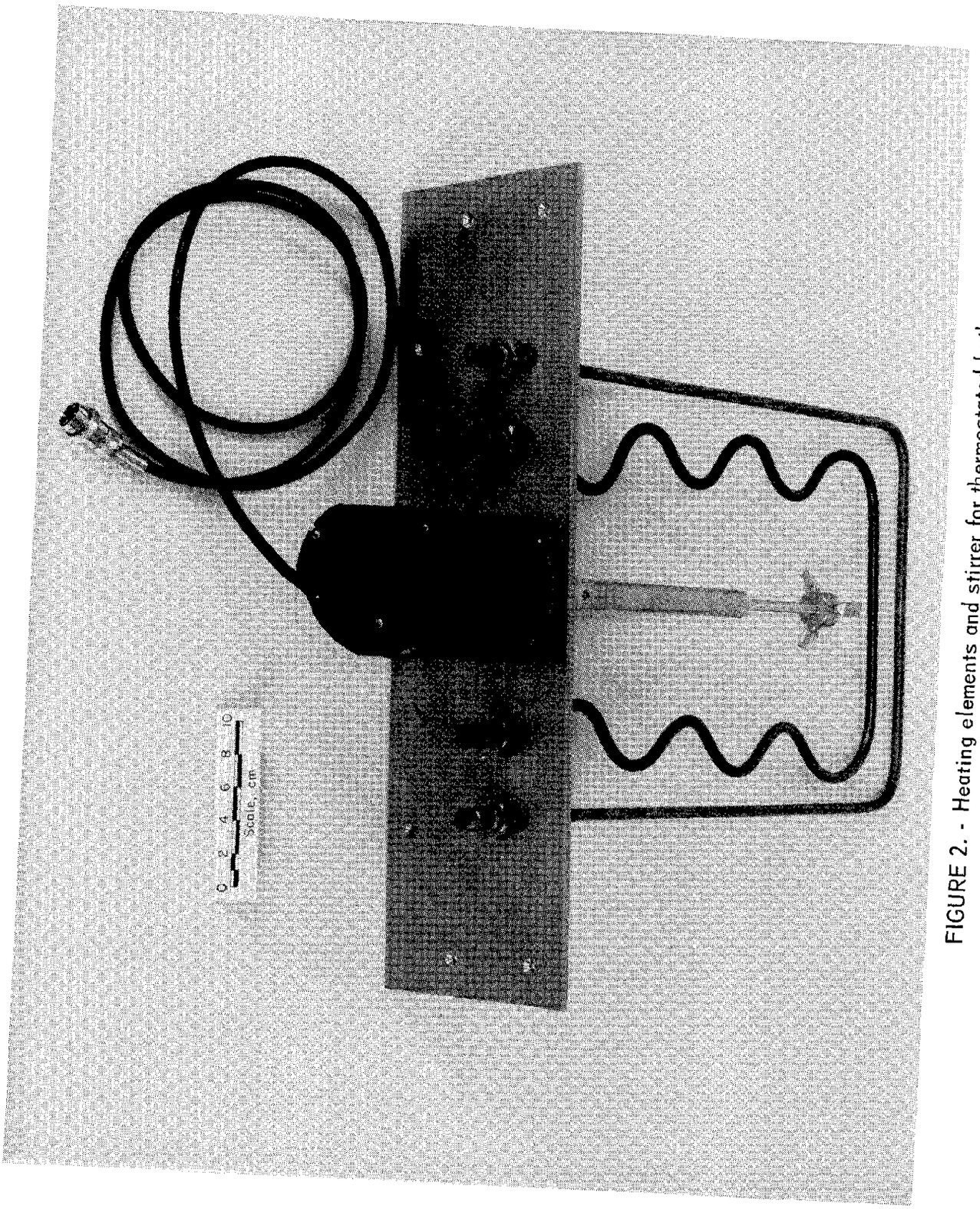


FIGURE 2. - Heating elements and stirrer for thermostated bath.

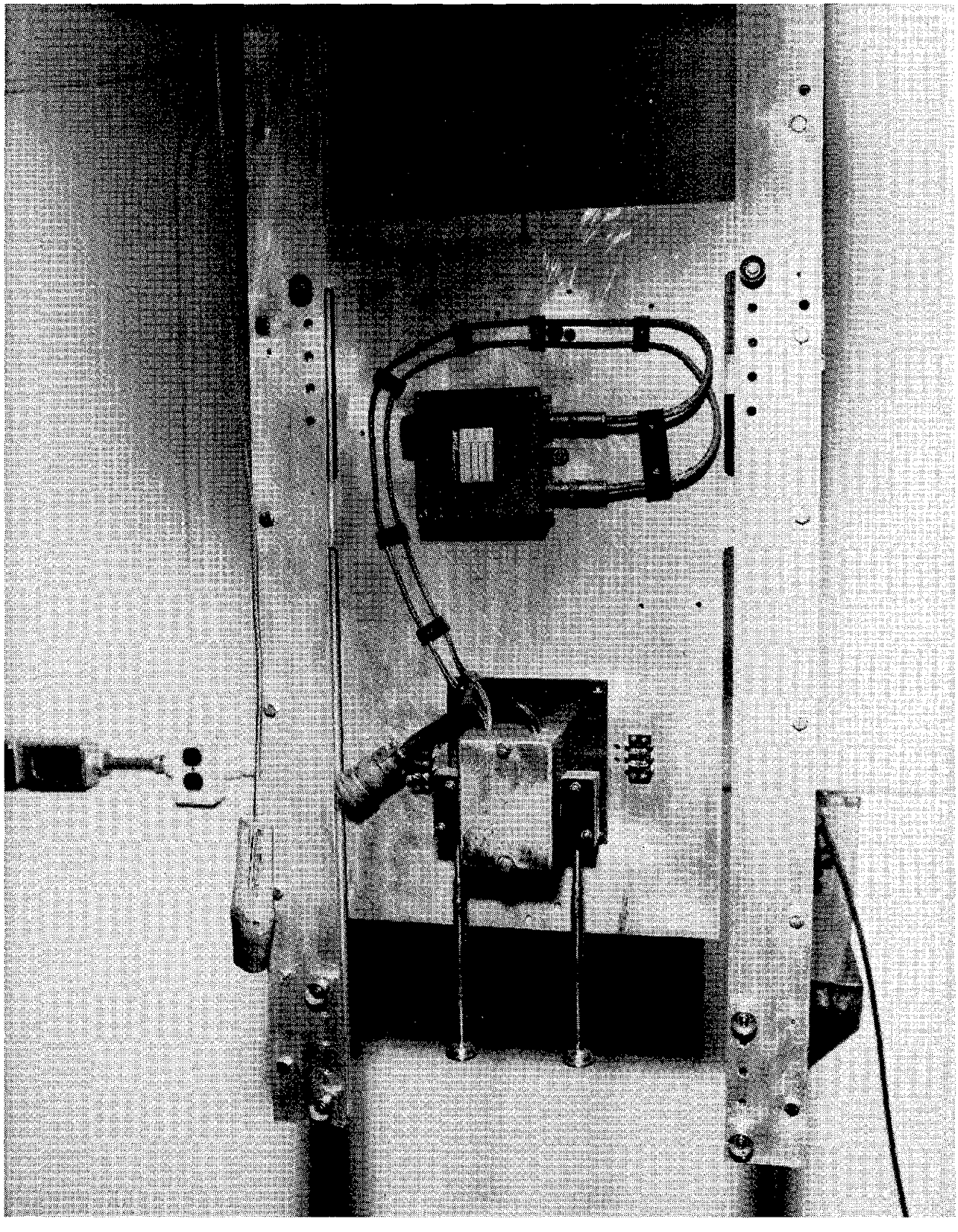


FIGURE 3. - Arrangement of differential pressure transducer (lower unit) and preamplifier (upper unit).

Differentiation of equation 7 with respect to the two variables, ΔP and P°, leads to the following relationship between the errors in ΔP and P° and the resulting error in a_w, da_w:

$$|da_w| = \frac{\Delta P}{P^\circ}\left[\frac{d(\Delta P)}{(\Delta P)} + \frac{dP^\circ}{P^\circ}\right]. \qquad (8)$$

Since $\Delta P/P^\circ = 1 - a_w$, it can be seen that the error in a_w will be smaller than the errors in ΔP and P° by the factor $(1 - a_w)$. For example, the activity of water of a 3 M solution of NaCl at 25° C is $a_w = 0.8932$ (8), and the factor $(1 - a_w)$ has a value of approxiy 0.1. The relative errors in ΔP and P° have been estimated to be 0.1 pct and 0.05 pct respectively, so that the error in the activity of water will be $da_w \simeq \pm 0.0001$.

ACKNOWLEDGEMENTS

The authors wish to express their appreciation to the staff of the Thermodynamics Laboratory of the Albany Research Center for their advice during the construction of the apparatus.

APPENDIX: GLOSSARY OF SYMBOLS

α	Debye-Hückel constant
a_i, a_j	Activities of cation i and anion j, respectively
a_{ij}	Mean ionic activity of electrolyte ij, defined by $a_{ij}^{\nu_{ij}} \equiv a_i^{\nu_i} \cdot a_j^{\nu_j}$
a_w	Activity of water (solvent)
f	Fugacity of water vapor over a solution at temperature T
f°	Fugacity of water vapor over pure water at temperature T
γ_i, γ_j	Activity coefficients of cation i and anion j, respectively
γ_{ij}	Mean ionic activity coefficient of electrolyte ij, defined by $\gamma_{ij}^{\nu_{ij}} = \gamma_i^{\nu_i} \cdot \gamma_j^{\nu_j}$
γ_w	Activity coefficient of water
i	Cation i (designated by odd numbers)
j	Anion j (designated by even numbers)
m_{ij}	Molality of electrolyte ij ($mol \cdot kg^{-1}$)
m_i, m_j	Molalities of cation i and anion j, respectively; related to m_{ij} by $m_i = \nu_i m_{ij}$ and $m_j = \nu_j \cdot m_{ij}$
$m_{ij\pm}$	Mean ionic molality of electrolyte ij, defined by $m_{ij\pm}^{\nu_{ij}} = m_i^{\nu_i} \cdot m_j^{\nu_j}$; $m_{ij\pm}$ is related to m_{ij} by: $m_{ij\pm} = m_{ij}\left(\nu_i^{\nu_i}\ \nu_j^{\nu_j}\right)^{1/\nu_{ij}}$
ν_i, ν_j	Stoichiometric coefficients of cation i and anion j, respectively
ν_{ij}	Sum of the stoichiometric coefficients ν_i and ν_j, defined by $\nu_{ij} = \nu_i + \nu_j$
P	Vapor pressure of water over an electrolyte solution at temperature T

P°	Vapor pressure of pure water at temperature T
ΔP	Pressure difference, defined by $\Delta P = P^\circ - P$
Σ	Summation symbol.
T	Absolute temperature (K)
x_w	Mole fraction of water
55.508	Number of moles of water in 1 kg of water

REFERENCES[5]

1. Benson, B. B., and D. Krause, Jr. Use of the Quartz Crystal Thermometer for Absolute Temperature Measurements. Rev. Sci. Instr., v. 45, No. 12, 1974, pp. 1499-1501.

2. Bromberg, J. P. Accurate Pressure Measurements in the Region 0.1-1000 mTorr; The Intercalibration of Two McLeod Gauges and a Capacitance Manometer. J. Vac. Sci. Technol., v. 6, No. 5, 1969, pp. 801-808.

3. Bromley, L. A. Thermodynamic Properties of Strong Electrolytes in Aqueous Solutions. AIChE J., v. 19, No. 2, 1973, pp. 313-320.

4. Curran, D. J. Pressure Transducers. J. Chem. Educ., v. 46, 1969, pp. A465-A480.

5. Gokcen, N. A. Determination and Estimation of Ionic Activities of Metal Salts in Water. BuMines RI 8372, 1979, 24 pp.

6. _____. Thermodynamics. Chapter XIII. Techscience, Inc., Hawthorne, Calif., 1975, 460 pp.

7. Haase, R. Analytische Darstellung der Gleichgewichtseigenschaften konzentrierter Elektrolytlösungen (Analytical Representation of the Equilibrium Properties of Concentrated Electrolyte Solutions). Z. Phys. Chem. (Frankfurt am Main), v. 39, 1963, pp. 360-382.

8. Hamer, W. J., and Y.-Ch. Wu. Osmotic Coefficients and Mean Activity Coefficients of Uni-univalent Electrolytes in Water at 25° C. J. Phys. Chem. Ref. Data, v. 1, No. 4, 1972, pp. 1047-1099.

9. Kirby, R. C., and J. A. Barclay. Extraction Processes for Low-Grade Ores. Min. Eng. v. 27, No. 6, 1975, pp. 42-47.

10. Kusik, C. L., and H. P. Meissner. Electrolyte Activity Coefficients in Inorganic Processing. AIChE Symp. Ser., v. 74, No. 173, 1978, pp. 14-20.

11. Pitzer, K. S. Electrolyte Theory - Improvements Since Debye and Hückel. Acc. Chem. Res., v. 10, 1977, pp. 371-377.

[5]Title enclosed in parenthesis is translation from the language in which the item was published.

12. Sohn, H.Y. Annual Review of Extractive and Process Metallurgy: Developments in Physical Chemistry and Basic Principles of Extractive Metallurgy in 1978. J. Metals. v. 31, No. 5, 1979, pp. 10-32.

13. Wadsworth, M. E. Annual Review of Extractive and Process Metallurgy: Review of Developments in Hydrometallurgy in 1978. J. Metals, v. 31, No. 5, 1979, pp. 12-35.

14. Wexler, A. Vapor Pressure Formulation for Water in Range of 0 to 100° C. A Revision. J. Res. NBS, v. 80A, Nos. 5-6, 1976, pp. 775-785.

DISCUSSION

Pamela Rogers: What is the maximum temperature at which the transducer can be operated?

J. P. Neumann: The maximum temperature is 250° C. There are two types of pressure gages available commercially. In one type, the sensor and the preamplifier form a single unit. These sensors can be operated only at ambient temperature because the semiconductor components of the preamplifier cannot withstand elevated temperatures. In the other type of pressure gage, the one we are using, the sensor and the preamplifier form separate units, which are connected by a cable. In order to reduce the electronic noise, the cable should be as short as feasible. In our case, the cable is about 2 feet long. We keep the sensor at a constant temperature of 100° C. We chose this temperature because it is above the highest temperature of our open water bath. I think we may be able to go up to 60° C with our vapor pressure measurements. However, as I said before, the sensor can actually be operated up to 250° C.

Pamela Rogers: Up to what concentration ranges do you intend to make measurements?

J. P. Neumann: We are interested in the concentration range from about 0.05 molal up to saturation.

E. J. Prosen: What type of transducers are used in your apparatus?

J. P. Neumann: We use a so-called "single-sided" differential capacitance transducer, which has two electrodes located on one side of the diaphragm. Other capacitance transducers have one electrode on each side. We selected for our applications a single-sided transducer because we will also be measuring solutions containing volatile, corrosive electrolytes like hydrochloric acid and nitric acid. This type of transducer is ideally suited for pressure measurements of corrosive gases since it is constructed of Inconel and stainless steel; the electrodes are located on the side of the diaphragm that is not exposed to the corrosive gases.

C. M. Criss: What is the full-scale range of the transducer?

J. P. Neumann: Presently, we have one sensor with a full-scale range of 1,000 torr, but two more sensors with full-scale ranges of 10 and 100 torr are on order. The smallest range that is available from this manufacturer is 1 torr.

E. J. Prosen: This may not concern you because you are interested in

concentrated solutions. What are you doing to take account of any gas solubility?

J. P. Neumann: I think the standard prodecure for removing dissolved gases is to alternately freeze and remelt the solution under vacuum. The gas solubility in the solid state is much lower than in the liquid state. Repeating this procedure three to four times should remove all the dissolved gases from the solution.

R. N. Goldberg: How do you intend to calibrate your instrument? Would there be any advantage gained by using the instrument in a "null" mode, i.e., by referencing your measurements to another solution having a well-known vapor pressure very close to that of the solution under investigation?

J. P. Neumann: We intend to test and calibrate our equipment in two ways: First, by measuring the absolute vapor pressure of pure water as a function of temperature and comparing our results with the latest compilation by Wexler of the National Bureau of Standards; second, by measuring the vapor pressure difference between pure water and NaCl solutions of various concentrations. The vapor pressure of NaCl solutions has been measured by several authors and is well known, although not with the same accuracy as that of pure water. The advantage of our method is that we measure directly the small difference between two large pressure values. At higher electrolyte concentrations, the pressure difference will be larger, and one could use for example a saturated solution of NaCl as reference; however, this would be a secondary standard.

N. A. Gokcen: We can always connect one side of the transducer to vacuum and then water will be our standard. The vapor pressure of water is very well known and it is a dependable standard.

J. P. Neumann: I would like to add that anybody interested in seeing the equipment is welcome to visit the laboratory.

CALORIMETRY OF IONIC SOLUTIONS

by

Cecil M. Criss[1]

ABSTRACT

Recent advances in electronics and basic designs of calorimeters have made it possible to measure thermal properties of electrolyte solutions with a precision and speed considered impossible two decades ago. Nowhere is this more evident than in the measurement of heat capacities. Although the newer techniques have not had such a dramatic effect upon the precision for enthalpies of solution and dilution, they have nevertheless led to an increased speed and ease in making the measurements. In addition, the commercial availability of calorimetric instruments has made calorimetry more convenient. Finally, the new technology is making it possible to study system that were not easily amenable to investigation a few years ago, such as solutions of high-vapor-pressure solvents and solutions under extreme conditions of temperature and pressure.

The greatest changes have occurred in the measurement of heat capacities. The techniques have evolved from the direct specific heat measurements prior to 1950, through the integral heat method, commencing in the early 1960's, to the recently developed differential flow technique. Developments in instruments and current practices in these and other areas of solution calorimetry are presented.

INTRODUCTION

Applications of calorimetry to the study of ionic solutions have occurred simultaneously with the development of chemical thermodynamics and ionic solution theory itself. In the latter half of the 19th century a large number of enthalpies of solution in water were measured by Berthelot, de Forc-

[1]Department of Chemistry, University of Miami, Coral Gables, Fla.

rand, Thomsen, Pickering, and others. These measurements were generally made at high concentrations using mercury thermometers and large bulky calorimeters. Many of the currently tabulated thermodynamic values are partially based on these data (27, 34).[2] From the outset it was recognized that enthalpies of solution were dependent upon the final concentration of the solution, and during the early part of the 20th century many attempts were made to accurately measure the concentration dependence and to explain the results theoretically. In order to improve the temperature sensitivities, calorimetrists turned increasingly to thermocouples and resistance thermometers. The thermocouple was introduced to solution calorimetry by White (39) in 1914.

However, the real impetus for accurate calorimetric measurements was the introduction of the Debye-Hückel theory of ionic solutions in 1923 (9). Soon after the publication of this theory, Bjerrum (3) and Adams (1) independently applied it to predict enthalpies of dilution of electrolytes in dilute aqueous solutions, and in 1929 Randall and Rossini (32) calculated the theoretical limiting slope for the concentration dependence of heat capacities of aqueous ionic solutions. The latter authors neglected to include the change in concentration with temperature in their derivation, but this term was included in a later derivation by La Mer and Cowperthwaite (22). Adequate tests of the predictions of the Debye-Hückel theory required calorimeters with even greater temperature sensitivities. The climax of these developments occurred in the 1930's with the extraordinarily sensitive enthalpy of dilution calorimeters of Lang and coworkers (23-24), Gulbransen and Robinson (16), and Gucker, Pickard, and Planck (15). These calorimeters had temperature sensitivities that exceeded 1×10^{-6}° C. At the same time calorimeters were developed that were capable of measuring direct specific heats to better than 0.01 pct. Among the more precise were the calorimeters of Randall and Rossini (32) and Gucker, Ayres, and Rubin (13).

These calorimeters and others of similar design were used to measure enthalpies of dilution to 1×10^{-4} molal (m) and specific heats to 0.1 m. In all but a few cases the experimental limiting slopes for enthalpies of dilution of strong electrolytes were shown to agree with the theoretical slope. However, as a result of the inability to measure specific heats accurately at concentrations less than 0.1 m, adequate comparisons with the theoretical slope were not possible for heat capacities, except for those few cases for which the temperature coefficients of the enthalpies of dilution were available. An excellent review of these precise calorimeters and the results obtained from them has been given by Gucker (12).

The very precise techniques used in enthalpy of dilution and specific heat calorimeters were also used to improve the sensitivity of solution calorimeters, although because of the necessity of introducing a solid into the calorimeter, considerable modifications had to be made. Furthermore, the

---

[2]Underlined numbers in parentheses refer to items in the list of references at the end of the paper.

sudden and rather large temperature changes caused by dissolution of a solute, and the heat generated by the sample introduction itself obviated the sensitivity one could obtain with thousand-junction thermopiles. One of the more precise of these calorimeters has been described by Slansky (37).

To review in detail the development and variations of the calorimeter during the 1930's is beyond the scope of the present paper, but one can summarize the general characteristics of the more precise instruments in the following terms: (1) The calorimeters were batch type, generally of twin (differential) construction and operated adiabatically, (2) they were large and bulky, frequently having a volume in the vicinity of a liter, (3) they employed resistance thermometers or multiple thermocouples, sometimes exceeding 1,000 junctions, along with bridges or potentiometers with their accompanying galvanometers for temperature measurements, (4) they were electrically calibrated using batteries as "constant-voltage" power sources, and (5) they were individually constructed, and generally complex to operate, and all data had to be recorded manually. Nearly all measurements during this period were confined to within a few degrees of room temperature. Developments in calorimetry reached a plateau by 1940 and remained dormant until new materials and electronic instrumentation became available in the 1950's.

Five important items became available since the early 1950's that have caused a rapid change in the technology of solution calorimetry. These are (1) thermistors and commercial thermopiles, (2) highly sensitive low-noise-level electronic amplifiers, (3) electronic constant-current power supplies, (4) data acquisition equipment and laboratory computers, and (5) commercially constructed calorimetric instruments. While none of these has increased the temperature sensitivity of the calorimeters, they have made the construction, maintenance, and operation of calorimeters much more convenient, and the required volumes of sample have been significantly reduced. The purpose of this paper is to examine some of the newer techniques that have been incorporated into calorimetry since about 1955, and with which the author has had some personal experience. The discussion is limited to calorimeters suitable for measuring enthalpies of solution, heat capacities, and enthalpies of dilution. Titration and other special types of calorimetry will not be discussed.

ENTHALPY OF SOLUTION CALORIMETERS

Most of the modern enthalpy of solution calorimeters are of the isoperibol (isothermally jacketed) type and use thermistors as temperature-sensing element. The substitution of thermistors for thermopiles made possible the construction of smaller calorimeters, with no significant loss in accuracy. One of the first reports of a calorimeter incorporating a thermistor is that by Coops, Balk, and Tolk (7) in 1956. Soon afterwards, Sunner and Wadsö (38) analyzed the efficienty of several calorimetric designs of about 100-ml capacity, all of which employed thermistors.

The commercial availability of low-noise-level dc microvolt amplifiers in the 1950's made it possible for the first time to amplify and record bridge output voltages so that continuous records of temperature variations in calorimeters could be made. Gunn (17) described such a system for a rocking-bomb solution calorimeter using a resistance thermometer, G-2 Mueller bridge, dc amplifier, and analog recorder. A saw tooth signal was superimposed upon the recorder trace as a result of oscillation of the thermometer circuit in the earth's magnetic field. Professor Cobble and his students (2, 8, 20, 26) described a series of calorimeters of different designs which employed thermistors or resistance thermometers, dc amplifiers, and strip-chart recorders. For the first time electronically controlled constant-current power supplies were used for electrical calibrations, and consequently current did not have to be continuously monitored during calibration periods. One of these calorimeters (2) had a total volume of about 7 ml and a thermal sensitivity of 5 x 10^{-5} cal.

Examples of two calorimeters incorporating modern designs and which we have used in our laboratory (18, 35) are shown in figures 1 and 2. The design in figure 1 has the advantages that it is easier to construct initially and easier to charge in operation. However, it has a relatively larger vapor phase volume which may require corrections for enthalpies of vaporization, especially for high-vapor-pressure solvents, and it requires a longer time to come to equilibrium. The all-metal calorimeter shown in figure 2 has a rapid equilibrium time and low-temperature modulus. This is accomplished by requiring the two stainless steel support tubes to have extremely thin walls so that the thermal conduction to the surroundings is minimized while at the same time the better conducting metal enables a faster establishment of thermal equilibrium. Thermistors are used as temperature-sensing elements in both calorimeters, and the bridge outputs are amplified and automatically recorded. In the case of the calorimeter shown in figure 2, no attempt is made to balance the bridge circuit during the calorimetric run; instead, the bridge unbalance is amplified by a very linear nanovolt amplifier, digitized, and fed into a data acquisition system or computer (35). The data are processed completely by computer, which corrects for the nonlinearity of the thermistor and bridge and removes all possibility of subjectivity in data analysis. This calorimeter has a noise level of 4 x 10^{-6}° C and has been used to measure the enthalpy of solution of Tris(hydroxymethyl-aminomethane) (TRIS) in HCl with a reproducibility of ±0.04 pct. The vapor seal at the top also makes it suitable for measurements in anhydrous solvents. Commercial instruments having a design similar to that in figure 1 are available from LKB Instruments, Inc., and from Tronac, Inc.

One of the few new adiabatic solution calorimeters to be described recently has been assembled at the National Bureau of Standards by Prosen and Kilday (30). The adiabatic shield temperature is automatically controlled through an electronic feedback system employing thermocouples, a microvolt amplifier, and a power amplifier. The temperature within the calorimeter is measured either by a platinum resistance thermometer and G-3 Mueller bridge or by a commercially available quartz-oscillator thermometer.

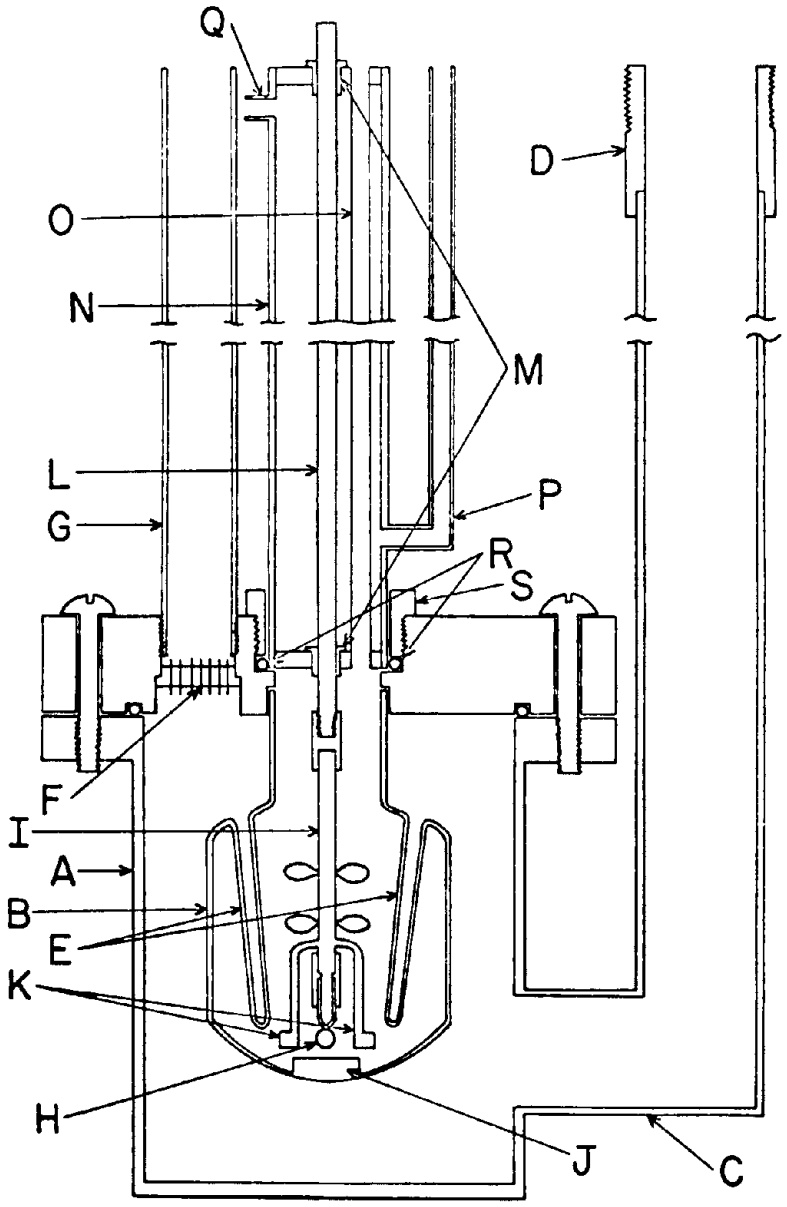


FIGURE 1. - Submarine solution calorimeter: A, brass vacuum jacket; B, reaction vessel; C, evacuating tube; D, threaded coupling; E, thermistor and heater wells; F, hermetic electrical seal; G, conduit; H, sample bulb; I, stirring shaft; J, anvil; K, forked paddle; L, steel shaft; M, Teflon bearings; N, shaft housing; O, filling tube; P and Q, tubes for purging with nitrogen; R, O-ring; S, threaded nut. *(Courtesy, American Chemical Society.)*

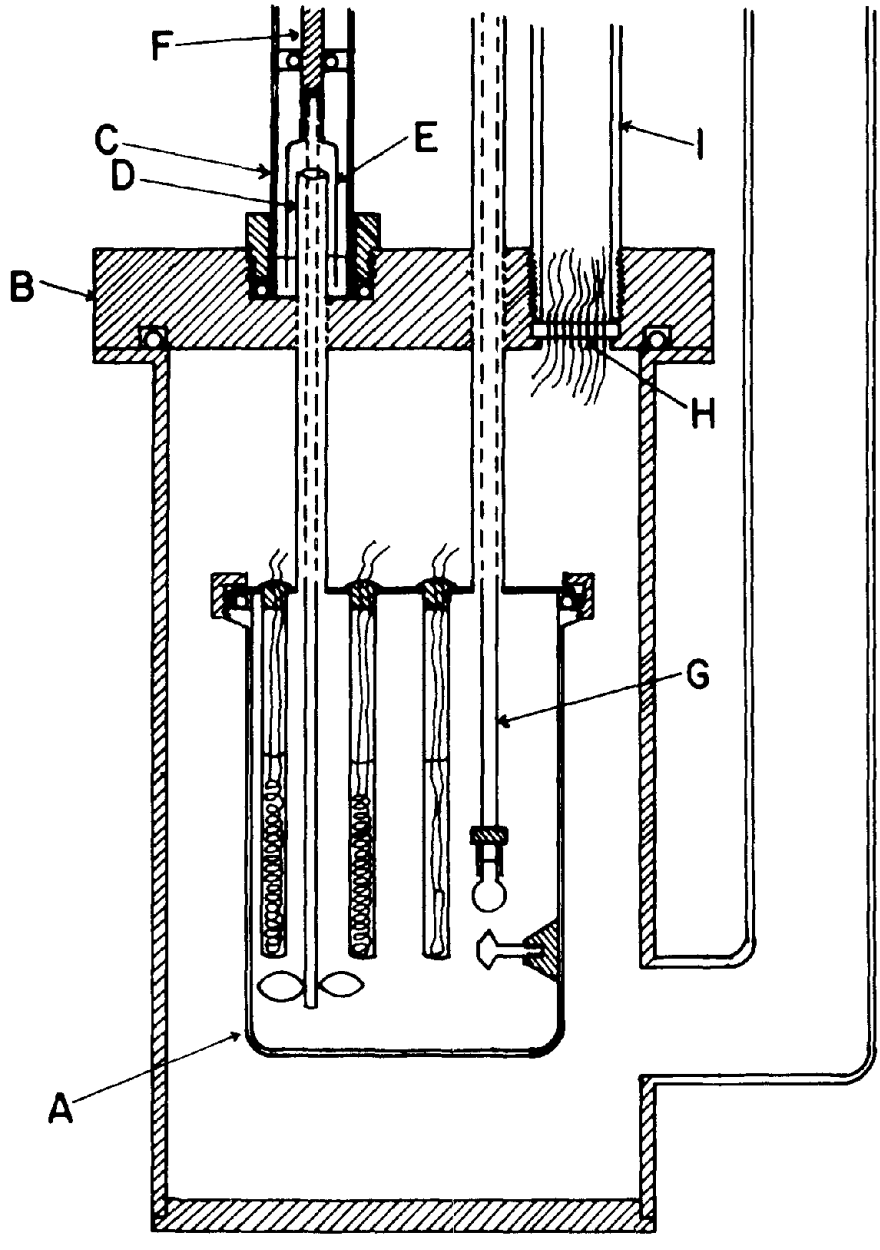


FIGURE 2. - Improved submarine solution calorimeter. A, reaction vessel; B, top of outer vacuum jacket; C, stirring shaft housing; D, inner tube of vapor trap; E, rotating hood of vapor trap; F, stirring shaft; G, bulb support and smasher; H, hermetic electrical feedthrough; I, conduit for heater and thermistor leads. *(Courtesy, American Institute of Physics.)*

Standard reactions for testing the precision and accuracy of solution calorimeters have been a continual problem. KCl has traditionally been used as a calibration standard for endothermic reactions. However, the discrepancies among the reported values are much greater than one would expect, either from the estimated accuracy (frequently <0.1 pct) or from the actual experimental reproducibilities of the calorimeters used in the measurements. Sunner and Wadsö (38) have examined several published enthalpies of solution for KCl and concluded that systematic errors are present in one or more of the determinations. They questioned whether KCl was really a suitable standard for solution calorimetry.

In 1964 Irving and Wadsö (19) proposed the use of the reaction of TRIS with 0.1 N HCl, and recommended a value of 29.723 kj $mole^{-1}$ (35). The National Bureau of Standards has issued TRIS as a standard reference material for solution calorimetry, SRM 724 and 724a, and Prosen and Kilday (31) at the Bureau have measured its enthalpy of reaction with 0.1 N HCl, using the adiabatic calorimeter described above (31). On the basis of their measurements and data from other laboratories, they have recommended 29.771 ± 0.031 kj $mole^{-1}$. The uncertainty assigned, which is disappointingly large, includes a reflection of the values reported from other laboratories. In another study from the Bureau of Standards, Brunetti, Prosen, and Goldberg (4), using an isoperibol solution calorimeter, obtained a value of 29.792 ± 0.031 kj $mole^{-1}$. Again, as in the case of KCl, the spread in results for TRIS is greater than the apparent inaccuracies of the high-precision calorimeters, and Prosen and Kilday (31) have concluded that it will probably be some time before the source of the spread of results is understood.

SPECIFIC HEATS OF IONIC SOLUTIONS

Until the early 1960's specific heats of ionic solutions were measured directly using highly precise calorimeters developed by Gucker and others, as described in the introduction. Although the precision of these calorimeters is superb, usually being better than 0.01 pct, measurements below about 0.1 m are useless for obtaining apparent molal heat capacities. This is easily understood from the definition of apparent molal heat capacity:

$$\phi_{cp} = \frac{C_p - n_1 \bar{C}^\circ_{p1}}{n_2}. \qquad (1)$$

In this equation C_p is the heat capacity of the solution, $\bar{C}^\circ_{p1}$ is the heat capacity of pure solvent, and n_1 and n_2 are the number of moles of solvent and solute, respectively. As the solution becomes more dilute in electrolyte, both the numerator and denominator approach zero and any error in C_p results in an astronomical uncertainty in ϕ_{cp}. The magnitude of this error for a 0.01 pct error in specific heat measurement can be seen in figure 3. Berthelot recognized this problem long ago and suggested that specific heats could be obtained at lower concentrations by combining specific heats at higher concentrations with the temperature coefficient of the enthalpy of dilution at lower concentrations. This approach was first actually used in

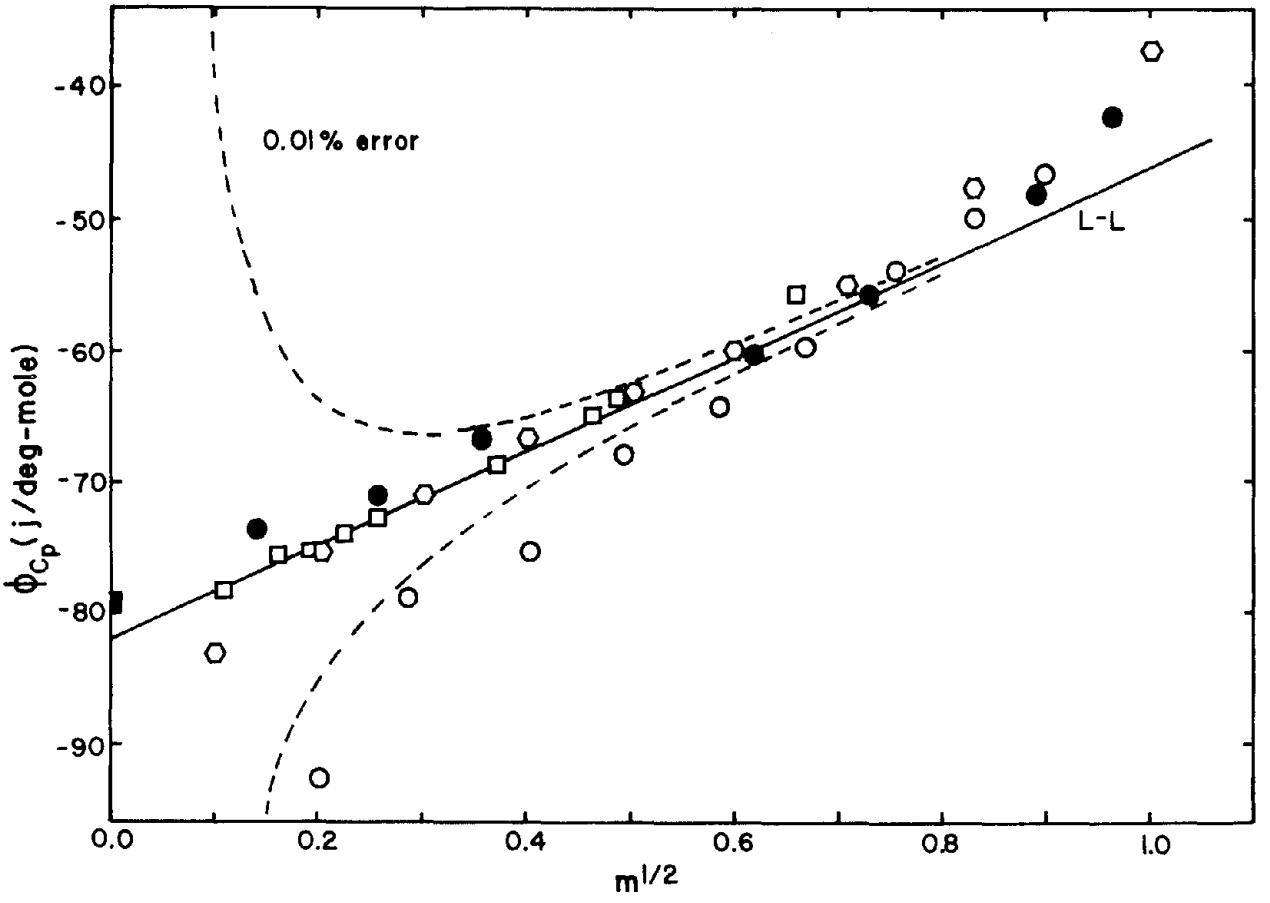


FIGURE 3. - Apparent molal heat capacities of aqueous NaCl. ○ Randall and Rossini; □ Pasztor; ○ Fortier, Leduc, Desnoyers; ● Lage; ▮ Criss and Cobble. Dashed line represents error in ϕ_{cp} for a 0.01 pct error in direct specific heat measurement. L-L refers to the Debye-Hückel limiting-law.

1905 by Richards and Lamb (33). In terms of modern thermodynamic treatment, the enthalpy of dilution is converted to the relative apparent molal heat capacity by means of the equation

$$\phi_{cp} - \phi^{\circ}_{cp} = \left(\frac{\delta \partial L}{\partial T}\right)_p = -\left(\frac{\delta \partial H_{Dil}}{\partial T}\right)_p \qquad (2)$$

from which ϕ°_{cp} can be obtained if ϕ_{cp} is known at a higher concentration.

This approach may lead to very accurate values of ϕ_{cp} at low concentrations, but it requires two different kinds of highly precise calorimeters an many time-consuming measurements. Further, in order to obtain the heat capa city at one temperature, the enthalpy of dilution must be measured at two or more temperatures. Consequently, very few measurements of this type have been reported.

To avoid having to make measurements with two types of highly sophisticated calorimeters, Criss and Cobble (8) suggested in 1961 that standard state heat capacities could be obtained in many cases by measuring enthalpies of solution at low concentrations (0.001 m to 0.01 m) and at rather close temperature intervals. Extrapolation of the enthalpies to infinite dilution by an extended Debye-Hückel equation gave standard enthalpies of solution, ΔH_s°, which were converted to standard partial molal heat capacities by the equation

$$\overline{C}_{p2}^\circ - C_p^\circ = \Delta C_p^\circ = \left(\frac{\partial H_s^\circ}{\partial T}\right)_p \approx \left(\frac{\Delta(\Delta H_s^\circ)}{\Delta T}\right)_p , \qquad (3)$$

where C_p° is the heat capacity of the crystalline solute and ΔC_p° is the change in heat capacity for the reaction process. The approximation in equation 3 is valid if the temperature interval is kept to 5° or 10° C for systems in which the heat capacity is varying rapidly, such as aqueous solutions. This approach, which is referred to as the "integral heat method," has been exploited extensively by Professor Cobble and his students. It has several advantages: (1) The calorimeter is less complicated to construct and operate than the specific heat and enthalpy of dilution calorimeters, (2) the measurements are all made at very low concentrations, so that extrapolation to infinite dilution is more reliable, and (3) limiting slopes for enthalpies are known relatively better than the slopes for heat capacities. The low concentrations also enable one to obtain heat capacities for electrolytes which are not sufficiently soluble to obtain by other methods. Furthermore, since the method is optimized by making measurements at several temperatures, one generally evaluates heat capacities over a significant temperature range. The method has three major disadvantages: (1) It is very time consuming to obtain data, (2) it is practical to obtain heat capacities only at infinite dilution, and (3) obtaining accurate data requires that the enthalpies of solution be small (<40 kj mole^{-1}). This last limitation arises because the method requires taking the difference in the enthalpies of solution at two temperatures, and even if these are known quite accutately (~0.1 pct), the uncertainties in absolute numbers will be large if the enthalpies are large. This becomes a serious limitation for high-temperature aqueous solutions and some nonaqueous solutions. In spite of these drawbacks, the author has used the technique extensively for nonaqueous solutions. It works well for solvents with low vapor pressures, but problems are encountered with high-vapor-pressure solvents. Heat capacities for $NaClO_4$ in water, methanol, and N,N-dimethylformamide (5) obtained by the integral heat method are shown in figure 4. These data illustrate the extreme temperature sensitivity of heat capacities of electrolytes in some solvents, such as water, and the relative insensitivity in other solvents.

More recently Picker and coworkers (29) have described a differential flow heat capacity calorimeter that removes many of the disadvantages of the two methods discussed above. In North America a commercial version of the instrument is sold by Sodov, Inc. The general principle of operation is shown schematically in figure 5. It consists of two identical parallel cap-

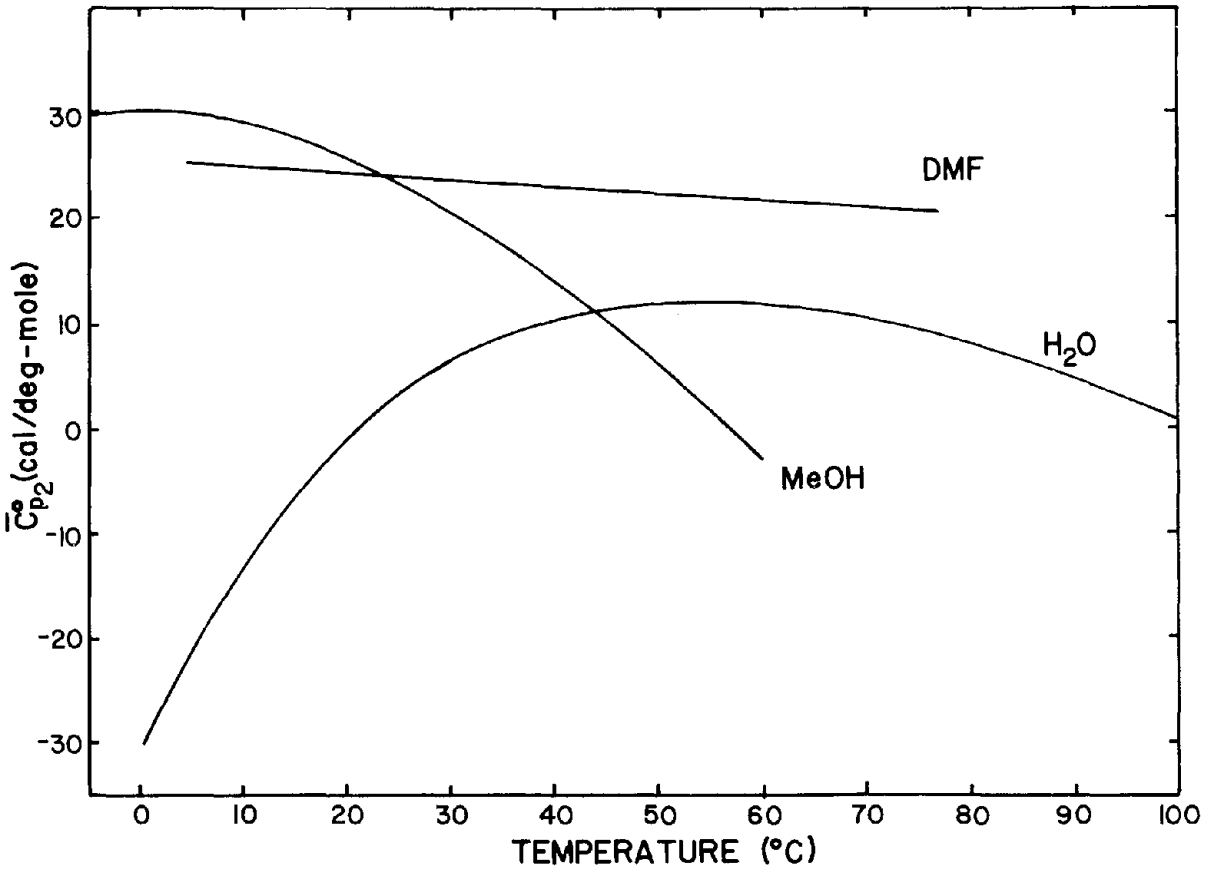


FIGURE 4. - Standard partial molal heat capacities of $NaClO_4$ in N, N-dimenthylformamide, methanol, and water, obtained by the integral heat method.

illary tubes inside a vacuum chamber. Inasmuch as possible the tubes are symmetrical; one acts as a reference cell and the other as a working cell. There are two heaters, H_r and H_w, and thermistors, T_r and T_w, for the corresponding tubes. The thermistors are in opposite arms of a bridge circuit so that any temperature deviation between T_w and T_r results in a bridge unbalance, which is amplified and fed back into H_w to bring the temperature at T_w back to its original temperature, which is the same as T_r. The change in power to H_w is reflected in a potential change across resistor R_w which is recorded. In operation, the valve, V, is adjusted so that pure solvent passes through the capillary, which is thermostated to temperature, T_i, and continuing through the reference cell, and the delay line, back through the thermostat and through the working cell. The heaters are adjusted such that the temperature changes at H_r and H_w are identical. The adjustment may range up to about 3° C depending upon the power setting. Once a base line is obtained on the recorder, the valve is adjusted to permit solution to pass through the reference cell. If the specific heat of the solution is different from that of the solvent, the temperature rise at H_r will be different from that at H_w through which pure solvent is

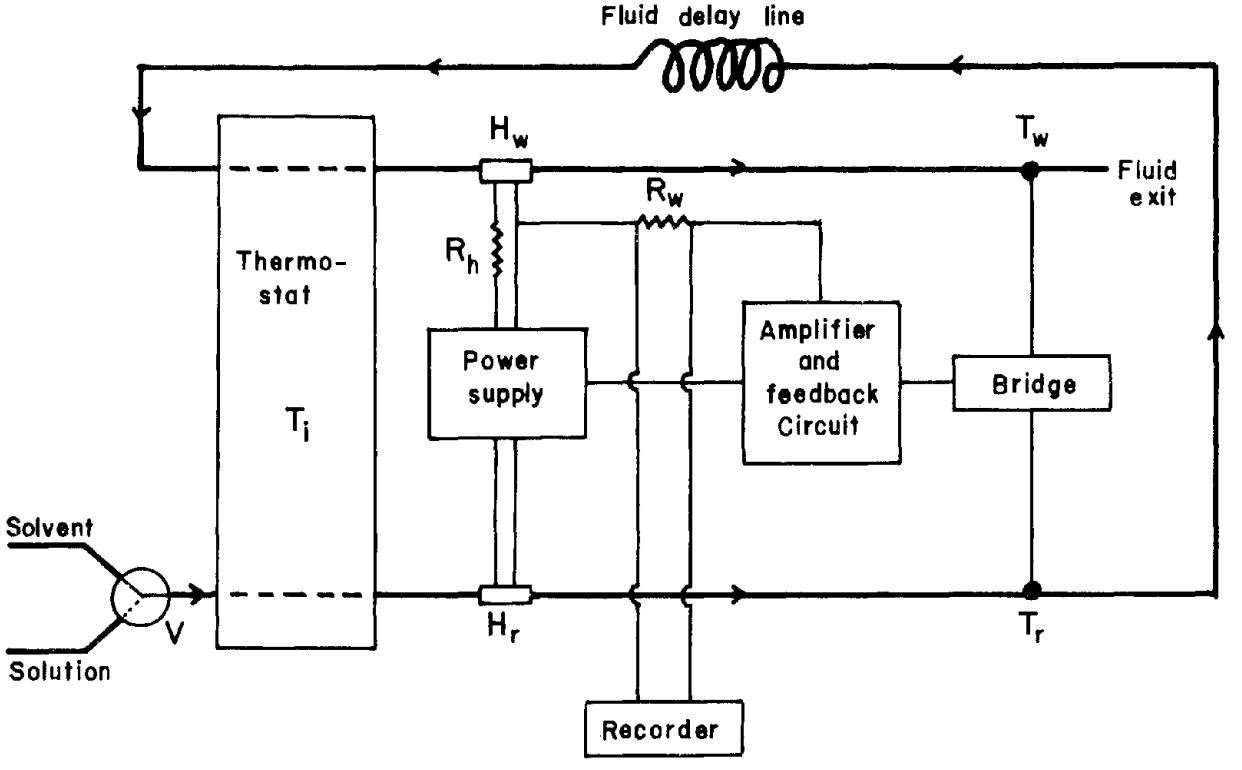


FIGURE 5. - Differential flow heat capacity calorimeter: H_w and H_r, heaters for working and reference cells; T_w and T_r, thermistors; R_h and R_w, resistors for measuring power to heaters; V, fluid selection valve.

still passing. The temperature difference will be detected at the thermistors, and a corresponding change will be made in the power to H_w; this change will be shown as a deflection at the recorder. After a period of time, solution is passing through both cells and the base line will be re-established; the valve can then be adjusted to permit pure solvent to pass through the reference cell, and a deflection in the opposite direction is obtained on the recorder. Comparing the deflections with standard deflections obtained by electrical calibrations enables one to calculate the heat capacity of the solution relative to that of the solvent:

$$\frac{c_p}{c_p^\circ} = \left(1 + \frac{\Delta P}{P}\right)\left(\frac{\rho^\circ}{\rho}\right), \qquad (4)$$

where c_p and c_p° are the specific heats of the solution and solvent respectively, P is the base power to the heaters, ΔP is the change in power to the heater in the working cell, and ρ° and ρ are the densities of the pure solvent and solution respectively. Professor Robert Wood at the University of Delaware has shown (40), and we have verified, that it is necessary only

to know the density ratio at the temperature of the delay line, and not at the temperature of the actual heat capacity measurements. Consequently the delay line should be thermostated during the calorimetric measurements and the densities measured at that temperature.

The differential flow calorimeter has three major advantages: (1) It enables one to measure specific heats for solutions about 10 times more dilute (0.01 m) than the direct specific heat method, (2) it is much more rapid than the integral heat method, and (3) it requires much less volume of liquid than either of the other methods. This last advantage becomes important when one is investigating nonaqueous systems. Additionally the flow system is particularly convenient to use for anhydrous solutions, and solvents exhibiting high vapor pressures, such as methanol. It has the disadvantages that the most dilute concentrations that can be measured are still about 10 times more concentrated than those required in the integral heat method, and one must measure precise densities. However, the densities are useful in themselves for calculating apparent molal volumes.

Figure 3 shows ϕ_{cp} for aqueous NaCl obtained by direct calorimetry (32) and several separate investigations by differential flow calorimetry (11, 21, 28), along with $\phi^{\circ}_{cp} (=\bar{C}^{\circ}_{p2})$ obtained from the integral heat method (8). One can observe a change in slope near the lower limit of the measurements by direct calorimetry.

Both the integral heat and the differential flow heat capacity techniques have been used in the author's laboratory to measure heat capacities of numerous electrolytes in several nonaqueous solvents. The results appear to be comparable in accuracy, uncertainties in the enthalpies of solution at several temperatures obtained in the integral heat method are balanced by the uncertainties in the extrapolations of the ϕ_p data from the differential flow method. The large differences in $\bar{C}^{\circ}_{p2}$ for selected electrolytes in four different solvents at 25° C are illustrated by the data in table 1. However, one must be careful in attaching a meaning to the differences in $\bar{C}^{\circ}_{p2}$ for a given electrolyte in various solvents, since the differences may vanish or even change sign at other temperatures as one can observe from figure 4.

As a result of the energy crisis there has been an increasing interest in the thermodynamic properties of aqueous solutions at higher temperatures. These values are most easily obtained by having accurate heat capacities for the aqueous electrolytes as a function of temperature, and it is worthwhile focusing our attention on the problems associated with measuring this function at higher temperatures.

Measurements up to 100° C present few problems, and numerous data now exist. Heat capacities for simple electrolytes in water exhibit the charac-

teristic curve of $NaClO_4$ shown in figure 4, except that they are negative over the entire temperature range. Above 100° C, $\bar{C}^{\circ}_{p_2}$ becomes rapidly negative with temperature; for example, $\bar{C}^{\circ}_{p_2}$ for aqueous NaCl becomes -837 j deg^{-1} $mole^{-1}$ at 300° C (25). Consequently if one desires accurate thermodynamic

TABLE 1. - $\bar{C}^{\circ}_{p_2}$ for electrolytes in various solvents at 25° C (j deg^{-1} $mole^{-1}$)

Electrolyte	$\bar{C}^{\circ}_{p_2}$			
	H_2O[1]	MeOH (28)	DMF[2]	Ethylene glycol (21)
LiCl	-65.2	-119.1	94.2	30.9
LiBr	-69.1	-99.8	70.3	-9.1
NaBr	-88.1	-34.6	116.1	11.0
KBr	-118.3	-20.4	119.0	4.0
KI	-108.7	.2	93.7	39.8

[1]Desnoyers, J. E., C. de Visser, G. Perron, and P. Picker. J. Sol. Chem. v. 5, No. 9, 1976, pp. 605-616.
[2]Choi, Y-S., and C. M. Criss. Disc. Faraday Soc., No. 64, 1978, pp. 204-219.

values at higher temperatures, it is important to measure accurately the temperature dependence of $\bar{C}^{\circ}_{p_2}$.

High-temperature (above 100° C) calorimetry of aqueous solutions generates several new problems. The resulting high pressures require calorimeters to have thicker walls with the result that the ratio of the mass of fluid to that of the calorimeter is reduced, causing a corresponding loss in sensitivity. Heat leaks from radiation are also much greater. Finally, materials that can withstand the corrosive action of ionic solutions at high temperatures are difficult to find. These problems are common to all three types of calorimeters used for heat capacities, although the first is not significant for the differential flow calorimeter because of its small volume.

In spite of these limitations, high-temperature calorimeters of each type have been constructed. Gucker and Christens (14) have described a direct specific heat calorimeter suitable for measuring specific heats to the critical temperature of water, but to the knowledge of this author no results from this calorimeter were ever published. Cobble and Murray (6) have described a solution calorimeter that they have operated at 300° C to measure heat capa-

cities by the integral heat method. More recently Wood (40) has constructed a differential flow heat capacity calorimeter which has been operated successfully at 325° C.

In addition to the experimental problems, there are problems in the treatment of data. The limiting slopes for heat capacities at higher temperatures are extremely large and uncertain (36). Consequently extrapolation of ϕ_{cp} from the lower concentration limit of 0.1 m obtained from direct specific heat measurements is impractical. Similar problems arise in extrapolating data from the differential heat capacity calorimeter, but the extrapolation is only from 0.01 m which gives some advantage. The integral heat method is even more advantageous in this respect since the concentrations covered range down to 0.001 m making the length of extrapolation to infinite dilution much less. Furthermore, the limiting slopes for enthalpies of dilution are known more accurately than those for heat capacities (36). However, enthalpies of solution generally become extraordinarily negative at high temperatures, more than 400 kj $mole^{-1}$ in some cases (6), so that even for 0.1 pct uncertainty, the uncertainty in absolute number of calories for ΔH_s° bebecomes large, with a correspondingly large uncertainty in the standard state heat capacity. Upon consideration of all factors, it is the opinion of this author that the differential flow calorimeter has the greatest advantages at high temperatures.

ENTHALPY OF DILUTION CALORIMETRY

Most of the recently published enthalpy of dilution data have been obtained from either flow or rotating batch enthalpy of mixing calorimeters. Both types of instruments are commercially available. The rotating batch calorimeter appears to be well suited for solvent systems having vapor pressures equal to or lower than water at room temperatures. It uses very small volumes of liquids (2 ml/4 ml) and has the major advantage that pumps are not required for its operation, as with flow calorimeters, but it has the disadvantage that corrections have to be made for the heat of wetting of the walls of the cells in precise work. Wood and coworkers have used a rotating batch calorimeter for both aqueous solutions and N-methylacetamide (10, 41) and have described the corrections for the enthalpy of wetting of the walls (10).

The author has employed an LKB-type flow calorimeter[3] for measuring enthalpies of dilution of several alkali metal halides in methanol, from near saturation to low concentrations. A schematic of the flow cell is shown in figure 6. Two cells of similar construction are placed in a large aluminum heat sink and the system is operated in a differential mode, with signals from the thermopiles being amplified by a microvolt amplifier and recorded on a strip-chart recorder. A base line is established when pure solvent is entering both capillaries of the cell. The system may then be calibrated electrically by means of a heater embedded in the cell, and the peak height obtained on the recorder compared with the peak height caused by mixing the pure solvent with solution. With care it is possible to measure enthalpies of dilution to 0.005 m.

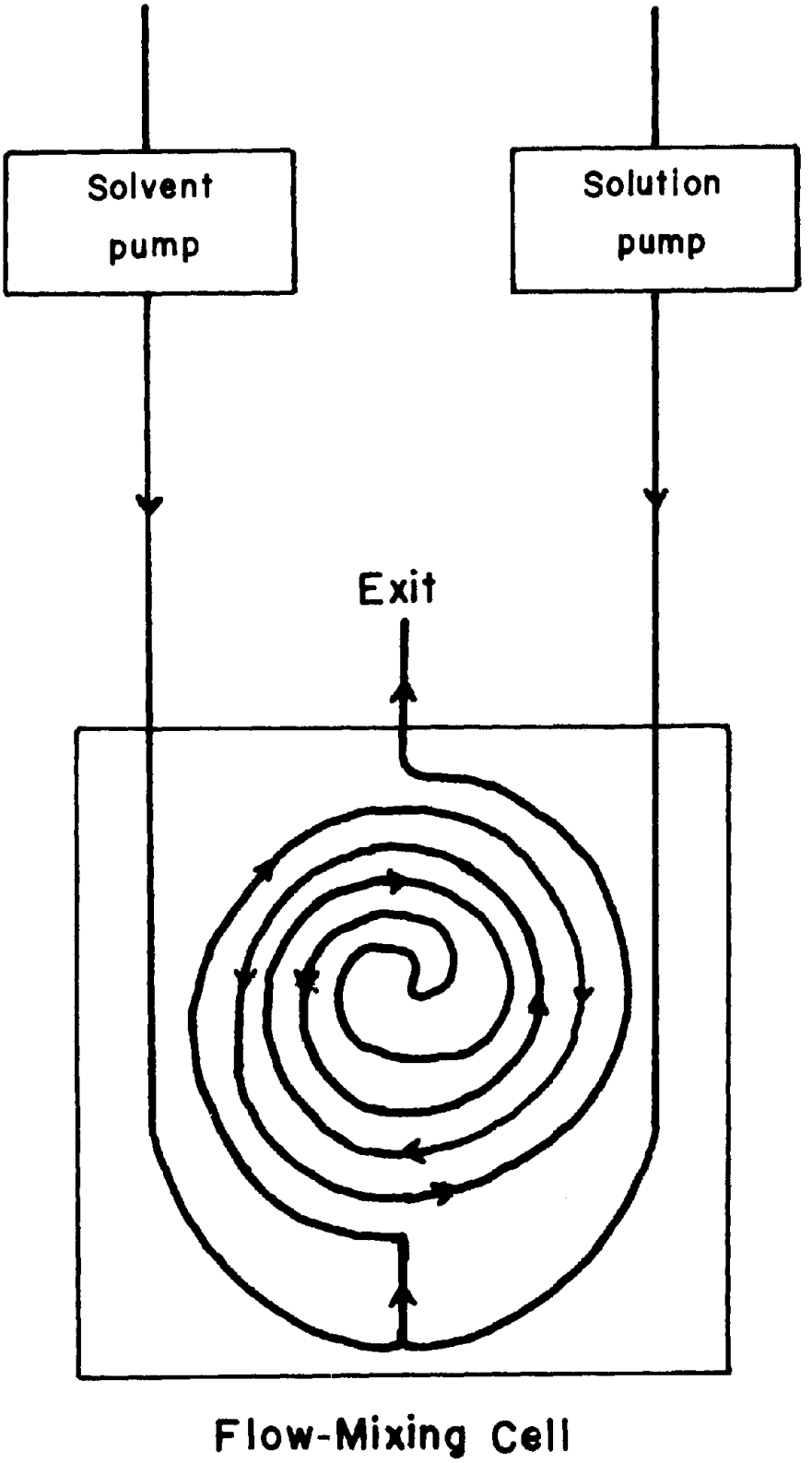


FIGURE 6. - Schematic of flow cell of heat of mixing calorimeter.

The major advantage of the flow-mixing calorimeter is the convenience and rapidity of measurement, especially for systems that must be maintained in anhydrous condition. The flow technique is especially suited for working with high-vapor-pressure solvents, since one need not be concerned with a change in concentration because of evaporation of solvent into the vapor phase. The major problem of the method is obtaining a reliable pump that can deliver the solvent and solution with 0.1 pct accuracy, without pulsation. Pumps are available that can deliver fluids with the necessary accuracy, but not totally without pulsation, which appears as noise in the signal.

Figure 7 shows the enthalpy of dilution of NaI in methanol and in water. The extraordinarily large enthalpies of dilution appear to be common in this solvent. Much of this is accounted for by the Debye-Hückel theory; nevertheless, the experimental slopes are about 30 pct greater than the theoretical slope. This appears to be caused by ion-pair formation.

REFERENCES

1. Adams, E. Q. J. Am. Chem. Soc., v. 48, No. 3, 1926, pp. 621-626.

2. Argue, G. R., E. E. Mercer, and J. W. Cobble. J. Phys. Chem., v. 65, No. 11, 1961, pp. 2041-2048.

3. Bjerrum, N. Z. physik. Chem., v. 119, Nos. 3-4, 1926, pp. 145-160.

4. Brunetti, A. P., E. J. Prosen, and R. N. Goldberg. J. Res. NBS, v. 77a, No. 5, 1973, pp. 599-606.

5. Chang, S., and C. M. Criss. J. Sol. Chem., v. 2, No. 5, 1973, pp. 457-466.

6. Cobble, J. W., and R. C. Murray, Jr. Disc. Faraday Soc., No. 64, 1978, pp. 144-149.

7. Coops, J., A. N. Balk, and M. W. Tolk. Rec. Trav. Chim., v. 75, No. 1, 1956, pp. 75-81.

8. Criss, C. M., and J. W. Cobble. J. Am. Chem. Soc., v. 83, No. 15, 1961, pp. 3223-3228.

9. Debye, P., and E. Hückel. Z. Phys., v. 24, 1923, pp. 185-206.

10. Falcone, J. S., Jr., and R. H. Wood. J. Sol. Chem., v. 3, No. 3, 1974, pp. 215-231.

11. Fortier, J. -L., P. -A. Leduc, and J. E. Desnoyers. J. Sol. Chem., v. 3, No. 4, 1974, pp. 323-349.

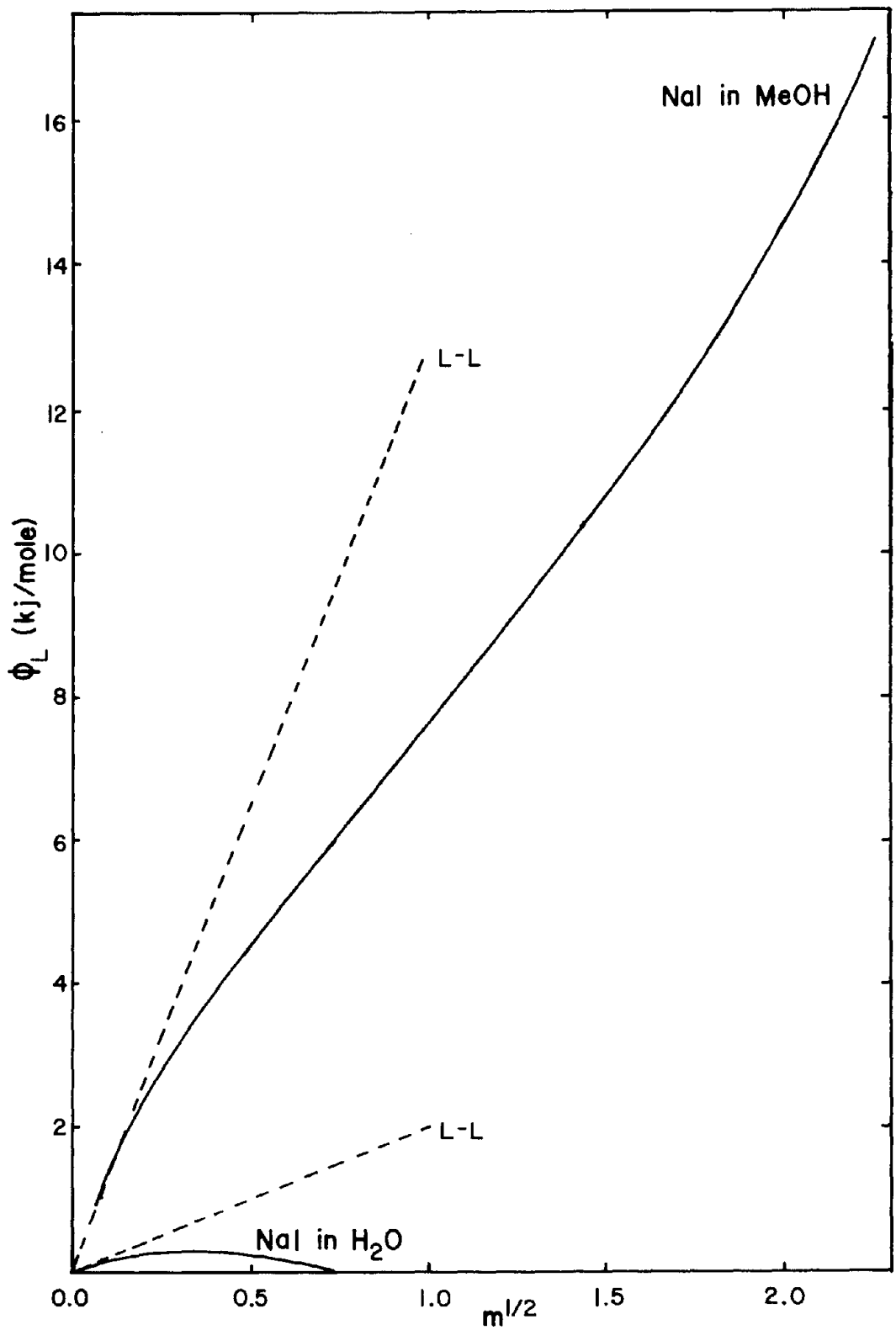


FIGURE 7. - Relative apparent molal enthalpy of NaI in water and methanol at 25° C. L-L refers to the Debye-Hückel limiting-law.

12. Gucker, F. T., Jr. Ann. N.Y. Acad. Sci., v. 51, No. 4, 1949, pp. 680-704.

13. Gucker, F. T., Jr., F. D. Ayres, and T. R. Rubin. J. Am. Chem. Soc., v. 58, No. 11, 1936, pp. 2118-2126.

14. Gucker, F. T., Jr., and J. M. Christens. Proc. Indiana Acad. Sci., v. 64, 1955, pp. 97-104.

15. Gucker, F. T., Jr., H. B. Pickard, and R. W. Planck. J. Am. Chem. Soc., v. 61, No. 2, 1939, pp. 459-470.

16. Gulbransen, E. A., and A. L. Robinson. J. Am. Chem. Soc., v. 56, No. 12, 1934, pp. 2637-2641.

17. Gunn, S. R. Rev. Sci. Inst., v. 29, No. 5, 1958, pp. 377-380.

18. Held, R. P., and C. M. Criss. J. Phys. Chem., v. 69, No. 8, 1965, pp. 2611-2617.

19. Irving, A. J., and I. Wadsö. Acta Chem. Scand., v. 18, No. 1, 1964, pp. 195-201.

20. Jeckel, E. C., C. M. Criss, and J. W. Cobble. J. Am. Chem. Soc., v. 86, No. 24, 1964, pp. 5404-5407.

21. Lage, G. A. B. Ph. D. Thesis, University of Miami, 1978.

22. LaMer, V. K., and I. A. Cowperthwaite. J. Am. Chem. Soc., v. 55, No. 3, 1933, pp. 1004-1013.

23. Lang, E., and J. Monheim. Z. physik. Chem., v. A149, Nos. 1-2, 1930, pp. 51-88.

24. Lang, E., and A. L. Robinson. Chem. Rev., v. 9, No. 1, 1931, pp. 89-116.

25. Liu, C., and W. T. Lindsay, Jr. J. Sol. Chem., v. 1, No. 1, 1972, pp. 45-69.

26. McDonald, J. E., J. P. King, and J. W. Cobble. J. Phys. Chem., v. 64, No. 10, 1960, pp. 1345-1346.

27. Parker, V. B. Thermal Properties of Aqueous Uni-univalent Electrolytes. NSRDS-NBS 2, 1965, 66 pp.

28. Pasztor, A. J., Jr., Ph. D. Thesis, University of Miami, 1976.

29. Picker, P., P. -A. Leduc, P. R. Philip, and J. E. Desnoyers. J. Chem. Thermodyn., v. 3, No. 5, 1971, pp. 631-642.

30. Prosen, E. J., and M. V. Kilday. J. Res. NBS, v. 77A, No. 2, 1973, pp. 179-203.

31. _____. J. Res. NBS, v. 77A, No. 5, 1973, pp. 581-597.

32. Randall, M., and F. D. Rossini. J. Am. Chem. Soc., v. 51, No. 2, 1929, pp. 323-345.

33. Richards, T. W., and A. B. Lamb. Proc. Am. Acad. Sci., v. 40, No. 20, 1905, pp. 661-680.

34. Rossini, F. D., D. D. Wagman, W. H. Evans, S. Levine, and I. Jaffe. Selected Values of Chemical Thermodynamic Properties. NBS Circ. 500, 1952, 1268 pp.

35. Shin, C., and C. M. Criss. Rev. Sci. Instr., v. 46, No. 8, 1975, pp. 1043-1046.

36. Silvester, L. F., and K. S. Pitzer. J. Phys. Chem., v. 81, No. 19, 1977, pp. 1822-1828.

37. Slansky, C. M. J. Am. Chem. Soc., v. 62, No. 9, 1940, pp. 2430-2434.

38. Sunner, S., and I. Wadsö. Acta Chem. Scand., v. 13, No. 1, 1959, pp. 97-108.

39. White, W. P. J. Am. Chem. Soc., v. 36, No. 9, 1914, pp. 1856-1868.

40. Wood, R. H. Private communication.

41. Wood, R. H., and J. S. Falcone, Jr. J. Phys. Chem., v. 79, No. 15, 1975, pp. 1540-1542.

AQUEOUS SOLUTIONS DATABASE TO HIGH TEMPERATURES AND PRESSURES, NaCl SOLUTIONS[1]

by

Sidney L. Phillips,[2] Roland J. Otto,[2]
Huseyin Ozbek,[2] and Mehdi Tavana[2]

ABSTRACT

A survey is made of available experimental data on sodium chloride solutions which are used in geothermal energy exploration and development for electrical power production and direct use. The data are classified as thermodynamic, transport, and physical; they are useful in the design and development of a geothermal area from brine production through utilization to brine disposal. An ideal data system for geothermal energy is described.

INTRODUCTION

The Lawrence Berkeley Laboratory (LBL) is funded by the U.S. Department of Energy to provide a single, comprehensive database of properties of aqueous solutions involved in basic geothermal energy. The compilation, which includes critical evaluation and correlation, constitutes a single source of recommended values to be used in research and development of both electrical power generation by and direct utilization of geothermal energy. In addition, the result of this work includes identification of areas where data are either lacking or inadequate, and recommendations for research designed to provide the needed data.

Reliable data are needed on the basic properties of geothermal brines covering a range of conditions up to high temperatures and pressures (8).[3] However, geothermal brines are site dependent in the concentration of dissolv-

[1]Supported by U.S. Department of Energy under Contract W-7405-ENG-48, Office of Basic Energy Sciences, Division of Engineering, Mathematical and Geosciences

[2]National Geothermal Information Resource, Lawrence Berkeley Laboratory, University of California, Berkeley, Calif.

[3]Underlined numbers in parentheses refer to items in the list of references at the end of the paper.

ed substances; the total dissolved solids vary over three orders of magnitude, depending on the site. Concentrations differ also for individual wells within the same geothermal area.

Since data on the basic properties of individual geothermal brines are virtually nonexistent, it is common practice to rely on those of sodium chloride solutions in water as a substitute.

The larger LBL project covers energy properties of the following aqueous solutions:

1. Substances that on dissolving in water change the basic properties of the resulting solution. Electrolytes such as NaCl and KCl and gases such as CO_2 are examples.

2. Substances that cause scaling, corrosion, or erosion when present in brines. Hydrogen sulfide, carbonates, and silicates are examples of such substances.

3. Materials that react with the brine and are dissolved by the brine. Examples are rocks in brine reservoirs and steel used in pipes and turbines.

This report is limited to a survey of the experimental data and correlations for NaCl solutions up to 350° C temperatures and 50-MPa pressures.[4] The objectives of the work are mainly to: (1) obtain correlation equations that closely reproduce the available experimental data on the basic properties of aqueous NaCl solutions over a range of temperatures up to 350° C and pressures to 50-MPa, (2) develop tables of smoothed data based on the correlation expressions and provide reasonable estimates of these properties through extrapolation, where necessary, into the region of geothermal interest, and (3) prepare a handbook containing equations, evaluation procedures, tables of smoothed data and recommendations for future research in areas where the current data are either lacking or inadequate.

The basic properties of NaCl solutions can be organized in several ways; it is convenient here to separate them into a number of categories, as indicated in table 1. The table lists these classes of basic energy data for NaCl solutions and the experimental measurement means commonly used to obtain the data.

In this paper it is not possible to cover all the data for each solution of interest. More complete information can be obtained from references 3-5, 10, 13-14, 16, 18, and 22.

---

[4] 1 atm = 101,325 Pascals (Pa).

TABLE 1. - Selected basic energy properties of sodium chloride solutions and commonly used methods of measurement to high temperatures

Basic property	Temperature, ° C	Method
Heat of solution	0-100	Calorimeter (glass).
	100-200	Calorimeter (Ti).
	300	Calorimeter (Ti-Pd).
Heat of dilution	10-100	Calorimeter.
		Flow calorimeter.
	184-712 (51;100MPa)	Calorimeter (Hastelloy).
Heat of solution at infinite dilution	0-300	Calorimeter; vapor pressure.
Heat capacity	1-85	Calorimeter (stainless steel).
		Flow calorimeter.
		Bomb calorimeter (gold-plated beryllium copper).
Vapor pressure	25-100	Manometer.
	75-700	Differential manometer (Pt cups).
		Isotensicope.
		Bomb (Stellite).
Viscosity	25-150	Cannon glass capillary.
		Ostwald and Ubbelohde.
		Oscillating disk.
Thermal conductivity	25-50	Coaxial cylinders.
	25-150	Continuous line source.
	25-330	Flat plate.
Electrical conductivity	0-800	Conductance cell (Pt-Ir).
		Four-electrode cell (ceramic,Pt).
Density	0-200	Sinker.
	20-75	Pycnometer.
	25-350	Hydrostatic weighing.
	150-500	Autoclave, filling temperature.
Solubility	0-300	Sample analysis.
	148-425	Pressure-temperature (Pt vessel).

Data Acquisition Systems for Solutions

Prospective users of aqueous solutions are faced with a formidable assortment of computer databases, theoretical and empirical correlation equations, publications in three major languages, differing units of concentrations and basic parameter, extrapolated and interpolated values, values calculated for 1 property using data for another contained in over 50 journals, and reports from over 25 laboratories.

The engineer or scientist needs to consider that for each property the following must be critically evaluated in selecting data or correlations: the purity of the water and NaCl used, the instrumental method employed in the measurement, the calibration procedures used, the number of replicate determinations, the temperature and pressure control, chemical reactions between the NaCl solution and the instrument, and the sampling and data processing procedures used. Each step is important, and the entire data acquisition system must be considered in selecting best values.

Both the discussion that follows and specific examples given will center around the more important geothermal energy properties that have been selected from those listed in references 3, 8, and 26. The data covered will be confined to those published since the International Critical Tables in 1929.

THERMODYNAMIC PROPERTIES

The thermodynamic properties covered here are enthalpy, heat capacity, and vapor pressure. Despite the need for experimental data to 350° C, 50-MPa, and saturation concentrations, the majority of thermodynamic data available are still below 100° C and at saturation vapor pressures (table 2). The lack of data at higher temperatures is so acute that only a few newly published values are sufficient cause for recalculation of correlation equations. To a large extent, tables of smoothed values are based on calculated and extrapolated data. In the following sections heat of solution, heat of dilution, heat capacity, and vapor pressure are discussed as examples of the current status of data on thermodynamic properties of NaCl solutions to high temperatures. These are the experimental data most often used to calculate the total specific enthalpy and entropy of NaCl solution.

Enthalpy

The total enthalpy of aqueous NaCl solutions changes with temperature. It is calculated from the standard state enthalpy of pure water, the standard state enthalpy of NaCl solutions, and the enthalpy differences between the standard state and real solution. The enthalpy of water is obtained from steam tables (11, 16). The two other terms are obtained from measurements of the heat of solution of NaCl crystals in water, and the enthalpy change when NaCl solutions are diluted from one concentration to a lower concentration. Table 2 contains selected references to experimental data which have been used

TABLE 2. - Selected experimental data of the basic energy properties of NaCl solutions to high temperatures

Temperature, ° C	Concentration, m	Pressure, MPa	Reference
	HEAT OF SOLUTION		
0-95	0.0009-0.02	Saturation	Criss 61.
10-65	≤4	ND	Abrosimov 77.
25	.05-1.3	Saturation	Benson 55,56.
114-200	.007-.04	do	Gardner 69.
200-300	1.7-10.3	do	Borodenko 75,76.
<327	ND	<100	Puchkov 78, Dimitriev 77.
300	.003-.018	Saturation	Cobble 78.
	HEAT OF DILUTION		
10-25	0.0002-0.6	Saturation	Gulbransen 34.
10-75	ND	do	Craft 75.
25	.39-1.2	do	Vaslow 71.
25	ND	do	Wood 69.
25-100	.04-5	do	Messikomer 75.
30	.1-1	do	Leung 75.
40-80	.1-6	do	Ensor 73.
183-712	.53-6	51: 100	Kasper 79.
	HEAT CAPACITY		
1.5-45	0.01-3	Saturation	Perron 75.
5-85	.04-6	do	Tanner 78.
6-48.9	High dilution	do	Arnett 70.
10-120	.5	do	Ackermann 58.
10-130	.4-1.1	do	Eigen 51.
24.15	.01-2	do	Picker 71.
25	.01-3	do	Fortier 74.
80-200	.35-2	do	Likke 73.
50-350	.43-6	do	Puchkov 76.
20	.1-2	100: 200	Liphard 77.
	VAPOR PRESSURE		
25.00	0-5.8	ND	Pepela 72.
20-30	2.0-4.0	ND	Olynyk 43.
25-100	1.0-6.1	ND	Gibbard 74.
167-265	.5-1	ND	Gardner 69B.
125-270	1-3	ND	Gardner 63.
150-350	1.2-5.6	ND	Mashovets 73.

ND - No data.

TABLE 2. - (continued)

Temperature, ° C	Concentration, m	Pressure, MPa	Reference
	VAPOR PRESSURE (continued)		
75-300	4.8-sat.	ND	Liu 72.
125-300	.2-1	ND	Liu 70.
125-300	.1-3.5	ND	Lindsay 68.
20.3	.03-.1	ND	Grollman 31.
75-150	.1-3.5	ND	Fabuss 67C.
350-400	3 pct-sat.	ND	Urusova 71C.
250-700	Saturated	ND	Sourirajan 62.
60-101	.05-1.0	ND	Smith 39.
61-105	1.5-4.0	ND	Smith 39B.
15-45	.1-6.0	ND	Robinson 59.
125-270	1.0-3.0	ND	Gardner 63.
200-400	2-15	ND	Urusova 71B.
450-550	3 pct-sat.	ND	Urusova 74.
183-646	.1-.5 mole fr.	ND	Keevil 42.
	THERMAL CONDUCTIVITY		
20	0.9-5.7	Saturation	Riedel 51.
20-80	2.7-5.9	do	Tufew 66.
25-150	.7-3.5	do	Korosi 68.
25	.7-5.5	do	Kapustinski 72.
25-50	1.9-4.5	do	Chernenkeya 72.
20-40	1-3	do	Chiquillo 67.
30	4.2	do	Vargaftik 56, Prudnikov 70.
	VISCOSITY		
0-25	0.002-2	Saturation	Jones 37.
10-40	.1-5.8	do	Lengyel 64.
12-42	.001-.5	do	Kaminsky 56.
18-154	.4-4	1-30	Kestin 77.
20-80	6	Saturation	Postnikov 70.
23	.3-2.5	do	Gaeta 66.
25-50	.007-5.8	do	Goncalves 77.
25	.09-1.2	do	Drucker 46.
25-150	.1-3.6	do	Korosi 68.
25	.1-5.6	do	Janz 70.
25	1.0-5.6	do	Ostroff 69.
25-60	1.1-6.1	do	Ezrokhi 52.
30-55	1.0-5.0	do	Suryanarayana 58.
35	.01-.07	do	Chacravarti 40.
20-350	1-20 wt-pct	⩽ 30	Pepinov 77.

ND - No data.

TABLE 2. - (continued)

Temperature, ° C	Concentration, m	Pressure, MPa	Reference
	ELECTRICAL CONDUCTIVITY		
0-800	0.001-0.1	1-400	Quist 68.
22-375	.2-4 M	30	Ucok 79.
370-600	.01-.0005 N		Lukasov 76.
	DENSITY		
0-25	0.002-1.0	Saturation	Jones 37.
0-55	.01-1	do	Millero 70.
0.20-100	6	do	Cornec 32.
5	.05-3.5	do	Vaslow 69.
5-25	4	do	Wirth 68.
40-280	.001-1.5	10	Gorbachev 74.
200-680	1-6	56-137	Ikornikova 71.
150-520	1-4	25-175	Lemmlein 61.
100-440	.1-6	1-35	Khaibullin 66.
185-414	1-2	1-30	Samoilovich 68.
385-396	.7-4	23-26	Copeland 53.
175-350	.5-3	ND	Ellis 63.
50-200	.1-1	ND	Ellis 66.
25-175	.1-2.5	Saturation	Fabuss 66.
	73.3-133.9ppm	ND	Masui 78.
25-350	20-24 wt-pct	0-1000 kg/cm^2	Zarembo 76.
25-150	.1-3.5	Saturation	Korosi 68.
20-300	.1-6	10-150	Polyakov 65.
25	.7-1	120	Millero 72.
50	.005-1	ND	Millero 72B.
20	.1-4	ND	Passynski 38.
25	.002-.7	ND	Kruis 36.
	SOLUBILITY		
148-425	29.62-48.42 pct	Saturation	Potter 77.
150-350			Schroeder 35.
285-455			Benrath 37.
183-646			Keevil 42.
75-300			Liu 72.
	CRITICAL TEMPERATURE		
383-462	0.1-1.8	ND	Marshall 74.
	CRITICAL PRESSURE		
374-700	0-26.4 pct	2-12	Sourirajan 62.

ND - No data.

in calculating the total enthalpy of NaCl solutions up to high temperatures. Most experimental measurements are below 100° C, and only two are at pressures different from saturation vapor pressure. However, there are sufficient data for development of correlation equations.

Bradley and Pitzer fit experimental thermodynamic data to a 30-parameter equation that reproduces the enthalpy and heat capacity data from 0° to 300° C. They provide tables of heats of solution at infinite dilution, partial molal enthalpy, and total enthalpy from 0° to 300° C. Values of the total relative molal enthalpy agree to within ±60 j/mole up to 75° C, and 250 j/mole at 100° C for 5 molal NaCl. The large value at 100° C is attributed to incompatibility between the various types of data. More information appears in reference 16. Earlier work includes that of Silvester and Pitzer (21) and Haas (3-4). A method for estimating the enthalpy of geothermal brines is given by Grens (2) and Potter and Haas (19). See table 3 and figure 1.

The effect of added NaCl is to lower the enthalpy of pure water over the temperature range 0° to 350° C (figs. 2 and 3). For example, at 300° C, a 5 molal NaCl solution has an enthalpy difference of about 500 kj/kg compared with pure water at this temperature (11).

In summary, the experimental data on heat of solution, heat of dilution, heat capacity, and vapor pressure are adequate for calculating the total specific enthalpy of NaCl solutions to 300° C; see the equation developed by Pitzer and coworkers (16). However, additional experimental data are needed to improve the fit of correlation equations above 100° C and data are especially needed on the effect of pressures to 50 MPa.

Heat Capacity

Experimental data on heat capacity are available to 350° C and 0.01-6 molal; however, only one set of data is available at pressures different from vapor saturation (table 2). The available data fit the Pitzer (16) equation well. The data below 100° C showed an error of less than 0.004 j/g-deg, but the error was as large as 0.01 j/g-deg at high molalities at temperatures of 45° and 65° C. Also the error in the fit to experimental data increased with increasing temperature and was ±0.03 j/mole-deg C at 250° C for concentrations below 5 molal, 0.05 j/mole-deg C at 275° C, and 0.17 j/mole-deg C at 300° C; the error had an average value of 0.56 j/mole-deg C at 325° and 350° C. Reference 16 gives more details.

The empirical correlation equation developed by Otto reproduces experimental values with an error less than ±2 pct from 5° to 300° C and less than ±5 pct between 300° and 350° C for concentrations between 0 and 6 molal at saturation vapor pressures (11).

Figure 4 shows the decrease in heat capacity of NaCl solutions for NaCl concentrations between 0 and 6 molal. At each concentration, the heat capacity increases with temperature; the magnitude of the increase is less as the concentration increases.

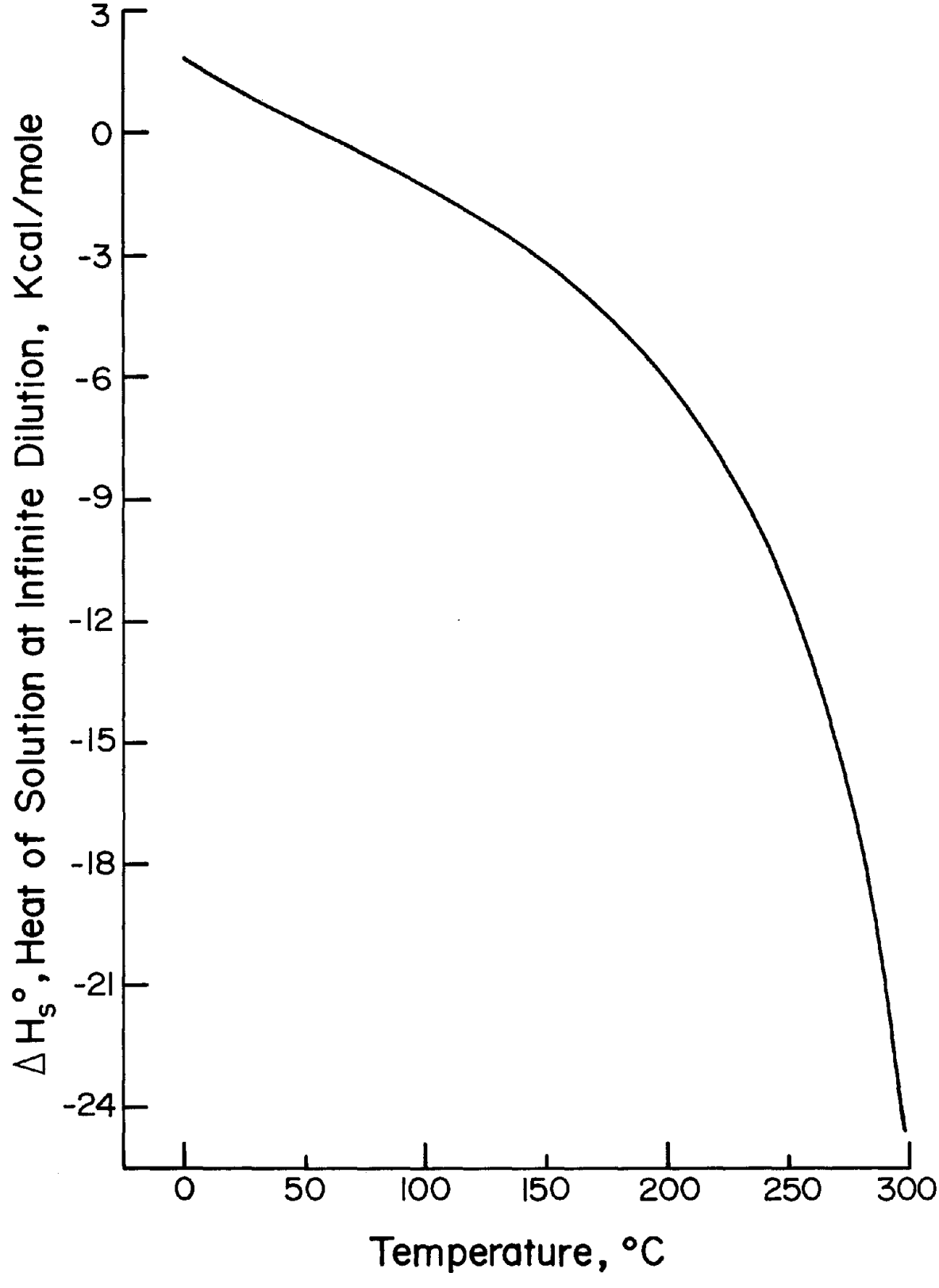


FIGURE 1. - Heat of solution at infinite dilution versus temperature.

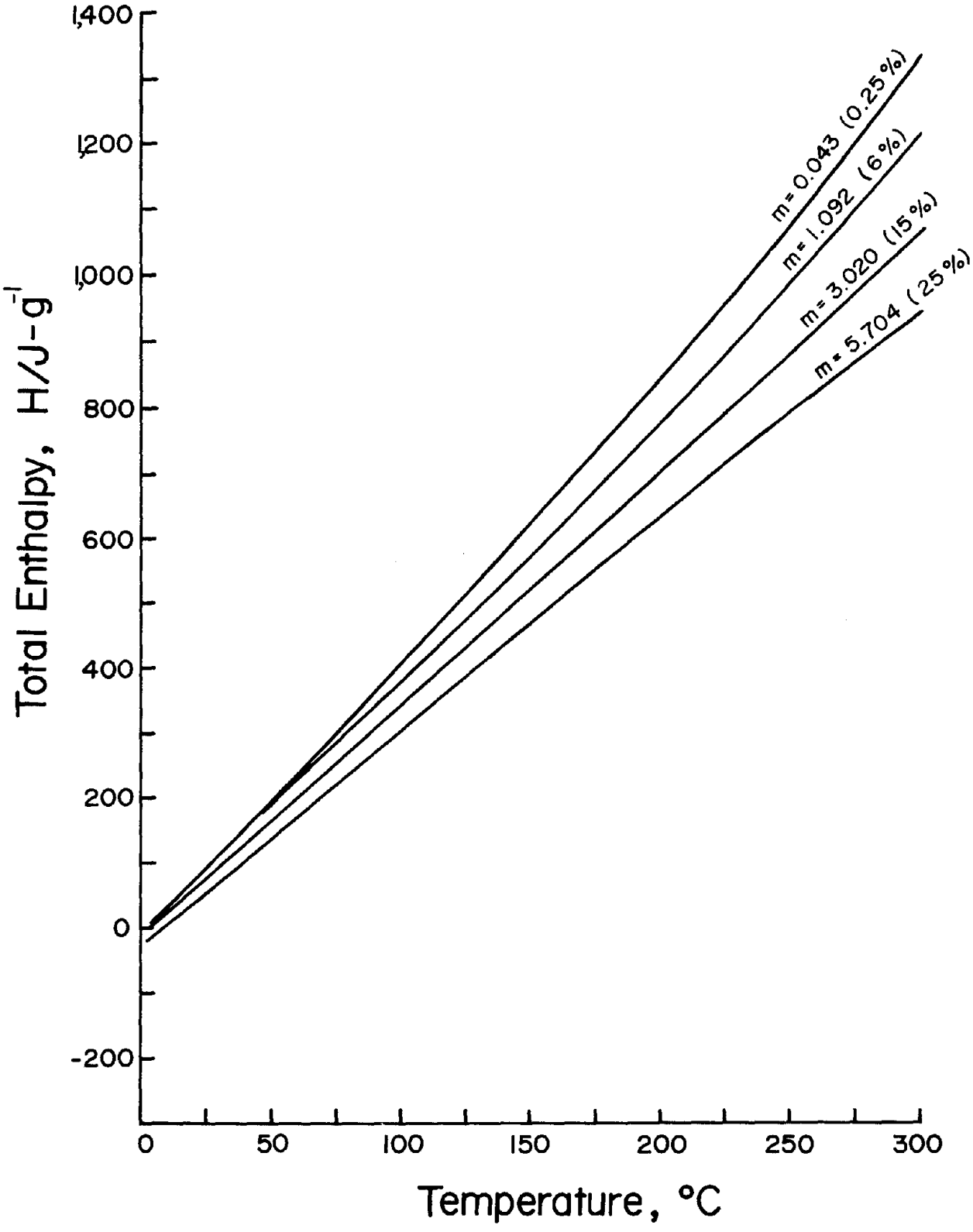


FIGURE 2. - Total specific enthalpy of NaCl solutions versus temperature (m = molal).

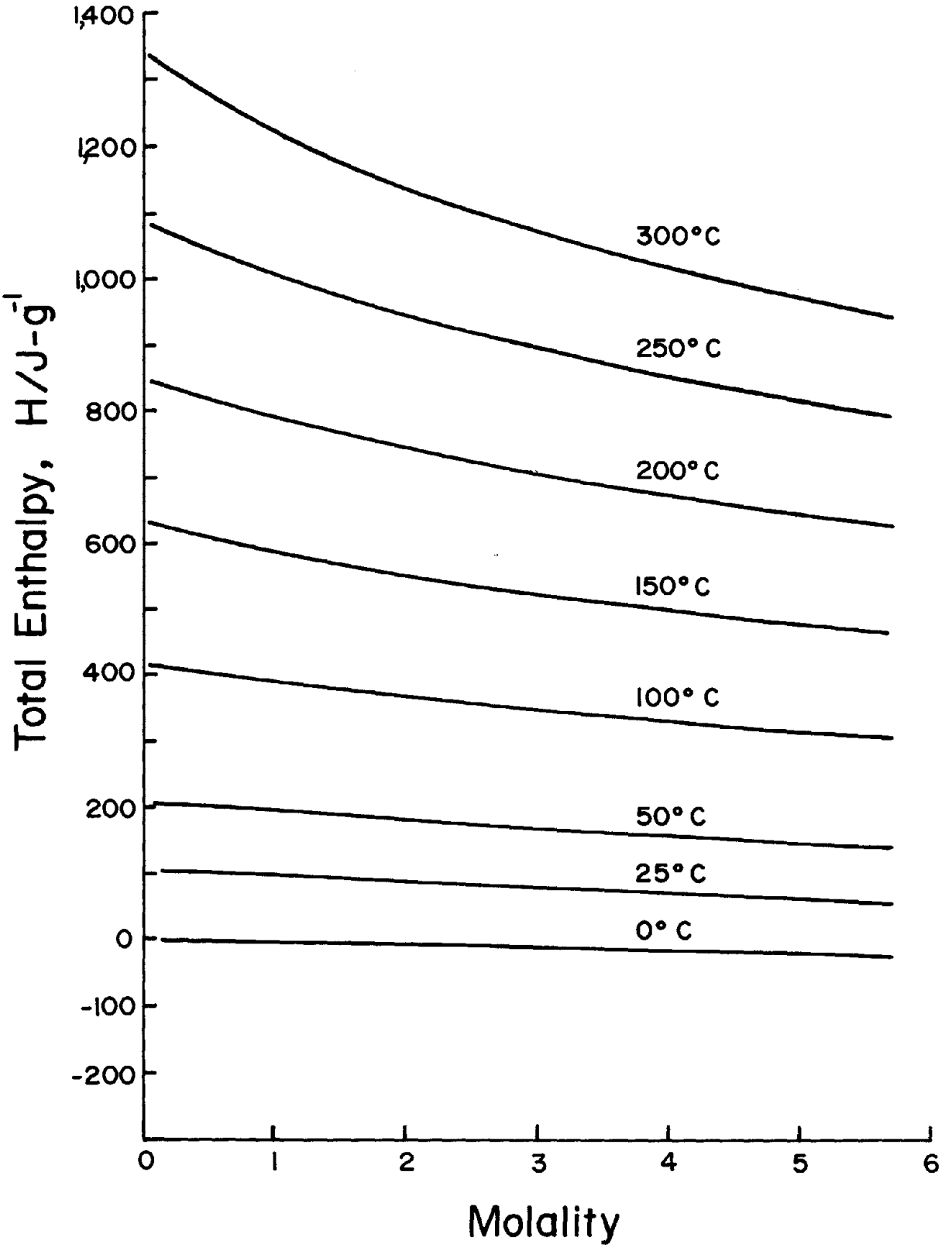


FIGURE 3. - Total specific enthalpy of NaCl solutions versus molality.

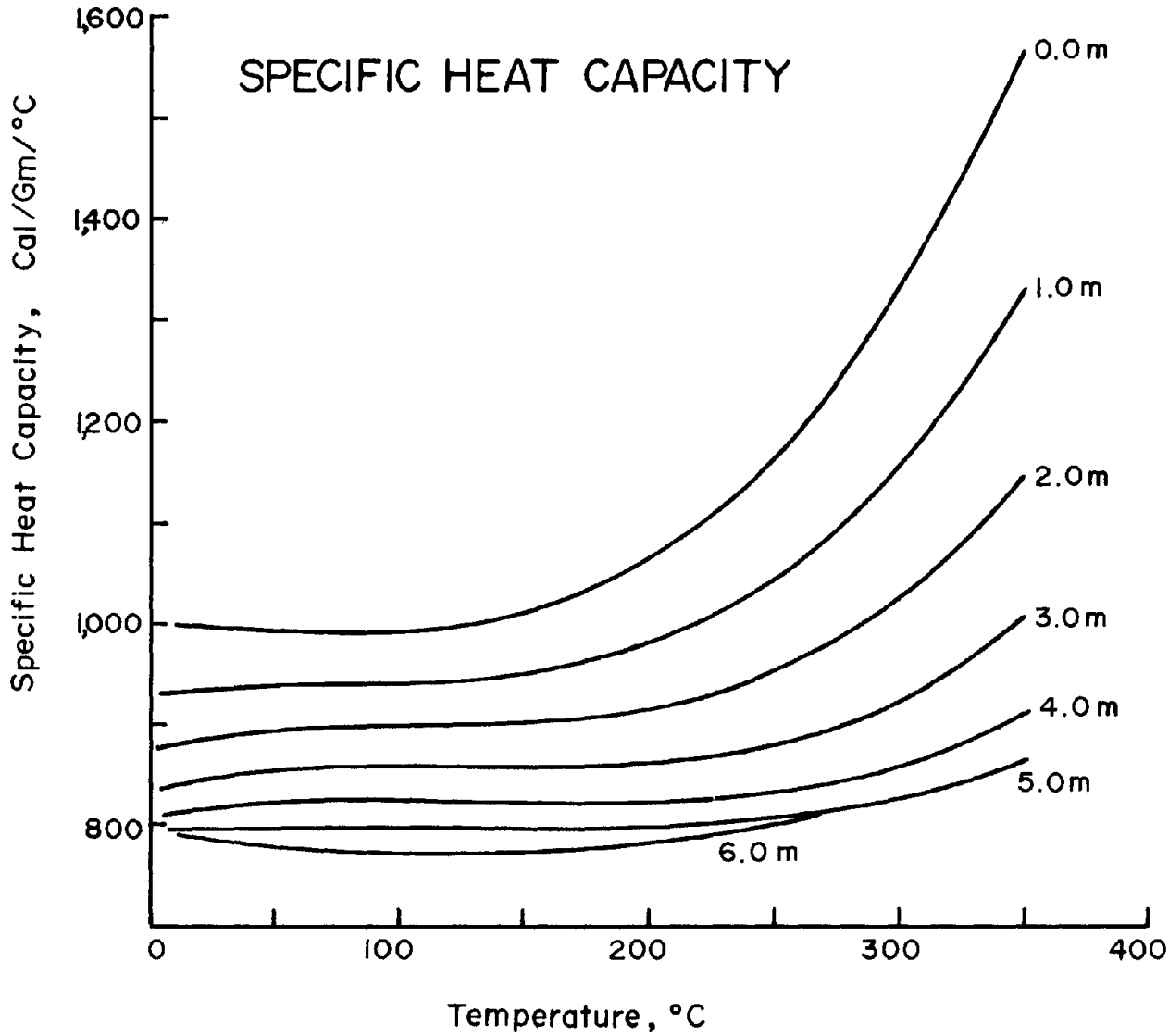


FIGURE 4. - Specific heat capacity of NaCl solutions versus temperature (m = molal).

TABLE 3. - Selected correlations for the basic energy properties of NaCl solutions and pure water to high temperatures

Property	Temperature, ° C	Concentration, molal	Pressure, MPa	Accuracy	Reference and date
			NaCl SOLUTIONS		
Thermal conductivity.	20-300	0-5	Saturation	±2%	Ozbek 79.
Viscosity	0-150	0.5-5	To 30	±1.5%	Ozbek 77.
	0-300	0-6	Saturation	±1%	Potter 78.
Electrical conductivity.	0-800	0.001-0.1	To 400		Quist 68.
Electrical resistivity.	22-375	0.2-4 molar	30	±2%	Ucok 79.
Solubility	0-600		Saturation		Potter 77.
Specific volume	40-280	0.001-1.5	10		Gorbachev 74.
	0-175	0-25 wt-pct	To 350 $kg-cm^{-2}$	1.5 ppt	Rowe 70.
Density	20-150	0-6	To 35		Kestin 77.
	80-325	0-30	Saturation	±0.002g/cm^3	Haas 75.
					Ozbek 79.
Vapor pressure	75-325	0-saturation		0.32 pct	Hass 75.
Heat of solution.	0.01-300	0.25-25 wt-pct	Saturation	<5KJ/mole	Pitzer 79.
Heat of solution at infinite dilution.	0-300		Saturation		Pitzer 79.
Heat of dilution					Pitzer 79.
Heat capacity	0-300	0.25-25 wt-pct	Saturation	0.004-0.17 J/mole -deg	Pitzer 79.
Total enthalpy	0-300		Saturation		Pitzer 79.
Specific heat capacity.	0-300		Saturation		Pitzer 79.
			WATER		
Thermal conductivity.	0<T<800	NAP	0.1<P<100		IAPS 78.
Viscosity	0<T<800	NAP	0<P<100		IAPS 76.
Specific enthalpy	0.01<T<374	NAP	0.0006113<P< 22.09		Keenan 78.
Specific volume	0.01<T<374	NAP	0.0006113<P< 22.09		Keenan 78.
Vapor pressure		NAP			Keenan 78.
Heat capacity	0<T<374	NAP	To 100 Mpa		Keenan 78.

NAP - Not applicable.

In summary, equations are available for providing tables of smooth values for heat capacity to 350° C and 6 molal. However, data are needed at temperatures above 275° C, especially from 300° to 350° C. Data at high pressures are also needed.

Vapor Pressure

The available vapor pressure data cover the temperature range 25° to 700° C and concentrations from 0 to saturation (table 2). The experimental results published by Liu and Lindsay have been widely used. See references 11, 16, and 21.

Correlation equations which reproduce vapor pressure data were developed by Haas (3-4), MacMullin (9), and Korosi and Fabuss (7). Vapor pressure estimates may be made as described by Potter and Haas (19) and Grens (2). Haas gives a table of data covering the temperature range 80° to 325° C and concentration from 0 to saturation; the standard error is 0.32 pct of the observed pressure. The vapor pressure decreases with increasing NaCl concentration and increases markedly at any particular concentration as the temperature increases. References 3 and 4 give additional information.

While the data on vapor pressure cover the range of geothermal interest, the correlation should be redone to include data published since 1971.

TRANSPORT PROPERTIES

Transport properties cover viscosity, thermal conductivity, and electrical conductivity.

Viscosity

The currently available experimental data on the viscosity of NaCl solutions is sparse and covers mainly pressures from atmospheric to 30 MPa, concentrations from 0 molal to saturation, and temperatures below 150° C (table 2). Above 75° C the available data are those of Korosi and Fabuss (7) and Kestin (6). An empirical correlation equation was developed which reproduces the experimental data with an error of less than 1.5 pct over the temperature range 10° to 150° C (13). The equation is convenient for interpolation and for machine calculations. Additional laboratory measurements on the viscosity of NaCl solutions between 150° and 350° C are needed. Laboratory data are also needed for pressures up to 50 MPa.

The viscosity has been correlated by a number of workers including Ozbek, Fair, and Phillips (13), Kestin (6), and Potter (17) as shown in table 3. The equation developed by Potter permits extrapolation to about 325° C. See figure 5.

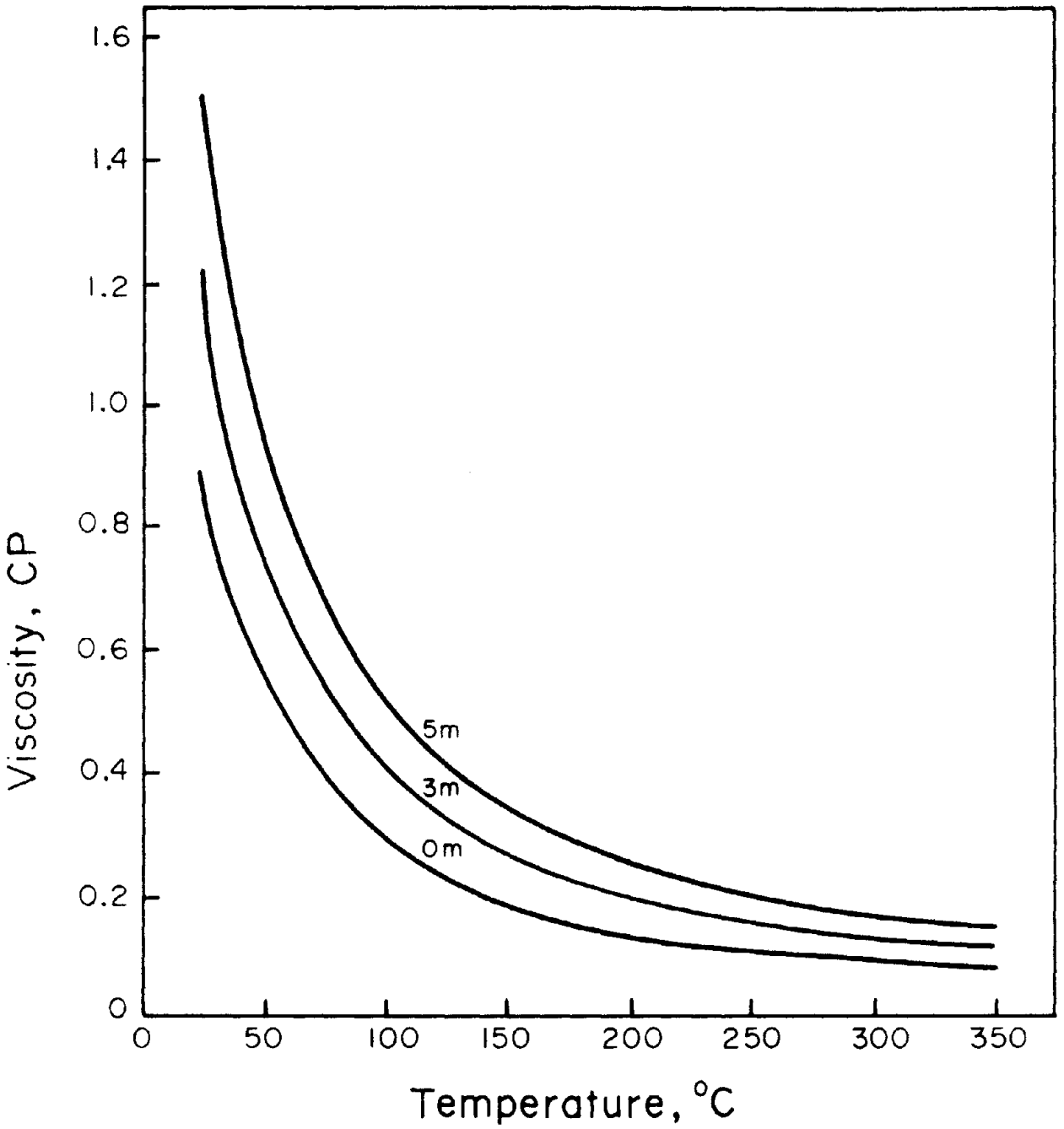


FIGURE 5. - Viscosity of NaCl solutions from 0°to 150° C, m = molal. A, 0.5m; B, 1m; C, 2m; D, 3m; E, 4m; F, 5m.

Thermal Conductivity

Published experimental data have been available for some time for the thermal conductivity of NaCl solutions up to 150° C, and data to 330° C, in the form of graphs and a correlation equation, were published recently (14). The correlation equation selected for our data base reproduces most of the published experimental data to better than 3 pct up to 80° C. The deviation is considerably larger (5 to 30 pct) for the data of Korosi and Fabuss (7) over the range 25° to 150° C. Unfortunately, the greatest number of experimental points are not available in tabular form but are published as a correlation equation or in graphical form. Based on this equation, which was applied to all the data used in the evaluation, the thermal conductivity of pure water is lowered by dissolved NaCl at all temperatures up to 330° C; the change at 140° C is about 7 pct for a 5 molal solution. For any NaCl concentration up to 5 molal, the thermal conductivity increases with increasing temperature to a broad maximum at about 140° C then decreases by more than 0.2 watt/m-° C as the temperature is further increased to 330° C. See figure 6.

Few experimental data points have been published on the thermal conductivity of NaCl solutions. From 100° to 150° C there are only the six measurements reported by Korosi and Fabuss (7). Data to 330° C reported by Yusufova and coworkers are not tabulated but must be calculated from the published correlation equation. No data are available on the effects of elevated pressures on the thermal conductivity of NaCl solutions (14).

Electrical Conductivity

Experimental data on electrical conductivity are available for NaCl solutions for temperatures from 0° to 80° C, a pressure range from 0 to 400 MPa, and concentrations up to 4 molal. Data were recently correlated as resistivity measurements to 375° C. The resistivity decreased with increasing concentration over the range 3 to 20 wt-pct NaCl. With temperature the resistivity decreased to a broad minimum between about 275° and 325° C. Beyond about 325° C, the resistivity increased to 375° C. At 25°, 100°, and 300° C, the resistivity falls rapidly when the NaCl concentration lies between 3 and 10 wt-pct, then more slowly between concentrations of 10 and 26 wt-pct. The data were correlated to ±2 pct for NaCl solutions for 3 to 20 wt-pct concentrations over the temperature range 25° to 375° C (25).

PHYSICAL PROPERTIES

Solubility

The solubility of NaCl in water increases continuously with temperature at saturated water vapor pressures to 800° C. Potter and coworkers (18) developed a correlation equation to fit data on the solubility of NaCl solutions from 0° to 800° C.

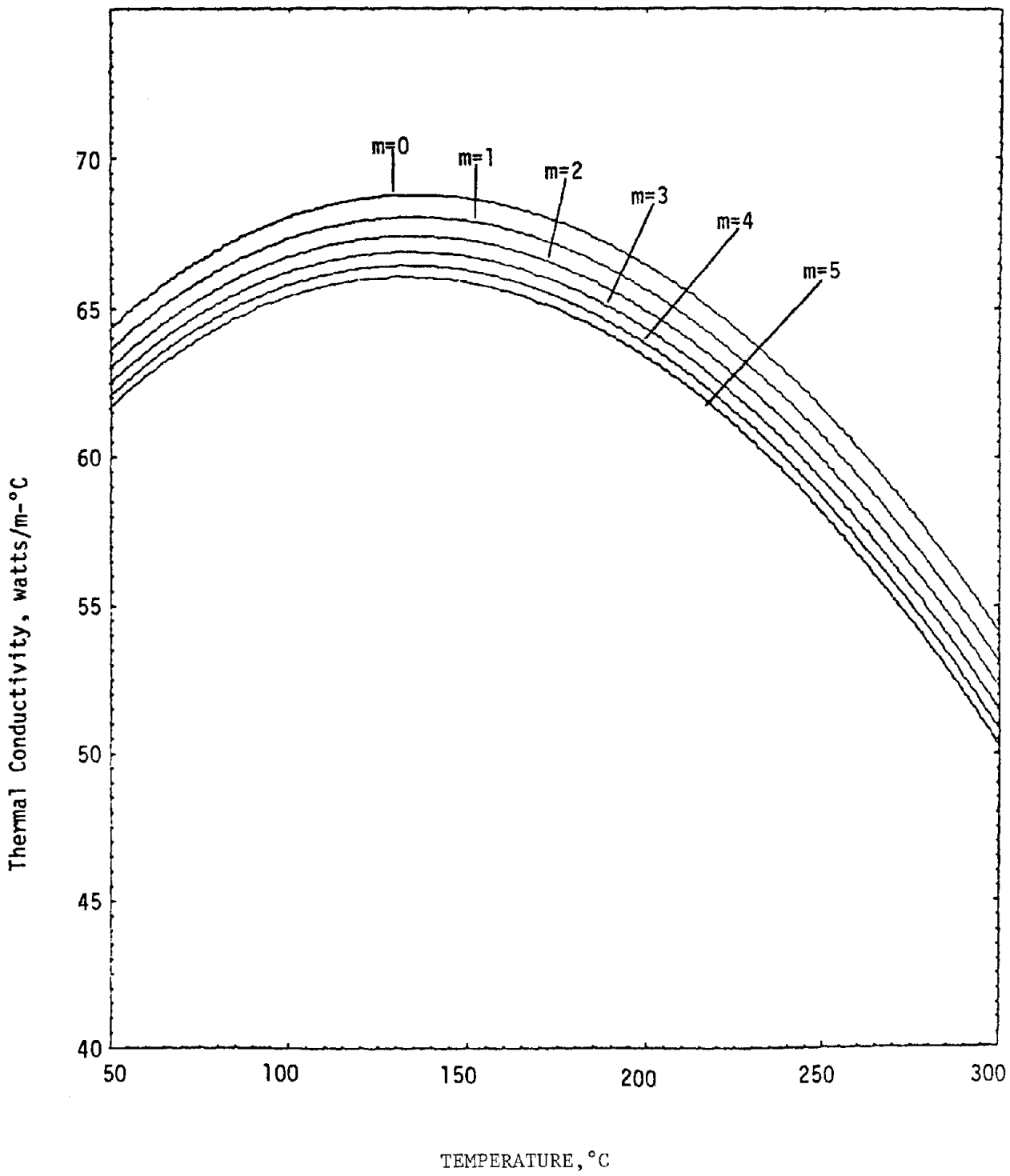


FIGURE 6. - Thermal conductivity of aqueous NaCl solutions as a function of temperature (m = molal).

Density

The data on density of aqueous NaCl solutions are extensive; over 1,300 experimental values have been compiled for temperatures up to 770° C and pressures to 270 MPa (table 2).

Correlation equations have been developed by a number of workers including Kestin (6), Rowe and Chou (20), Potter and Haas (19), Korosi and Fabuss (7), and Ozbek, Fair, and Phillips (12).

The density of NaCl solutions increases with increasing concentration from 0 to 6 molal over the temperature range 0° to 300° C. There is no significant effect of pressure over this range of temperature up to 20 MPa. Figures 7 and 8 show the change in density with temperature and pressure, respectively.

Critical Temperature and Pressure

The critical temperature and pressure of an aqueous electrolyte solution are functions of the concentration of the solution. At a fixed concentration, the critical temperature, pressure, and density define the critical point. It is at this point that the vapor and liquid phases of the solution have the same density, and, in effect, a one-phase fluid system is established for all temperatures and pressures above the critical point. Marshall and Jones (10) have measured the critical temperature of aqueous NaCl solutions, as well as for 20 other electrolyte solutions, in the concentration range of 0.1 to 1.8 molal. The electrolytes included both salts and acids. A review of the available data between 0 and 2 molal in concentration is also given (10). Sourirajan and Kennedy (23) reported the critical temperature and pressure for the NaCl-H_2O system for concentrations between 0 and 6.2 molal.

SUMMARY AND CONCLUSIONS

A review of the current status of data on selected properties of NaCl solutions in the temperature range 0° to 350° C and pressures up to 50 MPa shows that only limited data are available for providing tables of smoothed values. Experimental data are needed mainly for pressures different from vapor saturation, and at temperatures above about 150° to 200° C for viscosity, thermal conductivity, enthalpy, and heat capacity. All properties need to be correlated as new data are made available; this will result both in improved fits of the equations and in better extrapolation procedures.

RECOMMENDATIONS

After reviewing current data in light of the needs of the geothermal energy program, some general observations are appropriate. The "ideal" data obtainable from published literature should include the following:

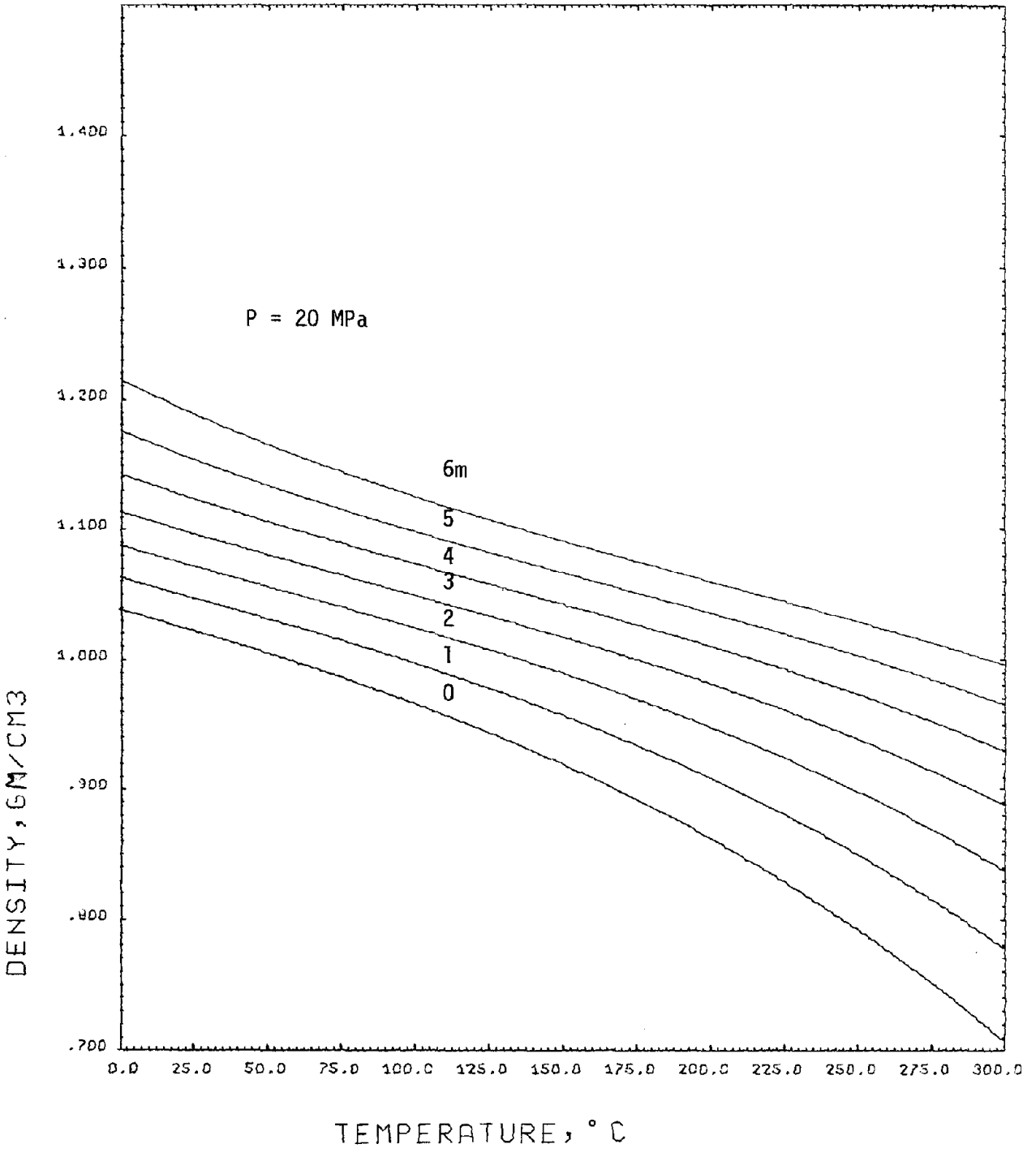


FIGURE 7. - Density of NaCl solutions from 0°to 300° C (m = molal).

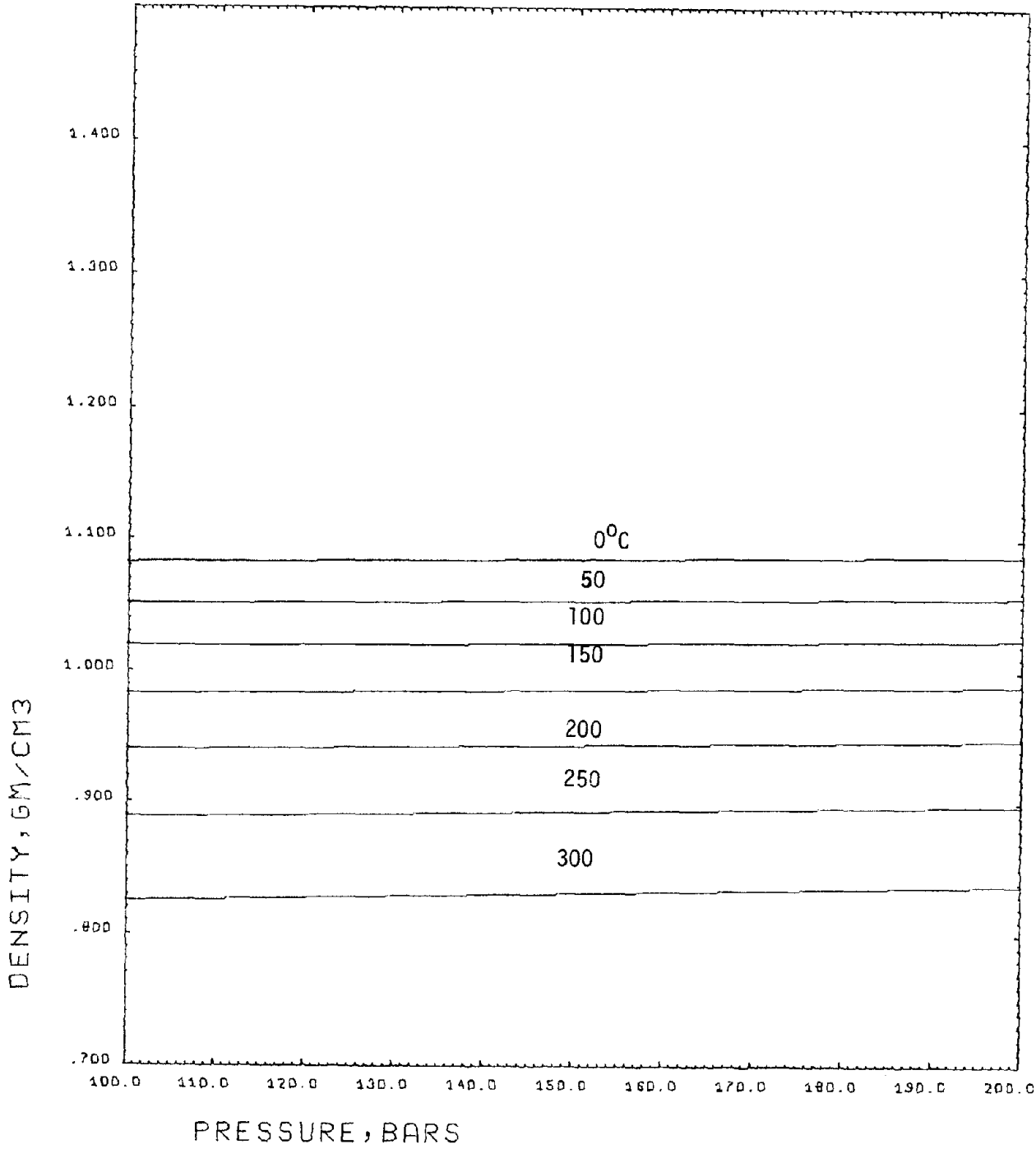


FIGURE 8. - Density of 2 molal NaCl solutions at 20-MPa pressure.

1. Experimental values in tabular form showing concentration, temperature, pressure, and the measurement of the basic property. The data can then be used to develop correlation expressions and for calculations of mean values and deviations from the mean.

2. Measurements on the basic properties of geothermal brines under operating conditions, or from samples that are preserved to the extent possible. These measurements would permit a comparison between NaCl solutions and the various brines.

3. Use of a consistent set of units for the various data. Experimental values are currently published using a variety of units for temperature, pressure, concentration, and property; these must then be converted to a standard form prior to evaluation. The Standard International set of units should be used.

4. A description of any special instrumentation or materials used in obtaining the experimental values. Sodium chloride solutions chemically attack some materials at high temperatures and pressures. This can cause undesirable side reactions and interfere with measurement of the property.

5. Data on the effects of the substances (e.g., KCl, $CaCl_2$, CO_2) on the properties of NaCl solution. Geothermal brines are complicated solutions which consist of a large number of substances besides NaCl; these are present in amounts that may significantly change a property of NaCl solution as the temperature and pressure are changed.

6. Foreign language publications with an English language abstract, and English language headings for both tables of data and graphs. There is much delay in evaluating data when there is a need for translations.

ACKNOWLEDGEMENT

Thanks are given to George A. Morton, Daniel J. Bradley, and Susan R. Lepman of the Lawrence Berkeley Laboratory for their comments.

REFERENCES

1. Fabuss, B. M., and A. Korosi. Properties of Sea Water and Solutions Containing Sodium Chloride, Potassium Chloride, Sodium Sulfate and Magnesium Sulfate. U.S. Department of the Interior, Office of Saline Water, Res. and Devel. Prog. Rept. 384, 1968.

2. Grens, J. Z. The Effect of Salinity on Geothermal Well Performance. Lawrence Livermore Laboratory, University of California, UCID-16791, May 14, 1975.

3. Haas, J. L., Jr. Physical Properties of the Coexisting Phases and Thermochemical Properties of the H_2O Component in Boiling NaCl Solutions. U.S. Geol. Survey Bull. 1421-A, 1976.

4. Haas, J. L., Jr., and R. W. Potter II. The Measurement and Evaluation of PVTX Properties of Geothermal Brines and the Derived Thermodynamic Properties. Proc., 7th Symposium on Thermophysical Properties, A. Cezairliyan, ed., ASME, New York, 1977.

5. Holmes, H. F., C. F. Baes, Jr., and R. E. Mesmer. J. Chem. Thermodyn., v. 10, 1978, p. 983.

6. Kestin, J., H. E. Khalifa, Y. Abe, C. E. Grimes, H. Sookiazian, and W. A. Wakeham. J. Chem. Eng. Data., v. 23, 1978, p. 328.

7. Korosi, A., and B. M. Fabuss. Thermophysical Properties of Saline Water. U.S. Department of the Interior, Office of Saline Water, Res. and Devel. Prog. Rept. 363, 1968.

8. Lyon, R. N., and G. A. Kolstad (eds.). A Recommended Research Program in Geothermal Chemistry. WASH-1344, October 1974. Available from U.S. Department of Commerce, National Technical Information Service, Springfield, Va.

9. MacMullin, R. B. Algorithms for the Vapor Pressure of Water Over Aqueous Solutions of Salt and Caustic Soda. J. Electrochem. Soc., v. 116, No. 3, 1969, pp. 416-419.

10. Marshall, W. L., and E. V. Jones. Liquid-Vapor Critical Temperatures of Aqueous Electrolyte Solutions. J. Inorg. Nucl. Chem., v. 36, 1974, pp. 2313-2318.

11. Otto, R. J. and S. L. Phillips. Enthalpy and Heat Capacity of Aqueous Sodium Chloride Solutions from 0.01° to 350° C. Lawrence Berkeley Laboratory, University of California, LBL-12810, June 1981.

12. Ozbek, H., J. A. Fair, and S. L. Phillips. Density of NaCl Solutions at High Temperatures and Pressures. Lawrence Berkeley Laboratory, University of California, LBL-12810, June 1981.

13. _____. Visocity of Aqueous Sodium Chloride Solutions From 0°-150° C. Lawrence Berkeley Laboratory, University of California, LBL-5931, December 1977.

14. Ozbek, H., and S. L. Phillips. Thermal Conductivity of Aqueous NaCl Solutions from 20° to 330° C. Lawrence Berkeley Laboratory, University of California, LBL-9086, May 1979.

15. Perron, G., J.-L. Fortier, and J. E. Desnoyers. The Apparent Molar Heat Capacities and Volumes of Aqueous NaCl from 0.01 to 3 Mol-Kg^{-1} in the Temperature Range 274.65 to 318.15 K. J. Chem. Thermodyn., v. 7, 1975, pp. 1177-1184.

16. Pitzer, K. S., D. J. Bradley, P. S. Z. Rogers, and J. C. Peiper. Thermodynamics of High Temperature Brines. Lawrence Berkeley Laboratory, University of California, LBL-8973, April 1979.

17. Potter, R. W., II. Viscosity of Geothermal Brines. Trans. Geothermal Res. Council, v. 2, July 1978, pp. 543-544.

18. Potter, R. W., II, R. S. Babcock, and D. L. Brown. A New Method for Determining the Solubility of Salts in Aqueous Solutions at Elevated Temperatures. J. Res. U.S. Geol. Survey, v. 5, No. 3, 1977, pp. 389-395.

19. Potter, R. W., II, and J. L. Haas, Jr. Models for Calculating Density and Vapor Pressure of Geothermal Brines. J. Res. U.S. Geol. Survey, v. 6, No. 2, 1978, pp 247-257.

20. Rowe, A. M., Jr., and J. C. S. Chou. Pressure-Volume-Temperature-Concentration Relation of Aqueous NaCl Solution. J. Chem. Eng. Data, v. 15, No. 1, 1970, pp. 61-66.

21. Silvester, L. F., and K. S. Pitzer. Thermodynamics of Electrolytes. 8. High Temperature Properties, Including Enthalpy and Heat Capacity with Application to Sodium Chloride. J. Phys. Chem., v. 81, No. 19, 1977, p. 1828.

22. Smith-Magowan, D., and R. N. Goldberg. A Bibliography of Sources of Experimental Data Leading to Thermal Properties of Binary Aqueous Electrolyte Solutions. NBS, 1978.

23. Sourirajan, S., and G. C. Kennedy. The System H_2O-NaCl at Elevated Temperatures and Pressures. Am. J. Sci., v. 260, 1962, pp. 115-141.

24. Tanner, J. E. and F. W. Lamb. Specific Heats of Aqueous Solutions of NaCl, NaBr, and KCl: Comparisons With Related Thermal Properties. J. Sol. Chem., v. 7, No. 4, 1978, pp. 303-316.

25. Ucok, H., I. Ershaghi, and G. R. Olhoeft. Electrical Resistivity of Geothermal Brines. SPE of AIME International Symposium on Oilfield and Geothermal Chemistry, Houston, Tex., Jan. 22-24, 1979, Paper SPE 7878.

26. U.S. Department of Energy. Summaries of Physical Research in the Geosciences. Division of Basic Energy Sciences, DOE/ER-0016, September 1978.

DISCUSSION

R. P. Beyer: Aren't the main constituents of the minerals that plate out in geothermal wells barium and strontium sulfates?

S. L. Phillips: It is possible, but there are several other compounds depending on the locations of the wells. I think in the case of oilfield brines the barium and strontium are more prevalent.

M. W. Chase: How does your NaCl work compare with John Haas' work at the Geological Survey?

S. L. Phillips: In this specific instance, we could use the most recent data. We would use whatever experimental data we might have and then select a correlation, the one that is hopefully widely accepted by the engineers and others that are working in industry. We provide data that have been evaluated by others. For the particular instance of heat capacity and the enthalpy, the most recent is this work. Included are some of the most recently available experimental data up to 1979.

B. R. Staples: How does this correlation compare with the work of Potter and Haas in the U.S. Geological Survey?

S. L. Phillips: We are in the process now of surveying the available data - the heat capacity and the enthalpy, etc. We believe that our correlation is quite satisfactory.

THERMODYNAMIC MEASUREMENTS OF CARBONATE EQUILIBRIA INVOLVING METAL IONS

by

John E. Bauman, Jr.[1]

ABSTRACT

The formation constants K_f for complexes involving bicarbonate ion and various divalent metal ions (Mg^{2+}, Ca^{2+}, Mn^{2+}, Cu^{2+}, Zn^{2+}) have been measured as a function of temperature between 10° and 90° C. In all cases the complexes become more stable at higher tempertures. The data fit a standard equation of the form $\log K_f = A + B \log T + C/T$ from which the standard enthalpy change $\Delta H°$ may be determined. A check on these enthalpy values determined by calorimetry shows no significant differences. Problems of activity coefficients, variations in ionic strength, liquid junction potentials, absolute pH, and P_{CO2} measurements as temperature changes occur are handled by a computer technique known as a "floating point method." Data from a titration are able to give convergent values of an equilibrium constant if the initial activity of HCO_3^- is properly selected. Although absolute values of activities cannot be thermodynamically measured, their ratios or changes can.

INTRODUCTION

Complexes between Ca^{2+}, Mg^{2+}, Cu^{2+}, and Zn^{2+} with CO_3^{2-} and HCO_3^- have been of interest to those concerned with models of electrolytes in studies appropriate to seawater and freshwater systems. In the pH range of primary interest (5-8) the principal form of the carbonate species is HCO_3^-. The aquated metal ions, except for Cu^{2+}, exist in the M_{aq}^{2+} or $M(OH)_{aq}^{+}$ form where M is a divalent metal. The purpose of this investigation is to determine the speciation and stability of divalent metal ion complexes in aqueous systems exposed to CO_2. Effects of temperature, ionic strength, and pH are shown. In additon to classical potentiometric measurements involving specific ion and glass electrodes, direct calorimetric measurements are made on the solutions to assess the thermodynamic properties as a function of temperature. Implications of these complexes on the Garrels-Thompson (3)[2] seawater model on the solubility of the carbonates are shown.

---

[1]Department of Chemistry, University of Missouri-Columbia, Columbia, Mo.

[2]Underlined numbers in parentheses refer to items in the list of references at the end of this paper.

For the formation of a M^{2+}-HCO_3^- complex

$$[M^{2+}] + [HCO_3^-] \rightleftharpoons [MHCO_3^+] \quad (1)$$

$$K_f=[MHCO_3^+]/[M^{2+}][HCO_3^-]. \quad (1a)$$

The molality of the complex is traditionally found by subtracting the free metal ion concentration, $[M^{2+}]$, from the total metal ion concentration. The $[M^{2+}]$ may be measured directly by specific ion electrodes or indirectly by making use of the mass balance equation for the bicarbonate:

$$[HCO_3^-]_T= [HCO_3^-] + [MHCO_3^+], \quad (2)$$

where $[HCO_3^-]$ is determined by its acid-base behavior via a pH electrode:

$$[HCO_3^-] = K(\underline{P}_{CO_2})/[H^+]. \quad (3)$$

If K, $\underline{P}_{CO_2}$, pH, and the specific ion electrode response can be known as a function of temperature and ionic strength, K_f can be evaluated. The situation is further complicated in case of bicarbonates by the very low solubility of the carbonate salts and by the extensive hydrolysis of some of the transition metals involved:

$$M^{2+} + H_2O \rightleftharpoons MOH^+ + H^+. \quad (4)$$

This paper describes a method by which the weak metal-bicarbonate interactions can be measured even though one does not have absolute measured values of pH, $\underline{P}_{CO2}$, pM^{2+}.

EXPERIMENTAL WORK

Potentiometry

A titration was made of $KHCO_3$ solution in equilibrium with pure CO_2 gas with alternating additions of MCl_2 and $KHCO_3$ solutions where M is Mg^{2+}, Ca^{2+}, Mn^{2+}, Fe^{2+}, Cu^{2+}, or Zn^{2+}. A thermostatic water bath for the runs has been described by Siebert, McGee, and Hostetler (12). The experimental pH was monitored with a Orion 801 digital meter and a Beckman 39000 glass electrode paired with an Orion 90-00-03 double-junction reference electrode. All materials were reagent grade and analyzed by conventional methods. Deionized, distilled water was used in all runs. Commercial buffers at pH 4.008 and 7.000 were used to standardize the meter. Reproducibility of ±0.005 pH unit was achieved on calibration.

Single-ion activity coefficients were calculated from the Debye-Hückel equation:

$$\log \gamma_i = Az_i^2 I^{1/2}/(1+\mathring{a}_1 BI^{1/2}) \quad (5)$$

with A and B values from Helgeson (4), å values from standard sources, and I, the molal ionic strength.

The data were calculated by a floating point method described by Siebert and Hostetler (11) and Hostetler and coworkers (5). In this method the HCO_3^- molality is considered to be unknown. However, the change in HCO_3^- activity between runs can be accurately calculated if P_{CO2} remains constant. For the nth point in a titration

$$[HCO_3^-]_n = [HCO_3^-]_1[\exp(pH_n - pH_1)], \quad (6)$$

where $[HCO_3^-]_1$ is the initial bicarbonate activity. This value was allowed to "float" to a value which permitted the K_f values (equation 1a) to be constant for the 10 points in a typical titration.

Calorimetry

Two calorimeters were used to measure the heats of formation. One based on the design of Robie and Hemingway (9) employed a digital quartz thermometer to measure temperature changes in an 800-ml stainless steel vessel equipped with a buret. The other was a commercial Tronac Model 450-4 isoperibol calorimeter consisting of a 100-ml glass Dewar vessel and a thermistor. Dilute $KHCO_3$ aqueous solution was added to 0.2 molal MCl_2 and/or $M(NO_3)_2$ solution. Corrections were made for heats of dilution, temperature differences between the buret and the calorimeter, and heats of deprotonation or hydrolysis of the metal ion. The calorimeters were calibrated electrically after standardization between dilute HCl and dilute tris hydroxymethylaminomethane (THAM). The corrected heat of protonation of THAM was found to be -11.23 ± 0.02 kcal/mole at 25° C.

RESULTS AND DISCUSSION

Table 1 contains typical reaction conditions for the titrimetric determination of log K_f for the $CaHCO_3^+$ ion pair (1). The average log K_f of 1.225 ± 0.009 represents a typical good convergence. Table 2 contains log K_f values for a number of complexes measured at different temperatures. The results for $FeHCO_3^+$ are available only at 25° C and appear to be log K_f = 1.3 ± 0.2 (6). Thus it is significantly less stable than Cu^{2+} and more in line between Mn^{2+} and Zn^{2+}.

It is noted that the stabilities of all of these complexes increase rapidly with temperature. The data were fit to the equation of Lesht and Bauman (7):

$$\log K_f = A + B \log T + C/T. \quad (7)$$

Table 3 shows the parameters for this equation as well as the calculated $\Delta H°$ form:

$$\Delta H° = R(BT - 2.303C). \quad (8)$$

TABLE 1. - Typical reaction conditions and species activities in a determination of the $CaHCO_3^+$ ion pair at 25° C (1)

Initial Conditions: 1607.6 g H_2O, 24.510 g 0.09883-M solution (K), 19.336 g 0.093519-M $CaCl_2$ solution (Ca) under pure CO_2 at 1 atm and initial pH = 4.804

			Activities ($x10^3$ molal)			
Grams	Solution	pH	HCO_3^-	Ca^{2+}	$CaHCO_3^+$	log K_f
10.21	K	4.93	1.62	5.26	0.14	1.22
22.08	Ca	4.88	1.45	9.40	.22	1.20
12.64	K	5.01	1.94	9.28	.31	1.23
24.66	Ca	4.97	1.77	13.0	.38	1.21
15.14	K	5.09	2.30	12.8	.51	1.24
27.47	Ca	5.05	2.12	16.4	.58	1.22
17.50	K	5.15	2.67	16.2	.75	1.24
30.21	Ca	5.12	2.48	19.8	.81	1.22
20.12	K	5.21	3.07	19.5	1.02	1.23

TABLE 2. - Log K_f values for $M^{2+} + HCO_3^- \rightleftharpoons MHCO_3^+$ at various temperatures

	10° C	25° C	40° C	55° C	70° C	90° C
Mg^{2+}	1.05	1.07	1.11	1.16	1.23	1.34
Ca^{2+}	1.23	1.23	1.26	1.31	1.38	1.50
Mn^{2+}	1.24	1.28	1.33	1.39	--	--
Cu^{2+}	1.91	2.08	2.32	2.58	--	--
Zn^{2+}	1.42	1.40	1.47	1.57	1.63	--

TABLE 3. - Parameters from the equation log K_f = A + B log T + C/T where T is in kelvins and $\Delta H°$ is at 298 K

	A	B	C	$\Delta H°$, cal/mole
Mg^{2+}	-59.85	21.14	2,567	779
Ca^{2+}	-79.08	27.71	3,497	213
Mn^{2+}	-80.63	28.41	3,462	983
Cu^{2+}	-168.7	60.13	6,560	5,610

An additional equation relating log K_f values for electrostatic ion pairs is due to Fuoss (2):

$$\ln K_f = A' - (B'/\varepsilon T), \tag{9}$$

where $A' = 4Na^3/3{,}000$ and $B' = Z_1Z_2e^2ka$ in which a is the ion size parameter, N is Avogadro's number, k is the Boltzmann constant, ε is the dielectric constant of water, e is the electronic charge, and Z_1 and Z_2 are charges on the cation and anion. The equation is fit at 25° C to calculate an "a" value. Table 4 shows the fit between experimental K_f values and those calculated from the Fuoss equation.

TABLE 4. - Comparison of experimental log K_f values for HCO_3^- ion pairs with those calculated from the Fuoss equation

Temperature, ° C	Mg^{2+}, a = 2.53A		Ca^{2+}, a = 2.24A		Zn^{2+}, a = 2.02A	
	Exp.	Calc.	Exp.	Calc.	Exp.	Calc.
10	1.05	1.03	1.22	1.18	1.42	1.34
25	1.07	1.07	1.23	1.23	1.40	1.40
40	1.11	1.11	1.26	1.28	1.47	1.48
55	1.16	1.17	1.31	1.34	1.57	1.56
70	1.23	1.23	1.38	1.41	1.63	1.65
90	1.34	1.32	1.50	1.51	--	1.73

Despite the good fit of the Mg^{2+} data to both equations 7 and 9, a calculation of $\Delta H°$ at 25° from equation 7 is 780 cal/mole and from equation 9 is 1,190 cal/mole. Furthermore, both equation show $\Delta H°$ to be increasing rapidly with temperature. Calorimetric determinations of $\Delta H°$ for HCO_3^- complexation are found to be 630 cal/mole for Ca^{2+} (1), 5.0 kcal/mole for Cu^{2+} (8), and 1.75 kcal/mole for Zn^{2+} (10). These do not differ significantly from the values determined from calculations based on equations 7 and 8. Table 5 gives the results for Ca^{2+}.

The log K_f and $\Delta H°$ data may be combined to calculate $\Delta S°$ for the formation of the complex. In all cases this increases from 6 cal/mole-deg at 25° C to 14 cal/mole-deg at 90° C. This indicates that the enhanced stability of the $MHCO_3^+$ unit at higher temperatures may be due to an increase in the number of water molecules released from the hydration sphere of the uncomplexed metal cation. Both the positive $\Delta S°$ term and the positive $\Delta H°$ support this model.

$$\text{Heat} + Ca(H_2O)_x^{2+} + HCO_3^- \rightleftharpoons [Ca(H_2O)_{x-y}HCO_3]^+ + yH_2O \tag{10}$$

TABLE 5. - Comparison of calculated and measured enthalpies of formation of $CaHCO_3^+$ complexes

Temperature ° C	ΔH° (calorimetric), kcal/mole	ΔH° (calculated), kcal/mole
10	0.13±0.03	-0.41±0.2
25	.63± .03	.41± .2
40	1.13± .04	1.24± .2
55	1.64± .06	2.06± .3
70	1.95± .31	2.89± .5
90	2.67± .20	3.99±1.0

The stabilities of the bicarbonate complexes appear to parallel the Irving-Williams stability series and to reflect the trends in solubility of the solid carbonates. The 1:1 bicarbonate-cation complex plays only a limited role in the solubility and mobilization of carbonates. Higher order bicarbonate and carbonate complexes also are expected to be important in natural water systems.

ACKNOWLEDGMENTS

This research was supported by the Earth Sciences Section, National Science Foundation, Grants GA31231 and EAR76-22327. The author is indebted to P.B. Hostetler, R.M. Siebert, D. Zebolsky, W.R. Almon, D.L. Leach, M.P. Ryan, D.Lesht, and D. Rages who did the work described here.

REFERENCES

1. Almon, W. R. M. A. Thesis, Univ. of Missouri-Columbia, 1973.

2. Fuoss, R. M. J. Am. Chem. Soc., v. 80, 1958, pp. 5059-5061.

3. Garrels, R. M., and M. E. Thompson. Am. J. Sci., v. 260, 1962, pp. 57-66.

4. Helgeson, H. C. Ch. in Researches in Geochemistry, ed. by P.H. Abelson. John Wiley & Sons, Inc., New York, v. 2, 1967, pp. 362-404.

5. Hostetler, P. B., and others. Manuscript in preparation.

6. Johnson, G. K., and J. E. Bauman. Inorg. Chem., v. 17, 1978, pp. 2774-2779.

7. Lesht, D., and J. E. Bauman. Inorg. Chem., v. 17 1978, pp. 3332-3334.

8. Rages, D. M.A. Thesis, Univ. of Missouri--Columbia, 1978.

9. Robie, R. A., and B. S. Hemingway. Calorimeters for Heat of Solution and Low-Temperature Heat Capacity Measurements. U.S. Geol. Survey Prof. Paper 755, 1972, 32 pp.

10. Ryan, M. P., and J. E. Bauman. Inorg. Chem., v. 17, 1978, pp. 3329-3331.

11. Siebert, R. M., and P. B. Hostetler. Am. J. Sci., v. 277, 1977, pp. 716-734.

12. Siebert, R. M., K. A. McGee, and P. B. Hostetler. J. Res. U.S. Geol. Survey, v. 5, 1977, pp. 597-602.

DISCUSSION

B. R. Staples: Variation in temperature changes the Kf values for these equilibria - what does one use for Kf values in these mixtures?

J. E. Bauman, Jr.: We can apply the traditional Kf for water as a function of temperature, but as far as they are in these solutions at this particular ionic strength, that is not at all clear. This is kind of allied with the activity coefficient question.

DETERMINATION OF APPARENT MOLAR HEAT CAPACITIES BY FLOW MICROCALORIMETRY: ΔC_p° FOR IONIZATION OF WATER AND HEAVY WATER AT 10°, 25°, and 40° C

by

Gregory C. Allred[1] and Earl M. Woolley[1]

ABSTRACT

A steady-state flow microcalorimeter and a vibrating-tube densimeter have been used to determine apparent molar heat capacities and volumes for NaCl, HCl, and NaOH in H_2O, and NaCl, DCl, and NaOD in D_2O, all at 10°, 25°, and 40° C. Solution concentrations ranged from 0.03 to 0.4 molal. Standard partial molar heat capacities and volumes were obtained by extrapolation. These results were used to calculate values of ΔC_p° for the ionization of H_2O and D_2O, and further, to obtain values for the standard enthalpy change and the equilibrium constant for ionization of D_2O over a range of temperatures.

INTRODUCTION

The partial molar heat capacity is a potentially useful tool in elucidating the nature of ion-solvent, ion-ion, and solvent-solvent interactions. The temperature dependence of these interactions may be determined from thermodynamic calculations based on heat capacities. Further, a knowledge of heat capacities over a range of temperatures permits the calculation of thermodynamic quantities at considerably higher and lower temperatures.

Within the last decade a new type of flow calorimeter (19-20)[2] has been developed which has helped to overcome some of the experimental difficulty associated with obtaining precise heat capacity data for dilute solutions. With a calorimeter of this type we have measured heat capacities of dilute (0.03 to 0.4 mol kg^{-1}) solutions of NaCl, HCl, and NaOH in H_2O and NaCl, DCl, and NaOD in D_2O with precision of about 0.006 pct. Measurements were made at 10.0°, 25.0°, and 40.0° C. Precise density measurements were also made. These results were used to derive standard partial molar heat capacities, $\overline{C}_2^\circ$, and volumes, $\overline{V}_2^\circ$, for the solutes and ΔC_p° and ΔV° for the ionization of water and of heavy water.

---

[1]Department of Chemistry, Brigham Young University, Provo, Utah.

[2]Underlined numbers in parentheses refer to items in the list of references at the end of this paper.

EXPERIMENTAL WORK

Materials

All water used to prepare stock solutions and as reference solvent was degassed once or twice by aspirating through a fritted glass disk. For measurements on D_2O Solutions at 25° C Pfaltz and Bauer, Inc. D_2O having an isotopic purity of 99.7_5 mole-pct was used. The average measured density of this D_2O at 25° C was found to be about 0.04 pct greater than the "best" value reported by Kell (10). It was assumed that this density difference was due to isotopic enrichment in ^{18}O. Since D_2O from the same bottle was used both as solvent for the solutions and as the reference solvent for both heat capacity and density determinations, the values of ϕ_c and ϕ_v[3] calculated from equations 3 and 4 were not significantly affected by small variations in the numerical value of d_1° used in the calculations. Several density measurements were performed on solutions of NaCl and DCl at 25° C in a mixture of D_2O from Sigma Chemical Co. and from Bio-Rad Laboratories, each having a specified isotopic purity of 99.8 pct. These results were used to calculate apparent molar volumes for NaCl and DCl, and to calculate densities of solutions used in heat capacity determinations at 25° C. For all measurements on D_2O solutions at 10° and 40° C, Bio-Rad D_2O was used. All D_2O solutions were prepared inside a polyethylene glove bag which was flushed with dry nitrogen.

Solute concentrations in stock solutions were determined either by gravimetric determination of Cl^- as AgCl, or by pH titration against dried primary standard potassium hydrogen phthalate using a weight buret. All replicate determinations agreed to within at least 0.07 pct. All dilutions of these stock solutions were made by weight, using degassed solvent.

The Picker Flow Microcalorimeter

Heat capacity measurements were made with a Picker flow microcalorimeter (19-20) built at the University of Sherbrooke, Sherbrooke, Quebec, Canada. This type of calorimeter, in which both the sample and a reference solvent or solution are made to flow simultaneously and in series through the instrument, seems to be better adapted to making high-precision measurements in very dilute solutions than the more traditional, static-type instrument.

The calorimeter itself consists of a pair of stainless steel flow cells constructed of 1.1-mm-OD tubing, each cell having a pair of Zener diode heaters and a thermistor detector. Each thermistor forms one arm of a Wheatstone bridge. In operation, the instrument acts as a thermal balance, adjusting the power input to the Zener heaters as required to maintain the thermistor bridge in balance. The two flow cells are connected in series so that, by means of a valve and a delay line, a solution may be caused to flow in one cell while a reference solvent or solution flows in the other. The ratio of the volumetric heat capacities of the two liquids is given by the ratio of the power input to the two Zener heaters. A calibration is performed after each measurement by

---

[3]See equations 3 and 4 for definitions of ϕ_c and ϕ_v.

means of a constant-current power source which is used to provide a known additional increment of power to one heater while a response of the instrument, which reacts to restore balance to the thermistor bridge, is recorded.

The calorimetric measurements were made at a flow rate of about 0.7 $cm^3 min^{-1}$ with a temperature rise of about 1.9 K. All measurements were made relative to the pure solvent (H_2O or D_2O). Solution densities, which are necessary to calculate c_p (J K^{-1} g^{-1}) with this instrument, were determined with a Picker vibrating-tube densimeter (21).

Heat Leaks

Desnoyers and coworkers (4) observed that results from a newer model of the Picker flow calorimeter were consistently different from those from an earlier, prototype version. They tentatively attributed this difference to an asymmetrical heat flow between the flow cells and the calorimeter jacket in the prototype. Several tests have been suggested (6, 20) to physically evaluate this asymmetry, but none has proved practical, since the uncertainty in such tests has always been greater than the overall uncertainty in the heat capacity measurements. Desnoyers suggested the use of the correction factor, f, which would relate the measured volumetric heat capacity σ^* (J K^{-1} cm^{-3}), to some standard value, σ:

$$f = \frac{(\sigma-\sigma^\circ)/\sigma^\circ}{(\sigma^*-\sigma^\circ)/\sigma^\circ} \qquad (1)$$

where σ° is the volumetric heat capacity of the pure solvent. Values for σ were determined for NaCl solutions at 25° C over a range of concentrations up to 1.0 mole kg^{-1} by combining measured values of σ from three different Picker calorimeters.

Olofsson (15) has combined non-flow calorimetric results reported by earlier investigators (9, 22, 25) with measurements made at the University of Lethbridge using a LKB[4] calorimeter to get a "best" set of data for apparent molar heat capacities of NaCl in the concentration range 0.5 to 3.2 mole kg^{-1} at 25° C.

In practice, σ^* is measured in two different ways. In the first case, a solution in the working cell is compared to solvent in the reference cell, and f would be defined as in equation 1. In the second case, where solvent is in the working cell and the solution is in the reference cell, the following definition would apply:

$$f' = \frac{(\sigma^\circ-\sigma)/\sigma}{(\sigma^\circ-\sigma^*)/\sigma^*}. \qquad (2)$$

We have calculated values for f and f′ for 23 solutions of NaCl at 25° C between 0.038 and 1.00 mole kg^{-1} using the values for σ recommended by

[4]Manufactured by LKB Produkter, Bromma, Sweden.

Desnoyers. Similarly, values for f and f′ were calculated from the data of Olofsson for eight solutions of NaCl at 25° C between 0.407 and 2.90 mole kg^{-1}. The results of these calculations are given in table 1.

TABLE 1. - Values for f and f′ from equations 1 and 2 for NaCl solutions at 25° C[1]

Concentration, mole kg^{-1}	f	f′
0.038 - 1.00	1.002 ± 0.008	1.006 ± 0.007
.407 - 2.90	1.000 ± .006	1.008 ± .004

[1]Uncertainty is ±1 standard deviation.

Use of the first pair of f values in table 1 would, in effect, only "calibrate" the present instrument against other instruments of the same design. Because of the close agreement between reported values of ϕ_c for NaCl solutions above 0.4 mole kg^{-1} and the nature of the calorimetric methods used for their determination, the method of Olofsson seems advantageous, except that it can give no information for solutions more dilute than about 0.4 mole kg^{-1}. Since the uncertainty in the f values calculated by either method is nearly as great as or even greater than the difference between f or f′ and 1, the present results were not corrected by either method. In any case, the above analysis shows that the present results for NaCl solutions at 25° C are in good agreement with the best results obtained by other workers.

RESULTS AND DISCUSSION

Apparent Molar Volumes and Heat Capacities

For a solution that contains 1,000 g of solvent, the apparent molar heat capacity of the solute is defined by the expression

$$\phi_c = \left(M_2 + \frac{1,000}{m}\right)c_p - \frac{1,000}{m}\,c_p^\circ \qquad (3)$$

and the apparent molar volume by

$$\phi_v = \frac{mM_2 + 1,000}{dm} - \frac{1,000}{d_1^\circ m} \qquad (4)$$

in which M_2 is the solute molecular weight, m is the molal concentration of the solute (mole kg^{-1}), c_p is the heat capacity per gram of solution, c_p° is the heat capacity per gram of the pure solvent, d is the density of the solution, and d_1° is the density of the pure solvent.

The ϕ_c and ϕ_v results obtained in this study were fit to equations of the form

$$\phi_y = \phi_y^\circ + A_y(d_1^\circ m)^{1/2} + B_y m, \quad (y = c \text{ or } v) \tag{5}$$

where A_y is the limiting slope derived from the Debye-Hückel theory and B_y is an adjustable parameter. The limiting slopes used in equation 5 were those given by Perron and coworkers (18) and are listed in table 2.

Included in table 2 are the values of c_p° and d_1° used in equations 3 and 4. Those for H_2O are from Kell (10), while the ones for D_2O were determined in the present study.

The parameters of equation 5 determined from least-squares analysis of $[\phi_x - A_y (d_1^\circ m)^{1/2}]$ versus m are given in table 3 for solutions in H_2O. The number of separate solutions used in each extrapolation is found under the columns headed "n."

The ϕ_c° values derived by Parker (17) in her review of earlier heat capacity data are more negative than the present results for NaCl, HCl, and NaOH by 6, 12, and 1.6 J $K^{-1}mole^{-1}$, respectively, at 25° C. Tanner and Lamb (25) have reported ϕ_c° = -83.3 J $K^{-1}mole^{-1}$ for NaCl at 25° C, and the integral heat of solutions work of Criss an Cobble (3) led to C_p° values of -121.3, -79.1, and -64.0 J $K^{-1}mole^{-1}$, at 10°, 25°, and 40° C, respectively. Desnoyers and coworkers (4) have used a Picker flow calorimeter to determine apparent molar heat capacities of NaCl solutions over a range of temperatures, resulting in values of ϕ_c° that are more negative than the present results by about 4, 0.7, and 1 J $K^{-1}mole^{-1}$ at 10°, 25°, and 40° C, respectively. Singh and coworkers (24) report ϕ_c° = -84.6 J $K^{-1}mole^{-1}$ for aqueous NaCl at 25° C. Flow calorimetric measurements have led Desnoyers to ϕ_c° = -127.0 J $K^{-1}mole^{-1}$ and Singh to ϕ_c° = -127.2 J $K^{-1}mole^{-1}$ for HCl at 25° C. The present result is in fair agreement. For aqueous NaOH at 25° C we have ϕ_c° = -94.6 J $K^{-1}mole^{-1}$ from Desnoyers and -96.2 J $K^{-1}mole^{-1}$ from Singh compared with -100.5 J $K^{-1}mole^{-1}$ from the present study. Flow calorimetric measurement for the present electrolytes other than NaCl at temperatures other than 25° C do not appear in the literature. It may be observed that the general agreement among different investigators using the Picker flow calorimeters is very good, with ϕ_c° results from different laboratories differing by usually not more than 2 or 3 J $K^{-1}mole^{-1}$ for 1:1 electrolytes.

The agreement between the present ϕ_v° values and most of those compiled by Millero (12) is within a few tenths of a cubic centimeter per mole. This agreement serves as a check on solution concentrations and densities.

The parameters of equation 5 determined from ϕ_c and ϕ_v values for NaCl, DCl, and NaOD in D_2O are given in table 4.

Our results for NaCl at 25° C may be compared with ϕ_c° = -120 J $K^{-1}mole^{-1}$ and ϕ_v° = -15.75 cm^3mole^{-1} from Fortier and coworkers (7) and ϕ_v° = 15.78 cm^3mole^{-1} from Conway and Laliberté (1).

TABLE 2. - Debye-Hückel limiting slopes, heat capacity, and density of H_2O and D_2O

t, ° C	H_2O				D_2O			
	$A_c d_1^{\circ 1/2}$	$A_v d_1^{\circ 1/2}$	c_p°, J $K^{-1}g^{-1}$	d_1°, g cm^{-3}	$A_c d_1^{\circ 1/2}$	$A_v d_1^{\circ 1/2}$	c_p°, J $K^{-1}g^{-1}$	d_1°, g cm^{-3}
10	24.229	1.612	4.1919	0.999700	25.180	1.695	4.2802	1.105957
25	28.945	1.865	4.1793	.997045	30.616	1.960	4.2227	[1]1.104903
40	33.805	2.131	4.1783	.992215	35.619	2.235	4.1944	1.099984

[1]For density determinations on NaCl and DCl solutions in D_2O at 25° C, d_1° was 1.104420.

TABLE 3. - Parameters of equation 5 for NaCl, HCl, and NaOH in H_2O[1]

Solute	t, ° C	$\phi_c^\circ=\overline{C}_2^\circ$, J $K^{-1}mole^{-1}$	B_c, J $K^{-1}mole^{-2}kg$	n	$\phi_v^\circ=\overline{V}_2^\circ$, cm^3mole^{-1}	B_v, $cm^3mole^{-2}kg$	n
NaCl	10	-128.6±0.2	41.4±1.0	8	14.89±0.02	0.60±0.08	10
	25	-83.7± .3	15.8±1.4	18	16.63± .02	-.07± .07	18
	40	-65.2± .5	-.4±2.6	20	17.40± .06	-.45± .27	20
HCl	10	-147.7± .8	7.0±4.0	13	17.15± .04	-.56± .21	13
	25	-124.7± .7	-6.5±3.5	10	17.89± .02	-1.11± .10	10
	40	-115.2± .5	-10.2±2.3	13	17.91± .02	-.91± .09	15
NaOH	10	-167.4± .8	82.4±4.1	14	-7.54± .03	2.24± .16	14
	25	-100.5± .5	41.2±2.2	12	-5.37± .02	1.35± .11	15
	40	-67.3± .7	15.7±3.3	10	-4.30± .03	.79± .13	10

[1]Standard deviations of slopes and intercepts (26) are indicated by ± values.

ΔC_p° and ΔV° of Ionization

The ionization of water is represented by

$$H_2O(liq) = H^+(aq) + OH^-(aq). \quad (6)$$

Because $\phi_c^\circ \equiv \bar{C}_{p2}^\circ$ for a solute at infinite dilution, we can obtain ΔC_p° for reaction 6 from

$$\Delta C_p^\circ = \phi_c^\circ (HCl) + \phi_c^\circ (NaOH) - C_p^\circ (H_2O) - \phi_c^\circ(NaCl). \quad (7)$$

An analogous equation applies for D_2O. Results of calculations based on equation 7 are summarized in table 5.

Olofsson and Olofsson (13-14) have reported calorimetric measurements leading to ΔH° for ionization of water at several temperatures and they have derived ΔC_p° values (16) of $-265(\pm 8)$, $-213.4(\pm 5)$, and $-190.5(\pm 8)$ J $K^{-1}mole^{-1}$ at 10°, 25°, and 40° C. Our more directly measured values agree to within at least 3 J $K^{-1}mole^{-1}$ in each case. Singh and coworkers (24) derived $\Delta C_p^\circ = -215.2$ J $K^{-1}mole^{-1}$ as a result of flow-calorimetric investigation of eight 1:1 electrolytes at 25° C. Similarly, Enea and coworkers (5) obtained $\Delta C_p^\circ = -214.6$ J $K^{-1}mole^{-1}$ at 25° C, while in another investigation, Singh and coworkers (23) obtained $\Delta C_p^\circ = -213.8$ J $K^{-1}mole^{-1}$. Covington and coworkers (2) have derived values for K, the ionization constant of D_2O, from very careful electromotive force measurements made over a range of temperatures. By successive differentiation they derived $\Delta C_p^\circ = -229$ J $K^{-1}mole^{-1}$ for the ionization of D_2O at 25° C.

Values of ΔV° for ionization of water and of heavy water calculated from our ϕ_V° results are listed in table 6. V° values are from Kell (10).

The following equations were found to represent the present ΔC_p° results over the range 5° to 45° C.

For H_2O:

$$\Delta C_p^\circ = -216.8 + 2.3133\ (t-25) - 0.046667\ (t-25)^2 \quad (8)$$

For D_2O:

$$\Delta C_p^\circ = -249.0 + 3.9533\ (t-25) - 0.076444\ (t-25)^2 \quad (9)$$

where t is the temperature in ° C. These equations may be used to integrate the Kirchhoff equation

$$\left(\frac{d\Delta H^\circ}{dT}\right)_p = \Delta C_p^\circ \quad (10)$$

and then the van't Hoff equation

$$\left(\frac{d\ \ln K}{dT}\right)_p = \frac{\Delta H^\circ}{RT^2} \quad (11)$$

TABLE 4. - Parameters of equation 5 for NaCl, DCl, and NaOD in D_2O[1]

Solute	t, ° C	$\phi_c^\circ=\overline{C}_2^\circ$, J $K^{-1}mole^{-1}$	B_c, J $K^{-1}mole^{-2}kg$	n	$\phi_v^\circ=\overline{V}_2^\circ$, cm^3mole^{-1}	B_v, $cm^3mole^{-2}kg$	n
NaCl	10	-203.0±0.5	75.0±1.9	8	13.53±0.03	0.85±0.12	10
	25	-124.8± .6	21.9±2.5	10	15.84± .03	-.41± .14	12
	40	- 93.8± .3	8.1±1.1	10	16.96± .01	-.41± .03	10
DCl	10	-188.4± .8	8.8±3.0	8	16.55± .08	-.70± .33	9
	25	-150.8±1.1	7.3±5.2	9	17.66± .06	-1.56± .32	9
	40	-125.6± .4	-18.3±1.6	8	17.75± .01	-1.08± .05	10
NaOD	10	-254.4±1.0	125.5±3.7	10	-9.66± .02	2.89± .08	10
	25	-138.3±1.0	44.6±4.1	10	-6.44± .01	1.35± .04	10
	40	-91.1± .3	28.9±1.3	10	-5.07± .01	.98± .04	10

[1]Standard deviations of slopes and intercepts (26) are indicated by ± values.

TABLE 5. - ΔC_p° of ionization of H_2O and D_2O[1], J $K^{-1}mole^{-1}$

t, ° C	C_p° (H_2O)	ΔC_p° (H_2O)	C_p° (D_2O)[2]	ΔC_p° (D_2O)
10	75.52	-262.0±1.2	85.72	-325.5±1.4
25	75.29	-216.8± .9	84.68	-249.0±1.6
40	75.27	-192.6±1.0	84.00	-206.9± .6

[1]± values represent standard deviations.
[2]$C_p^\circ(D_2O)$ at 10° and 40° C from present measurements using the molecular weight given by Kell (10). C_p° (D_2O) at 25° C from Kiyohara and coworkers (11).

TABLE 6. - ΔV° of ionization of H_2O and of D_2O[1], cm^3 $mole^{-1}$

t,	V° (H_2O)	ΔV° (H_2O)	V° (D_2O)[2]	ΔV° (D_2O)
10	18.021	-23.30±0.05	18.108	-24.75±0.09
25	18.069	-22.18± .03	18.134	-22.75± .07
40	18.157	-21.95± .07	18.208	-22.49± .02

[1]± values represent standard deviations.
[2]Reference 10.

to obtain relations for the standard enthalpy for ionization and the equilibrium constant for ionization as functions of temperature. Table 7 summarizes the results of such calculations for D_2O, using $\Delta H^\circ_{298} = 60,618$ J mole^{-1} from Goldberg and Hepler (8) and K_m (298.15) = 1.371 x 10^{-15} from Covington and coworkers (2). Included in table 7 are values of $\Delta H^{\circ\prime}$ and K_m' calculated assuming constant ΔC_p° and constant ΔH°, respectively. K_m is expressed in terms of moles of solute per 55.508 moles of solvent, the so-called aquamolal concentration scale.

It can be seen that equation 9 may be used to predict the value of K_m to within 2 or 3 pct of the measured value over the whole temperature range, while the error resulting from the assumption of constant ΔH° may be as much as 8 pct. The difference between ΔH° values predicted by means of equation 9 and those derived assuming constant ΔC_p° is as much as 1.5 pct. No experimentally determined values for ΔH° for the ionization of D_2O at temperatures other than 25° C are presently in the literature.

CONCLUSION

Flow microcalorimetry has been shown to be a valuable tool capable of determining heat capacities of dilute solutions which are precise enough to be used for extending thermodynamic calculations over a range of temperatures with reasonable accuracy.

ACKNOWLEDGEMENTS

We thank the Brigham Young University Research Division for partial support of this research. Thanks is extended to Loren G. Hepler and Inger Olofsson for providing copies of manuscripts prior to publication.

TABLE 7.- Standard enthalpy of ionization and equilibrium constant for $D_2O(liq) = D^+(aq) = OD^-(aq)$

t, °C	ΔH°[1], kJ mole^{-1}	$\Delta H^{\circ\prime}$[2], kJ mole^{-1}	K_m (2), x 10^{15}	K_m[3] x 10^{15}	K_m'[4] x 10^{15}
5	66.59	65.60	0.2249	0.217	0.236
10	64.88	64.35	.3681	.359	.375
15	63.33	63.11	.5834	.576	.587
20	61.92	61.86	.9036	.899	.903
25	(60.618)	(60.618)	1.371	(1.371)	(1.371)
30	59.42	59.37	2.032	2.04	2.05
35	58.30	58.13	2.951	2.99	3.03
40	57.24	56.88	4.207	4.28	4.42
45	56.23	55.64	5.888	6.03	6.38

[1]Using equations (9) and (10).
[2]Using equation (10) with ΔC_p° = -249.0 J K^{-1}mole^{-1}.
[3]Using equations (9), (10), and (11).
[4]Using equation (11) with ΔH° = 60,618 J mol^{-1}.

REFERENCES

1. Conway, B. E., and L. H. Laliberté. H_2O-D_2O Solvent Isotope Effects in the Volume and Expansivity Behaviour of Some Organic and Inorganic Ions. Trans. Faraday Soc., v. 66, 1970, p. 3032.

2. Covington, A. K., R. A. Robinson, and R. G. Bates. The Ionization Constant of Deuterium Oxide from 5 to 50°. J. Phys. Chem., v. 70, p. 3820.

3. Criss, C. M., and J. W. Cobble. The Thermodynamic Properties of High Temperature Aqueous Solutions. I. Standard Partial Molal Heat Capacities of Sodium Chloride and Barium Chloride from 0 to 100°. J. Am. Chem. Soc., v. 83, 1961, p. 3223.

4. Desnoyers, J. E., C. deVisser, G. Perron, and P. Picker. Reexamination of the Heat Capacities Obtained by Flow Microcalorimetry. Recommendation for the Use of a Chemical Standard. J. Sol. Chem., v. 5, 1976, p. 605.

5. Enea, O., P. P. Singh, E. M. Woolley, K. G. McCurdy, and L. G. Hepler. Heat Capacities of Aqueous Nitric Acid, Sodium Nitrate, and Potassium Nitrate at 298.15 K: ΔC_p° of Ionization of Water. J. Chem. Thermodyn., v. 9, 1977, p. 731.

6. Fortier, J.-L., G. C. Benson, and P. Picker. Heat Capacities of Some Organic Liquids Determined with the Picker Flow Calorimeter. J. Chem. Thermodyn., v. 8, 1976, p. 289.

7. Fortier, J.-L., P. R. Philip, and J. E. Desnoyers. Thermodynamic Properties of Alkali Halides. III. Volumes and Heat Capacities of Transfer from H_2O to D_2O at 25° C. J. Sol. Chem., v. 3, 1974, p. 523.

8. Goldberg, R. N., and L. G. Hepler. Thermodynamics of Ionization of Deuterium Oxide. J. Phys. Chem., v. 72, 1968, p. 4654.

9. Hess, C. B., and B. E. Gramkee. The Specific Heats of Some Aqueous Sodium and Potassium Chloride Solutions at Several Temperatures. I. J. Phys. Chem., v. 44, 1940, p. 483.

10. Kell, G. S. Thermodynamic and Transport Properties of Fluid Water. Ch. in Water - A Comprehensive Treatise, ed. by F. Franks. Plenum Press, New York, 1972, p. 376.

11. Kiyohara, O., P. J. D'Arcy, and G. C. Benson. Heat Capacities and Compressibilities of Deuterium Oxide - Water Mixtures at 298.15 K. Thermochim. Acta, v. 25, 1978, p. 379.

12. Millero, F. J. The Partial Molal Volumes of Electrolytes in Aqueous Solutions. Ch 13 in Water and Aqueous Solutions, ed. By R. A. Horne. John Wiley and Sons, Inc., New York, 1972.

13. Olofsson, G., and I. Olofsson. A Calorimetric Determination of the Enthalpy of Ionization of Water Between 273 and 323 K. J. Chem. Thermodyn., v. 5, 1973, p. 533.

14. _____. The Enthalpy of Ionization of Water Between 273 and 323 K. J. Chem. Thermodyn., v. 9, 1977, p. 65.

15. Olofsson, I., personal communication.

16. _____. Some Thermodynamic Properties of Water and Aqueous Electrolytes. Ph.D. Dissertation, Lund, 1979, p. 18.

17. Parker, V. B. Thermal Properties of Aqueous Uni-univalent Electrolytes. NSRDS-NBS 2, 1965.

18. Perron, G., N. Desrosiers, and J. E. Desnoyers. Thermodynamic Properties of Tetraalkylammonium Halides: Volumes, Heat Capacities, and Expansibilities in H_2O, D_2O and Urea - Water Mixtures from 278 to 328 K. Can. J. Chem., v. 54, 1976, p. 2163.

19. Picker, P. New Concepts in Design and Applications of Flow Microcalorimetry. Can. Res. and Devel., January 1974, p. 11.

20. Picker, P., P.-A. Leduc, P. R. Philip, and J. E. Desnoyers. Heat Capacity of Solutions by Flow Microcalorimetry. J. Chem. Thermodyn., v. 3, 1971, p. 631.

21. Picker, P., E. Tremblay, and C. Jolicoeur. A High-Precision Digital Readout Flow Densimeter For Liquids. J. Sol. Chem., v. 3, 1974, p. 377.

22. Randall, M., and F. D. Rossini. Heat Capacities of Aqueous Salt Solutions. J. Am. Chem. Soc., v. 51, 1929, p. 323.

23. Singh, P. P., K. G. McCurdy, E. M. Woolley, and L. G. Hepler. Heat Capacities of Aqueous Perchloric Acid and Sodium Perchlorate at 298 K: ΔC_p° of Ionization of Water. J. Sol. Chem., v. 6, 1977, p. 327.

24. Singh, P. P., E. M. Woolley, K. G. McCurdy, and L. G. Hepler. Heat Capacities of Aqueous Electrolytes: Eight 1:1 Electrolytes and ΔC_p° for Ionization of Water at 298K. Can. J. Chem., v. 54, 1976, p. 3315.

25. Tanner, J. E., and F. W. Lamb. Specific Heats of Aqueous Solutions of NaCl, NaBr, and KCl: Comparisons with Related Thermal Properties. J. Sol. Chem., v. 7, 1978, p. 303.

26. Young, H. D., Statistical Treatment of Experimental Data, McGraw-Hill Book Co., New York, 1962, pp. 115-126.

SECTION 5.- DATA COMPILATION

EVALUATION OF ACTIVITY AND OSMOTIC COEFFICIENTS FOR ELECTROLYTE SOLUTIONS, BASIC METHODOLOGY

by

Bert R. Staples[1]

ABSTRACT

A number of models and associated correlating equations used in electrolyte theory and critical evaluations of thermodynamic properties of aqueous solutions are discussed. The methodology and philosophy used in critical evaluation schemes are summarized.

INTRODUCTION

Studies of problems in the area of water quality control, the application of geothermal energy, the desalination of water, sewage treatment, industrial applications, and bioengineering all must treat aqueous solutions containing ionic species. A significant need for reliable quantitative data on the properties of aqueous solutions has become apparent in recent years, particularly with the development of large-scale models that attempt to simulate complex aqueous ecosystems (12, 32).[2] Reliable quantitative data must often be selected from discordant results of various experimenters. A critical evaluation is the best approach to providing "standard" sets of data.

Critical evaluations of activity and osmotic coefficient data were undertaken in the 1930's by Harned and Owen and by Robinson and Stokes. The most recent revised editions of their books (9, 23) were published in 1958 and 1965 respectively. Wu and Hamer (31) evaluated activity and osmotic coefficient data for a series of electrolytes until about 1968, but their work on polyvalent electrolytes was not completed. Their work on the 1:1 electrolytes (8) was published in 1972. The evaluation of polyvalent electrolyte data has been continuing in the Electrolyte Data Center at the National Bureau of Standards, and this and the subsequent paper will summarize the methods and philosophy used in evaluating data for over 100 aqueous polyvalent electrolytes. Models and the associated correlating equations will be discussed, as will the methodology for the correlating schemes.

---

[1]Electrolyte Data Center, National Measurement Laboratory, National Bureau of Standards, Washington, D.C.

[2]Underlined numbers in parentheses refer to items in the list of references at the end of this paper.

MODELS AND CORRELATING EQUATIONS

The Debye-Hückel limiting law was derived in 1923 and has served as an excellent model for simple salts at very low concentrations. The limiting form of this theory can be derived in several ways that give correct results at moderate (up to 0.5 or 1 mol-kg^{-1}) concentrations (2). The mathematics involved in proceeding beyond the limiting law stage are so formidable that the theories have been of very limited use in the experimental range of concentrations.

Friedman (3) has used the cluster theory of Mayer (11) to derive equations that give the thermodynamic properties of electrolyte solutions as the sum of convergent series. The first term in these series is identical to, and thus confirms, the Debye-Hückel limiting law. The second term is an IℓnI term whose coefficient, like the coefficient in the Debye-Hückel limiting law equation, is a function of the charge type of the salt and the properties of the solvent. From this theory, as well as from others referred to above, a higher order limiting law can be written as

$$\ell n\ \gamma_{\pm} = -\left|z_+ z_-\right| A_m I^{1/2} - \frac{(\Sigma \nu_i z_i^3 z)^2}{\nu \Sigma_i (\nu_i z_i^2)} A_m^2\ I \ell nI, \qquad (1)$$

where $\gamma_{\pm}$ is the mean ionic activity coefficeint, z is the ionic charge, A_m is the Debye-Hückel constant on the molality scale, I is the ionic strength, and ν_i is defined after equation 4. For symmetrical electrolytes the coefficient of the IℓnI term is zero.

Higher terms involve direct potentials corresponding to the forces between sets of ions and become mathematically very difficult.

Pitzer and coworkers (13-19) have proposed a set of equations based on the general behavior of classes of electrolytes. They write equations for the excess Gibbs energy ΔG^{ex}, the osmotic coefficient ϕ, and the activity coefficient $\gamma_{\pm}$ for single unassociated electrolytes as

$$(\Delta G^{ex}/n_w RT) = f^{Gx} + m^2\ (2\nu_M \nu_X) B_{MX}{}^{Gx} + m^3 [2(\nu_M \nu_X)^{3/2}]\ C_{MX}{}^{Gx} \qquad (2)$$

$$\phi - 1 = \left|z_M z_X\right| f^{\phi} + m\left(\frac{2\nu_M \nu_X}{\nu}\right) B_{MX}{}^{\phi} + m^2 \frac{2(\nu_M \nu_X)^{3/2}}{\nu} C_{MX}{}^{\phi} \qquad (3)$$

$$\ell n\gamma = \left|z_M z_X\right| f^{\gamma} + m\left(\frac{2\nu_M \nu_X}{\nu}\right) B_{MX}{}^{\gamma} + m^2 \frac{2(\nu_M \nu_X)^{3/2}}{\nu}) C_{MX}{}^{\gamma} \qquad (4)$$

where ν_M and ν_X are the numbers of M and X ions in the formula $M_{\nu_M} X_{\nu_X}$, and z_M and z_X are their respective charges in electronic units; also $\nu = \nu_M + \nu_X$

while n_w is the number of kilograms of solvent and m is the conventional molality. Other quantities have the form

$$f^{Gx} = - A_\phi(4I/b) \ln (1 + bI^{1/2}) \tag{5}$$

$$f^{\phi} = -A_\phi \frac{I^{1/2}}{1 + bI^{1/2}} \tag{6}$$

$$f^{\gamma} = -A_\phi[\frac{I^{1/2}}{1 + bI^{1/2}} + \frac{2}{b} \ln (1 + bI^{1/2})] \tag{7}$$

$$B_{MX}{}^{Gx} = \beta_{MX}(0) + \frac{2\beta_{MX}(1)}{\alpha^2 I} [1 - e^{-\alpha I^{1/2}} (1 + \alpha I^{1/2})] \tag{8}$$

$$B_{MX}{}^{\phi} = \beta_{MX}(0) + B_{MX}(1)e^{-\alpha I^{1/2}} \tag{9}$$

$$B_{MX}{}^{\gamma} = 2\beta_{MX}(0) + \frac{2\beta_{MX}(1)}{\alpha^2 I} [1 - e^{-\alpha I^{1/2}} (1 + \alpha I^{1/2} - (1/2)\alpha^2 I)]. \tag{10}$$

In addition, several other forms of correlating equations give comparable fits to the experimental data. One equation uses the higher order limiting law, equation 1, followed by an empirical polynomial in the square root of molality. Here, A_1 and A_2 are coefficients calculated from equation 1 and the B_i are adjustable parameters:

$$\ell n\ \gamma_{\pm} = -A_1 I^{1/2} - A_2 I \ell nI + \sum_{i=1}^{N} B_i m^{(i+1)/2} \tag{11}$$

$$\phi = 1 - \frac{A_1 I^{1/2}}{3} - \frac{A_2 I}{2} [\ell n\ I + 1/2] + \sum_{i=1}^{N} B_i \frac{(i+1)}{(i+3)} m^{(i+1)/2}. \tag{12}$$

Similarly, another equation uses the Debye-Hückel limiting law, with B (in equation 13) set equal to zero, followed by an empirical polynomial in the square root of molality.

Effective correlating equations should represent the experimental data adequately over a wide range of concentrations. They also should take into account the very dilute regions because they are used to evaluate the integral in the Gibbs-Duhem relation. Thus it is appropriate to include the Debye-Hückel limiting law as the first term. What is appropriate at slightly higher concentrations is difficult to determine. In our work, correlations are carried out using a variety of equations, but the tabulated and recommended values are generally based on the empirical form of an equation used previously by Hamer and Wu (8) and Leitzke and Stoughton (10):

$$\ell n\ \gamma_{\pm} = \frac{-|z_+z_-|A_m I^{1/2}}{1 + BI^{1/2}} + Cm + Dm^2 + Em^3 + \ldots \qquad (13)$$

The ionic strength I is given by $I = 1/2\Sigma_i m_i z_i^2$, and B is used to denote $B_m \cdot a$, with a being the distance of closest approach in the Debye-Hückel expression. The constants B, C, D, E, etc., are empirical.

The osmotic coefficient and excess Gibbs energy can be expressed in terms of the same parameters by

$$\phi = 1 + \frac{|z_+z_-|A_m}{B^3 I}\left[-(1 + BI^{1/2}) + 2\ell n(1 + BI^{1/2}) + 1/(1 + BI^{1/2})\right] +$$

$$(1/2)Cm + (2/3)Dm^2 + (3/4)Em^3 + \ldots, \qquad (14)$$

and

$$\Delta G^{ex} = \nu mRT\,\frac{|z_+z_-|A_m}{B^3 I}\left[(2-BI^{1/2})BI^{1/2} - 2\ln(1+BI^{1/2})\right]$$

$$+ (1/2)Cm + (1/3)Dm^2 + (1/4)Em^3 + \ldots \qquad (15)$$

Values for the parameters are determined by a least squares fit of experimental data using equation 13 for experiments such as galvanic cell measurements that measure solute activity and thus γ/γ_{ref} values, and equation 14 for experiments such as vapor pressure measurements that measure solvent activity and thus ϕ values. As explained below, these two types of measurements are used in a single fitting program to determine the best value for the parameters.

BASIC METHODOLOGY

An overview of all available data is necessary before a critical evaluation can be accomplished. All available reprints of original articles for each compound are assembled through a combination of the in-house files of the Chemical Thermodynamics Data Center, the files collected by Wu and Hamer, and a computer search of Chemical Abstracts and National Technical Information Service. A bibliography of data sources for activity and osmotic coefficient data has been compiled (7). Another bibliography on thermal properties (24) has also been published. In general, experimentally observed data are used as a starting point rather than smoothed or recalculated data. Thus for electromotive force data the observed compositions and cell voltages are the primary data, and for isopiestic vapor pressure measurements the observed isopiestic molalities of the salt being investigated and the reference salt are the primary data.

All the data are made consistent with the ^{12}C scale of atomic weights, and where necessary are corrected to the most recent recommended values of the physical constants (1).

To obtain values of $\ell n\ \gamma_{\pm}$ and $\gamma_{\pm}$ from the cell measurements, it is necessary to know a value for γ_{ref} at a reference molality for each set of experimental data. We arrive at the value of $\gamma_{\pm}$ by an iteration technique. Initial values for γ_{ref} are calculated by equation 13 using initial parameters given by Wu and Hamer (31). Using this reference value, a pair of values of m, $\gamma_{\pm}$ is obtained at each experimental point. These data are then combined with the pairs of m, $\gamma_{\pm}$ values from diffusion data, m, ϕ values from freezing point data, and vapor pressures, and a new set of parameters for equations 13 and 14 is calculated by a nonlinear least-square fit to minimize $\Sigma\omega_i[f_i - f_i(calc)]^2$, where ω is the assigned weight and the functions f are $\ell n\ \gamma_{\pm}$ or ϕ and are obtained from equations 13 or 14, respectively. The summation is over the number of experimental points. Using the new parameters, a new set of γ_{ref} are calculated, and the fitting procedure is repeated. This process continues until the parameters remain essentially unchanged. Many of the basic computer programs have been documented in a National Bureau of Standards Technical Note (30), although these have been refined over the past few years.

Initially all the experimental data are weighted equally and included in the fitting procedure. The data are divided into sets according to source, and an estimate of the standard deviation of each set is made by equating it to the root-mean-square deviation of the points in the set from the curve obtained in the initial fit. Using weights corresponding to these estimates of standard deviations, a second fit of the data is made. The results of these calculations, together with subjective evaluation of experimental procedures, are used to weigh the experimental points. After the first iteration, experimental points with deviation from calculated values of greater than 0.1 in ϕ or γ are usually given zero weight.

Using this iterative and selective approach, all of the available data are being correlated through the model equations. Recommended values of parameters of these correlating equations as well as standard tables of values are published.

Ongoing efforts in the Electrolyte Data Center include critical evaluations of osmotic and activity coeeficients for aqueous polyvalent electrolytes at 298.15 K. These compounds include $CaCl_2$, H_2SO_4, all of the 2:1 charge-type electrolytes of the periodic group II such as $MgCl_2$, and compounds of iron, nickel, cadmium, cobalt, lead, copper, manganese, uranium, and other charge types (alkali metal nitrites, sulfates, carbonates, and others) (4-6, 27-29). Some work has begun on the evaluation of other thermodynamic properties such as equilibrium constants (26) enthalpy of dilution and heat capacities of solutions.

Several investigators are engaged in the modern evaluation of data, such as Pitzer's group (13-19), who are covering a wide range of electrolytes and their properties, and Rard and coworkers (20-22, 25), who have recently pub-

lished evaluations of activity and osmotic coefficients for $CaCl_2$, H_2SO_4, and many of the rare earth salts.

The various experimental techniques that serve as a source of data and the results of correlations of thermodynamic properties for a number of aqueous polyvalent electrolytes are discussed in the succeeding paper by R. N. Goldberg.

REFERENCES

1. Cohen, E. R., and B. N. Taylor. J. Phys. Chem. Ref. Data, v. 2, 1973, p. 663.

2. Debye, P., and L. Hückel. Physik. Z., v. 24, 1923, p. 185.

3. Friedman, H. L. Ionic Solution Theory. Interscience Publishers, New York, 1962.

4. Goldberg, R. N. Evaluation Activity and Osmotic Coefficients for Aqueous Solutions: Bi-univalent Compounds of Lead, Copper, Manganese, and Uranium. J. Phys. Chem. Ref. Data.

5. Goldberg, R. N., and R. L. Nuttall. Evaluated Activity and Osmotic Coefficients for Aqueous Solutions: the Alkaline Earth Metal Halides. J. Phys. Chem. Ref. Data, v. 7, 1978, p. 263.

6. Goldberg, R. N., R. L. Nuttall, and B. R. Staples. Evaluated Activity and Osmotic Coefficients for Aqueous Solutions of Iron Chloride and the Bi-univalent Compounds of Nickel and Cobalt. J. Phys. Chem. Ref. Data.

7. Goldberg, R. N., B. R. Staples, R. L. Nuttall, and R. A. Arbuckle. A Bibliography of Sources of Experimental Data Leading to Activity or Osmotic Coefficients for Polyvalent Electrolytes in Aqueous Solution. NBS Spec. Pub. 485, 1977.

8. Hamer, W. J., and Y. C. Wu. J. Phys. Chem. Ref. Data, v. 1, 1972, p. 1047.

9. Harned, H. S., and B. B. Owen. The Physical Chemistry of Electrolytic Solutions. Reinhold Pub. Corp., New York, 3d ed., 1958.

10. Lietzke, M. H., and R. W. Stoughton. J. Phys. Chem., v. 66, 1962, p. 508.

11. Mayer, J. E. J. Chem. Phys., v. 18, 1950, p. 1426.

12. Morel, F., and J. J. Morgan. Envir. Sci. Technol., v. 6, 1972, p. 58.

13. Pitzer, K. S. J. Chem. Soc., Faraday Trans. II, v. 68, 1972, p. 101.

14. ____. J. Phys. Chem., v. 77, 1973, p. 268.

15. ____. J. Sol. Chem., v. 4, 1975, p. 249.

16. Pitzer, K. S., and J. J. Kim. J. Am. Chem. Soc., v. 96, 1974, p. 5701.

17. Pitzer, K. S., and G. Mayorga. J. Phys. Chem., v. 77, 1973, p. 2300.

18. ____. J. Sol. Chem., v. 3, 1974, p. 539.

19. Pitzer, K. S., and L. F. Silvester. J. Sol. Chem., v. 5, 1976, p. 269.

20. Rard, J. A., A. Habenschuss, and F. H. Spedding. J. Chem. Eng. Data, v. 22, 1977, p. 180.

21. ____. J. Chem. Eng. Data, v. 21, 1976, p. 374.

22. Rard, J. A., H. O. Weber, and F. H. Spedding. J. Chem. Eng. Data, v. 22, 1977, p. 187.

23. Robinson, R. A., and R. H. Stokes. Electrolyte Solutions. Butterworth and Co., London, 2d (rev.) ed., 1970.

24. Smith-Magowan, D., and R. N. Goldberg. A Bibliography of Experimental Data Leading to Thermal Properties of Binary Aqueous Electrolyte Solutions. NBS Spec. Pub. 537, 1979.

25. Spedding, F. H., H. O. Weber, V. W. Saeger, H. H. Petheram, J. A. Rard, and A. Habenschuss. J. Chem. Eng. Data, v. 21, 1976, p. 341.

26. Staples, B. R. Envir. Sci. and Technol., v. 12, 1978, p. 339.

27. ____. Activity and Osmotic Coefficients of Aqueous Alkali Metal Nitrites. J. Phys. Chem. Ref. Data (in press).

28. ____. Activity and Osmotic Coefficients of Aqueous Sulfuric Acid. J. Phys. Chem. Ref. Data (in press).

29. Staples, B. R., and R. L. Nuttall. The Activity and Osmotic Coefficients of Aqueous Calcium Chloride at 298.15 K. J. Phys. Chem. Ref. Data, v. 6, 1977, p. 385.

30. ____. Computer Programs for the Evaluation of Activity and Osmotic Coefficients. NBS Tech. Note 928, 1976.

31. Wu, Y. C., and W. J. Hamer. Osmotic Coefficients and Mean Activity Coefficients of a Series of Uni-Bivalent and Bi-Univalent Electrolytes in Aqueous Solutions at 25° C. NBS IR 10052, pt. 14, 1969, p. 83.

32. Zemaites, J. Equilibrium Compositions. Ind. Res., November 1975.

EVALUATION OF ACTIVITY AND OSMOTIC COEFFICIENTS FOR ELECTROLYTE SOLUTIONS: APPLICATIONS TO REAL SYSTEMS

by

Robert N. Goldberg[1]

ABSTRACT

Some of the philosophy that has guided the evaluation efforts in which the author has recently been engaged is presented. Consideration is given to the accuracy and the state of the art with which activity and osmotic coefficients for aqueous electrolyte solutions can be calculated using the following methods of measurement: vapor pressure measurements, direct and relative (isopiestic); electromotive force measurements with and without transference; freezing point depression measurements; vapor pressure osmometry measurements; diffusion measurements; solvent extraction measurements; and ultracentrifuge measurements. The role of the choice of the correlating equation(s) and the difficult problem of the proper merging of the experimental data with the Debye-Hückel limiting law are discussed.

INTRODUCTION

This workshop offers an excellent opportunity for the author to present some of the philosophy and opinions that have guided his recent work on the evaluation of activity (γ) and osmotic coefficients (ϕ) of aqueous electrolytes. The research in which I have recently been engaged (4-9)[2] is an extension and continuation of the earlier work of Wu and Hamer (13, 37-38) and has been performed both in collaboration with and parallel to the research of Staples and Nuttall (30-33) at the Electrolyte Data Center of the National Bureau of Standards. I would first like to state my belief that data evaluation is best undertaken on a systematic basis. From the logistical point of view, it takes considerable amounts of time to build up the necessary tools to be able to perform a competent evaluation of a given property of a given material. There is a large investment required (1) to establish the data base

[1]Electrolyte Data Center, National Bureau of Standards, National Measurement Laboratory, Washington, D.C.

[2]Underlined numbers in parentheses refer to items in the list of references at the end of this paper.

of literature references, (2) to devise the computational procedures and to write the necessary computer codes, and (3) to obtain a "feel" for the data and for the theory that (hopefully) ties the data together. Having made this investment, it is desirable to make the most progress both in a practical and in a scientific sense by systematically evaluating a large body of related data. This type of effort requires a commitment of time and facilities for a period of several years.

METHOD OF MEASUREMENT

The detailed procedures that we have used for the evaluation of the activity and osmotic coefficients have been described in detail elsewhere (8, 32-33). To summarize briefly, the values of the activity and osmotic coefficients that we calculate are largely based upon the following experimental methods: (1) vapor pressure measurements, direct and relative (isopiestic), (2) electromotive force (emf) measurements with and without transference, (3) freezing point depression measurements, and (4) vapor pressure osmometry. The emf measurements involving transference require accurately known values of the transference number as a function of the molality, while the freezing point depression measurements require a knowledge of the relative apparent molal enthalpy (Φ_L) and the apparent molal heat capacity (Φ_C). Miscellaneous methods which have also been utilized include diffusion measurements (14), solvent extraction measurements (17), and ultracentrifuge measurements (16, 29). Each of these methods has its utility, its place, and its own potential systematic errors. It is the tying together of the data and testing for consistency of these different methods of measurement that is both a crucial part of the methodology and an important product of the data evaluation process. Generally, one feels more confident in values of thermodynamic properties that have been obtained from different methods of measurement, and that are in agreement. We shall now consider the status of the various methods of measurement that have been used to obtain activity and osmotic coefficients.

Freezing Point Depression Measurements

This is a highly developed method of measurement which, in principle, is capable of high precision and accuracy. The reader is referred to the classic paper by Robertson and LaMer (27) for a discussion of the high degree of care that is required if systematic errors are to be minimized when using this method. These workers claimed an inaccuracy of about 10 μK in the temperature measurement and also described the proposed construction of an apparatus suitable for obtaining data good to 1 pct at 5×10^{-5} mole·kg^{-1}. If all inaccuracies are represented in the measured freezing point depression, this very high level of accuracy would correspond to an inaccuracy of about 3 μK in the measurement of the temperature depression. Although modern techniques permit the measurement of temperature differenes to a precision of a few μK, the author is not aware of any freezing point depression measurements on electrolyte solutions that have been performed to this degree of accuracy, and a more realistic estimate of error would be between 20 and 50 μK for very careful work. This propagates, using a representative inaccuracy of about 50 μK, to an uncertainty of about 1 pct in ϕ at 0.001 mole·kg^{-1} and 0.1 pct at 0.01 mole·kg^{-1} for a 1-2 or 2-1 type electrolyte. At higher molalities, the utili-

ty of the freezing point depression method for obtaining accurate values of the osmotic coefficient becomes very much dependent on the accuracy with which the auxiliary thermal data (Φ_L and Φ_C) are known.

Isopiestic Measurements

The development of this method is described in the many papers by Robinson and Stokes (28). The accuracy of this method is largely based upon the certainty with which the osmotic coefficient for the reference electrolyte is known (KCl, NaCl, $CaCl_2$, and H_2SO_4 are the traditional reference electrolytes). Current reviews (13, 23-24, 31, 33) of the status of these reference electrolytes indicates that $\emptyset$ is known for these systems to within a few parts per thousand. The isopiestic method is a reliable and general method for use from moderate molalities (0.1 mole$\cdot$kg^{-1}) to beyond saturation. It might be possible with extreme care in the weighings, equilibration, and thermostatting to extend the use of this method to molalities as low as 0.01 mole$\cdot$kg^{-1}. The practical lower limit to which the method may be utilized is probably determined by the extremely long time period required to reach equilibrium under such conditions and the care with which dissolved gases are removed from the solutions.

Direct Vapor Pressure Measurements

In assessing the inaccuracies inherent in the use of data obtained from direct vapor pressure measurements, we refer to the results of Bechtold and Newton (1) on aqueous $BaCl_2$ and our treatment (7) of their data. At a molality of 1.6001 mole$\cdot$kg^{-1} an error in the pressure measurement of 0.001 torr will cause an error of only 0.06 pct in $\emptyset$, while at a molality of 0.01017 mole$\cdot$kg^{-1} a similar error will cause an error in $\emptyset$ of 16 pct. Accordingly, and again depending upon our subjective judgement of the care with which the measurements have been performed, we have tended to give lower weight to vapor pressure measurements performed at molalities less than a few tenths mole$\cdot$kg^{-1}.

Electromotive Force Measurements

Electromotive force measurements can be performed with a very high degree of precision. In the analysis of data from such measurements, we view inaccuracies as generally not being associated with the precision of the emf measurements, but rather with the degree of certainty with which the chemical processes are known - specifically, the absence of side reactions and the attainment of a truly reversible electrode. Because of these possible systematic errors, which usually have not been investigated, we have generally tended to prefer the results of careful isopiestic measurements over emf measurements or, when there exist only emf measurements at low molalities, to examine closely just how well the emf measurements merge with the isopiestic measurements.

Vapor Pressure Osmometry

The basis of this method has been discussed in a recent review (8). The author's present views of this method are (1) in principle, the method should be valid at moderate molalities (a few hundredths to a few mole$\cdot kg^{-1}$ (2) the real accuracy and precision of this method have not yet been properly demonstrated and/or documented, and (3) data have been obtained for many systems using this method alone; in such situations, we have relied to date in our evaluations solely upon data from that one source. A detailed study of the utility of this method would be of real value.

Activity Coefficients from Diffusion Measurements

Harned (14) has described the basis of this method. From our point of view, the method has two important features: (1) Using the conductance method, the measurements can be performed at very low molalities (data exist at 0.0001 mole$\cdot kg^{-1}$), and (2) from a strictly phenomenological view point, it is not a rigorous method of measurement (18). Yet, because of the small magnitude and cancellation of higher order electrophoretic effects (28) and also since the method yields values of the activity coefficient that are in reasonable agreement with values obtained by other methods, we have used activity coefficients calculated by this method. It is interesting to note that since the cessation of these measurements in Harned's laboratory in the 1950's, few diffusion measurement that extend to such low molalities have been reported in the literature.

Solvent Extraction Measurements

To date, we have encountered only one set of data (17) obtained by this method. The data pertain to $UO_2(NO_3)_2$. When subjected to analysis, the data obtained by this method were found to be in reasonable accord (agreement to within a few percent in γ) with values of the osmotic coefficient obtained from careful isopiestic measurements.

Ultracentrifuge Measurements

This method has not been very widely used, and the reader is referred to the paper by Johnson, Krauss, and Young (16), and to the book by Robinson and Stokes (28) for a discussion of its basis. We have examined its application to only one system, $BaCl_2$ (7), and have found the results of measurements by this method to be in good agreement with results obtained from emf, direct vapor pressure, and isopiestic measurements.

MODEL DEPENDENCY OF ACTIVITY COEFFICIENTS

Choice of Correlating Equation

The calculational procedure requires the selection of a correlating equation. The three equations used to date for the activity coefficient are:

$$\ell n\ \gamma = -\frac{A_1 I^{1/2}}{1+BI^{1/2}} + Cm + Dm^2 + Em^3\ \ldots, \tag{1a}$$

$$\ell n\ \gamma = -A_1 I^{1/2} - A_2 I\ \ell nI + \sum_{i=1}^{N} B_i m^{(i+1)/2}, \tag{2a}$$

and

$$\ell n\ \gamma = -A_1 I^{1/2} + \sum_{i=1}^{N} B_i m^{(i+1)/2}. \tag{3a}$$

For the osmotic coefficient, the corresponding equations are:

$$\phi = 1 + \frac{A_1}{B^3 I}\{-(1 + BI^{1/2}) + 2\ \ell n(1 + BI^{1/2}) + 1/(1 + BI^{1/2})\} + 1/2\ Cm$$

$$+ 2/3\ Dm^2 + 3/4\ Em^3 + \ldots, \tag{1b}$$

$$\phi = 1 - \frac{A_1}{3} I^{1/2} - \frac{A_2}{2} I\ [\ell nI + 1/2] + \sum_{i=1}^{N} B_i \frac{(i+1)}{(i+3)} m^{(i+1)/2} \tag{2b}$$

and

$$\phi = 1 - \frac{A_1}{3} I^{1/2} + \sum_{i=1}^{N} B_i \frac{(i+1)}{(i+3)} m^{(i+1)/2} \tag{3b}$$

The essential thermodynamic parameter that is treated is the excess Gibbs energy (ΔG^{ex}) in $J \cdot kg^{-1}$, given by the relationship

$$\Delta G^{ex} = G_{real} - G_{ideal} = \nu mRT(1 - \phi + \ell n\gamma). \tag{4}$$

In the above equations, I is the ionic strength, m is the molality, R is the gas constant, T is the absolute temperature, and ν is the number of ions formed form one molecule of solute ($M_{\nu+}X_{\nu-}$) assuming complete dissociation.

A_1 is equal to $A\left|z+z-\right|$, A_2 is equal to $\frac{\Sigma\nu_i z_i^3)^2}{3\nu\Sigma(\nu_i z_i^2)} A^2$, A is the Debye-Hückel constant equal to 0.51084 $\log_e 10\ kg^{1/2} \cdot mole^{-1/2}$ at 25°, and z+ and z- are the charges of the cation and anion, respectively. Equations 1 have a long historical background (10-11,13), and in using them we have allowed the value of the B coefficient to be determined empirically via the fitting procedure. Equations 2 include an additional term that is theoretically predicted (3). Equations 3 use a Debye-Huckel first term with a zero B coefficient followed by a polynomial in $m^{1/2}$. This latter equation has a particular utility whenever the value of the B coefficient obtained in equations 1 becomes too negative, thus causing the osmotic coefficient to become an imaginary number.

It is important to realize that the values of the activity coefficient that one calculates will depend upon the correlating equation(s) or model that one selects and that one finds numerical differences between activity and osmotic coefficents calculated using different methods. Typically, over most of the molality range, we have found these differences to be less than 1 pct in γ and less than 0.010 pct in ϕ. One must expect the largest discrepancies at the highest molalities for which data exist. These differences can range as high as several percent. We have also examined the numerical differences between the values of γ that we have calculated and the values of γ that can be calculated from the coefficients given by Pitzer and Mayorga (20); in general, we have found the agreement to be quite good; i.e., differences of less than a few percent are typical.

I take note of a problem for which I presently have no solution. In this research we have attempted a detailed recalculation, evaluation, and representation of the experimental data by means of empirical virial equations to the highest molalities for which data exist. This has, for several systems, necessitated the use of a large number of empirical parameters (as many as 12). Because of the numerical coupling effects implicit in the fitting process, it is very difficult to ascribe physical significance to any individual virial coefficient. Pitzer and Mayorga (20) have ascribed physical significance to the three virial coefficients ($\beta^{(0)}$, $\beta^{(1)}$, and C^{ϕ}) they tabulate, but for many of the systems they investigated, this has precluded doing fits to the maximun molalities for which data exist.

MERGER OF THE EXPERIMENTAL DATA WITH THE DEBYE-HUCKEL LIMITING LAW

If accurate experimental measurements (ϕ and/or γ/γ_{ref} data) extending to very low molalities existed, the data evaluation procedure would be on a much surer footing than it presently is. In such a case, it would be possible to ascertain clearly the nature of the merger of the experimental curve with the Debye-Huckel limiting law and to perform rigorous calculations of the activity coefficients and the excess Gibbs energies at various molalities. Note that the absolute values of the experimentally determined osmotic coefficients stand independently of this issue. In the general absence of such data, we and others have frequently assumed a smooth merger of the experimental data with the Debeye-Huckel limiting law. This approach does not seem to be unreasonable provided that there is no complex chemical behavior in the solution such as ion association or hydrolysis, or if there is, that such behavior is not too extensive.

Some History

When such complicating chemical behavior does occur, it is very much a moot point as to just how such systems should be treated. Much of the past effort has focused on systems that undergo extensive ion pairing, such as the electrolytes of charge type 2-2, hydrofluoric acid, the cadmium halides, and sulfuric acid. Harned and Owen (15) simply estimated γ equal to 0.15 at a molality of 0.1 mole$\cdot$kg^{-1} for the 2-2 electrolytes and used this value as the basis for the assignment of activity coefficients. Brown and Prue (2) introduced an association model in treating six electrolytes of charge type 2-2.

Pitzer (19) refined and generalized upon the equilibrium model of Brown and Prue (2) and also introduced a triplet ion of the type $(M^+)(X^{2-})_2$ when treating the 2-2 electrolytes. Subsequently, Pitzer and Mayorga (21) discarded the explicit treatment of ion association and used a correlating equation which aids in the merger with the Debye-Hückel limiting slope - although it is still possible to demonstrate a relationship between the virial coefficients and an association constant. Hamer and Wu (12) treated the activity coefficients of HF by utilizing an equilibrium model and conductivity data and estimating the fractions of the various ionic species, H^+, F^-, HF°, and HF_2^-, present in solution. A very intricate, self-consistent equilibrium-type calculation was employed by Reilly and Stokes (26) in treating the data for $CdCl_2$. Pitzer, Roy, and Silvester (22) were able to extract a dissociation constant for sulfuric acid from their treatment of the activity and osmotic coefficient data for that system; and recently Wood, Lilley and Thompson (35) treated the $ZnSO_4$ electrochemical cell data of Rassiah (25) by utilizing a novel activity expansion approach, which, while it introduces a new kind of equation of state, still contains in it an equivalence to an ion-association model.

The Approach of Wu and Young

One very interesting approach, applied by Wu and Young (36, 39) to the analysis of the enthalpies of dilution of sulfuric acid, used Raman spectral data to obtain the fractions of the ions HSO_4^- and SO_4^{2-} in solution, and then estimated the relative apparent molal enthalpy for H_2SO_4 as follows:

$$\Phi_{L(H_2SO_4)} = \alpha\, \Phi_{L(1\text{-}1)} + (1-\alpha)\, \Phi_{L(1\text{-}1)} + \Delta_m H + \alpha\Delta H^\circ. \qquad (5)$$

In the above equation, α is the fraction of HSO_4^-, $\Phi_{L(1\text{-}1)}$ and $\Phi_{L(1\text{-}2)}$ are, respectively, the relative apparent molal enthalpies of relatively unassociated 1-1 and 1-2 electrolytes, $\Delta_m H$ is an enthalpy-of-mixing term, and ΔH° is the standard state enthalpy change for the process

$$H^+(aq) + SO_4^{2-}(aq) = HSO_4^-(aq). \qquad (5a)$$

Wu and Young (36, 39) took $\Delta_m H$ to be zero (40) and used Φ_L for HCl and LiCl for $\Phi_{L(1\text{-}1)}$, and Φ_L for Li_2SO_4 for $\Phi_{L(1\text{-}2)}$. ΔH° was obtained from calorimetric measurements (15). It should be noted that the single largest contribution to $\Phi_{L(H_2SO_4)}$ comes from the term $\alpha\Delta H^\circ$. Also, while $\Phi_{L(H_2SO_4)}$ must be considered an estimated quantity, the experimental data do not exist for the very low molalities at which Φ_L is being estimated. However, Wu and Young (36, 39) were able, using a "chord-area-type" plot, to compare estimated values of $(\overline{\Delta\Phi}_L/\Delta m^{1/2})$ with experimental data and found good agreement in the region $m^{1/2} = 0.03$ to 0.3 $mole^{1/2}\cdot kg^{-1/2}$.

Extension of the Approach of Wu and Young (36, 39) to the Excess Gibbs Energy

Applying similar reasoning to Gibbs energy data, one can obtain, for H_2SO_4, the equation

$$\Delta G^{ex} = \alpha\ \Delta G^{ex}_{1-1} + (1-\alpha)\ \Delta G^{ex}_{1-2} + \Delta_m G + \alpha m \Delta G^\circ, \qquad (6)$$

where ΔG^{ex} is the excess Gibbs energy in $J \cdot kg^{-1}$, α has the same meaning as above, $\Delta_m G$ is a Gibbs energy of mixing term which should largely be accounted for by an entropic term, $-T\Delta_m S$, and ΔG° is the standard Gibbs energy change for process 5 in $J \cdot mole^{-1}$. ΔG^{ex}_{1-1} and ΔG^{ex}_{1-2} are the excess Gibbs energies for relatively unassociated electrolytes of charge type 1-1 and 1-2, respectively. If one were dealing with a system more complex than sulfuric acid, involving multiple complex ion formation and/or hydrolysis, a generalized form of equation 6 would be

$$\Delta G^{ex} = \sum_i f_i \Delta G^{ex}_i + \Delta_m G + m \sum_i f_i \Delta G^\circ_i, \qquad (7)$$

Where the f_i's represent the fractions of the various ionic species, ΔG^{ex}_i and ΔG°_i are, respectively, the appropriate excess Gibbs energies and standard state Gibbs energy changes in $J \cdot mole^{-1}$, and m is the molality of the solution.

The application of equation 7 to real systems requires (1) an estimate of the ΔG^{ex}_i terms and the $\Delta_m G$ terms, (2) knowledge of the f_i's, and (3) knowledge of the ΔG°_i terms. Let us assume that (1) can be done reasonably accurately. Then, if the ΔG°_i's are known, but the f_i's are not, it becomes necessary to calculate values for the f_i terms by applying chemical equilibrium principles. (Note that, in general, it will be necessary to assume single-ion activity coefficients.) If the ΔG°_i's are <u>not</u> known, then one must either estimate the ΔG°_i's or perform a calculation where the ΔG°_i terms are guessed at and used to calculate the f_i's which, together with the estimated ΔG^{ex}_i and $\Delta_m G$ terms are used to calculate values of ΔG^{ex} for the solution using equation 7. Values for ϕ and (γ/γ_{ref}) may then be calculated from the estimated values of ΔG^{ex} and compared with the experimental values in a self-consistent and iterative-type calculation where the sums of the weighted squares of the differences between the experimental and calculated values are minimized.

It has been the purpose of this section of the paper to review some of the earlier approaches to a very difficult problem and to suggest a possible approach to it which builds upon the work of Wu and Young (<u>36</u>, <u>39</u>), Reilly and Stokes (<u>26</u>), Wood, Lilley, and Thompson (<u>35</u>), and others. It is a problem that, for many systems, is logically incapable of resolution in the absence of experimental data; i.e., osmotic coefficients (ϕ) and ratios of activity coefficients (γ/γ_{ref}) at much lower molalities than are presently accessible by current measurement techniques.

ACKNOWLEDGMENTS

This research was supported by the Division of Energy Storage Systems of the Department of Energy and by the Office of Standard Reference Data of the National Bureau of Standards.

REFERENCES

1. Bechtold, M. F., and R. F. Newton. J. Am. Chem. Soc., v. 62, 1940, p. 1390.

2. Brown, D. G. M., and J. E. Prue. Proc. Roy. Soc. London, Ser.A, v. 232, 1955, p. 320.

3. Friedman, H. L. Ionic Solution Theory. Interscience Publishers, New York, 1962.

4. Goldberg, R. N. Evaluated Activity and Osmotic Coefficients for Aqueous Electrolyte Solutions: Thirty-five Uni-bivalent Systems. J. Phys. Chem. Ref. Data (in press).

5. ____. Evaluated Activity and Osmotic Coefficients for Aqueous Solutions: Bi-univalent Compounds of Lead, Copper, Manganese, and Uranium. J. Phys. Chem. Ref. Data, v. 8, 1979, p. 1005.

6. ____. Evaluated Activity and Osmotic Coefficients for Aqueous Solutions: Bi-univalent Compounds of Zinc and Cadmium, and Ethylene Bis(trimethylammonium) Chloride and Iodide. J. Phys. Chem. Ref. Data, v. 10, 1981, p. 1.

7. Goldberg, R. N. and R. L. Nuttall. J. Phys. Chem. Ref. Data, v. 7, 1978, p. 263.

8. Goldberg, R. N., R. L. Nuttall, B. R. Staples. Evaluated Activity and Osmotic Coefficients for Aqueous Solutions: Iron Chloride and the Bi-univalent Compounds of Nickel, and Cobalt. J. Phys. Chem. Ref. Data, v. 8, 1979, p. 923.

9. Goldberg, R. N., B. R. Staples, R. L. Nuttall, and R. Arbuckle. A Bibliography of Sources of Experimental Data Leading to Activity or Osmotic Coefficients for Polyvalent Electrolytes in Aqueous Solution, NBS Spec. Pub. 485, 1977.

10. Guggenheim, E. A., Phil. Mag., v. 19, 1935, p. 588.

11. Guggenheim, E. A., and J. C. Turgeon. Trans. Faraday Soc., v. 51, 1955, p. 747.

12. Hamer, W. J., and Y. C. Wu. J. Res NBS Sec. A, v, 74, 1970, p. 761.

13. ____. J. Phys. Chem. Ref. Data, v. 1, 1972, p. 1047.

14. Harned, H. S. Diffusion and Activity Coefficients of Electrolytes in Aqueous Solutions. Ch. in The Structure of Electrolytic Solutions, ed. by W.J. Hamer. John Wiley and Sons, Inc., New York, 1959.

15. Harned, H. S. and B. B. Owen. The Physical Chemistry of Electrolyte Solutions. Reinhold Pub. Corp., New York, 3d ed., 1958.

16. Johnson, J. S., K. A. Krauss, and T. F. Young. J. Am. Chem. Soc., v. 76, 1954, p. 1436.

17. Mikhailov, V. A. and V. G. Torgov. Russ. J. Phys. Chem. (English Trans.) v. 38, 1964, p. 151.

18. Miller, D. G. J. Phys. Chem., v. 70, 1966, p. 2639.

19. Pitzer, K. S. J. Chem. Soc., Farady Trans. II, v. 68, 1972, p. 101.

20. Pitzer, K. S., and G. Mayorga. J. Phys. Chem., v. 77, 1973, p. 2300.

21. ____. J. Sol. Chem., v. 3, 1974, p. 539.

22. Pitzer, K. S., R. N. Roy, and L. F. Silvester. J. Am Chem. Soc., v. 99, 1977, p. 4930.

23. Rard, J. A., A. Habenschuss, and F. H. Spedding. J. Chem. Eng. Data, v. 21, 1976, p.374.

24. ____. J. Chem. Eng. Data, v. 22, 1977, p. 180.

25. Rassiah, J. The Activity and Osmotic Coefficients of Zinc Sulfate in Water and Heavy Water at 25° C. Thesis, Univ. of Pittsburgh, 1965.

26. Reilly, P. J., and R. H. Stokes. Aust. J. Chem., v. 23, 1970, p. 1397.

27. Robertson, C., and V. K. LaMer. J. Phys. Chem., v. 35. 1931, p. 1953.

28. Robinson, R. A., and R. H. Stokes. Electrolyte Solutions, Butterworth and Co., London, 3d ed., 1970.

29. Rush, R. M., and J. S., Johnson. J. Phys. Chem., v. 68, 1964, p. 2321.

30. Staples, B. R., Activity and Osmotic Coefficients of Aqueous Metal Nitrites. J. Phys. Chem. Ref. Data (in press).

31. ____. Activity and Osmotic Coefficients of Aqueous Sulfuric Acid. J. Phys. Chem. Ref. Data (in press).

32. Staples, B. R., and R. L. Nuttall. Computer Programs for the Evaluation of Activity and Osmotic Coefficients, NBS Tech Note 928, 1976.

33. ____. J. Phys. Chem. Ref. Data, v. 6, 1977, p. 385.

34. Stokes, R. H. Trans. Faraday Soc., v. 44, 1948, p. 295, and the papers cited therein.

35. Wood, R. H., T. H. Lilley, and P. T. Thompson. J. Chem. Soc., Faraday Trans. I, v. 74, 1978, p. 1301.

36. Wu, Y. C. Thesis, University of Chicago, 1957.

37. Wu, Y. C., and W. J. Hamer. Electrochemical Data - Part XIV. NBS Rept. 10052, July 2, 1969.

38. ____. Electrochemical Data - Part XVI. NBS Rept. 10008, Nov. 6, 1969.

39. Wu, Y. C., and T. F. Young. Enthalpies of Dilution of Aqueous Electrolytes: Sulfuric Acid, Hydrochloric Acid, and Lithium Chloride, J. Res. NBS, v. 85, 1980, p. 11.

40. Wu, Y. C., T. F. Young, and A. A. Krawetz. Disc. Faraday Soc., No. 24, 1957, p. 37.

DISCUSSION

C. M. Criss: How do you handle electrolyte solutions of the type which Loren Hepler calls "almost strong" electrolytes? Some electrolytes are not quite strong in nonaqueous solutions. We need an equation which will work over the entire range, and the form of equation is important for extrapolating data to infinite dilution. Normally, one type of equation is used for strong electrolytes and another for weak electrolytes, but if a system is studied which gradually shifts from a strong to a weak electrolyte, then there is a discontinuity in the extrapolated results when one shifts from one equation to the other.

R. N. Goldberg: One possibility would be to utilize the approach of Wood, Lilley, and Thompson (J. Chem. Soc. Faraday Trans. I, v. 74, 1978, p. 1301) in that it appears to avoid all arbitrary distinctions between weak and strong electrolytes. Another approach would be to use the extension of the method of Wu and Yound (see my symposium paper) where the association constants become an explicit part of the excess Gibbs energy function. It is important to realize that there is no definitive answer to the problem of how to ascertain the correctness of the absolute values of the excess Gibbs energy and enthalpy in the absence of experimental data at very low molalities and that in the absence of such data, it will probably be necessary to resort to estimation schemes and self-consistent type calculations in order to obtain approximate answers. In any case, it is important to preserve the experimental data, whatever evaluation scheme is utilized.

Anonymous: Can I give you one more thought? I notice a lot of people spend more time fussing about how to treat their data than generating them, and maybe I shouldn't knock data evaluation, or data treatment, but I am willing to bet that 50 years from now, people will come back and think of a different way of treating the data than we do right now. What really counts are the good experimental numbers. In other words, one thing we cannot do as data evaluators is to turn a bad experiment into a good one. I imagine we could do the reverse if we mess up on a calculation.

Pamela Rogers: I would like to make a comment on the use of the b parameter in the limiting law term

$$\ln = \frac{AI^{0.5}}{a + bI^{0.5}} + C_1 m + C_2 m^{1.5} + C_3 m^2 . . . . .,$$

where "b" is a constant value and absorb the temperature effect in the remaining fitting constants C_1, C_2, C_3, etc. The reason becomes apparent when you start taking temperature derivatives of this equation to obtain expressions for the enthalpy and heat capacity. Having a "b" term that varies with temperature complicates these derivatives.

SURVEY OF BUREAU OF MINES CRITICAL COMPILATIONS

by

A. D. Mah[1]

The U.S. Department of the Interior, Bureau of Mines, critical compilation history began in Berkeley, Calif., in 1932, when K. K. Kelley published the first volume of a long series of publications under the title "Contributions to the Data on Theoretical Metallurgy." His first work, subtitled "The Entropies of Inorganic Substances" (1)[2] was followed the next year by a second volume, "High-Temperature Specific Heat Equations for Inorganic Substances" (2), three more additions to the theoretical metallurgy series were published in the following 3 years, as follows: "The Free Energies of Vaporization and Vapor Pressures of Inorganic Substances" (3), "Metal Carbonates--Correlations and Application of Thermodynamic Properties" (4), and "Heats of Fusion of Inorganic Substances" (5).

By 1936, sufficient data had accumulated in the literature for Kelley to prepare a second edition of the first volume of "Contributions to the Data on Theoretical Metallurgy" subtitled "A Revision of the Entropies of Inorganic Substances" (6), and two more additions to the series appeared in 1937, "The Thermodynamic Properties of Sulfur and Its Inorganic Compounds" (7) and "The Thermodynamic Properties of Metal Carbides and Nitrides" (8).

As the years went by, Kelley's compilation work was interrupted, first by experimental low-temperature heat-capacity investigations and then by supervisory duties as chief of the Bureau of Mines thermodynamics group in Berkeley. In spite of added responsibilities, he continued his compilation interests, and in 1941 published a third edition of the popular entropy bulletin, calling it "The Entropies of Inorganic Substances. Revision (1940) of Data and Methods of Calculation" (9).

In 1949 to 1950, after several shorter compilations, Kelley published two

[1]Research Chemist, Albany Research Center, Bureau of Mines, Albany, Oreg.
[2]Underlined numbers in parentheses refer to items in the list of references at the end of this paper.

more volumes of the theoretical metallurgy series. "High-Temperature Heat-Content, Heat-Capacity and Entropy Data for Inorganic Compounds" (10) was the first revision of the 1933 high-temperature bulletin, and "Entropies of Inorganic Substances. Revision (1948) of Data and Methods of Calculations" (11) was the fourth edition of the widely circulated entropy bulletin.

As the volume of literature data expanded at an increasing rate, Kelley recognized the need for skilled evaluators and trained J. P. Couglin, A. D. Mah, and E. G. King in the critical evaluation and compilation of thermodynamic properties. In 1954, J. P. Coughlin published the 12th volume of the "Contributions to the Data on Theoretical Metallurgy" series, "Heats and Free Energies of Formation of Inorganic Oxides" (12).

Kelley continued with compilation work and in 1955 wrote a chapter titled "Thermodynamic Properties of Zirconium Compounds" for the book "Metallurgy of Zirconium" (17). In 1959, Kelley published with A. D. Mah "Metallurgical Thermochemistry of Titanium" (19).

Three compilations came out in 1960. The foremost was Kelley's third and final revision of the high-temperature work, Bureau of Mines Bulletin 584, "Contributions to the Data on Theoretical Metallurgy. XIII. High-Temperature Heat-Content, Heat-Capacity, and Entropy Data for the Elements and Inorganic Compounds" (13). This valuable work is still in use. Following the high-temperature bulletin came a chapter, "Thermodynamics of Hafnium and Its Compounds," written by Kelley and E. G. King for the Naval Reactor Handbook, "The Metallurgy of Hafnium" (18). This was followed by publication of "Thermodynamic Properties of Manganese and Its Compounds," by A. D. Mah (21).

In 1961, Kelley and King published the fifth and final revision of the popular entropy compilation, Bureau of Mines Bulletin 592, "Contributions to the Data on Theoretical Metallurgy. XIV. Entropies of the Elements and Inorganic Compounds" (14). Like Bulletin 584, this work is still in use. In 1962, in response to demand, four of Kelley's older bulletins were republished as Bureau of Mines Bulletin 601, "Contributions to the Data on Theoretical Metallurgy. XV. A Reprint of Bulletins 383, 384, 394, and 404" (15).

After Kelley's retirement, A. D. Mah; continued intermittently the critical compilation work and in 1966 published "Thermodynamic Properties of Vanadium and Its Compounds" (22). After the Berkeley Thermodynamics Laboratory moved to its present location in Albany, Oreg., E. G. King's computerization of compilation methodology provided techniques that have been useful up to the present time. Recently, N. A. Gokcen proposed further modernization of the compilation effort, using up-to-date data processing methods. An inhouse minicomputer system designed by J. M. Stuve for this purpose was successfully implemented, with adaptation of software by R. P. Beyer.

In 1973, by cooperative agreement with the International Copper Research Association, King, Mah, and Pankratz published a monograph "Thermodynamic Properties of Copper and Its Inorganic Compounds" (20), and in 1976 Mah and Pankratz published "Contributions to the Data on Theoretical Metallurgy. XVI.

Thermodynamic Properties of Nickel and Its Inorganic Compounds" (16).

The earlier compilations were made a part of the National Standard Reference Data System library collection when NSRDS was established. The last two volumes were reviewed by the Office of Standard Reference Data of the National Bureau of Standards at the time of publication and incorporated into the National Standard Reference Data System.

REFERENCES

Part I (Sequential)

Contributions to the Data on Theoretical Metallurgy series

1. Kelley, K. K. Contributions to the Data on Theoretical Metallurgy. I. The Entropies of Inorganic Substances, BuMines. Bull. 350, 1932, 63 pp.

2. _____. Contributions to the Data on Theoretical Metallurgy. II. High-Temperature Specific Heat Equations for Inorganic Substances. BuMines Bull. 371, 1933, 78 pp.

3. _____. Contributions to the Data on Theoretical Metallurgy. III. The Free Energies of Vaporization and Vapor Pressures of Inorganiz Substances. BuMines Bull. 383, 1935, 132 pp.

4. Kelley, K. K., and C. T. Anderson. Contributions to the Data on Theoretical Metallurgy. IV. Metal Carbonates--Correlations and Application of Thermodynamic Properties. BuMines Bull. 384, 1935, 73 pp.

5. Kelley, K. K. Contributions to the Data on Theoretical Metallurgy. V. Heats of Fusion of Inorganic Substances. BuMines Bull. 393, 1936, 166 pp.

6. _____. Contributions to the Data on Theoretical Metallurgy. VI. A Revision of the Entropies of Inorganic Substances. BuMines Bulle. 394, 1936, 55 pp.

7. _____. Contributions to the Data on Theoretical Metallurgy. VII. The Thermodynamic Properties of Sulfur and Its Inorganic Compounds. BuMines Bull. 406, 1937, 154 pp.

8. _____. Contributions to the Data on Theoretical Metallurgy. VIII. The Thermodynamic Properties of Metal Carbides and Nitrides. BuMines Bull. 407, 1937, 66 pp.

9. _____. Contributions to the Data on Theoretical Metallurgy. IX. The Entropies of Inorganic Substances. Revision (1940) of Data and Methods of Calculation. BuMines Bull. 434, 1941, 115 pp.

10. _____. Contributions to the Data on Theoretical Metallurgy. X. High-Temperature Heat-Content, Heat-Capacity, and Entropy Data for Inorganic Compounds. BuMines Bull. 476, 1949, 241 pp.

11. _____. Contributions to the Data on Theoretical Metallurgy. XI. Entropies of Inorganic Substances, Revision (1948) of Data and Methods of Calculation. BuMines Bull. 477, 1950, 147 pp.

12. Coughlin, J. P. Contributions to the Data on Theoretical Metallurgy. XII. Heats and Free Energies of Formation of Inorganic Oxides. BuMines Bull. 542, 1954, 80 pp.

13. Kelley, K. K. Contributions to the Data on Theoretical Metallurgy. XIII. High-Temperature Heat-Content, Heat-Capacity, and Entropy Data for the Elements and Inorganic Compounds. BuMines Bull. 584, 1960, 232 pp.

14. Kelley, K. K., and E. G. King. Contributions to the Data on Theoretical Metallurgy. XIV. Entropies of the Elements and Inorganic Compounds. BuMines Bull. 592, 1961, 149 pp.

15. Kelley, K. K. Contributions to the Data on Theoretical Metallurgy. XV. A Reprint of Bulletins 383, 384, 393, and 406. BuMines Bull. 601, 1962, 525 pp.

16. Mah, A. D., and L. B. Pankratz. Contributions to the Data on Theoretical Metallurgy. XVI. Thermodynamic Properties of Nickel and Its Inorganic Compounds. BuMines Bull. 668, 1976, 125 pp.

Part II

Other Series

17. Kelley, K. K. Thermodynamic Properties of Zirconium Compounds. Ch. 4 of Metallurgy of Zirconium, ed. by B. Lustman and F. Kerze, Jr. McGraw-Hill Book Co. New York, 1955, pp. 59-134.

18. Kelley, K. K., and E. G. King. Thermodynamics of Hafnium and Its Compounds. Ch. 9 of the Metallurgy of Hafnium, ed. by D. E. Thomas and E. T. Hayes. Naval Reactor Handbook, 1960 pp. 323-356.

19. Kelley, K. K., and A. D. Mah. Metallurgical Theremochemistry of Titanium. BuMines RI 5490, 1959, 48 pp.

20. King, E. G., A. D. Mah, and L. B. Pankratz. Thermodynamic Properties of Copper and Its Inorganic Compounds. INCRA Monograph Series II (sponsored by the International Copper Research Association and the U.S. Bureau of Mines), New York, 1973, 257 pp.

21. Mah, A. D. Thermodynamic Properties of Manganese and Its Compounds. BuMines RI 5600, 1960, 34 pp.

22. _____. Thermodynamic Properties of Vanadium and Its Compounds. BuMines RI 6727, 1966, 84 pp.

THERMODYNAMIC DATA EVALUATION

by

L. B. Pankratz[1]

One of the Bureau's current compilation projects is the revision of Bulletin 605, "Thermodynamic Properties of 65 Elements, Their Oxides, Halides, Carbides, and Nitrides," by Wicks and Block. The major effort of this revision is to completely reevaluate the high-temperature data for these substances. This reevaluation has been made easier by the continuing effort to maintain an up-to-date file of thermodynamic data from the literature. Related data such as vapor pressures, temperatures and enthalpies of transformation, decomposition studies, phase studies, and pertinent gas data are also collected. The major source of references is from a search of Chemical Abstracts. However, references in collected articles and bibliographies of compilations and review articles are also examined.

After collection, the first step of evaluation is to assess the method used to generate the data, that is, the calorimetric system. Though the following discussion centers on the copper-block drop calorimeter, it should illustrate the processes used. Particular points of the system examined are the temperature measurement of the sample, calibration techniques, the calorimeter itself, and the actual measurements.

The sample temperature-sensing device, usually a thermocouple, should be referred to some well-defined temperature scale by appropriate calibration. Also, the method of calibration must be able to show any changes if the thermocouple is used at higher temperatures; for example, above 1,500 K for platinum versus Pt-Rh couples. Needless to say, the equipment associated with the thermocouple should not degrade its accuracy. Regardless of the care taken to insure measurement accuracy, it is meaningless if the sensing device does not indicate the true temperature of the sample through poor positioning, or if part of the sample is hotter or colder than the indicated temperature because of an inadequate isothermal zone in the furnace.

Along with the calibration of the temperature-measuring device, an examination is made of the techniques used for other equipment, such as standard

[1] Research chemist, Albany Research Center, Bureau of Mines, Albany, Oreg.

cells, standard resistors, timers, and potentiometers.

The calorimeter and the actual measurements are studied from several points. First, is the method appropriate? For instance, drop calorimeters are not very precise below 400 or 500 K, nor are they suitable for cases where the sample does not return to the same well defined state upon cooling. Second, are the design and operation such that heat exchange between the calorimeter and its surroundings is well defined and accounted for? Obviously, any unknown or unaccounted heat leak will affect the accuracy of the measurements. Third, how was the calorimeter calibrated? This is usually done by direct electrical measurement and, if done often, will reflect any small, long-term changes. Comparison of measurements of standard substances, such as alpha alumina, with those of other workers can indicate the overall accuracy and precision of the system but should not be used as a calibration.

The second step of evaluation is to assess the sample and its treatment. Two particular areas are examined, characterization of the sample and possible reactions or changes occurring during measurements. Certainly, a careful analysis of the sample's chemical composition and stoichiometry should be made. Other data needed for a more complete characterization of the sample would be its crystal structure, the presence or absence of other phases, and the method of preparation. During measurements, some check should be made to determine if the sample is returning to the same state on cooling in the calorimeter. Also, during measurements, the possibilities of decomposition vaporization and reaction with the container or with impurities should be examined. Sometimes a complete reanalysis of the sample is necessary after completion of the measurements.

Some final points in assessing the data include corrections for the sample container, corrections for impurities, and other calculations.

Except for heat capacities, which are treated separately, all evaluated data are converted to enthalpies relative to 298 K and calories per mole for comparison. These data are plotted as the function $(H_T - H_{298})/(T - 298.15)$ versus temperature. This function is used because it emphasizes enthalpy differences; also, it is equal to the heat capacity at 298 K. All data for a single substance are plotted on the same graph with the enthalpy data derived from low-temperature data. Only a short range of low-temperature data, usually 50 degrees, is used, since the primary purpose is to achieve a reasonable merging of high- and low-temperature data.

The evaluation of the calorimetric systems and samples, the enthalpy function plot, and any other pertinent data, such as phase studies, transformation temperatures and enthalpies, and decomposition studies, are then used to select "best" values. These selected experimental values are fit with a polynomial expansion in terms of temperature, using a computer program. Several calculations with different parameters are usually needed before an acceptable fit is obtained. The program also calculates and tabulates, at even

temperatures and at transition points, heat capacities, entropies, Gibbs energy funtions, and relative enthalpies.

Two real problems may remain at this point. The first is that two apparently equally good studies disagree well outside their experimental errors. The resolution of this disagreement requires the complete reassessment of the evaluation and the examination of any other work not previously studied. This examination includes results for different substances by the authors under consideration, as well as those by other investigators. Estimation of unavailable data is the second problem. Though many methods of estimation have been published, none have seemed adequate. As a consequence, estimations are rarely made, and then only with some supporting evidence and consultation with others.

The collection and evaluation of data for the elements and oxides are essentially complete, and the results are in process for publication. The tabular data will include heat capacities, standard entropies, Gibbs energy functions, and enthalpies relative to 298 K. Tables for the oxides will also include heats and Gibbs energies of formation. Standard-form equations have been fit to the tabular relative enthalpies. These equations, along with those derived for heat capacities, heats of formation, and Gibbs energies, will also be given.

DISCUSSION

N. A. D. Parlee: What Bulletin were you revising?

L. B. Pankratz: It was Bulletin 605.

N. A. D. Parlee: This thing is tremendously important to us. This publication is very valuable because it could be purchased at our book store and then we could direct our students in materials science to buy it, if it were made available for purchase; they could use it in their classes. They go to the library and it is out. They bother the professor to borrow his copy, and pretty soon they are all lost. Some have been copied and sold. All I am pointing out is how tremendously valuable this material is. If the students did have something to use that was low priced, and have it available for them, it would be wonderful. I would like to request here that our Government try to provide our students with some type of modestly priced publication, keep it available, and not let it run out of print.

L. B. Pankratz: That is the intention of this publication. At the moment we do not propose to have all the elements and compounds in one volume. The first volume coming out will be the elements and oxides, and then the halides, carbides, and nitrides will follow in another volume. I sincerely doubt whether you will get it for a dollar anym number. I mean, the number is usually small, so if there are any sales at all, that is sold out early and normally they won't reprint it. Geological Survey Bulletin 1259 was that way. It was out of print for 5 years before the new version was printed. I would be willing to bet that the new version will be out of print. They just don't want to print it. It is the GPO, not the Bureau.

L. B. Pankratz: That's right. We've had many requests for Bulletin 605, and I have a copy which I lock up every night just so that I have a copy that I

can refer to. Otherwise, it might disappear. We intend to publish essentially the same type of data, with the equations, and as I said, heats and Gibbs energies of formation. It will be in a slightly different format, but it will all be there, and hopefully more.

N. A. Gokcen: Lou Pankratz has revised the oxides section of Bulletin 605 and it will be published probably within one year. Bulletin 605 was completed in 1961 and since then the available data for oxides yielded more tables than all the tables in Bulletin 605 for oxides, halides, carbides, and nitrides.

Y. A. Chang: Are you going to include phase diagrams? Thermodynamic data alone do not tell you the full story.

L. B. Pankratz: No, there will be no phase diagrams, but I agree with your remark. It comes down to how much one can do. It would be nice if I could include the phase diagrams if I had help, or more time; but I just don't, and that's what it amounts to. It is a matter of time.

Anonymous: Are there duplications in data evaluation and compilation?

L. B. Pankratz: There are efforts to eliminate duplication. Revision of Bulletin 605 was announced in the Bulletin of Thermodynamics.

M. W. Chase: I see Leo Brewer often enough, but I had no indication from the Bureau of Standards that they were working on molybdenum when I started. When I started molybdenum, I had done all the low temperature work before I saw the Bureau of Standards publication. When I was out to see Brewer and told him I was having trouble with molybdenum, then he told me that he had been working on it. Oftentimes it is just a case of everybody writing down what they are going to do for the next year, and exchanging it, but that is not happening. Normally, there is no overlap between myself and the Bureau of Standards. Recently, there was more overlap between JANAF and Brewer. I think we've ironed that out so as to eliminate duplication. For the work overseas, I know what they are doing now, so we won't overlap with them.

ANALYSIS OF {EQUILIBRIUM CONSTANT TEMPERATURE} DATA: NEW EQUATIONS FOR CALCULATION OF CHANGE IN PLANCK FUNCTION FROM ΔC_p°

by

Robert D. Freeman[1]

ABSTRACT

The general equation for analyzing (K, T) data by both second- and third-law methods is

$$\Gamma(T;T^h,T^s) \equiv \Delta Y^\circ(T;T^h,T^s) - R \ln K = T^{-1}\Delta H^\circ(T^h) - \Delta S^\circ(T^s).$$

Calculation of Γ from ΔC_p° data appears more complicated than calculation of the traditional Σ. For example, if the usual form $\Delta C_p^\circ = \Delta a + \Delta bT + \Delta cT^{-2}$ is substituted into the expression

$$\Delta Y^\circ(T;T_x,T_x) = \int_{T_x}^{T} (\Delta C_p^\circ/T)dT - T^{-1} \int_{T_x}^{T} \Delta C_p^\circ dT,$$

one obtains, on the right side

$$\Delta a[\ln(T/T_x) - (T - T_x)/T] + \Delta b[T - T_x - (T^2 - T_x^2)/2T]$$

$$+\Delta c[T^{-1}(T^{-1} - T_x^{-1}) - (T^{-2} - T_x^{-2})/2].$$

However, if one defines $\phi = (T - T_x)/T$, this result may, with no approximations, be put into the much simpler form

$$\Delta Y^\circ(T;T_x,T_x) = (\phi^2/2)[\Delta bT_x/(1 - \phi) + \Delta cT_x^{-2}] - \Delta a[\phi + \ln(1 - \phi)].$$

Further, if $\ln(1 - \phi)$ and $1/(1 - \phi)$ are represented by series, and ϕ is sufficiently small, this reduces to the remarkable form

$$\Delta Y^\circ(T;T_x,T_x) \simeq (\phi^2/2)\ \Delta C_p^\circ(T_x).$$

An appreciably better approximation is provided by

$$\Delta Y^\circ(T;T_x,T_x) \simeq (\phi^2/2)(1 + q\phi)\ \Delta C_p^\circ(T_x)$$

with $q = 0.6$ for $\phi < 0$ and $q = 1.0$ for $\phi > 0$.

[1]Department of Chemistry, Oklahoma State University, Stillwater, Okla 74078.

Availability of these last three equations renders obsolete the integrated van't Hoff equation--Σ-plot method, and the plotting of "uncorrected" ln K versus 1/T.

INTRODUCTION

Before describing the new results cited in the title, a brief summary of key points from earlier papers (7-8, 10-11)[2] in this series would seem to be in order. I shall use, without extended discussion, the compact functional notation (CFN) introduced in references (7-8) and described in detail in the Calorimetry Conference COSSSUN report (2).

THE COMPACT FUNCTIONAL NOTATION

The essential feature of the CFN is that it provides a simple, straightforward, flexible, compact, self-consistent scheme for representing the experimentally realizable portion of each of the seven common thermodynamic functions: U, S, H, A, G, J, Y. For example, the result of integration of C_p to obtain a value of H(T) is

$$H(T) = H(T^h) + \int_{T^h}^{T} C_p dT. \tag{1}$$

Since the enthalpy $H(T^h)$ at the reference temperature T^h [which typically is 0 or $\mathfrak{T}$ = 298.15 (2)] is unknown, the experimentally realizable portion of H(T) is the integral, which in CFN is represented by $H(T;T^h)$(2). It follows from equation 1 that

$$H(T;T^h) = H(T) - H(T^h). \tag{2}$$

Similarly, for the entropy one has

$$S(T) = S(T^s) + \int_{T^s}^{T} C_p d\ln T \tag{3}$$

and

$$S(T;T^s) \equiv \int_{T^s}^{T} C_p d\ln T = S(T) - S(T^s). \tag{4}$$

The usual convention for tabulating entropy assumes that for each substance there is at T = 0 a perfectly ordered state for which the entropy can be taken as zero. This perfectly ordered state may not be "actually attained" as T → 0. Hence, it is useful, even necessary, to distinguish between the entropy S(0) which the real system has as T → 0, and the entropy S(∅) which the system would have if, as T → 0, it became perfectly ordered. (The usual conventions about isotopes, nuclear spins, etc., remain in effect.) Hence,

---

[2]Underlined numbers in parentheses refer to items in the list of references a at the end of the paper.

$S(\emptyset)$ is the reference state for the conventional entropy (2): $S(T;\emptyset) = S(T) - S(\emptyset)$. The quantity $S(0) - S(\emptyset)$, if nonzero, corresponds to "residual entropy."

THE PLANCK FUNCTION

If the expressions in equations 1 and 3 for H(T) and S(T) are substituted into the defining equation for the Planck function (2)

$$Y(T) = S(T) - [U(T) + pV]/T = S(T) - H(T)/T, \tag{5}$$

one obtains

$$Y(T) = [S(T^s) - H(T^h)/T] + \int_{T^s}^{T} C_p d\ln T - T^{-1}\int_{T^h}^{T} C_p dT \tag{6}$$

$$= [S(T^s) - H(T^h)/T] + Y(T;T^h,T^s). \tag{7}$$

Clearly $Y(T;T^h,T^s)$ represents the two integrals of equation 6 and equally clearly it represents the experimentally realizable portion of the Planck function Y(T), since $S(T^s)$ and $H(T^h)$ in equations 6 and 7 are the unknown and unknowable terms from equations 1 and 3. From equations 7, 6, 4 and 2 one can immediately write

$$Y(T;T^h,T^s) = \int_{T^s}^{T} C_p d\ln T - T^{-1}\int_{T^h}^{T} C_p dT \tag{8}$$

$$= S(T;T^s) - T^{-1}H(T;T^h) \tag{9}$$

$$= Y(T) - [S(T) - H(T^h)/T]. \tag{10}$$

If in these last three equations one takes $T^s = \emptyset$ and $T^h = \text{Æ}$, and if one substitutes Y(T) = -G(T)/T, equation 10 becomes

$$Y(T;\text{Æ},\emptyset) = -G(T)/T - S(\emptyset) + H(\text{Æ})/T = -[G(T) - H(\text{Æ})]/T - S(\emptyset). \tag{11}$$

If the third-law convention $S(\emptyset) = 0$ is adopted, equation 11 may be written as

$$Y(T;\text{Æ},\emptyset) = -[G(T) - H(\text{Æ})]/T. \tag{12}$$

The right side of equation 12 is the familiar "free energy function" as tabulated, for example, in the JANAF Tables (3-6). Hence, the traditional "fef" is seen to be identical with the experimentally realizable portion of the Planck function. Use of the symbols $Y(T;\text{Æ},\emptyset)$, $Y(T;0,\emptyset)$, etc, and the name "Planck function (at T) wtih H referred to Æ (or 0) and S referred to $\emptyset$ is recommended (2).

THE GENERAL EQUATION RELATING K TO T

If the Δ operator is applied to equation 10 and standard-state pressure is specified, one obtains

$$\Delta Y^\circ(T;T^h,T^s) = \Delta Y^\circ(T) - \Delta S^\circ(T^s) + \Delta H^\circ(T^h)/T. \qquad (13)$$

It should be remembered that the left side of equation 13 is, with proper choice of T^h and T^s, identical with the familiar Δ("fef") or Δ("gef"). From the defining equations for $Y^\circ(T)$ and $G^\circ(T)$, one gets

$$Y^\circ(T) = -G^\circ(T)/T, \text{ and } \Delta Y^\circ(T) = -\Delta G^\circ(T)/T \qquad (14)$$

If this result is combined with the well-known expression for ln K, one has

$$\Delta Y^\circ(T) = -\Delta G^\circ(T)/T = R \ln K, \qquad (15)$$

and, if this equation is substituted into equation 13,

$$\Delta Y^\circ(T;T^h,T^s) - R \ln K = \Delta H^\circ(T^h)/T - \Delta S^\circ(T^s). \qquad (16)$$

This last equation is the general equation (8) relating ln K to T and subsumes all second- and third-law methods known to the author: 1. Differentiation of equation 16 with respect to T readily produces the van't Hoff equation (8). 2. If the left side of equation 16 is represented by $\Gamma^\circ(T^h,T^s)$ and if both T^h and T^s are taken to be Tc, one has

$$\Gamma^\circ(T;\text{Tc},\text{Tc}) = \Delta H^\circ(\text{Tc})/T - \Delta S^\circ(\text{Tc}), \qquad (17)$$

and it is clear that a "second-law plot" of Γ versus 1/T yields ΔH°(Tc) and ΔS°(Tc) from slope and intercept. 3. If T^h = Tc and $T^s = \emptyset$, as in the JANAF Tables, one has

$$\Gamma^\circ(T;\text{Tc},\emptyset) = \Delta H^\circ(\text{Tc})/T - \Delta S^\circ(\emptyset) \qquad (18)$$

or, if one invokes the third law and sets $\Delta S(\emptyset) = 0$,

$$\Gamma^\circ(T;\text{Tc},\emptyset) = \Delta H^\circ(\text{Tc})/T; \qquad (19)$$

the slope from a plot of Γ versus 1/T, with the line constrained to have intercept $\Gamma = 0$ at $1/T = 0$ [because $\Delta S(\emptyset) = 0$], provides the correct (8) third-law value for $\Delta H^\circ(T)$. 4. The conventional third-law value for ΔH°(Tc) is obtained as the average value of $T \cdot \Gamma^\circ(T;\text{Tc},\emptyset)$ (cf. equation 19 after multiplication by T), and is equivalent to the average slope $\Gamma/(1/T)$ of the various lines that connect the origin to each experimental (Γ, 1/T) point (8).

$Y^\circ(T;T^h,T^s)$ and $\Delta Y^\circ(T;T^h,T^s)$ From C_p°, ΔC_p° Data

It happens not infrequently that tabulated values of $Y^\circ(T;\text{Tc},\emptyset)$ or $Y^\circ(T;0,\emptyset)$ are not available for a particular substance. For this situation, calculation of $\Delta Y^\circ(T;T^h,T^s)$ and use of the general equation are conveniently discussed under three subheadings.

C_p° Data Available for All Desired Temperatures

This rather trivial case requires only that one evaluate $Y^\circ(T;\mathfrak{T},\emptyset)$ for each substance using equation 8 and the available C_p° data. It may be convenient to write equation 8 as

$$Y^\circ(T;\mathfrak{T},\emptyset) = \int_0^{\mathfrak{T}} C_p^\circ d\ln T + \int_{\mathfrak{T}}^{T} C_p^\circ \, d\ln T - T^{-1}\int_{\mathfrak{T}}^{T} C_p^\circ dT \qquad (20)$$

and to evaluate the first integral numerically or graphically and the other two integrals analytically from algebraic equations for C_p°. It may also be convenient to use equation 20 in the Δ-form:

$$\Delta Y^\circ(T;\mathfrak{T},\emptyset) = \Delta S(\mathfrak{T};\emptyset) + \int_{\mathfrak{T}}^{T} \Delta C_p^\circ d\ln T - T^{-1}\int_{\mathfrak{T}}^{T} \Delta C_p^\circ dT, \qquad (21)$$

and to evaluate $\Delta Y^\circ(T;\mathfrak{T},\emptyset)$ directly from ΔC_p° and the conventional entropy change for reaction at $\mathfrak{T}$: $\Delta S^\circ(\mathfrak{T};\emptyset)$.

C_p° Data Available Only for $T > 298.15$ K

The lower limit of both integrals of equation 8 would typically be chosen as $\mathfrak{T} = 298.15$ K, and

$$\Delta Y^\circ(T;\mathfrak{T},\mathfrak{T}) = \int_{\mathfrak{T}}^{T} \Delta C_p^\circ d\ln T - T^{-1}\int_{\mathfrak{T}}^{T} \Delta C_p^\circ dT \qquad (22)$$

would be evaluated analytically or numerically as required by the available data.

No C_p° or ΔC_p° Data Available

It is usually possible to make a "reasonable" estimate of ΔC_p°. If it can be done for the reaction of interest, then, rather than make no "ΔC_p corrections" to ln K, it is preferable (8) to evaluate

$$\Delta Y^\circ(T;T_x,T_x) = \int_{T_x}^{T} \Delta C_p^\circ d\ln T - T^{-1}\int_{T_x}^{T} \Delta C_p^\circ dT \qquad (23)$$

from the estimated ΔC_p°, and then to obtain $\Delta H^\circ(T_x)$ and $\Delta S^\circ(T_x)$ from

$$\Delta Y^\circ(T;T_x,T_x) - R \ln K = \Delta H^\circ(T_x)/T - \Delta S^\circ(T_x). \qquad (24)$$

The temperature T_x would typically be a convenient value near the middle of the experimental temperature range, a choice which minimizes the magnitude of the "ΔC_p° correction" $\Delta Y^\circ(T;T_x,T_x)$.

NEW EQUATIONS FOR EVALUATING $\Delta Y^\circ(T;T_x,T_x)$

It is apparent from equations 21, 22, and 23 that evaluation of $\Delta Y^\circ(T;T^h, T^s)$ from ΔC_p° data typically involves evaluation of two integrals with identical upper and lower limits, which are hereinafter designated by T and T_x; hence, the integrations produce a value for $\Delta Y^\circ(T;T_x,T_x)$. If the usual form $\Delta C_p^\circ = \Delta a + \Delta bT + \Delta cT^{-2}$ is substituted into equation 23, integration produces

$$\Delta Y^\circ(T;T_x,T_x) = \Delta a[\ln(T/T_x) - (T - T_x)/T] + \Delta b[T - T_x - (T^2 - T_x^2)/2T]$$
$$+ \Delta c[(T^{-1} - T_x^{-1})/T - (T^{-2} - T_x^{-2})/2], \qquad (25)$$

a form not particularly convenient for routine use. However, if one defines $\phi \equiv (T - T_x)/T$ - that is, ϕ is the "fractional temperature change" associated with "correction" of data from T to T_x - equation 25 can, with straightforward algebra and no approximations, be put into the considerably more convenient form

$$\Delta Y^\circ(T;T_x,T_x) = (\phi^2/2)[\Delta bT_x/(1 - \phi) + \Delta cT_x^{-2}] - \Delta a[\phi + \ln(1 - \phi)]. \qquad (26)$$

If $\ln(1 - \phi)$ and $1/(1 - \phi)$ are represented by series, one has, for $-1 < \phi < 1$,

$$\Delta Y^\circ(T;T_x,T_x) = (\phi^2/2)[\Delta a(1 + 2\phi/3 + \phi^2/2 + \ldots)$$
$$+ \Delta bT_x(1 + \phi + \phi^2 + \ldots) + \Delta cT_x^{-2}]. \qquad (27)$$

Retention of the quadratic terms in the series is often not justified (see below). If $\phi \ll 1$, the first power terms may also be deleted. The result is the remarkable form

$$\Delta Y^\circ(T;T_x,T_x) \simeq (\phi^2/2)[\Delta a + \Delta bT_x + \Delta cT_x^{-2}] = (\phi^2/2)\Delta C_p^\circ(T_x). \qquad (28)$$

From equation 27 one can readily deduce that the approximation represented by equation 28 would be improved by inclusion of a term of the form $(1 + q\phi)$ with $q \leq 1$:

$$\Delta Y^\circ(T;T_x,T_x) \simeq (\phi^2/2)(1 + q\phi)\Delta C_p^\circ(T_x). \qquad (29)$$

The import of equations 28 and 29 is especially noteworthy. From a value of ΔC_p° at one temperature T_x, values for $\Delta Y^\circ(T;T_x,T_x)$ can be calculated for any temperature T over a range which remains to be defined. It also bears repeating that equation 26 is rigorous; the only "approximation" lies in the degree to which the widely used algebraic expression for ΔC_p° reproduces experimental data.

To obtain information about the temperature range over which equations 28 and 29 are adequate approximations, calculations have been made (11) over the range 800 → 2,100 K, with T_x = 1,300 K, for the reaction

$$2\ Al(g) + 1.5\ O_2(g) \rightarrow Al_2O_3(s,\alpha),$$

which was chosen because reliable data are available and because ΔC_p° is relatively large. A sample of the results is given in table 1 as values of the change in rational standard Planck function $\Delta Y^\circ(T;T_x,T_x)/R$ (2) calculated from equations 26, 28, and 29 and from data in the JANAF tables. Heat capacities for O_2 and Al_2O_3 from Kubachewski, Evans, and Alcock (14) were combined with $C_p^\circ = 5R/2$ for Al(g)(3-6) to obtain $\Delta C_p = 4.80 + 2.75\overline{N3}\ T - 6.02P5\ T^{-2}$ (9)[3]. Entries in the column headed "From $Y^\circ(\bar{\epsilon};T,\emptyset)$" were calculated (8) from values of $Y^\circ(\bar{\epsilon};T,\emptyset)$ (that is, from values of the "free energy function," $[G^\circ(T) - H^\circ(298.15K)]/T$, values of $S^\circ(1,300\ K)$, and values of $H^\circ(1,300\ K; \bar{\epsilon}) = H^\circ(1,300\ K) - H^\circ(298.15\ K)$, from the JANAF Tables (3-6). This column is included solely to provide confirmation for the results from equation 26; differences in these two columns arise from the inability of a simple three-parameter equation to produce faithfully the variations of C_p° over a wide

[3] $2.75\overline{N3} = 2.75\times10^{-3}$; $6.02P5 = 6.02\times10^{5}$.

TABLE 1. - $\Delta Y^\circ(T;T_x,T_x)/R$ for $2\ Al(g) + 1.5\ O_2(g) \rightarrow Al_2O_3(s,\alpha)$, by various methods

T/K	ϕ[a]	$\Delta Y^\circ(T;1,300\ K, 1,300\ K)/R$					$\Delta Y^\circ(T;\bar{\epsilon},\bar{\epsilon})/R$	
			Eq. 29[a]					
		Eq 28a	q=0.6	qk=1.0	Eq. 26a	From $Y^\circ(T;\bar{\epsilon},\emptyset)$[b]	Eq. 4[c]	From $Y^\circ(T;\bar{\epsilon},\emptyset)$[b]
800	-0.62500	0.788	0.493	0.295	.518	0.539	0.416	0.416
900	-.44444	.399	.292	.221	.291	.300	--	--
1,000	-.30000	.182	.149	.127	.145	.149	.729	.755
1,200	-.08333	.0140	.0133	.0128	.0131	.013	1.055	1.105
1,400	+.07143	.0103	.0107	.0110	.0110	.011	1.379	1.450
1,600	+.18750	.0710	.0790	.0840	.0845	.085	1.698	1.784
1,800	+.27778	.155	.182	.199	.204	.203	2.009	2.105
2,100	+.38095	.293	.360	.405	.436	.427	--	--

[a] T_x = 1,300 K.

[b] Data for $Y^\circ(T;\bar{\epsilon},\emptyset)$ from JANAF Tables.

[c] T_x = 298.15 K ≡ $\bar{\epsilon}$.

temperature range. This is further illustrated in the last two columns of the table, where T_x is taken as 298.15 K ≡ ℭ rather than the value 1,300 K used in the remainder of the table; there is a consistently increasing discrepancy between values obtained from ΔC_p°, equation 26, and values obtained from data in the JANAF Tables (last column). It should be noted that results (omitted from table 1) of calculations using equation 25 agree exactly with those using equation 26, as expected.

Exploration of the new equations 26, 27, 28, and 29 has been limited, but several guides to their use may be offered: 1. Equation 26 is rigorous and may be used over any temperature range for which Δa, Δb, and Δc are valid. 2. The approximations given by equations 28 and 29 are poor for $\phi > +0.5$. Therefore, these approximate forms should not be used in correcting high-temperature data to 298.15 K; for T_x = ℭ and $\overline{T}$ = 600 K, ϕ = (600 - 298)/600 = 0.503, and for T_x fixed and $T > T_x$, ϕ increases as T increases. 3. The approximations given by equations 28 and 29 are inappropriate if ΔC_p° changes sign between T_x and T; for example, for the reaction given above, ΔC_p° = -1.16 at 298.15 K and +6.95 at 1,000 K. 4. The approximation of equation 28 appears to be valid within ±0.05 (or ±0.1 cal/K) over $-0.3 < \phi < 0.3$, but note that, stated in this form, the error in the approximation depends on the magnitude of $\Delta C_p^\circ(T_x)$. 5. The approximation of equation 29, with q = 0.6, appears to be valid within ±0.03 (or ±0.06 cal/K) over $-0.6 < \phi < 0.3$, but see the note under 4. 6. It appears that the approximation of equation 29 can be further improved for positive values of ϕ by taking q = 0.6 for $\phi < 0$ and q = 1.0 for $\phi > 0$.

The approximations for $\Delta Y^\circ(T;T_x,T_x)$ provided by equations 28 and 29 should be especially useful in evaluating $\Delta H^\circ(T_x)$ and $\Delta S^\circ(T_x)$ from ln K for reactions for which ΔC_p° is not known. The availability of equation 24, with $\Delta Y^\circ(T;T_x,T_x)$ provided by equation 28 or 29, makes unnecessary the resort to plotting "uncorrected" ln K versus 1/T and the subsequent ambiguity (12) about the temperature to which the derived ΔH° applies. With equations 24 and 28 or 29 one may have to estimate ΔC_p° at T_x, but there is no ambiguity in what is done; further, the probable range of error in the estimated value of ΔC_p° and the resultant error in $\Delta H^\circ(T_x)$ can be evaluated on a rational basis.

Finally, I would add that after the initial note (11) describing these equations had been submitted, I learned from Professor C. B. Alcock, in private conversation, that he has developed and described (1, 13) some related equations for calculating the error made in using the approximation $\Delta G^\circ(T) \approx \Delta H^\circ(ℭ) - T\,\Delta S^\circ(ℭ)$ rather than the correct version:

$$\Delta G^\circ(T) = \Delta H^\circ(T) - T\,\Delta S^\circ(T).$$

The nature of the error in this approximation is made clear if, in equation 13, one takes $\Delta Y^\circ(T) = -\Delta G^\circ(T)/T$ and $T^h = T^s = ℭ$:

$$\Delta Y^\circ(T;ℭ,ℭ) = -\Delta G^\circ(T)/T - \Delta S^\circ(ℭ) + \Delta H^\circ(ℭ)/T.$$

Multiplication by T and rearrangement produces

$$\Delta G^\circ(T) = \Delta H^\circ(\mathfrak{T}) - T\ \Delta S^\circ(\mathfrak{T}) - T \cdot \Delta Y^\circ(T;\mathfrak{T},\mathfrak{T}).$$

Hence, the approximation discussed by Alcock is a straightforward result of assuming $\Delta Y^\circ(T;\mathfrak{T},\mathfrak{T}) = 0$, that is, $\Delta C_p^\circ = 0$, and the error in the approximation, $T \cdot \Delta Y^\circ(T;\mathfrak{T},\mathfrak{T})$, may be evaluated readily from equations 26, 28, and 29, which are appreciably more convenient than those described by Alcock.

REFERENCES

1. Alcock, C. B. Nature, v. 209, 1966, pp. 198-199.

2. Calorimetry Conference Committee. Report of Calorimetry Conference Committee on Standard States, Symbols, Units, and Nomenclature (COSSUN Report). July 1979 (available from author of this article).

3. Chase, M. W., and coworkers. JANAF Tables, 1974 Supplement. J. Phys. Chem. Ref. Data, v. 3, 1974, pp. 311-480.

4. _____. JANAF Tables, 1975 Supplement. J. Phys. Chem. Ref. Data, v. 4, 1975, pp. 1-75.

5. _____. JANAF Tables, 1978 Supplement. J. Phys. Chem. Ref. Data, v. 7, 1978, pp. 793-940.

6. Dow Chemical Co., Thermal Research Laboratory. Janaf Thermochemical Tables, 2d Ed. NSRDS-NBS-37, S/N 003-003-00872-0, U.S. Government Printing Office, Washington, D.C., 1971, 1141 pp.

7. Freeman, R. D. Proc. 5th Bienn. Internat. CODATA Conf. Boulder, Color. July 1976. Pergamon Press, Oxford, England, 1977, pp. 585-591.

8. _____. Bull. Chem. Thermodyn., v. 21, 1978, pp. 505-520.

9. _____. J. Chem. Educ., v. 56, 1978, p. 103.

10. _____. High Temp. Science, v. 11, 1979, pp. 213-221.

11. _____. High Temp. Science, v. 12, 1980, pp. 133-138.

12. Horton, W. S. J. Res. NBS, v. 70A, 1966, p. 533.

13. Kubachewski, O. and C. B. Alcock. Metallurgical Thermochemistry, 5th ed. Pergamon Press, Oxford, England, 1979.

14. Kubachewski, O., E. L. Evans, and C. B. Alcock. Metallurgical Thermochemistry, 4th Ed, Pergamon Press, Oxford, England, 1967, table C.

DISCUSSION

R. N. Goldberg: What effects would changes in the numerical value of the gas constant, R, have on the values of the thermodynamic functions?

R. D. Freeman: I don't think that is really a problem. I will tell you why. Regardless of how you tabulate the data (that is, in conventional or in rational form), you have to use R. If you tabulate data in rational form, R is not used in obtaining values from partition functions, but it is used in converting experimental C_p and enthalpy data to the rational form. If you tabulate thermodynamic data in conventional form, R is not used with experimental data, but is required for conversion of statistical-mechanical values to dimensioned form. So, in a set of tables - the total compilation - you have to use R one way or another. The question is, for those statistical quantities that you get from the partition function, do you multiply those by R, or do you divide experimental heat capacity and enthalpy data by R? Either way, you have to use R in one place or another. You can't get away from it. The other part of the answer is that whoever puts R into a set of tables should state what the value of R is so that the original experimental data can be reacquired.

Anonymous: In your first slide, you talked about conversion from atmosphere, and you left calories in. I was wondering why.

R. D. Freeman: The reason I did it on the slides was because I thought more people are familiar with the calorie. In the paper on adoption of the bar (High Temperature Science, v. 11, No. 2,1979, pp. 73-79), I gave the error in both calories and joules.

Anonymous: Would you elaborate on your functional notation.

R. D. Freeman: The first symbol in the parentheses is an independent variable, and then you have a semicolon followed by the two constant parameters which describe a particular one of that family of functions. That is typical mathematical notation; to separate constant parameters from independent variables with a semicolon. Are we not in agreement? I thought we were saying the same thing.

SECTION 6.- HETEROGENEOUS PHASE EQUILIBRIA

THERMOCHEMICAL MEASUREMENTS OF GAS-SOLID REACTIONS PROPOSED FOR CHEMICAL HEAT PUMPS[1]

by

Robert W. Carling[2]

ABSTRACT

An apparatus has been assembled to measure pressure-temperature relationships and derive reaction energies for reactions of the type

$$\text{salt}\cdot n\text{L(s)} \rightleftarrows \text{salt}\cdot m\text{L(s)} + (n-m)\ \text{L(g)},$$

where L is water, ammonia, or methanol. These reactions have been proposed for use in chemical heat pump systems. A chemical heat pump performs all the functions of a conventional electric heat pump; however, solar energy is combined with energies of chemical reactions to replace electricity requirements.

One problem is the scarcity of pertinent thermochemical information to assist in selecting chemicals for use in a chemical heat pump system, and the apparatus discussed in this paper provides a convenient means for generating the information. Incorporated in this apparatus is a sensitive cantilever balance. This balance is used to prepare salt samples in situ so that the stoichiometry of the salt hydrate, ammoniate, or methanolate is known prior to the pressure measurements. A detailed description of the apparatus is given in addition to results on a system that has been studied in this apparatus: $CaCl_2 \cdot nNH_3$ (where n = 8, 4, 2, or 1).

INTRODUCTION

A chemical heat pump is similar to existing heat pumps in that it is used for heating and cooling applications in homes or industry. However, presently available heat pumps are driven by electricity, whereas a chemical heat pump is driven by solar energy. The chemical heat pump can perform all of the functions of a conventional electric heat pump only without the need for electricity. In

[1]Work supported by U.S Department of Energy under contract AT(29-1)-789.
[2]Sandia Laboratories, Livermore, Calif.

lieu of electrical energy, one harnesses the energy available in the chemicals stored in a chemical heat pump.

Present configurations of chemical heat pumps harness the energy available by employing reversible chemical reactions. The majority of the present chemical reactions proposed are gas-solid reactions of the type

$$MX \cdot n\ L(s) \rightleftarrows MX \cdot m\ L(s) + (n-m)\ L(g), \qquad (1)$$

where MX is a salt and L is a ligand such as water, ammonia, or methanol(2)[3]. In such a system, solar energy is used to drive the above reaction in the forward direction. The gas generated is condensed and stored within the chemical heat pump. To recover the energy at night or on cloudy days, the reaction is reversed.

Addressed in this paper are the pressure-temperature relationships and heats of reaction in the following $CaCl_2$-NH_3 reactions 2-5:

$$CaCl_2 \cdot 8NH_3(s) \rightleftarrows CaCl_2 \cdot 4NH_3(s) + 4NH_3(g) \qquad (2)$$

$$CaCl_2 \cdot 4NH_3(s) \rightleftarrows CaCl_2 \cdot 2NH_3(s) + 2NH_3(g) \qquad (3)$$

$$CaCl_2 \cdot 2NH_3(s) \rightleftarrows CaCl_2 \cdot NH_3(s) + NH_3(g) \qquad (4)$$

$$CaCl_2 \cdot NH_3(s) \rightleftarrows CaCl_2(s) + NH_3(g). \qquad (5)$$

Although it is theoretically possible to use any of the above reactions in a chemical heat pump, reaction 2 has been of particular interest (5). Unfortunately, the pressure-temperature data existing for the above reactions are either very old, of uncertain quality, or incomplete. For these reasons, a decomposition pressure apparatus has been built in which the starting materials can be prepared in situ and the pressure-temperature data taken. A complete description of the experimental setup is presented in this paper, along with the experimental results.

EXPERIMENTAL WORK

The apparatus will be described in the first part of this section. The second part will describe the interface between the desk-top calculator and the pressure measurement system. The final part documents the sample preparation procedures.

$CaCl_2$-NH_3 Experimental System

For the $CaCl_2$-NH_3 system, a pressure measurement system was designed in

[3]Underlined numbers in parentheses refer to items in the list of references at the end of this paper.

order to determine the sample stoichiometry independent of the measured decomposition pressure while retaining the ability to prepare salts in situ. This system incorporated a balance into the pressure measurement system. This balance is similar to an idea used in another application (1). A cross-sectional view of the balance is shown in figure 1. A schematic of the overall system is illustrated in figure 2.

The balance used a 2-mm quartz glass rod (A in figure 1) which acted as a cantilever. The salt was placed in a platinum dish (B) suspended from one end of the glass rod. As weight was lost or gained by the salt, the rod moved up or down. This motion was followed by employing a displacement gage. The system operates on the eddy-current principle. As the distance between the conductive surface (gold foil, D) and the displacement gage sensor (C) changes, more or fewer eddy currents are generated. The impedance variations produced are converted to dc voltage proportional to the distance being sensed.[4] Output from the sensor was read using a Hewlett-Packard 3455A digital voltmeter. The range of the sensor in the system was 0 to 1.3 mm. Calibration of the sensor with known weights indicated a sensitivity of about 5 mV g^{-1}.

The constant-temperature bath was insulated and contained Dow Corning 550 oil as the bath fluid. The pump (to stir the bath), bath heater, and thermostat were contained within one unit, a Thermomix 1480 made by B. Braun Melsungen AG of West Germany. The bath temperature controller and the fluid were both capable of temperatures to 523 K. The temperature of the bath could be held constant within a variation of ± 0.05 K. A copper cooling coil was used to cool the bath when needed. A thermocouple (Chromel-Alumel, type K) was held just below the platinum sample container. The output from the thermocouple went to a Hewlett-Packard 3455A digital voltmeter and was recorded using a Hewlett-Packard 9825A desk-top calculator.

To measure the decomposition pressure of the salts, a differential capacitance manometer (MKS Instruments, Inc., Baratron head type 310BH) was used with a range of 0 to 10,000 torr. The output from the manometer went to an electronics unit (MKS Instruments, 170M-6B) and then to a digital readout unit (MKS Instruments, 170M-25C) to provide pressure readings in units of torr. In order to record the pressure data on the desk-top calculator, an interface was required between the calculator and the digital readout. The interface was a Fairchild model 4883 instrument coupler. The bath temperature controller was monitored by the desk-top calculator via a Hewlett-Packard 6940B multiprogramer. Details of the control system and data collection procedure are presented in the next section.

Control and Data Acquisition System

The calculator control system was designed so that the HP 9825 calculator would control the entire experiment. That is, not only was the calculator to collect data, it was also to control the bath temperature, determine when

[4]A supplier for such equipment is: Kaman Sciences Corporation, 1500 Garden of the Gods Road, Colorado Springs, Colo. 80933.

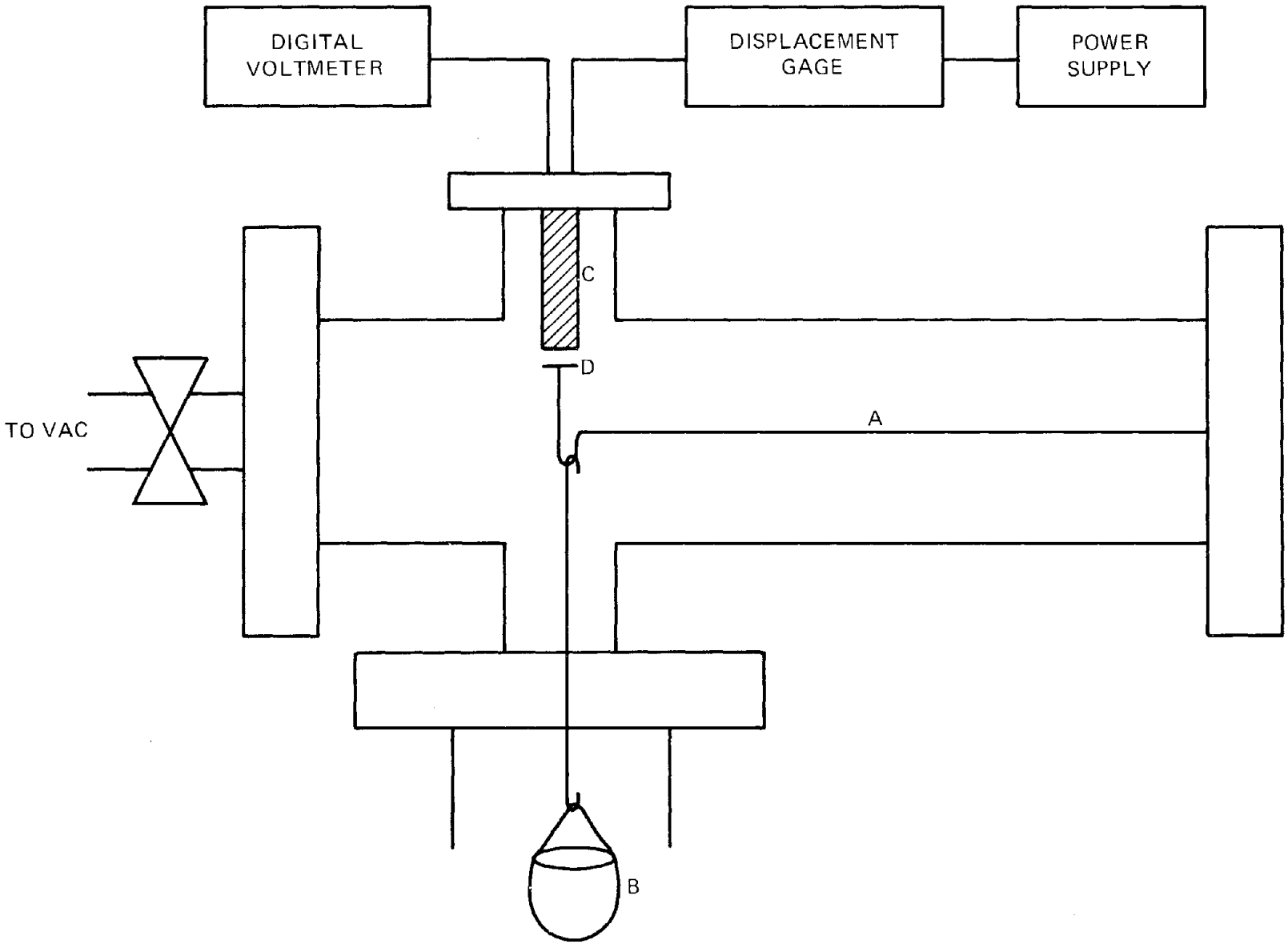


FIGURE 1. - Cross-sectional view of cantilever balance for $CaCl_2/NH_3$ dissociation pressure measurement system. A, Quartz rod; B, platinum sample holder; C, sensor; D, gold foil.

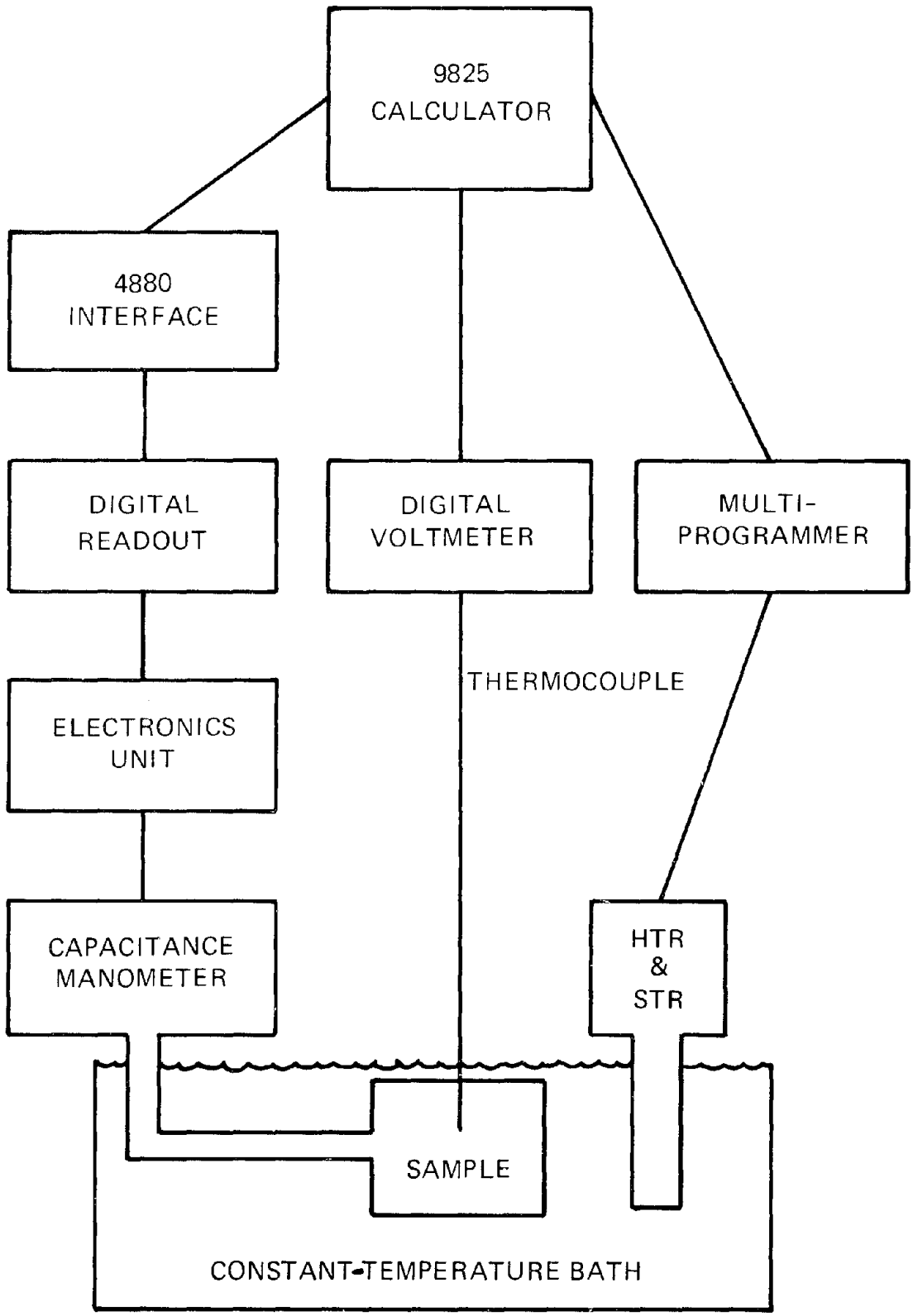


FIGURE 2. - Schematic of $CaCl_2/NH_3$ dissociation pressure measurement system.

pressure equilibrium had been reached, and then proceed to a new bath temperature for the next pressure measurement.

The link between the bath temperature controller and the calculator was a Hewlett-Packard 6940B multiprogramer. The multiprogramer mainframe holds plug-in cards that can be used for a variety of purposes including controlling a constant-temperature bath. In this case a Hewlett-Packard 69513A resistance output card provided known resistances to the Thermomix 1480 controller in the constant-temperature bath. The multiprogramer was cabled to the calculator using a Hewlett-Packard 98032A Option 040 16-bit interface kit. The calculator was programed to ask the operator for initial bath temperature (T_i), final bath temperature (T_f), and the change in temperature (ΔT) desired between each pressure-temperature equilibrium point.

Once T_i, T_f, and ΔT had been determined, the calculator then needed to know what it should consider equilibrium to be. In this system, temperature equilibria were always reached well before pressure equilibria. Therefore, the operator had to decide what the pressure equilibria conditions were to be. Pressure equilibria were dependent on two factors: time between pressure readings (time interval) and the percentage change of pressure during the time interval. Typical time intervals in this study values were 10, 20, 30, and 60 min. Once the programed temperature had been reached, a reading of time, temperature, and pressure was recorded on paper tape by the calculator. The initial pressure was the first reference pressure. After waiting the time interval programed, time, temperature and pressure were recorded again. If the pressure had changed by less than the percentage change programed (the default was 1 pct over the time interval programed), then the calculator recorded that equilibrium had been reached and then increased the bath temperature by ΔT. If the pressure change was larger than the percentage change programed, the most recently recorded pressure became the new reference pressure and the calculator waited the time interval before looking for pressure equilibrium again. This process was continued until pressure equilibrium had been reached at T_f, at which time the experiment was concluded. A flow chart for the experimental procedure is shown in figure 3.

Sample Preparation

Starting material for the $CaCl_2$-NH_3 system was purchased from Alfa Division of Ventron Corp. The salt obtained was $CaCl_2 \cdot 2H_2O$ labeled as analytical reagent.

Calcium chloride dihydrate was weighed, dried in vacuo at 423 K for 24 hours, and reweighed after cooling in a desiccator. The weight loss indicated the starting material to have a composition of $CaCl_2 \cdot 2.2H_2O$. The sample was then transferred, in air, to the pressure measurement apparatus. Reweighing the salt on the balance incorporated in the pressure measurement apparatus indicated a negligible weight change. The system was evacuated overnight to remove air and any water that might have adsorbed on the salt. To prepare the ammoniate, ammonia (Matheson, labeled anhydrous) was then introduced into the system. The ammonia pressure in the line was adjusted to about 310 torr. Lower

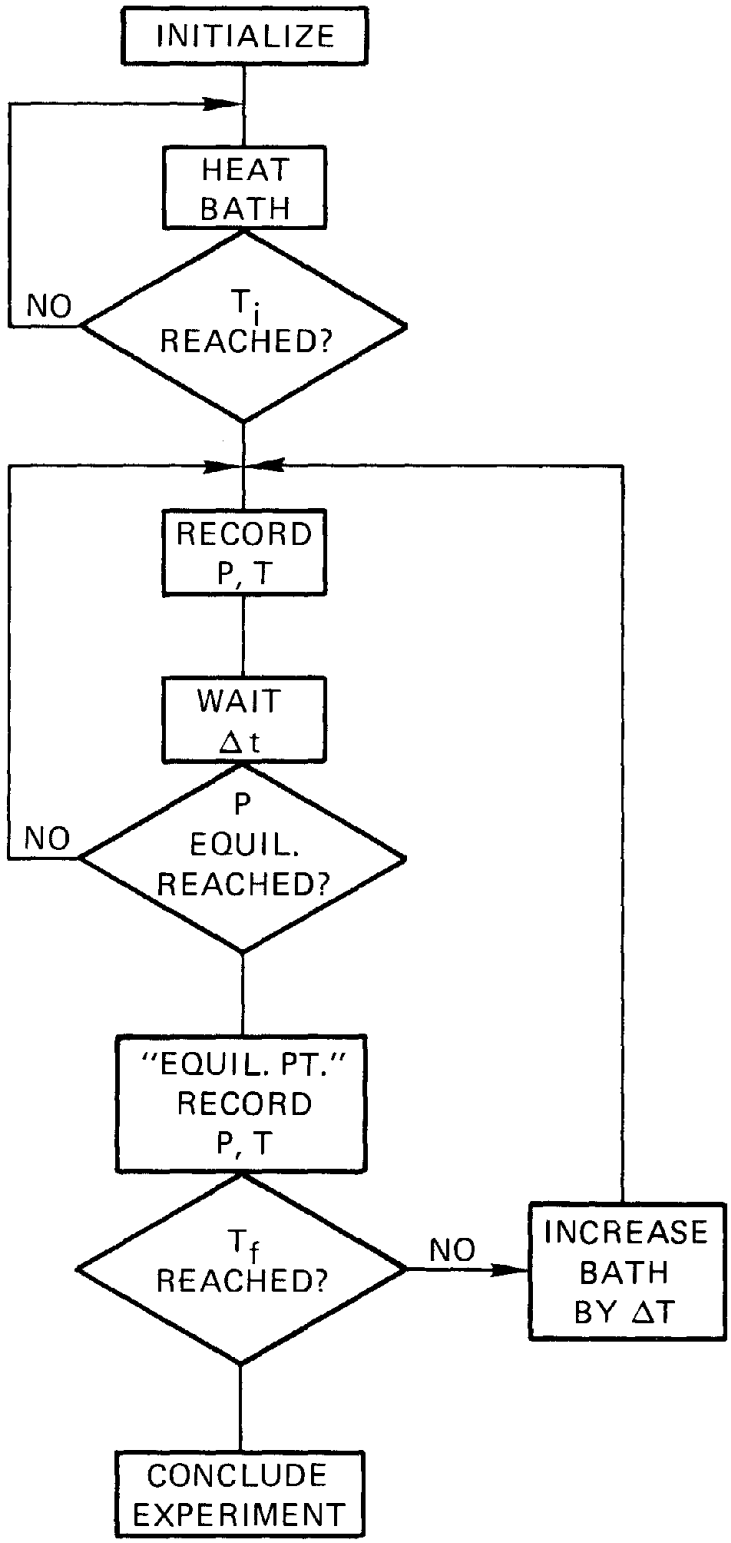


FIGURE 3. - Flow diagram of control and data acquisition system. T_i and T_f are initial and final temperature, respectively. P is pressure; t is time.

ammoniates of calcium chloride were prepared in situ by vacuum pumping on the high-ammoniate salt and watching the weight loss on the balance. Preparation of $CaCl_2 \cdot 2NH_3$ and $CaCl_2 \cdot NH_3$ required heating of the salt in addition to pumping.

RESULTS AND DISCUSSION

The results of the dissociation pressure measurements for $CaCl_2 \cdot 8NH_3$, $CaCl_2 \cdot 4NH_3$, $CaCl_2 \cdot 2NH_3$, and $CaCl_2 \cdot NH_3$ are illustrated in figure 4. A least-squares fit of the equilibrium data for each sample yielded the following equations

$$\ln P \text{ (torr)} = (23.33 \pm 0.12) - (50.6 \pm 0.4)10^2 \, T^{-1} \quad (6)$$

$$\ln P \text{ (torr)} = (22.71 \pm 0.13) - (50.5 \pm 0.4)10^2 \, T^{-1} \quad (7)$$

$$\ln P \text{ (torr)} = (25.13 \pm 0.26) - (81.4 \pm 1.0)10^2 \, T^{-1} \quad (8)$$

$$\ln P \text{ (torr)} = (26.05 \pm 0.30) - (94.0 \pm 1.2)10^2 \, T^{-1} \quad (9)$$

for reactions 2, 3, 4, and 5, respectively. The equations are valid over the temperature ranges of the experimental data. Enthalpies of dissociation were calculated at the average temperature of each series of pressure-temperature data and are presented in table 1 along with previously reported values. The previously reported values were obtained from three sources: the International Critical Tables (ICT)(6), Huttig (4), and a Martin Marietta Corp. report (3).

TABLE 1. - Enthalpies of dissociation for $CaCl_2$-NH_3, kcal $mole^{-1}NH_3$

Reactant	$\overline{T}$/K	ΔH_T[1]			
		This work	Washburn(6)	Hüttig(4)	Hall(3)
$CaCl_2 \cdot 8NH_3$	313.93	10.06±0.07	9.8	9.8	10.1
$CaCl_2 \cdot 4NH_3$	325.22	10.04± .08	10.1	10.1	11.1
$CaCl_2 \cdot 2NH_3$	394.81	16.2 ± .2	15.1	15.2	12.8
$CaCl_2 \cdot NH_3$	412.08	18.7 ± .2	16.5	17.0	12.6

[1]Errors are standard deviations.

The enthalpies of dissociation of $CaCl_2 \cdot 8NH_3$ and $CaCl_2 \cdot 4NH_3$ from this work agree with those of all investigators and need not be discussed further. However, the enthalpies of dissociation of $CaCl_2 \cdot 2NH_3$ and $CaCl_2 \cdot NH_3$ do not agree and require discussion. The data quoted in ICT for the two lower ammoniates are derived from the work of Hüttig. The reason for the discrepancies is not clear. The values for ΔH_{diss} found in Hüttig's paper were apparently obtained from a publication dated before 1900 in which solution calorimetry was used to determine ΔH_{diss}. The quality of the work is uncertain. It is still unclear how ICT arrived at their values of ΔH_{diss}. Fitting the ICT data to a straight line gives values of ΔH_{diss} = 14.8 kcal mol^{-1} NH_3 for $CaCl_2 \cdot 2NH_3$ and ΔH_{diss} = 19.4 kcal

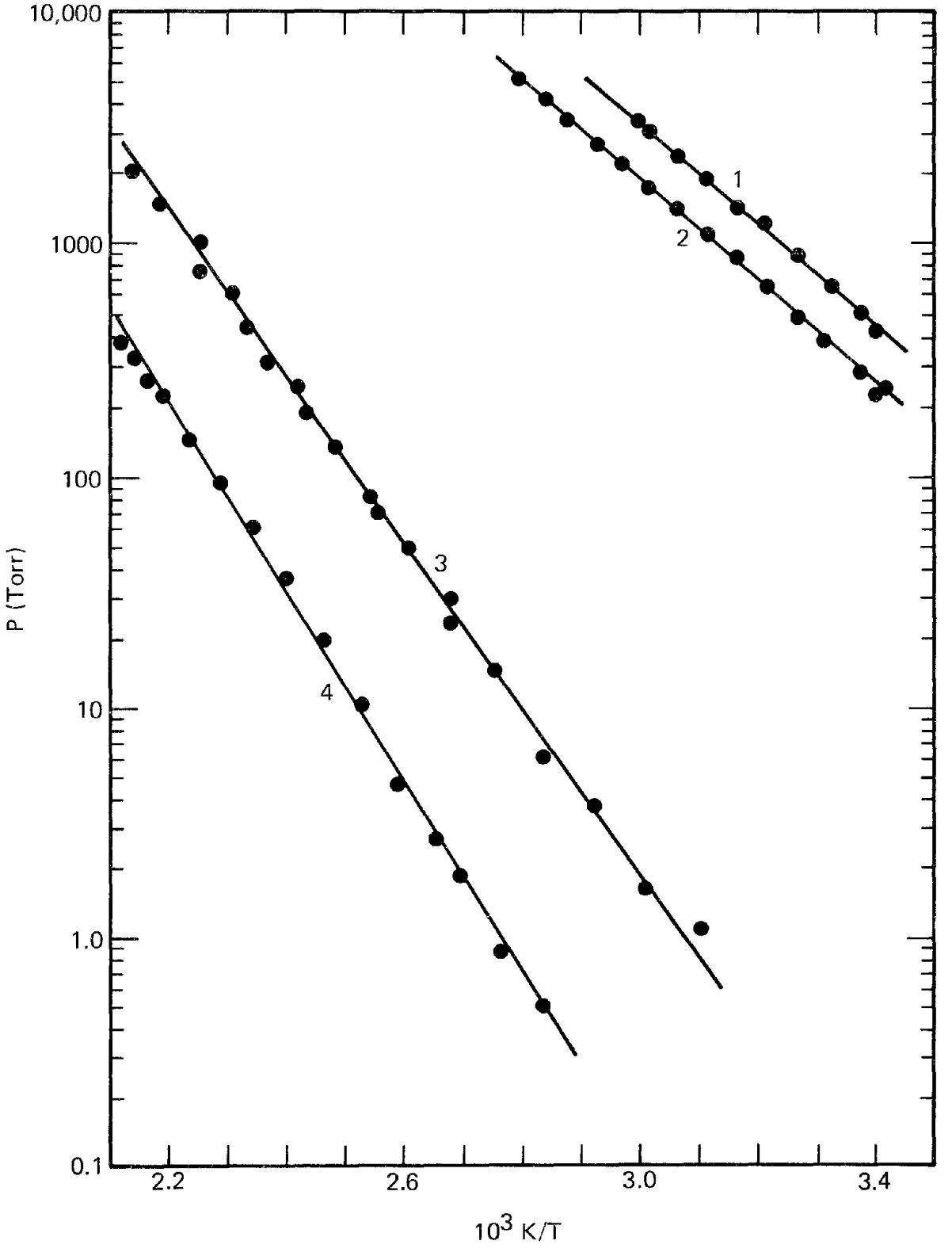


FIGURE 4. - Dissociation pressure data for $CaCl_2/NH_3$ system. 1, $CaCl_2 \cdot 8NH_3$; 2, $CaCl_2 \cdot 4NH_3$; 3, $CaCl_2 \cdot 2NH_3$ 4, $CaCl_2 \cdot NH_3$.

mole^{-1} NH_3 for $CaCl_2 \cdot NH_3$. These values do not agree with those presented in table 1. The ICT values may be derived from a graphical best fit of the data and, therefore, differ from the computer-generated best fit derived above.

The enthalpies of dissociation reported by Martin Marietta Corp. (3) were obtained by using differential thermal analysis (DTA). The results suffer because of the nature of DTA analyses. Data from DTA analyses are not taken under equilibrium conditions, whereas the data obtained in this work were. The reason ΔH_{diss} of $CaCl_2 \cdot 8NH_3$ and $CaCl_2 \cdot 4NH_3$ agree fairly well is probably due to the much faster equilibration times of the higher two ammoniates compared with $CaCl_2 \cdot 2NH_3$ and $CaCl_2 \cdot NH_3$. Pressure equilibrium times for $CaCl_2 \cdot 8NH_3$ and $CaCl_2 \cdot 4NH_3$ were about 4 hours. For $CaCl_2 \cdot 2NH_3$ and $CaCl_2 \cdot NH_3$ typical equilibrium times averaged about 24 hours when the temperature was increased. However, on decreasing temperature, it was not possible to return to previously recorded pressure readings even after several days. In fact it was not possible to establish reliable equilibrium pressure values below about 340 K for $CaCl_2 \cdot 2NH_3$ and 350 K for $CaCl_2 \cdot NH_3$; the pressures were too high. Even by reducing the temperature to, say, 300 K and pumping off "unequilibrated" ammonia, it was not possible to obtain reliable data. The lower temperature data obtained on cooling were scattered, unreproducible, and did not fall on an extrapolated line obtained from the higher temperature data; therefore, these data were not used to derive equilibrium values for the pressure-temperature curves and the resultant enthalpies of reaction.

SUMMARY

This paper has described the development of an experimental system in which materials proposed for chemical heat pump applications can be reliably prepared. Once prepared, pressure-temperature data can be obtained over large temperature (293 to 523 K) and pressure (10^{-3} to 10,000 torr) ranges. The entire experiment is controlled and data are recorded using a desk-top calculator.

Dissociation pressure measurements have been made on the $CaCl_2$-NH_3 system, and enthalpies of dissociation of the calcium chloride ammoniates have been determined; they are 10.06 ± 0.07, 10.04 ± 0.08, 16.2 ± 0.2, and 18.7 ± 0.2 kcal mole^{-1} NH_3 for $CaCl_2 \cdot 8NH_3$, $CaCl_2 \cdot 4NH_3$, $CaCl_2 \cdot 2NH_3$, and $CaCl_2 \cdot NH_3$, respectively. These data confirm previously reported values of ΔH_{diss} for $CaCl_2 \cdot 8NH_3$ and $CaCl_2 \cdot 4NH_3$ and establish reliable values for $CaCl_2 \cdot 2NH_3$ and $CaCl_2 \cdot NH_3$.

REFERENCES

1. Bertolotti, R. L., J. E. Shelby, and P. R. Coronado. Improved Beam-Bending Glass Viscometer. Sandia Laboratories, Livermore, Calif., SCL-DR-720352, October 1972.

2. Bramlette, T. T., and R. W. Mar. Fiscal Year 1978 Annual Operating Plan for the Thermochemical Energy Storage and Transport Program of the National Thermal Energy Storage Program, Sandia Laboratories, Livermore, Calif., SAND77-8288, May 1978.

3. Hall, C. A., Martin Marietta Corporation Report MCR-76-502. September 17, 1976.

4. Hüttig, G. F. Z. Anorg. Allgem. Chem., v. 123, 1922, p.31.

5. Jaeger, F. A. Thermochemical Energy Storage Systems. Proc. 2d Ann. Thermal Energy Storage Contractors' Information Exchange Meeting, Gatlinburg, Tenn., CONF-770955, Sept. 29-30, 1977, p. 325.

6. Washburn, E. W. (ed.). International Critical Tables. McGraw-Hill Book Co., Inc., New York, v. 7, 1930.

DISCUSSION

L. D. Hansen: How do you know that you have only two pure phases in the system?

R. W. Carling: Oh, you do, you have to. You will always have a mixture of two salts plus the vapor phase. At any one temperature the pressure remains constant when two salts and one gas are present.

M. W. Chase: Can you do the same for calcium and water?

R. W. Carling: There is no 8-hydrate. There are 6-, 4-, 2-, and 1-. You could do the same study. The hydrate system that has been of a real interest is magnesium chloride-water, which is a bad actor because of hydrolysis.

DIFFERENTIAL MASS SPECTROMETRY USING EFFUSION CELLS FOR ACTIVITY MEASUREMENTS IN COMPLEX LIQUID OXIDE MIXTURES

by

Michel Allibert[1] and Christian Chatillon[1]

ABSTRACT

Based on a very recent experience with more than seven binary or ternary oxide systems, the general feature of the differential mass spectrometry is presented. The special interest of this technique for complex oxide mixtures is outlined. A tentative definition of its operating range, accuracy, and reliability is made from experimental results. The emphasis is placed on problems related to mass spectrometry on effusion cells and physicochemical interactions between the cells and the liquids studied. The corresponding technical solutions developed by the authors at the University of Grenoble (France) are described. The given examples illustrate specifically the determination of liquid oxide activity as well as the measurements of the Gibbs energy of formation of solid stoichiometric compounds at high temperatures.

INTRODUCTION

The differential measurement using a mass spectrometer coupled to several effusion cells is not a new method for activity determination in inorganic mixtures (4, 18)[2]. However, it has not been extensively used until recently, perhaps because of its apparent technological complexity (13), but more surely because it is a demanding technique, the disadvantage of which can only be compensated for by the certainty of a wide measurement range and a sufficient accuracy. During the past years we focused our attention on the effusion cells and we found that many problems originated here and not from differential measurements or even mass spectrometry. Moreover, the ability of making comparisons provides an easy way to analyse the physicochemical behavior of the effusion cell-system under investigation. An attempt to define the accuracy and limit of differential mass spectrometry can be made from the results we obtained on liquid oxides and liquid alloys. The examples illustrating our point of view are taken from our work with liquid oxides.

[1]Laboratoire de Thermodynamique et Physicochimie Métallurgique, ENSEEG – Domaine Universitaire, St. Martin D'Heres, France.

[2]Underlined numbers in parentheses refer to items in the list of references at the end of this paper.

GENERAL FEATURES OF DIFFERENTIAL MASS SPECTROMETRY

Although several types of mass spectrometers can be used for thermodynamic studies with effusion cells, the description of our assembly illustrates the principles involved in the present investigation. If required, a detailed base can be found in books related to mass spectrometry with emphasis placed on oxides (6) or on evaporation and effusion cells (16). The progress of the technique could be followed in the series "Advances in Mass Spectrometry" (12, 19, 22).

Principles of Differential Mass Spectrometry

Fundamental Relationship

As schematically shown in figure 1, the mixture for which a measurement is needed is put in an effusion cell and heated under vacuum. The studied condensed phases are partially decomposed, giving gases, a part of which is allowed to escape the cell by effusion through a little orifice. The escaping gaseous species make up a molecular beam (without collisions) defined by a diaphragm-set and submitted to electron bombardment. The ions produced are accelerated by an electric field and scattered by a magnetic prism depending on their mass over charge ratio. The resulting ionic current I_i, for a given gaseous species i, is measured after amplification by a secondary electron multiplier. Such a chain leads to a simple relationship between the ionic current I_i, the cell temperature T, and the partial pressure P_i of the gaseous species at equilibrium with the condensed phases in the effusion cell:

$$P_i \times S_i = I_i \times T, \tag{1}$$

where S_i is the apparatus sensitivity with respect to the gaseous species i. This factor depends on the physical properties of i and on the apparatus design, so that the partial pressure P_i cannot be obtained without calibration.

Calibration by Differential Measurements

The calibration or elimination of S_i can be achieved by comparing the ionic intensities of the same gaseous species over two effusion cells, so that

$$\frac{P_i}{P_i^\circ} = \frac{I_i}{I_i^\circ} \times \frac{T}{T^\circ} \times \frac{S_i}{S_i^\circ} \tag{2}$$

where the superscript o designates a cell arbitrarily taken as a reference. When these two cells are present simultaneously in the same furnace and submitted to measurements under the same conditions (geometrically and electronically identical), the sensitivity as well as the temperature are eliminated, giving

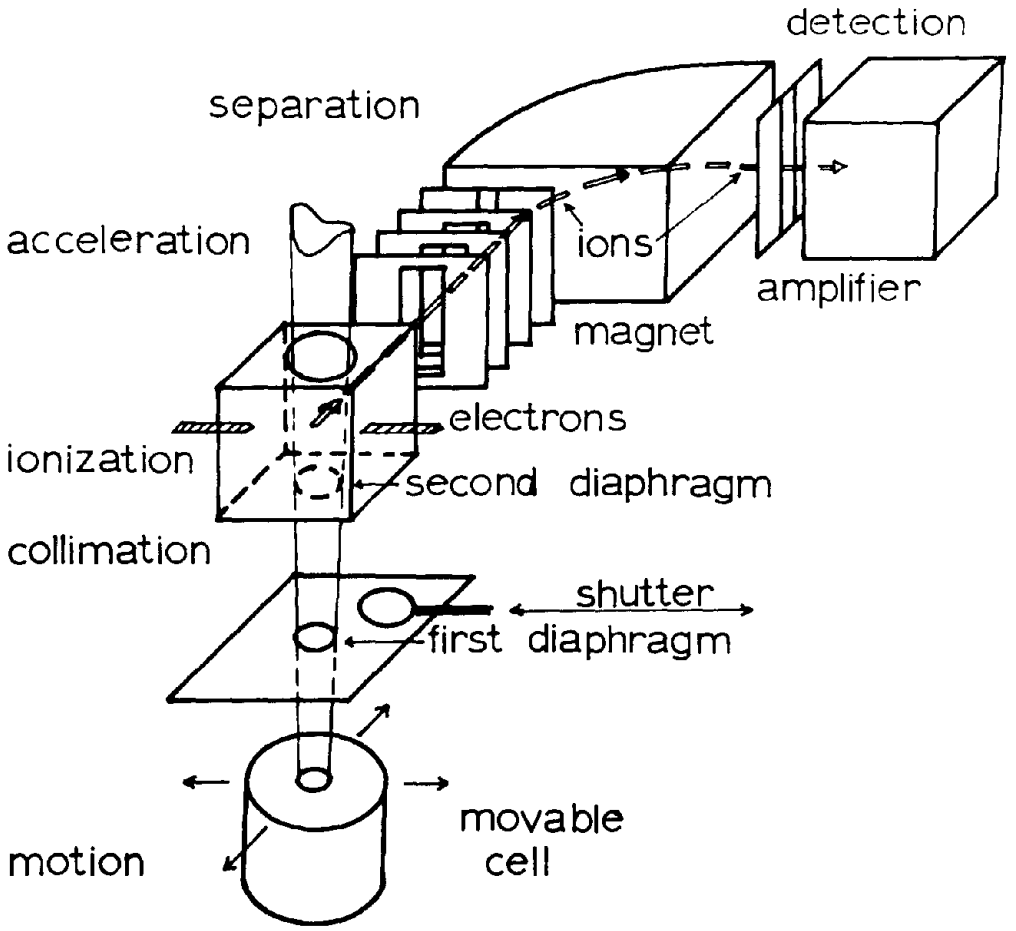


FIGURE 1. - Chain of functions in mass spectrometry on effusion cell. For differential measurements multiple-cell assembly (not shown on this diagram) is necessary, and each cell is placed in succession in front of the diaphragms that define the analysed molecular beam.

$$\frac{P_i}{P_i^\circ} = \frac{I_i}{I_i^\circ} . \qquad (3)$$

Activity Measurements

Assuming that the condensed species and the gaseous species are at equilibrium in the effusion cell, the activity of a given condensed species can be deduced from the ionic intensity measurements as shown in the following examples. In the CaF_2-CaO-Al_2O_3 slag study (1) the CaF_2 and CaO activities were deduced from the equilibria:

$$(CaF_2) \rightarrow CaF_2 \qquad (4)$$

$$\langle CaO \rangle + AlF + CaF_2 \rightarrow AlOF + 2CaF \qquad (5)$$

where ( ) and < > designate the liquid and the solid state respectively. From this,

$$a_{(CaF_2)} = \frac{I_{CaF_2}}{I^{\circ}_{CaF_2}}, \tag{6}$$

and

$$a_{<CaO>} = \left(\frac{I_{AlOF} \times I^2_{CaF}}{I_{AlF} \times I_{CaF_2}}\right) \Bigg/ \left(\frac{I_{AlOF} \times I^2_{CaF}}{I_{AlF} \times I_{CaF_2}}\right)^{\circ}. \tag{7}$$

Advantages of Differential Mass Spectrometry

The operating pressure range of mass spectrometry is large enough to allow measurements to be performed simultaneously on several gaseous species, the relative partial pressure of which ranges from 1 to 10^6. This potential for measuring activities of several components in complex mixtures is quite unique in physical chemistry. Such an advantage becomes specially important when studying multicomponent melts for which the Gibbs-Duhem integration technique is increasingly inaccurate and awkward to use as the number of components becomes higher.

Furthermore, because oxides decompose and give various gaseous species for a single condensed one, the amount of information collected by a mass spectrometer is great, increasing its advantage over other classical methods of activity measurement. A good example of this abundance of information is given in the study of the Ga_2O_3 - Gd_2O_3 system (3) where the Ga_2O_3 activity could be deduced from 10 different equilibria between $<Ga_2O_3>$ and the gaseous species: O, Ga, Ga_2O, GaO, and Ga_2O_2. This provides a cross-checking of the measured data and facilitates error detection.

Limitations and Identified Sources of Errors

General Limitations

As seen previously, the application of differential mass spectrometry relies on several assumptions, and every deviation from the conditions for which theory are valid creates errors and thus defines limits (as far as the operating conditions can be analyzed in terms of fulfilled conditions).

A typical figure for the activity accuracy is 1 to 5 pct, but there is no fundmental reason that prevents this being improved and becoming commonly better than 1 pct. Some usual sources of error for such measurements are presented in table 1.

TABLE 1. - General limitations for mass spectrometry

Limits	Limiting factor	Observations
Pressure, 10^{-3} atm. Pressure, 10^{-10} atm.	Molecular flow. Poor ionization efficiency.	Could be improved depending on technology (10^{-17} atm?).
Temperature difference between 2 cells.	Enthalpy of vaporization: $20 < \frac{\Delta P/P}{\Delta T/T} < 60$.	Isothermal conditions by heat pipes (7) at low temperatures ($T < 1,500$ K).
Molecular beam sampling.	Molecular species coming from outside the effusion cell (10).	Use of cold diaphragm set (9).
Irreversible evaporation and gas flow.	Apparent evaporation coefficient (6, 20), $\alpha \leq 1$ for liquids, to $\sim 10^{-3}$ for solids.	Motzfeldt approximation $\underline{P}=P$ meas. $(1+\frac{Ca}{A})$. C Clausing factor a effusion area A evaporation area
Compositional changes.	Selectivity of effusion process. Changes towards congruency (10).	Related to an upper pressure limit ($\sim 10^{-4}$ atm).
Relative volatility (10^6).	Sensitivity of the apparatus. Mass interferences.	-----
Interactions with effusion cell (10).	Chemical interaction. Creeping out. Diffusion.	Becomes important at high temperatures (1,500 to 2,500 K).
Stability and reproducibility of measurements.	Depends on apparatus design. Electronic stability is not a problem for differential measurements.	-----

Reading and Tuning Errors

A reading error for ionic intensities could result in improper tuning or in the impossibility of identifying the nature of a change. An estimate of this kind of stochastic error has been made for our mass spectrometer (Nuclide 90 H.T.) during a campaign of measurements on $CaO \cdot Al_2O_3$(15) and $CaO \cdot MgO \cdot Al_2O_3$ (2) systems. The results reported in figure 2 show a steep precision change when the partial pressure of the studied gaseous species drops below 10^{-8} atm. Under this limit, the lack of accuracy seems excessive (>6 pct). In fact a certain compensation of errors occurs during a comparative measurement. This

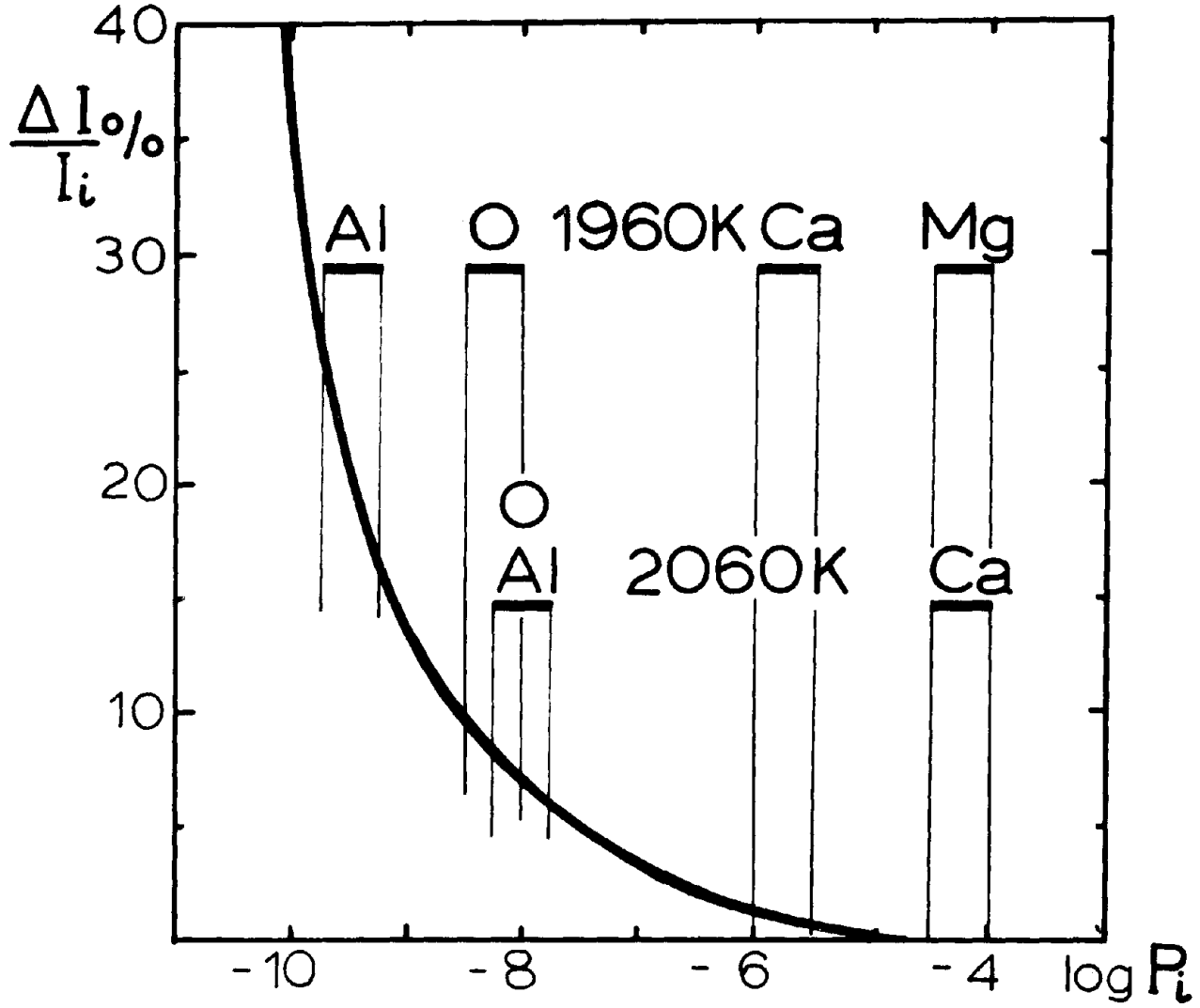


FIGURE 2. - Relative reading error as a function of partial pressure of the measured species. Vertical lines indicate actual measurement ranges for $CaO \cdot Al_2O_3$ liquids at 2,060 K and $CaO \cdot MgO \cdot Al_2O_3$ liquids at 1,960 K.

eliminates partially some systematic errors and explains the unexpected relative quality of the measurements down to 10^{-10} atm as well as the possibility of measurement of enthalpy of mixing. This latter property is very difficult to measure by mass spectrometry because the usual precision on enthalpy of vaporization or atomization is considered to be about ±4 or ±8 kJ/mole. However, in some exceptional cases (Ag-Ge alloys), the differential technique gives the partial enthalpy of mixing within ±1 kJ/mole (16). A precise knowledge of temperature could greatly improve such measurements (21).

The almost systematic use of complex equilibria, such as equation 5, instead of more direct measurements, such as equation 4, is an important accuracy limiting factor for oxides and salts because it is almost impossible to find conditions under which the accuracy is good for all the gaseous species involved. However, the control of one species in the gaseous phase gives a new degree of freedom to improve the activity determination using complex equilibra. It was one of the reasons that led us to use an oxygen pressure monitoring system.

An estimate of the reading precision as a function of oxygen pressure is reported in figure 3 for a hypothetical Al_2O_3 activity measurement using various equilibria such as

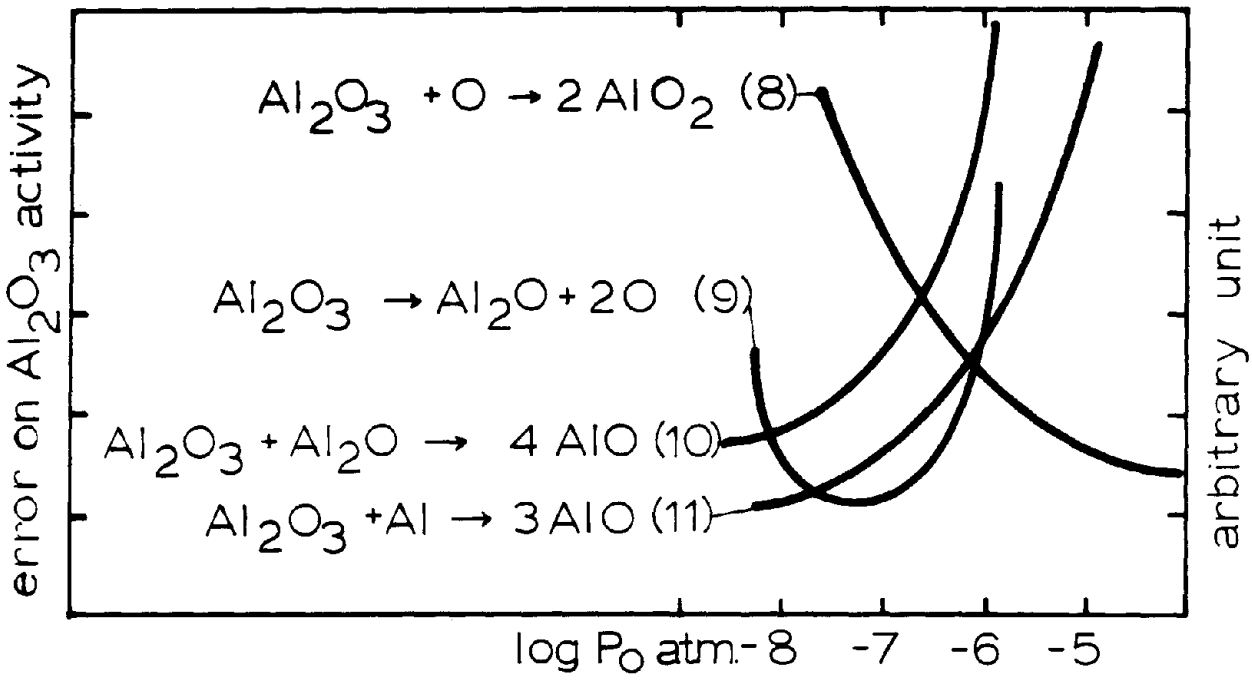


FIGURE 3. - Calculated reading error for Al_2O_3 activity measurements using various types of equilibrium between gaseous species and the condensed Al_2O_3. The error depends on the oxygen potential in the effusion cell.

$$\langle Al_2O_3\rangle + O \rightarrow 2AlO_2, \quad (8)$$

$$\langle Al_2O_3\rangle \rightarrow Al_2O + 2O, \quad (9)$$

$$\langle Al_2O_3\rangle + Al_2O \rightarrow 4AlO, \quad (10)$$

$$\langle Al_2O_3\rangle + Al \rightarrow 3AlO. \quad (11)$$

Cold Diaphragm and Furnace Motion

As already described (11), the solution we adopted to maintain the equality of S_i over several cells is to position them in succession in front of a single diaphragm-set (9). Thus the solid angle under which the inside of effusion cells is "seen" by the source is always the same and therefore independent of the effusion orifice size. This requires a very precise and reproducible positioning of each cell so that the effusion orifice diameter is not increased too much to obtain the same sensitivity, and affecting the reversibility of the vaporization process.

Figure 4 presents a convincing example of the importance of avoiding the ionization of species coming from outside the effusion cell. The molecular emissivity profile presented in this figure was obtained by moving the cell in front of the diaphragm-set. Because of the thickness of the area "seen" by the source, the intensity recorded does not exhibit changes as steep as they are for the molecular emissivity itself. However, it is obvious that, without the help of a cold diaphragm-set, the measurement error would have been catastrophically high, especially for aluminum. The same kind of behavior was found for a solid Ti_3O_5 study where emissivity, referred to the effusion orifice emissivity, was < 1 pct for TiO_2, 3 pct for TiO, 11 pct for O and 15 pct for Ti.

In some cases, the gaseous species coming into the ion source cannot be completely condensed at room temperature or source temperature. A background appears depending on the residence time of the species in the ionization area; that is, on the source design and the pumping system. Using a liquid nitrogen trap as source diaphragm and source envelope was confirmed to be a good solution for avoiding the Sb_4O_6 background during a study in progress on Sb_2O_3. This particular technique is not effective for N_2 or O_2 or other permanent gases, and the quality of O or O_2 pressure measurement could also be a limiting factor in oxide studies.

Irreversibility and Reference

In differential mass spectrometry, the apparatus calibration is made by using reference cells containing one or several components in a state that can be used as a reference state for activity or Gibbs energy determinations. For oxides this state is often the solid state even when the measurements are made on liquid mixtures. A multiphase reference is usually preferable because of the diffusion and evaporation problems with solids (6). A liquid phase ensures a good mass transport and a high evaporation coefficient (1). However,

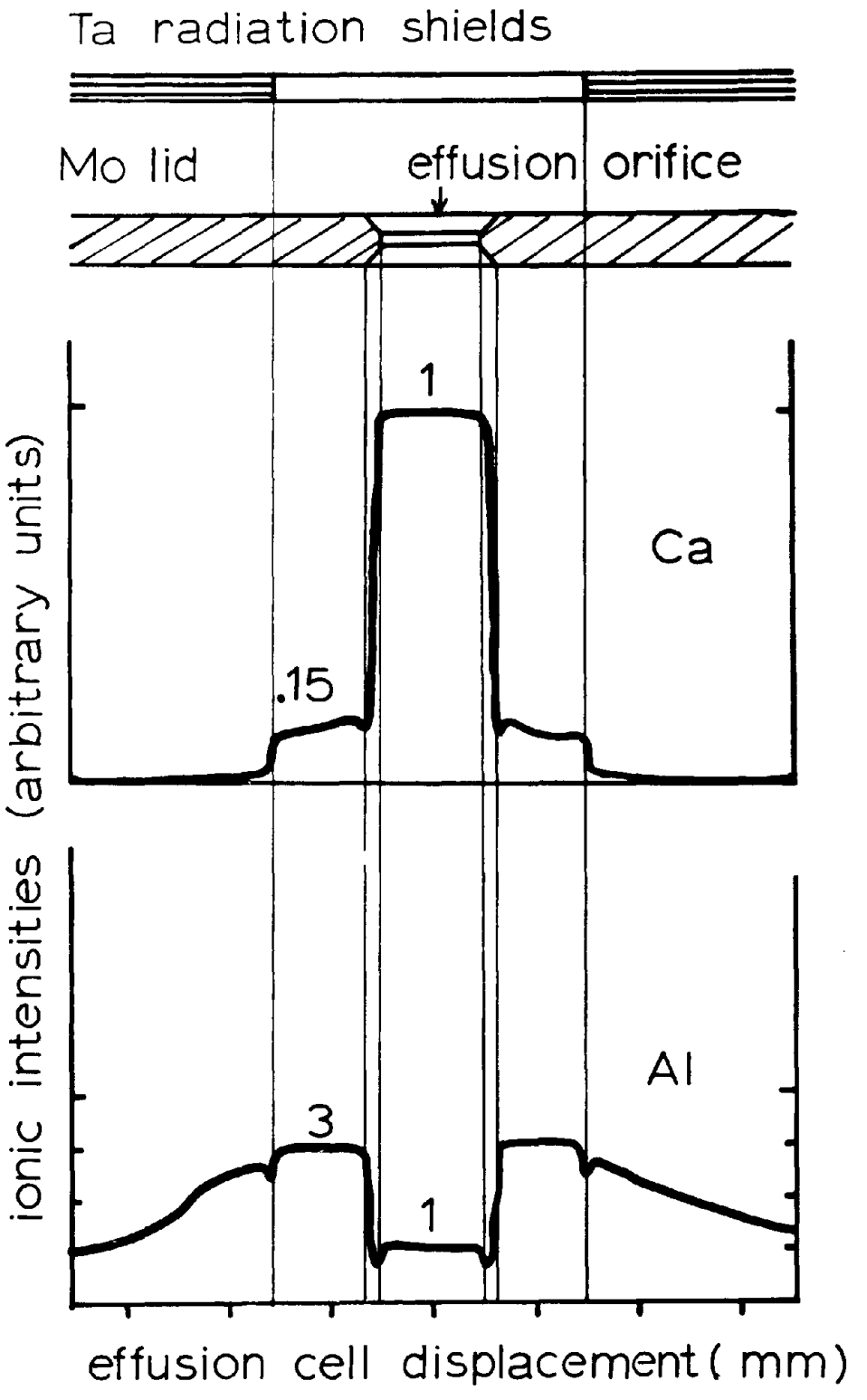


FIGURE 4. - Effect of change in the position of effusion cell on the measured molecular emissivity. The diagram illustrates the need for optimal collimation of the molecular beam to allow only molecules from the sample to enter the ionization chamber.

other examples can be found, such as the use of an Al_2O_3-saturated mixture rich in CaF_2 as reference in our study of the CaF_2-CaO-Al_2O_3 system. This reference cell exibited an irreversible behavior resulting in an apparent lowering of Al_2O_3 activity (which ought to be unity) by a factor as high as 5,000 in some cases. This could be due to the high CaF_2 activity in the liquid phase and the high solid-alumina-over-liquid ratio. The solid alumina was probably not well wetted by the liquid because of the reaction taking place between the two phases. This reaction was also occurring between the gaseous CaF_2 and the solid alumina, as confirmed by a decrease of CaF_2 pressure while the AlF pressure was increasing. The extremely low AlOF pressure could, with the previous observation, justify the assumption of reactions such as

$$\langle Al_2O_3\rangle + 3CaF_2 \rightarrow 3\langle CaO\rangle + 2AlF_3 \qquad (12)$$

and

$$\langle Al_2O_3\rangle + 4CaF \rightarrow 3\langle CaO\rangle + CaF_2 + 2AlF \qquad (13)$$

replacing

$$\langle Al_2O_3\rangle + AlF + 2CaF_2 \rightarrow 3AlOF + 2CaF. \qquad (14)$$

The strong interaction between lime and alumina is sufficient to give a very low CaO activity at the alumina surface because of Ca diffusion and formation of the CaO-Al_2O_3 compounds as already observed (14). This diffusion removes continuously the gaseous CaF_2 according to reaction 12.

The differential measurement provides a way of making a comparison between cells which are capable of various, but unknown, irreversible behavior. The choice of a proper cell design can be made after such a comparison has been made. An example of this is presented in figure 5 with TiNy in seven cells with an A-Ca ratio ranging from 50 to 710, corresponding to an effusion orifice diameter of 1.2 mm for an inner cell diameter from 9 to 32 mm. In this example, the irreversibility was due to surface depletion in solid TiNy (study in progress).

SPECIFIC FEATURES OF OXIDE MELTS

Although the previous discussion was illustrated by examples on oxide mixtures, the main character of oxygen was not really outlined. It lies in the multiple degree of oxidation of elements, either in the gaseous state or in both gaseous and condensed ones. But it also resides in some technical difficulties or facilities related to O_2 pressure control and measurement.

Gaseous Species

Complex Gaseous Species

When the total pressure of volatile species and the oxygen potential are high enough, many oxides give complex gaseous molecules in addition to single elements. This gives a special advantage to mass spectrometry because it

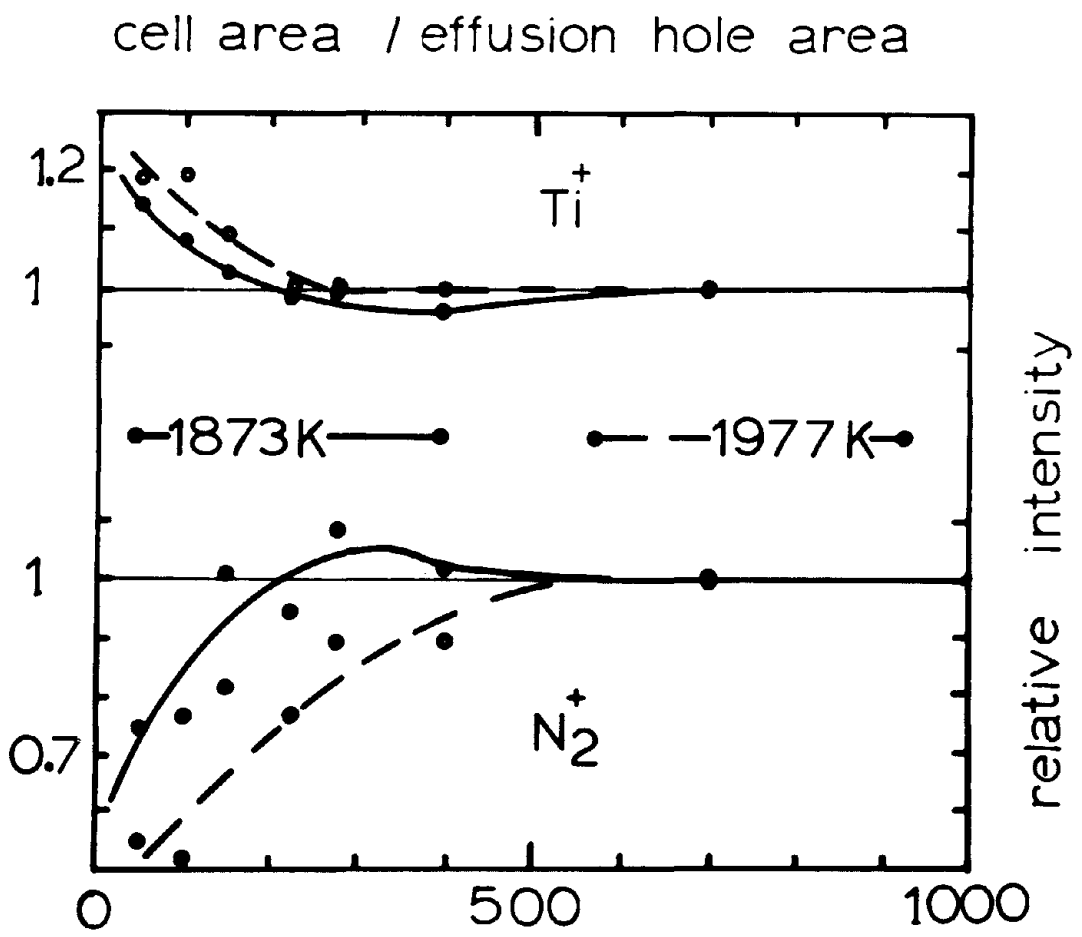


FIGURE 5. - Relative intensities of N_2^+ and Ti^+ measured over seven effusion cells with the ratio of cell area to effusion area ranging from 50 to 700. The departure from unity is due to a diffusion process in the nonstoichiometric TiNy lining the cell walls.

increases the amount of information about the condensed species producing these molecules. Furthermore, when the system under investigation is complex (three components or more), numerous mixed molecules can appear, again favoring mass spectrometry. As shown in table 2, there is a difference between the capabilities and the actual measurements; however, it is possible that this difference could be overcome.

Among the difficulties accounting for this difference is the fragmentation of complex molecules for a single ion. This problem is avoided by operating under different electron potentials in the ionizing electron beam, depending on the observed molecule. This is possible because the differential technique provides an immediate calibration of the apparatus, whatever the electronic conditions are. Some actual examples are reported in table 3.

Another problem arises with the complex molecules when the pressure is low because of the low encounter probability of the atoms making up such mole-

TABLE 2. - Practical and theoretical possibilities for mass spectrometry measurements[1]

System	Temperature, K	Gaseous Species Used	Other Possible Gaseous Species	Observations
$CaO-Al_2O_3$	2,060	Ca-Al-O	CaO, Al_2O-AlO-Al_2O_2-AlO_2.	Mass interference Fe56; T and P_{O_2} too low.
$MgO-CaO-Al_2O_3$	1,960	Mg-Ca-O	MgO	Mass interference Ca40; T and P_{O_2} too low.
$CaF_2-CaO-Al_2O_3$	1,700	CaF_2-CaF-AlF, AlOF	----	Fragmentation, creeping out.
$Cr_2O_3-CaO-Al_2O_3$	2,100	Cr-Ca-Al, CrO-CrO_2-Al_2O	CrO_3-O_2	Degree of oxidation of crucible.
$CaO-Ti_2O_3-TiO_2$	2,100	Ti-TiO-TiO_2 Ca-O	----	Do.
$Ga_2O_3-Gd_2O_3$	2,000	Ga-O-Ga_2O, GaO-Ga_2O_2	Ga_3O_3	Ga_3O_3 observed at the sensitivity limit.
$LiReO_4-CsReO_4$	700	$(LiReO_4)_2$, $(CsReO_4)_2$, $LiCs(ReO_4)_2$	----	Fragmentation.
In_2O_3	1,500	In-InO-In_2O-O_2	----	P_{O_2} controlled by electrochemical cell.

[1]Taken from studies made at the Laboratoire de Thermodynamique et Physicochimie Métallurgique, Grenoble, France.

TABLE 3. - Examples of operating potential for the ionizing electrons

Observed ion	Appearance potential (volts)	Operating potential (volts)	Parent gaseous specie
CaF^+	6	11	G.F
CaF^+	12.5	41	G.F_2(100 pct)
AlF^+	10	16	AlF
$AlOF^+$	10.5	26	AlOF
In^+	5.5	8.8	In (only)
In^+	9.5	---	In_2O
InO^+	13.3	23	InO
In_2O^+	8.4	23	In_2O
O^+	13	17	O cell
O^+	17.5	---	O_2 background

cules. This results in a very low evaporation coefficient, vitiating the measurement. But in fact, this kind of molecule is rather unusual and we never observed this problem except, perhaps, for the parasitic oxidation of the molybdenum container [$(MoO_3)_n$]. Nevertheless, special attention needs to be devoted to cell reversibility when using gaseous species with more than three atoms.

Compositional Changes

Because of the selective effect of effusion and the difference in composition between the gaseous and condensed phases, the effusion technique is always accompanied by a progressive change in the composition and/or amounts of the condensed phase.

Two parameters can be used to characterize this change, the oxygen-over-metals ratio in the gaseous flow, and the relative amount of each metallic element in the flow. This division is justified by the fact that the first steady state to be reached during the effusion process seems to be always the oxygen-over-metals congruence.

In fact, these two kinds of parameters are closely related and can be calculated provided the partial pressure of oxygen is known, that is, provided the leaking mechanism is known. At each given steady state, depending on the mixture composition and the nature of the container, there is a given set of oxygen potential, partial pressures, and flow composition parameters, as illustrated in figure 6.

From our experience, it appears that the actual partial pressure of oxygen is always lower than expected. This could be caused by mechanisms other

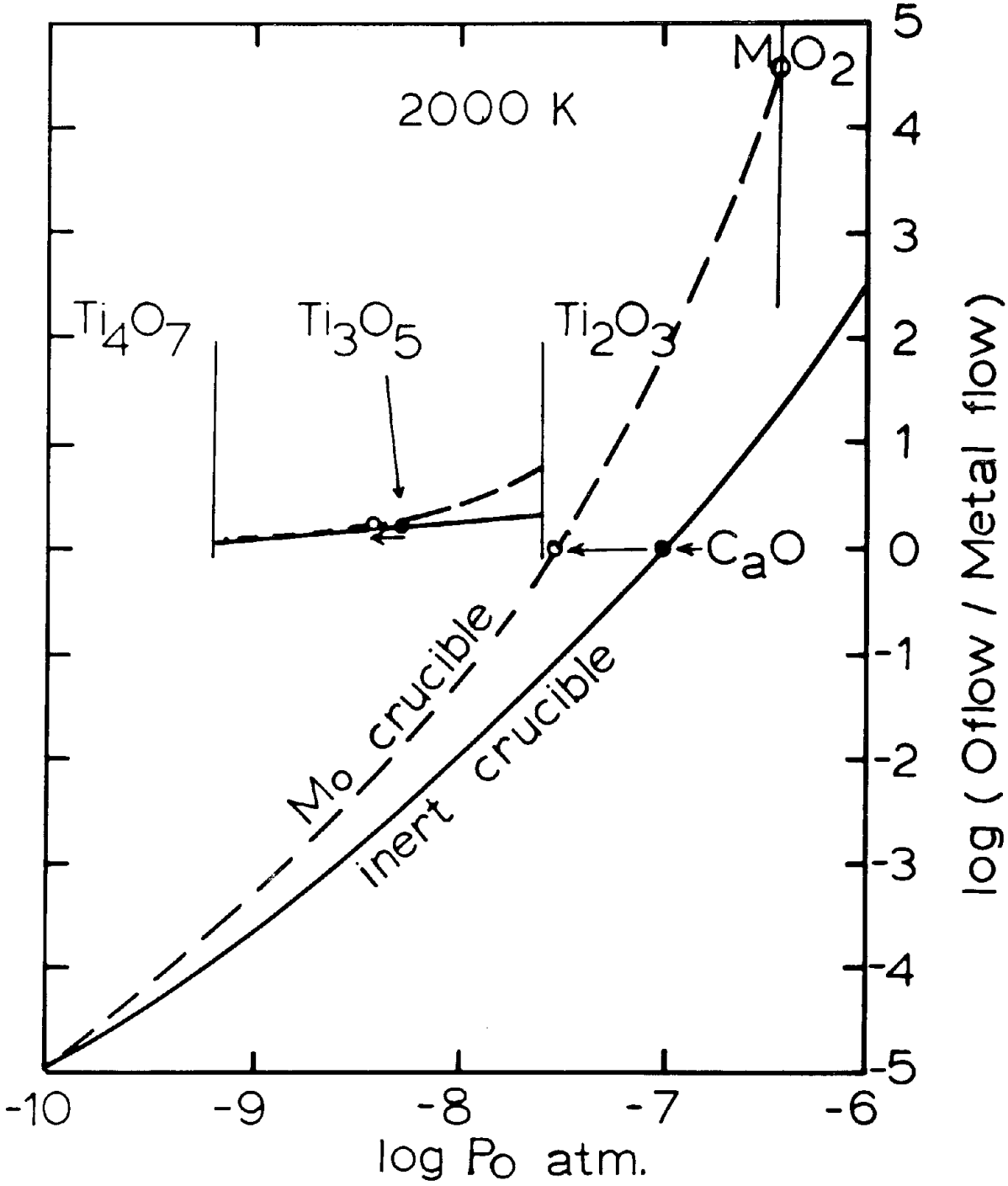


FIGURE 6. - Calculated ratio of oxygen flow to metal flow ratio, at 2,000 K, for pure CaO and pure Ti_3O_5 held in inert crucibles or molybdenum crucibles, as a function of partial pressure of monoatomic oxygen. The difference is due to Mo_2 and Mo_3 volatilization. The congruency points are shown, as well as the limits corresponding to Mo oxidation for CaO or appearance of other titanium oxides for Ti_3O_5. The lower limit at log P_O = -10 corresponds to the oxygen diffusion from the furnace chamber.

that effusion, such as various types of diffusion processes through the containers (Mo, Pt, Ir). As a result, the partial pressures of the metallic gaseous species are exceedingly high, and this reduces the operating temperature range. Such a problem could be overcome by controlling the oxygen partial pressure in the effusion cells, but only if the sample investigated is stoichiometric with respect to oxygen. When the sample contains multiple valency elements like Cr (II, III, IV, ...), Fe (II, III), or Ti (II, III, IV), another degree of freedon is given to the sample and it does not remain in the same oxidation state during effusion. We do not know yet if gaseous phase control can be achieved without changing too quickly the nature of the condensed phase. A simple oxide envelope around the metallic container was found to limit effectively any excessive oxygen leak, although this does not provide a real control over the vapor species.

Control and Measurement of Oxygen Pressure

The advantages of oxygen partial pressure control in effusion cells for oxide studies are as follows:

1. Observing more gaseous species and thus increasing the amount and the quality of information gathered on the oxide studied.

2. Decreasing the partial pressure of reduced species, which results in an increase of the upper temperature limit for the measurement.

3. Making measurements under optimum conditions for each equilibrium studied.

For this purpose we are developing two complementary devices, skimmer diaphragms and oxygen injection.

Skimmer Diaphragms

As outlined previously, uncondensed and unpumped O_2 represents a major background source and this constrains the oxygen partial pressure measurement. It leads to a "shutter effect" and decreases the practical sensitivity of the mass spectrometer towards this species. We successfully tried the skimmer diaphragm set shown in figure 7, improving the results for both N_2 and O_2 measurements. These conical diaphragms deflect the molecules coming from the cell area from their direct or indirect path towards the ionization zone. Thus, they decrease the local background in the source and the shutter area. A detailed analysis of this effect will be shortly presented for publication.

Oxygen Injection

We tried to monitor the oxygen flow in an effusion cell by controlling the intensity of a current passing through a piece of overoxidized zirconia placed beneath a platinum or alumina crucible loaded with In_2O_3 powder. The oxygen source and the crucible were placed inside an alumina effusion cell.

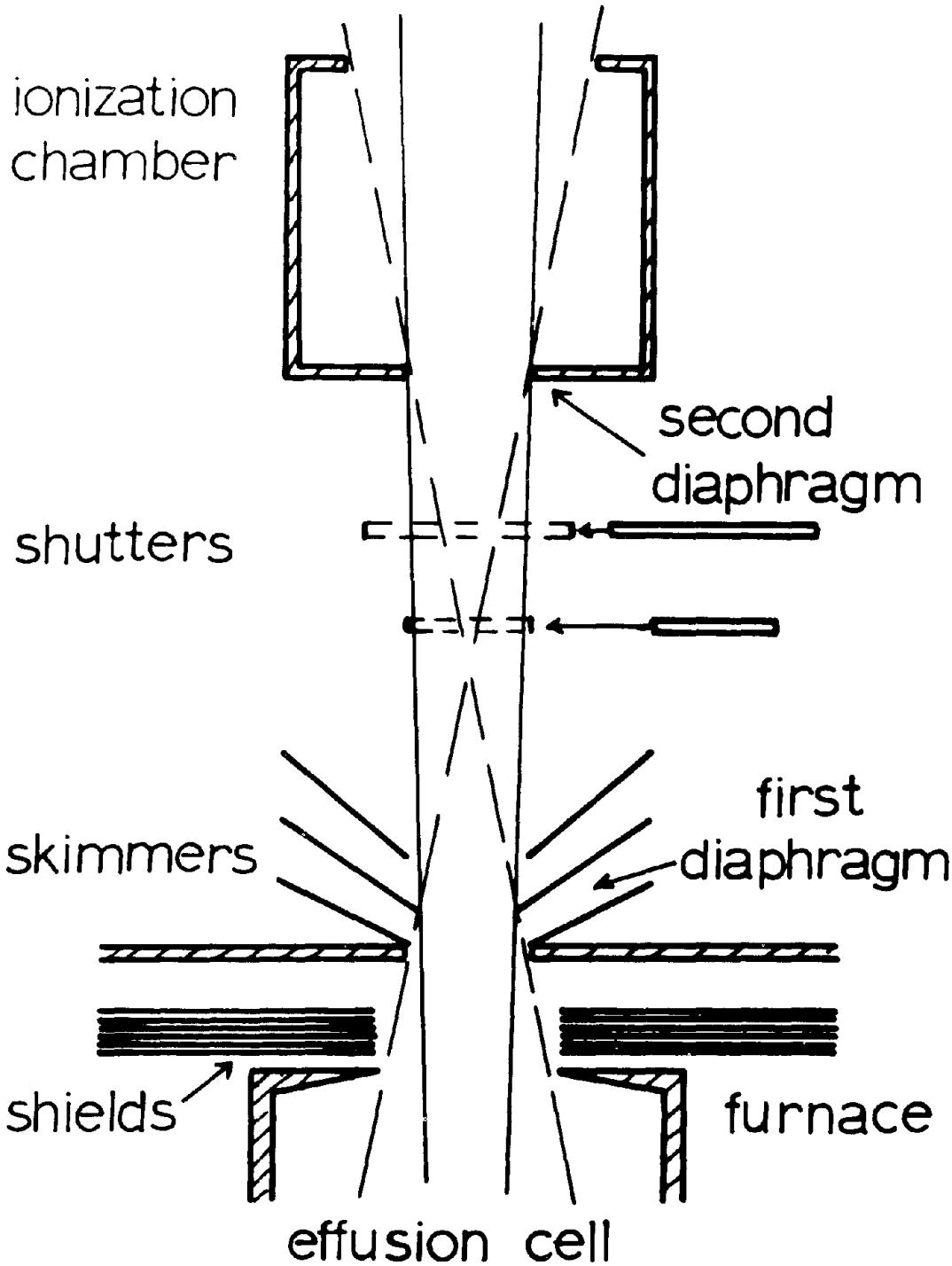


FIGURE 7. - Principle of the skimmer diaphragms. When the main molecular beam coming from the cell is intercepted by a shutter blade, the observed background is due to molecules traveling in the space between the second diaphragm and the upper skimmer. The skimmer's design decreases the amount of such molecules by reflecting away from the space molecules coming from the furnace zone.

The experiments were carried out at about 1,500 K. By changing the oxygen pressure in the cell by two or three orders of magnitude, it was possible to measure more accurately than usual the atomization energy of InO and In_2O. If compared with previous measurements, it seems that the accuracy was increased by a factor of 3, at least. The scattering of the results obtained by treatment according to the thermodynamic third law is about ± 0.3 pct. This corresponds to equilibria between solid In_2O_3 and several gaseous species within a temperature range of about 120 K and an O_2 pressure range from 5×10^{-9} atm to 10^{-5} atm.

If extended to higher temperatures, this kind of technique, whatever the nature of the oxygen supply, should certainly make mass spectrometry measurements easier to perform and also expand the field of applicability for this method.

CONCLUSION

The presentation of such a listing of error sources in thermodynamic measurements by mass spectrometry could give the impression that this is an unreliable method, whereas exactly the opposite is true. Indeed, it is the abundance of information provided by differential mass spectrometry that allows a very detailed analysis of various sources of error and therefore permits permanent improvements to be made. Some improvements are still necessary to bring the activity measurement accuracy into the 1 pct range whatever the system might be. Nevertheless, the general reliability of this method ought to be considered as high, particularly when cross-checking can be made.

As far as oxides are concerned, the mass spectrometry vapor pressure range corresponds roughly to temperatures stretching from eutectic points up to the melting points of pure oxides. This means that a wide range of liquid mixtures can be studied as well as their phase boundaries with solid compounds. Thus, both activity and Gibbs energy of formation data can be measured. This is specially true for alkaline earth oxides, transition metal oxides, and lanthanide and actinide oxides. The limitations are found in the relative thermal instability of some oxides (alkalines for instance) and in the high volatility of compounds such as metalloid or semimetal oxides.

Finally, differential mass spectrometry represents a unique method for studying thermodynamics of mixing of the most stable and nonvolatile oxides at temperatures in excess of 1,500 K.

REFERENCES

1. Allibert, M., and C. Chatillon. Can. Met. Quarterly, v. 18, 1979.

2. Allibert, M., C. Chatillon, and R. Lourtau. Proc. Colloque Internat. CNRS-IUPAC on Materials for High Temperature Energy Sources (French), June-July 1977, Odeillo, France.

3. Allibert, M., C. Chatillon, J. Mareschal, and F. Lissalde. J. Crys. Growth, v. 23, 1974, pp. 289-294.

4. Buchler, A., and J. B. Berkowitz-Mattuck. Ch. 2D in Physicochemical Measurements in Metals Research, v. IV, part 1, of the series "Techniques of Metals Research," ed. by R. F. Bunshah. John Wiley & Sons, Interscience Publishers, 1970.

5. Buchler, A., and J. L. Stauffer. Thermodynamics (AIEA, Vienna), v. 1, 1966, pp. 271-290.

6. Burns, R. P. J. Chem. Phys., v. 44, 1966, pp. 3307-3319.

7. Chatillon, C., M. Allibert, R. Moracchioli, and A. Pattoret. J. Appl. Phys., v. 47, 1976, pp. 1690-1693.

8. Chatillon, C., M. Allibert, and A. Pattoret. High Temp. Sci., v. 8, 1976, pp. 233-255.

9. _____. Advances in Mass Spectrometry, v. 7A, 1978, pp. 615-621.

10. _____. Proc. of Materials Research Symposium on Characterization of High Temperature Vapors and Gases, September 1978, Gaithersburg, Md.

11. Chatillon, C., C. Senillou, M. Allibert, and A. Pattoret. Rev. Sci. Instr., v. 47, 1976, pp. 334-340.

12. Daly, N. R. (ed.). Advances in Mass Spectrometry. Inorganic Application and High Temperature Chemistry. Heyden and Son Ltd., v. 7, 1978, pp. 545-692.

13. Ginsberg, M. J., Ph.D. Thesis, Univ. of Pennsylvania, 1969.

14. Kohatsu, I., and G. W. Brindley. Ztschr. Phys. Chem., v. 60, 1968, pp. 79-89.

15. Lourtau, R. Thesis, Université Scientifique at Médicale de Grenoble (France).

16. Margrave, J. L. (ed.). The Characterization of High-Temperature Vapors. John Wiley & Sons, Inc., 1967.

17. Martin-Garin, L., C. Chatillon, and M. Allibert. J. Less Common Metals, v. 63, 1979, pp. 9-23.

18. Pattoret, A., S. Smoes, and J. Drowart. Thermodynamics (AIEA, Vienna), v. 1, 1966, p. 377; Bull. Soc. Fr. Ceram., v. 77, 1967, pp. 75-90.

19. Quayle, A. (ed.). Advances in Mass Spectrometry. Inorganic Application and High Temperature Chemistry. Elsevier Pub. Co., v. 5, 1971, pp. 349-416.

20. Rutner, E., P. Goldfinger, and J. P. Hirth (eds). Condensation and Evaporation of Solids. Gordon and Breach Publishers, 1964.

21. Storms, E. K. Proc. Materials Research Symposium on Characterization of High Temperature Vapors and Gases, September 1978, Gaithersburg, Md.

22. West, A. R. (ed.). Advances in Mass Spectrometry. Inorganic Application and High Temperature Chemistry. Applied Science Publishers, v. 6, 1974, pp. 547-690.

DISCUSSION

N. A. Gokcen: What is the cell area versus orifice area? Do I understand that you had 1:1 ratio in one case?

M. Allibert: We have tried 1:1 just to see the effect, but we are not using it for this technique. We are just using it for comparison, this time we were comparing different values of the surface to orifice ratio ranging from 50-700.

N. A. Gokcen: You measure the equilibrium pressure over the bulk concentration, not the surface concentration, because the ratio of surface area to orifice area is large. Does this prevail in your cells?

M. Allibert: That is to say, the main assumption for the effusion technique is that the number of molecules leaving the surface and the number of molecules coming back to the same surface are almost the same. When this condition is satisfied, the analyzed gaseous phase is at equilibrium with the bulk condensed phase.

M. W. Chase: Are the data for aluminum oxide species measured or obtained from compilation?

M. Allibert. We used the JANAF tables.

M. W. Chase: Burns, at University of Chicago, has just done a mass spectrometric study on alumina, and there are indications that some of the data on gaseous aluminum oxides could be drastically changed.

M. Allibert: I have not seen the article, but that does not surprise me. Just because it is very difficult to look at all the oxide species from a technical point of view. As illustrated in my paper, each oxide species needs special conditions to be studied accurately. It was the main reason why we developed an oxygen injection technique.

N. A. Gokcen: I think this apparatus is well designed because it chops the molecular beam in such a way that it avoids the errors from surface diffusion. In other types of work, especially those involving oxygen, the atoms or molecules climb onto the sides and creep through the orifice and go to the side

and evaporate, but if the choppers are properly designed, they could eliminate the surface diffusion effect. Is that correct?

M. Allibert: Right, it was a very important problem.

VAPOR PRESSURE AND CALORIMETRIC STUDIES OF SELF-ASSOCIATION

by

J. Howard Rytting[1]

ABSTRACT

As examples of the many techniques that have been used to examine self-association, calorimetry and vapor pressure measurements are reviewed and compared. Calorimetry is attractive since it allows the calculation of both ΔG° and ΔH° simultaneously, is relatively rapid, and is applicable to a large variety of systems. A major disadvantage is that it requires the assumption that the enthalpy changes observed upon dilution are due only to the disaggregation of the polymeric species in solution. Vapor pressure measurements have the advantage that in most situations the vapor pressure of the solute is proportional to the monomer concentration in solution. Thus, the data directly reflect the concentration of a species of interest. For systems where both methods have been used, calorimetric data have usually been interpreted with association models of a lower order than corresponding data from pressure measurements. The combination of data derived from several techniques is probably desirable.

INTRODUCTION

Intermolecular interactions in various solutions have long been of interest to investigators in a number of disciplines. Consequently, a number of studies and techniques have been used to examine such interactions, including the solute-solute interactions that lead to self-association. For example, the breaking of hydrogen bonds that occurs on dilution of alcohols with a nonpolar solvent results in changes in enthalpies of mixing, partial molar volumes, dielectric properties, viscosities, infrared spectra, nuclear magnetic resonance, chemical shifts, ultrasonic absorption, vapor pressure, and other properties. Each of these has been used In studies of self-association, each has some disadvantages as well as advantages. Two of these methods will be considered in some detail in this presentation; namely, calorimetry and vapor pressure measurements.

CALORIMETRIC STUDIES

A number of studies have employed a calorimetric enthalpy of dilution technique to determine the thermodynamic quantities ΔG° and ΔH° for the self-

[1]University of Kansas, Lawrence, Kans.

association of compounds such as carboxylic acids (7, 17-19)[2] and alcohols (3, 14-16) where intermolecular hydrogen bonding can occur. It has also been used to study the self-association of 4,4',4",4'"-tetraoctadecylsulfonamido copper (II) phthalocyamine (6), and several trialkyl phosphates (10). This technique is attractive since it allows the calculation of both ΔG° and ΔH° simultaneously, is relatively rapid, and is applicable to many systems provided the heat evolved on dilution is sufficiently large. One disadvantage to the method is that it requires the assumption that the heat change measured upon dilution is due only to the disaggregation of the associated species in solution. There may be other contributions to the overall heat of dilution.

Heat of dilution studies have been made using various types of solution calorimeters including batch, titration, and flow microcalorimeters. The treatment of the data and calculation of the thermodynamic functions depend on the type of measurement made. For example, Woolley and Zaugg (17) describe calculations using apparent relative molar enthalpies, Φ_L. Anderson and coworkers (3) used a titration calorimeter to measure ΔH values for dilution from an initial concentration to a final concentration for several sets of concentrations, and then optimized the variables K and ΔH° until the best fit of the data was obtained. In all cases, the approaches involve fitting heat of dilution data obtained at various concentrations to yield constant K and ΔH° values.

Appropriate expressions can be developed to consider both monomer-single polymer models and monomer-multiple polymer models. Several of these have been described in the literature (3, 7, 14, 17).

VAPOR PRESSURE MEASUREMENTS

From a theoretical point of view, a method such as the determination of vapor pressure of a solute above a solution has advantages over many of the other available methods because the vapor pressure of the solute is proportional to the monomer concentration in solution, provided the polymer species are much less volatile than the monomer. Direct measurements of total vapor pressure have been made successfully for very volatile solutes (e.g., methanol) in nonvolatile solvents (e.g., n-hexadecanol) (11, 13). However, the determination of partial pressures of alcohols from measurements of total pressure is subject to greater error for longer chain alcohols having lower volatilities or in alkane solvents having shorter chain lengths and higher volatilities. Since we have been interested in studying a series of alcohols in more common volatile hydrocarbon solvents, a method involving the gas chromatographic analysis of the vapor in the headspace over solutions of alcohols in isooctane has been employed.

The gas headspace method has been used previously in the determination of

[2]Underlined numbers in parentheses refer to items in the list of references at the end of this paper.

alcohol content in blood, in the analysis of other volatile trace components, and in the estimation of activity coefficients of liquids in binary solution. The thermodynamic basis for the method is that, for a solution of a compound in equilibrium with vapor, the ratio between the fugacity of the substance in the vapor and its thermodynamic activity in the solution is a constant at a given temperature and pressure. At very low concentrations in a hydrocarbon solvent, alcohols are totally monomeric, and the ratio between the alcohol fugacity and its solution concentration is a constant. This constitutes a definition of Henry's law. The Henry's law constant, then, reflects the escaping tendency of monomer in a hydrocarbon environment. The techniques used in our laboratory are described in reference 2.

A primary assumption involved in determining monomer concentrations from vapor pressure data is that association of the monomer in the vapor is negligible. Cheam and coworkers (4) have shown that for methanol vapor at 25° C, self-association is negligible at vapor pressures lower than 30 to 40 torr. If other compounds behave similarly, nonideality in the vapor phase can be neglected provided the vapor pressures measured are less than 30 torr.

A second assumption that is made in this analysis is that the activity of the monomer is equal to its concentration (γ=1). This assumption is reasonable at low concentrations but may become less valid at higher concentrations. Therefore, generally only data at concentrations below 1 M are evaluated quantitatively in terms of a self-association model.

Several approaches can be used to derive association models and constants from vapor pressure data. In earlier studies (1-2, 9) of alcohol self-association, a monomer-single polymer model provided definite advantages in making comparisons among alcohols having different molecular structures. Although other, more complex models could be found to give slightly better fits of the data, a monomer-pentamer model provided a simple and reasonably accurate description of the primary alcohol and phenol vapor pressures at concentrations below 1 M. If a single polymer is dominant, the size of the polymer formed by self-association can be found graphically. A simple association constant can be written as

$$K_{1,n} = \frac{[n\text{-mer}]}{[\text{mon}]^n}. \qquad (1)$$

The total solute concentration (C_T) can be expressed as

$$C_T = [\text{mon}] + nK_{1,n}\,[\text{mon}]^n \qquad (2)$$

and

$$\log\,(C_T - [\text{mon}]) = \log(n \cdot K_{1,n}) + n \log\,[\text{mon}]. \qquad (3)$$

A plot of log (C_T-[mon]) versus log [mon] should yield a straight line with a slope of n, provided only one associated species is present. If more than

one polymer is present, upward curvature in the line will result.

The second approach used in analyzing vapor pressure data involved a least-squares computer-fitting technique similar to the simplex method reported by Deming and Morgan (5). The only constraint on the equilibrium constants using this method is the requirement that all values be positive. In all cases for primary alcohols a monomer-pentamer model gave significantly lower standard deviations than any other single-polymer model. In most cases a multiple-polymer model could be found that gave slightly better fits, and when chain branching occurs, we found that there was a gradual shift from pentamer to the dominance of tetramer and lower order polymers as the degree of branching increased (9).

The log-log plots and the least-squares fitting technique described above both require some assumptions regarding a self-association model. A model-independent method for estimating the average polymer size has been suggested by Tucker and Christian (12). This approach uses the following relationship:

$$C_T = [mon] + 2K_{1,2}\,[mon]^2 + 3K_{1,3}\,[mon]^3 + \ldots nK_{1,n}[mon]^n \qquad (4)$$

and the total species concentration

$$e = [mon] + K_{1,2}\,[mon]^2 + K_{1,3}\,[mon]^3 + \ldots K_{1,n}[mon]^n. \qquad (5)$$

Then

$$de/d[mon] = C_T/mon \qquad (6)$$

and

$$de = C_T/[mon]\; d[mon] \qquad (7)$$

$$e = \int_0^{mon} C_T/[mon]\; d[mon]. \qquad (8)$$

From the calculated e values, one can determine the average polymer size from

$$\text{polymer size} = \frac{C_T - [mon]}{e - [mon]}. \qquad (9)$$

We observed good agreement among all of these methods for the alcohol system studied.

COMPARISON OF CALORIMETRY WITH VAPOR PRESSURE MEASUREMENTS

A few systems have been studied using both a calorimetric technique and a vapor pressure method. Results of these studies are shown in table 1. In each of these cases the models preferred by the different techniques do not agree.

It is tempting to suggest that the calorimetric data are more suspect, since the assumption that there are no heat effects except disaggregation of associated species is probably less valid than the assumptions inherent in the vapor pressure measurements. The vapor pressure measurements should

TABLE 1. - Thermodynamic values for self-association of alcohols[1]

Substance	Calorimetry				Vapor pressure			
	Model	$K_{1,n}$	$\Delta H°$	Ref.	Model	$K_{1,n}$	$\Delta H°$	Ref.
Phenol	1-3	21.3	-10.95	14	1-5	2,660	[2]	1
1-Propanol	1-4	555	-21.4	3	1-5	8,600	[2]	2
1-Butanol	1-4	587	-21.4	3	1-5	8,700	-22.7	9
1-Pentanol	1-4	657	-21.1	3	1-5	9,400	[2]	2
1-Hexanol	1-4	673	-21.1	3	1-5	10,000	[2]	2
1-Heptanol	1-4	633	-21.2	3	1-5	10,900	[2]	2
1-Octanol	1-4	691	-21.2	3	1-5	10,300	[2]	2

[1]The phenol data are reported for solutions in cyclohexane. Isooctane was used as solvent for the primary alcohols. The $\Delta H°$ values are given in kilocalories per mole.
[2]No data.

directly reflect monomer concentration in solution and therefore should deserve more confidence. Unless the data have extremely high precision, however, it is probably unwise to place undue physical significance on the models derived from either approach. Rather small errors can have a profound effect on the best fit to various models. Even the choice of how to treat the data from the same experiment can influence the model chosen. For example, in a vapor pressure study of phenol self-association (1), we observed that the choice of the "best" multiparameter model depended on whether deviation between calculated and experimental values of monomer concentration or total phenol concentration was minimized. In that study variation between experimental and calculated values of monomer was minimized because monomer concentration was the experimentally determined quantity.

A recent study by Lin and coworkers (8) of the self-association of phenol in cyclohexane favored a 1-3-∞ model. We repeated the curve fitting of their data, modifying our computer program to minimize variation in either monomer or total phenol concentration. It was found that a 1-3-∞ model best fit their data when formal molarity is treated as the dependent variable, whereas a 1-5-∞ model is best when monomer molarity is treated as the dependent variable. This difference in "best" model is probably due to a difference in weighting of individual data points in different concentration ranges by the two methods. When only a single polymeric species is allowed, a monomer-pentamer model fits our data within experimental error.

When comparing data for similar compounds differing in molecular structure, the simplest model that gives a reasonable fit of the data offers distinct advantages, since such models tend to be less sensitive to subtle

changes and experimental errors. For example, the self-association of tert-butyl alcohol was studied at 15°, 25°, and 35° (9). The models giving the best fit were 1-4-5 at 15°, 1-3-4 at 25°, and 1-3-5 at 35° C. Since subtle changes influenced these choices, comparison using either a 1-4 model in all cases or a 1-4-5 model in all cases was preferred.

If one is primarily concerned with the relative differences among a group of compounds or environmental conditions, the choice of method is probably not critical as long as it is sensitive to those differences. One would expect that calorimetrically determined heats of self-association would be preferred to those determined from the slopes of plots of log $K_{1,n}$ versus 1/T. However, if there are significant heat effects other than disaggregation of the polymeric species, error could result.

The absolute choice of models with confidence in regards to a physical interpretation probably requires consideration of data obtained from several techniques.

ACKNOWLEDGEMENT

This work was supported by a grant from the National Institutes of Health (GM22357).

REFERENCES

1. Anderson, B. D., J. H. Rytting, and T. Higuchi. Influence of Self-Association on the Solubility of Phenol in Isooctane and Cyclohexane. J. Am. Chem. Soc., v. 101, 1979, pp. 5194-5197.

2. _____. Vapor Pressure Studies of Self-Association of Alcohols in Isooctane. I. The Effect of Chain Length. Internat. J. Pharm., v. 1, 1978, pp. 15-31.

3. Anderson, B. D., J. H. Rytting, S. Lindenbaum, and T. Higuchi. A Calorimetric Study of the Self-Association of Primary Alcohols in Isooctane. J. Phys. Chem., v. 79, 1975, pp. 2340-2344.

4. Cheam, V., S. B. Farnham, and S. D. Christian. Vapor Phase Association of Methanol. Vapor Density Evidence for Trimer Formation. J. Phys. Chem., v. 74, 1970, pp. 4157- 4159.

5. Deming, S. N., and S. L. Morgan. Simplex Optimization of Variables in Analytical Chemistry Anal. Chem., v. 45, 1973, pp. 278A-283A.

6. Graham R. C., G. H. Henderson, E. M. Eyring, and E. M. Woolley. Molecular Associations in Nonaqueous Solvents. 1. Thermodynamics of Dye-Dye Interactions in CCl_4 and C_6H_6. J. Chem. Eng. Data, v. 18, 1973, pp. 277-279.

7. Krishnan, T., W. C. Duer, S. Goldman, and J. L. Fortier. On the Use of Dilution Calorimetry in the Study of Hydrogen-Bonding Self-Association Reactions: Benzoic Acid in Benzene. Can. J. Chem., v. 57, 1979, pp. 530-537.

8. Lin, L-N., S. D. Christian, and E. E. Tucker. A Solute Activity Study of the Self-Association of Phenol in Cyclohexane and Carbon Tetrachloride. J. Phys. Chem., v. 82, 1978, pp. 1897-1901.

9. Rytting, J. H., B. D. Anderson, and T. Higuchi. Vapor Pressure Studies of Self-Association of Alcohols in Isooctane. 2. The Effect of Chain Branching. J. Phys. Chem., v. 82, 1978, pp. 2240-2245.

10. Rytting, J. H., A. Goldkamp, and S. Lindenbaum. Heats of Dilution of Trialkyl Phosphates in Isooctane and Carbon Tetrachloride: Interpretation in Terms of Self-Association. J. Solution Chem., v. 4, 1975, pp. 1005-1010.

11. Tucker, E. E., and E. D. Becker. Alcohol Association Studies. II. Vapor Pressure, 220-MHz Proton Magnetic Resonance and Infrared Investigations of tert-Butyl Alcohol Association in Hexadecane. J. Phys. Chem., v. 77, 1973, pp. 1783-1795.

12. Tucker, E. E., and S. D. Christian. Alcohol Association Studies. 3. Vapor Pressure Measurements for the Ethanol-n-Hexadecane System. J. Phys. Chem., v. 81, 1977, pp. 1295-1299.

13. Tucker, E. E., S. B. Farnham, and S. D. Christian. Association of Methanol in Vapor and in n-Hexadecane. A Model for the Association of Alcohols. J. Phys. Chem., v. 73, 1969, pp. 3820-3829.

14. Woolley, E. M., and L. G. Hepler. Molecular Association of Hydrogen Bonding Solutes. Phenol in Cyclohexane and Benzene. J. Phys. Chem., v. 76, 1972, pp. 3058-3064.

15. Woolley, E. M., and D. S. Rushforth. Molecular Association of Hydrogen Bonding Solutes, o-, m- and p-Cresol, in Carbon Tetrachloride. Can. J. Chem., v. 52, 1974, pp. 653-660.

16. Woolley, E. M., J. G. Travers, B. P. Erno, and L. G. Hepler. Molecular Association of Hydrogen-Bonding Solutes. Phenol in Carbon Tetrachloride. J. Phys. Chem., v. 75, 1971, pp. 3591-3597.

17. Woolley, E. M., and N. S. Zaugg. Thermodynamics of Intermolecular Self-Association of Hydrogen Bonding Solutes by Titration Calorimetry. Anal. Calorim., v. 3, 1974, pp. 479-488.

18. Zaugg, N. S., S. P. Steed, and E. M. Woolley. Intermolecular Hydrogen Bonding of Acetic Acid in Carbon Tetrachloride and Benzene. Thermochim. Acta., v. 3, 1972, pp. 349-354.

19. Zaugg, N. S., L. E. Trejo, and E. M. Woolley. Intermolecular Hydrogen Bonding of Chloro-substituted Acetic and Propionic Acids in Carbon Tetrachloride. Thermochim. Acta, v. 6, 1973, pp. 293-298.

DISCUSSION

L. D. Hansen: Does the choice of standard state, in this case we chose a molarity, affect the results, particularly at high concentrations?

J. H. Rytting: We have not analyzed our data in terms of a self-association model at concentrations above 1 molar because we felt that the potential activity coefficient corrections were sufficiently great that perhaps we could not distinguish between association and corrections. Although we have the data at high concentrations, we have only considered concentrations below 1 molar, and the choice did not seem to make any difference at these lower concentrations. There have been some reports (Ben-Naim, for example) that have suggested that molarity is the preferred standard state for these situations. However, Tanford and others have suggested the use of the mole fraction scale.

Anonymous: Are the nonideal heats of dilution closely related to the activity coefficient?

J. H. Rytting: They may well be. They may account for the fact that there are differences in terms of the results obtained using the vapor pressure technique compared with the calorimetric technique. We noticed that on occasion the model chosen is quite sensitive to small changes in the data. The differences in the fits that one finds when comparing the 1-4 model with the 1-5 model are not so great that small differences in experimental data couldn't account for them. Even though the two techniques seem to suggest different models, fairly small experimental differences could account for that.

Anonymous: Are there some density and volume measurements on these particular systems?

J. H. Rytting: In these solvents, I am not aware of any. Marsh and Burfitt have reported excess volumes for ethanol in several organic solvents.

N. A. Gokcen: The dissociation and association in solutions also includes the electrolyte solutions. I think that one can devise a model based on dilute solutions and consider that the model still exists at higher concentrations, and any change from that is then reflected in the activity coefficient. At the present time there is no absolutely dependable measurement technique for concentrations of different species except possibly in very dilute solutions.

J. H. Rytting: Mentioning again, for polar organic nonelectrolytes, such as the alcohols in hydrocarbon, it was found that there was greater association for the compounds having lower chain lengths; for instance, propanol seemed to exhibit greater association than did octanol at high concentrations. For those cases, one could suggest that one actually gets larger aggregates occurring at higher concentration. Because of the potential activity problems (which should not be as great as with electrolytes, however), it may be diffi-

cult to distinguish which effects are really related to association and which may be due to other deviations from ideality. By assuming still larger aggregates at higher concentrations, one can account for the data. However, we felt uncomfortable doing that.

C. M. Criss: I want to ask whether you have tried a series of hydrocarbons. Hydrocarbons are similar to the alcohols - you can't very well use propane - but perhaps, substituting octane for octanol as a solute compound, you can see what the properties of these model compounds are in your various organic solvents. In this way you can sort out the difference of what is happening because of the hydrogen bonding between solute molecules, and the effects because of interactions between the hydrocarbon groups in the alcohols.

J. H. Rytting: We have looked at the heat of mixing to some extent. Say, for example, one were to choose octane and iso-octane, the heat of mixing is much less than what one finds with the alcohols, so that it is insignificant compared with the other heat. We have not done any vapor pressure measurements of that type, and maybe it would be worthwhile doing some.

TORSION-EFFUSIVE STUDY OF THE CATALYZED THERMAL DECOMPOSITION OF MAGNESIUM SULFATE

by

D. R. Knittel[1], K. H. Lau[2], and D. L. Hildenbrand[2]

ABSTRACT

The simultaneous use of the torsion-effusion and gravimetric-effusion methods in our laboratory is discussed. This method is used to study the thermal decomposition and/or vaporization of $MgSO_4$, enabling us to distinguish between the decompostion paths $MgSO_4(s) = MgO(s) + SO_3(g)$ and $MgSO_4(s) = MgO(s) + SO_2(g) + 1/2\ O_2(g)$. In the temperature range of our measurements $MgSO_4$ decomposed by the first path with $SO_3(g)$ evolution. When mixed with a first-row transition metal oxide lying between Cr and Cu or a metal (namely Pt or Ru), $MgSO_4$ decomposed by the second path, yielding SO_2 and O_2 as the vapor species. Measurements of the decomposition pressure as a function of orifice area show that both steps are kinetically hindered. A Whitman-Motzfeldt plot was used to obtain equilibrium pressures which were used to obtain the standard enthalpy of formation for $MgSO_4$.

INTRODUCTION

The simultaneous measurement of torque angle (torsion-effusion method) and rate of weight loss (gravimetric-effusion method) is a combination method whereby one is able to measure both pressure and vapor molecular weight. This method is used to measure pressures below the molecular flow region (10^{-4} atm and less). In our laboratory we routinely make pressure measurement in the 10^{-8} atm range. The pressure measured using the torque angle along with the rate of weight loss is used to determine the vapor molecular weight. The temperatures at which these measurements can be made are limited only by the refractory material and the ingenuity of the investigator.

The torsion-effusion-gravimetric-effusion technique is a combination of

[1]Formerly with SRI International, Menlo Park, Calif; now with Standard Oil of Indiana, Naperville, Ill.
[2]SRI International, Menlo Park, Calif.

two classical effusion techniques--the Knudsen effusion method (7)[3] and the torsion-effusion method (11). The Knudsen effusion method involves determination of the weight loss $\dot{\omega}_i$ of the vapor effusing in unit time through an area A_i. The Knudsen effusion pressure P_k is related to $\dot{\omega}_i$ by

$$P_k = (2\pi RT/M)^{1/2} \sum_{i=1}^{n} (\dot{\omega}_i / A_i C_i) \tag{1}$$

where R is the gas constant, T is the absolute temperature, M is the molecular weight of the effusing species, and C_i is the orifice Clausing factor (1). The sum is carried over all n orifices. If we make the assumption that $\dot{\omega}_i$ is proportional to A_i times the probability term C_i, then equation 1 can be rewritten as

$$P_k = (2\pi RT/M)^{1/2} \dot{\omega} / \sum_{i=1}^{n} A_i C_i, \tag{2}$$

where $\dot{\omega} = \sum_{i=1}^{n} \dot{\omega}_i$. P_k is then obtainable from measureable quantities provided the molecular species are known. If more than one molecular species is present in the effusion vapor, M is a weighted average molecular weight

$$M = \left(\sum_{i=1}^{r} m_i M_i^{-1/2} \right)^{-2}, \tag{3}$$

where m_i is the mass fraction of species i and M_i is its molecular weight. The summation is over all the vapor species effusing from the sample. An obvious limitation to vapor pressure determination by this method is the required knowledge of the vapor molecular weight.

The second technique, the torsion-effusion method, does not require knowledge of the molecular composition of the effusing vapor to evaluate the effusion pressure. In this method a torque resulting from effusion of vapor through holes of area A_i and at distances d_i from the suspension axis of the cell is determined from the angle δ through which the torque twisted the torsion suspension faber. The torsion pressure of the P_T of the effusing vapro is related to the torque angle δ by

$$P_T = 2k\delta / \sum_{i=1}^{n} A_i f_i d_i, \tag{4}$$

where k is the fiber torsion constant, f_i is the ratio of the force from the

[3]Underlined numbers in parentheses refer to items in the list of references at the end of this paper.

effusion of vapor through orifice i of finite length to the expected force if the orifice had an infiniesimal length (3), and the sum is again carried over all orifices.

The torsion-effusion-gravimetric-effusion method involves simultaneously measureing the torque angle δ and the rate of weight loss $\dot{\omega}$. The measured torque angle δ is used in equation 4 to determine the torsion pressure. The torsion pressure obtained in equation 4 is identical to the Knudsen pressure defined in equation 2. By substituting P_T and the measured weight change $\dot{\omega}$ into equation 2, the weighted average molecular weight is determined. The resulting equation is

$$M = 2\pi RT \{ \dot{\omega} (\sum_{i=1}^{n} A_i f_i d_i) / (2k\delta \sum_{i=1}^{n} C_i A_i)\}^2. \quad (5)$$

For further discussion of the terms in equations 2 through 5 the reader is referred to Freeman (2) and Hildenbrand (4-5).

The measured effusion pressure P is a steady-state pressure and will at its maximum value be equal to the equilibrium pressure P_{eq}. In order to interpret P in terms of P_{eq}, the vaporization coefficients and resistance of gas flow through the effusion cell and out the orifice must be considered. This has been done very adequately by Whitman (12) and Motzfeldt (9). Their equation relating P_{eq} to P and cell constants is

$$P_{eq} = P (1+\beta \sum_{i=1}^{n} C_i A_i), \quad (6)$$

where β is a constant characteristic of a particular cell configuration. Equation 6 is used to extract equilibrium pressures from effusion data exhibiting pressure dependence on orifice size. Note that as the orifice size approaches zero the effusion pressure approaches P_{eq}. P_{eq} is obtained by plotting $1/P$ against the summation of $C_i A_i$ where the intercept is $1/P_{eq}$ and the slope is β/P_{eq}. The β value gives an indication of the kinetic hindrance of the vaporization process. To a first approximation β equals $(\alpha A_s)^{-1}$ where A_s is the effective vaporization surface area and α is the vaporization coefficient. If α equals one, there is no kinetic barrier and the pressure measured by the torsion-effusion method is independent of orifice area and equal to P_{eq}. A vaporization process for which no orifice area dependence is observed and thus possesses no detectable kinetic barrier is the thermal decomposition of KCl. A process that shows a substantial decrease in pressure with increasing orifice area is the thermal decomposition of metal sulfates (8).

EXPERIMENTAL WORK

In our experimental arrangement for the simultaneous torsion-effusion and gravimetric-effusion study, the torsion element and the effusion cell are

suspended directly from the arm of a Cahn RH electro-balance. The torsion apparatus is encased in a vacuum chamber since the effusion method is limited to the free-molecular-flow region. The region of the apparatus containing the effusion cell is equipped with temperature control to ±0.2° C. Heating in our system is accomplished using an electrical resistance furnace. In our torsion-effusion-gravimetric-effusion system the cell is placed between molybdenum heat shields in the central constant-temperature range of the furnace. The molybdenum heat shields help eliminate heat losses out the end of the furnace. The thermocouple junction is located adjacent to the sample chamber in this constant-temperature region.

In our experience a Pt-10 pct Ni ribbon with a 10-to-1 aspect ratio has proven to be the best type of torsion fiber in regard to reproducibility of the null point, uniformity of properties, strength, and ease of mounting. Others have used tungsten and quartz with varying degrees of success. (See reference 2 for a discussion of these fibers.) The fibers used in our torsion systems are typically 50 cm long and capable of holding at least 300g. We arrived at our torsion fiber constant k by using the torsion-pendulum treatment, which is normally done under dynamic conditions. The value for k obtained agrees within 0.5 pct of the value specified by the manufacturer, Sigmund Cohn Corp. The torsion angle δ is measured manually by sighting onto a mirror that is fixed on an aluminum damping disk with a telescope and scale. Harmonic oscillations of the suspension system induced by extraneous perturbations are damped by magnets placed on either side of the damping disk. During measurement of the torque angle δ, damping magnets are removed to avoid spurious torques that might arise from ferromagnetic deposits on the damping disk.

Common effusion cell fabrication material includes graphite, quartz, alumina, and platinum. The type of refractory material used depends upon the effusion process one wishes to study. From the standpoint of materials, graphite and quartz effusion cells are the cheapest to fabricate. In our sulfate work we used alumina cells because these cells did not interact with the sample. Our alumina cells were fabricated from resin-bonded alumina powder and subsequently fired. These cells consisted of two 1-cm-diameter cylindrical chambers 3 cm long mounted on either side of the suspension axis with two alumina bridges. The orifices were situated at the upper third of the sample chamber and alined so that the suspension axis is normal to the line connecting the orifices. Closure of the cells was provided by tight-fitting tapered alumina plugs. The geometrical factors, which include orifice area and distance of the orifice from the suspension axis, are measured using a traveling microscope. As a check on possible systematic errors, the vapor pressure of KCl is measured with each new cell. Acceptable cell constants are constants that yield pressures and molecular weights for KCl within 5 pct of pressure values reported by Pugh and Barrow (10) and the known vapor molecular weight. In our sulfate work, which exhibited pressure dependence on orifice size, we studied the decomposition process using cells with orifice sizes ranging between 0.2 and 0.03 cm.

The sample chambers of the cell should be evenly loaded with sufficient sample to provide a large enough vaporizing surface area. The sample loading

should be handled under anhydrous conditions. The rest or null point of the cell in the vacuum chamber is measured by sighting the angle through the telescope when no vapor is effusing through the orifice. The null point must be constant for a set of measured pressures. In our effusion studies normally 15 to 20 min. were required at a constant temperature before a torsion angle measurement could be made. The pressures measured varied only over a few tenths of a percent from the log P versus 1/T line defined by the measurements. The weight loss rate required more time to measure since it is not an instantaneous measurement, as is pressure. The vapor molecular weight calculated from the weight loss measurement is normally within 5 pct of the actual value. The additional errors in measuring tha vapor molecular weight arise from errors in both the pressure and weight loss measurements.

EXAMPLE

Table 1 summarized data obtained in our laboratory using the torsion-effusion and gravimetric-effusion methods simultaneously to study $MgSO_4$ decompositon. The table demonstrates the effect on pressure and vapor molecular weight of different catalyst additions to $MgSO_4$. The level of catalyst addition was 4 mole-pct in each instance. $MgSO_4$ with no catalyst addition has a vapor molecular weight of 81.5 ± 2. This is consistent with the process

$$MgSO_4(s) = MgO(s) + SO_3(g) \qquad (7)$$

whose average vapor molecular weight for $SO_3(g)$ is 80.1. With the addition of an appropriate metal or metal oxide catalyst (Pt, Zr, Cr_2O_3, CuO, Fe_2O_3, and Mn_2O_3), the average vapor molecular weight is about 55. This is consistent with the process

$$MgSO_4(s) = MgO(s) + SO_2(g) + 1/2\ O_2(g) \qquad (8)$$

whose average vapor molecular weight is 54.6. In addition to the lower vapor molecular weight, a substantially higher pressure is observed with the addition of the catalyst. In the case of a 4-mole-pct Pt addition to $MgSO_4$, a pressure of 32×10^{-6} atm at 1,000 K is obtained, compared with 0.54×10^{-6} atm for noncatalyzed $MgSO_4$. We have found using our torsion-effusion apparatus without the microbalance that CoO, NiO, and Ru also markedly increase the decomposition pressure and thus are effective catalysts. These results are presented in Series II of table 1. There are differences in the parameters of the two cells used, which make comparison between the two series impossible.

In the case of 4-mole-pct Fe_2O_3 additions to $MgSO_4$, we compared the effect on both pressure and vapor molecular weight of Fe_2O_3 mixed intimately and layered over the surface of $MgSO_4$. $MgSO_4$ with an Fe_2O_3 catalyst clearly decomposes to $SO_2(g) + 1/2\ O_2(g)$. However, in the case of Fe_2O_3 layered on $MgSO_4$, the partial catalysis of $SO_3(g)$ evidenced by a vapor molecular weight of 60.8±1 takes place in the gas phase and not at the site of $SO_3(g)$ evolution from $MgSO_4(s)$ lattice. A 1.5 times pressure increase compared with pure $MgSO_4$ decomposition is observed, which agrees with the volume change accompanying $SO_3(g)$ decomposing to $SO_2(g) + 1/2\ O_2(g)$.

TABLE 1. - Effect of various oxides[1] on gas composition over $MgSO_4$ and on decompositon pressure at 1,000 K

Additive	$P_{1000} \times 10^6$, atm	$\overline{M}$	A^2	B^2
	SERIES I (CELL Al_2O_3-I)[3]			
Pt	32.1	57.1±3	11.48±0.11	15,973± 98
Cr_2O_3	14.4	55.7±2	10.01± .16	14,846±144
CuO	13.6	56.4±1	10.92± .07	15,790± 63
Fe_2O_3	12.2	53.7±1	11.15± .07	16,068± 68
Mn_2O_3	7.8	53.3±2	10.38± .10	15,483± 96
Fe_2O_3 (surface layer)	.79	60.8±1	9.45± .68	15,555±662
None	.54	81.5±2	9.27± .12	15,542±120
	SERIES II (CELL Al_2O_3-II)			
Cr_2O_3	8.0	---	10.07±0.17	15,172±164
CoO	5.1	---	10.40± .04	15,692± 37
Ru	3.4	---	9.86± .05	15,324± 44
NiO	2.7	---	10.66± .08	16,228± 79
ZnO	.71	---	9.55± .10	15,699±105
V_2O_4	.65	---	10.73± .13	16,924±129
MgO	.30	---	10.12± .14	16,646±149
Al_2O_3	.35	---	9.61± .20	16,076±212
TiO_2	.41	---	10.15± .23	16,567±249
Y_2O_3	.28	---	8.48± .13	15,039±133
None	.34	---	7.86± .11	14,336±111

[1]For addition level of 4 mole-pct
[2]Coefficients of vapor pressure equation
log P(atm) = A - (B/T)
[3]Orifice diameter of cells Al_2O_3-I and Al_2O_3-II is 1.5 mm.

The last two columns of table 1 contain the coefficients of the vapor pressure equation log P (atm) = A - B/T. The temperature coefficient B is independent of the catalyst. The heat of reaction derived from each of these temperature coefficients coincides with the heat of reaction 6 derived in the noncatalyst case. This suggests that the thermal decomposition of $MgSO_4$ proceeds via reaction 7 followed by $SO_3(g)$ decomposition

$$SO_3(g) = SO_2(g) + 1/2\ O_2(g)$$

if a catalyst is present. If the catalyst is dispersed in the sulfate powder, reaction 9 can take place close to the site of SO_3 evolution, and the overall reaction rate is characterized by the equilibrium constant of reaction 8. If

the catalyst is removed from $SO_3(g)$ evolution sites, as in the case of Fe_2O_3 layered on $MgSO_4$, the overall reaction rate is characterized by the equilibrium constant of reaction 7 even though SO_2 and O_2 are the gas decompositon products.

An orifice size study was made with pure $MgSO_4$, $MgSO_4$ with 4 mole-pct Fe_2O_3, and $MgSO_4$ with 4 mole-pct Pt. The results for the first two systems are reported by K. H. Lau and coworkers (8). The change of pressure with hole size is given for the case of Fe_2O_3 and Pt catalyst additions to $MgSO_4$ at 1,000 K in a Whitman-Motzfeldt plot illustrated in figure 1. A substantial

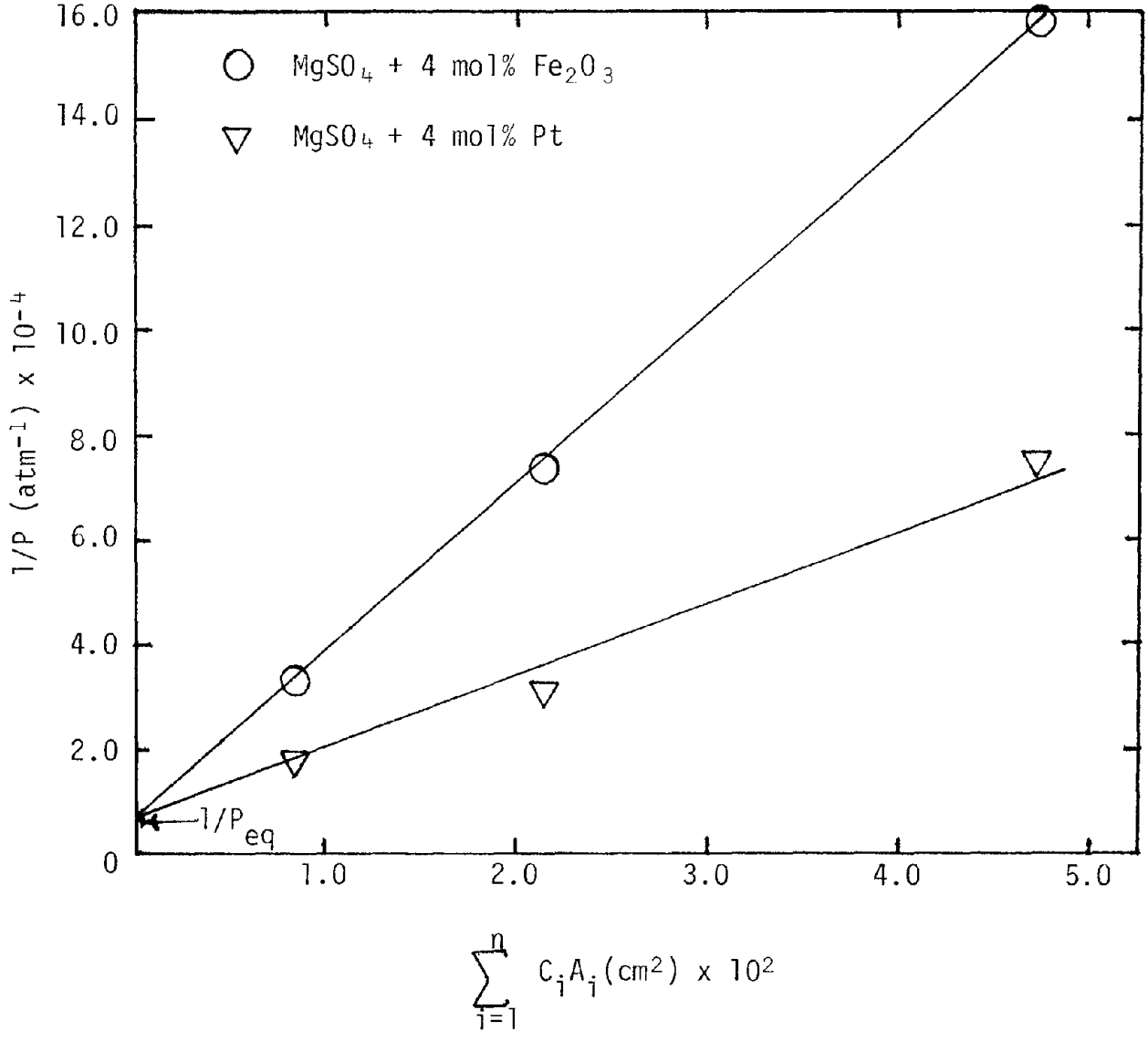


FIGURE 1. - Whitman-Motzfeldt plot for $MgSO_4$ decomposition pressures at 1,000 K.

trend of pressure with orifice area, as evidenced by the slope β, indicates the vaporization process is kinetically hindered. Extrapolation to zero hole size gives a total pressure of 1.08×10^{-4} atm at 1,000 K, which agrees closely with the value 1.07×10^{-4} atm at 1,000 K, calculated for reaction 8 from available free energy functions (10). As expected, these two catalysts, even though having vastly different steady-state torsion pressures, extrapolate to the same equilibrium pressure.

The standard enthalpy of decomposition of $MgSO_4$ is calculated using $\Delta H^\circ_{298} = -T(\Delta fef + RlnK)$, where Δfef is the free energy function and K is the equilibrium constant of reaction 7 or 8. In the case of $MgSO_4$ thermal decomposing without a catalyst, K = P, where P is the total effusion pressure. In the catalyzed process, because of different molecular weights of SO_2 and O_2 and the effect on effusion rates, the partial pressures within the cell require the ratio of $P_{(SO_2)}/P_{(O_2)} = 2\sqrt{2}$ rather than 2.0. With this requirement the stoichiometries of the solid phases and the effusing gas are maintained. The equilibrium constant in this case is related to the total effusion pressure P by the expression $K = P^{3/2}/2\sqrt{2}$. The $\Delta Hf_2{}^\circ{}_{98}(MgSO_4,s)$ = -310.0 ± 0.6 kcal/mole derived using $\Delta H^\circ_{298}(7)$ = 72.6 ± 0.5 kcal/mole, which was calculated using noncatalyzed $MgSO_4$ effusion data; and $\Delta Hf^\circ_{298}(MgSO_4,s)$ = -310.7 ± 0.6 kcal/mole using $\Delta H^\circ_{298}(8)$ = 97.0 ± 0.5 kcal/mole, which was calculated using effusion data for $MgSO_4$ catalyzed with 4 mole-pct Fe_2O_3. The standard enthalpy of decomposition of $MgSO_4$ calculated from effusion data agrees with -311.0 obtained from Kellogg's review (6).

This example demonstrates the usefulness of the simultaneous torque angle and weight loss rate measurements in enabling us to distinguish between the two vaporization processes. Without knowledge of the effusing vapor species, we never would have reached the present level of understanding of this complex decomposition process. The use of the torsion-gravimetric-effusion method to study a complex vaporization process such as the one described has not been reported previously by any other group.

SUMMARY

The effusion method with simultaneous torsion angle and weight loss rate measurements is an excellent method for studying the complex vaporization process and for extracting equilibrium data even for very kinetically hindered processes. This can be done within the limit of 5 pct of vapor molecular weight. By making careful analysis one can learn much about reaction mechanisms using this effusion method.

REFERENCES

1. Clausing, P. The Flowing of Very Dilute Gases Through Tubes of Any Length. Ann. Physik., 12, 1932, p. 961.

2. Freeman, R. D. Ch. in Characterization of High Temperature Vapors, ed. by J. L. Margrave. John Wiley & Sones, Inc., New York, 1967, pp. 152-192.

3. Freeman, R. D., and A. W. Searcy. The Effect of Channel Holes on the Force Exerted by Effusing Vapors. J. Chem. Phys., v. 22, 1954, p. 762.

4. Hildenbrand, D. L., and W. F. Hall. The Vaporization behavior of Born Nitride and Aluminum Nitride. J. Phys. Chem., v. 43, 1963, p. 888-893.

5. Hildenbrand, D. L., and D. T. Knight. Composition of Saturated Beryllium Chloride Vapor. J. Chem. Phys., v. 51, 1969, p. 1260.

6. Kellogg, H. H. A Critical Review of Sulfation Equilibriums. Trans. AIME, v. 230, 1964, p. 1622.

7. Knudsen, M. Effusion and the Molecular Flow of Gases Through Openings. Ann. Physik., 28, 1909, p. 999.

8. Lau, K. H., D. Cubicciotti, and D. L. Hildenbrand. Effusion Studies of the Thermal Decomposition of Magnesium and Calcium Sulfates. J. Chem. Phys., v. 66, 1977, p. 4532.

9. Motzfeldt, K. The Thermal Decomposition of Sodium Carbonate by the Effusion Method. J. Phys. Chem., v. 59, 1955, p. 139.

10. Pugh, A. C. P., and R. F. Barrow. Heats of Sublimation of Inorganic Substances. V. Alkali Metal Fluorides. Trans. Faraday Soc., v. 54, 1958, p. 671.

11. Searcy, A. W., and R. D. Freeman. Determination of Molecular Weights of Vapors at High Temperatures I. The Vapor Pressure of tin and the Molecular Weight of Tin Vapor. J. Am. Chem. Soc., v. 76, 1954, p. 5229.

12. Whitman, C. I. The Measurement of Vapor Pressures by Effusion. J. Chem. Phys, v. 20, 1952, p. 161.

DISCUSSION

R. W. Carling: Even though we observed from thermodynamic data that SO_2 and oxygen are the most favorable for reactions, why do we see SO_3 as the decomposition gas in your experiments?

D. R. Knittel: The reason is that the decomposition of SO_3 to SO_2 is the decomposition gas. A catalyst is needed to attain thermodynamically stable SO_2 and O_2.

G. T. Furukawa: Do you know by what route the JANAF table value was obtained, and can you account for the difference between your value and their value?

D. R. Knittel: I don't know by what route the JANAF table data were obtained. Their value is $\Delta H^\circ_{298} = -301 \pm$ kcal for $MgSO_4$.

M. W. Chase: The JANAF tabulation for $MgSO_4$ is outdated; the choice of the ΔH°_f value was incorrect.

D. R. Knittel: The NBS value for ΔH°_{298} is -307 kcal ± 5 kcal for $MgSO_4$. Our measurements are within their uncertainty limits. Kellogg's value for ΔH°_{298} is -311 kcal and is very close to -310.6 ± 0.6 kcal obtained in our laboratory.

M. W. Chase: Kellogg and the NBS apparently had the same data to analyze; I would be more concerned why those two studies differ. I am not disputing your number. The JANAF tabulation for $MgSO_4$ needs to be revised; there are at least three new studies relating to $\Delta G^\circ f$.

R. D. Freeman: What is the sensitivity of your balance with that load on it?

D. R. Knittel: We use 10 mg full scale. Weight loss rates of 0.5 mg/ph are easy to measure and give molecular weights to within 5 pct. The measurement requires about 2 hours.

R. D. Freeman: In your equation for torsion pressure, you had a symbol for the distance between the effusion orifices. I would have thought that it should be the distance between the effusion orifice and the rotation axis. There is a factor of two involved; maybe that is taken care of someplace, but it was not apparent to me that it was.

D. R. Knittel: You are correct. We have assumed, however, that the orifice area A_i and force factor f_i for each hole are identical. Thus, for the two orifices, the sum of $A_i f_i d_i$ becomes $Af(d_1 + d_2)$, where d_1 and d_2 are the distances between the orifice centers and the suspension axis. These two terms added give d, the distance between the orifice centers.

R. W. Carling: How do you measure your torsion angles?

D. R. Knittel: By sighting through a mirror onto a linear scale. By knowing the reading when no gas is effusing from the cell and comparing this number to the readings taken at a temperature where gas effuses, we are able to obtain pressure.

Anonymous: Have you any idea what the catalysts do?

D. R. Knittel: Currently we think that the catalyst catalyzes SO_3 to SO_2 plus oxygen, close to the sites where SO_3 is being expelled from the lattice. A more complete explanation is given in the paper.

N. A. Gokcen: If the orifice area to the inner area is fairly small, and the walls above the compound are perfectly reflecting, you should have equilibrium irrespective of the catalyst, but if the condensation coefficient is very small, then you have difficulties reaching equilibrium. Is it because of the orifice size, or the walls, or the condensation coefficient that you cannot obtain the sulfate - $SO_2 = SO_3 - O_2$ equilibrium?

D. R. Knittel: I think we attribute it to the condensation and vaporization coefficients.

J. B. Stephenson: Have you looked at vanadium pentoxide as a catalyst?

D. R. Knittel: Yes, but at $MGSO_4$ decomposition temperatures, vanadium pentoxide changed to V_2O_4, which does not appear to have much catalytic effect.

A. Adams: But there is no magnesium sulfate in the vapor phase.

D. R. Knittel: But there is solid magnesium sulfate in the cell, and I think what we are talking about is the ease with which the vapor can leave the solid. When it hits and sticks on the solid magnesium sulfate, the equilibrium in the gas phase is difficult to attain.

THE USE OF THE TORSION-EFFUSION AND THE MASS SPECTROMETRIC METHODS TO STUDY COMPLEX VAPORIZATION PROCESSES

by

K. H. Lau[1] and D. L. Hildenbrand[1]

ABSTRACT

This paper illustrates the technique of combining the torsion-effusion and mass spectrometry methods to study the complex vaporization process of $K_2SO_4(s)$. Both the sublimation and decomposition processes contribute to the total vaporization flux. The total vapor pressures and vapor molecular weights were measured by the torsion-effusion method. The vaporization processes were studied by use of mass spectrometry to identify and characterize the vapor species over the $K_2SO_4(s)$. The sublimation pressures, vapor composition, heats of sublimation, and decomposition pressure were calculated from directly measured total vapor pressures, known decomposition pressures, and the second-law slope heats derived from the temperature dependence of parent ions. Heat of formation and entropy of $K_2SO_4(g)$ were derived from this study. The advantages of this combined technique are discussed.

INTRODUCTION

It is difficult to determine the vaporization thermodynamics of substances that vaporize by molecular sublimation as well as by decomposition. Taking K_2SO_4 as an example, previous vaporization studies as reviewed recently by Eliezer and Howard (3)[2] had suggested the following possible reactions:

$$K_2SO_4(s \text{ or } \ell) = K_2SO_4(g), \tag{1}$$

$$K_2SO_4(s \text{ or } \ell) = 2K(g) + SO_2(g) + O_2(g), \tag{2}$$

and

$$K_2SO_4(s \text{ or } \ell) = K_2O(g) + SO_2 + 1/2\ O_2(g). \tag{3}$$

Halstead (2) studied the vaporization both by the transpiration method in

[1]SRL International, Menlo Park, Calif.

[2]Underlined numbers in parentheses refer to items in the list of references at the end of this paper.

which $SO_2 + O_2$ mixtures were used as carrier gas to suppress the decomposition reaction 2 and by the Knudsen effusion method with the assumption that the decomposition reaction 2 was negligible in the vapor pressure calculations. The reported vapor pressures from these two methods were conflicting with others (5, 10) not only in the vapor pressures values, which were different by an order of magnitude, but also in the assumption of vaporizatin by sublimation reaction. Recent mass spectrometric studies on K_2SO_4 vaporization were also in disagreement. Ficalora and coworkers (4) easily observed the decomposition reaction 2, while Kosugi (10) suggested reaction 3 as the major process from his studies. Total sublimation pressures were also reported from the mass spectrometric studies with uncertain accuracy because of uncertainty over the relative ionization cross sections of various vapor species. Clearly, the determination of the sublimation pressures of K_2SO_4 was complicated by the simultaneous decomposition reaction.

The purpose of this paper is to suggest a different approach to obtain accurate thermodynamic data for such complex vaporization processes. The total vapor pressures can be measured by the torsion-effusion method, a purely mechanical technique that requires no information about the vapor composition. The simultaneous mass effusion rate measurements allow one to determine the average molecular weight of the effusing vapor and to derive valuable information about vapor composition. The mode of vaporization was characterized and the heat of sublimation was determined by the mass spectrometric method.

For illustration of this combined method to determine vapor pressure as well as the vapor composition, our recent studies (11) on the vaporization of K_2SO_4 are given in this paper as an example. Two modes of vaporization reactions (1 and 2) were defined, and the composition of vapor was determined. The derived sublimation pressures and heat of sublimation measurements led to evaluation of the heat of formation and the entropy of K_2SO_4 vapor.

EXPERIMENTAL METHODS

Torsion-Effusion Plus Mass Loss Method

The apparatus used in these studies was the same as that described in earlier papers on ZrI_4 and $BeCl_2$ (1-2). Details of this method were given in our recent studies on metal sulfate decomposition (12). Briefly, the total pressures P in the effusion cell are evaluated from the measured angular displacement θ by means of the relation

$$P = 2\ K\ \theta/\Sigma\ af\ q, \qquad (4)$$

where k is the fiber torsion constant and a, f, and q are the area, force factor, and moment arm of each of the effusion orifices, respectively. When the mass effusion rate is measured simultaneously with the angular displacement, the vapor molecular weight of effusing vapor $\overline{M}$ can be calculated from the expression

$$\bar{M} = 2\pi RT\{[\dot{w}(\Sigma af\ q)]/[2\ k\ \theta(\Sigma\ Ca)]\}^2, \quad (5)$$

where R is the gas constant, T is the absolute temperature, $\dot{w}$ is the total rate of mass loss, and C is the orifice Clausing factor. In a complex vapor, $\bar{M}$ is a weight average molecular weight, evaluated from the relation

$$\bar{M} = [\Sigma m_i M_i^{-1/2}]^{-2}, \quad (6)$$

where m_i and M_i are the mass fraction and the molecular weight of the i gaseous species. Therefore, the vapor species and the mode of vaporization must be characterized in order to use the calculated molecular weight equation 6 and the measured molecular weight to evaluate the vapor composition and to derive the sublimation pressures from the total pressures measured by the torsion-effusion method.

The effusion cell material should be inert to the sample. In these studies the effusion cells were fabricated from Pt-30 pct Rh alloy. The cell configuration was described in our previous paper (11). Two effusion cells with orifice diameters of 0.06 and 0.11 cm were used in the vapor pressure measurements. The constants of each cell were checked by measuring the vapor pressure of KCl. Both cells gave results within 5 pct of the values reported by Pugh and Barrow (14). The measured molecular weights of KCl with the 0.06-cm-diameter cell were within 2 pct of the molecular weight of KCl. This cell was used for the average molecular weight measurement.

Mass Spectrometric Method

The mass spectrometer equipped with a high-temperature Knudsen cell molecular beam source was the same as described previously (8). A movable beam defining slit placed between the Knudsen cell and the ion source is used to distinguish between the vapor species generated from the Knudsen cell and those present as background. Vapor species generated from the platinum Knudsen cell were ionized by electron impact, and the mass spectra were recorded and identified by mass to charge ratio m/e, isotopic abundance, and measurements of appearance potential and ionization efficiency curves. After the sample had been outgassed, the measurements of the temperature dependence of ion intensity I_i^+ of each vapor species were made by varying the temperature randomly. The second-law heats of each vapor species are determined from least-squares fitting of log (I^+T) as a function of reciprocal temperature, since the ion intensity I_i^+ is related to the pressure P_i by the simple relation $P_i = \frac{kI^+T}{\sigma_i}$, where k is the mass spectrometer constant, T is the absolute temperature, and σ_i is the ionization cross section.

K_2SO_4 VAPORIZATION STUDIES

Material

The K_2SO_4 sample was reagent-grade material of 99.9-pct purity. X-ray diffraction patterns taken before and after the measurements showed only the presence of the low-temperature orthorhombic form of K_2SO_4, although our meas-

urements at 1,180 to 1,280 K were assumed to be on the equilibrium hexagonal. Chemical analyses of the decomposition residue gave no traces of sulfite, oxide, or sulfide, indicating that K_2SO_4 vaporized congruently.

Total Vapor Pressure

The vapor pressure measurements were made in the range 1,180 to 1,280 K with the Pt-30 pct Rh effusion cells PR-1 (0.11-cm-diameter orifice) and PR-2 (0.06-cm-diameter orifice). The results are given in figure 1. The measured vapor pressures show an orifice size dependence, indicating a kinetic barrier to the vaporization process. The derived equilibrium total pressures shown in figure 1 are obtained from the extrapolation of the vapor pressure data to zero Orifice area, using the Whitman-Motzfeldt model (1, 12-13, 15).

The average vapor molecular weights measured with the PR-1 cell are consistent and yield the average value M = 110 ± 5, independent to temperature. This measured value is lower than the molecular weight of K_2SO_4 (174.3) for sublimation reaction 1, but it is significantly higher than the value M = 44.3 for decomposition reaction 2, calculated from equation 6. As seen from figure 1, the derived equilibruim total pressure is a factor of about 2.7 larger than the calculated pressure P_D for decompostion reaction 2 evaluated from thermochemical data (10). It is clear from these results that both molecular sublimation and decomposition are major contributions to the total vaporization flux and to the resultant total vapor pressure.

Vapor Species Identification and Ion Intensity Measurements

The mass spectra of the vapor species over $K_2SO_4(s)$ were examined. The $K_2SO_4^+$, K^+, SO_2^+, O_2^+, and K_2O^+ ions were detected. The low appearance potentials $AP(K_2SO_4^+)$ = 8.4 ± 0.3 ev, $AP(K^+)$ = 4.5 ± 0.3 ev, and $AP(SO_2^+)$ = 12.4 ± 0.5 ev indicate that they are all parent ions. It was difficult to obtain an accurate AP for beam O_2^+ in the presence of normal background O_2^+, but the value was near 12 ev, close to the ionization potential of O_2. On the other hand, the appearance potential of K_2O^+ was measured as 11.5 ± 0.5 ev, clearly a fragment ion, since it is expected that the ionization potential $IP(K_2O) \cong IP(K)$. In fact, Gusarov and Gorokhov (6) have reported an approximate value of 5 ev for IP (K_2O). The decomposition reaction (3) concluded by Kosugi's studies (10) is in error. No SO_3 was detected in spite of a careful search. Therefore, the mode of vaporization can be described completely by sublimation reaction 1 and decomposition reaction 2.

The temperature dependences of the intensities of $K_2SO_4^+$, K^+, and SO_2^+ were measured over the range 1,170 to 1,300 K. Second-law heats of each ion were derived from least-squares analysis of log (I^+T) as a function of reciprocal temperature, with the results shown in table 1. Second-law heats of the three ions show very little variation and are in accord with the slope heats derived from the total pressures determined by the torsion method, ΔH_{1222} = 75.2 ± 0.4 kcal/mole (cell PR-1) and ΔH_{1240} = 75.9 ± 0.3 kcal/mole (cell PR-2). The second-law heats for K^+ and SO_2^+ agree closely with the corresponding slope heat of 75.1 ± 0.3 kcal/mole at 1,230 K calculated from accurate

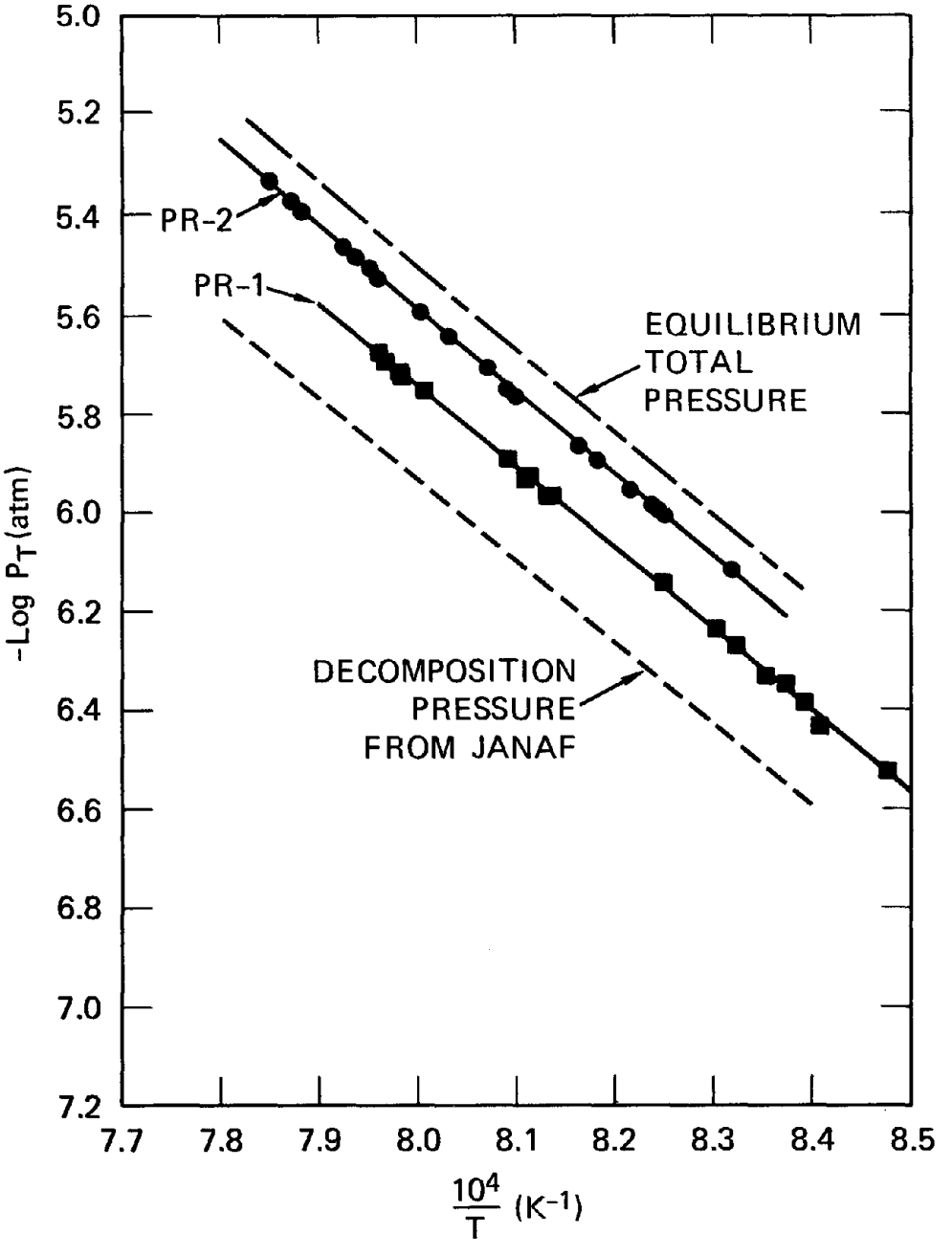


FIGURE 1. - Total pressure over $K_2SO_4(s)$ measured with two platinum-rhodium effusion cells, showing relation to extrapolated equilibrium pressure and calculated pressure for decomposition process $K_2SO_4(s) = 2K(g) + SO_2(g) + O_2(g)$.

thermochemical data (2) for reaction 2. Also the K^+ at 7 ev ionizing energy and the K^+ at 30 ev, which must include some fragmentation of K_2SO_4, show essentially the same temperature dependence. All these evidences point to the fact that reactions 1 and 2 have nearly equal temperature coefficients.

TABLE 1. - Second-law slope heats derived from ion temperature dependences

Ion	Electron energy, ev	Data points	Tavg, ° K	ΔH_T, Kcal/mole
$K_2SO_4^+$	15	9	1,218	76.3 ± 2.0
	15	10	1,252	73.9 ± 0.3
K^+	7	9	1,218	76.0 ± 1.0
	7	9	1,241	74.4 ± 0.7
	30	10	1,245	74.1 ± 1.6
SO_2^+	17	9	1,218	76.2 ± 0.8

Determination of Vapor Composition

Since the vaporization processes are now clearly established, it is possible to calculate the vapor composition from the total pressure data. The total pressure is contributed from the following sublimation and/or decomposition reaction of K_2SO_4:

$$K_2SO_4(s) = (1 - b)\ K_2SO_4(g) + 2b\ K(g) + b\ SO_2(g) + b\ O_2(g), \qquad (7)$$

where b is the fraction of K_2SO_4 decomposed. Then following the expression from equation 6, the average molecular weight M can be calculated in terms of b

$$\overline{M} = \left[\frac{(1-b)\ M_{K_2SO_4}^{1/2} + 2b\ M_K^{1/2} + b\ M_{SO_2}^{1/2} + b\ M_{O_2}^{1/2}}{(1-b)\ M_{K_2SO_4} + 2b\ M_K + b\ M_{SO_2} + b\ Mb_{O_2}}\right]^{-2}. \qquad (8)$$

The partial pressure of $K_2SO_4(g)$, $P_{K_2SO_4}$, and equilibrium total pressure, P_T, obtained from the Whitman-Motzfeldt extrapolation to zero orifice area are related to b by the expression

$$\frac{P_{K_2SO_4}}{P_T} = \frac{(1-b)\ M_{K_2SO_4}^{1/2}}{(1-b)\ M_{K_2SO_4}^{1/2} + 2b\ M_K^{1/2} + b\ M_{SO_2}^{1/2} + b\ M_{O_2}^{1/2}} \qquad (9)$$

The first approach to evaluate b is to use the directly determined vapor molecular weight data to solve for the b value from equation 8; the sublimation pressure can be calculated from equation 9, and vapor composition is then determined. Since the total effusion pressure P_D of the decompostion reaction (2) can be calculated accurately from thermochemical data (9), the second and better approach is used to determine the vapor composition. The partial pressure of K_2SO_4, $P_{K_2SO_4}$, is calculated from the relation $P_{K_2SO_4} = P_T - P_D$. The ratio $P_{K_2SO_4}/P_T$ is used to obtain the b value from equation 9, and the average molcular weight M is calculated from equation 4. the derived vapor pressure data are shown in table 2. In the range of measurements the values of

$R(P_{K_2SO_4}/P_T)$, b , and M vary little with temperature. the calculated molecular weight, M=116 ± 1, is in excellent agreement with the directly determined molecular weight, M=110 ± 5. The sublimation pressure of $K_2SO_4(g)$ accounts for 63 pct of the total pressure under the effusion conditions.

TABLE 2. - Derived vaporization data for $K_2SO_4(s)$

T(K)	$P_T \times 10^7$, atm	$P_D \times 10^7$, atm	$P_{K_2SO_4} \times 10^7$, atm	R	b	$\overline{M}$
1,180	5.07	1.94	3.13	0.618	0.237	114.6
1,200	8.74	3.31	5.43	.622	.235	115.1
1,220	14.79	5.55	9.24	.624	.233	115.5
1,240	24.60	9.16	15.44	.628	.230	115.9
1,260	40.26	14.88	25.38	.630	.228	116.3
1,280	64.90	23.81	41.04	.634	.226	116.8
1,300	103.08	37.55	65.53	.636	.224	117.0

The thermodynamic data of $K_2SO_4(g)$ were derived in detail in our previous paper (11). The heat of sublimation of $K_2SO_4(g)$ derived from mass spectrometric studies as given in table 1 leads to the standard heat of formation $\Delta H^\circ_{298}(K_2SO_4, g) = -257.0 \pm 1.5$ kcal/mole. From the slope heat and the absolute pressure of $K_2SO_4(g)$, one evaluates the entropy $S^\circ_{1200}(K_2SO_4, g) = 135.8 \pm 1.2$ cal/deg-mole.

REFERENCES

1. Cubicciotti, D., and K. H. Lau. J. Electrochem. Soc., v. 125, 1978, p. 972.

2. Dow Chemical Co., Thermal Research Laboratory. JANAF Thermochemical Tables, 2d ed. NSRDS-NBS 37, U.S. Government Printing Office, Washington, D.C, 1971, 1141 pp.

3. Eliezer, I., and R. A. Howard. J. Chem. Phys., v. 65, 1976, p. 3053.

4. Ficalora, P. F., O. M. Uy, D. W. Muenow, and J. L. Margrave. J. Am. Ceram. Soc., v. 51, 1968, p. 574.

5. Gorokhov, L. N. Annual Report, Institute for High Temperature. Academy of Sciences, U.S.S.R., 1975.

6. Gasarov, A. V., and L. N. Gorokhov. High Temp. (UUR), v. 4, 1966, p. 558.

7. Halstead, W. D. Trans. Faraday Soc., v. 66, 1970, p. 1966.

8. Hildenbrand, D. L. J. Chem. Phys., v. 48, 1968, p. 3657; v. 52, 1970, p. 5751.

9. Hildenbrand, D. L., and D. L. Knight. J. Chem. Phys., v. 51, p. 1260.

10. Kosugi, T. Bull. Chem. Soc. Japan, v. 45, 1972, p. 15.

11. Lau, K. H., D. Cubicciotti, and D. L. Hildenbrand. J. Electrochem. Soc., v. 126, 1979, p. 490.

12. _____. J. Chem. Phys., v. 66, 1977, pp. 4532.

13. Motzfeldt, K. J. Phys. Chem., v. 59, 1955, p. 139.

14. Pugh, A. C. P., and R. F. Barrow. Trans. Faraday Soc., v. 54, 1970, p. 671.

15. Whitman, C. I. J. Phys. Chem., v. 20 1952, p. 161.

DISCUSSION

R. W. Carling: Isn't the decomposition of SO_3 and SO_2 and oxygen the same way with potassium or magnesium sulfate? Once you get SO_3 into the gas phase, then it becomes the same problem.

K. H. Lau: I wanted to mention to you that this one decomposes at a lot higher temperature. We measured it at about 1,200 K, but in the magnesium sulfate we measured it at about 1,000 K. We also did some work on calcium sulfate; in that case, we detected SO_2 and oxygen. When you go up to high temperatures, for instance with calcium sulfate, barium sulfate, and strontium sulfate, you will see SO_2 and oxygen under equilibrium conditions.

R. W. Carling: Did you think this when you are evolving SO_2 and oxygen right from the cell?

K. H. Lau: This is what we propose. We did try very hard to look at the SO_3, but we could not find any.

N. A. Gokcen: I think the concentration of SO_3 is very small at low pressures and high temperatures. Probably less than 1 pct.

K. H. Lau: Yes.

A. Landsberg: Does the fact that you use an effusion cell and the escaping vapors are actually in the cell for a finite time have any effect on the SO_2, SO_3 ratio? What is the effect of the effusion orifice on the decomposition products?

K. H. Lau: We used two different orifice sizes to measure them and analyze them. One was 0.8 mm and the other 1.5. We found out there was essentially no change in the decomposition of the gas phase. Then we found a ratio of potassium sulfate to potassium and compared that with the larger orifice. We found essentially the same ratio.

M. W. Chase: Did you also study all the other alkali metal sulfates?

K. H. Lau: I am beginning to study sodium sulfate. I did observe the sodium sulfate molecules in the gas phase. But the ionization cross sections are very close to that of potassium sulfate. I think that the ratio for the sodium sulfate to sodium is a lot less than that for potassium sulfate to potassium. We believe that the sodium sulfate in gas phase would be about 15 to 20 pct. We are going to do that. This is our plan for the next year.

M. W. Chase: What about the other sulfates?

K. H. Lau: The other sulfates - calcium sulfate was done, but it decomposes to form an oxide. We feel that the result for calcium sulfate agrees very well, within 1 kcal.

M. W. Chase: You haven't published that have you?

K. H. Lau: We published that along with magnesium sulfate in 1977. It was our first paper. We used that as a model compound to check if this method really worked. We can derive highly accurate thermodynamic data on this sulfate.

L. D. Hansen: How is the catalyst distributed in your sample?

K. H. Lau: It does not matter in this case. The catalyst is what we want here. What we really measure is the total pressure. We derived that data from the vapor equilibrium.

R. W. Carling: In decomposition of potassium sulfate, would you expect to find SO_3?

K. H. Lau: We are looking at a much higher temperature. I think the temperature is the main effect; as Dr. Gokcen mentioned, at this high temperature, the ratio of SO_3 to SO_2 is very small. Also demonstrated in our work on magnesium sulfate, it does not matter what kind of steady-state pressure you get, the derived equilibrium pressure always gives you the correct equilibrium pressure. This is demonstrated by using different catalysts; platinum and chromium oxide give you different steady-state pressures, but you get the same derived equilibrium pressure.

Anonymous: Have you studied the alkali chromates?

K. H. Lau: No. The decomposition reactions for the chromates form chromium oxide as a solid phase. We hope to investigate it in the future.

N. A. Gokcen: After having spent more than 5 years on torsion cells, we went back to the gravimetric cell by using a microbalance; we thought that the advantages of the microbalance are far more than the few advantages that the torsion cell could have. The problem with the torsion cell is that the filament from which you hang the cell has to be calibrated each time, and often it has to be calibrated two or three times a year because it changes its characteristics. What are your reasons for preferring the torsion-effusion cells over the gravimetric-effusion cells?

K. H. Lau: I think people used a tungsten filament in the past. There were a lot of problems using it, - it was very brittle and easy to break. As Dr. Gokcen says, the torsion constant changes, but what we are using is a Pt-10 pct Ni fiber. This fiber is exceedingly stable. I have been working on the same fiber for about 2-1/2 years, and I constantly check the torsion constant. It always agrees within less than 0.1 pct. The beauty of this fiber is that you can hang very heavy weights on it. It does not change the constant at all. Of course, you take into account this possibility. We calibrate this fiber with the weight, which is almost equal to the weight of our torsion effusion cell. Because if you use the heavier weight you have a slightly larger torsion constant. One of the advantages for the torsion-effusion cell is that we are studying very complex vapors. Now in the regular weight loss you have the molecular weight term. You have to know what is in the vapor in order to get that molecular weight and calculate the total pressure. Of course, if you are looking at just a very simple sublimation, molecular weight would be equal to the molecular weight of the gas. In the torsion-effusion-plus-weight-loss method, it requires no knowledge of vapor composition to evaluate the total pressure.

M. W. Chase: When you do work on sodium sulfate, it seems to me you are going to have a horrendous problem knowing what the material is that you started with. In potassium sulfate, you have two crystal phases. I don't think there is any ambiguity at a certain temperature as to what you've got, but sodium sulfate has five different phases and when you get up above 1,000° they are not well characterized and you never know what you've got. What are you going to do to solve that problem?

K. H. Lau: According to the recently revised JANAF Tables, we are looking at a high-temperature phase, I forgot what phase it is. I believe that sodium sulfate has a lot lower vapor pressure. We have to melt it, so we study the liquid-gas equilibrium. When you are looking at a liquid phase, you always run into the problem of the liquid creeping out of the orifice and breaking off the cell. I think we can manage this problem by putting a packing of very fine platinum wire into the cell. Then when sodium sulfate melts, the surface tension will hold this liquid and platinum together. The same difficulty is also encountered with chromates.

J. Haygarth: Another complication appears to be in the liquid, and that is, as it decomposes, its composition will change. Do you foresee a problem in that?

K. H. Lau: I believe that potassium sulfate vaporizes congruently. In our potassium sulfate studies we are very careful in analyzing the residue materials. Take an X-ray, do some chemical analysis. What we find is that only the potassium sulfate is there. If we are going to do the sodium sulfate, we are going to do the same thing, make sure that the compound vaporized congruently.

EXPERIMENTAL METHODS FOR DETERMINING THE GIBBS ENERGIES OF METAL SULFIDES[1]

by

Kenneth C. Vlach[2] and Y. Austin Chang[2]

ABSTRACT

Experimental methods involving heterogeneous equilibria in the determination of Gibbs energies of formation of metal sulfides are reviewed. The methods covered include direct sulfur vapor pressure measurements, equilibrium with gas mixtures, and solid electrolyte galvanic cells. Calorimetry and techniques involving effusion into a vacuum are not covered.

INTRODUCTION

Determination of the Gibbs energy of formation of a metal sulfide is based on measurement of the equilibrium constant of the reaction

$$n\ M(s) + S_2(g) = n\ MS_{2/n}(s) \tag{1}$$

$$K = \frac{(a_{MS_{2/n}})^n}{(a_M)^n (a_{S_2})}. \tag{2}$$

As the activities of $MS_{2/n}(s)$ and $M(s)$ are unity,

$$\Delta G = -RT\ \ell n\ K = RT\ \ell n\ a_{S_2}. \tag{3}$$

For convenience, the standard state of sulfur is commonly chosen as $S_2(g, 1\ atm)$. Thus, ΔG_f° of the metal sulfide is found by determining its equilibrium sulfur partial pressure. As sulfur vapor may contain significant amounts of species other than S_2, a correction to the partial pressure p_{S_2} is

[1]This research is supported by the Division of Materials Research, National Science Foundation (DMR-78-04066).

[2]Formerly with the Materials Department, College of Engineering and Applied Science, University of Wisconsin - Milwaukee, Milwaukee, Wisc. Now with the Department of Metallurgical and Mineral Engineering, University of Wisconsin-Madison, Madison, Wisc.

sometimes necessary (especially at low temperatures and high pressures). Let it suffice here to say that this subject has been well covered; for example, see the work of Rau and coworkers (41)[3] and Wakihara and coworkers (56).

Means of determining the sulfur activity versus composition relationship (as a function of temperature) may be classified as to whether the sulfur activity is fixed by (1) the vapor pressure (or gas mixture), (2) the sample composition, or (3) the total amount of sulfur in a closed system.

Methods in which the sulfur activity is fixed by independently controlling the vapor pressure (or gas mixture) include static methods such as the buffered isopiestic types, dynamic methods such as thermogravimetric analysis (TGA) and buffered recirculatory systems, and some electromotive force (EMF) methods. (Buffered indicates the use of a two-phase reservoir to fix p_{S_2}.) The sample composition is the dependent variable that must be determined. These methods are best suited for single-phase (condensed) regions of binary systems.

Methods in which the sulfur activity is fixed by the sample include direct pressure measurement, the so-called indicator isopiestic-type methods, the dewpoint method, some EMF methods, and such dynamic methods as the gas entrainment method. Here the vapor pressure (or gas composition) must be determined. These methods are best suited for two-phase regions, but are useful for single-phase regions (where it may be necessary to determine the sample composition).

Methods in which the sulfur activity is controlled by the total amount of sulfur in a closed system include the static stepwise reduction method and dynamic systems such as nonbuffered recirculatory systems. These methods are suitable for both single- and two-phase regions. Either the gas or the sample composition (or both) may be measured, as one determines the other; generally, the gas composition is measured, since it may be done more easily and accurately.

The procedure that will be followed here is to classify the experimental methods as static, dynamic, or EMF techniques as outlined below:

Static Methods

Direct pressure measurement
- Mechanical methods
- Absorption methods

Isopiestic-type methods
- Buffer methods
- Indicator methods

Dewpoint method

Stepwise reduction method

[3]Underlined numbers in parentheses refer to items in the list of references at the end of this paper.

Dynamic Methods

Sulfur activity fixed by the gas stream
Means of controlling p_{S_2}
Gas mixtures
Carrier gas methods

Means of sample analysis (nondestructive)
Thermogravimetric analysis
Tarnish methods

Sulfur activity fixed by the sample
Circulating methods
Transportation and entrainment methods

Sulfur activity determined by mutual equilibration

Solid-Electrolyte EMF Methods

Conventional EMF methods
Isopiestic EMF method

STATIC METHODS

Direct Pressure Measurement

Direct measurement is theoretically the simplest means of determining the sulfur vapor pressure of a sample. However, it is complicated by the corrosiveness and the compositional makeup of sulfur vapor and the relatively high temperatures involved. Generally, a custom-made apparatus of silica glass is used, either partially or totally within a furnace.

Mechanical Methods

The most common means of measuring sulfur vapor pressure are the all-silica spiral and Bourdon gages. These almost identical instruments are operated by the same technique. The vapor pressure within the curved gage body causes a slight elastic deformation which moves the pointer from the null position. Then an externally measured gas pressure is applied to the outside of the gage until the pointer returns to the null position, at which time the sulfur vapor pressure is equal to the external gas pressure. Figure 1 shows a silica spiral gage used by Rau (35). A Bourdon gage differs only in that a broadened half-spiral is used. Since the sulfur vapor comes from the sample, the sample composition is corrected accordingly. To minimize error of this type, relatively large samples are used to reduce available vapor space. The gage may be kept either at the same temperature as the sample or at an arbitrarily fixed temperature. Sensitivity may be limited by thermal fluctuations in the vapor or the external gas (34). The Bourdon gage is usually used in

the pressure range 1 torr to 1 atm (29). By using a silica Bourdon gage in an isothermal furnace within a pressure vessel containing a viewing window, Rau (39) studied the $Co_{1-\delta}S$ system at pressures and temperatures up to 150 atm and 1,368 K.

A means of directly measuring lower sulfur vapor pressures is the Rodebush low-pressure manometer adapted by Leegaard and Rosenqvist (23) for use at high temperatures. Their apparatus, shown in figure 2, was used for measurements in the range 0.001 to 1 torr. The vapor pressure above the sample is determined by noting the decrease in the tension in the silica helix necessary to support the disk against the sealing flange. The stopcock and nylon thread at the top are used as a pulley to adjust the tension in the helix. This apparatus is only suitable for studying pressures above two-phase regions, since a small amount of sulfur vapor is lost during measurement.

Absorption Methods

Pemsler and Wagner (31) measured the equilibrium vapor pressure of sulfur for various Cu-Fe-S compositions using an ultraviolet absorption spectrometer. The silica sample vessel was placed in a multi-temperature zone furnace such that the sample temperature could be varied while the absorption path was kept at 700° C (fig. 3). Two absorption bands were used, so that a p_{S_2} range of of 1.5×10^{-5} to 0.04 atm could be measured.

Isopiestic-Type Methods

These methods depend upon sulfur vapor equilibration of a sample with a reference material (which either fixes or indicates the sulfur activity) within a sealed vessel. Isothermal methods are isopiestic; those that maintain different sample and reference temperatures are given the name pseudoisopiestic (30). Isopiestic-type methods can only be used for those systems where the metal is ~nonvolatile at the relevant temperature.

Buffer Methods

In the buffered isopiestic-type methods, the sulfur activity is fixed by a reservoir of buffer material (either liquid sulfur or a two-phase reference sulfide) at constant temperature, which maintains a constant sulfur vapor pressure. Buffer methods are most applicable to the study of single-phase regions. The experimental unknown is the sample composition. It may be monitored continuously by means of a balance or radioactive means, or it may be determined at the end of a run by quenching and analysis. The continuous methods have the advantage of showing when equilibrium has been reached; the disadvantage is the necessarily more intricate apparatus. Winn and Steele (60) used a sample vessel mounted on a pivot and attached to a recording microbalance to measure the transfer of sulfur between a standard sulfide and a Ti_xS_2 sample. A correction was made for the weight of vapor in the temperature gradient tube. The apparatus is shown in figure 4.

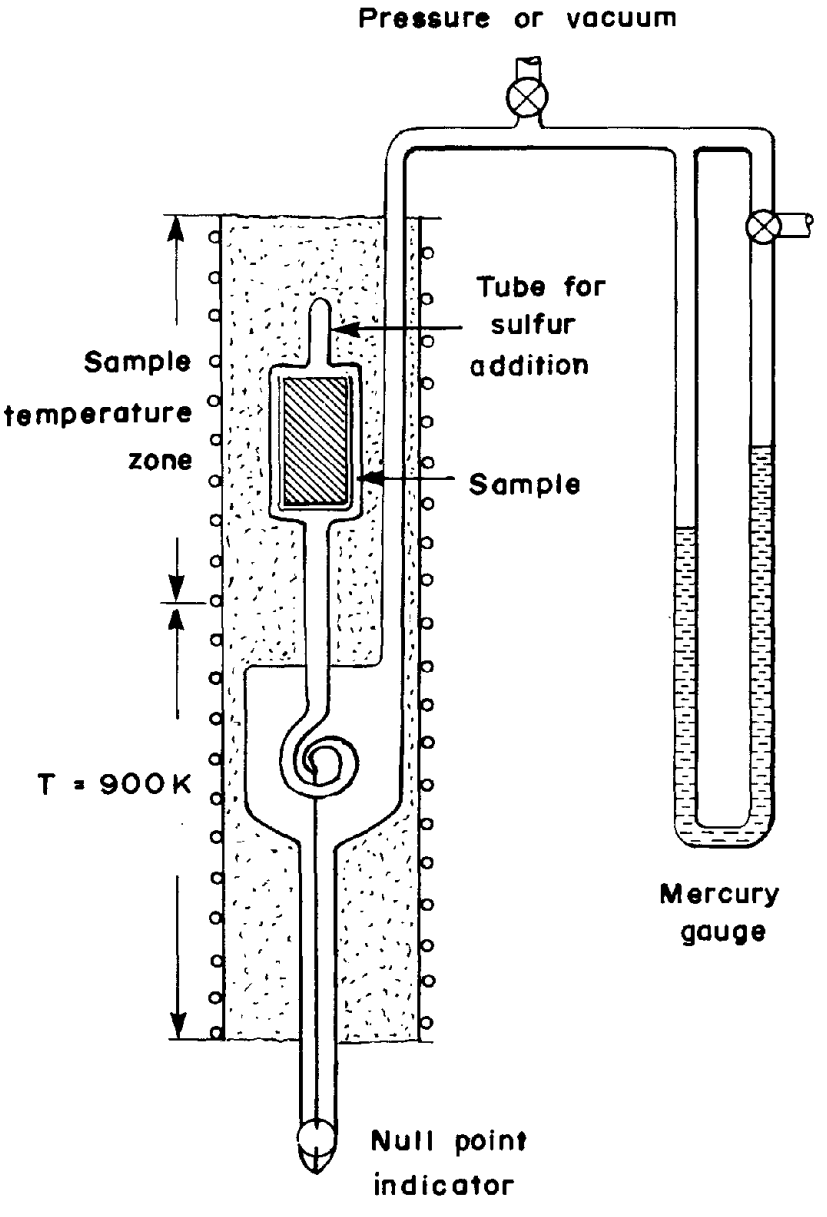


FIGURE 1. - Silica spiral gauge for sulfur vapor pressure (35).

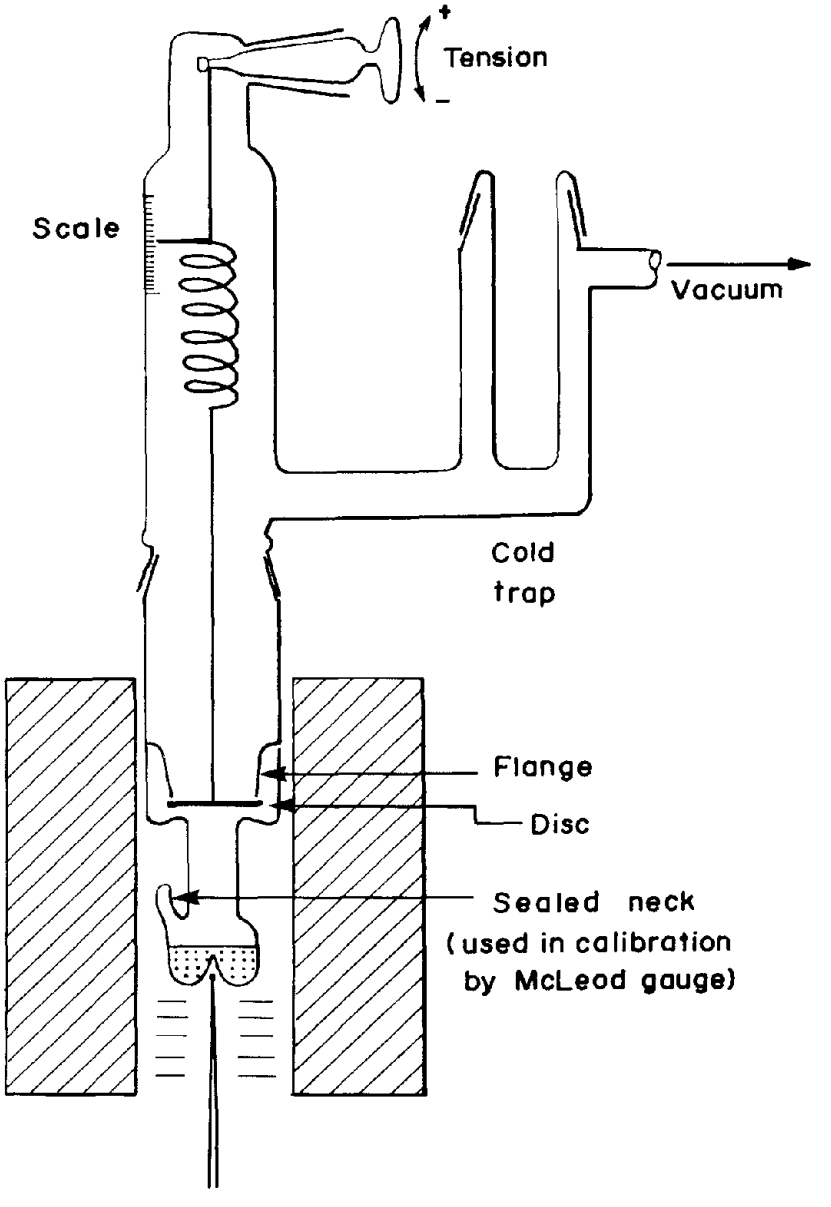


FIGURE 2. - High-temperature Rodebush manometer (23).

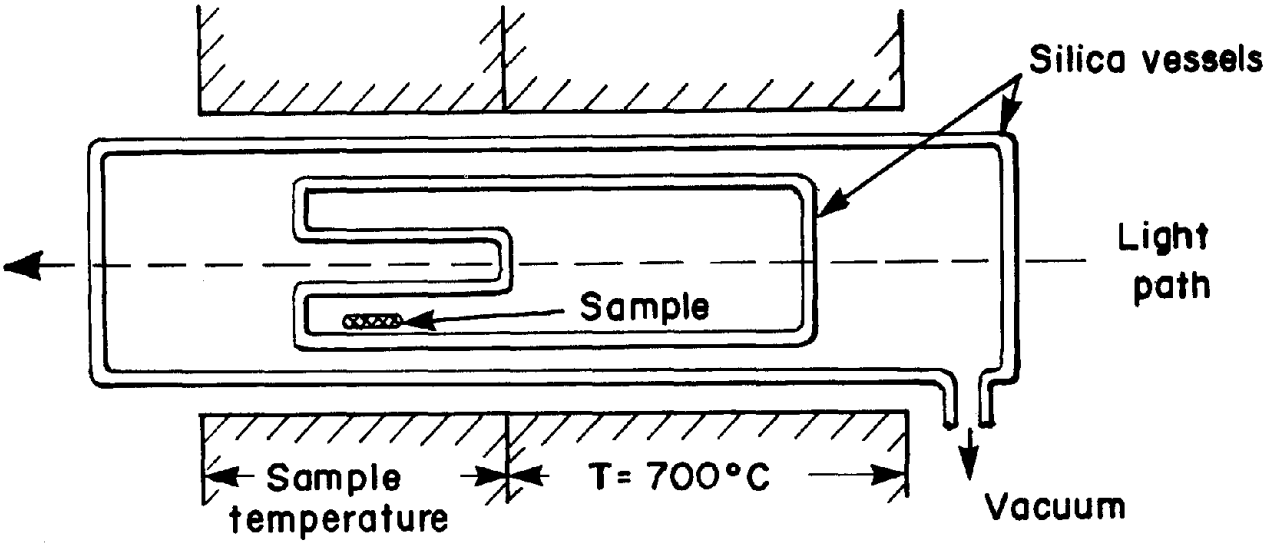


FIGURE 3. - UV absorption cell arrangement (31).

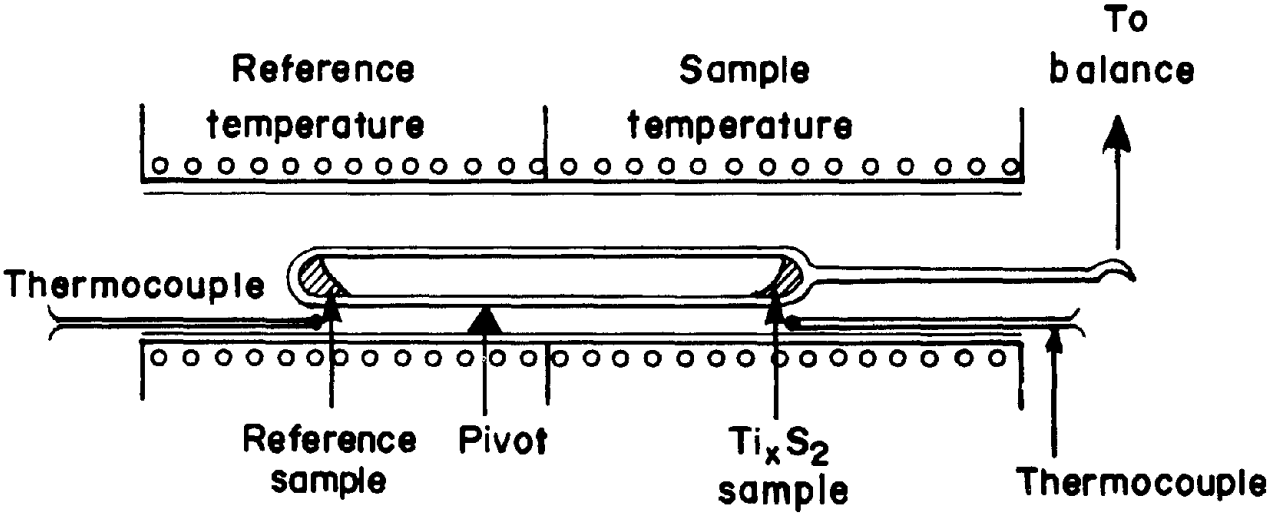


FIGURE 4. - Pseudoisopiestic balance (60).

Indicator Methods

In the indicator isopiestic-type methods, a small amount of standard indicator material is sealed in the sample vessel. The sample fixes the equilibrium sulfur activity which is determined by analysis of the indicator.

The pyrrhotite indicator technique is based on the wide range of sulfur activity over the $Fe_{1-\delta}S$ compositional range which has been well established and is summarized in references 24 and 25. After equilibrating the sample and the pyrrhotite indicator, the sample vessel is quenched and pyrrhotite composition is determined by X-ray analysis. This method has been used by Barton (3) in a study of the Cu-Fe-S system.

A simple means of testing the results for equilibrium is to "sandwich" the sample between two small amounts of pyrrhotite: one sulfur-rich and one sulfur-poor (fig. 5). At equilibrium the two pyrrhotites will have the same composition (5, 53).

Another indicator isopiestic-type method is the electrum-tarnish method developed by Barton and Toulmin (4). By visually determining the formation and decomposition temperatures of a sulfide layer on an electrum (silver-gold alloy) indicator sealed in a sample vessel, the sulfur activity of the sample could be determined.

The principal advantage of the method is its simplicity, which makes it possible to do many simultaneous runs for periods as long as months for low-temperature (T ~300° C) studies. A disadvantage is that the formation and decomposition temperatures can usually be determined only to a range of 5° to 10° C. Barton and Toulmin have compared the relative merits of different methods for determining sulfur activities at various temperatures (4).

Dewpoint Method

The dewpoint method is a simple yet accurate means of determining sulfur activity. It is based on the equality of the partial pressure of sulfur above a sample and the saturated vapor pressure of pure sulfur at lower temperature (the dewpoint). By determining the dewpoint, the sulfur activity of the sample may be found, as the P-T relationship for saturated sulfur vapor has been accurately determined (40). As it is necessary that the condensed sulfur be pure, the method cannot be used for metals that are appreciably volatile.

A typical dewpoint apparatus, as used by Mikkelsen (27) in a recent study of the Ti-S system, is shown in figure 6. A capillary tube extends from the sample vessel into an adjustable heating zone with a decreasing temperature profile. The dewpoint temperature is found by observing the condensation and evaporation of sulfur at the capillary tip in a series of heating and cooling cycles (with a successive narrowing of the temperature range).

The dewpoint method may be used for sulfur pressures in the range 2 torr to ~10 atm (27), which correspond to dewpoints of 200° to 600° C . The lower limit is due to the minimum amount of sulfur in the vapor that can produce detectable condensation; the upper limit is the approximate strength of silica sample vessels. It has been noted (11) that the sulfur transfer rates become very slow at vapor pressures less than 0.01 atm.

It is important to use relatively large samples (of single-phase condensed systems) to minimize compositional changes, which cause different heating and cooling dewpoint temperatures.

Stepwise Reduction Method

This method was developed and used extensively by Rau (35-39) for indirect measurement of low sulfur pressures (≪1 torr).

Basically, the method consists of adding H_2 to a sample in a silica vessel, equilibrating at a constant temperature, quenching, and then analyzing the resultant H_2S-H_2 mixture. The sulfur activity is calculated from the sample temperature and the H_2S-H_2 ratio using the following equation:

$$\ln a_S = 1/2 \ln P_{S_2} = \frac{\Delta G^\circ_{f,H_2S}}{RT} + \ln \frac{P_{H_2S}}{P_{H_2}} . \qquad (4)$$

The sample composition is calculated after measuring the amount of sulfur removed as H_2S (with a slight correction for sulfur present as vapor at the equilibrium temperature). This procedure is repeated until some metal-rich composition is reached, whereupon H_2S is added to return to a sulfur-rich composition.

The apparatus used by Vlach (54) is shown in figure 7. It consists of a silica sample vessel connected via capillary and stopcock to the H_2 and H_2S supplies and the gas analysis system. The analysis is carried out as follows: The H_2S-H_2 mixture is transferred (by raising and lowering the mercury in the Toepler pump, with appropriate opening and closing of the Teflon valve) to a known volume where its pressure is measured. Next, the H_2 is pumped away after freezing the H_2S with liquid nitrogen (poured in the surrounding flask). After warming up, the H_2S pressure is measured.

Advantages of the stepwise reduction method include

1. It is suitable for both single- and two-phase regions. Unlike most static methods, the sample composition is easily and precisely varied, which makes it suitable for single-phase regions. Unlike dynamic "once-through" flow systems, such as thermogravimetric analysis, it is ideal for two-phase regions. This makes it useful in determining transition (for example, eutectoid or peritectoid) temperatures between adjacent two-phase regions.
2. It is more exact than other static methods for measuring low

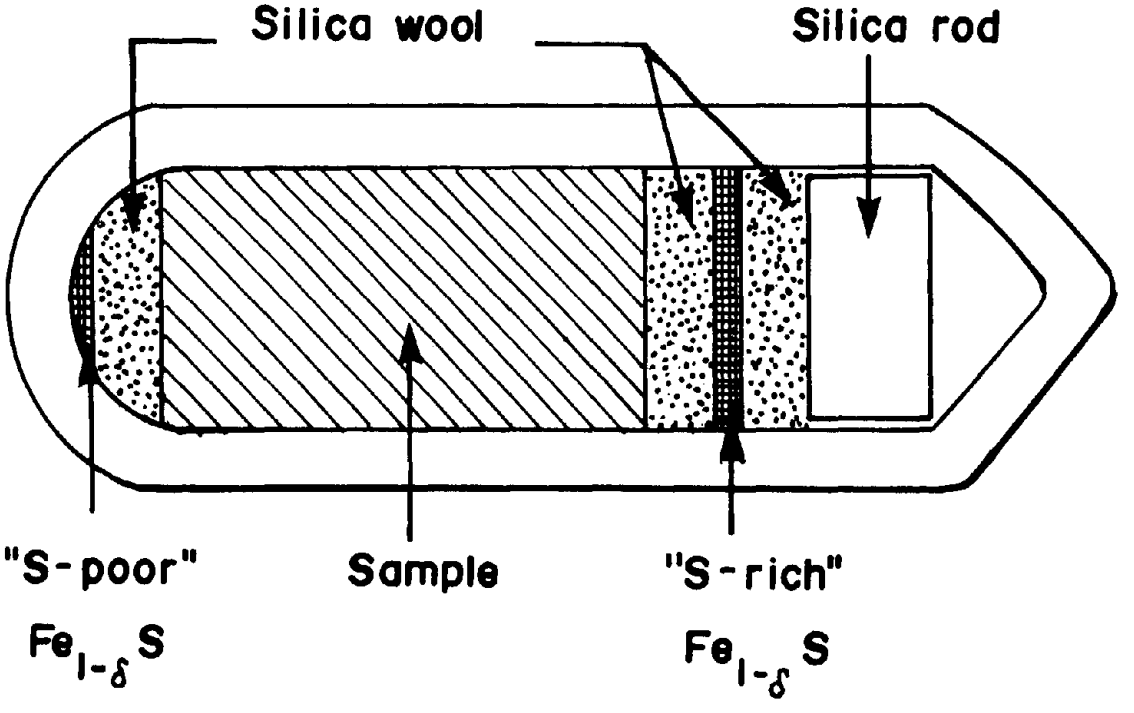


FIGURE 5. - Pyrrhotite indicator technique, using the "sandwich" arrangement (5).

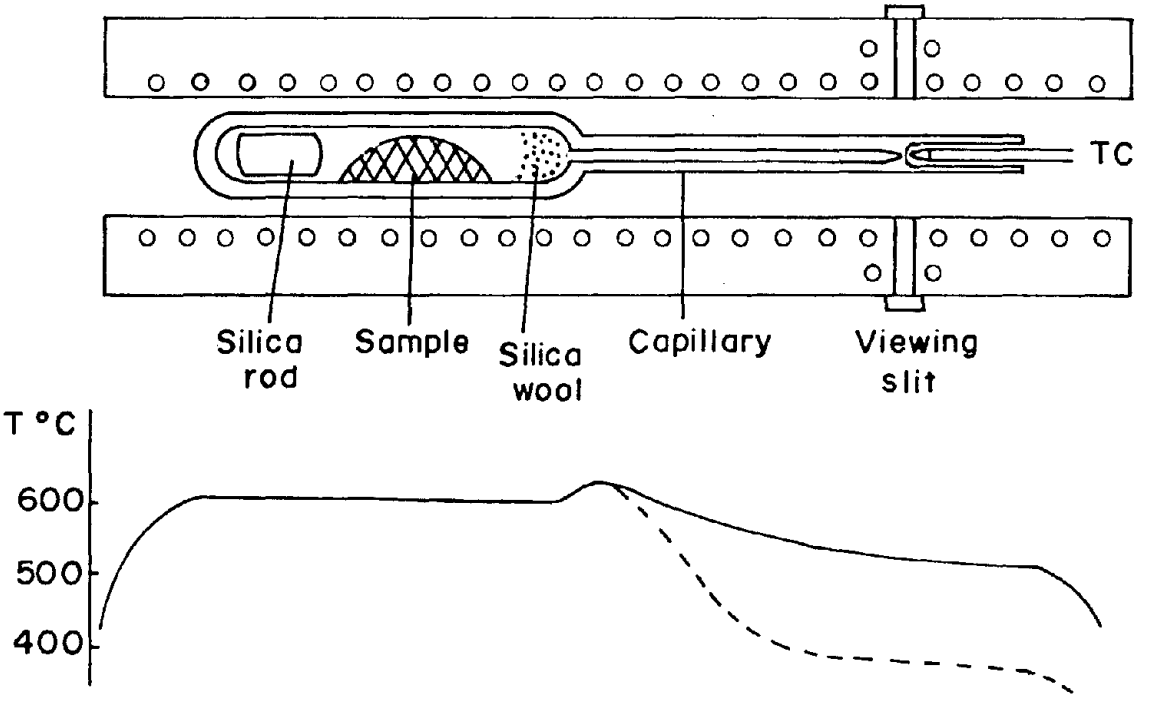


FIGURE 6. - Dewpoint apparatus, with typical temperature profile (27).

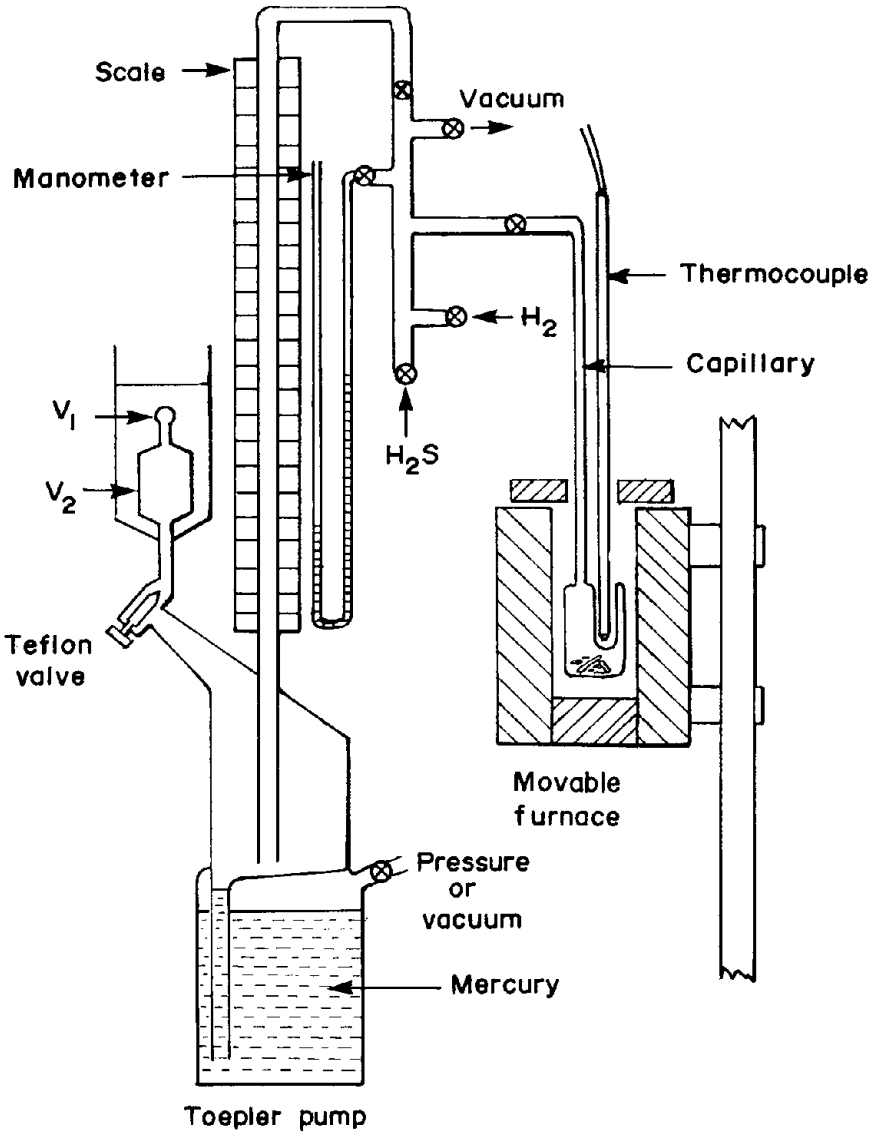


FIGURE 7. - Apparatus for static stepwise reduction (54).

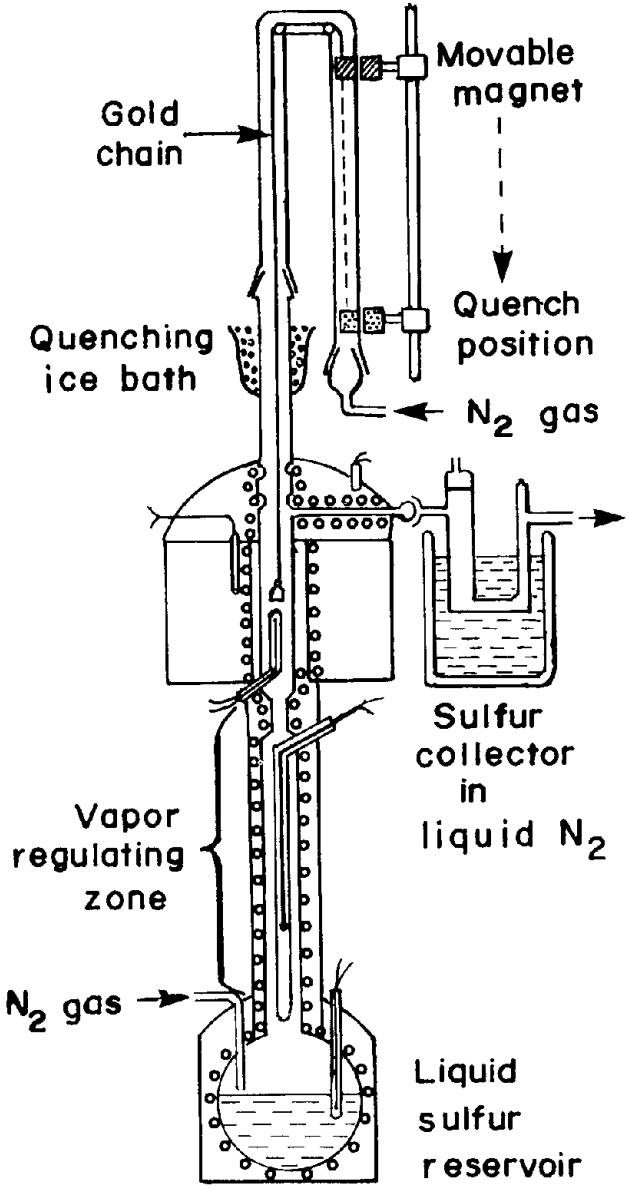


FIGURE 8. - Apparatus using N_2 carrier gas (57).

sulfur vapor pressure, since it uses the more easily measured H_2S-H_2 ratio.

3. Each change in composition is known very precisely. This makes it useful in determining the width of narrow phase regions.

4. Although there is a cumulative error in composition, this can be corrected (a) if there are already known data, such as a phase boundary, in the composition range being studied, or (b) by interconnecting series of data (35).

Disadvantages of the stepwise reduction method include

1. As mentioned above, there may be a cumulative error in composition.

2. It is limited to low sulfur pressures (α1.5 torr) to avoid sulfur condensation in the cooler portion of the capillary.

3. To reach lower sulfur compositions when the sulfur activity is very small is very time consuming, as the amount of H_2S formed each time is very small. This problem may be overcome by using smaller samples, or by starting with the metal and sulfidizing with H_2S.

4. Thermal segregation of H_2S (the heavier gas) may occur in the portion of the capillary outside the furnace. This is minimized by keeping this volume to $\underline{\alpha}$1 pct that of the sample vessel and by placing the capillary above the sample vessel.

DYNAMIC METHODS

The bulk of sulfur vapor pressure and Gibbs energy of formation data on metal sulfides has been obtained by dynamic methods involving equilibration of a sample and a gas stream. The various experimental techniques differ primarily in the means by which p_{S_2} is fixed and the type of analysis required. Methods in which p_{S_2} is controlled with a gas or vapor source require sample analysis. Methods in which p_{S_2} is fixed by the sample require gas analysis. Methods in which p_{S_2} is determined by mutual equilibration of the sample and a gas require either gas or sample analysis (sometimes both).

Sulfur Activity Fixed by the Gas Stream

These methods include once-through flow systems and buffered circulatory systems. Generally, data taking is limited to single-phase (condensed) regions. Sample analysis is required. It may be either nondestructive, such as thermogravimetric analysis and tarnish methods, or destructive, such as chemical or X-ray analysis. Only the nondestructive methods will be discussed, as they are part of the equilibration process (as opposed to destructive analysis, which is carried out afterwards).

Means of Controlling p_{S_2}

Gas Mixtures

Gas mixtures such as H_2S-H_2 are the most commonly used means of producing p_{S_2} values in the range 10^{-12} to 10^{-2} atm. At such low sulfur pressures, indirect control via the H_2S dissociation equilibrium (equation 4) is more exact than any direct means. Commercially available flowmeters and gases are ordinarily used, with purification as necessary. The H_2S-H_2 ratio may also be fixed by passage of H_2 or H_2S-H_2 through a buffer reservoir (liquid sulfur or a standard sulfide) at a controlled temperature. For example, H_2S-H_2 ratios from 4.5×10^{-4} to 2.4×10^{-3} can be produced by passing H_2 slowly over a mixture of Cu_2S and Cu at temperatures from 600° to 1,000° C (50). The buffer method may be used in either once-through or circulatory systems.

A wider range of H_2S-H_2 ratios (10^{-4} to 10) can be produced in the apparatus of Delmaire and LeBrusq (10), which passes an N_2-H_2 mixture containing a precisely controlled amount of H_2O vapor through a column of Al_2S_3, which converts the H_2O to H_2S. The relative error of the resultant H_2S-H_2 ratio is ±3 pct at a ratio of 10^{-4} (33).

Carrier Gas Methods

These are used for p_{S_2} values in the range 10^{-4} to 1 atm (57). The procedure is to use an inert gas to move sulfur vapor from a liquid sulfur reservoir past the sample. The sulfur vapor pressure is controlled by regulating the temperatures of the reservoir and the intermediate zone between the reservoir and the sample (fig. 8). The method is described in detail by Wakihara and coworkers (57-58) who studied the V-S system. Wada (55) has recently used the method in a thermogravimetric study of the Fe-V-S system.

An unusual carrier gas method was used by Tegman (51) in a pseudoisopiestic buffer technique. N_2 gas was circulated by means of a fan between the liquid sulfur reservoir and the sample, which were placed in two different temperature zones of the furnace.

Means of Sample Analysis (Nondestructive)

Thermogravimetric Analysis (TGA)

This method is used to determine the sample composition as a function of temperature and sulfur activity. The procedure is simple: The sample is suspended from a microbalance and equilibrated with a gas stream of known sulfur activity at a fixed temperature. The composition of the sample is then determined from its weight and the original composition and weight.

Advantages of the TGA method are

1. The composition is known very accurately because of the high sensitivity of microbalances.

2. There is no need to remove and analyze samples.

3. Many data points may be obtained with one sample, as only the temperature and/or gas ratio need to be varied.

4. The approach to equilibrium is easily observed.

Disadvantages of the TGA method are

1. Reliable data cannot be obtained in two-phase (condensed) regions, where the activity is independent of the composition.

2. Precautions must be taken to prevent the sulfur vapor from affecting the weighing mechanism (by condensation and/or corrosion).

Bale and Toguri (2) have discussed the application of TGA to sulfide studies. Their apparatus is shown in figure 9. To prevent corrosion of the electronic balance and sulfur deposition on the sample support, dry N_2 was passed through the balance and down the central column to the exit holes. A buoyancy correction was made for the densities of different H_2S-H_2 ratios.

Care should also be taken to avoid thermal diffusion. This is done by using high flow rates (sometimes with Ar as a diluent) and by preheating the gas mixture in a small-diameter tube (14).

Three basic types of weighing apparatus are used in TGA:

1. Automatic recording microbalances. - These provide automatic recording and balancing of the sample weight, as well as high accuracy (~1 ppm). Disadvantages are the high cost and vulnerability to corrosion. Balances are now available with all metal parts gold-plated for protection (8).

2. Silica springs. - These are simple, inexpensive, and not subject to corrosion. However, sensitivity is only about 1 part in 10^4, and measurements are usually made manually with a cathetometer. An automated recording method was used by Burgmann and coworkers (7). The position of a ferrite core included in the sample suspension was determined using a differential transformer.

3. The silica beam microbalance. - The microbalance designed by Gulbransen (15) was modified by Whittle (59) for photoelectric detection and electromagnetic balancing. Sensitivity of 10^{-6}g was achieved for a 0.5-g sample. This balance has both high sensitivity and corrosion resistance. However, the automated design is somewhat complicated.

Tarnish Methods

These are methods in which the H_2S-H_2 ratio and temperature for the metal-metal sulfide equilibrium are visually determined by observing the formation or decomposition of the sulfide phase on the metal.

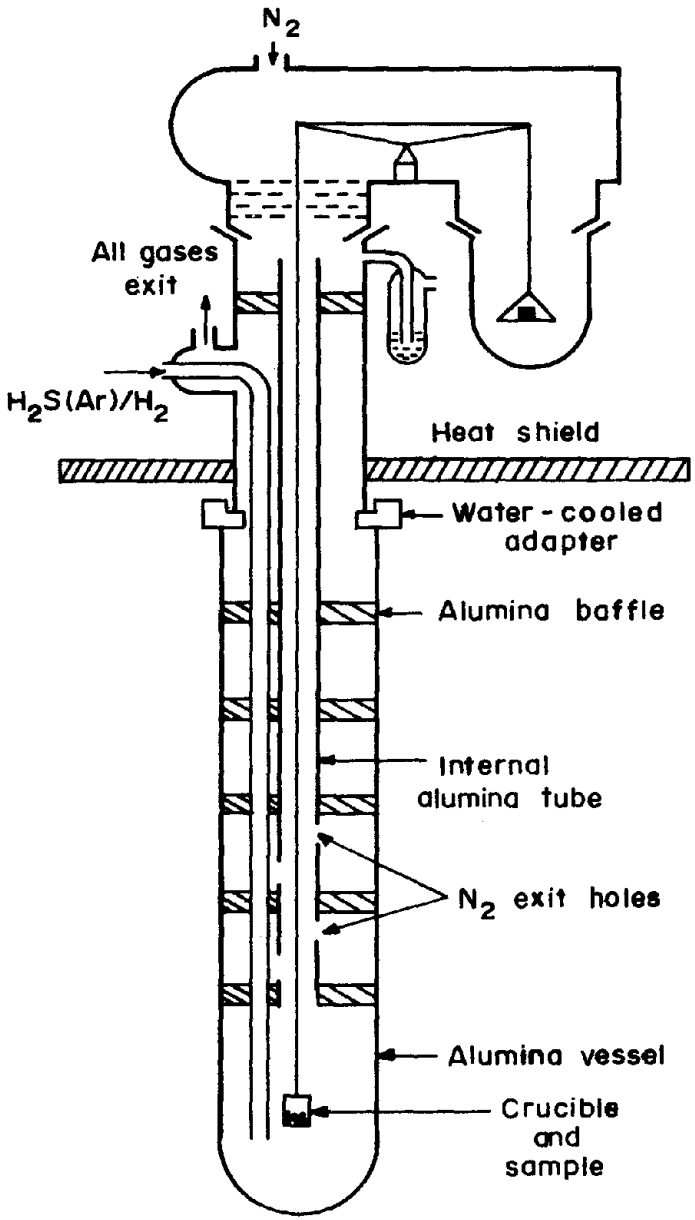


FIGURE 9. - TGA apparatus [furnace not shown] (2).

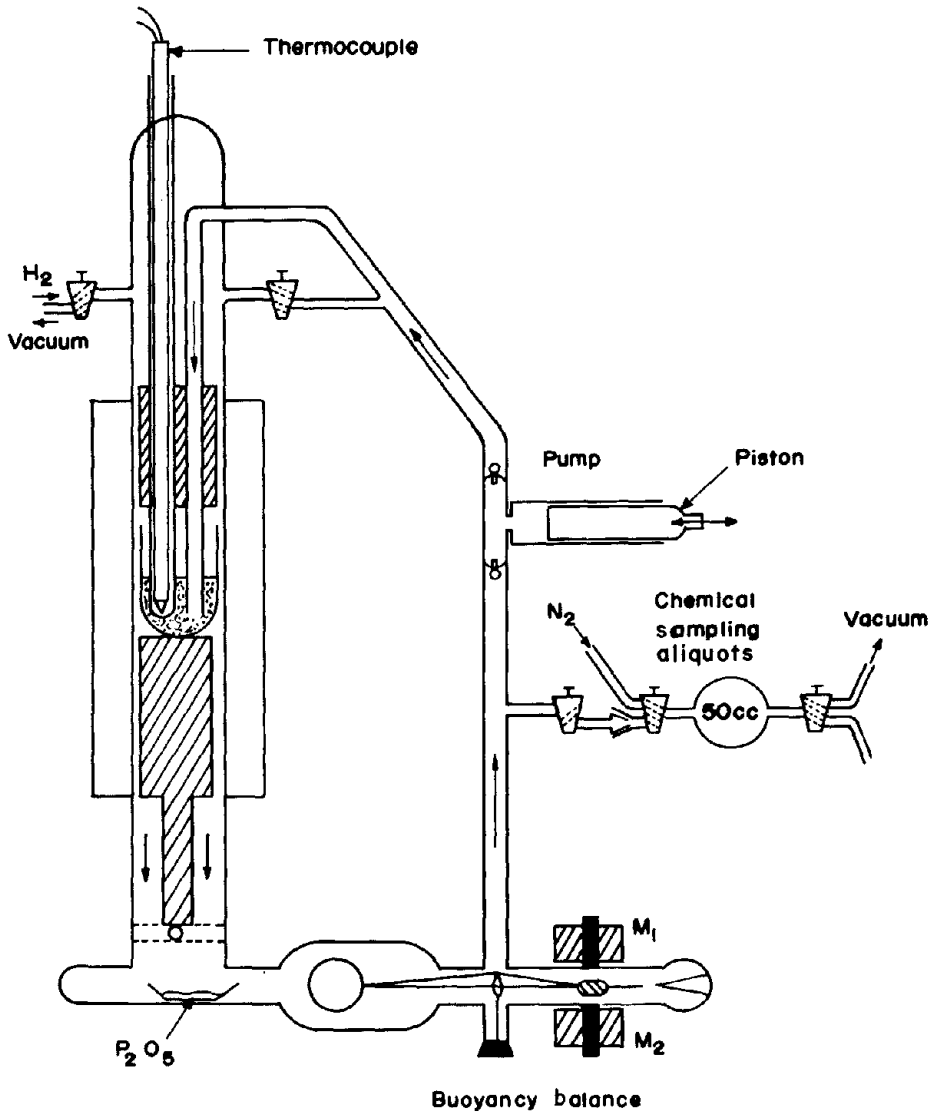


FIGURE 10. - Circulatory apparatus with buoyancy balance (46).

Kordes and Rackow (19) determined the sulfur vapor pressures (and heats of formation) of Cu_2S, FeS, and Ag_2S by observing the tarnishing of the metals in H_2-H_2S mixtures. By varying the sample temperature at fixed H_2-H_2S ratios and observing tarnish formation or decomposition, they determined the log p_{S_2} versus 1/T equations for the respective metal-metal sulfide equilibria (using literature data on the dissociation of H_2S).

Bielen (6) verified the accuracy of this method by comparing data on the Cu-Cu_2S system with data obtained by other means.

Hager and Elliott (16) used a slightly different procedure to obtain the same type of information. At a fixed temperature, mixtures with different H_2S-H_2 ratios were passed over metal samples until two adjacent ratios were obtained, one of which was sulfidizing and the other reducing.

Sulfur Activity Fixed by the Sample

Dynamic methods where the sulfur activity is fixed by the sample are used to investigate two-phase (condensed) equilibria as functions of temperature. They have also been used in single-phase studies by using sufficiently large samples so that changes in composition were insignificant; alternatively, such changes can be determined by special means (discussed below).

In all of these methods the gas is equilibrated with the sample and analyzed to determine the sulfur activity.

Circulating Methods

In these methods, H_2 (or an H_2S-H_2 mixture) is circulated over or through the sample until an equilibrium H_2S-H_2 gas mixture is produced, which is analyzed to determine the sulfur activity of the sample. The gas is ordinarily analyzed continuously (nondestructively), which allows the approach to equilibrium to be noted. Analytic methods include radioactivity measurement using ^{35}S [discussed extensively by Alcock (1)], density measurement using a buoyancy balance (45-46), as shown in figure 10, and optical interferometry (refractive index measurement) (9).

A novel method used by Meyer and coworkers (26) involved the operation of a once-through system in such a manner so as to give the results of a circulatory system in a much shorter time. An optical interferometer was used to compare the H_2S-H_2 ratios at the inlet and the outlet of the sample furnace. The inlet gas composition was adjusted until the inlet and outlet compositions were equal. At the high temperatures involved (up to 1,600° C) it was necessary to consider the partial dissociation of H_2S to H_2, S_2, S, and HS in order to calculate the equilibrium sulfur pressure p_{S_2}. The sample composition was analyzed chemically.

Transportation (Transpiration) and Entrainment Methods

In the transportation method, a slow-moving stream of inert gas is passed through the sample, becoming saturated with its equilibrium sulfur vapor which is condensed out and weighed after it leaves the sample furnace (20, 52). The partial pressure of sulfur p_{S_2} is calculated from the weight of the

condensate and the moles of carrier gas, with a correction being made for other sulfur species using the data of Rau and coworkers (41).

The entrainment method of Richards (42-44) is essentially the same except that reactant gases may also be used. An inert gas (N_2) was used, either alone or in mixtures with $S_2(g)$ and H_2, to study the vaporization, dissociation, and reduction equilibria, respectively, of SnS and ZnS. In these systems a stream of N_2 alone cannot give data for the Gibbs energies of formation because the vaporizing species will be SnS(g) and ZnS(g).

In both methods, equilibrium with the sample is theoretically attained at infinitely slow flow rates (20). In practice, flow rates of about 2ℓ/hr have been used, which is sufficient to avoid thermal diffusion (43-44, 52).

Sulfur Activity Determined by Mutual Equilibration

In this method, the sulfur activity is determined by the mutual equilibration of a sample and a fixed amount of gas in a closed circulatory system. It is the same in principle as the static stepwise reduction method and may be used for either single- or two-phase (condensed) regions. Both the sample and gas compositions are experimental unknowns, but measurement of one equilibrium composition permits calculation of the other, as the initial amounts and compositions are known. Frequently, the gas composition is analyzed continuously by the means covered in the previous section on circulating methods, such as the buoyancy balance (fig. 10) used in Rosenqvist's classic study (46). The gas composition may also be determined by chemical analysis of small volumes (21). Alternatively, the sample composition may be analyzed continuously, as done by Peronne and coworkers (32), who placed a silica balance within the reaction vessel to measure weight changes as small as 5 x 10^{-6}g in $Cu_{2-\delta}S$ of ~1.05 g. After equilibration, the H_2S-H_2 ratio was determined by manometric pressure measurements before and after freezing the H_2S in a cold trap.

The stepwise reduction technique is often used with this method in order that sulfur activities may be studied as the sulfur composition of the sample is gradually reduced by small, calculated amounts.

SOLID-ELECTROLYTE EMF METHODS

Conventional EMF Methods

The solid-electrolyte EMF method is an accurate means of determining the Gibbs energies of formation when the appropriate cells can be constructed. As metal sulfides are generally electronic conductors, the direct-reaction cell is not feasible. (The Nernst equation would not be obeyed.) Therefore, it is necessary to use an auxiliary electrolyte of ionic type. The most straight-

forward approach is to use an ionic salt of the metal, as in the well-known cells

$$Ag \mid AgI \mid Ag_2S, p_{S_2}$$

and

$$Cu \mid CuBr \mid Cu_{2-\delta}S, p_{S_2},$$

but there is a limited availability of such compounds with suitable properties. More generally, the use of several solid electrolytes of high chemical and thermal stability has been developed. These include CaF_2 and such oxides as CaO-stablized ZrO_2 and $ThO_2(Y_2O_3)$. In these cells, the sulfur potential is measured by converting it to an equivalent fluorine or oxygen potential. The CaF_2 electrolyte has been used by Moriyama (28) to determine $\Delta G^\circ_{f,Cu_2S}$ in the following cell (fig. 11):

$$Cu + Cu_2S, CaS/CaF_2 \text{ (single crystal)}/CaS, Ag + Ag_2S.$$

The sulfur activity at each electrode fixes the fluorine activity via the equilibrium

$$CaF_2(s) + 1/2\ S_2(g) = CaS(s) + F_2(g). \qquad (5)$$

The overall cell reaction is

$$Ag_2S + 2Cu = 2Ag + Cu_2S, \qquad (6)$$

for which

$$\Delta G^\circ_{Rx} = -nFE^\circ,$$

and the standard Gibbs energy of formation of Cu_2S is

$$\Delta G^\circ_{f,\ Cu_2S} = \Delta G^\circ_{f,Ag_2S} - 2FE^\circ. \qquad (7)$$

Jacob and coworkers (17) have studied the feasibility of using a similar CaF_2 cell for gas analysis. H_2S-H_2 mixtures were used to fix the electrode sulfur activities, which fixed the fluorine activities as above. Larson and Elliott (22) used stabilized zirconia ($Zr_{0.85}Ca_{0.15}O_{1.85}$) electrolyte in determining the Gibbs energies of formation of several metal sulfides. In what essentially are oxygen concentration cells, they used mixtures of the types (dependent upon the relative oxide-sulfide stability) MO, MS, and SO_2 (g, ~1 atm); MO, MS, and S_2 (g, ~1 atm); and M, MS, and SO_2 (g, ~1 atm) to fix the oxygen potential at the anode. The oxygen potential at the cathode was fixed by pure O_2 (g, 1 atm). For MO-MS-SO_2, the reaction for the reversible transfer of 1 mole O_2 is

$$2/3\ MO + 2/3\ SO_2(g) = 2/3\ MS + O_2(g)$$

and

$$\Delta G^\circ_{Rx} = 2/3\ (\Delta G^\circ_{MS} - \Delta G^\circ_{MO} - \Delta G^\circ_{SO_2}) = -4FE.$$

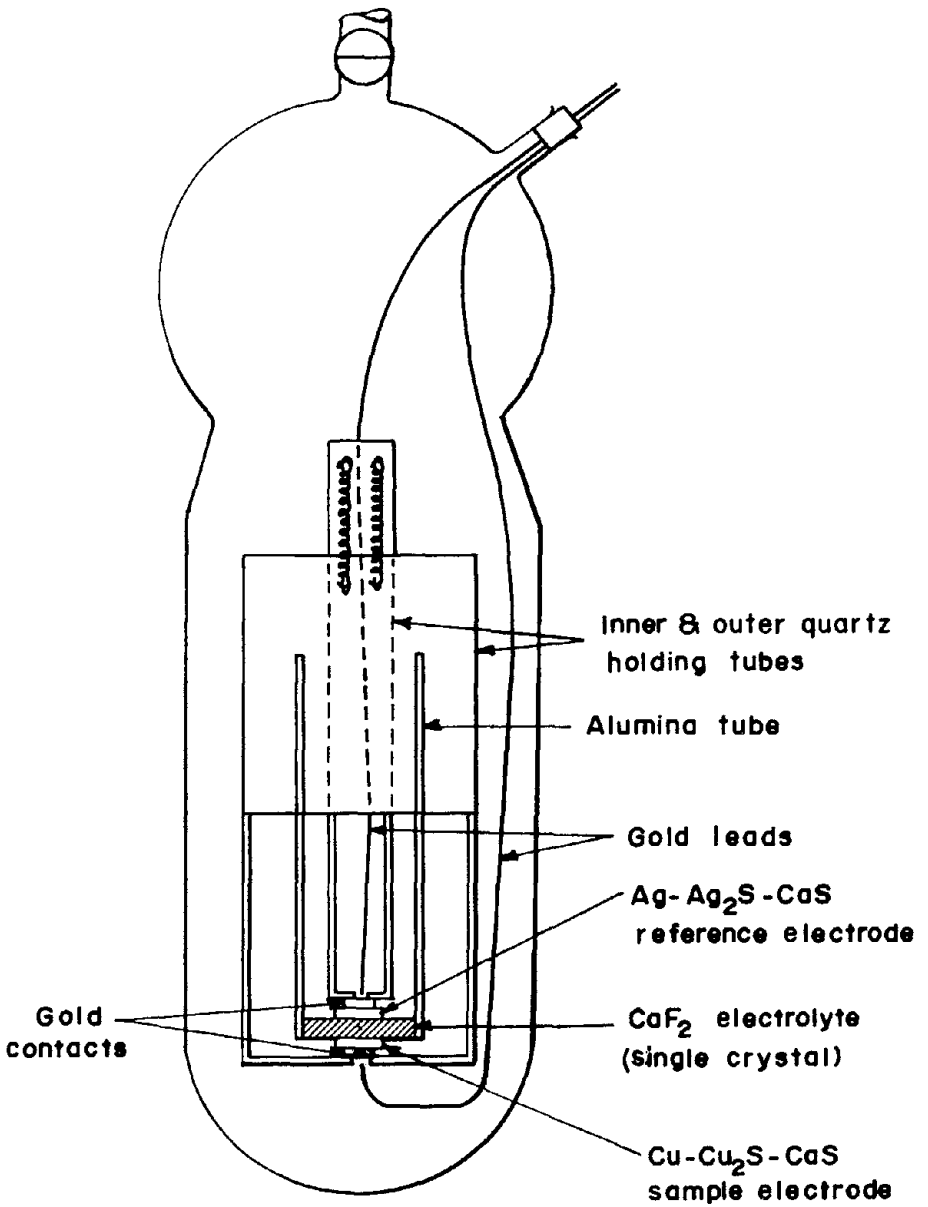


FIGURE 11. - Solid electrolyte EMF cell (28).

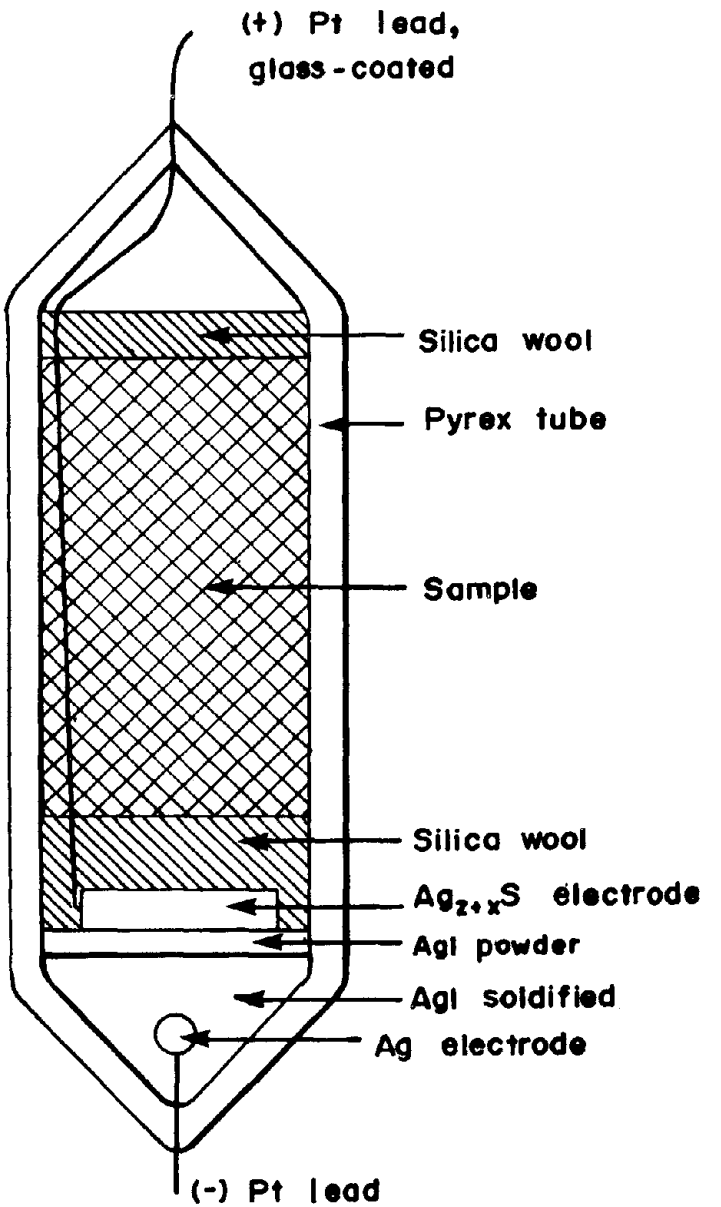


FIGURE 12. - Isopiestic EMF cell (49).

Their paper discusses experimental errors as well as uncertainty in the published data for $SO_2(g)$ and the relevant metal oxides. It should be noted that Rosenqvist and Haugom (47) have recently determined an accurate expression for ΔG°_f, SO_2 by high-temperature EMF measurements which is more positive than earlier expressions (12).

The stabilized ZrO_2 electrolyte has been used more recently by Espelund and Jynge (13) in a cell similar to that of Larson and Elliott (22) in a study involving ZnO-ZnS and Fe_3O_4-$Fe_{1-\delta}S$, and by Schaefer (48) in a study of ZnO-ZnS in which Cu + Cu_2O was used to fix the cathode oxygen potential.

Another oxide suitable for use as a solid electrolyte is ThO_2 (Y_2O_3) which has been used by Yuill and Cater (61) in a study of the U-O-S system and more recently by Hodouin (17) in a study of columbium sulfides.

Isopiestic EMF Method

Schneeberg (49) developed a method that uses the cell

$$Ag \mid AgI \mid Ag_{2+\delta}S,\ S_2(g)$$

to measure the sulfur activity of a sulfide mixture in isopiestic equilibrium with the $Ag_{2+\delta}S$ electrode (fig. 12). It may also be used for nonstoichiometric sulfides such as $Fe_{1-\delta}S$ and $Ni_{1-\delta}S$. It cannot be used for samples that can form iodides more stable than AgI.

The method has the advantages of simplicity and accuracy. Its disadvantages are the narrow temperature range in which the cell can be used (178° to ~445° C) and that the activity measurements are limited to those above that of the silver-silver sulfide equilibrium. The use of a more stable electrolyte should permit these limits to be extended (49).

REFERENCES

1. Alcock, C. B. Internat. J. Appl. Radiat. Isotopes, v. 3, 1958, pp. 135-142.

2. Bale, C. W., and J. M. Toguri. J. Thermal Anal., v. 3, 1971, pp. 153-167.

3. Barton, P. B. Jr. Econ. Geol., v. 68, 1973, pp. 455-465.

4. Barton, P. B., Jr., and P. Toulmin, III. Geochim. Cosmochim. Acta, v. 28, 1964, pp. 619-640.

5. _____. Econ. Geol., v. 61, 1966, pp. 815-849.

6. Bielen, H. Z. anorg. allg. Chem., v. 336, 1965, pp. 69-80.

7. Burgmann, W. Jr., G. Urbain, and M. G. Frohberg. Mem. Sci. Rev. Metall., v. 65, 1968, 567-578.

8. Cahn Instruments, Cerritos, Calif.

9. Dashevskiy, V. Ya., and A. Yu. Polyakov. Russ. Metall., No. 5, 1966, pp. 13-15.

10. Delmaire, J.-P., and H. Le Brusq. Bull. Soc. Chim. France, No. 3, 1973, pp. 879-881.

11. Ditman, A. V., and I. N. Vechko. Inorg. Mater., v. 1, 1965, pp. 1394-1399.

12. Dow Chemical Co. Thermal Research Laboratory. JANAF Thermochemical Tables, 2d ed., NSRDS-NBS-37, U.S. Government Printing Office, 1971, 1141 pp.

13. Espelund, A. W. , and H. Jynge. Scand. J. Metall., v. 6, 1977, pp. 256-262.

14. Gokcen, N. A., and J. Chipman. Trans. AIME, v. 194, 1952, pp. 171-182.

15. Gulbransen, E. A. Rev. Sci. Instr., v. 15, 1944, pp. 201-204.

16. Hager, J. P., and J. F. Elliott. Trans. TMS-AIME, v. 239, 1967, pp. 513-520.

17. Hodouin, D. Metall. Trans. B, v. 6B, 1975, pp. 223-228.

18. Jacob, K. T., D. B. Rao, and H. G. Nelson. J. Electrochem. Soc., v. 125, 1978, pp. 758-762.

19. Kordes, E., and B. Rackow. Z. physik. Chem., v. 200, 1952, pp. 129-157.

20. Kubaschewski, O., and E. Ll. Evans, and C. B. Alcock. Metallurgical Thermochemistry, Pergamon Press, Oxford, England, 4th ed., 1967, p. 169.

21. Larson, A. H., and A. W. Schlechten. Trans. TMS-AIME, v. 230, 1964, pp. 862-866.

22. Larson, H. R., and J. F. Elliott. Trans. TMS-AIME, v. 239, 1967, pp. 1713-1720.

23. Leegaard, T., and T. Rosenqvist. Z. anorg. allg. Chem., v. 328, 1964, pp. 294-298.

24. Libowitz, G. G., Ch. in Reactivity of Solids, ed. by J. B. Anderson, M. W. Roberts, and F. S. Stone. Chapman and Hall, London, 1972, pp. 107-115.

25. Lin, R. Y., H. Ipser, and Y. A. Chang. Metall. Trans. B, v. 8B, 1977, pp. 345-346.

26. Meyer, G. A., J. S. Warner, Y. K. Rao, and H. H. Kellogg. Metall. Trans. B, v. 6B, 1975, pp. 229-235.

27. Mikkelsen, J. C. Jr. Nuovo Cimento, v. 38 B, 1977, pp. 378-386.

28. Moriyama, J., T. Oishi, K. Ogino, and A. Egami. Proc. 4th Internat. Conf. Therm. Anal., Budapest, v. 3, 1974, pp. 867-872.

29. Nesmeyanov, A. N. Vapor Pressure of the Chemical Elements, Elsevier, Amsterdam, 1963, p. 9.

30. Norman, J. H., and P. Winchell. Measurement of Vapor pressures by Transpiration, Isopiestic, and other Techniques. Ch. 2C in Techniques of Metals Research, vol. IV, Physicochemical Measurements in Metals Research, Part 1, ed by R. A. Rapp, Interscience Publishers, New York, 1970, pp. 131-159.

31. Pemsler, J. P., and C. Wagner. Metall. Trans. B, v. 6B, 1975, pp. 311-320.

32. Peronne, R., D. Balesdent, and J. Rilling. Bull. Soc. Chim. France, No. 2, 1972, pp. 457-463.

33. Pouillard, G., and P. Perrot. C. R. Acad. Sci. Paris, Ser. C, v. 281, 1975, pp. 143-146.

34. Rau, H. Rev. Sci. Instr., v. 43, 1972, pp. 831-832.

35. _____. J. Phys. Chem. Solids, v. 35, 1974, pp. 1415-1424.

36. _____. J. Phys. Chem. Solids, v. 36, 1975, pp. 1199-1204.

37. _____. J. Phys. Chem. Solids, v. 37, 1976, pp. 425-429.

38. _____. J. Phys. Chem. Solids, v. 37, 1976, pp. 929-930.

39. _____. J. Phys. Chem. Solids, v. 37, 1976, pp. 931-934.

40. Rau, H., T. R. N. Kutty, and J. R. F. Guedes de Carvalho. J. Chem. Thermodynamics, v. 5, 1973, pp. 291-302.

41. _____. J. Chem. Thermodynamics v. 5, 1973, pp. 833-844.

42. Richards, A. W. J. Iron and Steel Inst., v. 173, 1952, p. 270.

43. _____. Faraday Soc. Trans., v. 51, 1955, pp. 1193-1197.

44. _____. J. Appl. Chem., v. 9, 1959, pp. 142-145.

45. Rosenqvist, T. Metals Trans., v. 185, 1949, pp. 451-460.

46. _____. J. Iron and Steel Inst., v. 176, 1954, pp. 37-57.

47. Rosenqvist, T., and J. Haugom. J. Chem. Soc., Faraday Trans. 1, v. 73, 1977, pp. 913-919.

48. Schaefer, S. C. BuMines RI 8301, 1978, 16 pp.

49. Schneeberg, E. P. Econ. Geol., v. 68, 1973, pp. 507-518.

50. Seybolt, A. U. Trans. TMS-AIME, v. 242, 1968, pp. 1955-1961.

51. Tegman, R. Chemica Scripta, v. 2, 1972, pp. 63-67.

52. _____. Chemica Scripta, v. 9, 1976, pp. 158-166.

53. Vaughan, D. J., and J. R. Craig. Mineral Chemistry of Metal Sulfides. Cambridge Univ. Press, Cambridge, England, 1978.

54. Vlach, K. C. M. S. Thesis, University of Wisconsin - Milwaukee, 1978.

55. Wada, H. Bull. Chem Soc. Japan, v. 51, 1978, pp. 1368-1373.

56. Wakihara, M., J. Nii, and M. Taniguchi. Chem. Letters, 1977, pp. 621-626.

57. Wakihara, M., T. Uchida, and M. Taniguchi. Mater. Res. Bull., v. 11, 1976, pp. 973-980.

58. _____. Metall. Trans. B, v. 9B, 1978, pp. 29-32.

59. Whittle, J. E. J. Sci. Instrum., v. 43, 1966, pp. 150-152.

60. Winn, D. A., and B. C. H. Steele. Mater. Res. Bull., v. 11, 1976, pp. 551-558.

61. Yuill, W. A., Jr., and E. D. Cater. J. Phys. Chem., v. 71, 1967, pp. 1436-1441.

DISCUSSION

R. D. Freeman: How do you get the composition of the gas? In this static technique you use to obtain the chemical potential of sulfur using H_2-H_2S mixture, how do you measure the volume or concentration of H_2S and H_2?

Y. A. Chang: In our gas analysis system, we have a vessel for which we know the total volume and also the volume of a small, upper portion. We transfer the entire gas mixture into the vessel and measure its pressure and temperature. After removing the H_2, the H_2S pressure is measured in the small volume.

R. D. Freemen: How do you separate the two?

Y. A. Chang: The H_2 is evacuated after freezing the H_2S (using liquid N_2 in a surrounding flask). The H_2S pressure is then measured after warming up.

Anonymous: How do you eliminate gas-phase segregation:

Y. A. Chang: If you use a sufficiently high velocity of H_2S-H_2 mixture, the segregation is minimized.

THERMODYNAMICS OF REACTIONS AND INTERACTION PROPERTIES IN SOME GAS-LIQUID METAL SYSTEMS

by

N. A. D. Parlee[1]

ABSTRACT

For simultaneous determination of solubilities (C) and diffusivities (D) of gases (H,N,O) by a combined "unsteady state-steady state" gas-liquid metal diffusion cell method, a gas-liquid metal diffusion cell is operated (at temp. T) first as an unsteady state cell yielding a linear plot of volume of gas absorbed versus $\sqrt{\text{time}}$; then, continuing the same run, it is operated as a steady state cell yielding linear plots of volume of gas absorbed versus time. The slopes of the two plots provide two equations that may be solved for C (1 atm) and D. Thermodynamics of gas dissolution reactions can be developed.

For determination of the thermodynamics of reactive metal nitride formation precipitation reactions in liquid metal solvent alloys, nitrogen is equilibrated in a Sieverts apparatus with liquid alloys (M-Sn, M-Fe, etc.) of fixed reactive metal (M) composition at T and at progressively increasing P_{N_2} values. Data derived from plots of $P_{N_2}^{1/2}$ versus volume of N_2 absorbed make it possible to establish the stoichiometry and the thermodynamics of $\underline{X}\underline{M} + \underline{Y}\underline{N} = M_XN_Y(s)$ reactions.

For determination of the thermodynamics of the carbothermic reduction of oxides of highly reactive metals in liquid metal solvent solutions, Sieverts apparatus is used to equilibrate charges of the oxide (for example, UO_2), C, and the solvent metal (for example, Sn) at different temperatures. The K_{eq} and thermodynamics of the reactions can often be determined.

SIMULTANEOUS DETERMINATION OF SOLUBILITIES AND DIFFUSIVITIES (D) OF GASES (H, N, O) BY A COMBINED "UNSTEADY STATE-STEADY STATE" GAS LIQUID DIFFUSION CELL METHOD

Solubilities of gases in liquid metals have long been determined by time-tested Sieverts methods (20)[2] with various modifications. Nearly all of our

---

[1]Professor of extractive metallurgy, Stanford University, Stanford, Calif.

[2]Underlined numbers in parentheses refer to items in the list of references at the end of this paper.

solubility data for H and N in metals like Ni, Fe, Cu, and their alloys, and for H, N, and O in metals like Ag, Au, and their alloys are derived from Sieverts work. Data are often reported in the literature as $C_{1\ atm}$, solubility at 1 atm at temperature T, or given in the form of $\Delta G^\circ = \Delta H^\circ - T\Delta S^\circ$ equations for reactions of the form $1/2G_2(g) = \underline{G}$, where $\underline{G}$ represents the dissolved gaseous component. Solubilities at other pressures are calculated, in simple cases, from the Sieverts relation $C_G = K\sqrt{P_{G_2}}$ where K is the equilibrium constant of the dissolution reaction. There are cases like O in liquid Cu and Fe where a liquid or solid oxide phase occurs at pressures below the level of pressure measurement by ordinary manometers in the standard Sieverts technique; in such cases indirect methods have generally been used to derive the gas solubility in the liquid phase. Even here, however, a modified Sieverts method sometimes can be used; for example El-Naggar, Horsley, and Parlee (6-7) measured the oxygen solubility relations in liquid copper and alloys, using a solid electrolyte cell to measure P_{O_2} in the gas-liquid copper range. However there are various other cases where the standard Sieverts method gives unreliable results. Sometimes the reasons are not fully accountable. One situation, however, is very common; this is where hydrogen or nitrogen solubility is so small that it cannot be measured with precision by any known Sieverts method or by the saturation-quench-chemical analysis method. The combined unsteady state-steady state method described below was developed because of the necessity of measuring both C and D values for H and N with good precision in a large number of simple and complex iron alloys. Both C and D at temperature T are calculated from the data taken in one long run. Very low values of C can be measured with considerable success.

The method evolved from the development of the first really satisfactory gas-liquid metal diffusion cell by Mizikar, Grace, and Parlee (15) and Shah and Parlee (19) for measuring D_O in liquid Ag, noble metals, and alloys, and later extended to the 1,750° C range by El-Tayeb and Parlee (9) and Sacris and Parlee (18) for measuring D_H and D_N in Sn, Cu, Fe, Ni, and their alloys. This was an unsteady state cell involving the diffusion of the gas component down into a cylindrical column of stagnant metal, after instant saturation of the surface by $1/2G_2(g)=\underline{G}$. Velho, El-Tayeb, Gani, and Parlee (21) discovered that the same type of cell could be operated as a steady state cell and that D_{gas} values for $\underline{O}$ in liquid Ag, essentially identical with unsteady state values, could be obtained if certain cell dimension restrictions were obeyed. They also demonstrated that it was possible to calculate sound C_{gas} values by combining the data from an unsteady state and a steady state run. This was confirmed by Sacris and Parlee (18) and Lee and Parlee (14) for C_H, D_H, and C_N, D_N for several liquid metals and alloys. They also found it most convenient and rapid to carry out the whole operation as one long run--the first part being the unsteady state stage followed immediately with the steady-state stage.

Apparatus

For the sake of brevity the apparatus and procedure are only outlined here. The reader is referred to original papers for details (9, 18, 21). The apparatus and procedure described below are those used for nitrogen in liquid iron alloys, but are nearly the same for other gas-liquid metal systems. Figure 1 shows the whole assembly.

The gas-liquid diffusion cell is at X inside of a vertical gas-impervious alumina combustion tube surrounded by a Pt-Rh wound Marshall furnace controlled at any desired temperature up to 1,800° C. Figure 2 shows the typical cell arrangement for unsteady state operation. The cell, when operating, is composed of a small-bore, vertical, gas-impervious alumina absorption tube (~0.5-cm diameter) open at the bottom and well immersed in the liquid metal held in an alumina crucible, resting on a support tube with a Pt-Rh thermocouple touching the bottom of the crucible. The metal is maintained stagnant by making certain that the crucible is 1° to 2° hotter at the top than the bottom, and also by making sure the absorption tube is not too large. Tests show that a 0.5- to 0.7-cm-diameter tube gives essentially the same results as a small capillary but with greater ease and precision; also fluid flow calculations show there is no convection with this size under these conditions. When in operation there is a slow flow of argon at 1 atm moving upward past the crucible. The cell and gas train are designed to make it possible to measure the rate of absorption of the gas by the originally gas-free metal. Figure 3 shows the arrangement for steady state operation. This is nearly the same except that the cell must be long and thin and the absorption tube must be close to the bottom, so that certain necessary approximations involved in the calculations will lead to only very small errors. Nevertheless the dimension L_2-L_1 must not be so small in relation to the tube diameter as to impose undesireable restriction upon diffusion. Obviously if one plans to run unsteady state-steady state in tandem for simultaneous C and D measurement, one must use the steady state cell arrangement with its dimension restrictions for the whole operation. The best way to tell if the dimensions are satisfactory for steady state operation is to compare the D values yielded by each operation separately. If both are the same, then the dimensions are satisfactory.

Procedure

The sample of metal is preferably a machined round or chunks, to reduce oxidized surface, and normally nearly fills the crucible. The charged crucible is inserted in the furnace, with the absorption tube in the retracted position above the crucible melt but connected by flexible tube P to the gas train as in figure 1. After melting in argon, sample is deoxidized with hydrogen by repeated treatments and evacuation, and by final evacuation and degassing to a stable "low-leak-rate" state. Upward argon flow is begun at slightly above 1 atm; a small nitrogen flow is started to flush the absorption tube at slightly above 1 atm, and then the absorption tube is immersed to the desired depth, quickly readjusting the nitrogen pressure to 1 atm. This is zero time. Nitrogen absorption at 1 atm (monitored by an oil manometer) with

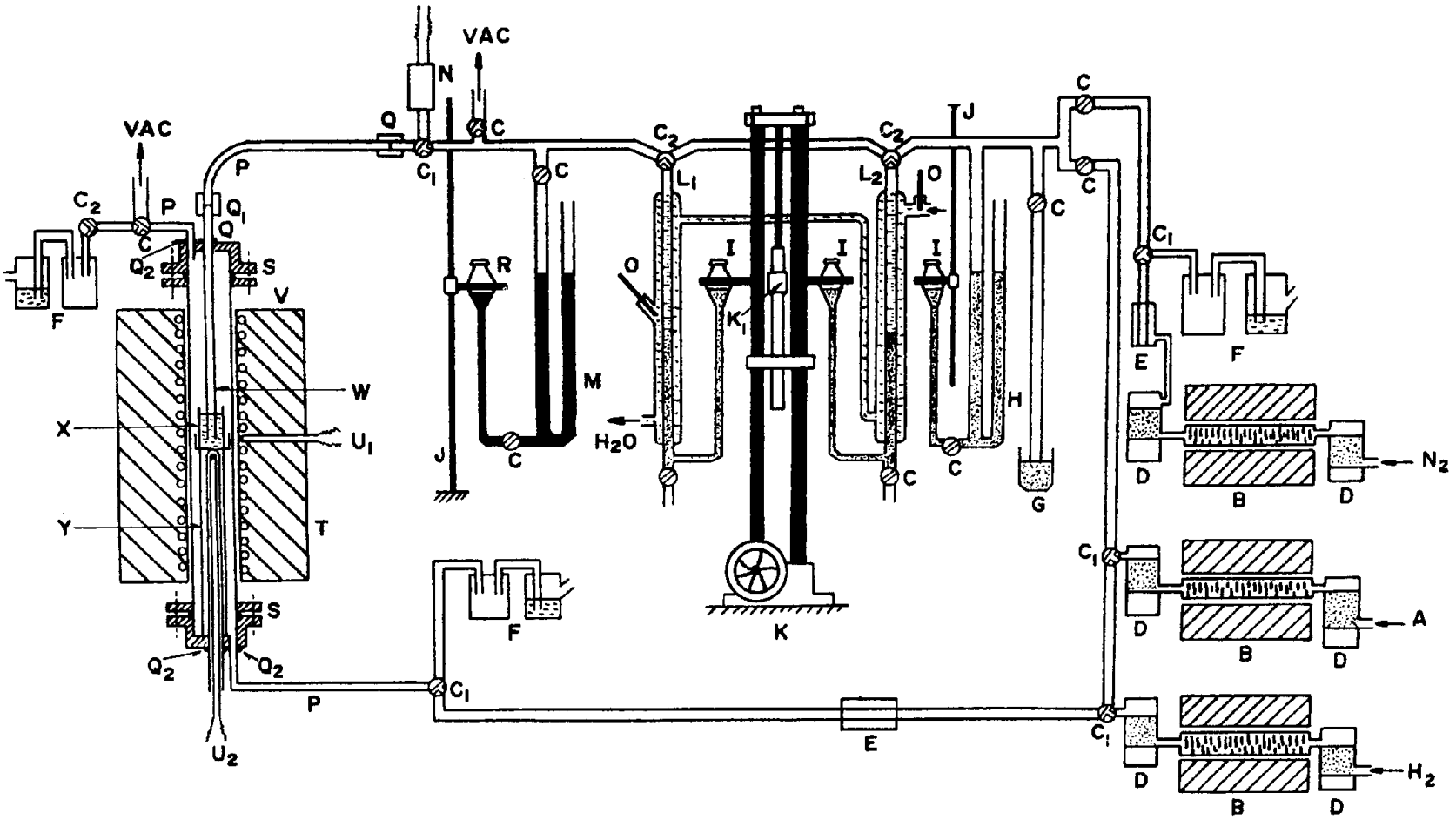


FIGURE 1. - Schematic diagram of the whole apparatus.

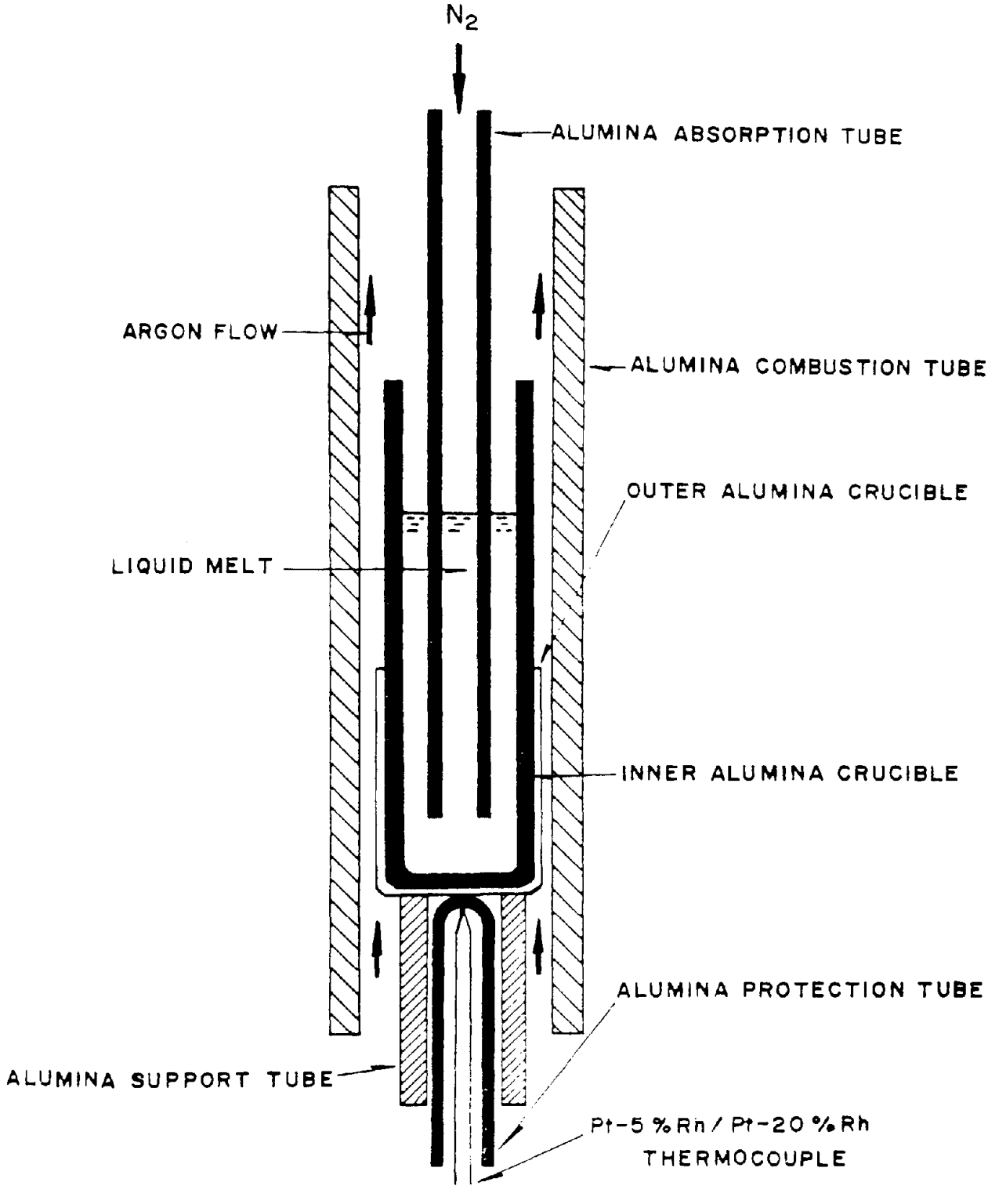


FIGURE 2. - The "unsteady state" cell operation.

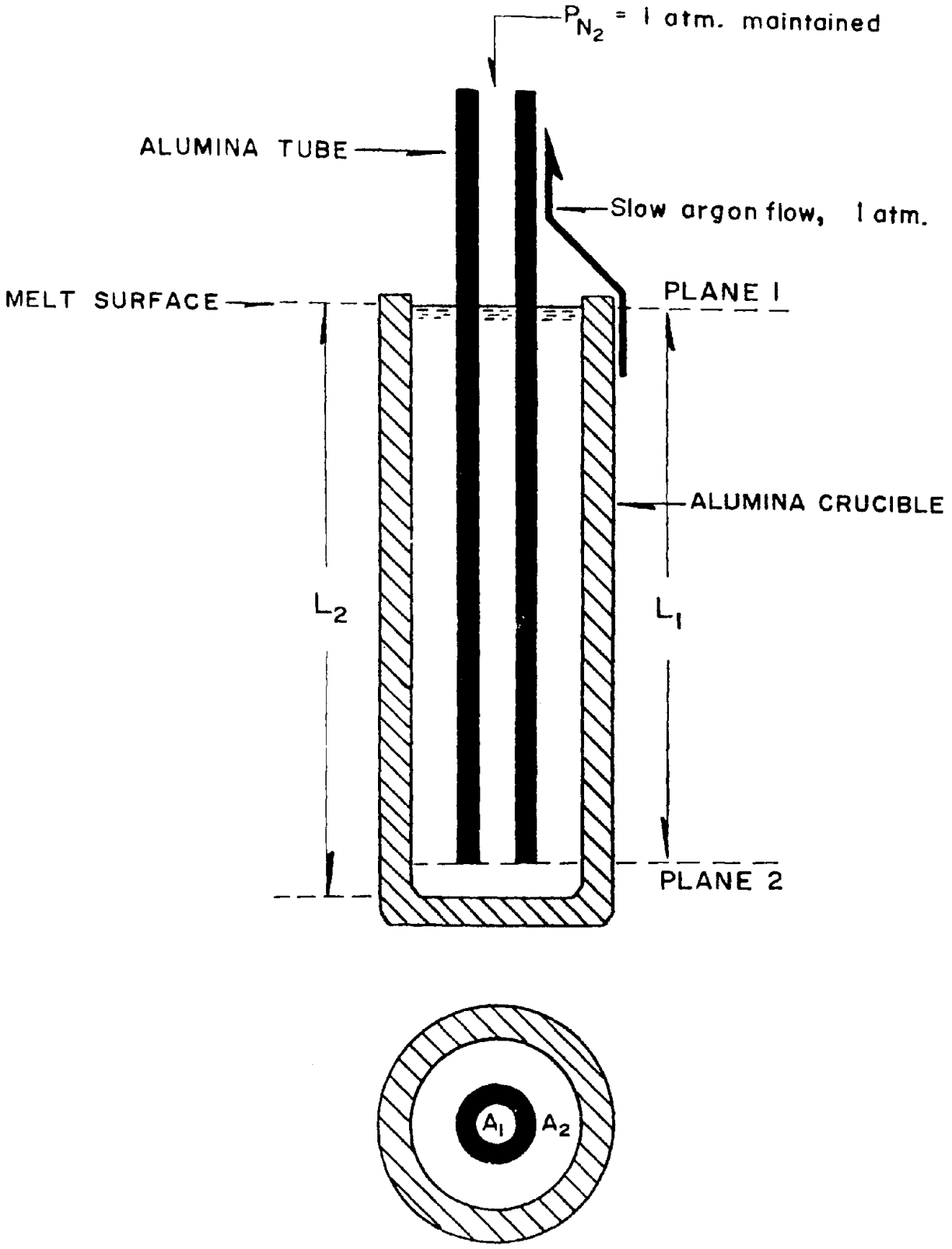


FIGURE 3. - Important cell dimensions for "steady state" operation.

time is observed from readings on a finely graduated small-diameter buret.

After sufficient readings for unsteady state interpretation of a V versus $\sqrt{t}$ (t=time) linear plot are complete, one may proceed to the steady state operation by simply waiting for the steady state absorption to develop at P_{N_2} = 1 atm. Normally, it is faster to retract the absorption tube, expose the metal and crucible to a flow of N_2 until saturation is approached, reinsert the absorption tube, restore argon flow around the crucible, and continue N_2 absorption measurements until the steady state is reached--as can be detected when volume of nitrogen absorbed is proportional to time. Readings are continued until a plot of V versus t is sufficiently linear to derive a reliable slope. Unsteady-state-run plots of V versus $\sqrt{t}$ show some "run-starting" phenomena discussed in reference 9, but (beyond this nonsignificant region) the significant part of the plot for measuring slope appears as in figure 4. The linear region exhibits Fick's second-law behavior extending up to the point B. P., which represents the point where deviation occurs due to the diffusing gas reaching and beginning to diffuse out of the bottom of the cell tube. The steady state plots are normally linear in V versus t, with no features worthy of illustration.

If C_s (1 atm saturation solubility) is already known, the slopes of both the unsteady state and steady state plots can be used to calculate D in square centimeters per second by the following equations (9, 21) derived from Fick's laws:

$$\text{Unsteady slope} = V/\sqrt{t} = \frac{d^2 \rho_m \, C_s \, \sqrt{\pi D}}{200 \, \rho_g}$$

$$\text{Steady slope} = V/t = D \, \frac{\rho m}{\rho g} \left| \frac{A_1 A_2}{A_1 L_2 + A_2 L_1} \right| \left| \frac{C_s}{100} \right|$$

where V is STP volume of hydrogen, in cubic centimeters absorbed at time t, in seconds; d is the diameter of the absorption tube in centimeters; ρ_m is the density of the liquid metal in grams per cubic centimeter; ρ_g is the density of STP gas in grams per cubic centimeter; C_s is saturation solubility (1 atm) in weight-percent; and A_1, A_2, L_1, L_2 are dimensions of cell as shown in figure 3. If everything is working properly, the two D values will agree reasonably well.

For calculation of both S and D the equations are written (21) as follows:

$$\text{Unsteady slope} = V/\sqrt{t} = S \cdot C_S \cdot \sqrt{D}$$

where S is the cell-system constant and

$$\text{Steady slope} = V/t = R \cdot C_S \cdot D$$

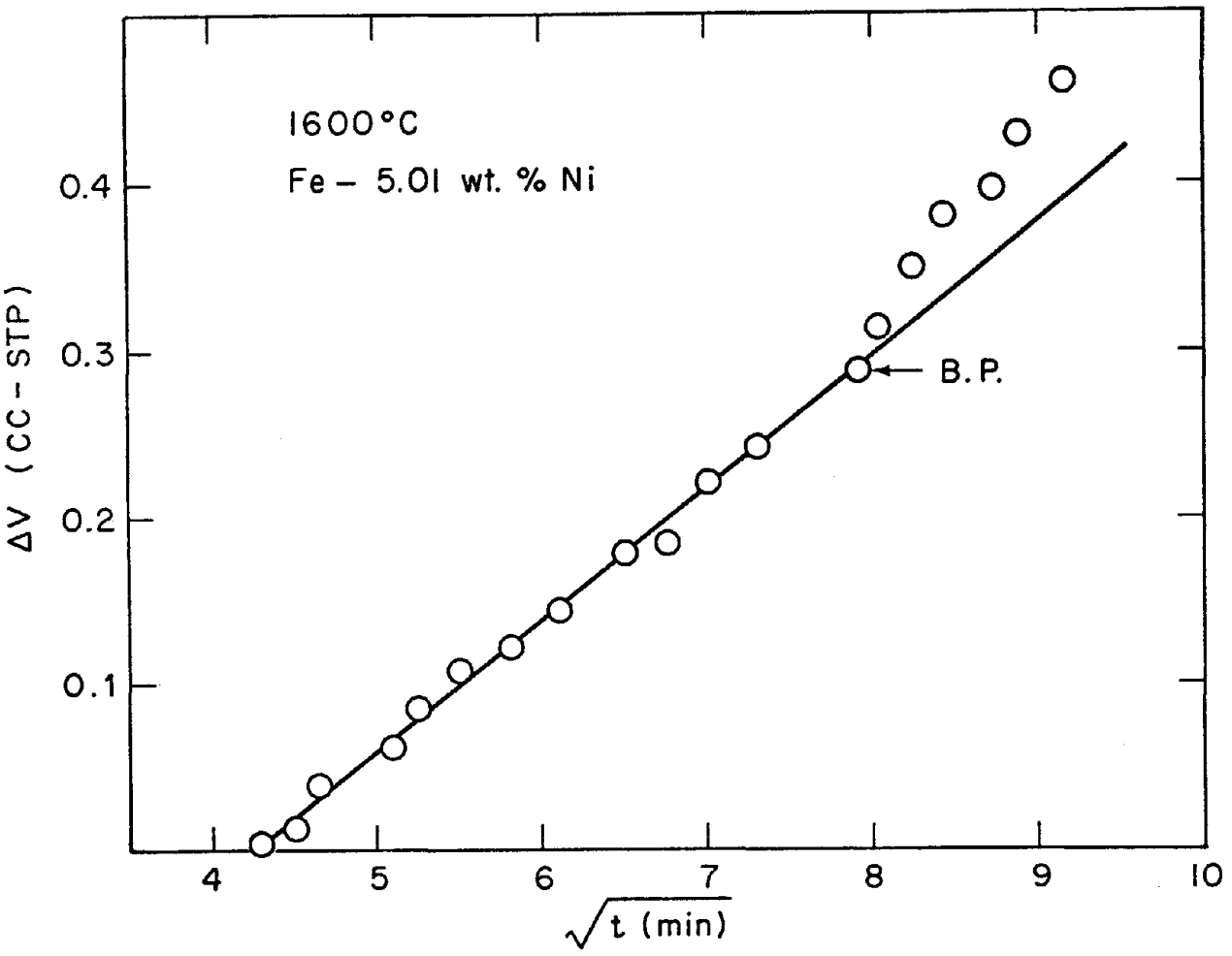


FIGURE 4. - Typical plot of volume of gas absorbed versus $\sqrt{\text{time}}$ for unsteady state operation (after initial stabilization period).

where R is the cell system constant. These two equations may be solved for the two unknowns C_S and D.

Applications

The method appears to have special promise where gas solubilities are too low for successful Sieverts work, such as for H and N in tin, where the results by the present method look good.

This technique is particularly useful in cases where it is desired to measure D but no values of C are available to make it possible to calculate D from a single-step method. Thus it was used extensively in the National

Science Foundation (U.S.-U.S.S.R.) program on the development of "Methods of Prediction of Solubilities and Diffusivities of Nitrogen and Hydrogen in Liquid Multi-Component Iron Alloys and Steels." This research is nearly complete--only a small part having been published (12). First a large number of C_S and D determinations on Fe-X alloys at 1,600° C were required for all commonly used alloying elements. This yielded useful plots of log f_N^X versus percent X and log f_H^X versus percent X for cases where literature data were scant (f_N and f_H being percent scale activity coefficients, that is, $a_N = f_N \cdot$ pcent N). Examples of such plots are found in the AIME book "Electric Furnace Steelmaking, Vol. II." Interaction parameters such as $e_N^X = \frac{\delta \log f_N}{\delta \text{ pct } X}$ at X→0 could be calculated from the plots. These same runs also yielded useful plots of log D_N^X versus percent X and log D_H^X versus percent X, representing the effects of single alloying elements on diffusivity. With these data it was possible to quickly test the simplest form of the Taylor expansion method of Wagner and Chipman for calculating log f_N^{alloy} and log f_H^{alloy}, and therefore C_S^N and C_S^H for a large number of complex alloys where C and D values had been determined by this or other research. This involves first-order terms of the equation

$$\log f_N^{alloy} = \log f_N^{Fe} + \frac{\delta \log f_N}{\delta(\text{pct}X)} (\text{pct}X) + \frac{\delta \log f_N}{\delta(\text{pct}Y)} (\text{pct}Y) + \text{etc}$$

where $\log f_N^{Fe} = 0$, and where X, Y, etc., are other solute elements.

This equation was found reasonably reliable for calculating solubilities (C_S^N, C_S^H) in the most complex alloys up to about 8 to 10 pct total alloy content as expected. Any method for highly concentrated alloys must somehow evaluate or take into account the higher terms of the series. This is obvious from the curvature of the log f_N and log f_H versus percent X curves. (A graphical vector method extended the predictability of C_S^N and C_S^H satisfactorily to the 15-pct-total-alloy-content range.) Graphical and computer methods were then used to develop equations (from the log f_{gas} versus percent X graphs) representing second-order and interaction terms for all alloying elements. When these were combined, it became possible to predict C_S^H or C_S^N in alloys of any complexity up to 50 pct total alloy content with a precision of ±5 pct. These alloys may, for example, contain one or more of the following elements: C, P, S, Al, Mn, Si, Co, Ni, Cr, Mo, W, Ti, V, Cb--which covers nearly all commercial iron alloys and steels made. Rather surprisingly, it was found that a variation of an older and different method of Kunze, Schurmann, and Parlee (13) gave rather good results for C_S^N up to quite high total alloy contents.

An important new discovery was that the same Taylor expansion principle could be made use of for calculating and predicting D_N and D_H values in complex alloys. This equation is analagous to the one above; namely

$$\log D_N^{alloy} = \log D_N^{Fe} + \frac{\delta \log D_N}{\delta (pct\underline{X})} (pct\underline{X}) + \frac{\delta \log D_N}{\delta (pct\underline{Y})} (pct\underline{Y}) + etc.$$

Here again evaluation of first terms--from the plots of log D_N versus percent $\underline{X}$ (see fig. 5) and log D_H versus percent $\underline{X}$, etc., gave good D_N^{alloy} values for all alloys up to 8- to 10-pct-total-alloy-element content. Graphical vector methods (12) were good for alloys of any complexity up to 15-pct-total-alloy-element content. However, the new sophisticated procedure involving graphical and computer-developed equations representing second-order and interaction terms for all alloying elements yielded a set of equations that would predict D_H and D_N with useful precision in liquid iron alloys and steels with any complexity and up to 50-pct-total-alloy content.

These experimental and calculated data on C_S^H, C_S^N, D_H, D_N, and these methods are now available to predict rate constants for the absorption, etc., of hydrogen and nitrogen in stirred liquid steels of any composition. The improved relations required to do this are being developed here and will soon be published.

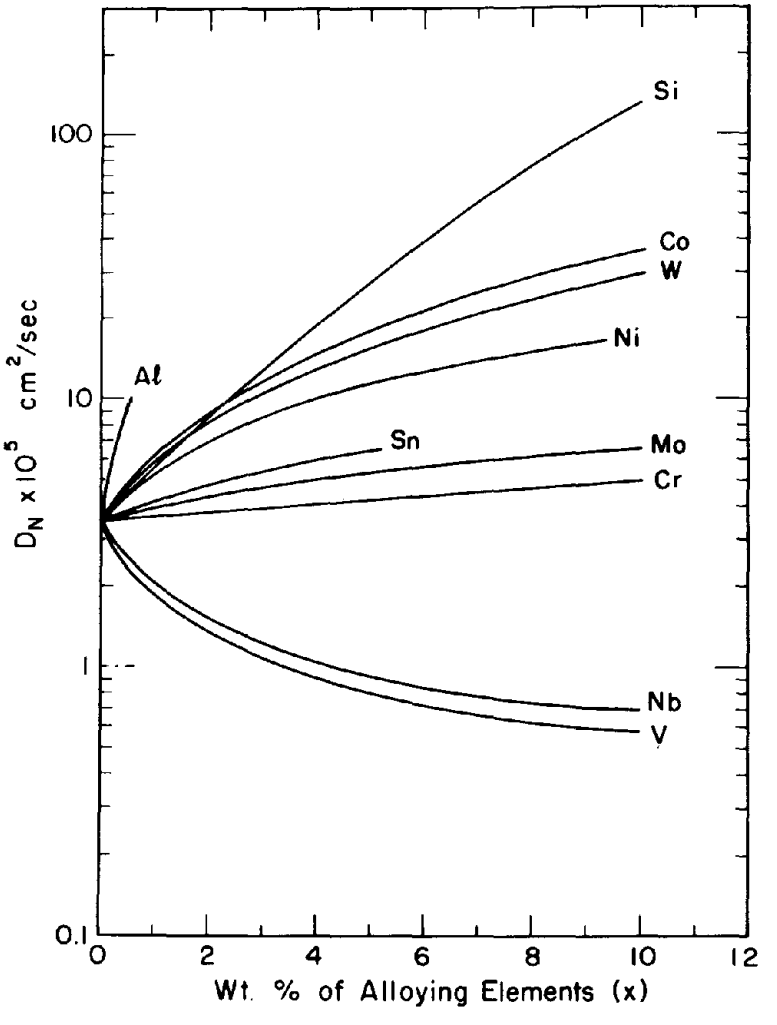


FIGURE 5. - Effects of alloying elements on the diffusion coefficient of nitrogen in liquid iron (D_N) at 1,600° C.

DETERMINATION OF THE THERMODYNAMICS OF REACTIVE METAL NITRIDE FORMATION--PRECIPITATION REACTIONS IN LIQUID METAL SOLVENT ALLOYS

The first recorded definitive study of a very reactive metal (Ti, V, U) nitride formation-precipitation reaction in a less reactive liquid solvent metal (Fe, Sn, Cu) was a paper by Rao and Parlee (16-17) presented in Paris at the Journeés d'Automne in 1959. This dealt with the titanium nitride formation in liquid iron-titanium alloys and established the basic techniques and methods of analysis of experimental equilibrium data that are employed today to provide the thermodynamics of nitride formation-precipitation reactions of the type

$$x\underline{M} + y/2\ N_2(g) = M_x\ N_y\ (s)$$

where $\underline{M}$ is the dissolved reactive metal, $N_2(g)$ is gaseous nitrogen, and $M_xN_y(s)$ is the solid nitride that precipitates at and above a critical partial pressure of nitrogen depending upon the equilibrium constant of the reaction. The work on Fe-Ti alloys was all done at 1,600° C, but the work on Fe-V alloys (8) which followed demonstrated that it was only necessary to repeat the same procedures at several temperatures to develop $\Delta G^\circ = \Delta H^\circ - T\Delta S^\circ$ values for reactions of this type. This was followed by work by Blossey and Pehlke (5), who used this technique to elucidate nitride formation in several Fe-M alloys such as Fe-Zr and Fe-Al, in the 1,600° to 1,700° C range. This work was all done in connection with the control of nitrogen in steelmaking. The ideas generated led to Anderson and Parlee's (1) work on the thermodynamics of the $\underline{U} + 1/2N_2(g) = UN(s)$ reaction in liquid tin, and other work by Fuwa, Anderson and Parlee (10) on Y-Sn, Pr-Sn, Gd-Sn, Th-Sn, Hf-Sn, etc., leading to the development of the proposed Parlee-Anderson selective nitriding process for reprocessing spent nuclear fuel. The techniques developed, once thought specialized, have more potential applications than generally realized. Solid hydride formation in several M-Sn alloys is being studied in the authors' laboratory, so far with only moderate success. In principle it should be profitable to elucidate oxide-formation-precipitation reaction stoichiometry and thermodynamics by this means in some liquid M-solvent systems. It should be easy in some M-Ag systems. In M-Cu systems it should be quite straightforward by using a solid electrolytic cell for P_{O_2} measurement. The potential of the technique is such that it should now be recognized as an important component of the thermodynamicist's "bag of tools."

Apparatus and Procedure

The apparatus is of the Sieverts type, now well known and described in literature in its various modernized forms (1, 5, 8), with the sample induction-heated to give as much stirring of the liquid as possible. The general procedure is equally well known but varies considerably from case to case. After melting, initial degassing, repeated deoxidation with hydrogen, degassing, dead-volume measurement with argon, reevacuation, and temperature adjustment, the run is begun. A small measured amount of nitrogen is admitted

adjustment, the run is begun. A small measured amount of nitrogen is admitted and equilibrated, and a reading of P_{N_2} is taken after taking special precautions to approach equilibrium from both sides. This procedure is repeated up to P_{N_2}=1 atm if desired. After applying dead-volume corrections, the results are plotted as percent N_2 absorbed (or cm^3 N_2/100 g) versus $\sqrt{P_{N_2}}$ $atm^{1/2}$. The upper curve in figure 6 shows the general form of all nitrogen absorption plots for reactive metal (Ti, V, U) nitride-formation-precipitation reactions in much less reactive solvent metals (Fe, Sn, Cu, Ni). Here iron is shown as the solvent. The lower curve shows the typical linear Sieverts relation for pure iron for comparison. The first leg of the plot for the alloy exhibits Sieverts behavior in the gas-liquid range (in some cases there may be some deviation as the solubility limit is approached) where the reaction is $1/2N_2(g) = \underline{N}$. If the solubility of nitrogen in the solvent metal (for example, tin) is too low to be detected, then this first (or Sieverts) region of the plot will lie along the base line. The sharp "break point" in the curve (labeled "solubility limit") represents the onset of nitride precipitation; in some systems, such as Fe-V, flecks of gold-colored nitride may be seen on the metal surface just above this point. At this point $x\underline{M} + y/2N_2(g) = M_xN_y(s)$ is in equilibrium. With added nitrogen the nitride precipitation continues until essentially all metal M is precipitated as the nitride (if P_{N_2} is high enough), at which place the curve becomes parallel with the pure solvent metal Sieverts line below.

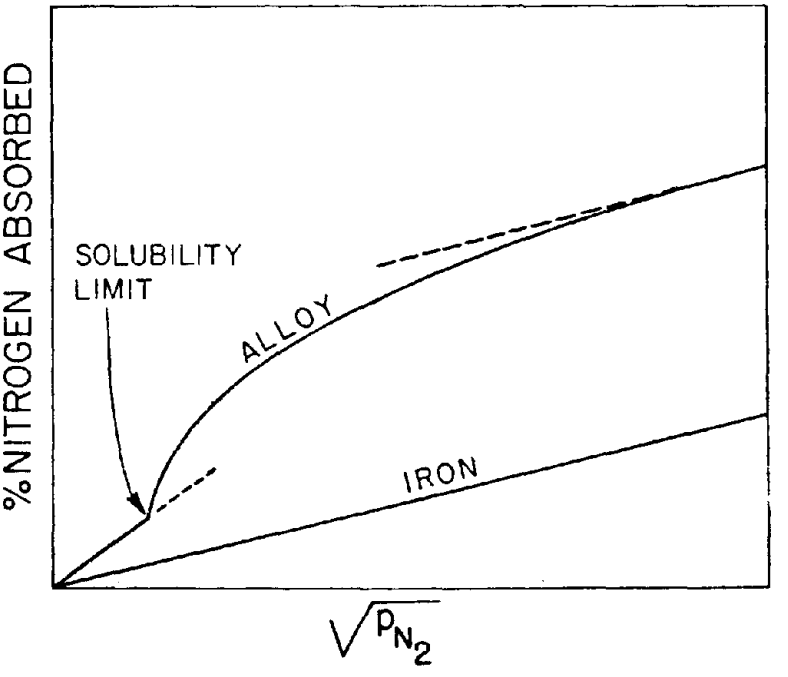


FIGURE 6. - Schematic diagram comparing nitrogen absorption curves of a pure metal (for example, iron) and of a nitride-forming alloy of the same metal.

When readings are complete, the power is shut off and the sample allowed to cool. If the nitride is lighter than the liquid, it will be on the top and surface; if it is much denser than the solvent metal, it will be at the bottom. In many cases X-ray work will establish the stoichiometry; otherwise it can be elucidated by plotting isoactivity lines (8, 10, 17) from runs made with charges of different initial percent M contents. The stoichiometry cannot just be assumed, because although it may be as simple as VN, it may be as surprising as $Ti_{1.7}N$.

If enough runs at different M compositions and different temperatures are made, then the thermodynamics of the reaction can be established. Let us consider the case of the following reaction in liquid iron (8), where the vanadium nitride stoichiometry is VN, as confirmed by both X-ray and isoactivity plots:

$$\underline{V}(pct) + 1/2\ N_2(g) = VN(s)$$

$$K = \frac{1}{a_V \cdot P_{N_2}^{1/2}} = \frac{1}{f_V \cdot pct\underline{V} \cdot P_{N_2}^{1/2}}$$

(The Henrian percent activity scale is used in this example, but the molecular fraction scale could be used). Values of percent V and P_{N_2} are taken from the "break points" from runs of several initial percent V compositions, and used to calculate values of K', the apparent equilibrium constant.

The true value of K is found by plotting log K' versus percent V and by extrapolating to 0 pct V, where K' = K. For example at 1,604° C, K is 0.122. Activity coefficients and interaction parameters can be calculated. It is possible to derive K from percent N_2 absorbed versus $\sqrt{P_{N_2}}$ data points along the curve above the break points, but the procedure is a good deal more complex. If the reaction $\underline{V}(pct) + \underline{N}(pct) = VN(s)$ is of interest, then values of percent V and percent N at the break point may be used in a similar, but somewhat more complex, manner to calculate K (8) for this reaction, which is 2.7 at 1,604° C. Plotting log K versus 1/T for several temperatures yield $\Delta G° = \Delta H° - T\Delta S°$ equations. For the latter reaction, the result is $\Delta G° = -58,000 + 29T(°K)cal$.

Figure 7 shows the form of nitrogen absorption curves for nitriding of U-Sn solutions at 1,567° C. The liquid-phase solubility is too small to detect; thus the break points appear to start at the base line. The numbers at the far right indicate that the uranium is almost completely converted to nitride at P_{N_2} = 1 atm for the 9 and 18 pct cases.

Isoactivity plots and X-rays showed stoichiometry to be U_2N_3 in the 1,475° range, and UN above 1,475° C. Figure 8, for GdN formation in liquid tin, is a good example of the use of absorption curve data to prepare isoactivity plots for stoichiometry determination. Values of K were determined at several temperatures for these reactions. Activity coefficient data were derived. The thermodynamics of the two reactions were developed as follows:

600° to 1,475° C:

$$2\underline{U}(pct) + 3/2\ N_2(g) = U_2N_3(s);\ \Delta G° = -3,890 + 7.5T$$

Above 1,475° C:

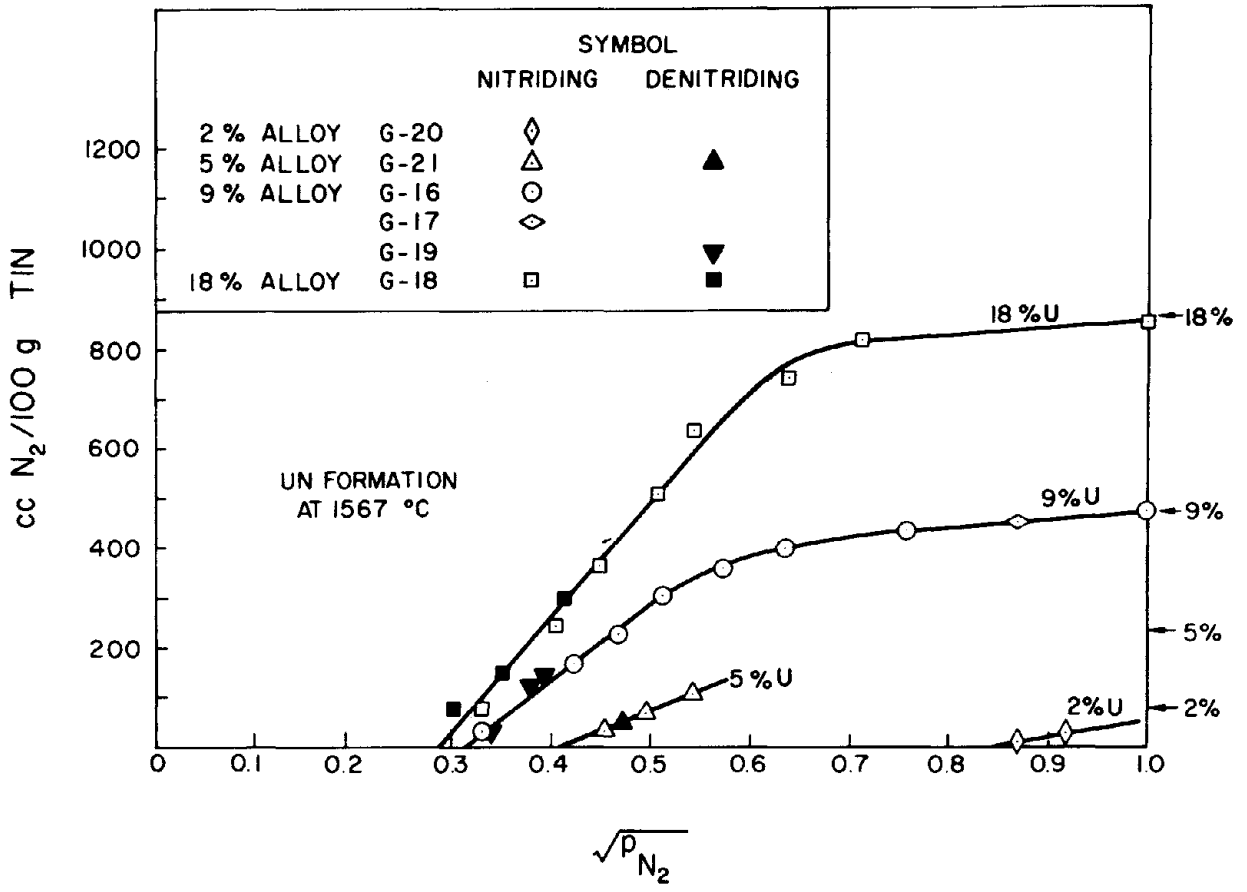


FIGURE 7. - Absorption of nitrogen by liquid U-Sn alloys at 1,567° C . (Alloy percentages refer to uranium, weight-percent concentration before nitriding.)

$$\underline{U}(pct) + 1/2N_2(g) = UN(s);\ \Delta G^\circ = -35{,}350 + 20.0T$$

When a second strong nitriding element is present, such as in U-Gd-Sn alloys (10), there will be two break points. For example, in 6.6 pct U-11.0 pct Gd alloy at 1,530° C the UN begins to precipitate at $P_{N_2}^{1/2} = 0.11$ $atm^{1/2}$ and continues to precipitate alone to $P_{N_2}^{1/2} = 0.22$ $atm^{1/2}$, where GdN begins (at a second break point) to coprecipitate with UN. A 6.6 pct U-0.1 pct Gd precipitates only UN up to $P_{N_2} = 1$ atm (and considerably beyond), leaving Gd unreacted in solution. Zr can be separated from Hf impurity by this method.

This kind of research led to the proposed Parlee-Anderson (3) process for reprocessing spent nuclear reactor fuel where the basic method of separation involves the selective precipitation of UN, leaving fission products behind in the tin solution, leading eventually--after subsequent steps--to three products; (1) reusable fuel, (2) waste, and (3) tin for recycling.

Thus, this general technique represents not only a method of deriving important thermodynamic information but also the basis of several potential metal-refining processes.

DETERMINATION OF THE THERMODYNAMICS OF THE CARBOTHERMIC REDUCTION OF OXIDES OF HIGHLY REACTIVE METALS IN LIQUID METAL SOLVENT SOLUTIONS

Anderson and Parlee (2) have demonstrated that the oxides of most highly reactive metals (U, Ti, Zr, Al, Mg, rare earths, etc.) can be reduced to the metal in certain liquid solvent metal solutions (Sn, Sb, Bi, etc.), without the formation of the carbides, which are the bane of conventional carbothermic processes when they are applied to the reduction of very reactive metals. The overall reaction is generally of the following simplified form

$$MO(s) + C(s) = CO(g) + \underline{M}$$

in favorable temperature and pressure ranges.

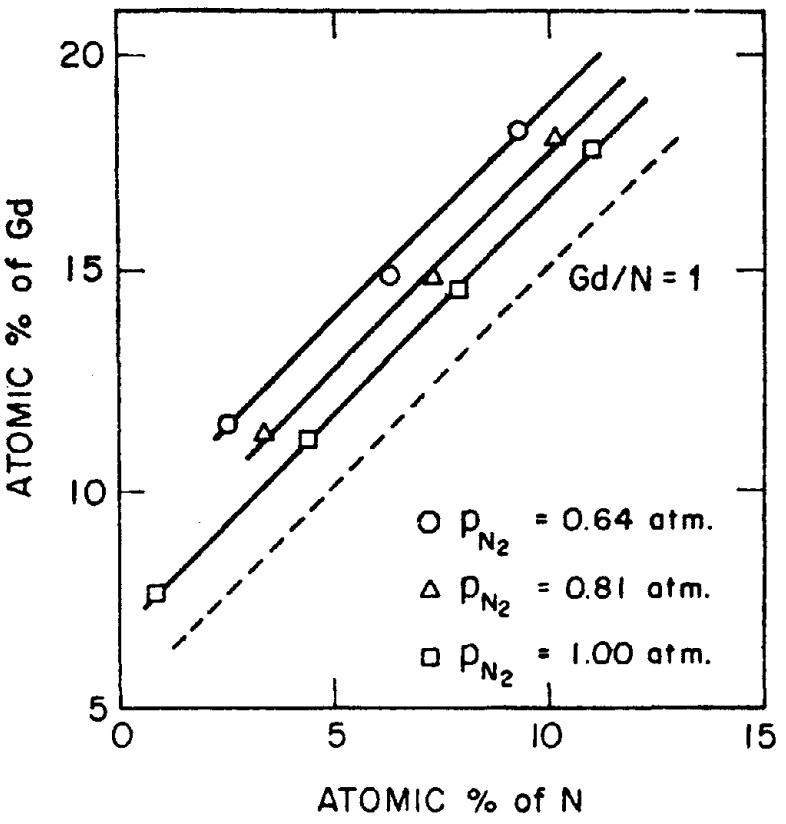


FIGURE 8. - Isoactivity plot for determination of the stoichiometry of the nitride compound precipitated from a Gd-Sn solution at 1,530° C.

Here $\underline{M}$ represents a very reactive metal dissolved in a much less reactive metal solvent, such as tin. The commercially pure reactive metal often may be recovered by phase separation and/or distillation. In the case of UO_2 reduction, the U-Sn solution produced can be cooled to near the eutectic, and the liquid-tin phase can be separated for recycling; then the solid phase can be remelted and the tin distilled off in vacuum. In Mg production, the final step is distilling off the Mg (2, 11, 4). The novel principle involved is that the solvent must be one that greatly reduces the activity of the reactive metal $\underline{M}$ in liquid solution--and reduces it to the point where carbides cannot form by reactions of the $x\underline{M} + yC(s) = M_xC_y(s)$ type. This also adds driving force to the reaction so that it may proceed at much lower temperatures and higher pressures (P_{CO}) than conventional carbothermic reduction. Refractory and other problems are reduced.

In principle, to carry out the reduction of an oxide, it is only necessary to heat a charge (M_xO_y + C + solvent metal) in a graphite crucible in vacuum to a temperature where the reaction proceeds; that is, where the gas comes off at a reasonable rate. However, in order to be able to design an industrial process, one needs to know the equilibrium pressures of the reaction under various conditions of charge and temperature. Thus it is desirable

to develop equilibrium constants and the thermodynamics of the reactions, as well as to determine the temperature and pressure ranges for the most rapid reduction.

The apparatus designed for this purpose by Bakshani, Anderson, and Parlee (4) therefore represents a thermodynamic technique that should be useful for studying the equilibria and thermodynamics of all "carbothermic reduction in solvent metal" reactions--particularly as applied to very reactive metals. The example used to illustrate the method is the reduction of UO_2. Figure 9 is a schematic drawing of the apparatus--which is of a modified Sieverts type. ABCD is the induction-heated reactor. The remainder is conventional except that an electronic manometer (pressure sensor and analog readout) and leak valve are added for more accurate measurement of pressures, also to measurement of rates of gas evolution at controlled operating pressure when desired. Figure 10 shows the reactor. A graphite rod is used to hold a pressed pellet of UO_2 + C powder mixture at the bottom and make sure it is below the liquid tin after meltdown. This is not necessary for the reduction but gives more consistent equilibrium pressures and operation for thermodynamic measurement. After evacuation and "dead volume" measurement (corrected for temperature by previous calibration), the power is turned on and the temperature is raised to the desired point. If the rate of reaction is reasonable at this temperature, the equilibrium can be measured. If desired, vacuum may be applied and the reaction allowed to proceed at a desired fixed pressure with measurement of gas produced. Measurement of gas involved (analyzed and shown to be essen-

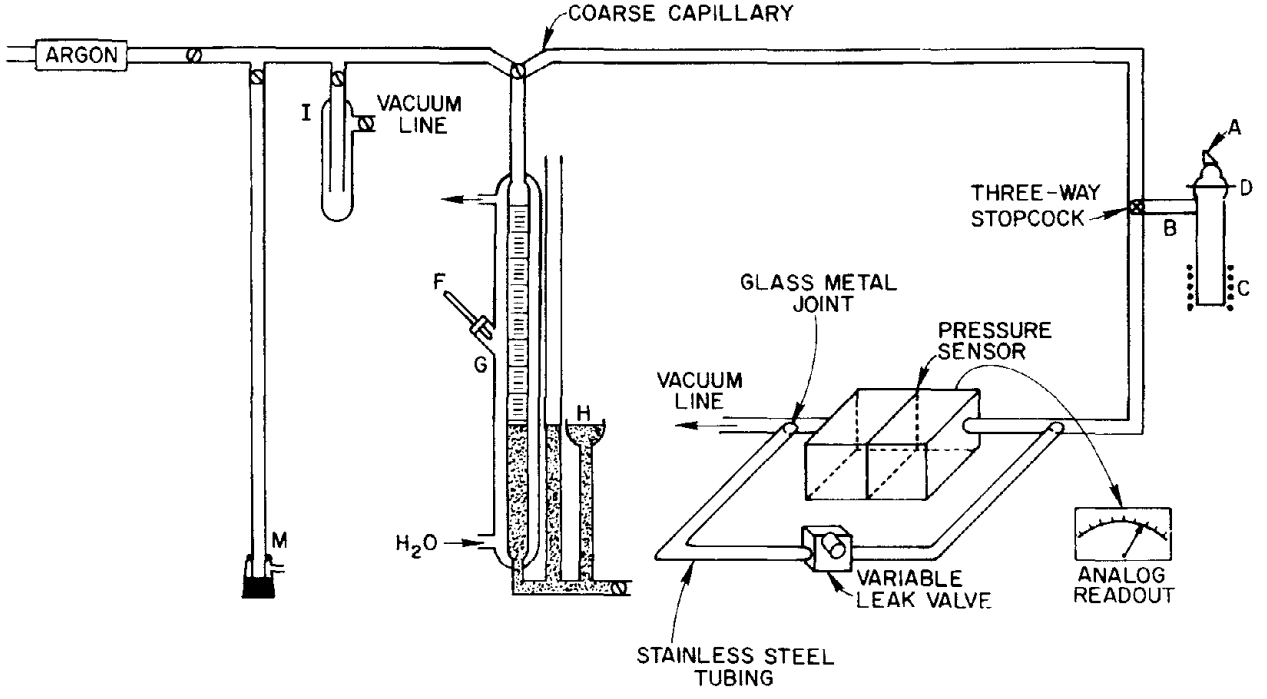


FIGURE 9. - Schematic drawing of apparatus used in studying carbothermic reduction of oxides of very reactive metals in liquid metal solvent solutions.

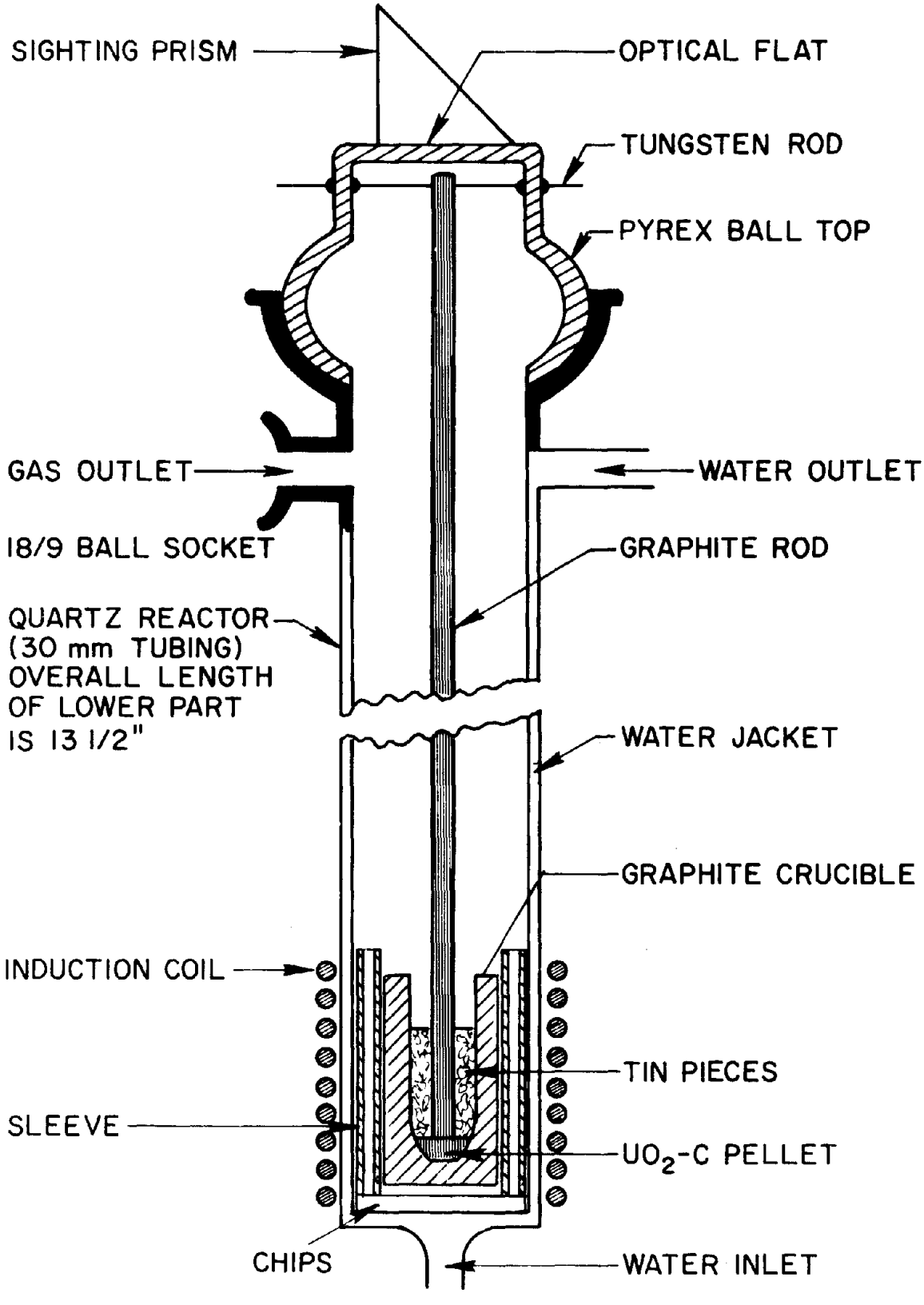


FIGURE 10. - The reactor assembly.

tially 100 pct CO) and analysis of solidified reaction product (in several runs after various degrees of reduction had occurred) showed the stoichiometry of the overall reation to be

$$UO_2(s) + 2C(s) = 2\ CO(g) + \underline{U}\ (\text{dissolved}).$$

This made it possible to calculate the extent of the reaction, in any particular case, from the amount of CO evolved, which in turn gave the amount and concentration of $\underline{U}$ produced. After measurement of equilibrium P_{CO} values under a number of different conditions, it became possible to calculate pseudoequilibrium constants, $K' = X_U \cdot P_{CO}^2$, where X_U is the equilibrium mole fraction of $\underline{U}$ dissolved in the tin and P_{CO} is the equilibrium pressure of CO. Plotting log K' versus 1/T yielded the following relation for the 1,450° C to 1,650° C range:

$$\log K' = -(28{,}600/T) + 12.17.$$

This relation makes it possible to calculate P_{CO} for any fixed extent of reaction (4). For example, at 1,650° C and 5.21 pct $\underline{U}$, the equilibrium P_{CO} (or total equilibrium) pressure is 208 torr in the presence of both UO_2 and C.

It should be quite possible to obtain true K by taking enough equilibrium measurements at different values of X_U and by extrapolating plots of log K versus X_U to $X_U = 0$. (Carbon solubility in tin is extremely small.) Then values of $\Delta G° = \Delta H° - T\Delta S°$ could be obtained.

However, in this research this was not done because a very large number of equilibrium measurements would be required, and several other objectives took priority--such as determining optimum operating conditions for the reduction (4). These were temperature 1,550° C to 1,630° C, pressure 1 to 10 torr, yielding 99 pct reduction in 5 hours without added stirring (which accelerates it). Carbon and oxygen contamination was low, typically 0.0008 pct C and 0.0015 pct O. A product that is very close to 100 pct U can be produced by evaporation at 1,300° C to 1,500 ° C. This may turn out to be the most economical method of producing several expensive metals. Industrial metal evaporation and distillation methods are developing rapidly.

A number of other reactive metal oxide-carbon systems have received one- or two-run "spot" studies by this method. They appeared to behave in a similar manner. Obviously there will be more complex cases, mostly below 1,000° C, where appreciable CO_2 will also be produced, but rates may be too slow to be of industrial interest. The technique appears to be a sound one for establishing the overall thermodynamics of many reactions of this kind in the more important temperature ranges.

ACKNOWLEDGMENTS

The first part of this study was initially funded by the Advanced Research Projects Agency (ARPA) through the Stanford University Center for

Materials Research (CMR), later by the American Iron and Steel Institute (AISI) and the National Science Foundation (NSF), and more recently by the US-USSR Co-operative Research Program through NSF. The second part was initially funded by Purdue University, then by ARPA through Stanford CMR, then by the Atomic Energy Commission, and more recently by NSF-Materials Research Laboratories (MRL) through CMR at Stanford. The third part was funded by NSF-MRL through CMR at Stanford University.

REFERENCES

1. Anderson, R. N. and N. A. D. Parlee. Met. Trans., v. 2, 1971, pp. 1599-1604.

2. ____. J. Vac. Sci. and Technol., v. 13, no. 1, January-February 1976, pp. 526-529.

3. Anderson, R. N., N. A. D. Parlee, and J. Gallagher. Nuclear Technol., v. 13, 1972, pp. 29-35.

4. Bakshani, N., N. A. D. Parlee and R. N. Anderson. Ind. Res./Devel., February 1979, pp. 122-126.

5. Blossey, R. G., and R. D. Pehlke. Trans. TMS-AIME, v. 236, 1966, pp. 566-569.

6. El-Naggar, M. M. A., G. B. Horsley, and N. A. D. Parlee. Trans. AIME, v. 239, December 1967, pp. 1994-1995.

7. El-Naggar, M. M. A. and N. A. D. Parlee. V. 1, October 1970, pp. 2975-2977.

8. El-Tayeb, N. M. , and N. A. D. Parlee. Trans. TMS-AIME, v. 227, 1963, pp. 929-933.

9. ____. Trans. TMS-AIME, v. 239, 1967, pp. 1345-1351.

10. Fuwa, A., R. N. Anderson, and N. A. D. Parlee. High Temp. Sci., v. 7, 1975, pp. 249-258.

11. Graves, C. Liquid Metals as Process Solvents: Design Techniques for Oxide Reduction. Ph.D. Dissertation, Univ. of Illinois at Urbana-Champaign, 1978.

12. Jayarajan, A., and N. A. D. Parlee. High Temp. Sci., v. 8, 1976, pp. 317-337.

13. Kunze, H. D., E. Schurman, and N. A. D. Parlee. Met. Trans., v. 1, 1970, pp. 281-290.

14. Lee, J. Y., and N. A. D. Parlee. High Temp. Sci., v. 4, No. 2, 1972, pp. 147-159.

15. Mizikar, E. A., R. E. Grace and N. A. D. Parlee. Trans. Am. Soc. Metals, v. 56, 1963, pp. 101-106.

16. Rao, M. M., and N. A. D. Parlee. Mem. Scientifiques Rev. Metallurg., v. 58, No. 1, 1961, pp. 52-60.

17. ____. Trans. Can. Min. and Met. Bull., v. 66, 1963, pp 123-129.

18. Sacris, E. M., and N. A. D. Parlee. Met. Trans., v. 1, 1970, pp. 3377-3382.

19. Shah, I. D., and N. A. D. Parlee. Trans TMS-AIME, v. 239, 1967, pp. 763-764.

20. Sieverts, A., and N. Hagenacker. Z. Physik. Chem., v. 68, 1910, p. 115.

21. Velho, L. R., N. M. El-Tayeb, J. Gani, and N. A. D. Parlee. Trans. TMS-AIME, v. 235, 1969, pp. 185-186.

HEATS OF MIXING OF HYDROGEN-BONDED SPECIES

by

K. D. Williamson[1]

ABSTRACT

Heats of mixing of several hydrogen-bonded pairs of liquids have been measured with a Tronac flow calorimeter at 25° to 75° C. Some qualitative comparisons of the data are given. The apparatus, operating techniques, and data reduction methods used in these studies are reported in detail.

INTRODUCTION

Heats of mixing have been determined on a variety of binary mixtures in our laboratory. There are several reasons for wanting such data. In some cases, the heat of mixing is large enough to be an appreciable engineering consideration. In other cases it is small but is useful in correlating with other physical data - for example, in deducing micelle formation or other molecular orientation in solutions of polymers. Still another use of heats of mixing has been in calculating other related thermodynamic data, through equations of state or through relations involving activity coefficients. For example, vapor-liquid equilibria data have been determined from the heats of mixing with or without other supporting data.

EXPERIMENTAL WORK

In the course of this work, data have been obtained on the heats of mixing of several pairs of liquids, each member of which undergoes hydrogen bonding. Although other factors such as configuration affect the heats of mixing, hydrogen bonding must be the predominant effect. With pairs that form hydrogen bonds in the neat components, the net effect upon mixing may be making additional hydrogen bonds, breaking previously existing hydrogen bonds, or exchanging hydrogen bonds of one strength for those of another. Making more or stronger hydrogen bonds is exothermic. Reducing the number or the average strength of the hydrogen bonds is endothermic. The present state of the art does not permit a priori predictions of the heat of mixing for cases as complex as the present. Whereas nearly quantitive prediction can be made for a simpler case like the mixing of a linear alcohol and a hydrocarbon, methods such as "group contributions" are very approximate here.

[1]Union Carbide Corp., South Charleston, W. Va.

The systems reported here are indicated below:

Methanol + Ethylene glycol	(130)
Methanol + Glycerol	(315)
Ethanol + Ethylene glycol	(475)
Ethylene glycol + Glycerol	(26)
Glycerol + Water	(-725)

The heats of mixing in all cases were positive except for glycerol + water. The extreme values (joules/per mole) for the various pairs at 25° C are shown in parentheses in the diagram. As might be expected, similar molecules mix with little heat effect (for example, ethylene glycol + glycerol). Increasing dissimilarities in size (for example, methanol + glycerol) versus (methanol + ethylene glycol) or in hydroxyl concentration (for example, methanol + ethylene glycol versus ethanol + ethylene glycol) cause the heat of mixing to increase. Water added to any highly hydroxylated hydrocarbon (as illustrated here by water-glycerol) seems to be exothermic. The present systems are illustrative of the data that we have obtained recently with a Tronac flow calorimeter. More complete data on the present systems will be presented in a later paper, along with comparisons with other published data.

EXPERIMENTAL SETUP

The emphasis in this report is on the equipment, the experimental procedure, and data processing incidental to obtaining heats of mixing. The inatrument and its accessories are similar to the equipment described by Christensen (1-2)[2]. A semischematic diagram of the apparatus is shown in figure 1. The apparatus consists of (1) a flow cell maintained isothermally with a closely controlled constant-temperature bath, (2) a pair of pumps for programed flow of the two components being mixed, (3) a back-pressure regulator, and (4) supporting electronic equipment for maintaining and monitoring conditions.

The calorimeter cell consists of input tubes, a junction for mixing, and a 6-foot coil of tubing for heat exchange with an isothermal slab. This aluminum slab is mounted on insulating spacers within a watertight shell that is mounted within the thermostatted bath. A working heater and a Peltier device are also in thermal contact with the slab. The Peltier device works in opposition to the heater, to maintain a steady state when no thermal incident is occurring within the calorimeter. The heater is controlled by a thermistor attached to the slab. The heater fires in equienergetic pulses (several thousand per second). When the slab tends to cool, the heater fires more frequently; when the slab tends to heat, the heater fires less frequently. The change in heater output is a measure of the magnitude of the thermal event taking place at a given instant within the calorimeter. This change is monitored by a counting circuit, which registers the number of pulses per second. A calibrating heater attached to the slab can be turned on at will. The wattage output of the calibration heater (obtained by measuring the cur-

[2]Underlined numbers in parenthese refer to items in the list of references at the end of this paper.

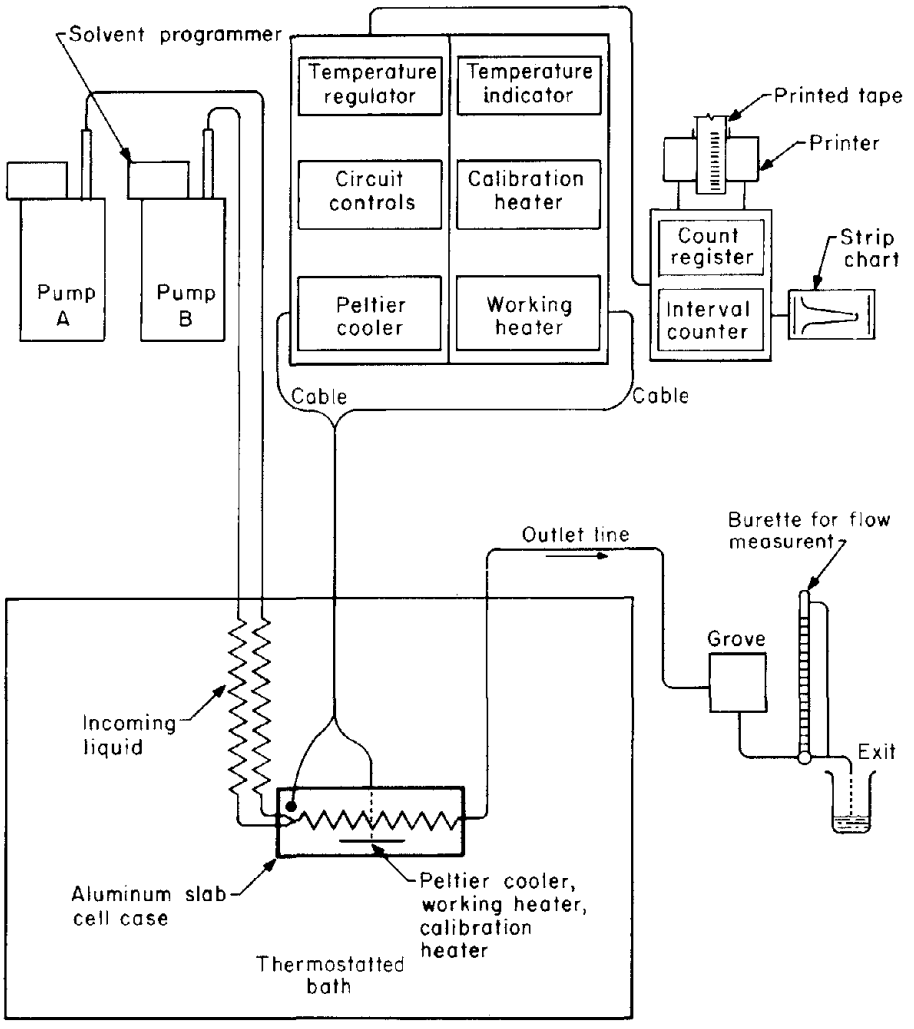


FIGURE 1. - Schematic of Tronac flow calorimeter.

rent and the potential) is matched against the pulse rate of the working heater to obtain joules per pulse. A final monitoring device within the calorimeter cell is a second thermistor, by which the temperature of the slab at any instant is determined.

The calorimeter is fed by a pair of Varian pumps, model 8500, direct-displacement pumps of the type used for liquid chromatography. These pumps can be set to feed from 1 to 900 cm^3/hr. The flow can be set manually for steady output from each pump. Alternatively, the flow can be programed by a Solvent Programmer for linearly variable feed--for example, to process from 0 to 100 pct of a component over a period of time--10 min to several hours. Thus a heat-of-mixing run may be made by manual adjustment of the pumps in a succession of steps to cover the desired concentration range--or by programing through the concentration range linearly over time. Feed from pumps flows through 1/16-inch-OD stainless steel tubing which passes through the

bath to the calorimeter junction. The tubing in the bath serves as a heat exchanger to bring the liquids to bath temperature (essentially calorimeter temperature) before the mixing occurs.

Flow exiting from the pump passes through a back-pressure Grove valve, which controls the pressure within the flow tube. Downstream from the Grove is a liquid buret, into which effluent can be diverted for measured time intervals, for direct determination of flow. Pressure can be maintained in the flow cell from slightly above 1 bar to as high as 138 bars. Temperature in the cell can be maintained, by means of the thermostat, at any temperature from 273 to 348 K. The output of the calorimeter is followed by a strip chart recorder, an especial aid in setting up initial conditions with the proper range and baseline. A more exact output is afforded by a printed tape, onto which averages rates of heater pulsing for increments of time are printed out consecutively. Periods from 2 to 50 seconds are normally used.

Runs are made in both continuous and stepwise mode. In the continuous mode, the controls are set to traverse the desired concentration range, usually in 1 to 2 hours, so that the change of concentration passing through the calorimeter is about 0.5 to 1.0 pct/min--a rate of change compatible with the time constant of the instrument. With this type of run, the forward run is followed by a reverse run. Small differences due to instrumental time lag and random disturbances are averaged out between the forward and reverse runs. In the stepwise mode, measurements are usually made at each 0.05 or 0.1 mole fraction, with the flow being left at a given concentration for 10-20 min. Whichever type of run is made, the preparations for the run, the run itself, and the calculations on the run can be made comfortably in a day's time, if all goes well. Professor Christensen has shown, and this has been verified by our own experience, that one type of run is about as accurate as the other, if proper precautions are taken in each case. A basic difficulty has been in operating at extreme concentrations--from 0 to 10 pct or from 90 to 100 pct of a component. Special means, such as feeding diluted samples, have been necessary to provide accurate data in these regions.

REDUCTION OF DATA

A computer program was written for calculating the heat of mixing at different mole fractions from the raw data. The input to this program from the calorimeter is pulses per second and joules per pulse. The other experimental quantities entered are flow rates of the two components. Auxiliary data, such as densities and molecular weights of the two components, are entered by teletype on a tutorial-type program. The output from this program can be manipulated in various ways by a second program. The data are fitted by a spline function, after which

1. The heat-of-mixing data can be calculated at arbitrary mole fractions; for example, at each 0.05 mole fraction.

2. First derivatives can be calculated at any point, thereby providing differential heats of mixing.

3. Various statistical tests can be run, to estimate uncertainty in the original data or in the derivatives.

CALIBRATION AND TESTING OF APPARATUS

The heat of mixing is calculated from two basic measurements: the energy requirement and the flow rate. The energy requirement in joules per second is calculated as the product of pulses per second times joules per pulse. The pulses per second is obtained directly from the counter at a given instant during a run. The joules per pulse is obtained from observations with the calibration heater on, before and after a run. The accuracy of this latter measurement depends on the constancy of resistance of the calibration heater and on the accuracy of calibration of this heater when the instrument was built.

The flow rate is checked by direct measurement of the output of the pumps. The flow of each pump is measured separately at the pressure of the experiment. Extensive checking has shown that the flow of one pump is independent of the flow of the other. Extensive checking has also shown that the Solvent Programmer proportions the flow as accurately as we can measure it, volumetrically or gravimetrically. That is, if the pump delivers 50 cm^3 /hr at the 100 pct setting, it will deliver 12.5 cm^3/hr on a 25 pct setting. The nominal setting of the Varian pumps is usually within 1 to 2 pct of the directly measured setting. Direct measurements made before and after a run generally agree within 1 pct.

The ultimate test for accuracy of the overall operation is measuring the heat of mixing for a system of accepted value. To check the accuracy of the entire calorimeter assembly during flow measurements, we measured the heat of mixing of n-hexane and cyclohexane at 298.15 K. This reaction has become a standard for heats of mixing throughout the world. Table 1 shows the comparison between our own work and that deemed to be most accurate from other laboratories. Our data are about 2 pct lower than the standard set, through most of the concentration range. Probably most of this apparent inaccuracy is in flow control and measurement. With the flow method, the points at extreme concentrations are inherently less accurate than those at intermediate concentrations.

CONCLUSIONS

A Tronac flow calorimeter has been used to measure heats of mixing for several pairs of hydrogen-bonded compounds. The data collection has been largely automated. Computer programs have been devised for reducing the raw data, statistically analyzing the data, and calculating derivative data. Check runs on a standard system indicate the data are accurate to about 2 pct (or 5 j/mole) with the greatest inaccuracy being due to uncertainty in flow.

TABLE 1. - Heats of mixing of n-hexane + cyclohexane at 298.15 K

Mole fraction cyclohexane	Heat of mixing, j/mole	
	Standard[1]	Present Work[2]
0.1	64.03	
.2	118.95	119.38
.3	163.50	163.57
.4	196.43	191.05
.5	216.17	211.95
.6	220.51	215.83
.7	206.31	203.01
.8	169.15	165.76
.9	103.02	97.00

[1]Standard data for exact values of mole fraction calculated by means of Redlich-Kister equation furnished in reference 3.

[2]Data for exact values of mole fraction calculated by means of Taylor-series equation fitted to the raw data.

REFERENCES

1. Christensen, J. J., L. D. Hansen, D. J. Eatough, and R. M. Izatt. Isothermal High Temperature Flow Calorimeter. Rev. Sci. Instr., 47, 1976, pp. 730-734.

2. Christensen, J. J., R. M. Izatt, R. W. Izatt, R. W. Hanks, and K. O'Neill. Prediction of Vapor-Liquid Equilibrium for Hydrocarbon - Alcohol Systems From Heat of Mixing Data. 33d Ann. Calorimetry Conf., Logan, Utah, July 26, 1978.

3. Thermodynamics Research Center, Texas A & M University. Selected Data on Mixtures. Internal DATA Series, 1976.

DISCUSSION

C. M. Criss: Did you have any problem with pulsing in the pumps?

K. D. Williamson: We had problems when we were using Waters pumps. They were supposed to have all sorts of fancy compensators in them that lagged out the flow, but we could see perturbations no matter what we did and no matter what the company tried to do for us. We changed over to the Varian pumps. They are direct displacement pumps. The pumps have massive pistons in them. These do not show any cycling whatsoever. Another question you might ask is,

how good are the pumps? Again, we had quite a bit of trouble with the Waters pumps, trying to maintain any accuracy or any consistency with them. We had to calibrate very specifically for them, and yet, the next day they might not be delivering quite what we had calibrated them to the day before. The Varian pumps are delivering very nearly the nominal flow. We checked the flows directly with a buret at the exit, but they are within 1 to 2 pct of the nominal flow at all conditions. The two pumps are independent of each other so that there is no interaction there; that is, if one pump is started up, the other one does not slow down or anything like that. However, I suspect that there is still the factor that we need to trim out in order to get the very best data. The inconsistency that I showed you here on the normal hexane-cyclohexane is mainly attributable to that. We will probably develop some fancier systematic scheme for determining our flow.

C. M. Criss: How do you get very viscous materials to mix properly in the flow cell.

K. D. Williamson: Sometimes we don't. That is the limiting factor in using them. As a rule of thumb, we seem to do all right if the viscosity of one of the feeds is not more than 100 centipoise and the viscosity of the other is more like water. We can tell when there are difficulties in handling the viscous fluids. One is the pressure drop, which goes up enormously if a fluid is just too viscous to put through a very small tube in our cell. The other is that we start seeing irregularity; that is, if we are running a 30:70 mixture at a steady state, the output (counts per second) will fluctuate. That way we will see irregularities in the plot that we get, rather than a straight line, if we do have poor mixing.

K. J. Breslauer: How much time do you need to get a steady state? How much overshoot and undershoot is there?

K. D. Williamson: This depends somewhat on the conditions of the operation. Speaking generally, the time constant for the instrument is about 2 min to make an abrupt change of some magnitude. If the step change is small, then it may be only 30 sec to get essentially the new value. We checked this out by our calibration heater. We turn on the heater for a step function and then turn it off again later, and we pretty well see what the response time is through that. I have also run some stop-flow experiments with the cell, and that also helped me to evaluate that factor.

K. J. Breslauer: I guess what I am getting at is, if your minimum flow rate is 10 cm^3/min and you have response built in with the overshooot and undershoot, what total volume, including volume of the flow tube, does one need to get an effective steady state run?

K. D. Williamson: I think it is best stated in terms of the time required to get very good data. That requires at least an hour. So that if we are running 10 cm^3/hr, that would be 5 cm^3 of each component.

GENERAL DISCUSSION: GAS-CONDENSED PHASE EQUILIBRIA

Y. A. Chang: (In reply to questions on variation of ΔG with temperature) My experience with substances of metallurgical interest is that for most of these substances the Gibbs energy of formation may be represented by the following equation:

$$\Delta G = A + BT + CT \ln T.$$

Very often, A + BT is sufficient to represent the Gibbs energy of formation data.

R. P. Beyer: How long does the platinum furnace winding last?

N. A. D. Parlee: Not very long. I mentioned that you could use it up to 1,800° C, and we've done quite a lot of work up to about 1,750°, but we've been doing less and less up to these high temperatures. The winding is actually pt-40 pct Rh alloy. At one time, at the rate a graduate student works, it took about two relinings a year with new windings. The trouble is, whereas a few years ago it only cost $4,000 to reline the furnace, now it costs $8,000. I have been in trouble with this work because I can't get enough money. It has taken us about a year to get a Super Kanthal furnace going. It is being developed by the Marshall Furnace Co., a small factory near us. They have been bringing furnaces around, burning them out, and finally after many months we think we've got one that works pretty well. This is an expensive business.

We think that the Super Kanthal is going to be the answer. At 1,800° C it sure won't last very long. It is not a platinum furnace. We prefer the pt-40 pct Rh winding which will last sometimes for 6 months if you don't go beyond 1,750° C.

J. C. Barclay: Does hydrogen sulfide react with mercury? Your use of the Topler pump means that the H_2S-containing gas mixture is exposed to a large mercury area and it wouldn't take much reaction to give erroneous pressure points.

Y. A. Chang: I think we have not run long enough to give you a good answer.

J. A. Barclay: Did I understand you to say that you had some some experiments on the carbothermic reduction of magnesium oxides?

N. A. D. Parlee: Some of my collegaues have. Professor Anderson and I were the ones that devised this scheme for making reactive metals by carbothermic reduction in solvent metals; there are a number of us involved, such as Professor Eckert of the University of Illinois. Yes, magnesium has been produced in the laboratory by this method. Quite a lot of studies have been made, and tin, antimony, and bismuth have been tested as solvent metals. For example, you can take MgO and reduce it into tin, and then, after you have reduced it into tin, you can raise the temperature and distill magnesium out of the tin. I don't know what more has been done about the commercial development of the process. There is a very large company that is interested in this; they do not wish to be named. In fact, a number of companies are doing work on it and all are very secretive. Professor Anderson and I have a patent on this pro-

cess. We know these companies are doing things, but we don't know exactly what. Certainly magnesium has been worked on by one of my colleagues, and it looks very favorable for a possible new method of making magnesium. The regular carbothermic method of making magnesium never really worked. It was tried during the war and it was never found feasible.

J. C. Haygarth: You have published and patented a separation technique for Zr and Hf based on formation of their nitrides from a solution of Zr and Hf in liquid Sn. In your patent, it is claimed that separation is achieved because ZrN is less dense than liquid Sn and floats, whereas HfN is more dense and sinks. My intuition leads me to suspect that mixed nitrides, that is, $Zr_xHf_{(1-x)}N$, would form and would sink or float according to density, which would depend in turn on x. Thus, I would expect the floated nitride to contain some Hf, and the sinking nitride to contain some Zr. Yet, your published results indicate total separation within analytical sensitivity. How do you account for this?

N. A. D. Parlee: You mean the nitrides as a solid solution? That is a good point that I hadn't thought about. I have considered that in certain cases this might be happening and wondered if it could happen. In some of the cases where I feared that it would happen, it had not. In this particular case, that work itself was done by Anderson. We both have a patent on it because it is an outgrowth from a previous basic patent by us. I am not sure about this. I would wonder about that myself. As I say, we have found situations like this, where I have feared that you might run into a solid solution. Recently, we found in the case of hafnium and zirconium, that there is a simpler way to actually make the separation. If you really want to do that separation, you are generally starting with something that contains quite a lot of zirconium and a small amount of hafnium. Generally, you are trying to get the hafnium out of the zirconium to improve its cross section for fuel, making fuel rods, or cylinders for nuclear fuel. We have found that we can separate by precipitating the zirconium and just leaving the hafnium behind in the solution; that is, without precipating quite all the zirconium; that appears to work. There again, one could ask the same question, "Why don't I get the two together?" However, the X-ray people simply reported only zirconium as a zirconium nitride in the precipitate and did not report any hafnium in the precipitate.

Anonymous: What are the basic reasons for this separation?

N. A. D. Parlee: The reason is just based on the concentration. If you have a small concentration of something it remains in solution. The one that is present in high concentration precipitates first. Actually, this is the basis of nuclear fuel separation. You have a high concentration of uranium; you have very low concentration of fission products. Nearly all the uranium is precipitated, but there is still some there in solution. You leave that behind with the fission products. In the case of the separation of natural amounts of Hf from Zr, you precipitate the Zr first, and you go on until the zirconium is nearly all precipitated before the hafnium will precipitate. The hafnium isn't high enough in concentration to precipitate. You stop at that point and you leave the Hf in solution. So that can be done. Another strange thing is that the nitrides that you get often aren't what you would predict at all. I remember working with titanium and expecting TiN. This was before I looked at the phase diagram and later discovered that you could get $Ti_{1.7}N$ which iso-activity analyses showed we were getting. One of the strange things

CLOSING REMARKS

by

N. A. Gokcen[1]

This three-day "Workshop on Techniques for Measurement of Thermodynamic Properties" has accomplished its main objectives for exchanging information on various experimental methods and discussing novel concepts. As a result, we feel better equipped to generate, correlate, and disseminate thermodynamic data useful in broad areas of research and technology, particularly in mineral technology advancement. These goals are consistent with the Bureau of Mines mission, which is

> To insure the continued viability of the domestic mineral and material economy and the maintenance of an adequate mineral base, so that the Nation's economic, social, strategic, and environmental needs can better be served.

I am deeply grateful to the participants for their stimulating presentations and discussions, and for making this workshop a success. All of us involved in various aspects of planning, organizing, and directing this effort are indebted to Dr. Thomas A. Henrie, Chief Scientist, and Ralph C. Kirby, Director, Mineral Resources Technology, Bureau of Mines, for their support and encouragement.

The task of planning and organizing was not a light labor. Local arrangements were made by Louis B. Pankratz and Stephen O'Hare with valuable help from Howard O. Poppleton and Robert J. Burch. Kenneth O. Bennington and John M. Stuve were responsible for programing the technical presentations. James F. Hendricks (now deceased), Stephen T. Anderson, George Daut, and Michael Barrett managed numerous details backstage and offstage. Sharon L. Brittain was in charge of all correspondence and retyping the proceedings for editing. Robert R. Brown and George E. Daut provided transportation between the motels and the campus room. (All these persons are from Albany Research Center, Bureau of Mines.)

Special thanks are due to Robert A. Miller of the Linn-Benton Community College for providing all the facilities and the food.

Again, I wish to express my sincere appreciation for your participation, presentations, and discussions.

---

[1]Research Supervisor, Thermodynamics Laboratory, Albany Research Center, Bureau of Mines, Albany, Oreg.

APPENDIX.- LIST OF ATTENDEES AND AUTHORS[1]

*Allibert, M.	University of Grenoble, France.
*Allred, G.	Brigham Young University, Provo, Utah.
Anderson, B. W.	University of Kansas, Lawrence, Kans.
Barclay, J.	Bureau of Mines, Washington, D.C.
*Bauman, J. E.	University of Missouri - Columbia, Columbia, Mo.
Bennett, R. R.	Consultant, Eugene, Oreg.
*Bennington, K. O.	Albany Research Center, Albany, Oreg.
*Beyer, R. P.	Albany Research Center, Albany, Oreg.
*Biltonen, R. L.	University of Virginia, Charlotte, Va.
*Breslauer, K.	Rutgers University, New Brunswick, N. J.
Brown, R. R.	Albany Research Center, Albany, Oreg.
*Bulas, K.	Rutgers University, New Brunswick, N. J.
Bulau, J. R.	University of Oregon, Eugene, Oreg.
*Carling, R. W.	Sandia Laboratories, Livermore, Calif.
*Criss, C. M.	University of Miami, Coral Gables, Fla.
*Chang, Y. A.	University of Wisconsin - Milwaukee, Milwaukee, Wisc.
Chase, M. W.	Dow Chemical, Midland, Mich.
*Chatillon, C.	University of Grenoble, France.
*Christensen, J. J.	Albany Research Center, Albany, Oreg.
Daut, G. E.	Albany Research Center, Albany, Oreg.
*Eatough, D. J.	Albany Research Center, Albany, Oreg.
*Ferrante, M. J.	Albany Research Center, Albany, Oreg.
*Freeman, R. D.	Oklahoma State University, Stillwater, Okla.
Friedman, H.	General Foods, Tarrytown, N. Y.
*Furukawa, G. T.	National Bureau of Standards, Washington, D.C.
*Gammon, B. E.	Bartlesville Energy Technology Center, Bartlesville, Okla.
*Gokcen, N. A.	Albany Research Center, Albany, Oreg.
*Goldberg, R. N.	National Bureau of Standards, Washington, D.C.
*Good, W. D.	Bartlesville Energy Technology Center, Bartlesville, Okla.
*Hansen, J.	Albany Research Center, Albany, Oreg.
Herrgott, J.	Hewlett-Packard, Mt. View, Calif.
Higuchi, T.	University of Kansas, Lawrence, Kans.
*Hildenbrand, D. L.	Stanford Research Institute, Menlo Park, Calif.
Hon, R.	Boston College, Boston, Mass.
*Izatt, R. M.	Albany Research Center, Albany, Oreg.
Kirby, R. C.	Bureau of Mines, Washington, D.C.
*Knittel, D. R.	Stanford Research Institute, Menlo Park, Calif.
*Ko, H. C.	Albany Research Center, Albany, Oreg.
Landsberg, Arne	Albany Research Center, Albany, Oreg.
*Lau, K. H.	Stanford Research Institute, Menlo Park, Calif.
Leavenworth, H.	Albany Research Center, Albany, Oreg.
*Mah, A. D.	Albany Research Center, Albany, Oreg.
*Mangum, B. W.	National Bureau of Standards, Washington, D.C.
*Mountcastle, D. B.	University of Virginia, Charlottesville, Va.
Mrazek, R. V.	Oregon State University, Corvallis, Oreg.
*Neumann, J. P.	Albany Research Center, Albany, Oreg.

[1]* indicates author.

O'Hare, S. A.	Albany Research Center, Albany, Oreg.
*Otto, R.	University of California, Berkeley, Calif.
*Ozbek, H.	University of California, Berkeley, Calif.
*Pankratz, L. B.	Albany Research Center, Albany, Oreg.
*Parlee, N. A.	Stanford University, Stanford, Calif.
*Phillips, S. L.	University of California, Berkeley, Calif.
Poppleton, H. O.	Albany Research Center, Albany, Oreg.
*Prosen, E. J.	National Bureau of Standards, Washington, D.C.
Ritchey, J. L.	University of Oregon, Eugene, Oreg.
Rogers, P.	Lawrence Berkeley Laboratory, Berkeley, Calif.
Romans, P.	Albany Research Center, Albany, Oreg.
Russell, J. H.	Albany Research Center, Albany, Oreg.
*Rao, Y. K.	University of Washington, Seattle, Wash.
*Rytting, J. H.	University of Kansas, Lawrence, Kans.
*Schaefer, S. C.	Albany Research Center, Albany, Oreg.
Schenz, T.	General Foods, Tarrytown, N. Y.
Shaffer, M.	University of Oregon, Eugene, Oreg.
*Staples, B. R.	National Bureau of Standards, Washington, D.C.
Stephenson, J. B.	Bureau of Mines, Rolla, Mo.
*Stuve, J. M.	Albany Research Center, Albany, Oreg.
*Suurkuusk, J.	University of Virginia, Charlottesville, Va.
*Tavana, M.	University of California, Berkeley, Calif.
Thomas, R.	Department of Energy, Bartlesville, Okla.
*Vlach, K. C.	University of Wisconsin - Milwaukee, Milwaukee, Wisc.
*Walls, F. L.	National Bureau of Standards, Boulder, Colo.
Weill, D. F.	University of Oregon, Eugene, Oreg.
*Westrum, E. F.	University of Michigan, Ann Arbor, Mich.
*Williamson, K. D.	Union Carbide, South Charleston, W. Va.
*Witkowski, L.	Rutgers University, New Brunswick, N. J.
*Wooley, E.	Brigham Young University, Provo, Utah.

☆U.S. GOVERNMENT PRINTING OFFICE: 1981-703-002/58 INT.-BU.OF MINES,PGH.,PA. 25566